

NASW-4435

1N-11-CR  
111-63

P-587

# Project Columbiad

## Mission to the Moon

(NASA-CR-192019) PROJECT  
COLUMBIAD: MISSION TO THE MOON.  
BOOK 1: EXECUTIVE SUMMARY. VOLUME  
1: MISSION TRADE STUDIES AND  
REQUIREMENTS. VOLUME 2: SUBSYSTEM  
TRADE STUDIES AND SELECTION (MIT)  
587 p

N93-18233

Unclass

G3/91 0141653

Massachusetts Institute of Technology  
Space Systems Engineering  
Spring 1992

### Book I

#### Executive Summary

Volume I: Mission Trade Studies and Requirements

Volume II: Subsystem Trade Studies and Selection

NASA / University Space Research Association  
©Massachusetts Institute of Technology, MCMXCII. All rights reserved.

## **Contributors**

### **Systems Engineering**

Michael Clarke  
Johan Denecke  
Suzanne Garber  
Beth Kader  
Celia Liu  
Ben Weintraub

### **Crew Capsules**

Patrick Cazeau  
John Goetz  
James Haughwout  
Erik Larson

### **Propulsion Stages**

Jed Dennis  
Kathryn Fricks  
Edward Walters  
Scot Cook

### **Surface Payloads**

Mark Bower  
Debabrata Ghosh

### **Launch Vehicles**

Henri Fuhrmann  
Aaron Newman  
Jon Strizzi

### **Propulsion**

George Nagy  
Jose Ortiz  
Charles Roburn

### **Program Planning**

Kathryn Fricks  
Debabrata Ghosh  
Celia Liu  
Jon Strizzi

### **Command, Control, Communications**

Jacqueline Moore  
Victor Owvour  
Jean Yoshii

### **Crew Systems**

Paul Tompkins  
John Woyak  
Jane Yu

### **Guidance, Navigations, Control**

Jonathan Kossuth  
Lou Macalou  
Michael O'Connor

### **Power and Thermal Control**

Debabrata Ghosh  
Simone Missirian  
Paul Stach

### **Status**

Maresi Berry  
Ralph Vixama

### **Structures and Thermal Protection**

Charles Bruen  
Larry Kaye  
Patrick Malone

## **Faculty**

Professor Joseph Shea  
Professor Harold Alexander  
Professor Peter Belobaba  
Professor Stanley Weiss  
Teaching Assistant: Greg Loboda

## **Acknowledgments**

The authors would like to gratefully acknowledge the assistance and information provided by the following people and companies: Allied Signal (AiResearch Division) for technical information on environmental control and life support components; William Suit and Lynda Foernster of NASA Langley Research Center for Shuttle trajectory information, launch vehicle information and technical assistance; Pratt & Whitney Government Engines for technical information on the RL10A-4 engine; and Kaiser Marquardt Corporation for technical information on the R4-D rocket.

Special thanks to Kathryn Fricks for undertaking the huge task of editing this report.

## **PROJECT COLUMBIAD**

*Reestablishment of Human Presence on the Moon*

**Massachusetts Institute of Technology  
Department of Aeronautics and Astronautics  
Cambridge, MA**

**Professor Joseph Shea  
Professor Stanley Weiss  
Professor Harold Alexander  
Professor Peter Belobaba  
Greg Loboda, Teaching Assistant**

**Maresi Berry  
Mark Bower  
Charles Bruen  
Patrick Cazeau  
Michael Clarke  
Scot Cook  
Johan Denecke  
Joseph E. Dennis  
Kathryn Fricks  
Henri Fuhrmann**

**Suzanne Garber  
Debabrata Ghosh  
John Goetz  
James Haughwout  
Beth Kader  
Lawrence Kaye  
Jonathan Kossuth  
Erik Larson  
Celia Liu  
Alou Macalou**

**Patrick Malone  
Jacqueline Moore  
George Nagy  
Aaron Newman  
Michael O'Connor  
Jose Ortiz  
Victor Owour  
Charles Roburn  
Paul Stach  
Jon Strizzi**

**Paul Tompkins  
Ralph Vixama  
Edward Walters  
Ben Weintraub  
John Woyak  
Jean Yoshii  
Jane Yu**

### **Abstract**

In response to the Report of the Advisory Committee on the future of the U.S. Space Program and a request from NASA's Exploration Office, the MIT Hunsaker Aerospace Corporation (HAC) conducted a feasibility study, known as Project Columbiad, on reestablishing human presence on the Moon before the year 2000. The mission criteria established were to transport a four person crew to the lunar surface at any latitude and back to Earth with a 14-28 day stay on the lunar surface. Safety followed by cost of the Columbiad Mission were the top level priorities of HAC. The resulting design has a precursor mission that emplaces the required surface payloads before the piloted mission arrives. Both the precursor and piloted missions require two National Launch System (NLS) launches. Both the precursor and piloted mission have an Earth orbit rendezvous (EOR) with a direct transit to the Moon post-EOR. The piloted mission returns to Earth via a direct transit. Included among the surface payloads preemplaced are a habitat, solar power plant (including fuel cells for the lunar night), lunar rover and mechanisms used to cover the habitat with regolith (lunar soil) in order to protect the crew members from severe solar flare radiation.

### **Executive Summary**

In 1990, the Report of the Advisory Committee on the future of the U.S. Space Program proposed a plan known as Mission from Planet Earth which included the establishment of a lunar exploration base. Under the direction of NASA's

Exploration Office, the MIT Hunsaker Aerospace Corporation performed a feasibility study on the reestablishment of human presence on the Moon before the end of the decade. The project became known as Project Columbiad, named after the fictional cannon in Jules Verne's From the Earth to the Moon.

The primary objectives of Project Columbiad were to transport a four person crew to the lunar surface and back with a 28 day stay on the lunar surface. Project Columbiad was also designed to have the capacity to land at any latitude on the lunar surface and be able to abort at any time -- meaning within the next lunar launch window. Other goals of the mission were to provide the foundation for the aforementioned future lunar exploration base and in the meantime to provide an opportunity for preliminary lunar exploration and scientific research. Still other goals of a high profile mission such as this are to boost national confidence and at the same time to promote international cooperation.

Safety of the crew members was always the primary concern during the design of the mission. Redundancy standards for the mission were set at two levels for mission success and three levels for crew safety. High levels of subsystem reliability were achieved through the use of proven technologies. Results of the initial studies indicate an expected human survivability probability of 99.7%. It is expected that in the next design iteration of Project Columbiad, this probability will reach the targeted 99.9%. At this stage in the design the overall mission probability of



success reached the targeted 95% probability.

Beyond safety, cost was the primary driver of the mission design. The final estimate for the complete first mission cost, including research, development, testing, and evaluation (RDT&E), was \$12.8 billion -- a relatively low cost for a mission of this size. With the cost spread out over the remaining decade, the cost per year is within the scope the NASA budget. The primary factor contributing to this low project cost is the use of already well-developed and tested technology.

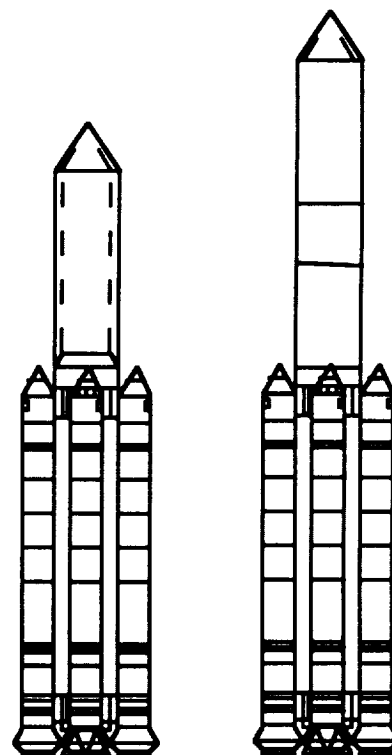
In order to make many of the design choices, a trade study regarding Columbiad's trajectory was made. In the Apollo missions of twenty years ago, a lunar orbit trajectory was used in order to reduce the initial weight and, hence, cost of the missions. Given the constraints for Columbiad to land at any latitude and to stay on the Moon for 14-28 days, the lunar orbit trajectory has several complications due to the mission goal for abort at any time. For this reason, a direct transit from the Earth is a better choice and was selected for the Columbiad missions.

The second critical trade study that was conducted was the choice of launch vehicle. The National Launch System (NLS) was chosen first for its high reliability and second for its launch capacity. The NLS has a high expected reliability due to the large number of flight tests that have already occurred for much of its hardware. Despite the fact that the NLS does not match the Saturn V's launch capabilities, it will be the largest reasonable launch vehicle available by the end of the decade. Another reason to use the NLS instead of reviving the Saturn V or designing an entirely new launch vehicle is that the NLS can be used for other types of missions and would not be a launch vehicle built and designed solely for these lunar missions as the Saturn V was. These other markets for the NLS aid in bringing down the cost of the NLS vehicle and raising the reliability.

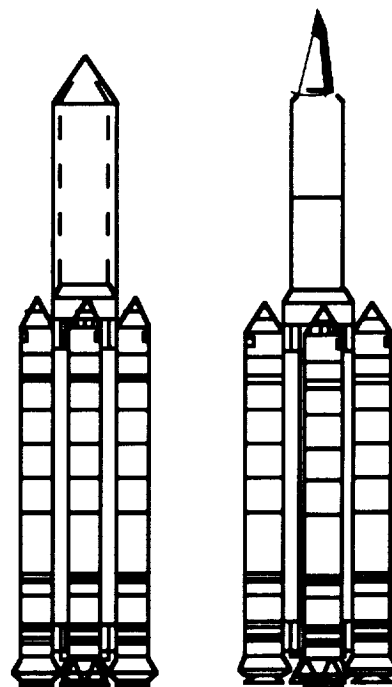
The current design for the NLS allows only a 72 metric ton payload to a 200 km circular orbit. Therefore two additional Redesigned Solid Rocket Motors (RSRM) were added on to the baseline NLS for a total of four RSRMs. This NLS configuration allows the insertion of a 100,000 kg payload (including a 10% margin) into a 200 km apogee launch trajectory. With this launch capacity, a minimum of two launches is required for a single piloted mission and an additional two launches is required for a precursor mission. Therefore an Earth orbit rendezvous is necessitated.

A total of four NLS launches is required for a complete Columbiad mission. Each precursor and piloted mission launch has a payload mass of approximately 95,600 kg. The packaging of the two missions is shown in Figure 1. The first two launches in quick succession are for the precursor while the third and fourth launches for the piloted mission are launched only after the success of the precursor mission has been confirmed. All launches are scheduled

from Kennedy Space Center, Launch Pads 39A and 39B.



**Precursor Mission**



**Piloted Mission**

**Figure 1 NLS Launches for Columbiad**

The precursor mission was designed to be as modular as possible with the piloted mission for cost considerations. Therefore, each precursor mission vehicle is composed of three propulsive elements (two are identical with the piloted mission stages) in addition to the surface payloads: Primary Trans-Lunar Injection (PTLI), Lunar Braking Module (LBM), and Payload Landing Module. Again, the PTLI is by itself on the first launch for the precursor mission (Launch 1) while the LBM, PLM, and surface payloads are on the second launch for the precursor mission (Launch 2). The surface payloads includes a habitat (BioCan) and a payload bay for other equipment.

The piloted mission is composed of three propulsive elements in addition to the Crew Module: Primary Trans-Lunar Injection (PTLI) stage, Lunar Braking Module (LBM), and Earth Return Module (ERM). The PTLI is the only component on the first launch for the piloted mission (Launch 3) while the LBM, ERM, and CM are grouped together on the second launch for the piloted mission (Launch 4).

Before translunar injection the vehicle must be established in a circular LEO for rendezvous. The NLS vehicle does not perform the circularization burn into a 200 km altitude for any of the four launches. In the precursor mission, the PTLI performs a circularization burn, and then raises its altitude to 275 km at the desired trajectory window where it will await rendezvous with the surface payload in the second launch. For the surface payloads launch, it is the LBM that performs both the circularization burn and the burn to higher orbit. Once again, for the piloted mission, the PTLI performs the circularization burn and, then, raises its altitude to 275 km at the desired trajectory window where it will await rendezvous with the piloted launch. For the piloted launch, it is the LBM that performs both the circularization burn and the burn to higher orbit.

**Table 1: Precursor Mission Profile**

Event	Location	$\Delta V$ (m/s)
Circularization of Launch 1	200 km LEO	177
Launch 1 burn to higher LEO	200-275 km LEO	43
Circularization of Launch 2	200 km LEO	177
Launch 2 burn to higher LEO	200-275 km LEO	43
Earth Orbit Rendezvous	275 km LEO	60
Trans-Lunar Injection	LEO	2460
Trans-Lunar Injection	LEO	680
Midcourse Corrections	Midcourse	120
Lunar Braking into LLO	Prior to LLO	1060
Lunar Braking to Moon	LLO to Moon	1700
Hover and Land	Moon	500

Once the vehicles have completed rendezvous, the Trans-Lunar Injection is performed by two stages: the PTLI and the LBM. The PTLI separates from the remaining stages upon the completion of its burn. The LBM completes the

burn and then performs midcourse corrections that are required during the 3 day transit. Upon lunar arrival, the LBM inserts the vehicle into LLO, and then performs the major portion of the descent burn before it is staged and crashed safely away from the landing site. For the precursor mission, the PLM then performs the final descent and hover burn before landing and deploying the habitat. A brief mission profile along with propulsive requirements for each stage is featured in Table 1.

Once the piloted mission, the ERM performs the final descent and hover burn before landing. After the 28 day lunar stay, the ERM launches the CM into LLO and then into the Earth transfer orbit. The ERM also performs any midcourse corrections. The ERM separates from the Crew Module (CM) just before reentry into the Earth's atmosphere, and then the CM proceeds to reenter the atmosphere safely. The piloted mission is completed when the CM lands at Edwards Air Force Base. A brief mission profile along with propulsive requirements for each stage is featured in Table 2. An outline of the trajectory that Columbiad vehicles will follow is shown in Figure 3.

**Table 2 : Piloted Mission Profile**

Event	Location	$\Delta V$ (m/s)
Circularization of Launch 3	200 km LEO	177
Launch 3 burn to higher LEO	200-275 km LEO	43
Circularization of Launch 4	200 km LEO	177
Launch 4 burn to higher LEO	200-275 km LEO	43
Earth Orbit Rendezvous	275 km LEO	60
Trans-Lunar Injection	LEO	2460
Trans-Lunar Injection	LEO	680
Midcourse Corrections	Midcourse	120
Lunar Braking into LLO	Prior to LLO	1060
Lunar Braking to Moon	LLO to Moon	1700
Hover	Moon	500
Lunar Launch	Moon to LLO	2200
Earth Return Injection	LLO	1060
Midcourse Corrections	Midcourse	120
Reentry	Earth's Atmosphere	100

In order to minimize the thermal stresses that the vehicle structures encounter during the mission, a decision was made to spin the transit vehicle at a rate of approximately once per hour. If a launch slippage occurs for either Launches 2 or 4, then the PTLI may initiate a spin while it waits in LEO. The PTLI would despin shortly before docking occurred with Launch 2 or Launch 4.

To equalize the payload weights of the launches, the TLI burn was split between two stages. The four launch weights were roughly equalized by allocating approximately 85% ( $\Delta V = 2460$  m/s) of the TLI burn to the Primary TLI stage. This left a  $\Delta V = 680$  m/s to be included in the next stage.

A separate stage was not designed for this small  $\Delta V$ . Instead, the propellant was included in the following stage, the LBM.

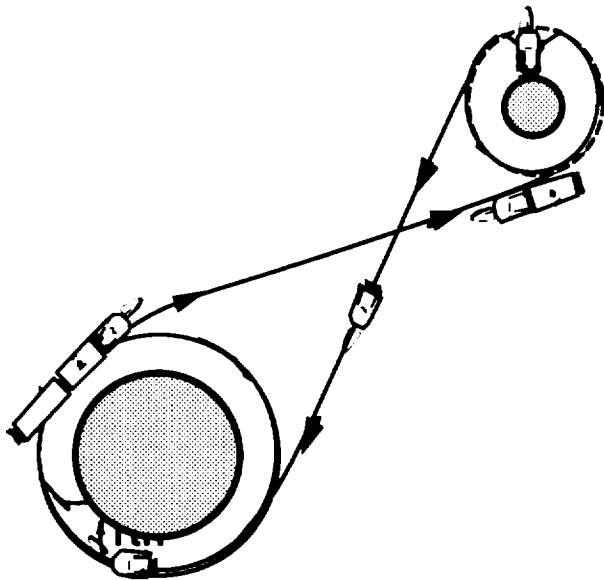


**Figure 3**  
**Columbiad Mission Trajectory**

To reduce the height of the vehicle landing on the surface of the Moon, a decision was made to stage just prior to the hover and landing phase of the lunar descent. Therefore, for both missions, the LBM is staged after completing the major portion of the descent. The ERM and PLM are both equipped with landing gear and propulsion systems to conduct the final descent phase. This is a significant aid as it reduces the height of the landing vehicle by 12-13 m.

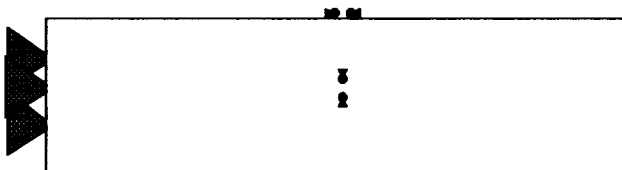


**Figure 4**  
**Primary Trans-Lunar Injection Stage**

The PTLI stage, shown in Figure 4, has five RL10 engines and performs four burns. The first PTLI burn circularizes the PTLI's Earth Orbit at 200 km. The second burn is the initial burn to transfer to a higher orbit, and the third burn completes the higher orbit transfer at 275 km. The fourth burn is the only burn occurring when the PTLI is attached to the other stages. When this burn is complete the PTLI has expended its fuel and is staged off.

The dry mass budget for this stage is 11,587 kg and the wet mass budget is 94,825 kg. Since the PTLI must remain in orbit about the Earth for up to 40 days, independently of the rest of the vehicle, it has its own power, Guidance, Navigation, and Control (GNC), and Command, Communications, and Control (C<sup>3</sup>) systems on board. Included among its apparatus is a low gain antenna for communication with Earth and a Reaction Control System (RCS) for stationkeeping.

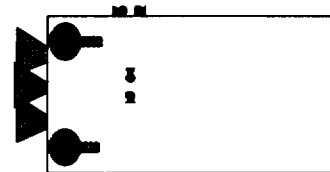


**Figure 5**  
**Lunar Braking Module**

The LBM, shown in Figure 5, has three RL10 engines and performs six burns plus midcourse corrections. The first LBM burn circularizes the vehicle's Earth Orbit at 200 km. The second burn is the initial burn to transfer to a higher orbit and the third burn completes the higher orbit transfer at 275 km, where docking with the PTLI occurs. The fourth burn is the Secondary Trans-Lunar Injection burn that occurs just after the PTLI stage is staged off. The fifth burn brakes the module into LLO, and the sixth and final burn completes most of the lunar descent burn before it is staged.

The dry mass budget for this stage is 6,731 kg and the wet mass budget is 62,285 kg. The LBM does not have its own power source. Either the ERM or the PLM provides the necessary power for it during its burns.

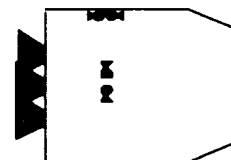


**Figure 6**  
**Earth Return Module**

The ERM, shown in Figure 6, utilizes three RL10 engines to perform three burns plus midcourse corrections. The first ERM burn is extremely critical because it prevents the CM from crashing into the lunar surface after the LBM has initiated the descent to the lunar surface. The second burn is the launch from the lunar surface into LLO and the third burn injects the vehicle into an Earth return trajectory.

The dry mass budget for the ERM is 5,553 kg, including 500 kg for landing legs that are jettisoned off after lunar launch. Within the stage, an additional payload weight of 3000 kg to the lunar surface can be stowed. This weight is twice the minimum necessary to resupply the habitat for future piloted missions. Therefore the total wet weight budget is 26,210 kg. The ERM has an RCS for both rendezvous and midcourse correction burns. It also contains a high gain antenna so that the crew can communicate with Earth in the vicinity of the Moon. The ERM supplies power to both the LBM and the CM in addition to itself.



**Figure 7**  
**Crew Module**

The crew module, shown in Figure 7, is designed as a biconic reentry vehicle with a maximum lift to drag ratio of 1.1. The lift to drag ratio allows for reentry maneuvering and extends the downrange and cross range distances of the vehicle. The vehicle safely houses the four crew members for the transit to the Moon and back to Earth, including the reentry phase. The budgeted mass of the CM is 6330 kg which includes the 730 kg heat shield.

**Table 2: Piloted Mission Mass Summary**

Stage	$\Delta V_{total}$ (m/s)	Wet Mass (kg)	Length (m)
PTLI	2680	94,825	15.96
LBM	3780	62,285	12.7
ERM	3880	22,710	9.97
Piloted Payload to Moon		3500	(in ERM)
Crew Module		6330	7.69
Nose Cone (Launch 3)		820	5
Total Mass		190,470	

Total length  
Total Mass for Launch 3 (PTLI stage) - 94,825 kg  
20.96 m  
Total Mass for Launch 4 (Piloted launch)- 95,645 kg  
27.66 m (plus 2.7 m)

The total height allowance for an NLS payload is 35 m including a nose cone. The height of Launch 4 is less than the total height of the LBM, ERM, and CM because the LBM stage is recessed into the launch vehicle by 2.7 m. This height adjustment is not needed for Launch 4, however,

it is needed for Launch 2, and in the interests of modularity, the height adjustment occurs on both Launches 2 and 4. There was no need to recess the PTLI stage for launches 1 and 3.

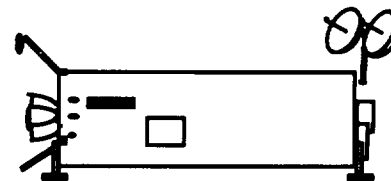


**Figure 8**  
**Payload Landing Module and BioCan**

The PLM, shown in Figure 8, has three RL10 engines and performs only one burn. The PLM burn is extremely critical in that it prevents the surface payloads from crashing into the lunar surface after the LBM has initiated the descent to the lunar surface. The PLM is also involved with the deployment of the surface payloads.

The dry mass budget for this stage is 2,743 kg. This dry mass budget does not include the weight of the landing legs. The landing legs are part of the surface payloads budget of 26,500 kg. The propellant mass is 3,582 kg although a greater amount of LOX and LH2 are stored in the propellant tanks because the tanks share the space with the lunar base fuel cell system. The total wet weight budget of the PLM is 6,325 kg. With the fixed propellant mass, the total wet weight budget of the combined PLM and surface payloads is 32,825 kg.

The PLM, also shown in Figure 8, has an RCS for both rendezvous and midcourse correction burns. It also has a high gain antenna in order that the crew can communicate with Earth while on the Moon. The PLM is responsible for providing power to itself and to the LBM during transit to the Moon in addition to its power duties on the surface. A self-deploying power system was designed for the power requirements of the habitat during the "hibernation state" (the period between the PLM touchdown and arrival of the crew). 2.5 kW of continuous usable power is supplied by two 10 m<sup>2</sup> arrays that partially track the sun and are deployed from an external surface of the PLM.

The surface payloads, shown in Figures 10 to 13, are either packed into the payload bay located just on top of the PLM, or they are packed into the habitat (BioCan) which is located above the payload bay. The payload bay has a large door on the side so that the crew members can access the packaged payloads. The payload bay is also connected to the habitat's emergency exit/entry airlock. The pathway for this airlock is only clear after the payload bay has been emptied out. The primary airlock is unobstructed on the opposite end of the BioCan.

One of the primary requirements for the lunar habitat is to provide protection against radiation from solar flares. For extended operations on the lunar surface, precautions are mandatory. In particular, Project Columbiad's 5-year campaign plan overlaps with the period 1999 to 2004 which is predicted to be a peak period in the solar flare cycle. Thus solar flare protection of the habitat is given a high priority in the surface operation requirements of the piloted mission. For Project Columbiad applications, a 25 Radiation Exposure Man (REM) *maximum* was set for the entire mission duration (36 earth-days). For almost all of the solar flares that will occur, the radiation dosage is much lower than the 25 REM with the amount of protection that the BioCan provides.

Columbiad's strategy for solar flare protection is to cover the habitat with regolith, the lunar soil. A depth of 50 cm is needed to provide the desired level of protection. This operation is performed by a regolith collecting machine that brushes the dirt from the lunar surface and dumps it into a dump-bucket attachment on the rover. The rover, in turn, pours the regolith onto a drivable conveyer, which dumps it to different heights on the side and top of the habitat. A regolith support structure is also designed, to hold the regolith on a 45° incline along the sides of the habitat. See Figure 9.

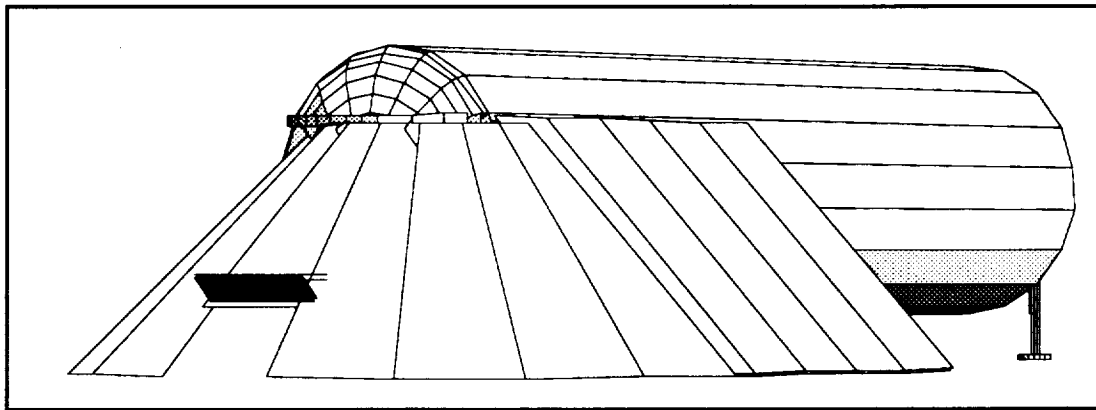


**Figure 9 Habitat with Regolith Support Structure**

The habitat, shown in Figure 9, is the lunar home for four astronauts. It is a 10 m long and 6 m diameter double-walled cylinder. The external skin is integrated with the external structure of the PLM. The internal cylinder, made of composite material is separated by a thin layer of sealed vacuum from the external cylinder and is pressurized with 5 psi of breathable atmosphere. The internal space is arranged to optimize the layout of all subsystems based on their predicted need and frequency of use. A 2 m by 1 m airlock door on one end of the habitat provides the primary access to the habitat. In case of an emergency, a secondary airlock that opens into the cargo bay from the crew quarters can be used. The total estimated mass of the habitat is less than 10,000 kg.

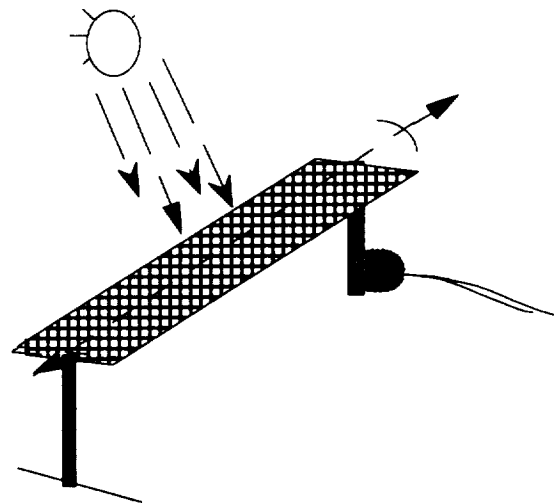


**Figure 10 Solar Lunar Power Plant**

A solar power plant, shown in Figure 10, is designed to meet the power requirements of running all the base operations. A 250 m<sup>2</sup> photovoltaic array provides 35 kW of continuous daytime usable power during the lunar day. The

rest of the power goes into charging up alkaline fuel cells system for 35 kW of night power. The fuel for the fuel cells are stored along with the propellant for the PLM. The total mass of the power system hardware is approximately 1000 kg. All fuel cells and other power conditioning hardware are located inside the PLM and the cargo bay.

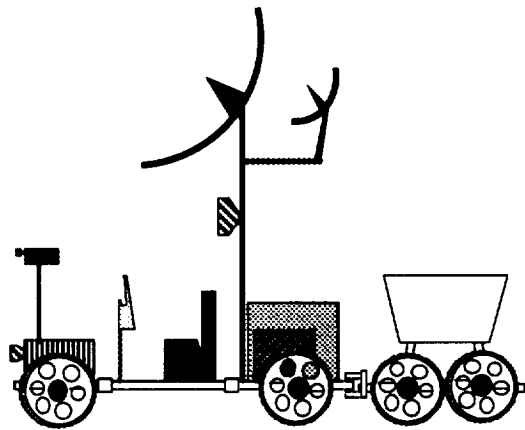


**Figure 11 Lunar Rover**

The Rover, shown in Figure 11, is the surface transportation vehicle, capable of ferrying 1500 kg of payload. It is a six-wheel drive, four-wheel steered vehicle. The fully deployed rover is 5 m long and 2.5 m wide. The height of the vehicle is 2.5 m, including the height of its fully deployed high gain antenna. The vehicle is battery powered for a 120 km nominal mission range at an maximum velocity of 20 km/hour. To ensure the walk-back capability of the astronauts, all missions are limited to within a 50 km radius of the habitat. The maximum mission duration is 8 hours. The vehicle is unpressurized, but the astronauts can hook up their EVA suits to the Portable Life Support System (PLSS) packs onboard the rover. The astronauts' PLSS backpacks are held in reserve for off-the-vehicle activities and for emergency procedures. Essentially, the rover is the workhorse for all surface operations. The regolith collector and the conveyor both require the rover for their operation.

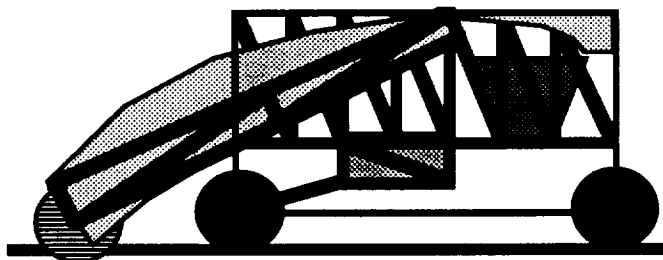


**Figure 12 Regolith Collector**

The regolith collector is quite similar in operation to a street sweeper. Loose lunar soil is swept up by a brush at a

nominal rate of  $0.05 \text{ m}^3$  per minute. The regolith particles slide up shroud and collect in a  $1 \text{ m}^3$  hopper. After every twenty minutes of soil collecting, the hopper dumps the collected regolith into a dump-bucket attached to the rover. The armature arm can be raised to lift the brush above 50 cm obstacles on the collector's way. The drive mechanism of the wheels can be preprogrammed and/or operated remotely within line of sight. The regolith collector runs on 7.5 kW of power, stored on board in Sodium-Sulfide cells. Maximum operating time of the machine, limited by the total stored power, is 8 hours. The cells require 12 hours to charge up to the maximum power levels.

The Lunar conveyor, shown in Figure 13, is a multipurpose conveyer system. The main use of the conveyer is to transport loose regolith to any height on the regolith support structure. The expandable design consists of four segments, each 4 m long for a total length of 16 m. The belt width is 1 m. The entire system sits on 16 wire-mesh wheels and can be driven around as an articulated, 4-wheel-drive vehicle. The power required to run the conveyor is 5 kW. This determines a maximum feed rate of  $0.28 \text{ m}^3$  of regolith over a 16.00 m distance in one minute. Each connection point is a pin which gives the conveyor the flexibility to deliver its payload up inclines and over obstacles. With torsional clamps, the joints can be made rigid to allow for transport over trenches.

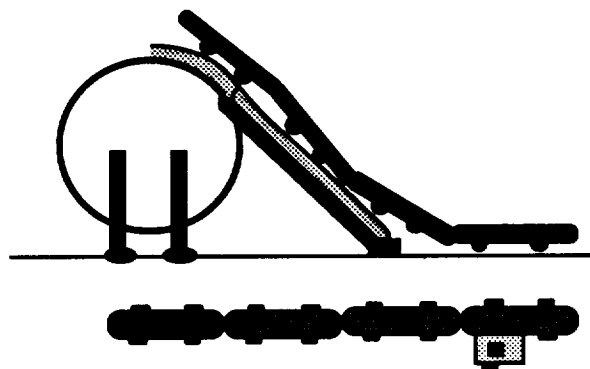


**Figure 13  
Regolith Conveyor on top of Regolith  
Support Structure**

**Table 3: Precursor Mass Summary**

Stage	$\Delta V_{\text{total}}$ (m/s)	Wet Mass (kg)	Length (m)
PTLI	2680	94,825	15.96
LBM	3780	62,285	12.7
PLM	500	6325	6.77
Surface Payloads		26500	12.5
Nose Cone (Launches 1, 2)		820	5
Total Mass		190,755	

**Total Length**

Total Mass for Launch 1 (PTLI stage)      94,825 kg  
20.96 m

Total Mass for Launch 2 (Piloted launch)      95,930 kg  
34.27 m (plus 2.7 m)

The total height allowance for an NLS payload is 35 m including a nose cone. The height of Launch 2 is less than the total height of the LBM, PLM, and the surface payloads because the LBM stage is recessed into the launch vehicle by 2.7 m. This height adjustment brings the total height of the launch within the 35 m limit.

**VOLUME I**  
**Mission Trade Studies and Requirements**



## Table of Contents

<b>1 Program Overview</b>	<b>1</b>
1.1 Introduction	1
1.2 Design Criteria	1
1.2.1 Crew Safety and Mission Success	2
1.2.2 Cost	2
1.2.3 Performance	2
1.2.4 Schedule	2
1.2.5 Expandability	2
1.3 Mission Overview	3
1.3.1 Launch Vehicle	3
1.3.2 Conceptual Mission Design	3
1.3.3 Conceptual Lunar Base Mission	4
1.4 Summary of Report	4
1.5 Mission Requirements	5
1.5.1 Mission Objectives	5
1.5.2 Mission Phase Requirements	6
1.5.2.1 Top Level Requirements for All Mission Phases	6
1.5.2.2 Launch to Low Earth Orbit	6
1.5.2.3 Earth Orbit Rendezvous	6
1.5.2.4 Low Earth Orbit to Lunar Transfer Orbit	6
1.5.2.5 Lunar Transfer Orbit to Low Lunar Orbit	7
1.5.2.6 Low Lunar Orbit to Lunar Surface	7
1.5.2.7 Lunar Stay	7
1.5.2.8 Lunar Surface to Low Lunar Orbit	7
1.5.2.9 Low Lunar Orbit to Earth Transfer Orbit	7
1.5.2.10 Reentry	8
1.5.3 Project and Subsystem Requirements	8
1.5.3.1 Launch Vehicles	8
1.5.3.2 Propulsion Stages	8
1.5.3.2.1 Propulsion	9
1.5.3.3 Crew Capsules	9
1.5.3.4 Crew Systems	9
1.5.3.5 Surface Payloads	10
1.5.3.5.1 Pre-positioned Payloads	10
1.5.3.5.2 Manned Capability	10
1.5.3.5.3 Surface Vehicle	10
1.5.3.6 Guidance Navigation and Control (GNC)	10
1.5.3.7 Command, Control, and Communications (C3)	11
1.5.3.8 Power and Thermal Control	11
1.5.3.9 Structure and Thermal Protection	12
1.5.3.10 Status	12
<b>2 Mission Modes</b>	<b>13</b>
2.1 Introduction	13
2.2 Launch Vehicle Capabilities Comparison	13
2.2.1 Energiya Launch System	13
2.2.1.1 Launch Vehicle Configuration	14
2.2.1.2 Reliability and Safety	15
2.2.1.3 Cost	15
2.2.1.4 Launch site	16
2.2.1.5 Summary	16
2.2.2 The National Launch System	16

2.2.2.1	Launch Vehicle Configuration .....	17
2.2.2.2	Reliability and Safety .....	19
2.2.2.3	Cost .....	19
2.2.2.4	Payload Interface .....	19
2.2.2.5	Launch Site.....	20
2.2.2.6	Alternate Configurations.....	20
2.2.2.7	Summary .....	20
2.2.3	Saturn V Launch Vehicle.....	22
2.2.3.1	Launch Vehicle Configuration .....	22
2.2.3.2	Reliability and Safety .....	22
2.2.3.3	Modifications .....	22
2.2.3.4	Cost .....	23
2.2.3.5	Summary .....	23
2.2.4	Heavy Lift Delta.....	24
2.2.4.1	Launch Vehicle Configuration .....	24
2.2.4.2	Reliability and Safety .....	24
2.2.4.3	Cost .....	26
2.2.4.4	Payload Interface .....	26
2.2.4.5	Summary .....	27
2.2.5	Shuttle-C.....	27
2.2.6	Conclusion.....	27
2.3	Mission Mode Considerations .....	27
2.3.1	Spacecraft Descriptions .....	27
2.3.1.1	Spacecraft Configurations.....	28
2.3.1.1.1	Service Module (SM).....	28
2.3.1.1.2	Lunar Braking Module (LBM).....	28
2.3.1.1.3	Lunar Touchdown Module (LTM).....	28
2.3.1.1.4	Command Module (CM).....	28
2.3.1.1.5	Trans-Lunar Injection Module (TLI) .....	28
2.3.1.1.6	Habitat.....	28
2.3.2	Reusability of Modules.....	29
2.3.2.1	Reusable Lander.....	29
2.3.2.2	Reusable Transfer Vehicle.....	29
2.3.2.3	Reusable Re-entry Vehicle .....	29
2.4	Definition of Modes Compared.....	29
2.4.1	Direct Flight (DF).....	29
2.4.1.1	Launch to Trans-Lunar Injection .....	29
2.4.1.2	Trans-Lunar Orbit.....	29
2.4.1.3	Lunar Approach and Landing.....	31
2.4.1.4	Lunar Launch to Trans-Earth Orbit.....	31
2.4.1.5	Earth Approach and Landing.....	31
2.4.2	Earth Orbit Rendezvous (EOR) .....	31
2.4.2.1	Launch to Trans-Lunar Injection .....	31
2.4.2.2	Trans-Lunar Orbit.....	31
2.4.2.3	Lunar Approach and Landing.....	33
2.4.2.4	Lunar Launch to Trans-Earth Orbit.....	33
2.4.3	Lunar Orbit Rendezvous Mode (LOR) .....	33
2.4.3.1	Launch to Trans-Lunar Injection .....	34
2.4.3.2	Trans-Lunar Orbit.....	34
2.4.3.3	Lunar Approach, Lunar Orbit, and Lunar Landing.....	35
2.4.3.4	Lunar Launch to Trans-Earth Orbit.....	35
2.4.3.5	Earth Approach and Landing.....	35
2.4.4	Earth/Lunar Orbit Rendezvous (ELOR).....	36
2.4.4.1	Launch to Trans-Lunar Injection .....	36

2.4.4.2	Trans-Lunar Orbit .....	36
2.4.4.3	Lunar Approach, Lunar Orbit, and Lunar Landing.....	36
2.4.4.4	Lunar Launch to Trans-Earth Orbit.....	36
2.4.4.5	Earth Approach and Landing .....	38
2.4.5	Reusable Modules .....	38
2.4.5.1	Re-entry Vehicle.....	38
2.4.5.2	Lunar Lander.....	38
2.4.5.3	Transfer Vehicle .....	38
2.4.6	Orbiting Lunar Station.....	38
2.4.7	Space Shuttle .....	39
2.4.7.1	Piloted Mission Shuttle .....	39
2.4.7.2	Orbiting Lunar Station .....	39
2.5	Mode Elimination.....	39
2.5.1	Launch Capability Limitations.....	39
2.5.2	Reusability Limitations.....	39
2.5.3	Orbiting Lunar Station.....	39
2.5.4	Space Shuttle .....	40
2.5.4.1	Piloted Mission Shuttle .....	40
2.5.4.2	Orbiting Lunar Station.....	40
2.6	Conclusion .....	40
3	<b>Piloted Mission Mode Comparison .....</b>	<b>41</b>
3.1	Requirements and Assumptions for Piloted Mode Analysis .....	41
3.2	Earth Orbit Rendezvous Design .....	43
3.2.1	Configuration Description .....	43
3.2.1.1	Trans-Lunar Injection Stages .....	44
3.2.1.2	Lunar Braking Module.....	45
3.2.1.3	Earth Return Module.....	46
3.2.1.4	Crew Module .....	46
3.2.1.5	EOR Mass Summary.....	47
3.2.2	Safety.....	47
3.2.3	Cost.....	47
3.2.4	Performance Issues.....	49
3.2.4.1	Design Complexity.....	49
3.2.4.2	Commonality with Precursor .....	50
3.2.5	Expandability Issues.....	50
3.2.6	Conclusion.....	50
3.3	Earth and Lunar Orbit Rendezvous Design.....	51
3.3.1	Configuration Description .....	51
3.3.1.1	Trans-Lunar Injection Stages .....	51
3.3.1.2	Service Module .....	51
3.3.1.3	Lunar Excursion Module .....	52
3.3.1.4	Crew Module and Heat Shield.....	52
3.3.1.5	Mission Profile Summary .....	55
3.3.1.6	ELOR Mass Summary.....	57
3.3.2	Safety.....	58
3.3.2.1	Abort Complexity .....	58
3.3.2.2	Rendezvous and Separation Complexity .....	59
3.3.3	Cost.....	60
3.3.4	Performance Issues.....	61
3.3.4.1	Design Complexity.....	61
3.3.4.1.1	Heat Shield Separation and Rendezvous in LLO.....	61
3.3.4.1.2	No Heat Shield Separation.....	64
3.3.4.1.3	Design Complexity Conclusion .....	65

3.3.4.2	Maintenance in LLO.....	65
3.3.4.3	Efficiency.....	66
3.3.4.4	Lunar Landing Advantage.....	66
3.3.4.5	Precursor Commonality .....	66
3.3.5	Expandability Issues.....	66
3.3.6	Conclusion.....	67
3.4	Mode Comparison.....	67
3.4.1	Introduction.....	67
3.4.2	Reliability and Mission Success.....	68
3.4.3	Performance.....	68
3.4.3.1	Crew Module Study.....	68
3.4.3.2	Mass Comparison .....	70
3.4.3.3	Performance Margins .....	70
3.4.4	Cost and Scheduling.....	71
3.4.5	Expandability .....	74
3.4.6	Crew Capsules Comparison.....	74
3.4.6.1	EOR Capsule Designs .....	74
3.4.6.1.1	EOR (Direct Flight Style) Capsule.....	74
3.4.6.1.2	The Landable Base Module.....	76
3.4.6.1.3	EOR Conclusions.....	77
3.4.6.2	ELOR Capsule Designs.....	77
3.4.6.2.1	Closed Cockpit Lunar Lander (CCLL).....	78
3.4.6.2.2	Open Cockpit Lunar Lander (OCLL).....	79
3.4.6.2.3	ELOR Conclusions .....	81
3.4.6.3	The EOR/ELOR Hybrid Capsule.....	81
3.4.6.4	The Final Capsule Selection.....	81
3.4.7	Conclusions on Mode Comparison.....	82
4	<b>Precursor Mission</b> .....	83
4.1	Lunar Landing Configuration.....	83
4.2	Vertical Stack .....	84
4.3	Horizontal Stack.....	85
4.4	Folded Horizontal Configuration.....	86
4.5	Hybrid Configuration.....	87
4.6	Side-Saddled Configuration.....	88
4.6.1	Vertical .....	88
4.6.2	Horizontal.....	89
4.7	Candidate Landing Configuration .....	89
4.8	Conclusion .....	91
5	<b>Columbiad Mission</b> .....	93
5.1	Piloted Mission Design .....	94
5.1.1	Piloted Mission Profile Overview.....	94
5.1.2	Design Choices.....	95
5.1.3	Primary Trans-Lunar Injection Stage.....	96
5.1.4	Lunar Braking Module .....	97
5.1.5	Earth Return Module .....	98
5.1.6	Crew Module.....	98
5.1.7	Piloted Mission Mass Summary .....	99
5.2	Precursor Mission Design .....	99
5.2.1	Precursor Mission Profile Overview .....	99
5.2.2	Commonality with Piloted Vehicle Stages .....	101
5.2.3	Payload Landing Module .....	102
5.2.3.1	Propulsion Stage .....	102
5.2.3.2	Landing and Deployment.....	102
5.2.4	Payloads Description .....	103

5.2.4.1	Habitat	103
5.2.4.2	Power Supply	103
5.2.4.3	Rover	104
5.2.4.4	Regolith Collector	104
5.2.4.5	Lunar Conveyor	104
5.2.5	Precursor Mission Mass Summary	106
5.2.6	Solar Protection	106
5.2.6.1	Radiation Exposure Limit	106
5.2.6.2	Determination of protection level	107
5.2.6.3	Protection Strategy	108
5.3	Mission Trajectory Analysis	108
5.3.1	Earth Launch	108
5.3.1.1	Launch Windows	108
5.3.1.2	Launch Window Periods	109
5.3.1.3	Orbital Drag on the PTLI Stage	109
5.3.1.4	NLS Ascent Trajectory	110
5.3.1.4.1	Sequenece of Events	111
5.3.1.4.2	Altitude, Downrange, and Pitch Profile	112
5.3.1.4.3	Orbital Insertion and Circularization	114
5.3.2	Rendezvous	115
5.3.3	Lunar Transfer Orbit	117
5.3.3.1	Three Body Problem Formulation	118
5.3.3.2	Designated Lunar Landing Site	120
5.3.3.3	Selected Transfer Trajectory	120
5.3.3.3.1	Trajectory Search Algorithm	120
5.3.3.3.2	Planar Transfer	122
5.3.3.3.3	Polar Transfer	124
5.3.3.4	Abort Considerations	126
5.3.4	Lunar descent	127
5.3.4.1	Gravity Turn Trajectory	127
5.3.5	Lunar Ascent	130
5.3.6	Earth Transfer Orbit	131
5.3.7	Reentry into Earth's Atmosphere	131
5.3.7.1	Reentry Configuration	132
5.3.7.2	Lunar Launch Windows and Trajectories	133
5.3.7.2.1	Entry Corridor	133
5.3.7.2.2	Earth Return Window	135
5.3.7.2.3	Initial Reentry Trajectory	136
5.3.7.2.4	Reentry Trajectory	136
5.3.7.2.5	Parachute Operations	139
5.4	Mission Timeline	141
5.4.1	Nominal Precursor Mission Event Timeline	141
5.4.1.1	Premission Operations	141
5.4.1.2	Earth Surface Operations	142
5.4.1.3	Prelaunch Checkout to EOR	142
5.4.1.4	Trans-Lunar Injection to LLO	144
5.4.1.5	LLO to Precursor Landing and Deployment	145
5.4.2	Nominal Piloted Mission Event Timeline	145
5.4.2.1	Earth Surface Operations	145
5.4.2.2	Prelaunch Checkout to EOR	146
5.4.2.3	Trans-Lunar Injection to LLO	147
5.4.2.4	LLO to Piloted Vehicle Landing	148
5.4.2.5	Lunar Surface Operations	148
5.4.2.6	Lunar Launch to Return Midcourse Corrections	149

5.4.2.7	Reentry and Landing.....	150
5.4.3	Abort Sequences (Precursor Mission).....	150
5.4.4	Abort Sequences (Piloted Mission).....	151
5.4.4.1	Conditions for Abort.....	151
5.4.4.2	Redundant-Set-Launch Sequencer Abort.....	152
5.4.4.3	SRB-Powered Flight Ejection Abort.....	153
5.4.4.4	Capsule Release and Ejection Abort.....	153
5.4.4.5	Trans-Atlantic/Abort-Once-Around/Abort-To-Orbit Abort.....	154
5.4.4.6	Earth Orbit Abort.....	154
5.4.4.7	Trans-Lunar Injection Abort .....	154
5.4.4.8	Trans-Lunar Abort .....	155
5.4.4.9	Lunar Orbit Insertion Abort.....	155
5.4.4.10	Descent Abort .....	155
5.4.4.11	Surface Abort.....	156
5.4.4.12	Ascent Abort.....	156
5.4.4.13	Trans-Earth Injection Abort.....	156
5.4.4.14	Post-Reentry Abort .....	156
5.5	Loading Profile.....	156
5.5.1	Launch Vehicle Loading .....	156
5.5.2	PTLI Propulsion Stage.....	157
5.5.3	The LBM Loading Profile .....	158
5.5.4	ERM Loading Profile.....	160
5.5.5	Reentry Loading of the Command Module.....	162
5.5.6	Parachute Loading .....	163
5.5.6.1	Drogue Parachute.....	163
5.5.6.2	Parafoil Deployment .....	164
5.6	Mission Reliability Analysis .....	165
5.6.1	Event Breakdown.....	165
5.6.2	Component or Subsystem Break-up.....	167
5.6.3	Reliability Analysis Summary.....	169
REFERENCES .....		173
APPENDIX I.....		174
APPENDIX II		
	Human Limitations of Multiple G.....	182
APPENDIX III.....		184

## List of Figures

Figure 1-1 Requirements Tree.....	5
Figure 2-1 Energiya Launch Vehicle.....	14
Figure 2-2 National Launch System.....	18
Figure 2-3 Alternate NLS Configuration.....	21
Figure 2-4 Heavy Lift Delta.....	25
Figure 2-5 Mission Profile, Direct Flight Mode.....	30
Figure 2-6 Mission Profile, Earth Orbit Rendezvous Mode .....	32
Figure 2-7a Mission Profile, Lunar Orbit Rendezvous Mode .....	34
Figure 2-7b Mission Profile, Lunar Orbit Rendezvous Mode .....	35
Figure 2-8 Mission Profile, Earth/Lunar Orbit Rendezvous Mode.....	37
Figure 3-1 Trans-Lunar Injection .....	44
Figure 3-2 Lunar Braking Module .....	45
Figure 3-3 Earth Return Module .....	46
Figure 3-4 Crew Module.....	46
Figure 3-5 Trans-Lunar Injection .....	51
Figure 3-6 Service Module.....	52
Figure 3-7 Lunar Excursion Module.....	52
Figure 3-8 Crew Module and Heat Shield .....	53
Figure 3-9 LLO Separation .....	54
Figure 3-10 LLO Rendezvous.....	55
Figure 3-11 Polar Orbit Alignment.....	58
Figure 3-12 Lock and Key Docking Method .....	62
Figure 3-13 Jaws and Swivel Docking Method .....	63
Figure 3-14 Roofer Docking Method.....	64
Figure 3-15 EOR Capsule Configuration .....	75
Figure 3-16 Landable Base Configuration .....	76
Figure 3-17 Return Vehicle and Propulsive Modules.....	78
Figure 3-18 Closed Cockpit Lander Configuration .....	78
Figure 3-19 Open Cockpit Lander Configuration .....	80
Figure 4-1 Vertical Landing Configuration .....	85
Figure 4-2 Horizontal Landing Configuration.....	86
Figure 4-3 Folded Horizontal Landing Configuration.....	86
Figure 4-4 Hybrid Landing Configuration.....	87
Figure 4-5 Side-Saddled Landing Configuration (vertical) .....	88
Figure 4-6 Side-Saddled Landing Configuration (horizontal) .....	89
Figure 4-7 Deployment of Surface Payloads .....	91
Figure 5-1 NLS Launches for Columbiad .....	93
Figure 5-2 NLS Launches for Piloted Mission.....	94
Figure 5-3 Primary Trans-Lunar Injection .....	96
Figure 5-4 Lunar Braking Module .....	97
Figure 5-5 Earth Return Module .....	98
Figure 5-6 Crew Module.....	98
Figure 5-7 NLS Launches for Precursor Mission.....	100
Figure 5-8 Payload Landing Module .....	102
Figure 5-9 Omitted Intentionally .....	
Figure 5-10 Surface Payloads .....	105
Figure 5-11 NLS Altitude vs. Down Range Trajectory .....	113
Figure 5-12 NLS Pitch Profile with Time.....	114
Figure 5-13 NLS Trajectory to 200km LEO.....	115
Figure 5-14 Rendezvous Orbit .....	117
Figure 5-15 Rotating Coordinate System of Three Body Problem.....	119

Figure 5-16 Lunar Transfer Orbit.....	122
Figure 5-17a Planar Injection Trajectory.....	124
Figure 5-17b Polar Injection Trajectory.....	125
Figure 5-18 Lunar Descent Profile.....	128
Figure 5-19 Lunar Ascent Profile.....	131
Figure 5-20 Biconic Design of the Entry Vehicle.....	132
Figure 5-21 Entry Corridor.....	133
Figure 5-22 Corridor Sizing.....	134
Figure 5-23 3-D View of the Reentry Window.....	134
Figure 5-24 Time-geometry Relationship.....	135
Figure 5-25 Motion of Landing Site.....	136
Figure 5-26 Reentry Trajectories.....	137
Figure 5-27 Altitude vs. Time for Reentry Trajectory.....	138
Figure 5-28 Velocity vs. Time for Reentry Trajectory.....	138
Figure 5-29 Acceleration vs. Time for Reentry.....	139
Figure 5-30 Graphical Representation of the Parachute Profile.....	140
Figure 5-31 Launch Loading.....	157
Figure 5-32 PTLI Loading from Trans-Lunar Injection Burn.....	158
Figure 5-33 PTLI Loading from Circularizing Burn.....	158
Figure 5-34 LBM Loading during LEO Circularization.....	159
Figure 5-35 LBM Loading due to the TLI Burn.....	159
Figure 5-36 LBM Loading from Midcourse Burn.....	160
Figure 5-37 LBM Loading from Lunar Orbit Braking Burn.....	160
Figure 5-38 ERM Loading during Lunar Hover.....	161
Figure 5-39 ERM Loading during Lunar Launch.....	161
Figure 5-40 ERM Loading during Trans-Earth Burn.....	162
Figure 5-41 ERM Loading during Midcourse Maneuvers.....	162
Figure 5-42 Reentry Loading.....	163
Figure 5-43 Drogue Parachute Loading.....	164
Figure II-1 Acceleration Vector Convention.....	182
Figure III-1 Geometry of Reentry.....	184
Figure III-2 Acceleration Profile during Reentry.....	186
Figure III-3 Energy Conversion Factor with Respect to Altitude.....	187
Figure III-4 Flow Field around Blunt Body and Streamlined Body.....	188



## List of Tables

Table 2-1: Energiya Specifications and Dimensions .....	14
Table 2-2: NLS Failure Probability .....	19
Table 2-3: Heavy Lift Delta Costs.....	26
Table 3-1: Mission Profile .....	44
Table 3-2: Mass Summary .....	47
Table 3-3: R&D and Manufacturing Costs.....	48
Table 3-4: Total Flight Costs .....	49
Table 3-5: Commonality Comparison between Precursor and EOR.....	50
Table 3-6: Mission Profile Summary .....	56
Table 3-7: Additional Mission Profile Summary .....	56
Table 3-8: Stage Mass Budgets.....	57
Table 3-9: Stage Summary.....	57
Table 3-10: R&D and Manufacturing Costs .....	60
Table 3-11: Mission and Long-Term Costs.....	61
Table 3-12: Summary of Crew Module Mass Studies.....	69
Table 3-13: Mass and $\Delta V$ Summary.....	71
Table 3-14: Commonality in Design of Components .....	72
Table 3-15: Cost Comparison for the Piloted Mission.....	73
Table 4-1: Summary of Landing Configurations.....	90
Table 5-1: Mission Profile .....	95
Table 5-2: Mass Summary .....	99
Table 5-3: Mission Profile .....	101
Table 5-4: Commonality Comparison between Precursor and EOR.....	101
Table 5-5: Mass Summary .....	106
Table 5-6: NASA Flight Rules for Crew Radiation Exposure Limits.....	107
Table 5-7: Required Protection for Different Levels of Solar Flare .....	107
Table 5-8: Altitude Loss of the PTLI Stage During a One Month Orbital Stay .....	110
Table 5-9: NLS Ascent Event Sequence.....	112
Table 5-10: Planar Transfer Specifications.....	123
Table 5-11: Polar Transfer Specifications.....	126
Table 5-12: Event Profile.....	140
Table 5-13: Parafoil Load Factors.....	164
Table 5-14: Precursor Mission Event Break-up .....	165
Table 5-15: Piloted Mission Event Break-up .....	166
Table 5-16: Component/Subsystem Reliabilities .....	167
Table 5-17: Precursor Mission Success Probability .....	170
Table 5-18a: Probability of Piloted Mission Success and Survivability .....	171
Table 5-17b: Probability of Piloted Mission Success and Survivability.....	172
Table II-1: Human Limitations of Multiple Acceleration .....	183

# **1. Program Overview**

## **1.1 Introduction**

Over twenty years ago Americans embarked on the most audacious and complex technological journey of the twentieth century: landing humans on the Moon and returning them safely to Earth. The many flights in the Apollo Program clearly demonstrated the superiority of the space technology in the United States. Now, it is time to demonstrate that the dream of permanent human presence in space can become an affordable reality.

Like its namesake, the fictional cannon which fired humans to the moon in Jules Verne's From the Earth to the Moon, Project Columbiad undertakes the challenge of designing an efficient and low-cost piloted mission to the lunar surface. Not only will meeting this challenge provide great scientific and technological advancement for the United States and the world, it can also invoke national pride in the American people. Such social benefits may include a betterment of the educational system as youngsters strive to achieve in science and technology, and economic benefits resulting from these morale changes. The question, then, should not be why this challenge is worth pursuing, but how this challenge is to be accomplished so that the most benefits can be reaped. Here, the Columbiad team of The Hunsacker Corporation proposes a space campaign which maximizes crew safety and minimizes national spending.

The goals of Project Columbiad include those set forth by Michael Griffen. The first is to transport a minimum of four people to the Moon with a landing coverage at any latitude. The humans must stay on the Moon for 14-28 days before returning back to Earth. The second goal is to establish an expandable foundation for a lunar base. Other mission objectives are to provide an environment for scientific research and exploration which would benefit longer duration missions such as a piloted Mars mission. International cooperation is considered, but boosting national confidence is the major concern in this period of disappointing and expensive space projects.

## **1.2 Design Criteria**

Public and political interests play an important part in the considerations which drive the design of the launch system, space vehicles, and lunar operations. Five main issues govern the entire mission and they are, in order of importance: crew safety and mission success, cost, performance, scheduling, and expandability.

### **1.2.1 Crew Safety and Mission Success**

A 99.9% crew survivability rate in all portions of the mission will be the top design priority. Therefore, all equipment, testing, and abort aspects which affect the crew safety need to provide the reliability and redundancy to meet this requirement. A 95% minimum mission success is desired, which can provide means to avoid over-redundancy in all subsystems to save on vehicle weight and cost. Safety is also an important issue in deciding between nuclear and solar power for the lunar habitat over the long term.

### **1.2.2 Cost**

Cost is an important issue in today's economy. No longer is the public willing to overlook spending to accomplish a goal, no matter how prestigious. Commonality between systems and low-risk technology will be used in the design whenever possible to cut down on development and integration costs as well as technological uncertainty factors. In the case where advanced technology is required, a method of risk management will be used to insure that over-runs are minimized.

### **1.2.3 Performance**

Good performance is necessary to accomplish any mission. Here, performance drives the mission mode profile chosen, the types of propulsion systems used, and the many factors which affect human activities. This design should accomplish the mission task in an efficient manner. The payload to initial mass ratio should be maximized. In order for the lunar base to be staffed and maintained, repeated flights will require a design that strives to do far more than what was done in the Apollo program for only a modest increase in effort.

### **1.2.4 Schedule**

NASA is aiming for a lunar mission by the turn of the century, so scheduling is also an important determination of the kind of technology which is chosen and the amount of testing and development which is needed. Program planning is required to minimize the time span of over-runs and to minimize costing spikes.

### **1.2.5 Expandability**

The goal for permanent human presence in space makes this design factor necessary. The lunar habitat must have a modular design, so that expansion units can be easily attached during later missions. The mission design also needs to have the capacity to have a second

piloted mission return to the lunar establishment *without* a second precursor mission also being required. This requires that the piloted vehicle have the capacity to resupply the habitat with food, water, air, clothing and any other 'used' items. Not only do lunar habitats need to provide ways for reusability and expandability, the crew capsule is also designed to be reusable. Expandability plays an especially important role in the design of the lunar habitat, the lunar landing configuration, and the shape of the crew capsule.

### **1.3 Mission Overview**

#### **1.3.1 Launch Vehicle**

The capability of the mission relies substantially on the launch vehicle which is chosen. This not only determines the amount of mass which can be transferred to Low Earth Orbit (LEO) and, therefore, the number of launches which is required for the mission, but it also determines when the mission can be reasonably launched. Project Columbiad chose to incorporate the National Launch System (NLS) into the lunar mission design both for its high expected reliability and also its compatibility with other space missions. With its extensive use of existing components, it was determined that the NLS would be able to fulfill the safety requirement with less testing than a completely new launch vehicle. Its possible application to other space programs would also add to the effort for development (see Section 2.2 for complete launch vehicle trade-off.).

The NLS is currently designed to be able to put 72 metric tons into LEO with two rocket boosters, but Hunsacker's Launch Vehicles team estimates that another 28 metric tons may be added with two additional boosters and the absence of a full external fairing. Even with plans to use all of the 100 metric ton capability, a minimum of two launches is required for every piloted mission in order to put into orbit all injection stages, the lunar lander, and the crew capsule.

#### **1.3.2 Conceptual Mission Design**

The space vehicles are designed within the weight and space limit set by the NLS. A constraint of 8 m diameter is the budget for all propulsion stages, and total spacecraft height is set at a 35 m maximum. The spacecraft transports the crew capsule from LEO to the Moon, performs lunar braking, and a lander allows the crew capsule to hover and land on the Moon. At the end of the lunar mission, the crew capsule will be transported back to the Earth, undergo aerobraking, and para-glide into Edwards Air Force Base.

### **1.3.3 Conceptual Lunar Base Mission**

Due to the length of the desired 28 day mission, extensive habitation, rovers, power and radiation protection, consumables, and life support must be provided for the astronauts. These requirements are met by landing an unpiloted precursor mission onto the moon before the arrival of the astronauts. It is desired that the equipment deployment is semi-automated so that portions of living conditions can be set up before the arrival of the crew. NLS is also used to launch this precursor mission to provide commonality, and the same spacecraft stages are utilized wherever possible to save on development and integration costs for the entire mission.

### **1.4 Summary of Report**

This report is set up to include not only the final designs for the lunar mission, but also any trade studies which were accomplished to arrive at these designs. Volume I describes the top-level mode studies. Starting with a brief description of all the options which were considered, it goes into detail about the two most feasible mode profiles, Earth Orbit Rendezvous (EOR) and Earth-Lunar Orbit Rendezvous (ELOR). After the descriptions of the EOR and ELOR modes, a mode comparison summarizes the factors that were considered in making the final choice of EOR. Then a detailed description of each possible precursor configuration is studied and the top-level design choice is described. Finally, trajectory analyses for the mission and the final piloted mission design is presented, followed by the design process which includes the requirements for the mission.

Volume II includes all subsystem trade studies and design choices. Volume III describes the individual modules in detail. This includes the lunar surface operations which are performed by the astronauts.

Finally, the pre-mission factors will be described in Volume IV. This includes all the cost analysis and estimation for the mission, the schedule for the entire program, and the acceptance testing which needs to be accomplished in the development process.

## **1.5 Mission Requirements**

This section outlines the requirements for Project Columbiad. Table 1-1 shows the format from the top-level to each subsystem. The supplemental text explains the details of each box.

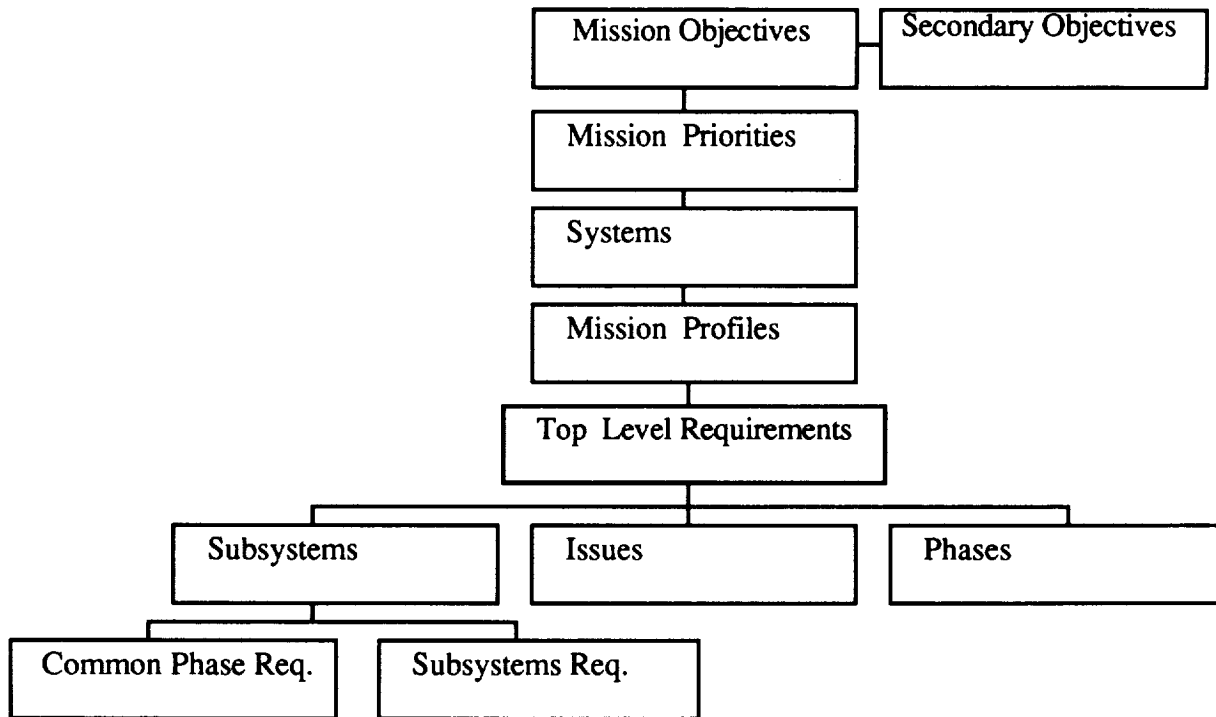


**Figure 1-1**  
**Requirements Tree**

### **1.5.1 Mission Objectives**

The following primary objectives were the foundation of Project Columbiad:

- Transport a minimum of four people to the Moon and back.
  - Land at any latitude
  - Mission duration of 14 - 28 days
- Establish a foundation for a lunar base.

Secondary objectives include:

- Project Columbiad will provide a stepping stone for the manned mission to Mars.
- Provide scientific research and exploration on the Moon.
- This project could be used to establish international cooperation for space exploration.
- Project Columbiad will be used to boost national confidence.

## **1.5.2 Mission Phase Requirements**

### **1.5.2.1 Top Level Requirements for All Mission Phases**

- 99.9% reliability for human survival
  - Three levels of redundancy
- 95% Mission Success
  - Two levels of redundancy
- Maximum loading for piloted flights
  - Axial = 3.5 g's
  - Lateral = 3.0 g's
  - Abort Modes = 7 g's
- Maximum loading for precursor = 7 g's

### **1.5.2.2 Launch to Low Earth Orbit**

- Provide a minimum of 190, 000 kg to LEO
- Set accuracy specifications for LEO
- Determine launch windows
- Design for immediate abort capabilities during this phase

A trade defined for this level is the trajectory to LEO and determining the optimum LEO altitude.

### **1.5.2.3 Earth Orbit Rendezvous**

- Design for rendezvous capability, with each stage and hardware having their own independent GNC and RCS system
- Maintain payload orbital and attitude stability
- Rendezvous hardware of unpiloted launches able to survive LEO environment for up to 40 days

### **1.5.2.4 Low Earth Orbit to Lunar Transfer Orbit**

- Determine injection and aiming requirements
- Start TLI burn assuming a velocity change of 3140 m/s

#### 1.5.2.5 Lunar Transfer Orbit to Low Lunar Orbit

- Provide midcourse correction burns
- Aiming requirements (TBD)
- Execute lunar retro burn assuming a velocity change of 1060 m/s
- Specify abort capabilities during this phase

#### 1.5.2.6 Low Lunar Orbit to Lunar Surface

- Ability to land at any latitude, including polar landing capability
- For landing, assume a velocity change of 2200 m/s
- Provide a landing accuracy of 50 meters within the predetermined landing site
- Restrict landing shock to less than 1.5 g's
- Specify abort capabilities during this phase

A trade defined at this level is to consider the options of human versus computer control of landing.

#### 1.5.2.7 Lunar Stay

- Provide a reusable habitat initially supplied for 1.5 months
- Provide near-continuous communication with Earth
- Provide immediate abort capability
- Provide effective propellant storage for return vehicle

#### 1.5.2.8 Lunar Surface to Low Lunar Orbit

- Determine launch windows
- Execute lunar launch burn assuming a velocity change of 2200 m/s
- Aiming requirements (TBD)

#### 1.5.2.9 Low Lunar Orbit to Earth Transfer Orbit

- Execute lunar escape burn assuming a velocity change of 1060 m/s
- Execute midcourse correction burns



#### 1.5.2.10 Reentry

- Determine re-entry trajectory
- Capability to land at Edwards Air Force Base
- Design for an accuracy of 5000 meters within landing site
- Design for aerobraking in order to save propellant for re-entry
- Provide thermal protection for re-entry vehicle and crew
- Re-entry capsule will be capable of autonomous operation during communications blackout

A trade defined at this level is the reusability of the re-entry vehicle.

### 1.5.3 Project and Subsystem Requirements

#### 1.5.3.1 Launch Vehicles

- Minimize the number of launches
- Maximize crew safety and reliability
- Minimize cost with loss of performance
- Minimize time and cost of development
- Ensure full political and scientific cooperation of contractor
- Provide reliable on-time launches

#### 1.5.3.2 Propulsion Stages

- Minimize weight
- Minimize cost
- Design for capability to abort at any time
- Design geometry and configurations for integration with the launch vehicle
- Staging failures - one engine: crew and mission safe
- Design piloted module for moon landing and earth re-entry
- Provide guidance for rendezvous in LEO
- Design for no in-orbit fueling
- Provide RCS for correction burns and rendezvous maneuvers
- Minimize power requirements

#### 1.5.3.2.1 Propulsion

- Minimize weight at LEO
  - Maximize Isp
  - Minimize propulsive structural weight
- Maximum weight = 190,000 kg for LEO
  - Maximum of 95,000 to LEO per launch
- Redundancy in:
  - Ignition systems
  - Staging or separation systems
- Monitor status of:
  - Chamber temperature and pressure
  - Flow rate and propellant mixture
- Factor of Safety: 1.5% reserve fuel

A trade defined at this level is the reusability of stages and number of stages.

#### 1.5.3.3 Crew Capsules

- Design a capsule that is more technologically advanced than Apollo
- Minimize weight for lunar vehicle
- Optimize abort modes, determine points of single redundancy
- Minimize complexity of mission and increase ease of operation
- Minimize cost

#### 1.5.3.4 Crew Systems

- Ensure a 99.9% reliability for human survival
- Minimize adverse physiological effects of space flight
- Promote psychological well-being of crew
- Limit radiation exposure to 25 REM for 34 days
- Specify and maintain composition of atmosphere
- Maintain temperature between 64 degrees and 81 degrees Fahrenheit
- Supply sufficient consumables for mission duration of 34 days and emergency extension
- Provide spacesuits for protection and life support during all EVA phases
- Accurately monitor human activities
- Specify all environmental conditions for human survivable limits
- Factor of Safety: 1.5

#### 1.5.3.5 Surface Payloads

- Specify proper environmental conditions
  - Provide a minimum living space of 30 m<sup>3</sup> for the lunar habitat
  - Provide protection from Level F solar flares during lunar stay
- Provide an excursion vehicle for the lunar mission
- Define scientific research and equipment
- Monitor status of payload
- Maximum parameters of 28,500 kg for final payload to lunar surface

##### 1.5.3.5.1 Pre-positioned Payloads

- Semi-autonomous monitoring and control
- Two year survivability without loss of function
- Ensure compatibility between lunar systems

##### 1.5.3.5.2 Manned Capability

- Four hour shutdown without loss of function
- Design for a minimum lifetime of ten years

##### 1.5.3.5.3 Surface Vehicle

- Design for a semi-autonomous operation
- Capable of a 100 km range from the habitat
- Provide attachments for various lunar operations
- Design vehicle with shielding from nominal radiation levels
- On-board Communication/Navigation system

#### 1.5.3.6 Guidance Navigation and Control (GNC)

- Utilize reusable components when possible
- Specify launch vehicle maneuvering accuracy and launch windows
- Minimize cost and weight
- Determine lunar orbital accuracy
- Pre-determine lunar approach trajectory
- Provide autonomous GNC during blackout
- Determine spacecraft positioning, attitude and velocity
- Compute trajectory and correction burns as well as propulsion cutoff timing

A trade defined at this level is the feasibility and usefulness of predeployed navigation beacons either on the lunar surface or orbiting the Moon. This group is also to conduct a trade between ground based GNC and autonomous GNC.

#### 1.5.3.7 Command, Control, and Communications (C3)

- Provide near continuous communication with Earth
- Provide inter-vehicle communications where necessary
- Provide communication system for lunar rover
- Provide on-board computational capability
- Specify location of antennas
- Specify heat dissipation for electronics
- Collect and process telemetry information
- Specify computation requirements
- Specify fault tolerant components and architecture
- Minimize power consumption

There are several trades defined at this level. This group is to conduct a trade between the level of autonomy and ground based control. Another trade study will determine the utility of predeployed communications aids. Finally, a survey should be conducted to determine whether the crew prefers HBO or Cinemax for crew entertainment.

#### 1.5.3.8 Power and Thermal Control

- Design hardware for power generation and conditioning
- Design thermal control hardware for on-site heat removal, collection and radiation
- Ensure safety and reliability of power subsystem
- Minimize mass of power and thermal systems
- Minimize hardware cost
- Provide adequate power for all systems
- Specify temperature range for payload and electronics
- Develop power budgets for all systems
- Minimize maintenance

A trade defined at this level the type of power source to be use for the lunar habitat. This group will also conduct a trade study between global and local thermal control.

#### 1.5.3.9 Structure and Thermal Protection

- Assure structural integrity by designing for no failure, no buckling, and no permanent deformations
- Provide environmental protection for crew and equipment from radiation, micrometeorites, corrosion, and out-gassing
- Provide thermal protection during re-entry against aerodynamic heating and landing impact
- Minimize structural weight of all systems
- Design for no plastic deformation under maximum specified stress
- Provide heat shielding for specified human survival limits
- Provide shielding from solar flare radiation in transit vehicles
- Protect structures from environmental hazards
- Factor of Safety: 1.4

A trade defined at this level is to consider modularity between stages.

#### 1.5.3.10 Status

- Specify tests for components at all stages of assembly and operation
- Evaluate mission success including abort decisions
- Capable of obtaining immediate and accurate data on the operation of the spacecraft
- Set error and error detection specifications
- Assemble a list of critical parameters from all subsystems
- Assemble a decision tree for all mission phases, including minimum requirements for mission continuation.
- Define and run system integration tests
- Monitor all systems for fault detection
- Execute subsystem checks before critical phases
- Define and execute decision about abort modes during the mission

## **2 Mission Modes**

### **2.1 Introduction**

Due to the scope of the project, it was determined immediately that Project Columbiad will need a precursor mission to fulfill the mission requirements. Therefore, mode selection was driven by the launch vehicle, complexity of mode, and safety. This chapter will look at both launch vehicle and spacecraft configurations considered, and mission profile options. Finally, this chapter will conclude with a comparison and how the number of choices were narrowed down.

### **2.2 Launch Vehicle Capabilities Comparison**

The launch vehicle is a major driving factor in the selection of modes. For selection of the launch vehicle, the payload assumptions used were 25,000 kg for the precursor mission and 2,000 kg for the piloted mission. This mass is additional to the landing vehicle and crew capsule. Also, due to scheduling concerns, launch vehicles were limited to existing systems, or those that are in a planning stage according to NASA. There were several vehicles looked at for this mission.

The following is a review of the launch vehicles considered for the Columbiad Project: Shuttle-C, Energiya, National Launch System (NLS), Saturn V, and the Heavy Lift Delta.

#### **2.2.1 Energiya Launch System**

Energiya is the most modern Heavy Lift Launch Vehicle (HLLV) of the former Soviet Union, now Commonwealth of Independent States (CIS). Its design allows for a number of uses, ranging from heavy lift to LEO to interplanetary exploration. It is also the launch vehicle for the Buran shuttle.

An overall view of the Energiya is shown in Figure 2-1. Its first stage is composed of four strap-on liquid fuel boosters with four engines each. Its second stage is the core of the vehicle (four engines) to which the boosters are attached.

The configuration of the Energiya considered for Columbiad would be the HLLV with the cargo container mounted on the side. Both boosters and cargo are lock-fastened to the

core. Unless stated otherwise, this memo reports information for the current Energiya HLLV configuration with four strap-on boosters.

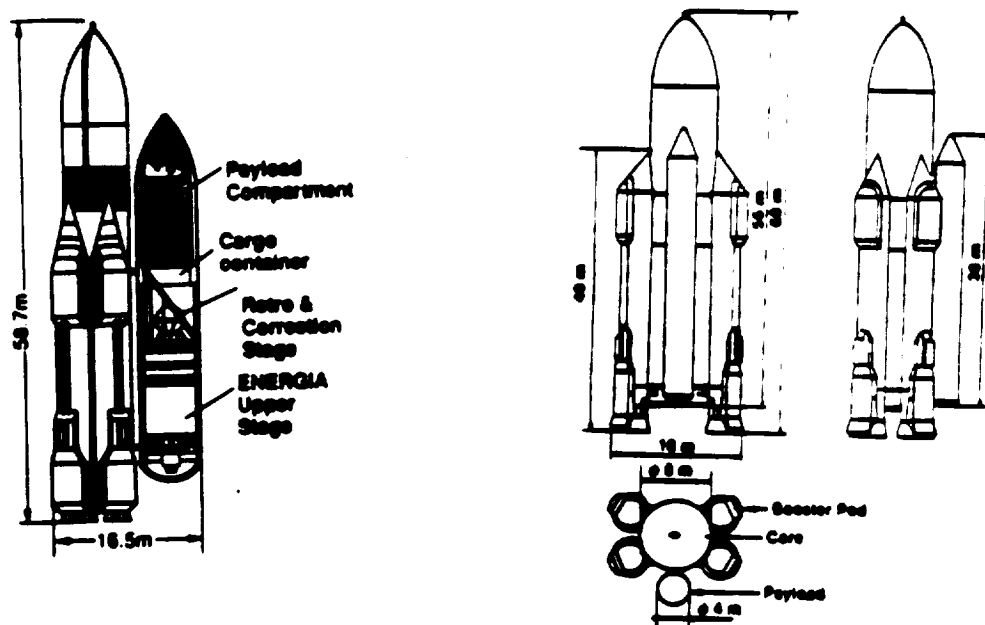


**Figure 2-1**  
**Energiya Launch Vehicle**

#### 2.2.1.1 Launch Vehicle Configuration

**Table 2-1: Energiya Specifications and Dimensions**

Vehicle Length	60 m
Vehicle Diameter	16 m
Booster Length	40 m
Booster Diameter	4 m
Payload Diameter (1987)	4 m
Payload Diameter (1989)	5.5 m
Payload Container Length	38 m
Min. Liftoff Acceleration	1.48 g's
Max. Liftoff Acceleration	1.77 g's
Max. Liftoff Mass	2400 metric tons
Max. Liftoff Thrust	
Initial Total Liftoff Power	132,000,000 lbs

Energiya is capable of delivering 105 t to LEO and 32 t to Low Lunar Orbit (LLO). Based on the 125-160 t to LEO requirements, it would take a maximum of two launches.

Energiya has four boosters in the current HLLV configurations with four thrust chambers per booster. The thrust chambers are fed by one engine and turbopump. The engines used for the boosters is the RD-170 developed by V.P. Glushko. The engines supply a total sea-level thrust of 2960 t.

The core is powered by four single-chambered engines of an unspecified type. The core provides a sea-level thrust of 592 t.

#### 2.2.1.2 Reliability and Safety

There have been two operational launches to date. The first launch of the Energiya used the HLLV configuration. The launch was a success as far as the Energiya was concerned. The second launch was with the unmanned Buran shuttle. That mission was a complete success. These two launches, with nothing else is not enough to make a reliability statement.

Numerous tests have been done on the system itself, which may relate to its success thus far. Before its first operational launch, there were over 6000 tests of 200 different experimental units. There were also 34 tests of large blocks of assembled sub-systems. Five full-scale mock-ups were tested before the first launch of the Energiya.

The computers are designed to perform a continuous safety diagnosis on all systems during the launch process. It has also been proven that the Energiya can meet lift requirements with one engine not functioning in either stage.

#### 2.2.1.3 Cost

There is little or no information available in this area. As an initial estimate, the Energiya could be said to cost as much per launch as the proposed NLS.



#### 2.2.1.4 Launch site

The current launch site for the Energiya is the Baikonur spaceport. The Energiya is assembled and tested horizontally in the technological facility near the launch pad. The turn-around time between successive launches is unknown.

#### 2.2.1.5 Summary

The Energiya is a good choice with regards to lift capability. However, there are a lot of specs that are still unknown or undisclosed. The reliability of the integrated system is unclear at this point. More launches are needed for an accurate study. There are also the political complications that could arise out of the use of the Energiya.

The fact that the payload is attached to the side of the core is important. This allows for independent development of the spacecraft. There is no need for the complicated integration that can happen when working with a stacked rocket.

### 2.2.2 The National Launch System

The National Launch System (NLS) is considered by some to be the next logical step in the continuing development of a reliable American launch vehicle fleet. The particular configuration examined in this report consists mostly of components derived from the Space Transportation System (STS).

At the core of the NLS is a new engine derived from the Space Shuttle Main Engine (SSME), known as the Space Transportation Main Engine (STME). The STME will offer vacuum thrust levels of approximately 2630 kN (sea level thrust of 2280 kN), with a vacuum specific impulse of 428 seconds (371.4 sec at sea level).

There has been some concern that the STME will not have enough power to meet the needs of a Heavy Lift Launch Vehicle (HLLV). On the other hand, the STME configuration makes maximal use of existing technology, a big advantage from the point of view of Project Columbiad. It is not likely that the project can drive the development of an entirely new launch system. However, a derivative HLLV like the STME requires a minimum of developmental cost.

#### 2.2.2.1 Launch Vehicle Configuration

The core vehicle for the NLS consists of a modified Space Shuttle External Tank (ET) and engines at the bottom. A payload of approximately 27 metric tons is shrouded by a Titan IV-derived fairing. The payload and fairing are then mounted on an avionics package and payload adapter above the ET standard LOX tank. An engine module consisting of four STME's, providing a total of 10,520 kN of (vacuum) thrust, is mounted beneath the LH<sub>2</sub> tank, completing the vehicle. Such a vehicle could be flight-ready by 1999.

Obviously, the core vehicle does not provide sufficient payload capacity for the needs of Project Columbiad. However, an extension of the core planned for 2002 would accommodate 72 t of payload to LEO. Two such vehicles would be needed to launch an entire mission profile. This NLS configuration is shown in Figure 2-2.

This extension vehicle has a larger fairing, and two side-mounted Advanced Solid Rocket Motors (ASRM's) providing the additional required thrust. The ASRM's, which are currently under development, are derived from the Space Shuttle's Solid Rocket Boosters (SRB's). Each ASRM provides 11,900 kN of vacuum thrust .

The dimensions of the ET from which this vehicle is derived are approximately 47 m long by 8.4 m in diameter. By extrapolation, it is assumed that the fairing for this vehicle is approximately 30 m long by a maximum of 8 m in diameter, offering a total payload volume of approximately 1,500 m<sup>3</sup>.

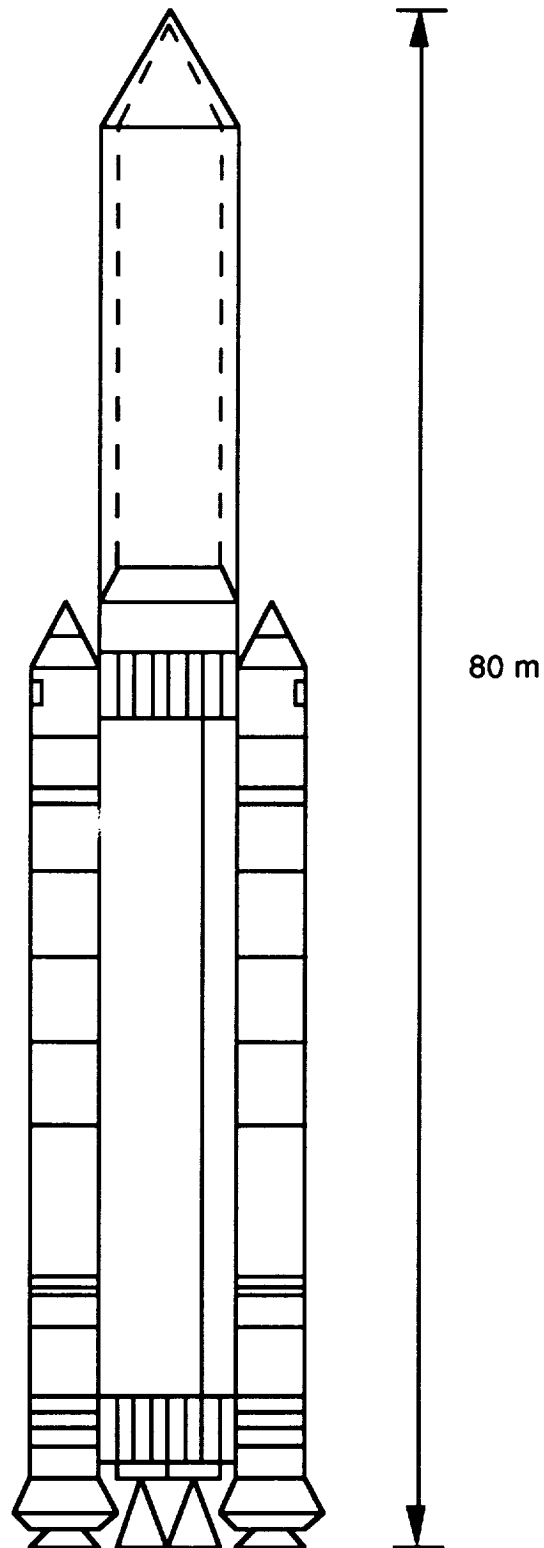


**Figure 2-2**  
**National Launch System**

### 2.2.2.2 Reliability and Safety

The document "Projected Launch Vehicle Failure Probabilities with and without Engine Segment-Out Capabilities", prepared by L Systems, Inc. provides estimates of NLS reliability based on historical data of the systems from which it is derived. The figures presented below are for a 4 STME system, with a one engine-out capability. The overall system reliability is calculated to be 97.5%.

**Table 2-2: NLS Failure Probability**

System	Failure Probability
ASRM	0.010
STME (Benign)	0.000
STME (Catastrophic)	0.004
Stage Level	0.002
Engine-Out Control	0.002
Guidance	0.002
Other Subsystems	0.005

Unfortunately, these numbers are for a system that has been tested for 100 flights. In fact, it is quite possible that the system reliability would not break 90% before the tenth flight which will affect scheduling and testing costs.

### 2.2.2.3 Cost

An estimate can be obtained by summing the procurement costs of the following STS components: one ET, two SRB's, and four SSME's.

### 2.2.2.4 Payload Interface

A maximum launch system acceleration values have been chosen from Wertz and Larson for the Space Shuttle since there have been no concrete figures developed.

At liftoff, the Shuttle maximum loads are as follows:

<b>Axial</b>	Steady State:	3.2 g's
	Dynamic:	3.5 g's
<b>Lateral</b>	Steady State:	2.5 g's
	Dynamic:	3.4 g's

#### 2.2.2.5 Launch Site

The NLS will be launched from the Kennedy Space Center in Florida, probably using one or both of the launch pads at Launch Complex (LC) 39, from which Space Shuttles are currently launched with minor modifications.

#### 2.2.2.6 Alternate Configurations

NASA has been studying a configuration of the NLS different than the one examined here. Their version makes use of two core vehicles (a total of eight STME's). This configuration will have the capability of launching 90 t to LEO. While it is a possibility for Project Columbiad, it offers little or no improvement over the 72 t payload capability of the original vehicle.

This configuration has no ASRM's. Instead, an additional reconverted ET is attached to the side of the vehicle. With all eight STME's firing, a total of 21,040 kN of vacuum thrust is provided. This vehicle is shown in Figure 2-3.

Another possible modification for the NLS is adding extra boosters. One extra booster will increase the payload to 83 metric tons in LEO. Two extra boosters will increase the payload to 91 metric tons in LEO.

#### 2.2.2.7 Summary

The facts in favor of the NLS are as follows: the system makes use of existing technology, and can be a reliable launch system when mature. In addition, it is a system heavily favored by NASA. On the other hand, maturity of the system requires 100 flights, which could not occur until well into the 2020's, given the planned flight rate per year, and the costs of this vehicle have not been well established.

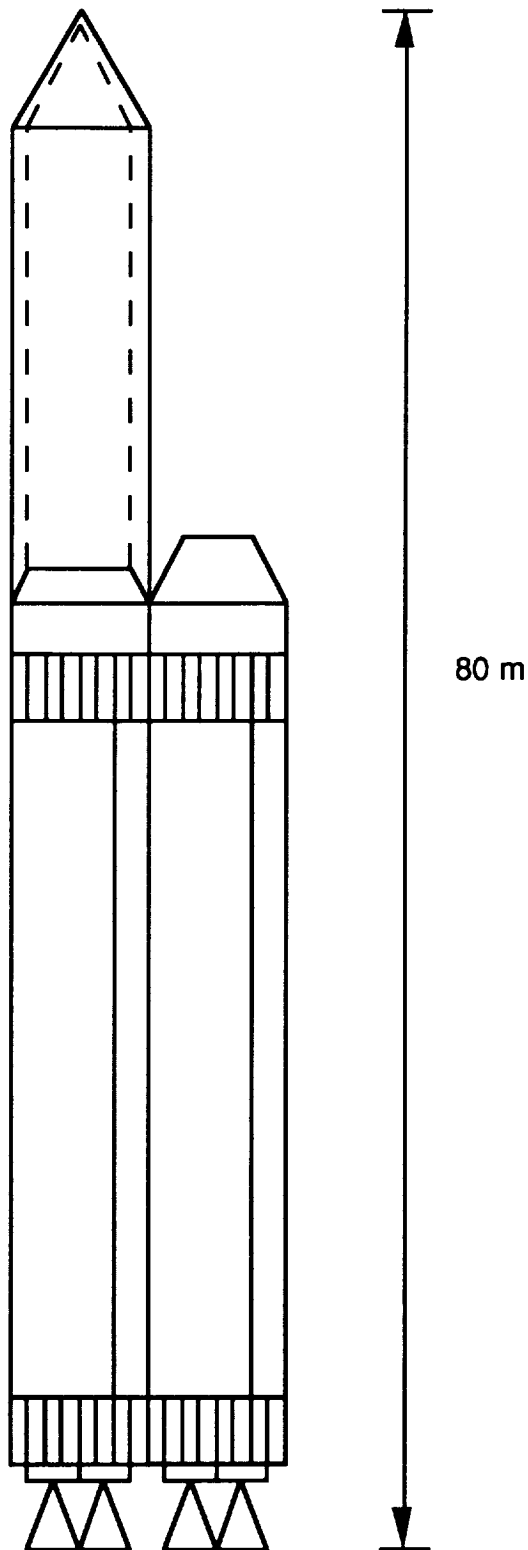


**Figure 2-3**  
**Alternate NLS Configuration**

### **2.2.3 Saturn V Launch Vehicle**

Another possible system considered is the resurrection of the Saturn V launch vehicle for the Columbiad Project. The Saturn V in both the lunar and skylab mode is able to launch 125 metric tons into LEO.

#### **2.2.3.1 Launch Vehicle Configuration**

The Saturn V is a three stage vehicle. The first stage (S-IC) is constructed by the Boeing Company and is powered by five F-1 Rocketdyne engines each delivering 6800 KN of thrust. The outer four engines can be gimbaled for thrust vectoring and course correction. After a 260 second burn an explosive charge separates the S-IC stage which in turn fires small retro rockets to aid in a smooth separation.

The second stage (S-II) is constructed by North American (Rockwell) and powered by five J-2 Rocketdyne engines each producing 1000KN of thrust. Similar to the S-IC, the outer four engines can be gimbaled. After 390 seconds the S-II stage is released with both retro rockets firing on the S-II stage and ullage rockets firing on the final stage.

The third stage (S-IVB) is constructed by McDonnell Douglas and powered by one J-2 Rocketdyne engine producing 1000KN of thrust. This stage gives the final boost to a 190 km orbit, sends the payload into translunar orbit, and is responsible for course corrections and go around abort. This stage is ejected and sent into a lunar collision trajectory.

#### **2.2.3.2 Reliability and Safety**

The Saturn V has never had a launch failure for 10 lunar flights plus several unmanned tests. The Saturn I and Saturn IB used for boilerplate testing and orbit rendezvous have had very successful launch histories. The Saturn V is a derivative of these vehicles and thus the reliability is enhanced. The F-1 and J-2 engines themselves have never had a catastrophic failure. Quality testing and high redundancy have given the Saturn V tremendous launch success but at a high cost.

#### **2.2.3.3 Modifications**

Extensive redesign and correlation of previous Saturn V data will have to be done before component manufacturing is begun. This project would be much more than simply piecing

together parts from a storage room. In many cases the parts, technology, and manufacturing know how have been lost or changed dramatically.

There are F-1 and J-2 engines in cold storage that could be utilized with substantial redevelopment costs. These engines are also being considered for certain NLS modes.

Launch Complex 39 will have to have major renovations to accommodate the Saturn V once again. The pad tower will have to be extended as well as reinforced. A 130 m mobile service structure for checkout functions, servicing and fueling will have to be assembled or reconstructed. The VAB will have to be modified to allow for the assembly of the Saturn V while not hindering Shuttle assembly. Various ground support facilities will have to be modified or reconstructed.

#### 2.2.3.4 Cost

Cost estimates for reviving the Saturn V vehicle and launch facility lie in the 1.3 billion dollar range (1988). This cost includes redevelopment and acquisition. Hardware alone would cost about 500 million. Refurbishing the F-1 and J-2 engines by Rocketdyne would cost about 11 million dollars and 5 million dollars respectively per engine.

#### 2.2.3.5 Summary

The Saturn V proven history and high reliability would make it by far the best system to date if it were still in operation. The Saturn V would use a modified launch complex 39 and would not push the state of the art. The system is also built in the United States which may become a large political factor. The Saturn V also uses the highly reliable and powerful F-1 engines.

The cons of reviving the Saturn V are that the system has very little margin for adaptability or expendability. The technology that built these systems is either out dated or lost, and the costs of bringing back the program would be excessive. Finally, it does not support prospective payloads outside of delivering 125 metric tons to LEO.

The Saturn V vehicle was one of the most reliable human-rated systems. Redevelopment and reassembly may or may not hinder the Saturn V reliability. The costs of such a redevelopment program will demand that the vehicle be used for other than lunar precursor missions. This will impose adaptability and expendability constraints on the Saturn V



which were not accounted for in the initial design. The Saturn V vehicle is the last vehicle in a long evolutionary chain of Saturn vehicles and does not allow for expansion. The only way to increase capability is to increase engine thrust, increase fuel Isp, or reduce structural weight. The engines used on the Saturn V are still the largest engines available, increasing Isp and reducing structural weight would result in a total redesign of the vehicle.

#### **2.2.4 Heavy Lift Delta**

McDonnell Douglas Corporation (MDC) is studying the feasibility of a low-cost, rapidly available heavy lift launch vehicle (HLLV), using a maximum of existing components. The result of this study was the Heavy Lift Delta (HLD), a vehicle which could go from paper to the launch pad in 42 months. An example of the HLD is shown in Figure 2-4.

##### **2.2.4.1 Launch Vehicle Configuration**

The first stage of the HLD consists of six Delta first stages, strapped together in three clusters of two each. Each of these stages uses the Rocketdyne RD-27 engine providing more than 900 kN of thrust. The fuel tanks of these stages are interconnected, such that if one engine fails, the other five will burn that engine's fuel.

Surrounding the first stage cluster are three Space Shuttle Solid Rocket Boosters (SRB's), placed at the corners of an equilateral triangle surrounding the vehicle. Each SRB provides over 11,000 kN of thrust. The second stage of the HLD uses a single Delta first stage. The 45 t of payload is placed on top, shrouded in an extended Titan IV fairing.

##### **2.2.4.2 Reliability and Safety**

The HLD uses components from the Delta launch vehicle, the most reliable system ever flown in any country. There have only been 11 launch failures in over 190 attempts. There has been no failure since 1986. One can use a reliability for the Delta stages of anywhere from 98% to 100%.

The SRB's used for the HLD will be the post-Challenger Redesigned Solid Rocket Motors (RSRM). These have not, as yet, experienced any problems in flight. They have a predicted reliability of over 98%.

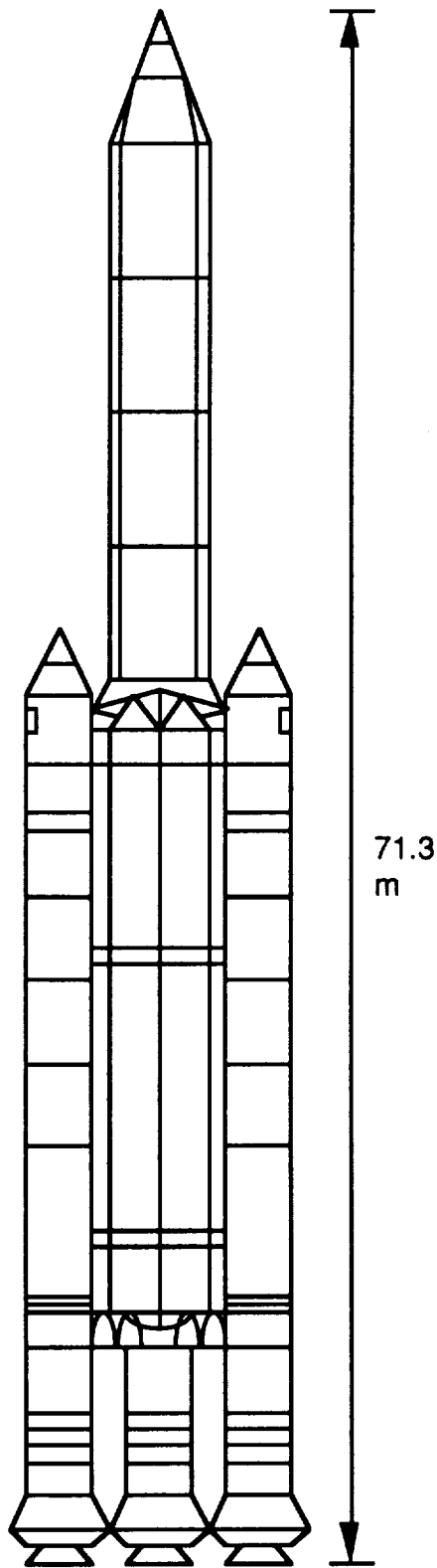


**Figure 2-4**  
**Heavy Lift Delta**

Overall, the individual components comprising the HLD all share extremely high levels of reliability (all greater than 98%), so the combination should produce a relatively high system reliability. At the present time, it is not clear exactly how reliable the system is. Future contact with McDonnell Douglas should resolve the situation.

#### 2.2.4.3 Cost

In constant 1990 dollars, the costs is as follows:

**Table 2-3: Heavy Lift Delta Costs**

<b>Non-Recurring Costs</b>	
HLD Vehicle	316 million
Tooling	91 million
Launch Facilities	222 million
GSE	71 million
<b>Total</b>	<b>700 million</b>
<b>Recurring Costs (per vehicle)</b>	
HLD Vehicle	188 million
Launch Support/ Payload Integration	17 million
<b>Total</b>	<b>205 million</b>

The total vehicle procurement costs would come to approximately \$615 million per mission.

#### 2.2.4.4 Payload Interface

Since there was no loading figures provided for HLD it was replaced by the Delta II Payload Planner's Guide which states that payloads experience loading in the range of 2 to 3 g's in both the axial and lateral directions, with a peak of 6 g's at main engine cutoff (MECO). The HLD will use load relief, by gimbaling both the SRB engines and the RS-27 engines. The gimbaling will reduce loads by changing the direction and magnitude of the thrust.

#### **2.2.4.5 Summary**

The HLD has the advantage of the unsurpassed reliability of the Delta system throughout its history, and the high use of existing technology in its development. In addition, the cost of the vehicle has been well established, and offers one of the lowest costs per kilogram of any launch system. Finally, the HLD can be on the pad within 42 months of inception of the program.

#### **2.2.5 Shuttle-C**

The Shuttle-C is a derivative of the Space Shuttle which conceptually carries 50 metric tons into LEO. It uses the familiar External Tank (ET) and Solid Rocket Boosters (SRB), replacing the Shuttle orbiter with a cargo carrier outfitted with 2-3 Space Shuttle Main Engines (SSMEs) or Space Transportation Main Engines (STMEs) which are under development.

This option was eliminated early because it is not a viable option and it was confirmed by NASA that it is no longer an entry in the National Launch System competition.

#### **2.2.6 Conclusion**

The Energiya was eliminated due to the uncertainty of its design and political situation. The Saturn-V was eliminated due to the lack of feasibility in reviving the launch vehicle. Between the NLS and HLD, the NLS was chosen as the better choice because of its higher payload to LEO capability and it was also rated as a more likely launch system to be designed and tested to meet the mission requirements and designs.

### **2.3 Mission Mode Considerations**

This section gives a brief description of all the mission profiles that was considered for Project Columbiad. There is a discussion of the assumptions for the spacecraft and stages and then a brief description of all the modes considered.

#### **2.3.1 Spacecraft Descriptions**

This section describes the preliminary assumptions for spacecraft configurations and weight requirements. These assumptions were used for the mode decisions.

#### 2.3.1.1 Spacecraft Configurations

Similar configurations were used for the mission modes. With exception of the modes utilizing the Space Shuttle, the spacecraft used for the modes are the following: the Service Module (SM), the Lunar Braking Module (LBM), the Lunar Touchdown Module (LTM), the Command Module (CM), the Habitat, and the Trans-Lunar Injection Stage (PTLI). Performance criteria have led to the use of these modules as described in the next section. The maneuvers, performance and names of these modules may have changed when the final mode is decided, so the following descriptions are the assumptions for the preliminary design. [Manned, 1962a]

##### 2.3.1.1.1 Service Module (SM)

The SM will supply the lunar escape capability and will execute trans-Earth midcourse maneuvers.

##### 2.3.1.1.2 Lunar Braking Module (LBM)

The LBM will be ignited for lunar orbit retro, re-ignited for lunar descent, and staged before lunar landing.

##### 2.3.1.1.3 Lunar Touchdown Module (LTM)

The LTM will land and launch the vehicle from the Lunar surface. Furthermore, it will execute midcourse maneuvers in the trans-lunar flight phase.

##### 2.3.1.1.4 Command Module (CM)

The CM contains the crew and all their supporting equipment for the flight to the moon and back.

##### 2.3.1.1.5 Trans-Lunar Injection Module (TLI)

The TLI will execute the escape burn and propel the spacecraft towards the moon.

##### 2.3.1.1.6 Habitat

The habitat contains the crew support equipment and the scientific equipment for the duration of the stay on the moon. There are three possible general configurations that were considered for landing the habitat. There is the vertical stacking, horizontal landing, and a hybrid configuration. The hybrid configuration redocks in LLO and then landed. These configurations are discussed in Volume I, Chapter 4.

### **2.3.2 Reusability of Modules**

This section describes the various options that were considered for reusability of various stages and/or modules. Reusability was considered as an option for future expendability of the primary lunar habitat and mission.

#### **2.3.2.1 Reusable Lander**

A reusable LTM would be used for the mode in which a stage is left in LLO. The LTM would then be capable of shuttling back and forth from the lunar surface and LLO. This variation of the LTM will be left in LLO for future missions to the Moon.

#### **2.3.2.2. Reusable Transfer Vehicle**

A reusable SM would be capable of shuttling back and forth from the Earth and the Moon.

#### **2.3.2.3 Reusable Re-entry Vehicle**

A reusable re-entry vehicle will be capable of repeated landings on Earth's surface.

### **2.4 Definition of Modes Compared**

This section defines the modes compared for Project Columbiad. All modes described in this section is applicable for both the precursor mission and the piloted mission. The two mission will not be clarified and will be referred as the "payload" in this section. Spacecraft will refer to the payload and the propulsive modules that have not yet been jettisoned.

#### **2.4.1 Direct Flight (DF)**

Figure 2-5 gives a graphical view of the mission profile for a DF mode. [Manned, 1962b]

##### **2.4.1.1 Launch to Trans-Lunar Injection**

During launch, the launch vehicle will stage as necessary in order to park the payload with the propulsive modules (LTM, LBM, and) in LEO. While in orbit, the spacecraft will orient for trans-lunar escape. The TLI will ignite for trans-lunar trajectory insertion.

##### **2.4.1.2. Trans-Lunar Orbit**

The TLI will be staged from the spacecraft. The spacecraft will then orient for navigation and a midcourse maneuver as necessary. For a midcourse maneuver, the LTM will ignite the midcourse engines. The spacecraft will reorient for coast.

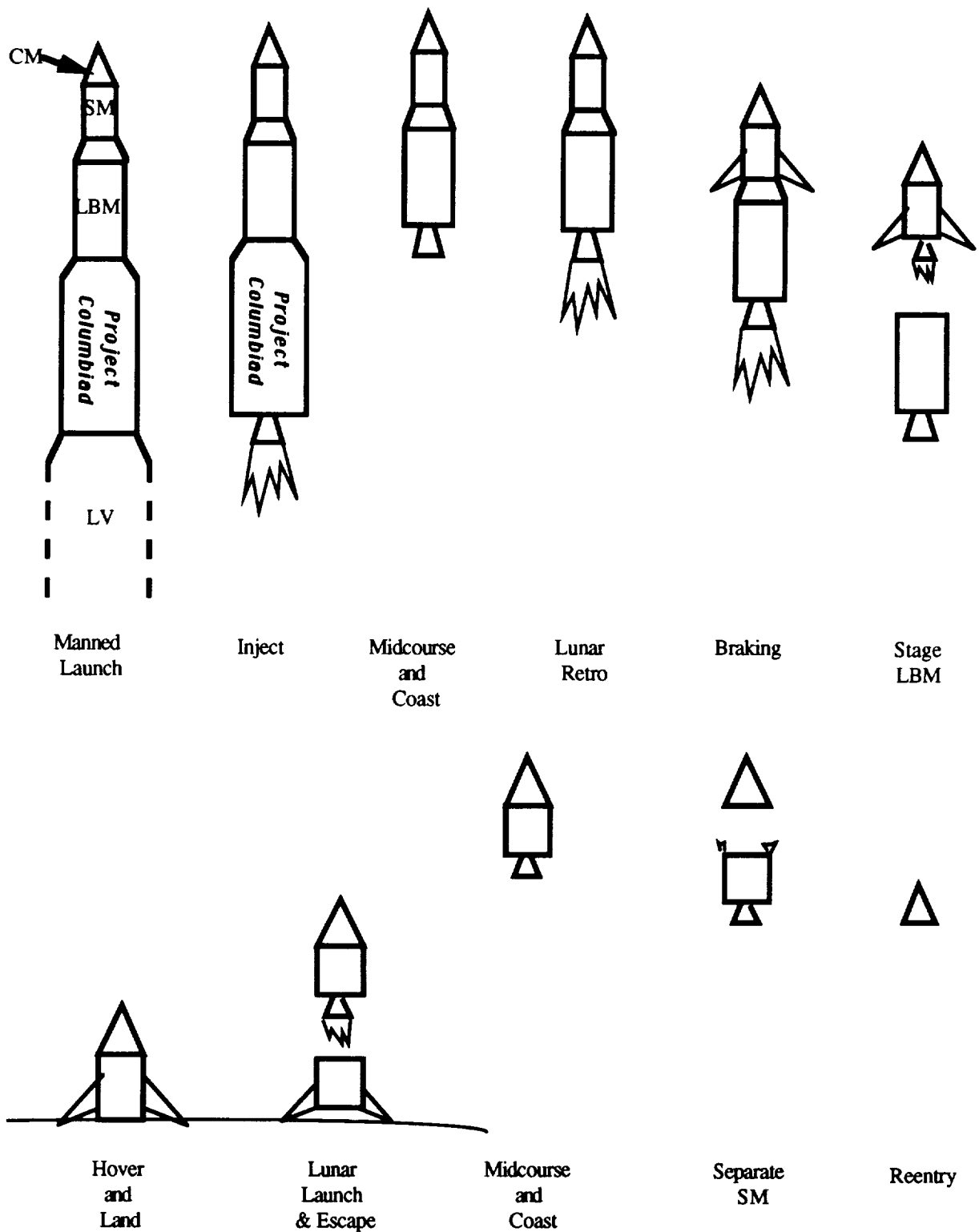


**Figure 2-5**  
**Mission Profile, Direct Flight Mode**

#### 2.4.1.3 Lunar Approach and Landing

The LBM will ignite for lunar orbit retro and establishing lunar orbit. The spacecraft will reorient for landing. The LBM will then re-ignite for braking and lunar descent. Just before landing the LBM will be staged. The landing engines of the LTM will be used to hover and translate to the landing site. The payload will then continue onto surface operations. If this is the precursor, the mission profile ends here.

#### 2.4.1.4 Lunar Launch to Trans-Earth Orbit

The LTM engines will ignite for launch. Once the spacecraft has establish LLO, the spacecraft will orient for lunar orbit escape. The LTM engine will be ignited and cutoff. The trajectory will be determined and the spacecraft will reorient for navigation a midcourse maneuver. The SM will ignite for the midcourse maneuver and then reorient for coast.

#### 2.4.1.5 Earth Approach and Landing

As the spacecraft approaches the Earth, GNC will determine the re-entry parameters. The SM will be separated from the command module. The spacecraft will reorient for re-entry and begin the re-entry flight. The vehicle will then land and the crew recovered.

### 2.4.2 Earth Orbit Rendezvous (EOR)

Figure 2-6 gives a graphical view of the mission profile for a EOR mode. [Manned, 1962c]

#### 2.4.2.1 Launch to Trans-Lunar Injection

This mode will require two launches. The first launch will transport the TLI in to LEO. The second launch will transport the payload into LEO. The TLI and payload will rendezvous and dock. While in orbit, the spacecraft will orient for trans-lunar escape. The TLI will ignite for trans-lunar orbit insertion.

#### 2.4.2.2. Trans-Lunar Orbit

The TLI will be staged from the spacecraft. The spacecraft will then orient for navigation and a midcourse maneuver if necessary. For a midcourse maneuver, the LTM will ignite the midcourse engines. Then the spacecraft will reorient for coast.



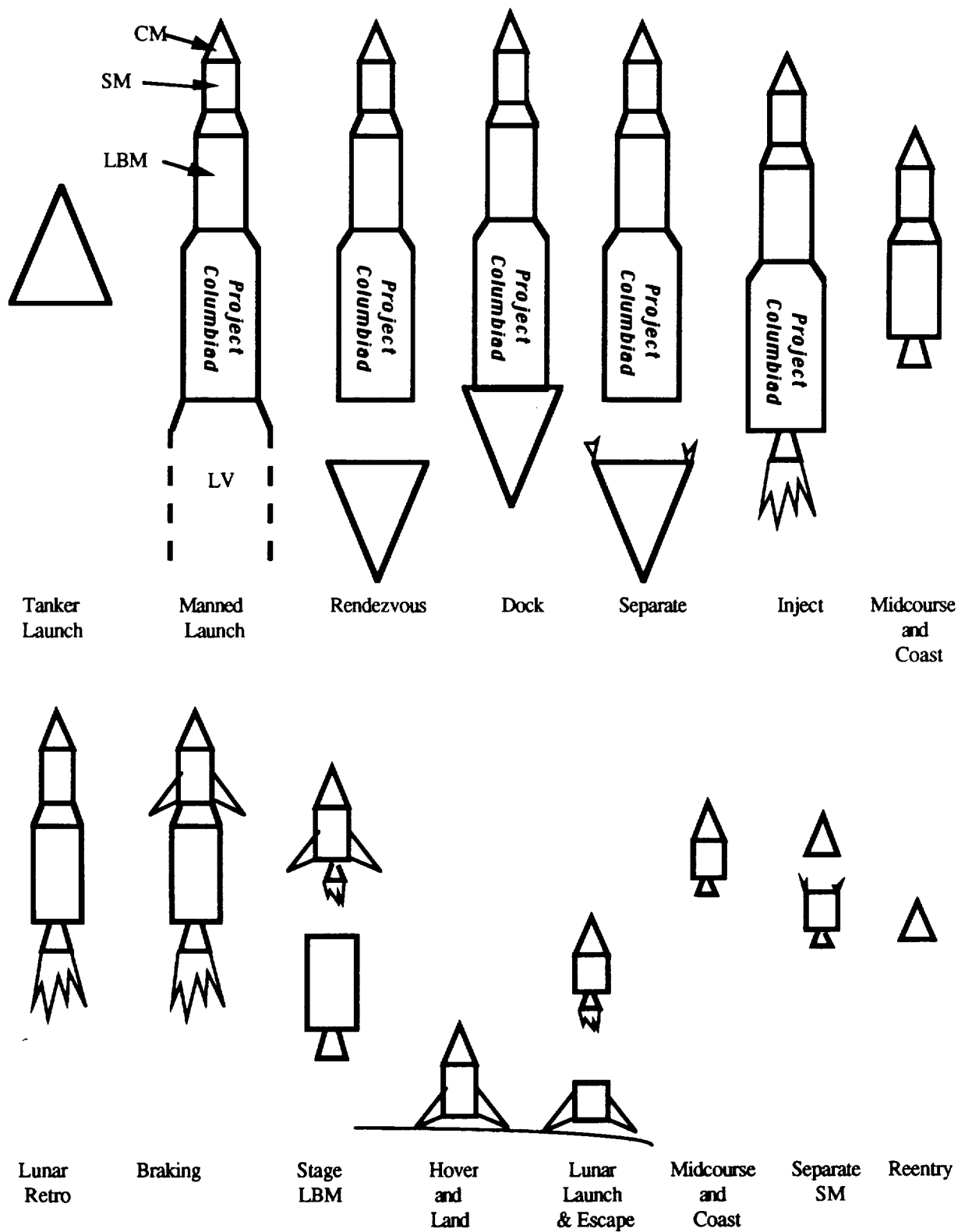


**Figure 2-6**  
**Mission Profile, Earth Orbit Rendezvous Mode**

#### 2.4.2.3 Lunar Approach and Landing

The LBM will ignite for lunar orbit retrofire and lunar orbit establishment. The spacecraft will reorient for landing. The LBM will then re-ignite for braking and lunar descent. Just before landing the LBM will be staged. The landing engines of the SM will be used to hover and translate to the landing site. The payload will then continue onto surface operations. If this is the precursor mission, the mission profile ends here.

#### 2.4.2.4 Lunar Launch to Trans-Earth Orbit

The SM will ignite the launch engines. Once the spacecraft has established LLO, the spacecraft will orient for lunar orbit escape. The SM engine will be ignited and cutoff. The trajectory will be determined and the spacecraft will reorient for navigation a midcourse maneuver. The SM will ignite for the midcourse maneuver and then reorient for coast.

#### 2.4.2.5 Earth Approach and Landing

As the spacecraft approaches the Earth, GNC will determine the re-entry parameters. The SM will be separated from the re-entry vehicle. The spacecraft will reorient for re-entry and begin the re-entry flight. The vehicle will then land and the crew recovered.

#### 2.4.3 Lunar Orbit Rendezvous Mode (LOR)

The configuration of the LOR spacecraft differs from the DF and EOR modes. The LOR spacecraft contains the CM, the Lunar Excursion Vehicle (LEV), and a two-stage SM. The first stage of the SM (SM-B) executes the trans-lunar midcourse and lunar orbit braking maneuvers. The SM second stage (SM-A) executes the lunar orbit escape maneuver and provides for midcourse maneuvers in the trans-Earth phase. The LEV is composed of a manned capsule which is the Lunar Excursion Module (LEM) and two fully-staged propulsion systems. The first stage (LEV-B) is used for lunar descent, hovering and touchdown, and the second stage (LEV-A) provides for lunar launch. A separate rendezvous propulsion system has been provided in the LEV-A stage. In addition to the LEV rendezvous capability, the CM has a redundant capability for rendezvous utilizing the SM-A. For this mode, it will only be considered for a piloted mission. Thus, if this mode is chosen, it has the disadvantage of loss of modularity with the precursor mission. Figure 2-7 gives a graphical view of the mission profile for a LOR mode. [Manned, 1962d]

#### 2.4.3.1 Launch to Trans-Lunar Injection

During launch, the LV will stage as necessary in order to park the payload with the propulsive modules (TLI, LEV, and SM) in LEO. While in orbit, the spacecraft will orient for trans-lunar escape. The TLI will ignite for trans-lunar orbit insertion. Then there will be a SM-LEM separation, the spacecraft will turn 180 degrees and the CM will dock with the LEM.

#### 2.4.3.2 Trans-Lunar Orbit

The TLI will be staged from the spacecraft. Then there will be a SM-LEM separation, the spacecraft will turn 180 degrees and the CM will dock with the LEM. The spacecraft will then orient for navigation and a midcourse maneuver if necessary. For a midcourse maneuver, the SM-B will ignite the midcourse engines. The spacecraft will then reorient for coast.

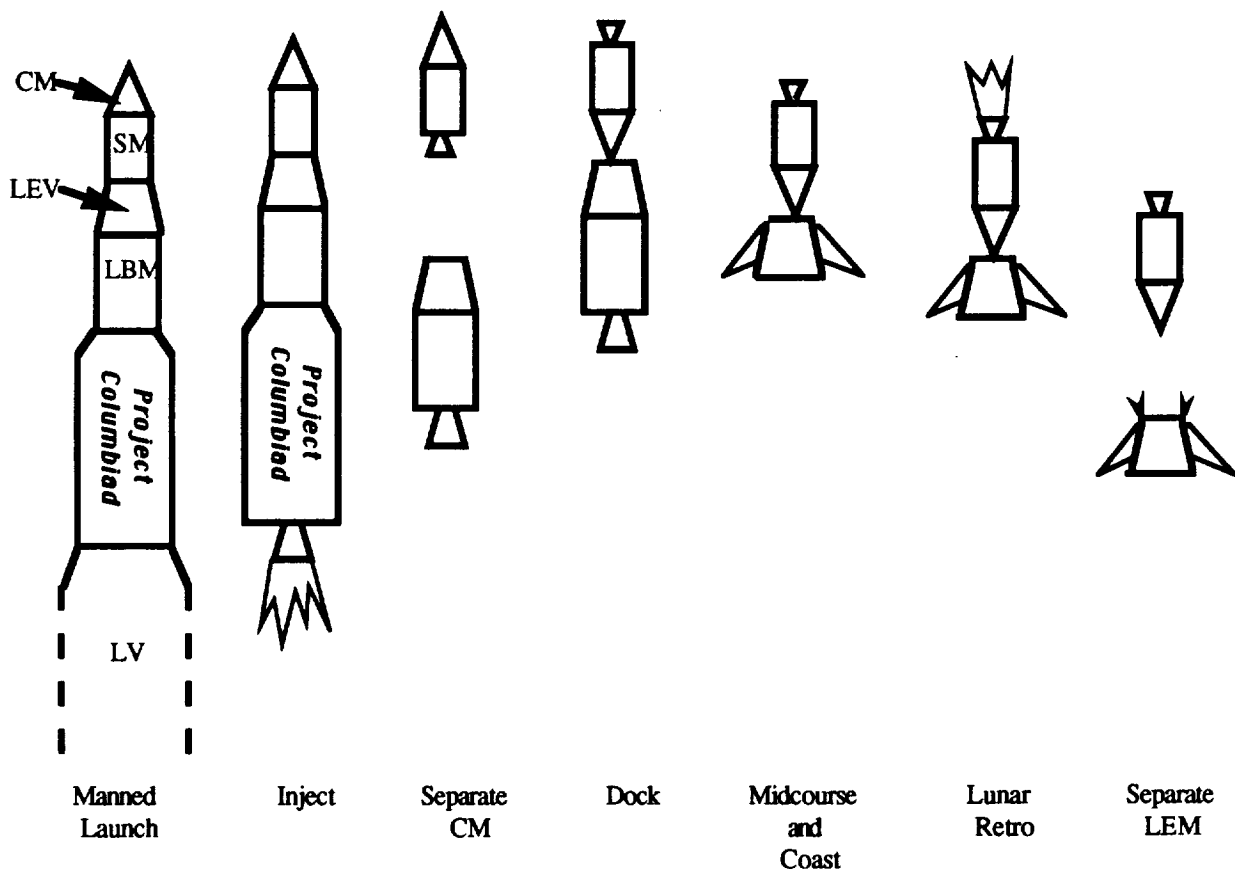


**Figure 2-7a**  
**Mission Profile, Lunar Orbit Rendezvous Mode**

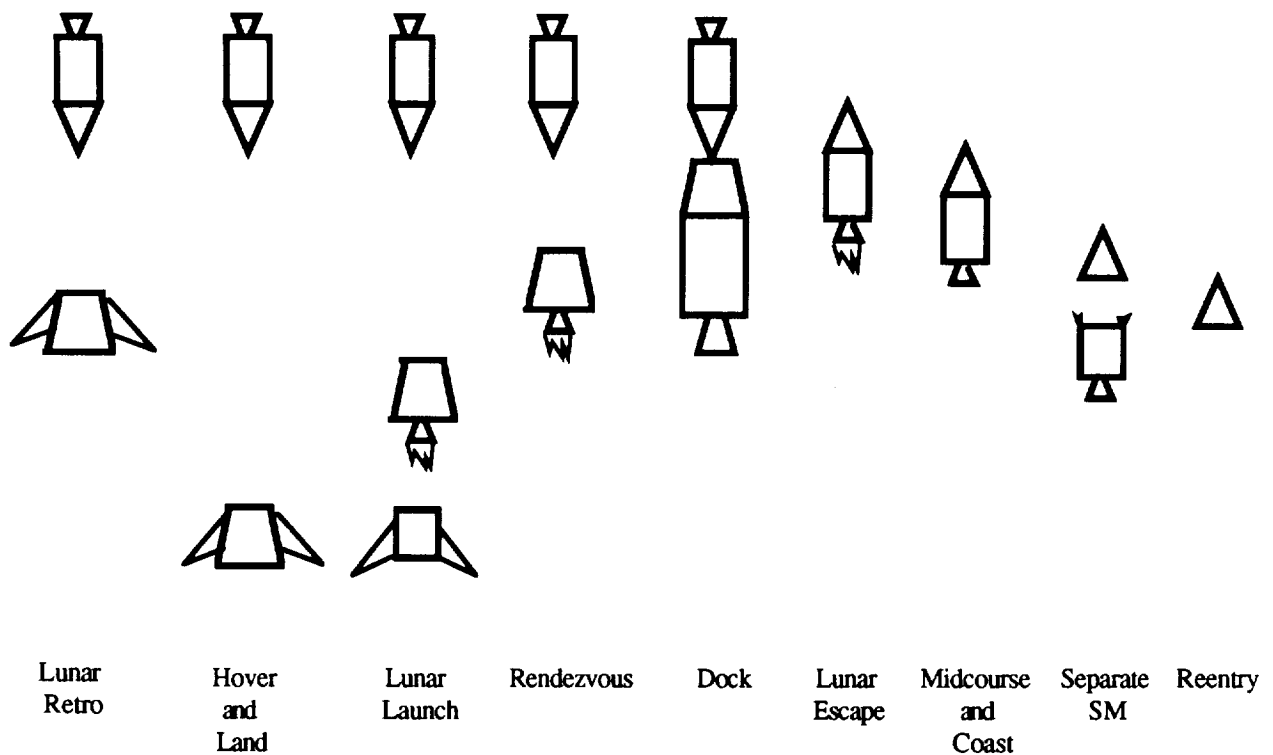


**Figure 2-7b**  
**Mission Profile, Lunar Orbit Rendezvous Mode**

#### 2.4.3.3 Lunar Approach, Lunar Orbit, and Lunar Landing

The SM-B will ignite for lunar orbit retro and establishing lunar orbit. The crew will then transfer to the LEM and the LEV will separate from the CM-SM configuration. The spacecraft will reorient for landing. The LEV-B will then ignite for braking, lunar descent, hover, and touchdown. The crew will then begin surface operations.

#### 2.4.3.4 Lunar Launch to Trans-Earth Orbit

The LEV-A will ignite the launch engines. Once the spacecraft has establish LLO, the spacecraft will orient for rendezvous with the CM. After docking the crew will transfer to the CM and the separate from the LEM. The trajectory will be determined and the spacecraft will reorient for navigation and midcourse maneuver. The SM-A will ignite for the lunar obit escape, provide for any midcourse maneuvers and reorient for coast.

#### 2.4.3.5 Earth Approach and Landing

As the spacecraft approaches the Earth, GNC will determine the re-entry parameters. The SM will be separated from the re-entry vehicle. The spacecraft will reorient for re-entry and begin the re-entry flight. The vehicle will then land and the crew recovered.

#### **2.4.4 Earth/Lunar Orbit Rendezvous (ELOR)**

See Figure 2-8 for the mission profile of ELOR.

##### **2.4.4.1 Launch to Trans-Lunar Injection**

This mode will require two launches. The first launch will transport the TLI in to LEO. The second launch will transport the spacecraft into LEO. The TLI and spacecraft will rendezvous and dock. While in orbit, the spacecraft will orient for trans-lunar escape. The TLI will ignite for trans-lunar orbit insertion.

##### **2.4.4.2 Trans-Lunar Orbit**

The TLI will be staged from the spacecraft. Then there will be a SM-LEM separation, the spacecraft will turn 180 degrees and the CM will dock with the LEM. The spacecraft will then orient for navigation and a midcourse maneuver if necessary. For a midcourse maneuver, the SM-B will ignite the midcourse engines. The spacecraft will then reorient for coast.

##### **2.4.4.3 Lunar Approach, Lunar Orbit, and Lunar Landing**

The SM-B will ignite for lunar orbit retro and establishing lunar orbit. The crew will then transfer to the LEM and the LEV will separate from the CM-SM configuration. The spacecraft will reorient for landing. The LEV-B will then ignite for braking, lunar descent, hover, and touchdown. The crew will then begin surface operations.

##### **2.4.4.4 Lunar Launch to Trans-Earth Orbit**

The LEV-A will ignite the launch engines. Once the spacecraft has establish LLO, the spacecraft will orient for rendezvous with the CM. After docking the crew will transfer to the CM and the separate from the LEM. The trajectory will be determined and the spacecraft will reorient for navigation a midcourse maneuver. The SM-A will ignite for the lunar obit escape, provide for any midcourse maneuvers and reorient for coast.

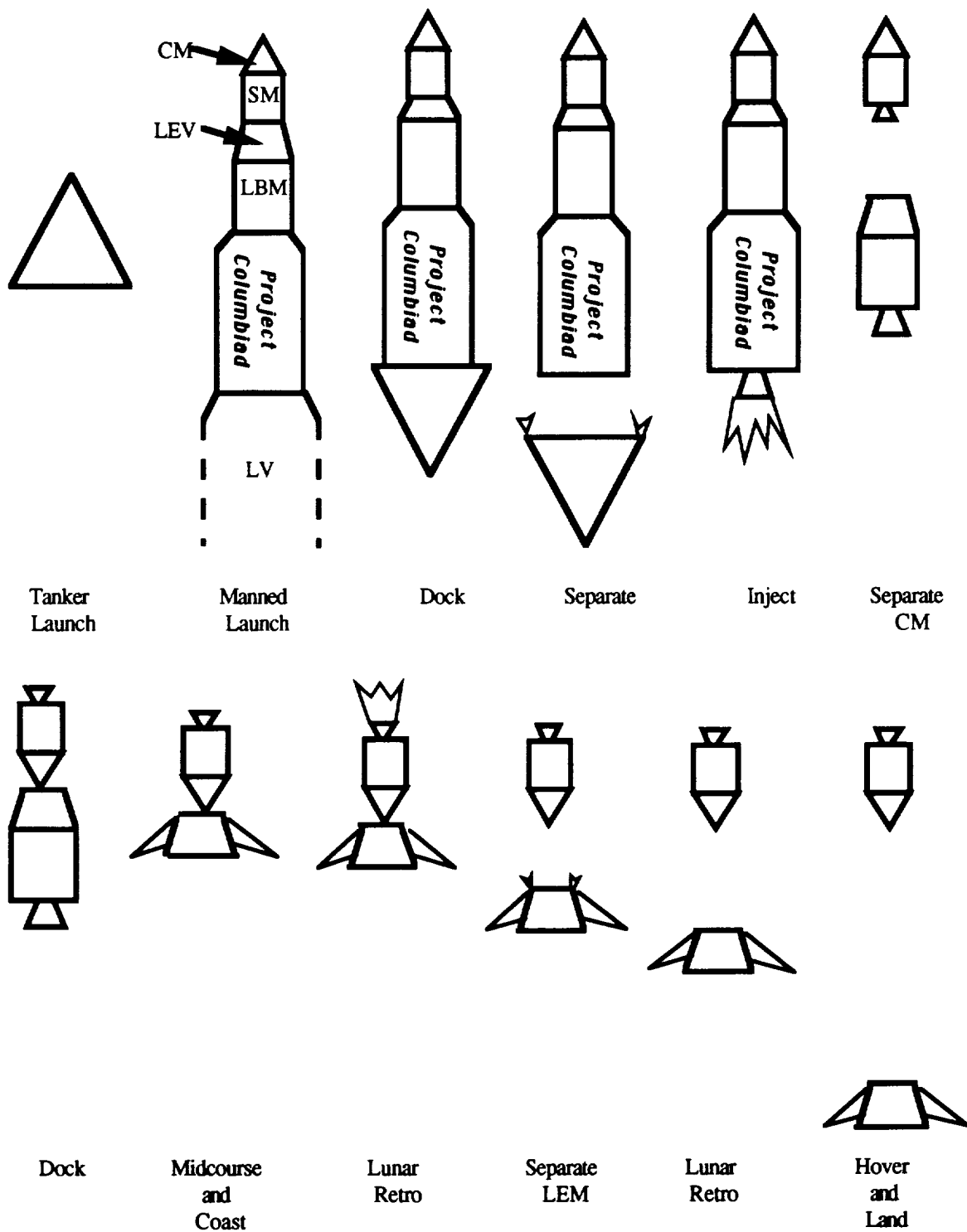


**Figure 2-8**  
**Mission Profile, Earth/Lunar Orbit Rendezvous Mode**

#### **2.4.4.5 Earth Approach and Landing**

As the spacecraft approaches the Earth, GNC will determine the re-entry parameters. The SM will be separated from the re-entry vehicle. The spacecraft will reorient for re-entry and begin the re-entry flight. The vehicle will then land and the crew recovered.

#### **2.4.5 Reusable Modules**

This section describes the variations of the four previous mission profile using the possible reusable modules.

##### **2.4.5.1 Re-entry Vehicle**

The reusable re-entry vehicle will modify all the mission modes only in the sense that it will supposedly be time-saving and cost-saving to re-use this vehicle.

Another option for EOR or ELOR is to leave the re-entry vehicle in LEO while the rest of the spacecraft continues on to the Moon. This was considered as a fuel saving option.

##### **2.4.5.2 Lunar Lander**

The reusable lunar lander will modify all the mission modes only in the sense that it may be cost-saving to re-use this vehicle. It will also allow the flexibility of shuttling to LLO for the LOR mode.

##### **2.4.5.3 Transfer Vehicle**

A reusable transfer vehicle would modify the ELOR mode as a shuttle between LEO and LLO. It would need to be refueled everytime it parks in LEO for the next lunar mission.

#### **2.4.6 Orbiting Lunar Station**

The orbiting lunar station would use a combination of the EOR and LOR mode, depending on whether it is more feasible to assemble the lunar station in LEO or LLO. EOR mode would be used for LEO assembly. The lunar station would be established in LLO. The reusable lunar lander will be important in this mode for excursion to the lunar surface. The advantage of the lunar station would be its expendability options and provide a possible node for the future Mars mission.

### **2.4.7 Space Shuttle**

#### **2.4.7.1 Piloted Mission Shuttle**

For EOR and ELOR, the Space Shuttle could be used to transport the crew to the previously launched spacecraft. Parking the Shuttle in LEO for the duration of the lunar mission provides the advantage of a reliable re-entry vehicle and the spacecraft saves fuel by not carrying the re-entry vehicle to the moon.

#### **2.4.7.2 Orbiting Lunar Station**

Another option considered for the mission modes was transporting the Space Shuttle to the moon. This would be done by two launches. One launch for the tanker, and the second launch with the LEM in the cargo bay. In LEO, the Space Shuttle will rendezvous with the tanker and refuel for the trans-lunar injection. At the Moon, the Space Shuttle will park in LEO and the LEM will transport the crew to the lunar surface. The Space Shuttle will also return the crew to the Earth and provide a reliable re-entry vehicle.

## **2.5 Mode Elimination**

### **2.5.1 Launch Capability Limitations**

Due to the weight comparisons for landing a payload of 25,000 kg precursor mission and 2,000 kg piloted mission, LOR and DF were eliminated because there is currently no single launch vehicle capable of putting into LEO the required mass. Therefore, since more than one launch will be necessary for each mission, there must be rendezvous in LEO.

### **2.5.2 Reusability Limitations**

The reusable modules were eliminated due to the complexity and development cost for each reusable stage. Reusable modules were determined to be out of the scope of this project.

### **2.5.3 Orbiting Lunar Station**

This option was also eliminated due to the complexity and development cost.



### **2.5.4 Space Shuttle**

#### **2.5.4.1 Piloted Mission Shuttle**

This option was eliminated due to the cost of a Space Shuttle launch and the reliability of timely Space Shuttle launches.

#### **2.5.4.2 Orbiting Lunar Station**

This option was eliminated due to the weight of the Space Shuttle. With a Space Shuttle weight of 160,000 kg, the amount of fuel calculated to transport the Space Shuttle to the Moon and back was far beyond the capability of even multiple launches of the launch systems previously discussed.

### **2.6 Conclusion**

For the scope of this project, the mode profiles was narrowed down to EOR and ELOR using the NLS system. The rest of this report describes how the mode was narrowed down to one and continues onto a more finalized design of the spacecraft, which in many cases differs dramatically from the assumptions used in this section.

### **3. Piloted Mission Mode Comparison**

For the piloted mission Earth Orbit Rendezvous (EOR) and Earth and Lunar Orbit Rendezvous (ELOR) were the two modes chosen for further detailed study after the initial investigations into mission modes and launch vehicle capabilities. The object of this study was to gain sufficient understanding of the safety, cost, and performance issues to perform a modal choice. The study sought to design a vehicle for each mode that would minimize the weight required in LEO for each.

At the end of the study, it was found that EOR actually required less weight in LEO than ELOR. This was contrary to some earlier expectations derived from Apollo mission mode comparisons. The two driving factors in the different results were, first, the land at any latitude requirement (coupled with the abort at any time requirement) and, second, the high Crew Module weight.

It is important to note when reading through the mode comparison section that the staging configuration used for the EOR mode is a different configuration than the one that was chosen as the final EOR configuration. The mode comparison configuration uses four propulsive stages in addition to the Crew Module while the final EOR configuration only uses three propulsive stages in order to reduce the cost of production.

#### **3.1 Requirements and Assumptions for Piloted Mode Analysis**

The first priority in the vehicle design process was to satisfy the top level requirements specified for the mission. There were five requirements that became the drivers for this step in the Columbiad design process. The five requirements were:

- High reliability -- mission survivability > 99.9%
- A minimum crew of four
- A "controlled crash" landing at Earth
- A propulsion system with  $I_{sp} > 440$  sec
- Expandability for future piloted missions

The requirement to have a 4 person crew and the requirement to have a "controlled crash" landing (Lift to Drag ratio  $\sim 1.1$ ) drove the initial weight estimates for the crew capsule to be  $\sim 6500$  kg and a heat shield weight of 730 kg. The combined Crew Module weight of

7230 kg drove the weight of the whole design. Small weight improvements in the Crew Module made large improvements in the initial weight needed at LEO.

The  $I_{sp}$  of the vehicle is one of the most important drivers in terms of minimizing the propellant mass required for the mission. Therefore, due to the high  $I_{sp}$  and high reliability requirement, the RL10 engines were chosen for the Columbiad mission. The RL10 engine  $I_{sp}$  ranges from 444 sec to 449 sec depending upon whether the throttleable or unthrottleable engine is used. Both the EOR and ELOR vehicle designs used a specific impulse of 449 sec. The fuel for the RL-10's is LOX/LH<sub>2</sub> which means that a cryogenic storage system had to be designed for the vehicle. For RCS burns, since the velocity change is minimal, performance equivalent to Apollo's RCS or better was required as opposed to the high performance required of the main engines. Therefore the Marquardt R4-Ds were assumed for the design. These RCS thrusters have an  $I_{sp}$  of 312 sec.

For the expandability requirement, the mission mode designs had to have the capacity to have a second piloted mission return to the lunar establishment *without* a second precursor mission also being necessary. This requires that the piloted vehicle have the capacity to resupply the habitat with food, water, air, clothing and any other 'used' items. The required resupply weight at the time of mode decision was 2000 kg and is labeled Moon Payload (MP) in the tables. This weight is transferred to the lunar surface only -- it is not brought back.

In addition to mission requirements being met, some design assumptions had to be made in order to calculate the stage weights for both the EOR and ELOR staging configurations. In order to estimate non propulsive masses of the stages, a mass estimate of 10% of total stage propellant and a mass estimate of 5% of total stage propellant estimate for cryogenic storage, power systems, GNC and C<sup>3</sup> systems on each stage. Therefore a 15% mass estimate for nonpropulsive weights was used. Along with this mass estimate, the known weights of the RL-10 engines were used. The number of engines for each stage was decided based upon burn times and thrust to weight ratios.

The other estimates used in the mode decision calculations were the reserve propellant carried with each stage. Two percent extra fuel margin at the end of each burn was the goal. Therefore, for each burn before the lunar landing of the piloted mission, 2% extra propellant was included in mass estimates. Since the propellant for the main engines is

cryogenic, and a certain level of uncertainty exists for thermal control of the cryogenic propellants, all burns occurring after the lunar stay budgeted for 8% extra propellant. The 8% came from the 4% propellant boil off per month estimate that existed at the time and an extra 2% for the case that departure from the lunar surface was delayed for two weeks beyond the planned four week stay. This would ensure the desired 2% extra propellant at the end of all of the burns. Later during our design phase, after mode decision was made, the propellant boil-off estimate dropped dramatically to ~0.2%.

### **3.2 Earth Orbit Rendezvous Design**

This chapter is a description of the Earth Orbit Rendezvous mission that was used in the piloted mode decision for Project Columbiad. The pros and cons relating to the top level mission requirements that are associated with the EOR mode are also detailed.

#### **3.2.1 Configuration Description**

Due to the assumed non propellant mass fraction of each stage (15% of propellant mass), and in particular the mass fraction for a stage to perform the Trans-Lunar Injection, if the entire burn ( $\Delta V = 3140$  m/s) is conducted in one stage, the payload of the TLI burn can only be 40% of the initial weight of the burn given the  $I_{sp}$  of the RL-10 Engines. This has unfortunate consequences when the distribution between two NLS launches is considered. The TLI stage alone weighs 60% of the total weight needed in LEO -- i.e. it is greater than half the weight so there is no way that the payloads on the two launches can be distributed evenly. This is a waste since one launch vehicle will be put to its limit while the other will be underused. Hence, in order to maximize the usage of the launch vehicle capacity, the TLI burn was divided among two stages. With the 15% non propellant mass fraction for each stage, the two launch weights were equalized when the Primary TLI stage (PTLI) had performed a  $\Delta V = 2415$  m/s propulsive maneuver; this left a  $\Delta V = 725$  for a Secondary TLI stage. This stage configuration is the one that was used at the time of mode decision for both the EOR and ELOR modes. Since then the Secondary TLI stage was incorporated into the following stage (LBM) in order to save on production costs for the vehicle.

So for the mode comparison, the EOR configuration was composed of four propulsive elements in addition to the crew capsule. The injection into the Lunar transfer orbit is performed by two stages: the PTLI and the STLI. Each stage separates from the stack upon the completion of its burn. A Lunar Braking Module (LBM) inserts the vehicle into Low Lunar Orbit (LLO), decircularizes the orbit, hovers, and lands. The Earth Return Module (ERM) launches the crew capsule into LLO and then into the Earth transfer orbit.

The ERM also performs any midcourse corrections. The ERM separates from the Crew Module (CM) just before reentry into the Earth's atmosphere and then the CM proceeds to reenter the atmosphere safely. This mission is completed when the CM lands at a predetermined landing site. A brief mission profile along with propulsive requirements for each stage is featured in Table 3-1.

**Table 3-1: Mission Profile**

<u>Event</u>	<u>Location</u>	<u>Propulsive Stage(s)</u>	<u><math>\Delta V</math> (m/s)</u>
Trans-Lunar Injection	LEO	PTLI	2415
Trans-Lunar Injection	LEO	STLI	725
Midcourse Corrections	Midcourse	LBM	120
Lunar Braking into LLO	Prior to LLO	LBM	1060
Lunar Braking to Moon	LLO to Moon	LBM	2020
Hover	LLO to Moon	LBM	180
Lunar Launch	Moon to LLO	ERM	1925
Earth Return Injection	LLO	ERM	1060
Midcourse Corrections	Midcourse	ERM	120
Reentry	Earth's Atmosphere	CM	100

### 3.2.1.1 Trans-Lunar Injection Stages

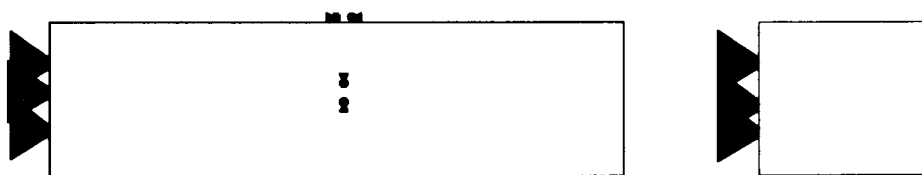


**Figure 3-1**

**Trans-Lunar Injection 1**

**Trans-Lunar Injection 2**

The two TLI stages perform the burn into Lunar transfer orbit. Each stage is jettisoned upon the completion of their respective burn. The Primary TLI stage with a  $\Delta V$  of 2415 m/s will require its own launch due to its wet mass of 84,400 kg. Once in orbit, it will await rendezvous and docking with the second launch which consists of the STLI, LBM, ERM, and CM.

In addition to the main propulsion system consisting of five nonthrottleable RL10 engines, the orbital waiting period and rendezvous and docking will require a reaction control system (RCS). The RCS uses monomethyl hydrazine and nitrogen tetroxide as fuel achieving an Isp of 312 sec. The structure must be able to dock with the STLI stage and maintain structural integrity until the completion of the burn.

The Secondary TLI stage completes the injection burn by supplying the remaining  $\Delta V$  of 725 m/s. The STLI stage also houses five nonthrottleable RL10 engines but does not require a separate RCS system. The total budgeted wet mass of the stage was 15,900 kg.

#### 3.2.1.2 Lunar Braking Module

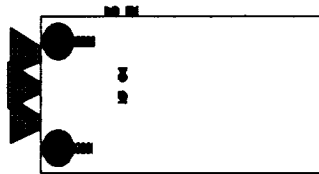


**Figure 3-2**  
**Lunar Braking Module**

The primary function of the Lunar Braking Module was to inject the spacecraft into a circular orbit and then to proceed to land upon the surface of the Moon. The current design actually stages the LBM just before the hover phase in order to reduce the landing height (see section 5.1 for more detail). The LBM features three throttleable RL10 engines which perform the braking  $\Delta V$  of 1060 m/s, the lunar descent  $\Delta V$  of 2020 m/s, and the hover and landing  $\Delta V$  of 180 m/s. The module requires an RCS to facilitate the landing process. Once the lunar stay is completed the module is left on the surface of the Moon. The wet mass budget of the vehicle was 43,700 kg. This wet weight was to include the landing legs in addition to the standard structural, power, GNC and C<sup>3</sup> weights.

### 3.2.1.3 Earth Return Module

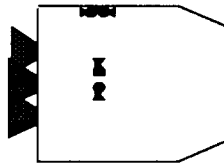


**Figure 3-3**  
**Earth Return Module**

The ERM returns the Crew Module back to the Earth. (See section 5.1 for a description of the new ERM functions.) This process required three maneuvers. The module provides the initial injection into LLO burn totaling a  $\Delta V$  of 2200 m/s. Second, the module performs the Earth orbit injection burn requiring a  $\Delta V$  of 1060 m/s. Lastly, the ERM performs any necessary midcourse corrections with a maximum  $\Delta V$  budget of 120 m/s. The ERM utilizes 3 throttlable RL10 engines and an RCS system. Just prior to reentering the Earth's atmosphere, the module is jettisoned and burns up upon reentry. The total budgeted wet mass of the ERM was 16,100 kg.

### 3.2.1.4 Crew Module



**Figure 3-4**  
**Crew Module**

The crew module is designed as a biconic reentry vehicle with a maximum lift to drag ratio of 1.1. The lift to drag ratio allows for reentry maneuvering and extends the downrange and cross range of the vehicle (the landing footprint). The primary function of the vehicle is to safely house the astronauts for the transit time to the Moon and back and to protect the crew during reentry, a total of six days. This function requires the vehicle to provide life-support and consumables for the trip time and a heat shield during the reentry phase. The vehicle is also designed to control the entire craft including sophisticated guidance, navigation, and control equipment. The design mass estimate for the CM at the time of mode comparison was 7230 kg.

### 3.2.1.5 EOR Mass Summary

A summary of the masses and the predicted lengths for each stage is shown in Table 3-2.

**Table 3-2: Mass Summary**

<u>Stage</u>	<u><math>\Delta V</math></u>	<u>Dry Mass</u> <u>(kg)</u>	<u>Propellant</u> <u>Mass (kg)</u>	<u>Wet Mass</u> <u>(kg)</u>	<u>Length (m)</u>
Trans Lunar Stage 1	2415	11,735	72,665	84,400	20
Trans Lunar Stage 2	725	2,800	13,100	15,900	5.9
Lunar Braking Module	3380	6,140	37,560	43,700	10.1
Earth Return Module	3105	2,550	13,550	16,100	7.7
Crew Module (with heatshield)	RCS	7,230	0	7,230	10
Payload to Moon	NA	2,000	0	2,000	2
Total Mass				169,330	

		Total length
Total Mass for Launch 1 (PTLI stage) -	84,400 kg	20 m
Total Mass for Launch 2 (Piloted mission)-	84,930 kg	35.7 m

This EOR configuration requires two NLS launches for the piloted mission with the addition of an extra SRM booster on each launch. The final piloted EOR configuration requires two NLS launches with two additional SRM boosters on each launch instead of one. This launch vehicle design is described in detail in Volume III, Chapter 2.

### 3.2.2 Safety

The EOR mission profile evaluated during the mode decision was designed to comply with all of the top level mission safety requirements. The standard redundancy level set in order to ensure this was three levels of redundancy for mission survivability and two levels for mission success. The EOR mission was also designed to comply with the requirement to be able to abort from the mission at any time -- including during the lunar stay.

### 3.2.3 Cost

The main drivers of the cost issue are the nonrecoverable research, development, and testing costs (R&D). Once a stage has been developed and tested the manufacturing cost is an order of magnitude lower than R&D. The priority therefore becomes to establish as



much commonality in staging as possible thereby lowering the R&D costs. Furthermore, common or similar stages benefit from a learning curve. Both design and manufacture improve with the experience gained by the initial flight and manufacturing. Designs can be improved and manufacturing techniques can be perfected. This learning curve becomes increasingly beneficial with increased production.

The cost estimation is a particularly difficult process for a mission on the scale being discussed here. Very little data exists from similar programs due to the unique nature of a Lunar mission. Apollo is the closest comparison available, offering outdated cost data. The two most common methods which could apply for the current situation are parametric cost analysis and analogous estimation. Both these methods require complex costing algorithms based upon previous data which is dubious at best and too complex for an initial cost study. In light of these facts, a costing procedure based upon data from a proposed lunar base costing estimate was used. Volume IV, Chapter 2 describes this costing procedure in detail.

The final results of the cost estimates are displayed in Table 3-3 for the first mission. As illustrated by these figures the R&D costs are a magnitude higher than the production costs. The analysis of the entire mission is displayed in Table 3-4. These figures include estimates for the precursor mission, launch vehicle costs, and operational costs. The precursor missioned costs included design commonality with EOR for both the Primary and Secondary TLI stages and the landing stage (LBM). Launch vehicle costs were assumed to be 600 million per launch.

**Table 3-3: R&D and Manufacturing Costs**

<u>Stage</u>	<u>R&amp;D Cost (millions )</u>	<u>Manufacturing Cost (millions )</u>
PTLI	Combined for 1,860	Combined for 180
STLI		
LBM	1,270	130
ERM	500	50
CM	1,500	200

The total cost estimates for a five year campaign is 46.7 billion dollars. This number shows a substantial learning curve effect from the first flight which totals about 12 billion dollars. These numbers illustrate the importance of long range planning and the substantial savings which may be obtained due to commonality between systems.

**Table 3-4: Total Flight Costs**

<u>Cost Factors</u>	<u>First Flight Cost</u> <u>(millions )</u>	<u>First Year Cost</u> <u>(3 piloted &amp; 1</u> <u>precursor)</u>	<u>Five Year</u> <u>Campaign (15</u> <u>piloted 5 precursor)</u>
Piloted Mission	5690	6,330	9,260
Precursor	2,300	2,300	4,160
Launch Vehicles	2,400	4,800	24,000
Operations	800	1,600	8,000
<b>Total</b>	<b>11,190</b>	<b>15,030</b>	<b>45,420</b>

### **3.2.4 Performance Issues**

#### **3.2.4.1 Design Complexity**

The EOR is a design utilizing the function of all the components to the maximum efficiency. Each stage serves a specific function and is then jettisoned once that function has been served. The simplicity of EOR has a number of beneficial effects upon the program. The vehicle does not need to be overly complex with multiple navigation and control system for different stages. The entire vehicle is self contained except for the Primary TLI stage which needs to rendezvous and dock with the piloted vehicle.

However, there is one area which provides complications for the design, namely lunar landing stability. The landing stability is a challenge due to the height of the landing configuration -- 29.8 m. The stability issue is largely dependent upon the ability to control the lateral motion of the craft, detailed knowledge of the landing site, and the landing accuracy. A solution that was designed after the mode decision and is, hence, not included in this EOR description was to have the Lunar Braking Module stage just prior to the hover maneuver which is performed by the ERM. This configuration still utilizes the LBM as the primary descent module and adds a limited amount of fuel and mass to the ERM. See

section 5.1 for more details. The design complication has therefore been transferred from the landing stability challenge to being able to stage successfully shortly before landing.

#### 3.2.4.2 Commonality with Precursor

EOR has the advantage of high commonality with the Precursor mission. The current masses for a Precursor mission landing a payload of 25,000 kg upon the surface of the moon are compared to the corresponding stages in Table 3-5.

**Table 3-5: Commonality Comparison between Precursor and EOR**

	<b>PRECURSOR</b>		<b>EOR</b>	
<u>Propulsion Stage</u>	<u><math>\Delta V</math> (m/s)</u>	<u>Mass (kg)</u>	<u><math>\Delta V</math> (m/s)</u>	<u>Mass (kg)</u>
PTLI	2415	84,400	2415	84,400
STLI	725	15,900	725	15,900
Lunar Landing	3380	43,700	3380	43,700

The velocity and masses are identical for each stage. With the current design above, there would be close to 100% commonality between the two TLI stages. A difference in landing stage configuration may exist between the the two missions due to nature of the delivered payloads. However, the precursor mission needs to land a tall stack consisting of the habitat and power system. The current configuration calls for a vertical landing of the precursor payload which is inherently similar to the EOR landing configuration. Therefore the level of commonality was correctly expected to be high at the time of mode decision.

#### 3.2.5 Expandability Issues

The expandability issue was mentioned earlier as a system requirement. Currently, there is a payload allotment of 2000 kg for the mission. The weight of consumables for the first mission is 2000 kg. The payload allotment therefore allows for future piloted missions to return to the Moon without the requirement for another precursor.

#### 3.2.6 Conclusion

EOR is a simple and elegant design in that each portion of the vehicle serves its purpose purely and simply. This EOR design allows for the use of two NLS launches with a total mass to orbit of 169,330 kg. Technically, the most challenging area was the landing stability (and is now the LBM staging reliability).

### **3.3 Earth and Lunar Orbit Rendezvous Design**

This chapter is a description of the Earth and Lunar Orbit Rendezvous mission that was used in the piloted mode decision for Project Columbiad. The pros and cons relating to the top level mission requirements that are associated with the ELOR mode are also detailed.

#### **3.3.1 Configuration Description**

For the reasons mentioned in 3.2.1, there are two stages that perform the Trans-Lunar Injection burn: the Primary TLI and the Secondary TLI. Therefore in the ELOR design that was used for the mode decision for the piloted mission of Columbiad, there are four propulsive stages in addition to a Crew Module. The four stages are PTLI, STLI, Service Module (SM), and Lunar Excursion Module (LEM).

##### **3.3.1.1 Trans-Lunar Injection Stages**

The PTLI stage is launched alone on the first NLS vehicle while the rest of the piloted vehicle is launched on a second NLS shortly after success of the first launch is confirmed. Once both launches have been successful, a rendezvous in Low Earth Orbit occurs. Thus docking interfaces exist on the top of the PTLI and the base of the STLI. Both launch pieces will have RCS and GNC systems on board in order to perform the maneuver. The role of the two stages is to provide the propulsive burn in order to inject onto the lunar transfer orbit. PTLI is staged when it completes its  $\Delta V$  burn of 2415 m/s and STLI is staged after it completes its  $\Delta V$  burn of 725 m/s. Both of the TLI stages have five nonthrottleable RL10 engines to perform their burns. The wet mass budget for the PTLI is 90,525 kg and is 16,970 for the STLI.



**Figure 3-5**

**Trans-Lunar Injection 1**

**Trans-Lunar Injection 2**

##### **3.3.1.2 Service Module**

The role of the Service Module is compound. It first brakes the piloted vehicle into LLO ( $\Delta V = 1060$  m/s). It then waits in LLO during the lunar stay (28 days) and is capable of performing a  $90^\circ$  plane change ( $\Delta V = 2300$  m/s) in the event that an abort is required.

Since it will be an independent vehicle during the Lunar Orbit Rendezvous, the SM has its own RCS and GNC systems. The SM is then responsible for the injection of the Crew Module onto the Earth return trajectory ( $\Delta V = 1060$  m/s). The SM is also responsible for midcourse correction burns on both the lunar transfer orbit and the earth return orbit. The wet mass budget for the SM is 38,250 kg.

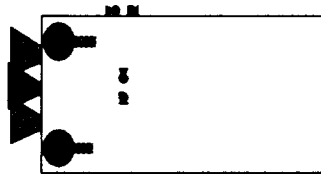


**Figure 3-6**  
**Service Module**

#### 3.3.1.3 Lunar Excursion Module

The first function of the LEM is to transfer the CM from LLO to the lunar surface ( $\Delta V = 2200$  m/s). After the lunar stay, the LEM brings the CM back up to LLO so that the CM can rendezvous with the waiting SM ( $\Delta V = 2200$  m/s). The wet mass budget of the LEM is 26,190 kg and includes the landing legs in addition to the standard structural, power, GNC and C<sup>3</sup> weights.

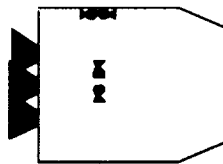


**Figure 3-7**  
**Lunar Excursion Module**

#### 3.3.1.4 Crew Module and Heat Shield

The Crew Module houses the four person crew for the entire transit to and from the Moon. The CM includes a heat shield (HS) to protect the crew when the CM reenters the Earth's atmosphere. It is capable of performing RCS maneuvers during all separation and rendezvous maneuvers along the phases of the mission in addition to during reentry.

In order to reduce initial weight in LEO, a trade was conducted on whether to leave the reentry heat shield for the Crew Module in LLO. The removable heat shield would be comparable to a slipper for the biconic crew capsule. Leaving the heat shield in LLO reduces the propellant weight that is required to transfer the crew capsule from LLO to the lunar surface and back to LLO. There is a small weight penalty for removing the heat shield. The weight of the shield and shield interface increases by approximately 30% of the nonremovable heat shield. The effect of this penalty is small enough that the propellant weight for all burns previous to separation in LLO is still reduced. For the ELOR stage weights mentioned in this chapter, a design that separated the heat shield was used. The CM mass budget for the ELOR mode analysis was 7230 kg.



**Figure 3-8**  
**Crew Module and Heat Shield**

The necessary separation and rendezvous maneuvers resulting from the removable heat shield are rather complex. First the LEM( with the CM and HS in front) detaches from the SM. The LEM, CM, and, HS combination reorients itself with respect to the SM so that the heat shield can attach onto the SM. The deshielded CM and LEM then slips out from the shield and heads toward the lunar surface.

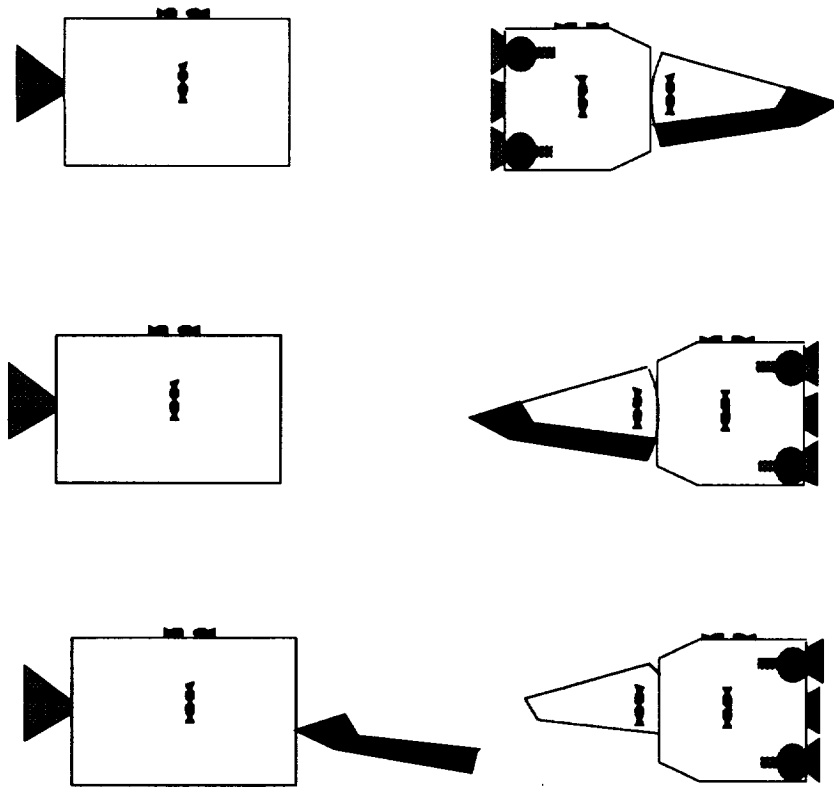


**Figure 3-9**  
**LLO Separation**

For rendezvous the LEM and deshielded CM return to LLO. The LEM then separates from the CM. The CM then slips back into its heat shield. The reshielded CM then detaches from the SM and reorients itself with respect to the SM so that the base of the CM can attach onto the SM before the SM performs the earth return injection burn.

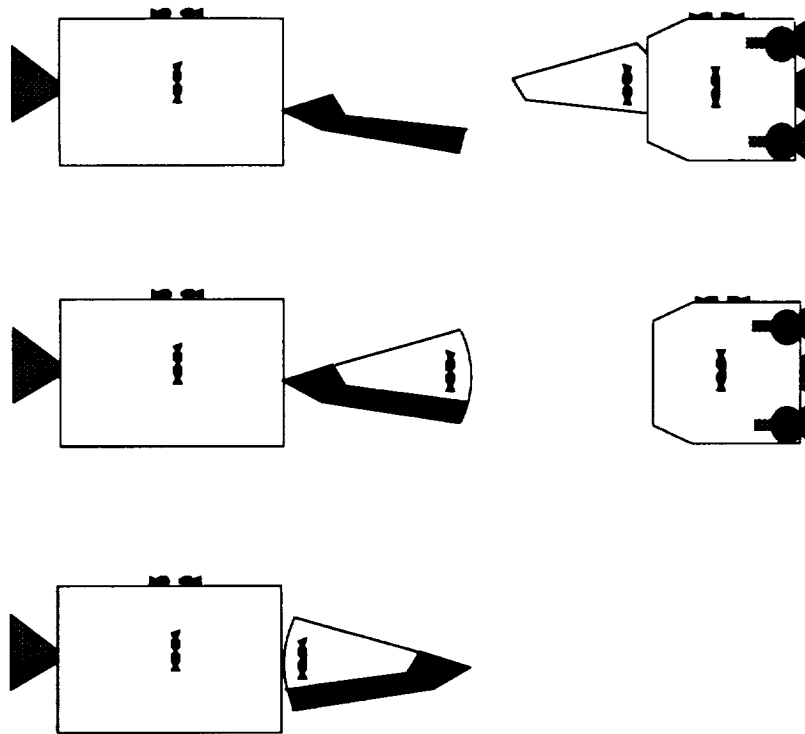


**Figure 3-10**  
**LLO Rendezvous**

#### 3.3.1.5 Mission Profile Summary

A summary of the mission profile is shown in Tables 3-6 and 3-7.



**Table 3-6: Mission Profile Summary**

<u>Event</u>	<u>Location</u>	<u>Propulsive Stage(s)</u>
Trans-Lunar Injection	LEO	PTLI
Trans-Lunar Injection	LEO	STLI
Midcourse Corrections	Midcourse	SM (RCS only)
Lunar Braking into LLO	Prior to LLO	SM
Lunar Braking to Moon	LLO to Moon	LEM
Hover	LLO to Moon	LEM
Lunar Launch	Moon to LLO	LEM
Abort ONLY	LLO	SM
Lunar Orbit Rendezvous	LOR	SM,LEM,CM
Earth Return Injection	LLO	SM
Midcourse Corrections	Midcourse	SM (RCS only)
Reentry	Earth's Atmosphere	CM (RCS only)

**Table 3-7: Additional Mission Profile Summary**

<u>Event</u>	<u>Propulsive Stage(s)</u>	<u><math>\Delta V</math> (m/s)</u>	<u>Non propulsive Sections</u>
LEO	PTLI	2415	STLI,SM,LEM,MP,CM,HS
LEO	STLI	725	SM, LEM, MP,CM, HS
Midcourse	SM (RCS only)	120	LEM, MP, CM, HS
Prior to LLO	SM	1060	LEM, MP, CM, HS
LLO to Moon	LEM	2020	MP, CM
LLO to Moon	LEM	180	MP, CM
Moon to LLO	LEM	1925	CM
Abort ONLY	SM	2300	HS
LOR	SM,LEM,CM	275	HS
LLO	SM	1060	CM, HS
Midcourse	SM (RCS only)	120	CM, HS
Reentry	CM (RCS only)	100	HS

### 3.3.1.6 ELOR Mass Summary

The specifics for each stage resulting from the aforementioned requirements and assumptions are shown in Tables 3-8 and 3-9.

**Table 3-8: Stage Mass Budgets**

<u>Stage</u>	<u>Dry Mass (kg)</u>	<u>Propellant Mass (kg)</u>	<u>Wet Mass (kg)</u>
PTLI	12,534	77,991	90,525
STLI	2,939	14,031	16,970
SM	5,685	32,565	38,250
LEM	3,852	22,338	26,190

**Table 3-9: Stage Summary**

<u>Stage</u>	<u><math>\Delta V_{TOTAL}</math> (m/s)</u>	<u>Wet Mass (kg)</u>	<u>Length (m)</u>
PTLI	2415	90,525	20
STLI	725	16,970	5.7
SM	4540	38,250	10
LEM	4400	26,190	7.6
CM	Reentry RCS	7230	10
Moon Payload	N/A	2000	2

<u>Launch 1</u>	Payload to LEO = 90,525 kg	Payload Length = 20 m
<u>Launch 2</u>	Payload to LEO = 90,640 kg	Payload Length = 35.3 m

Total Payload to LEO = 181,165 kg

Each launch weight is greater than the NLS capacity of 89,000 kg with 4 boosters for a 10% margin. This means that either the estimated mass fractions need to come down during the design process, the Moon Payload weight needs to come down, or the 10% margin desired by the Launch Vehicles group would have to be compromised. [Or a third option would be to eliminate the kick motor on the NLS and to have the PTLI and LBM perform the necessary circularization burns for each of their launches instead. This is what

is currently being done in the final EOR configuration. This tradeoff increases the overall payload achievable in LEO.]

The high initial weight at LEO has one advantage in that the corresponding precursor mission has a high surface payload delivery weight: 26,900 kg.

### **3.3.2 Safety**

#### **3.3.2.1 Abort Complexity**

The requirement for Project Columbiad to land at any latitude on the Moon's surface leads to an interesting orbital mechanics problem for the ELOR mode. The any latitude requirement means that polar orbits must be considered in addition to equatorial ones. Equatorial orbits are straightforward. If a vehicle is placed in an equatorial orbit about the Moon, it will remain in that orbit as the Moon rotates about the Earth. But, if a vehicle is placed in a polar orbit about the Moon, the orbit will appear to rotate longitudinally about the Moon's surface. The reason for this lies in the fact that the Moon always has the same side facing the Earth as it rotates about the Earth. The vehicle, however, while it rotates about the Earth with the Moon, maintains the orientation of its orbit with respect to inertial space. Figure 3-11 will help to clarify the orbit orientation.

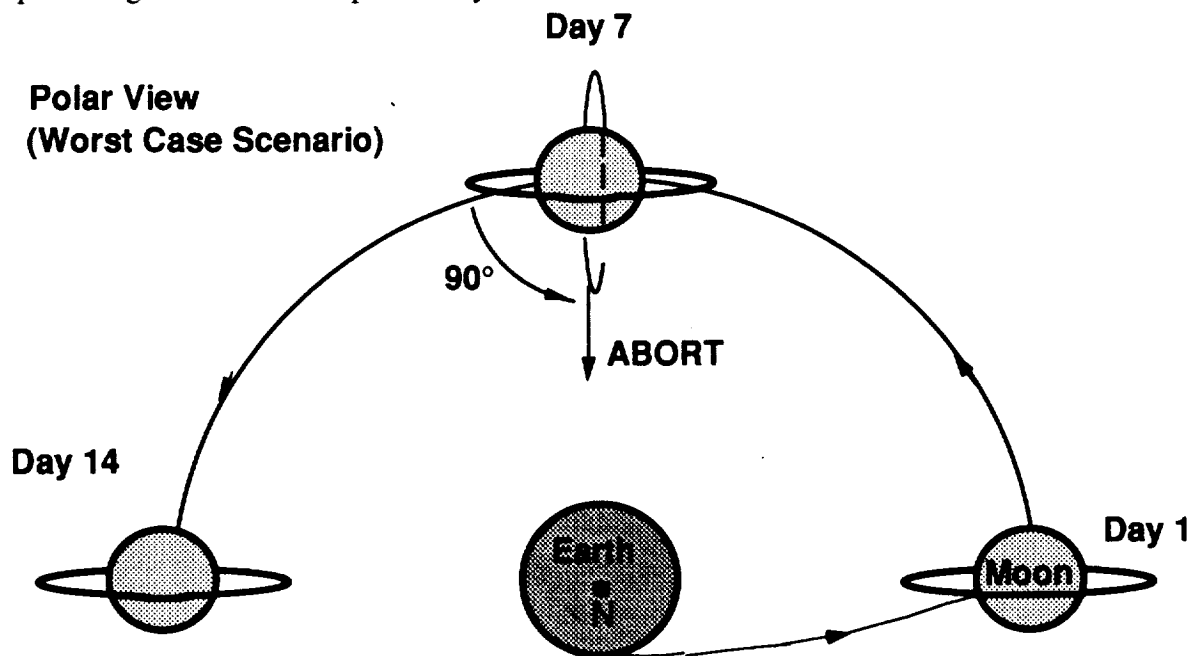


**Figure 3-11**  
**Polar Orbit Alignment**

Since the Moon's orbit around the Earth is 28 days, the polar orbit also has a period of 28 days to return to the original longitude that the polar orbit was initiated at. At both the 14 day point and the 28 day point the polar orbit is line with an Earth return trajectory. Rather convenient as one of the primary mission specifications was for a 14 to 28 day stay on the lunar surface.

However, mission safety must be taken into account. The 14 and 28 day positions are the only times that a return to Earth trajectory is possible without additional propellant. A system requirement, though, is that abort be possible at any time. From the any time requirement the worst case scenario must be evaluated. Both the 7 day and 21 day points the are the worst case scenario points. At these positions, the polar orbit of the SM and HS are 90° out of phase with the Earth return trajectory. To perform a standard plane change, a  $\Delta V = 2300$  m/s is required. Orbit maneuvers exist that would need less  $\Delta V$  to perform the plane change, however, these optimized trajectories take *time* to perform -- on the order of a day. But, since this is an *abort* mode, time is critical. Therefore the analysis of the ELOR mode needs to budget for 2300 m/s in order to be able to abort at any time.

The abort at any time requirement is slightly misleading. The requirement from the lunar surface is to be able to abort at any time within the next existing launch window. To arrive at the correct landing site on Earth, the launch windows occur approximately once a day. Hence, if at all possible, the return to Earth trajectory would be delayed until the launch window. If it is not possible, then alternate landing sites will be considered and then crash landing sites will be considered. The 1.1 L/D ratio of the reentry vehicle does allow some choice of the crash landing site.

### 3.3.2.2 Rendezvous and Separation Complexity

In ELOR not only is there a rendezvous in Low Earth Orbit, but there is also both a separation and rendezvous in Low Lunar Orbit as was detailed previously. This is a disadvantage because there are now two additional complex events that need to occur successfully. The additional complex events comes into the reliability and safety of the mission. Either the ELOR mission is less reliable than a mission without the additional separation and rendezvous maneuvers or the mission gets "beefed up" so much in order to be just as reliable that the weight (and cost) of the mission goes up. There is no simple way out of the increased complexity.

### **3.3.3 Cost**

Section 3.2.3 described the first-cut cost estimation of EOR and the important considerations which went into the analyses. Here, the same assumptions are used:

- All costs in 1990 dollars
- Research and Development costs include the design and construction of operational prototypes for test integration
- Manufacturing cost is the cost of building one complete design
- Per launch vehicle manufacturing cost is estimated at 600 million
- Per launch operations cost is estimate at 200 million
- No operations estimation on fuel and status monitoring beyond launch

The results of the cost estimates for ELOR are displayed in Table 3-10 for the first mission. As illustrated by these figures the R&D costs are a magnitude higher than the production costs. The analysis of the entire mission is displayed in Table 3-11. These figures include estimates for the precursor mission, launch vehicle costs, and operational costs. The precursor costs included design commonality with ELOR for both the PTLI and STLI stages.

**Table 3-10: R&D and Manufacturing Costs**

<u>Stage</u>	<u>R&amp;D Cost (millions )</u>	<u>Manufacturing Cost (millions )</u>
PTLI	2,000	200
STLI	500	50
SM	900	90
LEM	800	80
CM	1,500	200

The total cost estimate for a five year campaign is 46.3 billion dollars. This is assuming the launch of three piloted missions and one precursor mission a year. The numbers show a substantial learning curve effect and illustrate the importance of long range planning and the substantial savings which may be obtained due to commonality between systems.

**Table 3-11: Mission and Long-Term Costs**

<u>Cost Factors</u>	<u>First Flight Cost</u> <u>(millions )</u>	<u>First Year Cost</u> <u>(3 piloted &amp; 1</u> <u>precursor)</u>	<u>Five Year</u> <u>Campaign (15</u> <u>piloted 5 precursor)</u>
Piloted Mission	6,320	7,060	10,430
Precursor	2,230	2,230	3,850
Launch Vehicles	2,400	4,800	24,000
Operations	800	1,600	8,000
<b>Total</b>	<b>11,750</b>	<b>15,690</b>	<b>46,280</b>

### **3.3.4 Performance Issues**

#### **3.3.4.1 Design Complexity**

In order to perform a Lunar Orbit Rendezvous, docking interfaces, as opposed to simple staging interfaces, must be designed between three modules: the CM, the LLM, and the SM.

##### **3.3.4.1.1 Heat Shield Separation and Rendezvous in LLO**

Crew Capsules performed a study on types of heat shield detachment and attachment mechanisms. There were three primary designs considered.

### Lock and Key Method

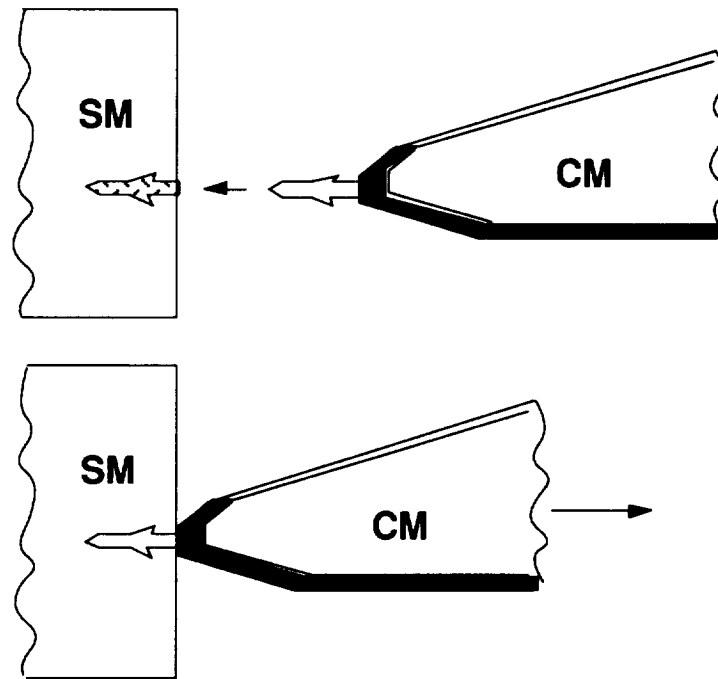


**Figure 3-12**  
**Lock and Key Docking Method**

This design has the advantage of being simplistic since it is merely an oversized "key" attached to the heat shield that slips into a "lock" located on the SM. There are problems associated with it however. One problem is how to actually attach the key onto the heat shield since the heat shield layer should not be compromised. It is important not to breach the integrity of the heat shield so that it is still able to protect the CM during reentry. In addition, if the attachment could be made successfully, a concern is the high stress concentrations that would be encountered at the heat shield interface during docking, undocking, and an abort maneuver should it be necessary.

### Jaws and Swivel Method

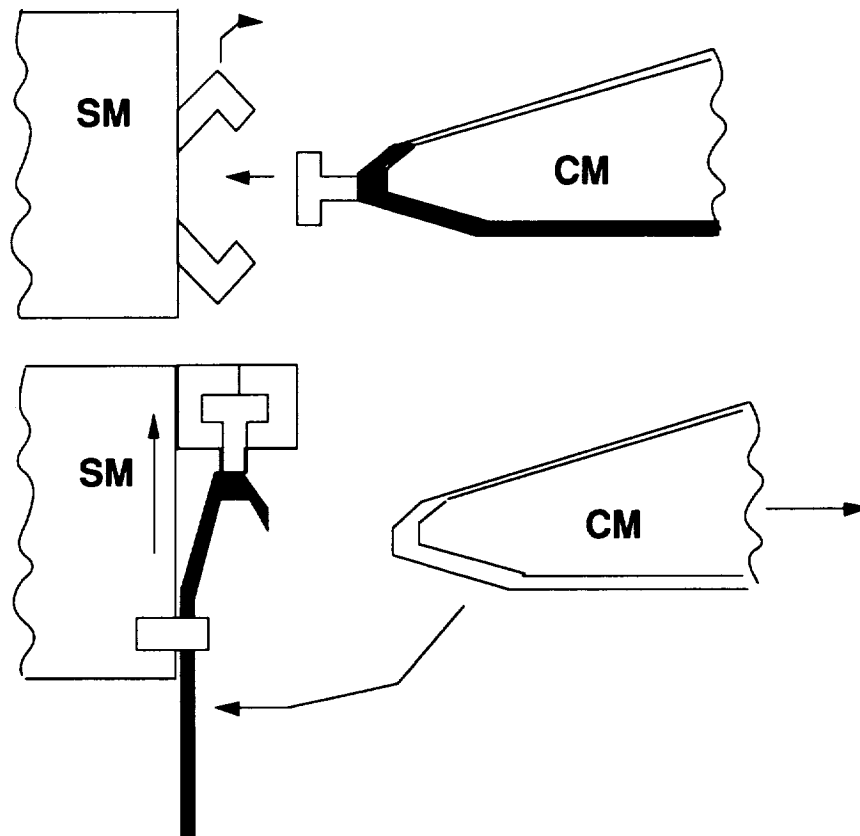


**Figure 3-13**  
**Jaws and Swivel Docking Method**

The jaws and swivel method is an improvement upon the lock and key in that an attempt to secure the heat shield is made in the event that an abort maneuver becomes necessary. There is still a slightly modified key attached onto the heat shield with the same stress concentration problem during docking and undocking and with the same attachment problem as with the lock and key method. The improvement comes in the fact that the key is now grabbed by jaws that then rotate the shield 90° so that the base of the shield rests against the SM. Another attachment mechanism from the SM then attaches onto the center region of the shield. There is now more contact area between the shield and the SM. This should help alleviate the stress concentrations felt during an abort maneuver.



Other disadvantages include the heavy mechanical design required for the jaws and the track for the jaws to swivel on. The mechanism is inherently more complex than the lock and key and hence would tend to be less reliable.

#### Roofer Method

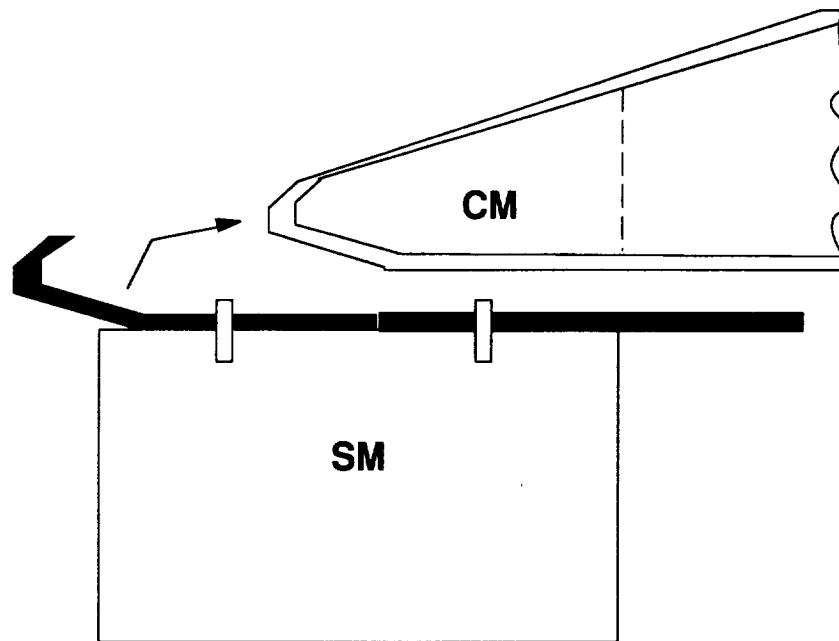


**Figure 3-14**  
**Roofer Docking Method**

The third design, the roofer docking method, involves attaching the base of the heat shield to the length, or "roof," of the SM. This option provides a large contact area for reduced stress concentrations and it does not require heavy mechanical designs as the jaws and swivel method did. One undesirable trait with the design, though, is that interfaces on the bottom of the heat shield are required. Another difficulty is that the base of the heat shield is curved, not flat. And still another deterring point is that maneuvering into this docking configuration is more difficult because more than one attachment point exists and visibility in that direction is poor (cameras could aid the pilot).

#### 3.3.4.1.2 No Heat Shield Separation

This interface and docking design is much simpler. The Service Module only needs to have an interface between the LEM and the base of the CM; no interface with a shield is

needed. The LEM's interface equipment remains essentially the same as it still needs to undock from the SM at LLO separation and stage off of the CM just before LLO rendezvous. The Crew Module is much simpler as the crew capsule does not have to slip out of its heat shield and the heat shield is not designed to interface with the Service Module. The base of the Crew Module, though, still needs to have interfaces compatible with both the LEM and the SM.

#### 3.3.4.1.3 Design Complexity Conclusion

The ELOR mode is overly complex when the shield detachment option is taken into account. There are problems with no clear solutions to each method of heat shield docking that was analyzed by Crew Capsules. Their recommendation was, therefore, despite the lower initial weight in LEO, and despite the fact that the mode study was based upon the detachable heat shield, to leave the heat shield attached. In the interests of simplicity, this is a wise recommendation.

There is yet another advantage with designing the heat shield to remain attached. The design of any landing wheels or skids that need to come through the bottom of the CM for landing on the Earth's surface is much easier if the base of the heat shield is not already designed to interface with the SM.

#### 3.3.4.2 Maintenance in LLO

A drawback to the ELOR mode is that the SM and HS must remain in LLO during the lunar stay. This means that both a communications system and a guidance, navigation and control system must be on-board. This dictates that a minimum of two independent (not redundant) power systems exist on the piloted mission since the SM can use neither the Crew Module's power supply nor the precursor's power supply during the lunar stay. The additional weight from this separate system was estimated to be roughly 400 kg for the design calculations.

There is one advantage to having the SM in LLO. The SM can be used to aid rover communications with the habitat when the rover is out of direct line of sight of the habitat. At the times when the SM is on the distant side of the moon from the habitat, the Earth ground control will be providing the communications transfer between the rover and habitat. This is undesirable due to the time delay in communications, hence the nearby orbiting SM could be a bonus for surface activities.

#### 3.3.4.3 Efficiency

As a performance issue, the amount of *waste* involved in the ELOR mode should be considered. For a nominal mission, the abort maneuver is *never* performed. For all nominal piloted missions the extra propellant, roughly 9100 kg, is never used. There is no practical way to leave this extra propellant in orbit for the next piloted mission to use. Even if the staging details to leave behind a separate abort stage were worked out, the abort stage's orbit would be non optimal for later missions. In fact, it could reduce the launch windows to the moon so severely that scheduling constraints would begin to drive all the piloted missions much more than is reasonable for a mission to the Moon.

Not only are there launch window problems, but there is also the problem with propellant boil-off. The abort stage would either have to carry enough cryogenic insulation to reduce boil-off to an acceptable level over a period of 2-10 years or a severe reduction in  $I_{sp}$  would be incurred by using a non cryogenic fuel.

It comes down to the fact that the land at any latitude requirement and the abort at any time requirement combine to create a very wasteful ELOR mode.

#### 3.3.4.4 Lunar Landing Advantage

The ELOR mode has a significant advantage over the EOR mode by virtue of the fact that it does not have to land an extremely tall vehicle when it lands on the Moon's surface. The expected landing height is 19.6 m with a 5 m base.

#### 3.3.4.5 Precursor Commonality

For all modes, the precursor mission is designed to have the highest commonality possible with the piloted mission. In this staging configuration of ELOR, the stages common to both the precursor and piloted mission are the PTLI and STLI stages. The commonality between the two missions is good because it reduces the development and production costs of the whole mission.

#### 3.3.5 Expandability Issues

The ELOR mode has been designed to be expandable in accordance with the top level requirements. It is capable of resupplying the habitat with 2000 kg of payload for any piloted missions beyond the first. The 2000 kg was the minimum set by Crew Systems at the time of mode decision.

### **3.3.6 Conclusion**

In order to reach Low Earth Orbit, the ELOR mode requires four NLS launches with two extra boosters: two for the piloted mission and two for the precursor. However, the margin of the NLS launch vehicles is slightly compromised. The precursor has two stages that are modular with the piloted mission and its delivery payload is 26,900 kg. The optimized weight (detachable heat shield) ELOR mode is extremely complex in terms of both docking maneuvers and docking interfaces. The non optimized weight (integral heat shield) is better, yet still complex. The abort at any time requirement is costly in terms of initial weight at LEO. The additional weight required for the abort is wasted in a nominal mission; there is no practical way to put the abort propellant to good use.

## **3.4. Mode Comparison**

### **3.4.1 Introduction**

The selection of the primary mode for achieving the piloted lunar landing has been the driving factor in the design process and resulting scheduling, since the choice of the mode affects design requirements for many system and subsystem elements. Differences between the mission profiles are compared in this section and priorities follow somewhat the order of the design criteria. The major factors in the mode selection are comparison of the modes by:

1. Reliability and mission success
2. Performance and weight
3. Cost and scheduling
4. Expandability

As a result of the initial stages of the design process, two major modes were considered as possibilities for the piloted lunar mission. They were:

1. Earth Orbit Rendezvous (EOR)
2. Earth-Lunar Orbit Rendezvous (ELOR).

Both options would require two NLS (National Launch Systems) launches in order to deliver the required mass to Low Earth Orbit (LEO), to meet the mission objectives set by Project Columbiad. The required mass at LEO is an important driver for mode decision. The ELOR mission profile requires additional propellant for a plane change necessary for an anytime abort capability set by Project Columbiad. As a result, the ELOR mode design requires additional fuel mass and in turn, requires more mass at LEO. Because of this extra

fuel which is required to perform anytime abort for the ELOR, In the current design, the mass difference at LEO between the EOR and the ELOR modes is no longer a factor of two as was expected from Apollo studies. This factor in addition to several other factors considered, the decision was made to use the EOR as the candidate mission profile for the piloted lunar mission.

In addition to the mode comparison, a discussion of the various crew capsule configurations suitable for each EOR and ELOR are presented, and comparisons based on the above design criteria are made. In summary, the mode selection will be presented, based on the various design comparisons considered, and the designs described in previous sections (3.1 through 3.3).

### **3.4.2 Reliability and Mission Success**

The reliability of the Piloted Lunar Mission depends on the large number of major events which must take place successfully and sequentially for the mission, or even an abort, to be completed successfully. This extreme system complexity places an unusual requirement on subsystem reliability. Reliability is an inverse, exponential function of the complexity of the component.

Although both the EOR and ELOR designs incorporate the 99.9% crew survivability rate, ELOR involves more abort complexity and, therefore, greater components and redundancy in order to meet the reliability and mission success. Additional complexities which are associated with the ELOR include docking for the lunar orbit rendezvous and injection of the service module for a lunar orbit plane change. Extra redundancies which must be built into the subsystems may very well increase the ELOR vehicle mass at LEO even more.

### **3.4.3 Performance**

#### **3.4.3.1 Crew Module Study**

The heating problem associated with reentry to the Earth's atmosphere on return, is one of major importance to the crew module since it affects the heat shield and its sub-structures, the internal insulation, and its cooling requirements. Several comparisons were made to study the amount of payload which can be added into the piloted mission and how this mass affects the mass at LEO. Here, design budgets must be allocated to insure that both EOR and ELOR can be launched within two launches, and they must also be allocated so

that additional payload can be launched in the piloted mission. Table 3-12.a through Table 3-12.c summarizes this study. All numbers are in kilograms.

**Table 3-12: Summary of Crew Module Mass Studies**

**Table 3-12.a**

Crew Capsule	Payload	EOR mass at LEO	ELOR mass at LEO
6000	0	150,000	159,500
	1000	156,500	167,700
	2000	163,000	175,900
	2500	166,200	180,000
	2000	163,000	137,200
no fuel for plane change			

**Table 3-12.b**

Crew Capsule	Payload	EOR mass at LEO	ELOR mass at LEO
6500	0	159,900	169,700
	1000	166,400	178,900
	2000	172,900	186,200
	2500	176,100	190,200
	2000	172,900	145,500
no fuel for plane change			

**Table 3-12.c**

Crew Capsule	Payload	EOR mass at LEO	ELOR mass at LEO
7475	0	179,200	189,600
	1000	185,700	197,900
	2000	192,200	206,100
	2500	195,400	210,200

The mass study at LEO illustrates the amount of performance margin which is left in the launch vehicle. One can see that in order to stay within the launch capabilities of the NLS launch system (approximately 180,000 kg), the crew module's mass (excluding the heat shield) cannot exceed a budget of 6500. It is also illustrated that the with the extra fuel needed for abort in the ELOR, the NLS system's margin is compromised.

#### 3.4.3.2 Mass Comparison

Throughout the design process, several mass comparisons were conducted, primarily on the design of the piloted mission. All mass estimations were based on a structural mass fraction of 0.15, and an additional fuel mass fraction of 0.08.

In all past lunar missions, spacecrafts have landed within a few degrees of the lunar equator. Project Columbiad, however, is requested to have capabilities to be able to land at any latitude, and it must stay on the Moon for a period of a month. This creates an additional abort complexity for the ELOR which past LOR missions have not encountered (as explained in Section 3.3.2). The Service Module (SM) which is left in orbit around the Moon for the ELOR profile must be able to align itself with the path of return to the Earth before injection for Earth return. After considering the worst case scenario in Section 3.3.4.1, the ELOR has been designed with the capability to perform a 90° plane change, expending a  $\Delta V$  of around 2300 m/s. Table 3-13 summarizes the mission profiles for the two modes, outlining the mass and  $\Delta V$  required for each major stage.

The mass comparison showed that the EOR mode would require less mass at LEO, in order to achieve the objectives of Project Columbiad. In addition, the mass required for each launch could be accommodated by modified NLS configurations using four solid rocket boosters (SRB's), to provide a maximum launch capability of 90,000 kg, in excess of the anticipated mass values.

#### 3.4.3.3 Performance Margins

The primary performance parameter in the mode comparison was the mass capabilities of each mode. In general, it was observed that the total mass delivered to the lunar surface was directly proportional to the mass at LEO. However, a limitation was set by existing launch vehicles on the actual amount payload that could be delivered to LEO. This in turn, limited the actual surface payload that could be delivered to the lunar surface. From the preliminary mass study, it was determined that the maximum surface payload that could be delivered to the lunar surface was 26,900 kg using an ELOR mission profile.

**Table 3-13: Mass and  $\Delta V$  Summary**

Stage	$\Delta V$ (m/s)	EOR Mode		ELOR Mode	
		Wet Mass (kg)	Length (m)	Wet Mass (kg)	Length (m)
PTLI	2415	84,400	20	90,525	20
STLI	725	15,900	5.9	16,970	5.7
LBM	3380	43,700	10.1	n/a	n/a
ERM	3105	16,100	7.7	n/a	n/a
SM	4540	n/a	n/a	38,250	10
LEM	4400	n/a	n/a	26,190	7.6
CM	n/a	7,230	10	7,230	10
Payload	n/a	2000	2	2,000	2
<i>Total Payload at LEO</i>		169,330		181,165	
Launch 1		84,400	20	90,525	20
Launch 2		84,930	35.7	90,640	35.3
Surface Payload		25,000		26,900	

**Table Legend:**

PTLI Primary Trans Lunar Injection stage  
 STLI Secondary Trans Lunar Injection stage  
 LBM Lunar Braking Module  
 ERM Earth Return Module  
 SM Service Module  
 LEM Lunar Excursion Module  
 CM Crew Module

**3.4.4 Cost and Scheduling**

The design and development phases of a space mission are heavily influenced by technological advances and the availability of the workforce to meet the demand that is defined by the mission. In addition, these phases are regulated by the availability of funding as most mission design require a budget in the billions of dollars. In the preliminary design process of Project Columbiad, various issues relevant to the overall cost of the project were considered in an effort to conduct a mode comparison for the design of the mission profile. These were commonality, developmental complexity and overall costs.



Throughout the design process, the issue of modularity and equipment commonality were drivers in the design of the various components for the mission. The component breakdown of the preliminary design for each mission profile, is outlined in Table 3-14. The table shows the level of commonality in the design of the piloted mission and the precursor mission.

**Table 3-14: Commonality in design of components**

Option	Case 1		Case 2	
Mission Profile	Precursor EOR	Piloted EOR	Precursor EOR	Piloted ELOR
Component				
PTLI	same design		same design	
STLI	different design		different design	
Lunar Lander	similar design		different design	

**Legend:**

PTLI Preliminary Translunar Injection Stage  
STLI Secondary Translunar Injection Stage

The precursor mission was designed for an Earth Orbit Rendezvous (EOR) profile and as a result, the EOR mission profile of the piloted mission had a slightly higher level of commonality than the case with the ELOR profile. In addition, the precursor landing configuration would be inherently similar to that of the piloted EOR mission profile. In each case, the design of the precursor mission was a derivative of the design of the piloted mission. As a result, the main propulsion stages were common in both designs.

One of the requirements of the project was that the designs were to be based on existing technologies that have been space rated. This would greatly reduce the developmental costs and complexity, as most designs would be derivatives of existing systems. These considerations are common to both mission profiles, however, it was evident that the design for the ELOR mission would be inherently more complex than that for the EOR mission profile.

The complexity of the ELOR mission profile is reflected both in its actual execution and the required development necessary to design the mission. As such, the ELOR mission would require more developmental time which would greatly influence the development costs. In addition, the manufacturing and quality assurance phase of the development process would be more complex for the ELOR case as the designs for this profile require special tooling that have to be developed and manufactured in addition to the primary components.

The main drivers in the cost analysis are the non-recoverable research, development, and equipment certification costs (R&D). For the mode comparison, an extensive costs analysis was conducted for both the ELOR and EOR mission profiles. The total costs estimates were divided into seven main categories as compared for both cases. A summary of the cost analysis is given in Table 3-15, each entry in the table is in millions of (1990) dollars. All assumptions are the same as those described in sections 3.2.3 and 3.2.3.

**Table 3-15: Cost Comparison for the Piloted Mission**

Design	1	2
Mission Profile	EOR	ELOR
Development	\$ 6890	\$ 7460
Production	1100	1090
Launch vehicle	2400	2400
Operation	800	800
Mission Cost		
Total launch	11,190	11,750
Total first year	15,030	15,690
Five Year Campaign	45,420	46,270

It was established that a EOR mode for the piloted mission would require a smaller project budget as there is a marginal difference in the developmental and production costs for this mode. The total cost over a five year campaign would have a difference of almost one billion (1990) dollars.

### **3.4.5 Expandability**

A major objective of the project is to establish a permanent lunar base at a predetermined location on the lunar surface. The overall design of each component for the project incorporates both modularity and commonality. In addition to the immediate benefits of reduced developmental costs, modularity in the design would permit both easy expandability and if necessary, modifications to existing components at various stages throughout the mission.

The designs for both ELOR and EOR mission profiles were based on the requirements of the anticipated lunar stay. The mission has been designed for a twenty eight day stay on the surface and a round-trip transit time of six days. Most of the subsystems in the spacecraft were designed for a lifetime more than the total mission duration of thirty -six days. The designs of the surface payloads were for a minimum lifetime of two years on the lunar surface. In addition, the crew capsule has been designed for reusability.

### **3.4.6 Crew Capsules Comparison**

For space applications, weight drives all aspects of design. However, for a piloted mission of Project Columbiad's magnitude, other drivers such as safety, reliability, and complexity must be taken into consideration. For this reason, the Crew Capsules project group considered many design profiles for the two considered mission modes, ELOR and EOR. These capsule designs are discussed below for each mission mode in which they apply.

#### **3.4.6.1 EOR Capsule Designs**

Capsule configurations for EOR missions function essentially the same as the old-style direct flight (DF) capsule designs. Crew Capsules considered two types of capsules for the EOR mission: a standard capsule which lands near a habitat a precursor and returns directly to Earth, and a landable bases with a smaller return vehicle and .

##### **3.4.6.1.1 EOR (Direct Flight Style) Capsule**

The EOR Capsule is the design chosen by Systems Engineering to be used by Project Columbiad. A single module design, the EOR capsule delivers a manned crew to a habitat precursor. This same capsule directly returns the crew to the Earth's surface with the propulsive aid of an Earth Return Module (ERM). To aid in this capsule's ability to safely reenter the Earth's atmosphere and land, it has a biconic lifting-body design which uses

deployable wings for dynamic stability and a parasail arrangement to slow its descent. Figure 3-15 shows the EOR capsule configuration.

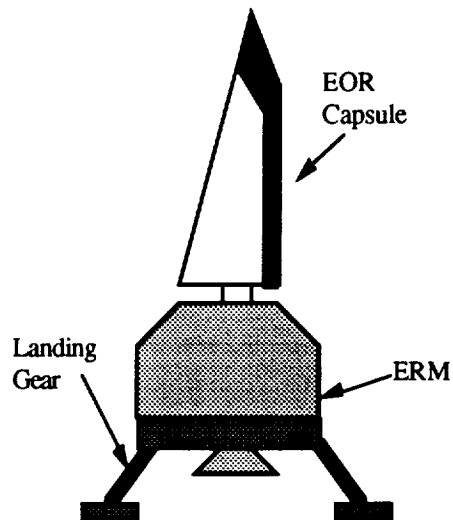


**Figure 3-15**  
**EOR Capsule Configuration**

Alone, the EOR capsule has a relatively low dryweight because it only contains one temporary habitat (with its life support, power, guidance, and communications systems) designed to support the astronauts during the journey to and from the lunar surface. However, the EOR must bring enough propellant with it to the Moon's surface in order to return it to the Earth. This amount of propellant is much larger than would be required if the ERM was left in lunar orbit. However, in light of the mission requirement for instantaneous abort, and the propellant savings is not as significant.

The EOR capsule serves as an environment for the astronauts to and from Earth, a lunar lander, a temporary lunar habitat, and a reentry vehicle capable of landing on a glide. These requirements still make the capsule very complex, requiring high development time and cost. However, some of this design complexity is alleviated because only one life supporting environment is needed, lowering the number of redundant systems associated with a separate return vehicle and excursion module.

The EOR Capsule is a very safe vehicle. It allows the astronauts to abort the mission more easily than if they were traveling with the habitat, or rendezvousing with a landing module. Also, the astronauts do not have to leave Earth until the Status group has verified that the

habitat is operational on the Moon. The major safety bonus of this design is seen in comparison to designs with separate return and landing vehicles. The EOR capsule does not require any EVAs until the capsule lands on the Moon, and the crew is ready to transfer to the main habitat. This is the primary safety feature of the EOR capsule

Although the EOR capsule is quite complex, its design offers many mission points where aborts may be made and low-weight redundant systems may be placed. Thus, the EOR can be made into a relatively reliable vehicle when the proper redundant systems and design complexities are considered.

#### 3.4.6.1.2 The Landable Base Module

The landable base module (LB) consists of a main module and a return module. The main module contains a descent stage, landing gear mechanism and a habitat capable of supporting four men for twenty-eight days. The return module contains a smaller capsule with an ascent stage and a Earth return module capable of returning the capsule to the Earth. Figure 3-16 shows the LB configuration.

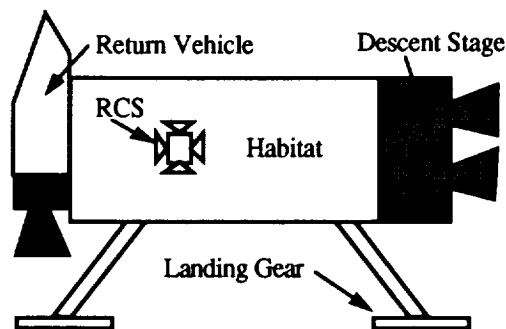


**Figure 3-16**  
**Landable Base Configuration**

The LB configuration, with its habitat and return vehicle, represents an enormous amount of payload weight which must be delivered to the lunar surface. This payload is far above the capabilities of all launch vehicles both currently produced as well as those scheduled to be constructed in the next decade. This reason alone rules out the LB option, raising the number launches required to place the astronauts and their habitat on the Moon to a minimum of two. Furthermore, the two launch profile changes the direct flight mode to an Earth-orbit rendezvous mode.

The LB design is also enormously complex. Ease of vehicle design is coupled with the required uses of the vehicle. This coupling does not produce a linear relationship when adding complexity to a design, i.e. designing a vehicle which is both a lander and a base does not have the same complexity as designing a lander and a base, but more. Landing a base safely on the Moon with astronauts inside, while carrying a return vehicle is highly complex. This complexity level increases both cost and development time as well as decreases the mission's reliability.

Highly complex missions such as the LB, have reduced reliability and mission safety. One abort option is lost by combining both the lander and base in one vehicle. If a major component of the habitat fails during landing, the astronauts must leave immediately. With a separate deployment, a second habitat could be deployed before the astronauts leave Earth. This loss of safety is somewhat alleviated by allowing the astronauts to land with their habitat. This reduces the number of habitats which must be developed and the number of dangerous EVAs the astronauts must make for habitat transfers.

The added complexity of the LB design also significantly increases the number of vehicle part which could fail during the mission. For each added part, reliability is reduced by the product of the overall project reliability and that particular part's reliability. The loss of reliability requires use of additional redundant design parameters, increasing mission weight, complexity, and cost. For the LB configuration, with its many parts and components, these increases in weight, cost, and complexity are magnified to a greater degree than it is in all other capsule designs.

#### 3.4.6.1.3 EOR Conclusions

Due to the unrealistically high mass of the LB, it cannot be considered a reasonable design choice. This leaves the EOR direct flight styled capsule as the only choice for an EOR mission. This choice is complicated, somewhat heavy, and costly, but it still is a reliable, very safe capsule design.

#### 3.4.6.2 ELOR Capsule Designs

All of the ELOR designs require a habitat precursor. Additionally, each design uses a return vehicle which houses the astronauts on their journey to and from the Moon. The return vehicle consists of two parts: a command module (CM) which contains the life-

supporting environment and serves as a reentry vehicle; and a service module (SM) which contains the propulsive section and major power systems.

This tri-modular configuration is similar to the Apollo design. The CM is a cone-shaped blunt body, similar to Apollo, but larger because of the four man crew. The SM contains more fuel so that it will be able to make a  $90^\circ$  lunar plane change. This will satisfy the overall mission requirements of landing the crew at any latitude and aborting at any time during the lunar stay. Figure 3-17 shows the CM and SM configuration.

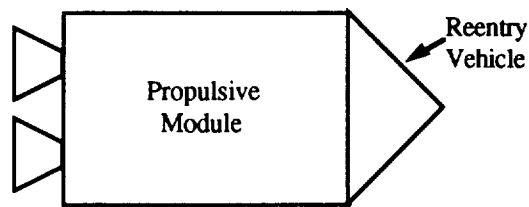


**Figure 3-17**  
**Return Vehicle and Propulsive Modules**

Below are descriptions for the landers considered for the ELOR mission.

#### 3.4.6.2.1 Closed Cockpit Lunar Lander (CCLL)

The CCLL consists of a enclosed life-supporting environment mounted upon ascent and descent stages. During initial lunar orbit, the lander docks with reentry vehicle, allowing the crew to enter via an EVA. Later, as the lander leaves the lunar surface, it leaves its landing gear and descent stage behind, docking with the reentry vehicle a second time. Figure 3-18 shows the CCLL configuration.

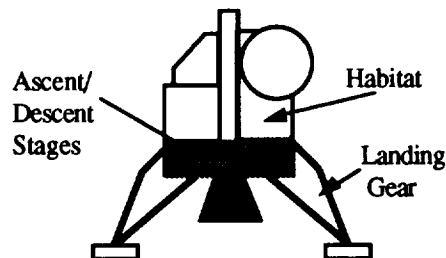


**Figure 3-18**  
**Closed Cockpit Lander Configuration**

Because the CCLL serves purely as a landing unit, it has a very low weight. The mass savings from this reduced weight becomes even greater when the required propellant mass to deliver the lander is considered. It is interesting to note that although the mass of all three modules, plus the propellant is less than the mass of the EOR capsule, plus its propellant weight, the dry weight of the ELOR system is heavier due to system redundancies.

As previously stated, overall vehicle complexity is coupled with the required uses of the vehicle. The modular CCLL arrangement greatly reduces design complexity because each component serves one basic function: reentry vehicle, propulsion stage, and lander. This modularity also reduces development time and cost. However, there is a significant increase to mission complexity due to the extra lunar orbit rendezvous. Command, control, and communications; guidance and navigation; structures; and propulsion stages groups must account for extra RCS maneuvers, complex vehicle dynamics, docking mechanisms, and EVAs in order to perform safe rendezvous.

The CCLL design suffers from a basic loss in safety because of the two extra required lunar orbit EVAs. Astronauts must first leave the reentry vehicle to enter the lander, and later, leave the lander after it has docked with the return vehicle. These extra EVAs expose the astronauts to radiation, micrometeors, and a dangerous zero-g environment in which the astronauts could "float away." Therefore, in comparison to the EOR capsule, the CCLL still offers a temporary habitat, but compromises safety with additional EVAs during rendezvous.

The CCLL unit, because of its single function, is very reliable. The additional temporary habitat also adds reliability to the mission. However, the lunar orbital rendezvous offers two mission points where failure will cause total mission failure and possible crew casualties. Overall, the CCLL increases design reliability but reduces mission reliability.

#### 3.4.6.2.2 Open Cockpit Lunar Lander (OCLL)

The OCLL consists of an "open" cage placed on top of a propulsion unit with landing gears. The cage contains the crew (wearing spacesuits), instrumentation, and emergency quantities of air, food, and water. The configuration of the OCLL is shown in Figure 3-19.



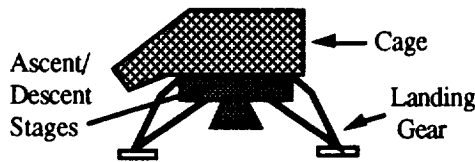


**Figure 3-19**  
**Open Cockpit Lander Configuration**

The OCLL offers the lowest weight of all of the capsule/lander options. When considering propellant weight also, the OCLL has a significantly lower total mass than any other system, even when compared to the CCLL.

Because it requires no structural mass and life support systems, the OCLL has remarkably low design complexity. Furthermore, the open cage structure of the OCLL gives excellent 360 degree visibility. This reduces the complexity of the orbital rendezvous and aids in landing the OCLL safely. The only complexities of the system derive from the dangers of the open capsule, the dependence on the space suits for life support, and the EVAs. However, these are more safety considerations than complexities, making the OCLL the least complex design.

Unfortunately, although the OCLL is the lightest and least complex system, it is also the most dangerous. The multiple EVAs, inherent in the ELOR mission mode, pose dangers similar to those of the CCLL. Additionally, the OCLL has no habitat, causing further critical dangers. The astronauts must depend upon their spacesuits for survival, limiting mobility, and fine motor control as well as exposing them to micrometeors and radiation. In the event of an emergency, the crew has a very limited surface survival time in which they can assemble a habitat or fix components. Also, if a crew member of the crew is injured, there is no location where he can remove his spacesuit and be treated. These dangers far outweigh the safety benefits of the open cage's increased visibility. According to Crew Systems, this lander is too dangerous to be considered a feasible design.

Due to the OCLL's low complexity, it is a reliable design. However this reliability is offset by the many dangers posed by mission events associated with its design. This makes the overall system unreliable in satisfying a major mission requirement: crew safety.

#### 3.4.6.2.3 ELOR Conclusions

The CCLL design offers low weight, low design complexity, safety, and good reliability. The OCLL offers extremely low weight and complexity, but offers little safety for the crew. In light of this, CCLL is the better choice for an ELOR mission. This design has a high mission complexity, but delivers a sizable payload safely to the Moon with good reliability and low design complexity.

#### 3.4.6.3 The EOR/ELOR Hybrid Capsule

In order to make a mode comparison based upon the majority of the Project Columbiad's stages, Systems Engineering developed a hybrid mode between EOR and ELOR. This mode uses a capsule very similar to the EOR capsule. However, this capsule lands on the Moon without the ERM, using a descent stage similar to that used in the ELOR mode.

Crew capsules has conducted various trade studies regarding this mission. The most significant of these studies with respect to this section of Project Columbiad's report was a study between leaving the 732 kg heat shield in orbit, with the ERM, or bringing it to the lunar surface. As discussed in the Crew capsules part of this report, the complexity of storing the heat shield, coupled with bringing it along with the ERM for a 90 degree lunar plane change, has ruled out the benefits of this option.

As discussed in the final mode selection procedures for this report. The complexity of the orbital rendezvous, the 90 degree plane change, and the redundant systems required in both the ERM and the capsule (especially the heavy RCS needed for the rendezvous) has shown that the hybrid mode is not beneficial. It contains the worst of the both modes: the heavy lunar payload and design complexity of the EOR, and the complicated rendezvous and redundant systems of the ELOR.

#### 3.4.6.4 The Final Capsule Selection

In light of all choices: EOR, EOR landable base, ELOR CCLL, ELOR OCLL, and the hybrid capsule, only one choice satisfies all of the mission requirements with the best combination of weight, safety, complexity, and reliability. That capsule is the EOR capsule. It has a reasonable mass, balanced combination of design and mission complexities, good margin of safety, and a good reliability. The specifics of this capsule are discussed in the Crew Capsules section of this report (Volume III, Chapter VI), while the mode selection process is discussed by Systems Engineering within this volume.

#### **3.4.7 Conclusions on Mode Comparison**

Based on the information ascertained in the mode comparison, the decision was made to utilize an EOR mission profile for the Piloted mission of Project Columbiad. It was determined that this mode would outperform the EOR mode in three of the four categories considered in the analysis. The most important being, the mass required at Low Earth Orbit in order to complete the mission, specified for Project Columbiad.

These designs reflect the initial stages of the design process and the preliminary designs which are presented in the report are derivatives of these designs. One of the major modifications was to incorporate the second translunar injection stage into the lunar braking module.

## **4. Precursor Mission**

The primary responsibility of the precursor mission is to deliver most of the surface payload required for a initial outpost on the lunar surface. The surface payloads consists of a pressurized lunar habitat, a power generation and storage system, a lunar surface excursion vehicle (rover) and equipment for other surface operations. Most of the support systems and consumables necessary for the piloted mission will be delivered in the precursor mission. The rest of the payload will be taken in the cargo bay of the piloted mission. In accordance to the general design philosophy of maintaining modularity and commonality in the overall design, the design of the precursor mission is conducted with the established design parameters of the piloted mission.

Maximum allowed mass of the surface payloads is 25,000 kg. Using the National Launch System (NLS), two launches will be necessary to deliver the precursor mission to the lunar surface. In the first launch, the primary Trans-lunar Injection (TLI) stage would be delivered to LEO . This would be followed by a second launch, in which the payloads, in an optimum stacking configuration, would be delivered to Low Earth Orbit (LEO). In low earth orbit, rendezvous and docking maneuvers would be performed to join the trans-lunar injection stage to the payloads in final preparation for the injection stage.

### **4.1 Lunar Landing Configuration**

The primary purpose of the lunar landing stage is to deliver the surface payloads to the lunar surface. The lunar landing and deployment of the surface payload posed a design challenge. As a result, the design of the lunar lander for the precursor mission went through an intensive iteration process based on several design parameters.

- Landing stability and control problems
- Structural requirements and complexity
- Docking requirements and complexity
- Modularity of stage with lunar landing stage of piloted mission
- Surface payload deployment and functional requirements

Throughout the design process, a total of six different designs have been considered for the configuration of the lunar lander. The following sub-sections outline brief description of each configuration and are accompanied by a schematic diagram of the design. The final design is considered as the best possible synthesis of the different special features each design offered.

In all the cases which requires docking procedures in low lunar orbit, the maneuvers are conducted after the staging of the lunar braking module at a predetermined low lunar orbit.

#### **4.2 Vertical Stack**

In this configuration , the entire payload stack and precursor lunar lander rest vertically on the lunar surface. The main problem of this configuration is the high center of gravity which results from the uneven mass distribution at the time of lunar landing. The surface payloads rests atop the almost empty propellant tanks. In addition, the mass of the surface payloads sets a requirement on the structural design of the containment used to house the propellant tanks. The overall height of the landed structure would result in a stability problem due to the difficulty of controlling the stack during landing. In addition, this would create problems in the deployment of the surface payloads unto the surface. On the positive side, the design of this configuration would not require any additional docking procedures besides that of the primary trans-lunar injection stage docking with the entire surface payload stack in low earth orbit, which is common to all cases.

The deployment of the surface payloads would require additional surface vehicles such as cranes or a lunar lander design which incorporates a lowering mechanism in its design. The design of the lunar landing stage in the stack would be identical to that of the piloted mission, in an effort to promote modularity in the overall mission design. Figure 4-1 outlines two possible layouts for this configuration.

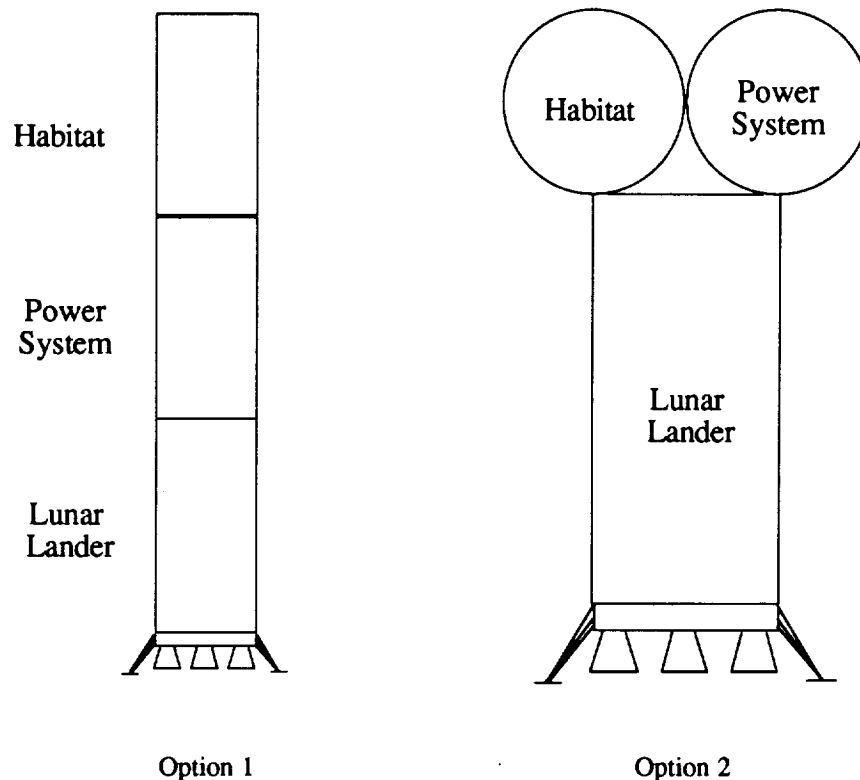


**Figure 4-1**  
**Vertical Landing Configuration**

### **4.3 Horizontal Stack**

In this configuration, the landing stability problem is resolved. However, with the given orientation of the rocket motors relative to the mid-plane of the stack, there is an added structural problem due to the excessive bending loads that the stack would experience on landing. This would necessitate additional structural components for increased structural integrity decreasing the allowed mass for the surface payloads. The design of this configuration would not require any additional docking procedures. The deployment of the payloads could be incorporated into the landing process and would not add any major complexity or difficulty to the design.

The design of the propulsion systems necessary for the landing would however require new designs, independent of the lunar lander designed for the piloted mission. In addition, it would require more engines, once again resulting in reduced payload capacity and a lower reliability. One added complexity resulting from this design was the effects of the overall configuration on the functional requirements of the surface payloads. For example, the ability to access the

airlocks of the lunar habitat after the deployment creates a problem, since the airlocks are blocked by the propulsive units. Figure 4-2 outlines this configuration.

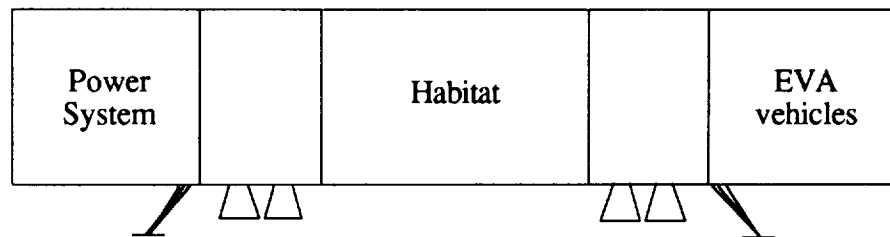


**Figure 4-2**  
**Horizontal Landing Configuration**

#### **4.4 Folded Horizontal Configuration**

This configuration is similar in design to the horizontal stack, however with added complexity because of the complex mass distribution requirement for control. In addition, it would require additional structural components for the folding and docking procedures. This configuration would require one additional docking procedure in low lunar orbit (LLO), in addition the docking procedures in low earth orbit. All maneuvers would necessitate additional reaction control systems (RCS) rocket motors at numerous locations of the containers housing the surface payloads.

The propulsion systems required for the design would be similar to the design for a horizontal stack, with some added complexity resulting from the mass distribution of the payloads. As a result, there would have been no modularity between the design and that of the lunar lander of the piloted mission. As in the horizontal case, the deployment of the payloads would have been incorporated into the landing process. In this configuration, at least one airlock in the habitat would be accessible. Figure 4-3 outlines this configuration.

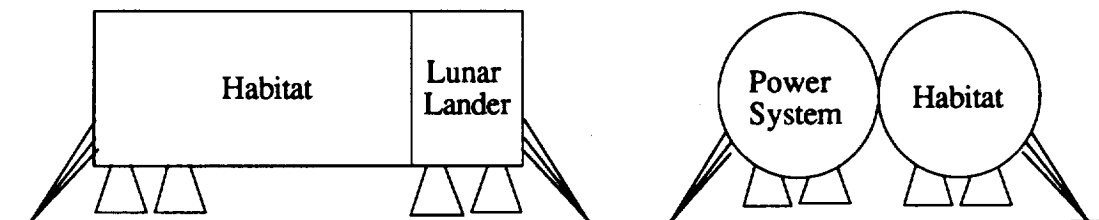


**Figure 4-3**  
**Folded Horizontal Landing Configuration**

#### **4.5 Hybrid Configuration**

In this configuration, the landing stability problem is resolved. The design incorporates the benefits of both the vertical and horizontal landing configurations. The relocation of the surface payloads lowers the center of gravity relative to the base of the lander. However, the complexity of the design has a significant impact on the structural mass of the lander as well as the need to design numerous mechanisms to assist in the attachment of the payloads to the lunar lander. The area between the power system and the habitat needs considerable structural reinforcement to handle the loading environment increasing the mass budget.

The design of this configuration would require additional docking procedures in low lunar orbit. All maneuvers and docking procedures would necessitate reaction control systems (RCS) rocket motors at numerous locations of the containers housing the surface payloads. In this particular case, the docking procedures would require extremely accurate guidance systems as well as many other complex support systems which would add to the overall complexity of the design.

The deployment of the surface payloads requires additional control systems, as well as additional structural components to assist in the deployment. The actual deployment process would utilize numerous mechanisms such as oxygen inflated balloons and winches to regulate the rate of deployment. The structural design of the propulsion stages necessary for the landing would require new designs, independent of the lunar lander designed for the piloted mission. Figure 4-4 outlines this configuration.

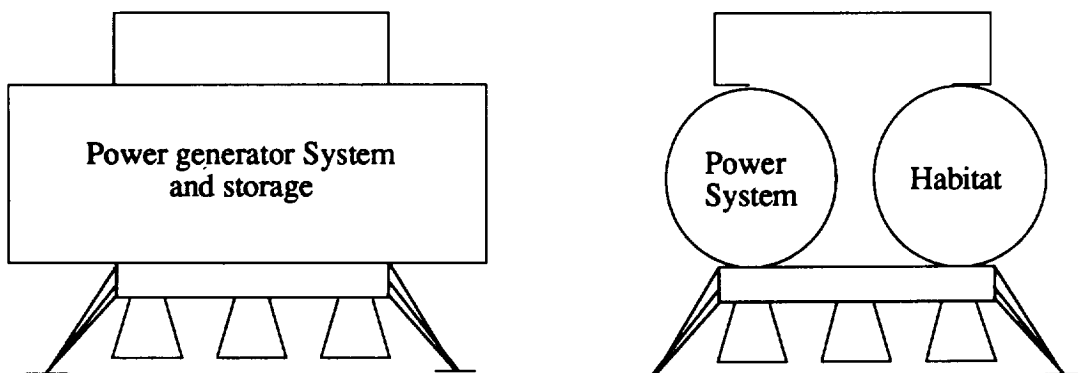


**Figure 4-4**  
**Hybrid Landing Configuration**



## **4.6 Side-Saddled Configuration**

### **4.6.1 Vertical**

This configuration is similar in design to the vertical stack, however the main problem of stability resulting from the high center of gravity is eliminated by the redistribution of the mass of the surface payloads on the lunar lander. The design of this configuration would require additional structural elements for the additional loads which would result from the payloads in this given case, attachments for the payloads, and mechanisms to assist in the deployment of the surface payloads. These components would add to the complexity of the design. Furthermore, this configuration would require additional docking procedures in low lunar orbit to configure the stack for landing. The complexity of the docking procedure would be greatly influenced by the external shape of the lunar habitat and containers used to store the other surface payloads throughout the mission.

The deployment of the surface payloads would require a lunar lander design which incorporates a lowering mechanism in its design. The design of the propulsion systems in the lunar landing stage of the stack would be identical to that of the piloted mission, thus maintaining modularity in the overall mission design. After the deployment of the surface payloads, there would be adequate accessibility to the lunar habitat and the surface payloads would be able to meet all their functional requirements. Figure 4-5 outlines this configuration.

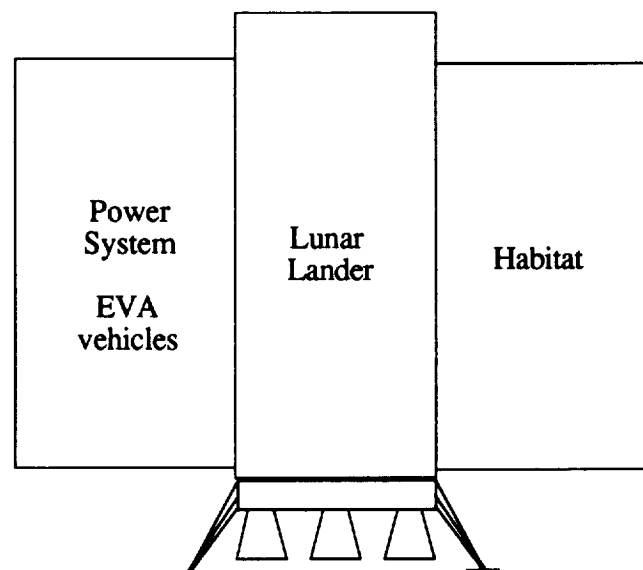


**Figure 4-5**

### **Side-Saddled Landing Configuration (vertical)**

#### 4.6.2 Horizontal

This configuration is similar in design to the horizontal landing stack, with the added complexity and structural problems resulting from the distribution of the surface payloads on the lander. As in the case of the vertical side-saddled configuration, the design would have to incorporate additional structure for the mechanical attachments for the payloads, mechanisms to assist in the deployment of the surface payloads, and to provide adequate structural integrity to meet all anticipated loadings. This configuration would require additional docking procedures in low lunar orbit to configure the stack for landing. These factors would add to the overall complexity of the design.

The deployment of the payloads could be incorporated into the landing process and would not add any major complexity or difficulty to the design. The surface payloads would be able to meet their functional requirements soon after deployment. The design of the propulsion systems necessary for the landing would require new designs, independent of the lunar lander designed for the piloted mission. In addition, it would require more engines, resulting in reduced payload capacity and a lower reliability.

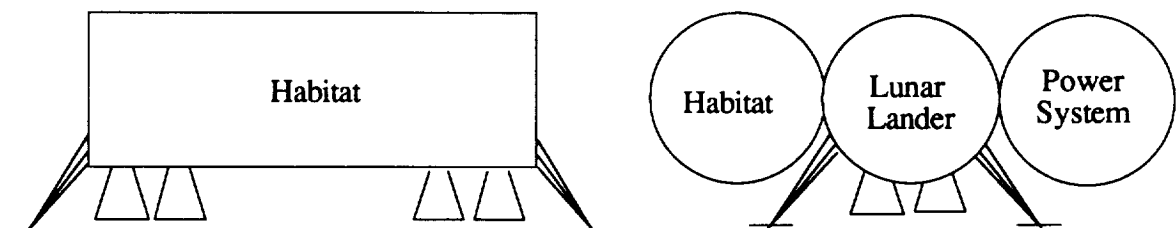


**Figure 4-6**  
**Side-Saddled Landing Configuration (Horizontal)**

#### 4.7 Candidate Landing Configuration

Based on numerous trade studies, we established a design for the lunar lander based on the proven vertical landing configuration. Table 4-1 summarizes all the deciding factors in the configuration choice. However, due to the complexity of the payload deployment associated with this configuration, the design incorporates additional mechanisms into the lander to facilitate the surface payloads deployment.

**Table 4-1: Summary of Landing Configuration**

Issues	Docking	Landing		Payload Deployment	Piloted mission
Candidate	<i>Complexity</i>	<i>Structural</i>	<i>Complexity</i>	<i>Complexity</i>	<i>Commonality</i>
Vertical	None	None	**	***	***
Horizontal	None	**	None	None	None
Folded Hori.	*	**	*	None	None
Hybrid	***	***	*	**	*
Side-saddled (vertical)	*	*	*	None	**
Side-saddled (horizontal)	**	***	None	**	None

- \* - increases mass/complexity/commonality
- \*\* - between the lower and upper increase
- \*\*\* - increases mass /complexity significantly

The deployment phase of the lunar landing is considered the main driving factor in the design of the lunar lander. The design of the lunar lander incorporates a set of retractable landing gear and a cluster of thrusters at the top of the payload stack to aid in the lowering of the payload. The engines would be used to provide any necessary force required to tip the stack, as well as to regulate the rate of fall of the payload stack as it lands horizontally on the lunar surface. A more detailed description of the surface payload deployment will be given volume II of the report. Figure 4-7 outlines the deployment phase of the lunar landing of the surface payloads.

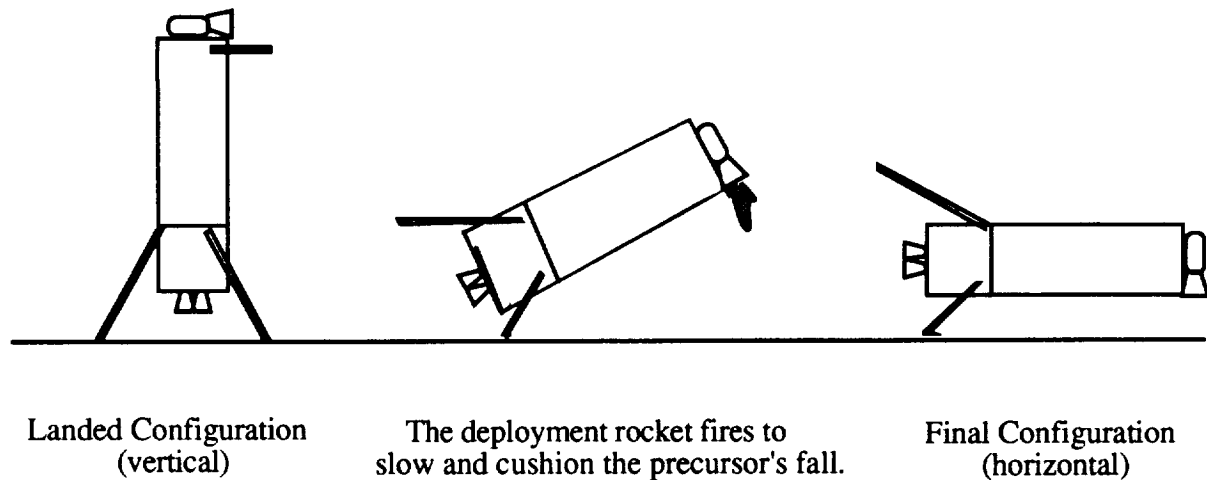


**Figure 4-7**  
**Deployment of Surface Payloads**

#### **4.8 Conclusion**

In summary, the primary objectives and requirements of the Project Columbiad dictated the need for a precursor mission to enable mission success. One of the deciding factors in the design process was the capability of existing launch vehicles. In order to deliver the required mass to the lunar surface, it was determined that the minimum mass in low earth orbit surpassed the capacity of any existing launch vehicle. As a result, the project had to be broken down into two mission: the precursor and the piloted missions. Further each mission had to be broken down to two launches.

In an effort to promote modularity and commonality in the overall design, the design of the precursor mission incorporated as much technology and developmental concepts as possible from that of the piloted mission. This was done in an effort to reduce developmental and manufacturing costs which would incur during the execution of Project Columbiad. The precursor mission has a similar staging profile as in the piloted mission and utilizes the same primary trans-lunar injection (PTLI) stage and lunar braking module (LBM) as that mission.

The precursor mission has a vertical landing configuration which incorporates various mechanical systems to facilitate the deployment of the surface payloads after landing. The design of the lunar landing stage will be similar, but not identical, in design to that of the piloted mission. The functional requirements of the lander in the precursor mission is less

than that of the piloted mission. It is not required to return the payload to the Earth. As a result, the required capability is reflected in its design. In addition, the design of the lunar lander incorporates reusability considerations of various subsystems within the lander. Such as reusing the propellant tanks for the power supply.

One of the major considerations in the design of the surface payloads was the anticipated length of stay on the lunar surface. The issue of primary concern was that of solar radiation, as crew safety is the top priority for the project. The safety requirement drove the design of the lunar habitat, and the survivability requirement, the designs of the various surface payloads. The final designs of the surface hardware and the lunar lander will be fully described in volume III of the report.

## **5. Columbiad Mission**

This chapter is a description of the Earth Orbit Rendezvous mission that was used in both the piloted and the precursor mission modes for Project Columbiad.

The NLS with 4 strap on solid rocket boosters was chosen as Columbiad's launch vehicle. This NLS configuration allows a pre-LEO circularization burn payload of 100,000 kg which includes a 10% margin. Both the precursor and the piloted mission require two launches each with launch payload masses of ~ 95,600 kg. Therefore, for a complete Columbiad mission, a total of four launches will be required. The first two launches in quick succession will be for the precursor while the third and fourth launches for the piloted mission will be launched approximately one month later. All launches will be from Kennedy Space Center and will rendezvous at a low Earth altitude of 275 km. Both missions are designed to be able to land at any latitude on the lunar surface. After the scheduled 28 day lunar stay, the Crew Module is scheduled to land at Edwards Air Force Base.

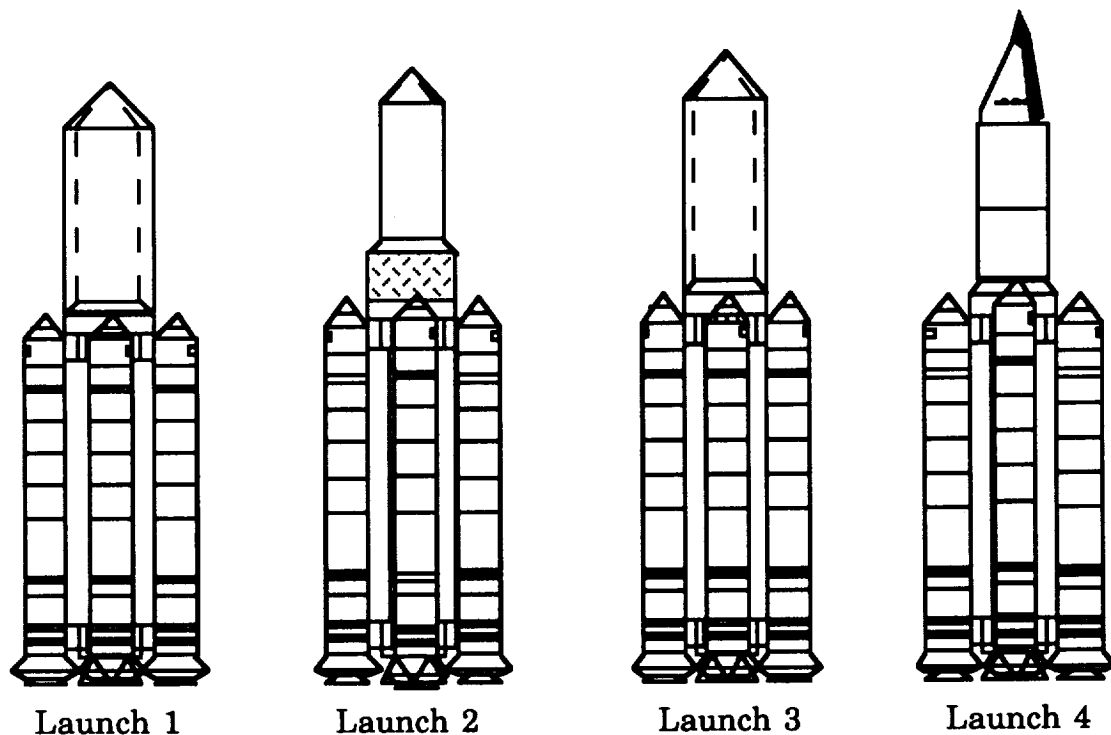


**Figure 5-1**  
**NLS Launches for Columbiad**

## **5.1 Piloted Mission Design**

### **5.1.1 Piloted Mission Profile Overview**

The EOR configuration for the piloted mission is composed of three propulsive elements in addition to the Crew Module: Primary Trans-Lunar Injection (PTLI), Lunar Braking Module (LBM), and Earth Return Module. The PTLI is by itself on the first launch for the piloted mission (Launch 3) while the LBM, ERM, and CM are on the second launch for the piloted mission (Launch 4).

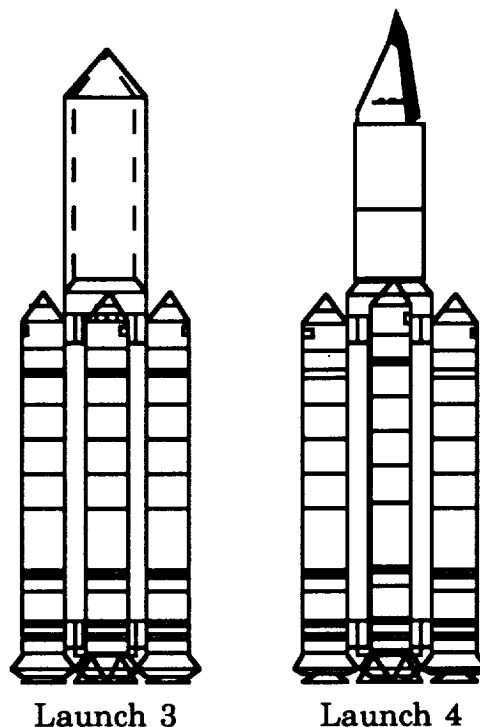


**Figure 5-2**  
**NLS Launches for Piloted Mission**

The NLS vehicle does not perform the circularization burn into a 200 km altitude for either launch. The PTLI performs the circularization burn and, then, raises its altitude to 275 km at the desired trajectory window where it will await rendezvous with the piloted launch. For the piloted launch, it is the LBM that performs both the circularization burn and the burn to higher orbit. Once the vehicles have completed rendezvous, the Trans-Lunar Injection is performed by two stages: the PTLI and the LBM. The PTLI separates from the stack upon the completion of its burn. The LBM completes the burn and then performs any

midcourse corrections that are required during the 3 day transit. At which point the LBM inserts the vehicle into LLO, and then performs the major descent burn before it is staged. The ERM performs the final descent and hover burn before landing. After the 28 day lunar stay the ERM launches the CM into LLO and then into the Earth transfer orbit. The ERM also performs any midcourse corrections. The ERM separates from the Crew Module (CM) just before reentry into the Earth's atmosphere and then the CM proceeds to reenter the atmosphere safely. The piloted mission is completed when the CM lands at Edwards Air Force Base. A brief mission profile along with propulsive requirements for each stage is featured in Table 5-1.

**Table 5-1: Mission Profile**

<u>Event</u>	<u>Location</u>	<u>Propulsive Stage(s)</u>	<u><math>\Delta V</math> (m/s)</u>
Circularization of Launch 3	200 km LEO	PTLI	177
Launch 3 burn to higher LEO	200-275 km LEO	PTLI	43
Circularization of Launch 4	200 km LEO	LBM	177
Launch 4 burn to higher LEO	200-275 km LEO	LBM	43
Earth Orbit Rendezvous	275 km LEO	LBM & PTLI	60
Trans-Lunar Injection	LEO	PTLI	2460
Trans-Lunar Injection	LEO	LBM	680
Midcourse Corrections	Midcourse	LBM	120
Lunar Braking into LLO	Prior to LLO	LBM	1060
Lunar Braking to Moon	LLO to Moon	LBM	1700
Hover	Moon	ERM	500
Lunar Launch	Moon to LLO	ERM	2200
Earth Return Injection	LLO	ERM	1060
Midcourse Corrections	Midcourse	ERM	120
Reentry	Earth's Atmosphere	CM	100

### ***5.1.2 Design Choices***

When the trade study was done to determine whether or not to have a kick motor on the NLS perform the circularization burn into a Low Earth Orbit at 200 km, it was found that having the PTLI in Launches 1 and 3 and the LBM in Launches 2 and 4 perform the circularization burn was more efficient weightwise. Just after these circularization burns,



the PTLI and the LBM stages perform burns to raise the LEO altitude from 200 km to 275 km. This choice was made after an analysis was done on the orbit decay rate and the RCS system necessary to keep the PTLI up in orbit for any reasonable length of time in the case of launch schedule slippage for Launches 2 and 4.

For the reasons mentioned in 3.2.1, the TLI burn is split between two stages. With the non propellant to propellant mass fraction equal to 14.8%, the four launch weights were roughly equalized when the Primary TLI stage (PTLI) was allocated a  $\Delta V = 2460$  m/s propulsive maneuver. This left a  $\Delta V = 680$  m/s to be included in the next stage. A separate stage was not designed for this small  $\Delta V$ . Instead, the propellant was included in the following stage, the LBM.

In order to even out the thermal stresses that the vehicle structures encounter during the mission, a decision to spin the transit vehicle at a rate of approximately once per hour was made. If a launch slippage occurs for either Launches 2 or 4, then the PTLI may initiate a spin while it waits in LEO. The PTLI would despin shortly before docking was to occur with Launch 2 or Launch 4.

Due to the landing height problem mentioned in section 3.2.2 (landing on the lunar surface presents a problem because the vehicle height is so tall), a decision was made to stage the LBM with just enough time to hover and land safely. This is a major improvement in the landing problem as it reduces the height of the landing vehicle by 12-13 m. Therefore the ERM has the vehicle's landing legs and performs the hover burn.

### **5.1.3 Primary Trans-Lunar Injection Stage**

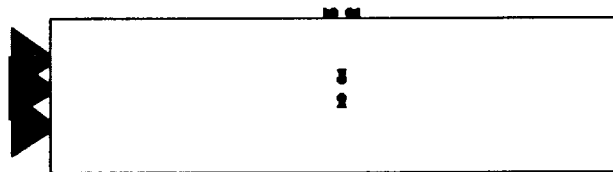


**Figure 5-3**  
**Primary Trans-Lunar Injection**

The PTLI has five RL10 engines and performs four burns. The first PTLI burn circularizes the PTLI's Low Earth Orbit at 200 km. The second burn is the initial burn to transfer to a higher orbit and the third burn completes the higher orbit transfer at 275 km.

The fourth burn is the only one with the other stages attached in front; it is the Primary Trans-Lunar Injection burn. When this burn is complete the PTLI has expended its usefulness and is staged off.

The dry mass budget for this stage is 11,587 kg. The wet mass budget is 94,825 kg. The propellant weight allows for a 1.5% extra propellant for each burn plus an additional 0.2% that is budgeted for propellant boil-off. Therefore 1415 kg of the 83,237 kg of propellant is extra. The expected length of the PTLI is 16 m. Therefore the Launch 1 and 3 heights are well below the 35 m height restriction even when a 5 m tall nose cone is added.

#### **5.1.4 Lunar Braking Module**

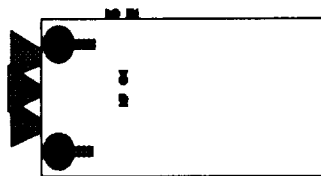


**Figure 5-4**  
**Lunar Braking Module**

The LBM has three RL10 engines and performs six burns plus midcourse corrections. The first LBM burn circularizes the LBM's Low Earth Orbit at 200 km. The second burn is the initial burn to transfer to a higher orbit and the third burn completes the higher orbit transfer at 275 km. The fourth burn is the Secondary Trans-Lunar Injection burn that occurs just after the PTLI stage is staged off. The fifth burn brakes the module into LLO and the sixth and final burn completes most of the lunar descent burn before it is staged off.

The dry mass budget for this stage is 6,731 kg. The wet mass budget is 62,285 kg. The propellant weight allows for a 1.5% extra propellant for each burn plus an additional 0.2% that is budgeted for propellant boil-off. Therefore 944 kg of the 55,554 kg of propellant is extra. The expected length of the LBM is 12.7 m.

### **5.1.5 Earth Return Module**

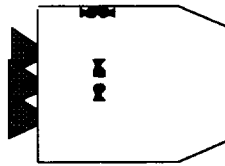


**Figure 5-5**  
**Earth Return Module**

The ERM has three RL10 engines and performs three burns plus midcourse corrections. The first ERM burn is extremely critical in that it prevents the CM from crashing into the lunar surface after the LBM has initiated the descent to the lunar surface. The second burn is the launch from the lunar surface into LLO and the third burn injects the vehicle onto an Earth return trajectory.

The dry mass budget for this stage is 5,053 kg. This dry mass budget, though, does not include the weight of the payload to the lunar surface even though this payload weight is contained in this stage. Neither are the landing legs which are budgeted 500 kg. The landing legs are exploded off the ERM at the time of lunar launch. Therefore the landing legs can be considered as lunar payload weight. The total budget for the lunar payload is 3500 kg which leaves 3000 kg for the payload -- twice the minimum resupply weight for a later 28 day stay. The propellant mass is 17,657 kg. Therefore the total wet weight budget is 26,210 kg. The propellant weight allows for a 1.5% extra propellant for all three burns plus an additional 0.2% that is budgeted for propellant boil-off for the first burn and 0.5% extra that is budgeted for propellant boil-off for burns after the lunar stay.

### **5.1.6 Crew Module**



**Figure 5-6**  
**Crew Module**

The crew module is designed as a biconic reentry vehicle with a maximum lift to drag ratio of 1.1. The lift to drag ratio allows for reentry maneuvering and extends the downrange and cross range of the vehicle (the landing footprint). The vehicle safely houses the

astronauts for the transit time to the Moon and back to Earth, including the reentry phase. The budgeted mass of the CM is 6330 kg which includes the 730 kg heat shield.

### **5.1.7 Piloted Mission Mass Summary**

A summary of the masses and the predicted lengths for each stage is shown in Table 3-2.

**Table 5-2: Mass Summary**

<u>Stage</u>	<u><math>\Delta V_{total}</math></u> (m/s)	<u>Dry Mass</u> (kg)	<u>Propellant</u> Mass (kg)	<u>Wet Mass</u> (kg)	<u>Length</u> (m)
PTLI	2680	11,587	83,237	94,825	15.96
LBM	3780	6731	55,554	62,285	12.7
ERM	3880	5053	17,657	22,710	9.97
Piloted Payload to Moon		3500		3500	(in ERM)
Crew Module		6330		6330	7.69
Nose Cone (Launches 1-3)		820		820	5
Total Mass				190,470	

		Total length
Total Mass for Launch 3 (PTLI stage) -	94,825 kg	20.96 m
Total Mass for Launch 4 (Piloted launch)-	95,645 kg	27.66 m (plus 2.7 m)

The total height allowance for an NLS payload is 35 m including a nose cone. The height of Launch 4 is less than the total height of the LBM, ERM, and CM because the LBM stage is recessed into the launch vehicle by 2.7 m. This height adjustment is not needed for Launch 4, but it is needed for Launch 2 and in the interests of modularity, the height adjustment will occur on both Launch 2 and 4. There is no need to make the PTLI stage recessed.

## **5.2 Precursor Mission Design**

### **5.2.1 Precursor Mission Profile Overview**

The EOR configuration for the precursor mission is composed of three propulsive elements in addition to the surface payloads: Primary Trans-Lunar Injection (PTLI), Lunar Braking Module (LBM), and Payload Landing Module. The PTLI is by itself on the first launch for

the precursor mission (Launch 1) while the LBM, PLM, and surface payloads are on the second launch for the precursor mission (Launch 2).

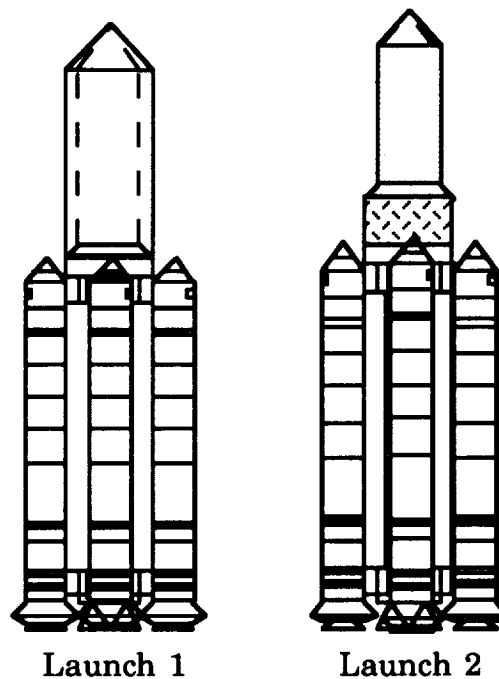


**Figure 5-7**  
**NLS Launches for Precursor Mission**

The NLS vehicle once again does not perform the circularization burn into a 200 km altitude for either precursor launch. The PTLI performs the circularization burn and, then, raises its altitude to 275 km at the desired trajectory window where it will await rendezvous with the surface payloads launch. For the surface payloads launch, it is the LBM that performs both the circularization burn and the burn to higher orbit. Once the vehicles have completed rendezvous, the Trans-Lunar Injection is performed by two stages: the PTLI and the LBM. The PTLI separates from the stack upon the completion of its burn. The LBM completes the burn and then performs any midcourse corrections that are required during the 3 day transit. At which point the LBM inserts the vehicle into LLO, and then performs the major descent burn before it is staged. The PLM performs the final descent and hover burn before landing and deploying the habitat. A brief mission profile along with propulsive requirements for each stage is featured in Table 5-3.

**Table 5-3: Mission Profile**

<u>Event</u>	<u>Location</u>	<u>Propulsive Stage(s)</u>	<u><math>\Delta V</math> (m/s)</u>
Circularization of Launch 1	200 km LEO	PTLI	177
Launch 1 burn to higher LEO	200-275 km LEO	PTLI	43
Circularization of Launch 2	200 km LEO	LBM	177
Launch 2 burn to higher LEO	200-275 km LEO	LBM	43
Earth Orbit Rendezvous	275 km LEO	LBM & PTLI	60
Trans-Lunar Injection	LEO	PTLI	2460
Trans-Lunar Injection	LEO	LBM	680
Midcourse Corrections	Midcourse	LBM	120
Lunar Braking into LLO	Prior to LLO	LBM	1060
Lunar Braking to Moon	LLO to Moon	LBM	1700
Hover and Land	Moon	PLM	500

### **5.2.2 Commonality with Piloted Vehicle Stages**

The precursor mission was designed to be as modular as possible with the piloted mission. For the Columbiad design, the two initial stages are exactly the same on both the precursor and piloted mission. As shown in Table 5-4, the velocity and masses are identical for each stage. See sections 5.1.3 and 5.1.4 for details on PTLI and LBM budgets. The choice to drive the precursor in this manner was made for developmental cost considerations.

**Table 5-4: Commonality Comparison between Precursor and EOR**

<u>Propulsion Stage</u>	<u>Precursor</u>		<u>Piloted</u>	
	<u><math>\Delta V</math> (m/s)</u>	<u>Mass (kg)</u>	<u><math>\Delta V</math> (m/s)</u>	<u>Mass (kg)</u>
PTLI	2680	94,825	2680	94,825
LBM	3780	62,285	3780	62,285

### **5.2.3 Payload Landing Module**

#### **5.2.3.1 Propulsion Stage**

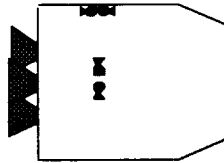


**Figure 5-8**  
**Payload Landing Module**

The PLM has three RL10 engines and only performs three one burn. The PLM burn is extremely critical in that it prevents the surface payloads from crashing into the lunar surface after the LBM has initiated the descent to the lunar surface. The PLM is also involved with the deployment of the surface payloads.

The dry mass budget for this stage is 2,743 kg. This dry mass budget does not include the weight of the landing legs. The landing legs are part of the surface payloads budget of 26,500 kg. The propellant mass is 3,582 kg although a greater amount of LOX and LH2 are stored in the propellant tanks because the tanks share the space with the lunar base fuel cell system. The propellant weight allows for a 1.5% extra propellant for the hover burn plus an additional 0.2% that is budgeted for propellant boil-off. The total wet weight budget of the PLM is 6,325 kg. With the fixed propellant mass, the total wet weight budget of the combined PLM and surface payloads is 32,825 kg.

#### **5.2.3.2 Landing and Deployment**

After staging from the LBM, the PLM slowly progresses towards the Lunar surface. Once close to the surface, the PLM provides enough thrust for hover during the final maneuver for landing. The landing legs are extended and the PLM finally touches down gently, in a vertical configuration. After touch down, the PLM is responsible for tipping itself into a horizontal configuration. This aspect of the mission is performed in two stages : 1) an impulse from solid impulse rockets (Star 48/TE-M 236) to tip the lander to an unstable position, and 2) a controlled angular reorientation to horizontal position by liquid rocket thrusters (XLR-132).

#### **5.2.4 Payloads Description**

The payloads sent in the precursor mission is stowed in a well-integrated manner with the PLM. The major payload systems are the habitat, a rover, a regolith collector, a lunar conveyer, and a solar lunar power plant (SLurPP). The SLurPP hardware is primarily located in the PLM propulsion stage. The rover, in stowed configuration, and the unassembled parts of the conveyer and the bagger are packed in the Cargo Bay between the habitat and the propulsion stage.

##### **5.2.4.1 Habitat**

The habitat, also known as the BioCan, is the lunar home for 4 astronauts. It is a 10 m long and 6 m in radius double-walled cylinder. The external skin is integrated with the external structure of the PLM. The internal cylinder, made of composite material, is separated by a thin layer of sealed vacuum from the external cylinder and is pressurized with 5 psi of breathable atmosphere. The internal space is arranged to optimize the layout of all subsystems based on their predicted need and frequency of use. A 2 m by 1 m airlock door on one end of the habitat, provides the primary access to the habitat. In case of an emergency, a secondary airlock that opens into the cargo bay from the crew quarters can be used. The total estimated mass of the habitat is less than 10,000 kg.

##### **5.2.4.2 Power Supply**

A solar power plant is designed to meet the power requirements of running all the base operations. A 250 m<sup>2</sup> photovoltaic array (GaAsSb cells) provides 35 kW of continuous daytime usable power during the lunar day. Rest of the power goes into charging up alkaline fuel cells system for 35 kW of night power. The fuel for the fuel cells are stored along with the propellant for the PLM. The total mass of the power system hardware is about 1000 kg. All fuel cells and other power conditioning hardware are integrated inside PLM and the cargo bay.

A smaller, self deploying system is also designed for the power requirements of the habitat during the "hibernation state" (the period between the PLM touchdown and arrival of the crew). A 2.5 kW continuous usable power is supplied by two 10 m<sup>2</sup> array, deployed from the external surface of the PLM.



#### 5.2.4.3 Rover

The Rover is the surface transportation vehicle, capable of delivering 1500 kg of payload. It is a six-wheel drive, four-wheel steered vehicle. The fully deployed rover is 5 m long and 2.5 m wide. The height of the vehicle is 2.5 m, including its antenna deployed. The vehicle is powered for a 120 km nominal mission range at an maximum velocity of 20 km/hour. To ensure the walk-back capability of the astronauts, all missions are limited within a 50 km radius of the habitat. The maximum mission duration is 8 hours. The vehicle is unpressurized, but the astronauts can hook up their EVA suits to the PLSS packs on-board the rover. The astronauts' PLSS backpacks are held in reserve for off-the-vehicle activities and for emergency procedures.

The rover is the workhorse for all surface operations. The Regolith Collector and the conveyer requires the rover for their operation.

#### 5.2.4.4 Regolith Collector

The regolith collector is quite similar in operation to a street-sweeper. Loose lunar soil is swept up by a brush at a nominal rate of  $0.05 \text{ m}^3$  per minute. The regolith particles slide up a Teflon coated shroud and collects in a  $1 \text{ m}^3$  hopper. After every twenty minutes of soil collecting, hopper dumps collected regolith into a dump-bucket, attached to the rover. The armature arm can be raised to lift the brush above 50 cm obstacles on the collector's way. The drive mechanism of the wheels can be preprogrammed and/or operated remotely within line of sight.

The regolith collector runs on 7.5 kW of power, stored on-board in Sodium-Sulfide cells. Maximum operating time of the machine, limited by total stored power, is 8 hours. The cells take about 12 hours to charge up at the same power levels.

#### 5.2.4.5 Lunar Conveyer

The Lunar conveyer is a multipurpose conveyer system. The main use of the conveyer is to transport loose regolith to any height on the regolith support structure. The expandable design consists four segments, each 4 m long to give a total length of 16 m. The belt width is 1 m. The entire system is sitting on 16 wire-mesh wheels and can be driven around a articulated, 4-wheel-drive vehicle. See Figure 5-10.

The power required to run the conveyer is 5 kW. That determines a maximum feed rate of  $0.28\text{m}^3$  of regolith over a 16.00 m distance in one minute. Each connection point is a pin which gives the conveyer the flexibility to deliver its payload up inclines and over obstacles. With torsional clamps, the joints can be made rigid to allow for transport over trenches.

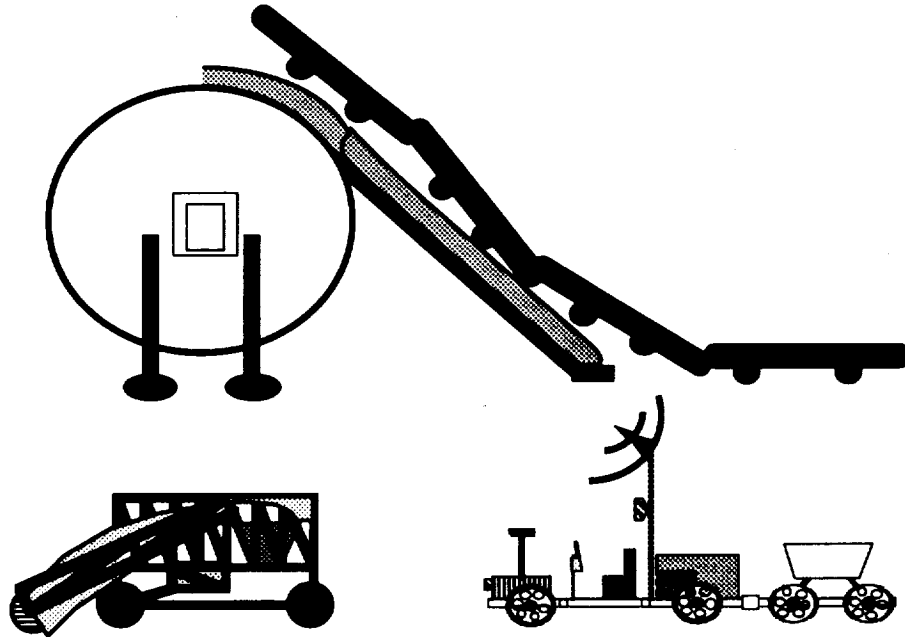


**Figure 5-10: Surface Payloads :  
Habitat with radiation protection, Lunar Conveyer, Rover,  
and Regolith Collector.**

### **5.2.5 Precursor Mission Mass Summary**

A summary of the masses and the predicted lengths for each stage is shown in Table 5-5.

**Table 5-5: Mass Summary**

Stage	DV <sub>total</sub> (m/s)	Dry Mass (kg)	Propellant Mass (kg)	Wet Mass (kg)	Length (m)
PTLI	2680	11,587	83,237	94,825	15.96
LBM	3780	6731	55,554	62,285	12.7
PLM	500	2743	3582	6325	6.77
Surface Payloads		26500		26500	12.5
Nose Cone (Launches 1-5)		820		820	5
Total Mass				190,755	

		Total Length
Total Mass for Launch 1 (PTLI stage)	94,825 kg	20.96 m
Total Mass for Launch 2 (Piloted launch)	95,930 kg	34.27 m (plus 2.7 m)

The total height allowance for an NLS payload is 35 m including a nose cone. The height of Launch 2 is less than the total height of the LBM, PLM, and the surface payloads because the LBM stage is recessed into the launch vehicle by 2.7 m. This height adjustment brings the total height of the launch within the 35 m limit.

### **5.2.6. Solar Protection**

One of the primary requirements for the lunar habitat is to provide protection against solar flares. The chances of encountering a solar flare during Apollo missions was small and no unexpected major event was encountered. However, for extended operations on the lunar surface, additional precaution is mandatory. In particular, Project Columbiad's 5-year campaign plan overlaps with the period 1999 to 2004 which is predicted to be a peak period in solar flare cycle. Thus solar flare protection of the habitat is given a high priority in the surface operations of the piloted mission.

#### **5.2.6.1 Radiation Exposure Limit**

The allowed doses of radiation under current NASA flight rules are shown in Table 5-6. These rules are designed to minimize carcinogenic effects later in the life. During Apollo or Space Lab missions same rules were applied, but during those missions no major flare event was expected or experienced and consequently the doses received were minimal.

Both the 30-day and 1-year allowed levels under current flight rules appear too high for long-time exposure in a lunar surface application. Thus it is likely that in the future a more stringent set of dose limits will be set for lunar base missions. However for Project Columbiad applications, we followed the current rules and set 25 REM limit for the entire mission duration (36 earth-days). A 25 REM/36 day (20 day in sun) exposure limit corresponds to a 0.625 REM for every 12 hours.

**Table 5-6 : NASA Flight Rules for Crew Radiation Exposure Limits**

Constraint	REM
30 days	25
Annual	50
Career	100-400*

\* Dose =  $200 + 7.5 \times (\text{Age}-38)$  for females  
=  $200 + 7.5 \times (\text{Age} -30)$  for males, both up to a maximum of 400

#### 5.2.6.2. Determination of protection level

The following table (Table 5-7) shows amount of protective layer required for different levels of solar flare along with the risk associated with not protecting for stronger flares beyond a certain level. The table was compiled from the data presented in the Project Artemis Final Report, MIT Space System Engineering, 1990.

**Table 5-7: Required Protection for Different Levels of Solar Flare**

Level of Solar Flare (protons/cm <sup>2</sup> )	Required Thickness for .1 REM/12 hr. of max. allowable dosage	Maximum Probability of occurrence of a higher level solar flare during the mission time
D (5.0 x 10 <sup>8</sup> )	1.1 g/cm <sup>2</sup>	3.4 %
E (2.0 x 10 <sup>9</sup> )	5.6 g/cm <sup>2</sup>	0.6 %
F (2.0 x 10 <sup>10</sup> )	56 g/cm <sup>2</sup>	0.2 %
G (2.0 x 10 <sup>11</sup> )	560 g/cm <sup>2</sup>	< 0.02 %

From the above data, we concluded a level F solar flare protection is optimum for the Project Columbiad missions.

#### **5.2.6.3 Protection Strategy**

Two basic strategy has been considered for flare protection. One is to carry a in-built solar storm shelter inside the habitat. The other is to cover the habitat with regolith. The estimates of additional mass required for a in-built safe haven shows that it is not a very economical option - a 3-day shelter for four persons could add 6-7 tons to the mass of the habitat. On the other hand providing the required 50 cm regolith (average density 1.2 g/cm<sup>2</sup>) cover would require bringing additional equipment to move regolith. Few different options of handling the regolith has been considered. Trenching and burying the habitat was ruled out because those operations ask for heavy-duty construction utility vehicles. Under the current design the job is performed by a regolith collecting machine, that brushes off dirt from the lunar surface and dumps it into a dump-bucket attachment on the rover. The rover, in turn, pour the regolith onto a drivable conveyer, which dumps it to different heights on the side and top of the habitat. A regolith support structure is also designed, to hold the regolith on a 45 ° incline along the sides of the habitat. See Figure 5-10.

### **5.3 Mission Trajectory Analysis**

Trajectory calculations for all phases of project Columbiad are presented in this chapter. The goal of these trajectories is to describe, in as great as detail as possible, the path that the spacecraft will follow from Earth launch until Earth touchdown. Over its course, the spacecraft must touchdown on the lunar surface at the designated point. The trajectory descriptions include characteristic velocity ( $\Delta V$ ) requirements, ideal thrusting directions, and a description of event times in as great detail as possible. A brief description of the paraglide Earth landing is also included. Though this presentation describes the trajectories in the context of the manned flight, the precursor mission follows identical phases with the exception that its flight program terminates at lunar touchdown. Possibilities for abort trajectories are also described.

#### **5.3.1 Earth Launch**

##### **5.3.1.1 Launch Windows**

The launch windows are the times allowable for launching into a successful orbit. Typically, the parameters of the desired orbit determine when, during the day (month or

year), a launch can occur. The amount of extra  $\Delta V$  carried on the vehicle for plane changes determines the length of the launch window. To reduce the amount of extra  $\Delta V$  required, it is necessary to match the EOR orbital plane with the Moon's orbital plane about the earth if the landing site is somewhere on the lunar equatorial plane. However, this may not necessarily be true for other landing sites on the moon.

The orbital inclination,  $i$ , of the Moon is  $28.5^\circ$  which specifies the target orbital plane. From a given latitude on earth it is only possible to achieve an orbital inclination greater or equal to  $i$ , without making any plane changes from orbit. Thus one of the reasons for choosing Cape Canaveral (at  $28.5^\circ$  latitude) as the launch site. From this latitude, the target orbit can be obtained with minimum fuel cost during launch. There is only one launch window per 24 hours such that the target orbit is coplanar to the lunar orbit. The Earth launch window is also determined by the lunar landing window, however, it precedes the lunar landing window by the amount of time required for rendezvous and transit.

There are two launch windows under consideration. The first is for the PTLI and the second for the lunar landing assembly. The major constraint is that the second launch window must follow within thirty days of the first. The other constraints are placed by rendezvous dynamics.

#### 5.3.1.2 Launch Window Periods

Using basic equations of orbital mechanics it is possible to determine the potential length of the launch windows. A  $\pm 15$  min. launch period would require 135 m/s  $\Delta V$  for an orbital plane change, whereas a  $\pm 7.5$  min. launch period would require 68 m/s  $\Delta V$ . The transfer trajectory may also have some flexibility in the requirement for the pre-injection orbital inclination. This will be the dominant factor in determining window size. Initial calculations estimate that a window of  $\pm 40$  minutes will provide an acceptable inclination. The decision of the final launch window size will be a trade between cost and launch period flexibility.

#### 5.3.1.3 Orbital Drag on the PTLI Stage

Since the PTLI stage will begin orbiting the Earth perhaps one month before the payload arrives, drag on the PTLI stage might require a higher orbit than the 200 km orbit provided by the launch vehicle. For comparison of the drag, Table 5-8 compares a 200 km orbit to a

275 km orbit. The 275 km alternative entered consideration due to GNC's preference for that altitude.

$$d = \rho A C_D v^2 / 2m \quad (5-1)$$

Specific drag on the stage, calculated with Equation 5-1 makes several assumptions. The standard atmosphere chart provides the densities listed in Table 5-8. The assumed vehicle area is 50 m<sup>2</sup>, a value slightly larger than the minimum possible exposed area. The vehicle mass is 100 metric tons. A standard coefficient of drag of 1.5 is assumed.

$$\Delta h = \left( (R_E + h) - \mu / \left( \left[ \mu / (R_E + h) \right] + 2 \Gamma d (R_E + h) \right) \right) \times \# \text{ of orbits} \quad (5-2)$$

The altitude loss is determined from the energy loss per orbit. The energy loss per orbit is the drag force times the orbital circumference. The energy loss per orbit results in a loss of orbital altitude over the orbit. Although the slightly lower orbit would increase the drag, hence increasing the altitude loss, this first cut analysis assumed that the drag remained constant. Finally, the altitude loss is approximately the altitude loss per orbit times the number of orbits per day ( 16 orbits) and the number of days (30 days). Equation 5-2 lists the altitude loss given the specific drag force. Table 5-8 lists the altitude loss for one month.

**Table 5-8: Altitude loss of the PTLI stage during a one month orbital stay.**

Altitude	Air Density	Velocity	Specific Drag	Altitude Loss
200 km	2.789x10 <sup>-10</sup>	7,786 m/sec	6.340x10 <sup>-6</sup>	13.648 km
275 km	4.126 x10 <sup>-11</sup>	7,742 m/sec	9.275x10 <sup>-7</sup>	2.065 km

#### 5.3.1.4 NLS Ascent Trajectory

The NLS capability and trajectory analysis was done using a planar trajectory model over a non-rotating, spherical earth. (Rotational effects were considered by changing the initial conditions to reflect an easterly velocity.) The thrust, component weights, and total vehicle weight was modeled using Shuttle thrust profiles, g limits and a constant fuel flow rates. The analysis assumed a constant pitch rate after clearing the tower at t=6.0 sec. until a pitch of 0° was reached. A coefficient of drag based on Shuttle values was used with a vehicle cross sectional area of 100.8 m<sup>2</sup>. Temperature and gravity were assumed to be constant.

The equations of motion, as presented in Griffin and French, [Griffin, 1991] are as follows:

$$dV/dt = (T \cos a - D) / m - g \sin g \quad (5-3)$$

$$V \, dg/dt = (T \sin a + L) / m - (g - V^2 / r) \cos g \quad (5-4)$$

$$ds/dt = (R/r) V \cos g \quad (5-5)$$

$$dr/dt = dh/dt = V \sin g \quad (5-6)$$

$$D = 1/2 \rho V^2 S C_D \quad (5-7)$$

where:	V = Inertial velocity	m = mass @ time = t
	R = Earth Radius	D = Drag force
	h = Height above surface	C <sub>D</sub> = Drag force
	r = Radius from earth center	$\rho$ = Atmospheric density
	s = Down-range travel	S = Drag reference area
	g = Flight path angle	a = Thrust vector angle
	T = Thrust @ time = t	

Table 5-9 shows the results of the ascent analysis for a 91 mt payload to be placed in an elliptical orbit with eccentricity of 0.045 at MECO. This orbit will allow the vehicle to coast to its initial orbital altitude of 200 km where the circularization burn will take place. This analysis assumes that the ascent trajectory specified will place the vehicle in the 200 km elliptical orbit. The NLS analysis gives a baseline trajectory from which loading, velocity, and trajectory information can be obtained.

The NLS will follow a similar launch profile to the Shuttle. SRB burnout and staging will occur at 123 sec. Main Engine Cut Off (MECO) will occur at t=416.5 sec, at an altitude of 127 km. The first circularization burn will take place at approximately t=967.5 sec after launch at an altitude of 200 km. Later, at a time determined by ground control, an additional burn sequence is performed, leaving the vehicle in a circular orbit at an altitude of 275 km.

#### 5.3.1.4.1 Sequence of Events



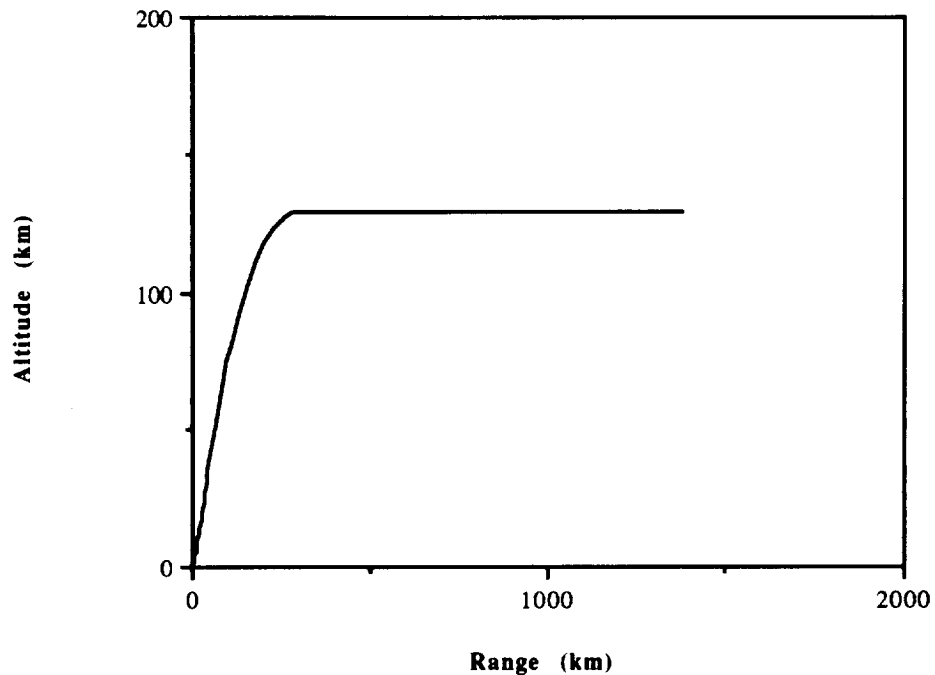
Table 5-9 is a chronology of ascent events for the NLS vehicle. The ascent is similar to the Shuttle's. [Suit, 1992]

**Table 5-9: NLS Ascent Event Sequence**

Time	Altitude (km)	Event
t = -3 sec	0	Space Transportation Main Engines (STME) ignite
t= 2.64 sec	0	SRB's ignite
t= 3 sec	0	Lift-off
t= 6 sec	0.126	Tower cleared, start constant pitch rate trajectory
t= 45 sec	11.3	STME's throttle back to 75% for max. Q
t= 64 sec	23.4	STME's throttle back to 100%
t= 123 sec	86	SRB burnout
t= 134 sec	98	SRB's jettisoned
t= 401 sec	128.4	STME's throttle back to 75% to remain in g limit
t= 416.5 sec	128.4	MECO, Elliptical orbit with $e = 0.045$
t= 432 sec	131	Core stage and nose cone jettisoned
t= 967.4 sec	198	Circularization burn starts
t= 1000 sec	200	Circularization burn complete

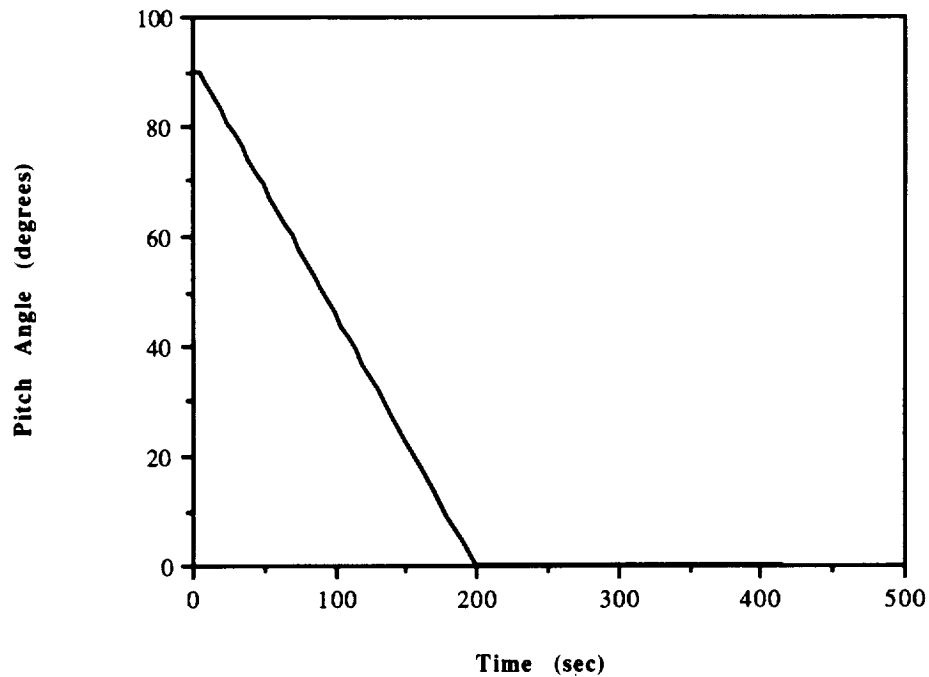
#### 5.3.1.4.2 Altitude, Downrange, and Pitch Profile

Figure 5-11 shows a plot of launch vehicle altitude vs. downrange distance through MECO. After MECO, the core vehicle burns up over the Indian Ocean while the SRBs are retrieved in the Atlantic. The SRBs free-fall to an altitude of 4.6 km where the nose cone is ejected and the drogue and parachute are pulled out. The SRB's splash down at about a velocity of approximately 88 m/s and a down range distance of 150 km. [Kaplan, 1978].



**Figure 5-11**  
**NLS Altitude vs. Down Range Trajectory**

Figure 5-12 gives the pitch profile of the NLS vehicle. The pitch profile is determined by MECO altitude, vehicle orientation, and weather conditions. In most cases the sole factor driving pitch variation is the wind. Mean wind data is available for each month at KSC. The pitch profile used by the guidance system is a result of these mean winds, the type and size of the payload, and the final vehicle orientation. For this analysis, a constant pitch rate trajectory was used. This trajectory can be modified subject to atmospheric conditions at launch, and to obtain the necessary elliptical orbit at MECO.



**Figure 5-12**  
**NLS Pitch Profile with Time**

#### 5.3.1.4.3 Orbital Insertion and Circularization

Orbital insertion will be accomplished by using the PTLI stage or the LBM stage, depending on the mission.

At MECO, the vehicle is in an elliptical orbit with an eccentricity of 0.045 with apogee at 200 km altitude. The insertion burn will be performed near apogee, at 967.4 sec into the flight, for 37 sec with the PTLI or 73 sec with the LBM, leaving the vehicle in a circular orbit of 200 km. Boost to the 275 km orbit will be conducted at an appropriate time. Figure 5-13 shows the total trajectory to the 200 km LEO as well as the SRB and core vehicle trajectories. The SRBs are recoverable approximately 150 km downrange.

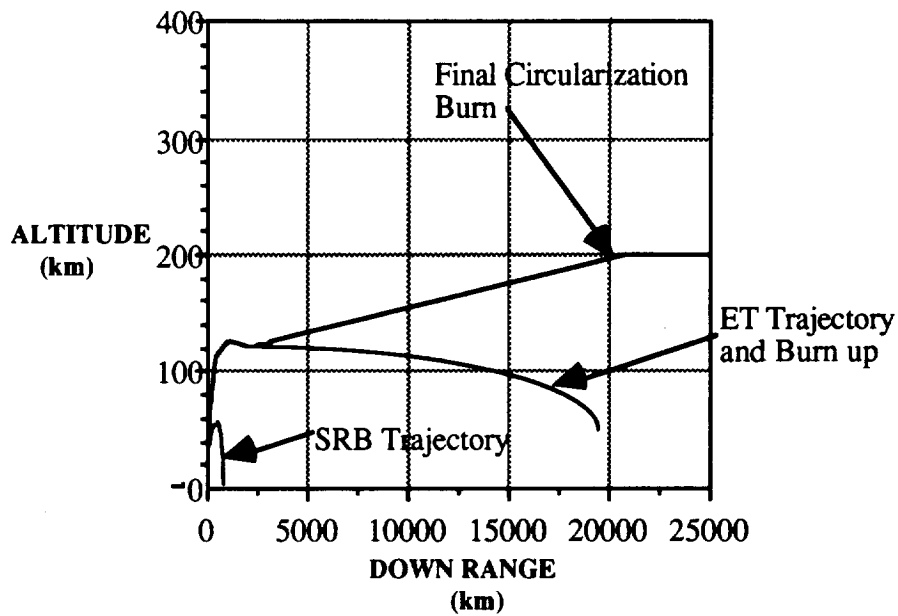


**Figure 5-13**  
**NLS Trajectory to 200 km LEO**

### **5.3.2 Rendezvous**

The rendezvous scenario described here, launch-to-rendezvous (LTR), is a modified version first developed by NASA through the Gemini and Apollo space programs [Griffin, 1991, Larson, 1991, Wiesel, 1989]. Because our mission does not require a plane change from launch to LEO (200 km), the rendezvous will automatically take place in a co-planar co-elliptical orbit. The preliminary task is to achieve an initial altitude of 200 km. Upon reaching a 200 km altitude, the vehicle is boosted to a 275 km altitude. The secondary task is to achieve proper vehicle phasing. The scenario is outlined below:

- 1) Any out-of-plane component in the chaser vehicle (CV) is removed by waiting until  $z=0$  in Hill's equations,

$$\frac{d^2 r}{dt^2} - 2n \frac{ds}{dt} - 3n^2 r = a_r$$

$$\frac{d^2 s}{dt^2} + 2n \frac{dr}{dt} = a_s$$

$$\frac{d^2 z}{dt^2} + n \frac{dz}{dt} = a_z$$

(5-8 through 5-10)

and thrusting with acceleration  $a_z$  to yield  $dz/dt = 0$ . Where  $r$  is in the orbit plane but normal-out to the target vehicle (TV),  $s$  is in normal to  $r$  in the orbit plane, and  $z$  is  $r \times s$ . This maneuver is usually not the first in the sequence and may only involve small adjustments [Griffin, 1991].

2) The second stage of rendezvous is to establish a phasing orbit relative to the orbit of the TV. In the case of the co-planar, circular orbits, this phasing orbit is actually the orbit of the CV (see Figure 5-14). Normally, the phasing orbit will have a different orbital period such that the CV can "catch-up" or "wait" for proper alignment between TV and CV. However, it has been noted that this sort of "rendezvous usually takes 1 to 2 days," [Wiesel, 1990] which is unacceptable in Project Columbiad.

The rendezvous scheme requires a boost from 200 km to 275 km. The altitude of 275 km was chosen so that the CV launching one sidereal day (24 hr 4s) later will be approximately 114 km behind the TV.

3) Once the TV and CV are along the same orbital path, the phasing sequence begins. It is possible to use the drift equation [Larson, 1991] given in equation 5-11.

$$\text{drift rate} = 1080 \frac{\Delta V}{V} \text{ (degrees/orbit)} \quad (5-11)$$

to close the 114 km gap. A total of 14.4 m/s will be required to maneuver the  $1^\circ$  difference, which will be completed in one orbital period. The CV should then be within a 1 km of the TV which is defined as the docking zone.

If the launch schedule for the second launch should be delayed, it is possible that the TV will not be within 114 km upon insertion into the 275 km orbit. A worst case scenario would be if the two rendezvous vehicles were  $180^\circ$  out of phase. This would require 144 m/s to obtain a drift rate of  $10^\circ/\text{s}$  and 18 hr rendezvous time. Though the time is long, it represents a worst case scenario using the maximum  $\Delta V$  that can be spared for this mission.

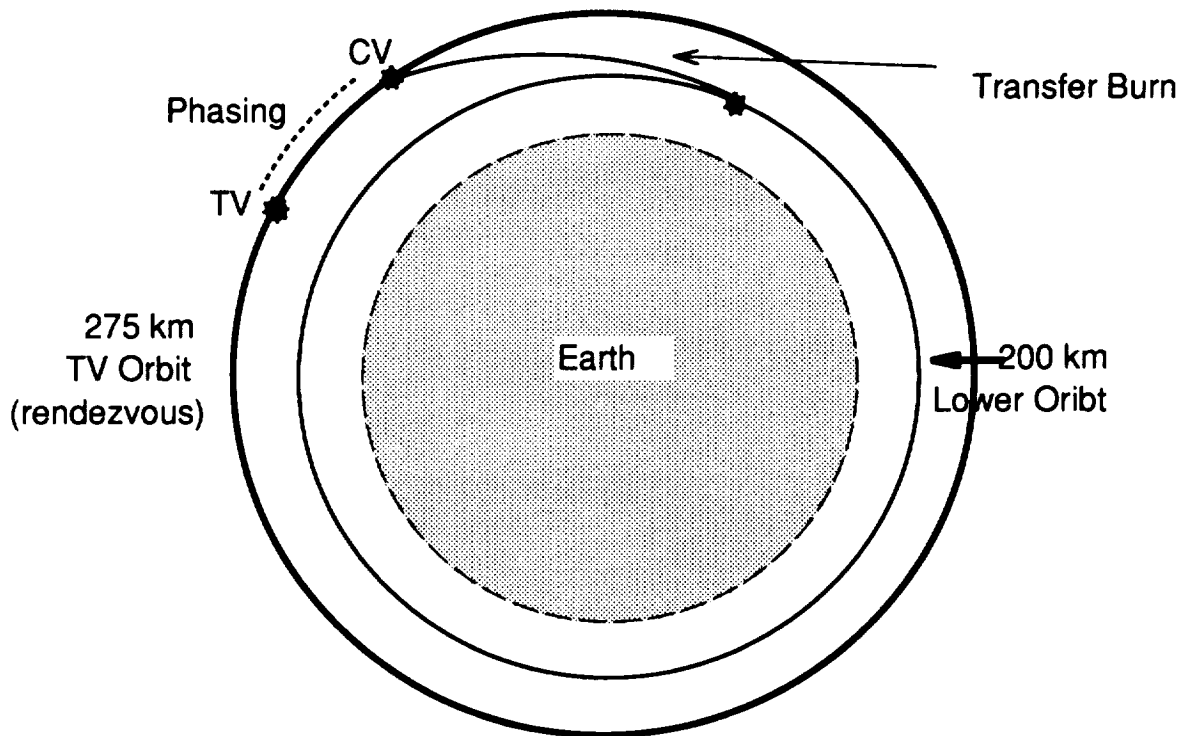


**Figure 5-14**  
**Rendezvous Orbit**

### **5.3.3 Lunar Transfer Orbit**

Once established in LEO, the spacecraft must await the proper point to complete the trans-lunar injection (TLI) burn that sets it on the trajectory to the moon. The goal of this trajectory is to reach the moon such that the desired lunar orbit (altitude and inclination) can be entered with a minimal TLI burn. Another criteria that we wish to satisfy is that the lunar trajectory take less than three and one half days because of crew considerations. This means that the total mission time for a 28 day stay, from takeoff to touchdown is approximately 35 days. The correct lunar orbit has an inclination such that the designated landing site passes under it. Unlike the Apollo mission, this requires that our spacecraft have the ability to arrive at the moon at any inclination out of the Moon-Earth plane. There are two methods of solving for a trajectory between two planetary bodies. One is to use the method of patched conics, where the motion of the spacecraft is considered to be affected by only one body at a time. Because of the Moon's proximity to the Earth, this method is inappropriate for the discussion of this trajectory [Weisel, 1989]. The second method, which is more valid, is to use the equations of motion for the restricted three body problem that the Earth-Moon system implies. Even though many trajectories for this problem are well documented, none were found to describe arrival at the moon significantly out of the

MEP. As will be discussed, this has required us to formulate a numerical solution to the three body problem.

The transfer trajectories that are presented here are only approximate solutions. As will be explained, they are intended only to provide an estimate of the fuel required to satisfy our mission requirement of landing at any latitude of the moon. The two solutions presented both begin in a 275 km LEO that has zero inclination to the MEP. One case brings the spacecraft to an equatorial lunar orbit, while the other results in a polar lunar orbit. These extreme cases were used as a proof of concept that Columbiad can land at any point on the lunar surface. Further study must include a more detailed trajectory analysis. Exact trajectory solutions would need to take into account the specific lunar landing site, the inclination of LEO to the MEP, and burn times. At this time the maximum acceptable inclination from which injection can occur is not known. Another point is that no claim is made as to the optimality of these trajectories. Trajectories were iterated upon to search for improvements, but a more comprehensive analysis may find more efficient routes. Due to the lack of a single, exact trajectory, the characteristic velocities used in the description of the mission in the volumes that follow were approximated and standardized early on in order to carry out the mission design. The standardized trajectory includes a 3140 m/s injection  $\Delta V$  and a 1060 m/s lunar orbit insertion. All components of the mission design are equally capable of carrying out either the polar or planar solutions presented in this section and in fact, this will require less  $\Delta V$  than in the standardized trajectory.

#### 5.3.3.1 Three Body Problem Formulation

The formulation of the restricted three body problem begins with the consideration of the rotating Earth-Moon system. This system is shown in figure 5-15. In this restricted system, only the combined effects of the Earth and the Moon are accounted for. Perturbation effects from the oblateness of the Earth, the Sun, and eccentricity of the Moon's orbit are not included in this preliminary trajectory analysis.

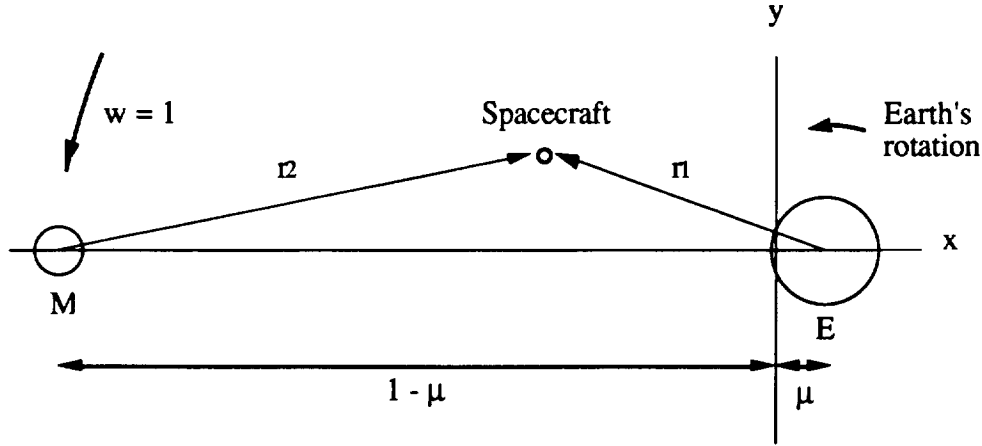


**Figure 5-15**  
**Rotating Coordinate System of Three body Problem**

Measurements in this system are nondimensionalized. Distances are in terms of Earth-Moon distances (D), and time is normalized by the Moon's orbital period. Equations 5-12 through 5-14 describe the flight of the spacecraft in the rotating coordinate system.

$$\ddot{x} - 2\dot{y} - x = -\frac{(1 - \mu_3)(x - \mu_3)}{r_1^3} - \frac{\mu_3(x + 1 - \mu_3)}{r_2^3} \quad (5-12)$$

$$\ddot{y} - 2\dot{x} - y = -\frac{(1 - \mu_3)y}{r_1^3} - \frac{\mu_3 y}{r_2^3} \quad (5-13)$$

$$\ddot{z} = -\frac{(1 - \mu_3)z}{r_1^3} - \frac{\mu_3 z}{r_2^3} \quad (5-14)$$

These non-linear, coupled differential equations do not have a solution in closed form. Numerical integration of the equations can produce the flight path of the spacecraft given one point of the trajectory (initial conditions). A thrust term is not included in these equations since for this preliminary analysis, propulsive burns are idealized to be impulses that take zero time. Numerical integration is computed using a Runge - Kutta method.



#### 5.3.3.2 Designated Lunar Landing Site

In order to satisfy the primary requirement of landing anywhere over the lunar surface, Columbiad will first establish a circular lunar orbit that passes over the desired landing site. One goal of the approach was to use a minimal amount of extra fuel in selecting various landing sites. In order to accomplish this, the lunar orbit should be established directly from the transfer trajectory so that a fuel expensive plane change is not necessary. This requires a specific transfer trajectory for each landing site. Fuel used for descent to the lunar surface is independent of the position of the site (more fuel may be used, however, for rough terrain where the lander may require extra maneuvering to a smooth landing site).

In order to enter an orbit such as this, the transfer trajectory must bring the spacecraft to the close proximity of the selected LLO with a velocity vector closely aligned with the correct velocity vector for that circular orbit. For a 100 km LLO, orbital velocity is 1.632 km/s. Such an arrival at the moon should not use significantly more fuel than the equatorial arrival used by Apollo. Varying arrival speeds, due to the inclination of the orbit, should not be significantly larger than the arrival speed of Apollo.

#### 5.3.3.3 Selected Transfer Trajectory

Selection of a transfer trajectory is based on several criteria, as mentioned above. The spacecraft must start in LEO, and be delivered to the lunar vicinity in the appropriate manner. Travel time should be kept close to three days because of considerations for life support weight and crew comfort. For abort reasons, a trajectory should require minimum additional thrusting to return to Earth once on the transfer path. Along with these considerations a minimum total amount of fuel should be used to complete the TLI and decelerate into LLO. The trajectory to meet this criteria is found by analyzing the three body problem described above. Initially both low, constant and high, impulsive thrust systems were considered, but low thrust orbits were ruled out due to the travel time requirement. All trajectory analysis was performed on MATLAB.

#### 5.3.3.3.1 Trajectory Search Algorithm

Transfer trajectory analysis was based on selecting initial conditions in LEO (post injection velocities) and then numerically integrating these forward. The equations of motion are very sensitive as demonstrated by the fact that a change of one m/s at injection will change the spacecraft's position at the moon by up to 100 km. In order to find a satisfactory set of initial conditions, a simplex search routine was used. This routine simply varies the input

parameters of a function in order to minimize it. The results of this analysis include many approximations, but they provide an appropriate estimation of the trajectories required for the Columbiad mission.

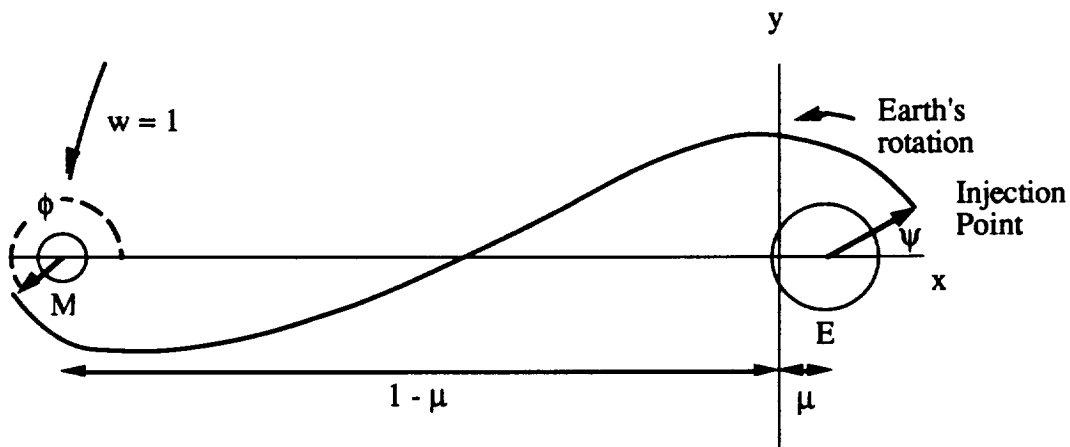
Simplex is implemented in MATLAB as the function “fmins”. Fmins was implemented by having it vary parameters which represent the initial conditions of a trajectory. These parameters were passed to a cost function which was created for each desired trajectory. This function converted the parameters to initial conditions that the three body numerical integration routine (Appendix I) could interpret. Effectively, the parameters that could be varied were the velocity components in each direction, the point during LEO (275 km altitude) where the injection occurred, and, in the case of the polar transfer, the point of a second injection burn. The results of the integration are returned to the cost function where the conditions at the closest point of approach to the moon are compared to the desired lunar approach conditions. This point was chosen because of simplicity, and the consideration that it is not desirable to approach the moon closer than the altitude of the orbit. The cost value was computed as a weighted combination of errors from the ideal end point conditions. Fmins would vary the input parameters and select sets that reduced the cost function, thereby finding a satisfactory set of initial conditions. The cost functions for the planar and polar approach are included in Appendix II.

There are several points to note about the simplex algorithm and the resulting trajectories. Most importantly, the trajectories that were produced were not exact, in that they did not match the end point criteria identically. For both the planar and polar case, the trajectories approached the moon at a distance significantly higher than LLO. The velocity vectors are also not exactly parallel to the velocity desired for a lunar orbit, which results in slightly higher  $\Delta V$ 's to brake into the orbit. These results are expected, since fmins only minimizes errors, and makes no guarantee to eliminate them, although it should, if it is possible for the system being dealt with. For the planar case, the number of free parameters is equal to the number of constraining variables in the cost function, but for the polar case, fmins must try to minimize five cost items while only varying four parameters. This may help to explain the fact that fmins would appear to find local minima in the cost function. This was demonstrated by changing the initial guess that fmins iterates on, and observing it return a different convergent solution. This leads to the point that it is entirely possible that more optimal trajectories exist.

There are several changes that could be made to the search algorithm which might result in a more efficient trajectory. Changing the cost function so that there are fewer endpoint constraints may change the problem so that it is under-constrained. Both cost functions currently look for an orbit in one plane only. This is not necessary since an orbit in any plane that passes over the desired landing point is acceptable. The relative weights of the constraints in the cost function can also have a large effect on the outcome of  $f_{mins}$ . Although some experimentation was done in changing these values, more should be conducted, especially with other modifications to the terms in the cost function. Also, increasing the number of parameters that  $f_{mins}$  can vary may help it to converge to the endpoint criteria. This greater freedom in selecting initial conditions could take the form of varying the altitude of LEO, and varying the position around the Earth at the injection point. It may also prove to be efficient to allow multiple burns along a course, although this may be considered undesirable due to reliability constraints. A final improvement may be made to the integration routine by having it include motion during thrusting periods rather than considering the thrusts as impulsive.

#### 5.3.3.3.2 Planar Transfer

The planar trajectory describes the path of the spacecraft for an insertion into an orbit around the moon within the MEP. The planar search routine and cost function are included in Appendix II.  $f_{mins}$  was allowed to vary four parameters:  $V_x$ ,  $V_y$ ,  $V_z$ , and the point along the LEO where injection takes place. The cost function was structured to minimize  $\Delta V$ , distance from a LLO radius, and distance and velocity out of the MEP. The results of the simplex search can be interpreted by the use of Figure 5-16.



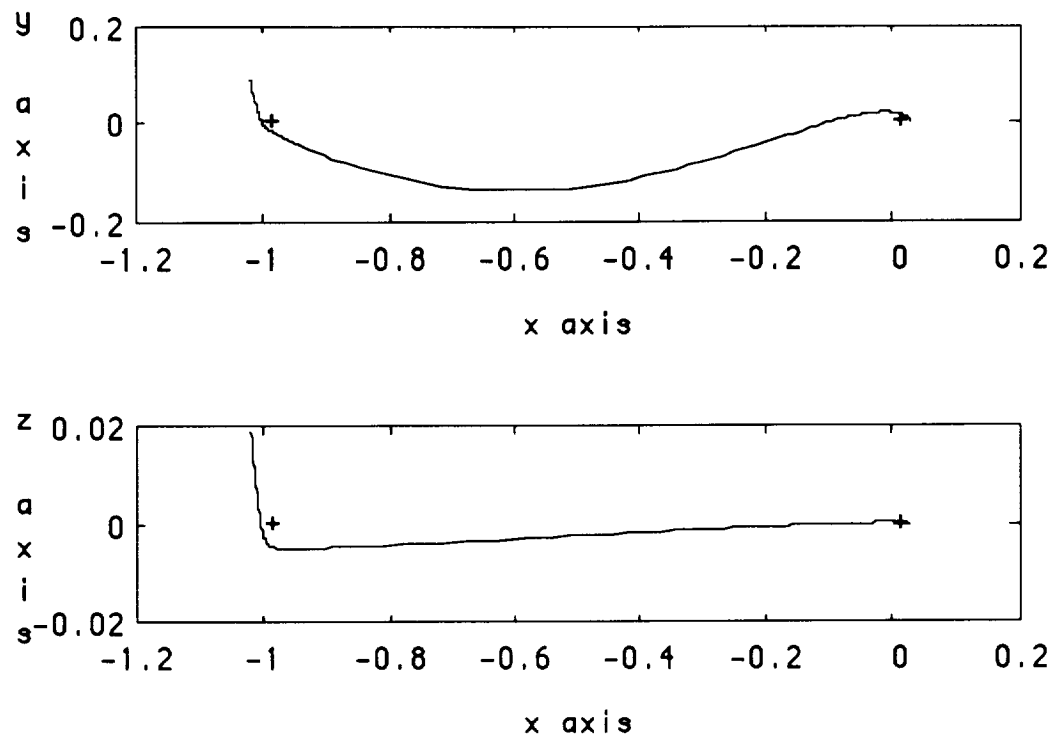
**Figure 5-16**  
**Lunar Transfer Orbit**

Table 5-10 lists the results in terms of injection and arrival conditions. The radius is measured from the appropriate body and the angles describe the points of arrival and injection.  $V_x$ ,  $V_y$ ,  $V_z$ , and  $V_{total}$  all describe the velocity of the spacecraft at the injection or arrival point. All measurements are made in the rotating coordinate frame described earlier. Time is expressed in hours and minutes. Arrival time is the time at the point of arrival and does not include the transfer ellipse which is described below.

**Table 5-10: Planar Transfer Specifications**

PARAMETER	INJECTION	ARRIVAL
psi	0.6°	N/A
phi	N/A	212°
Radius	6655 km	4100 km
time	00:00	57:23
$V_x$	-4.0398 km/s	-1.1753 km/s
$V_y$	9.8416 km/s	1.673 km/s
$V_z$	0.1046 km/s	0.2537 km/s
$V_{total}$	10.6389 km/s	2.062 km/s
$\Delta V_{total}$	2.8997 km/s	986 m/s

The velocity in LEO (275 km altitude) is 7.7392 km/s which gives an approximate  $\Delta V$  for injection of 2.8997 km/s. A plot of this post injection trajectory is shown in Figure 5-17a. No braking burn is included. Because the trajectory does not reach the moon at a 100 km altitude, an elliptical transfer to a circular LLO must be done. Upon reaching the lunar arrival point, the spacecraft must conduct a 497 m/s braking burn. This results in an elliptical orbit with a 100 km periselenium altitude. When periselenium is reached after 3 hours, the spacecraft must conduct a second burn of 489 m/s. This will circularize the spacecraft into the desired 100 km orbit from which descent can be initiated.



**Figure 5-17a**  
**Planar Injection Trajectory**

#### 5.3.3.3.3 Polar Transfer

The polar transfer describes the injection trajectory which will result in a polar circular orbit around the moon. In this case the search routine was used to find a second injection burn which would complete the polar injection burn. The parameters consisted of  $V_x$ ,  $V_y$ ,  $V_z$ , and  $t$ . The velocities were the component magnitudes of the second burn's characteristic velocities and  $t$  was the time at which the second burn took place. This time described a point along the planar trajectory. In other words, starting from LEO, the polar trajectory is identical to the planar trajectory until time  $t$ . At this point the second burn occurs, and the spacecraft follows the unique polar trajectory. The post injection trajectory is plotted in figure 5-17b.

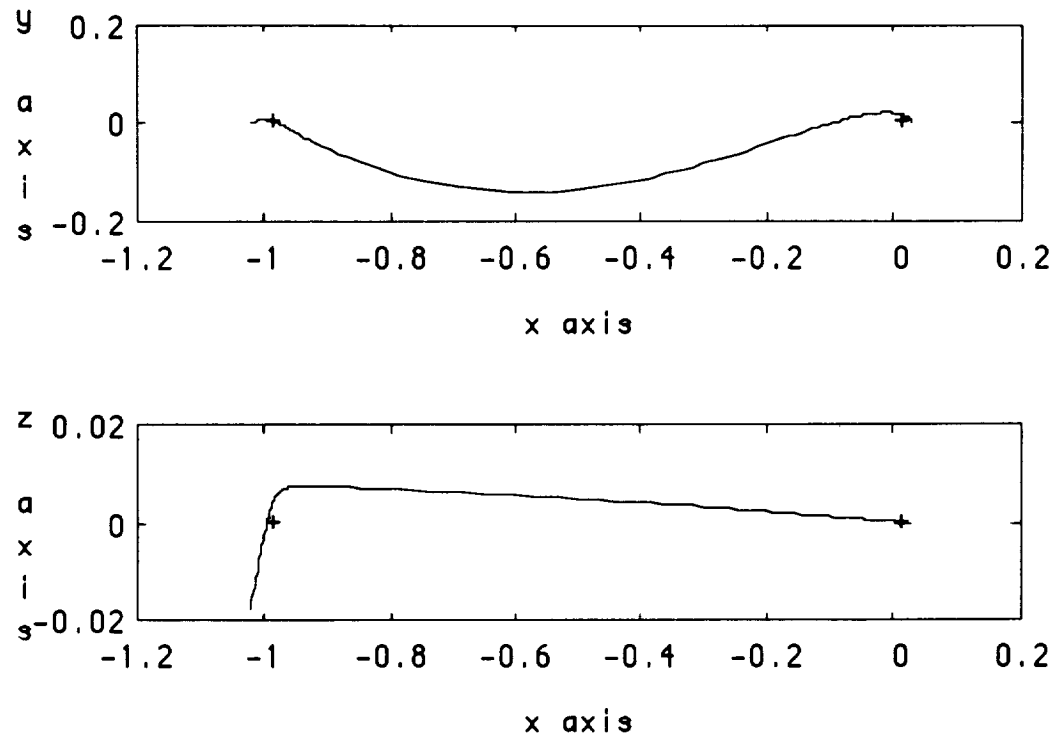


**Figure 5-17b**  
**Polar Injection Trajectory**

This method was chosen because it resulted in a total  $\Delta V$  of injection less than the  $\Delta V$  found for a single injection burn from LEO. This was the case even though the single burn polar injection was given an additional degree of freedom in the parameter alpha, which is included in the cost function MATLAB code, but is unused. Alpha is the latitude of the injection point, so effectively, injections could be made at any point over the Earth's surface. The fact that this was not sufficient to find a low  $\Delta V$  trajectory may indicate that the search function fell into local minima or some error was made in the implementation of alpha. At this time, no explanation has been confirmed. The results of the polar transfer are listed in Table 5-11. The second burn takes place 22 minutes after the initial injection. At the second burn, the angle psi is also approximated by assuming that the spacecraft is still in the MEP (it is actually 85 km above the MEP). In this case, phi is also measured in the x-z plane, clockwise from the x axis.

**Table 5-11: Polar Transfer Specifications**

PARAMETER	INJECTION	2nd BURN	ARRIVAL
psi	0.6°	88.3°	N/A
phi	N/A	N/A	268.6°
Radius	6655 km	8058 km	2840 km
time	00:00	00:22	61:57
V <sub>x</sub>	-4.0398 km/s	-8.9062 km/s	-1.9945 km/s
V <sub>y</sub>	9.8416 km/s	1.3809 km/s	0.5527 km/s
V <sub>z</sub>	0.1046 km/s	0.1165 km/s	-0.7313 km/s
V <sub>total</sub>	10.6398 km/s	9.0132 km/s	2.195 km/s
$\Delta V_{total}$	2.8997 km/s	0.1047 km/s	1.0810 km/s

Again, the radius at lunar arrival is above the 100 km LLO. This requires an initial burn of 645 m/s to brake into an elliptical orbit, followed by a circularization burn of 436 m/s. The time spent in the transfer ellipse is 1 hour 25 minutes. This transfer will bring the spacecraft into a polar oriented LLO.

#### 5.3.3.4 Abort Considerations

The requirement of the trajectory to provide a return to Earth with minimal additional thrusting has been made for safety reasons. The intent is that only partial propulsion systems need to be operable for Earth return due to a critical failure that occurs before insertion into LLO. These aborts are completely dependent upon the trajectory that the spacecraft is in and the extent of operability of the propulsion system. At this time, no specific calculations for an "around the moon" abort have been made. Another type of abort that our spacecraft is capable of is a "turn around". In a turn around abort, the spacecraft uses its propulsion system to decrease its velocity towards the moon. This will result in the spacecraft falling into an orbit around the Earth where additional small burns can initiate reentry. Because of the DF configuration which has all stages propelling the entire vehicle, the spacecraft has enough energy to complete this turn around at any point along the trajectory. However, after passing the cis-lunar Lagrange point, less  $\Delta V$  is required if an "around the moon" abort is conducted.

#### **5.3.4 Lunar descent**

A gravity turn descent trajectory is used by the spacecraft to descend from LLO to the lunar surface. In this trajectory, the spacecraft is braked into an elliptical orbit. At a specific point along this transfer ellipse, the terminal descent is initiated. This is a constant thrust maneuver, during which the LBM is staged. After the LBM is staged, the PLM/ERM will complete the descent with an additional horizontal thrust to reach the habitat, which is 860 meters to the side of the trajectory. This is done to prevent the staged LBM from overflying the habitat. In the PLM/ERM, a constant thrust is directed against the velocity vector which brings the lander down to an altitude of 400 m with zero horizontal velocity and a vertical velocity of 4m/s down. From this point, engines are throttled to provide a constant velocity vertical descent to the surface, with a final deceleration just before touchdown. This method was selected for several reasons. First the steering law is not complex, since it must only measure velocity direction, and then null any angular errors in vehicle coordinates. Secondly, the descent path will tend toward vertical as the spacecraft approaches zero velocity. This also provides good ground obstacle avoidance since horizontal velocity is low close to the surface. The third point is for a thrust to pre-descent earth weight ratio of 0.30 the characteristic velocity loss due to gravity is approximately 200 m/s [Akridge, 1963].

##### **5.3.4.1 Gravity Turn Trajectory**

The terminal descent phase is started from LLO. First an impulse is applied against the velocity vector to attain a transfer ellipse which has its periselenium altitude at 10 km. This altitude provides clearance in the event that powered descent is not initiated. For 100 km LLO, this requires a burn of  $\Delta V = 21$  m/s. Powered descent is initiated at  $r_0$  in Figure 5-18.



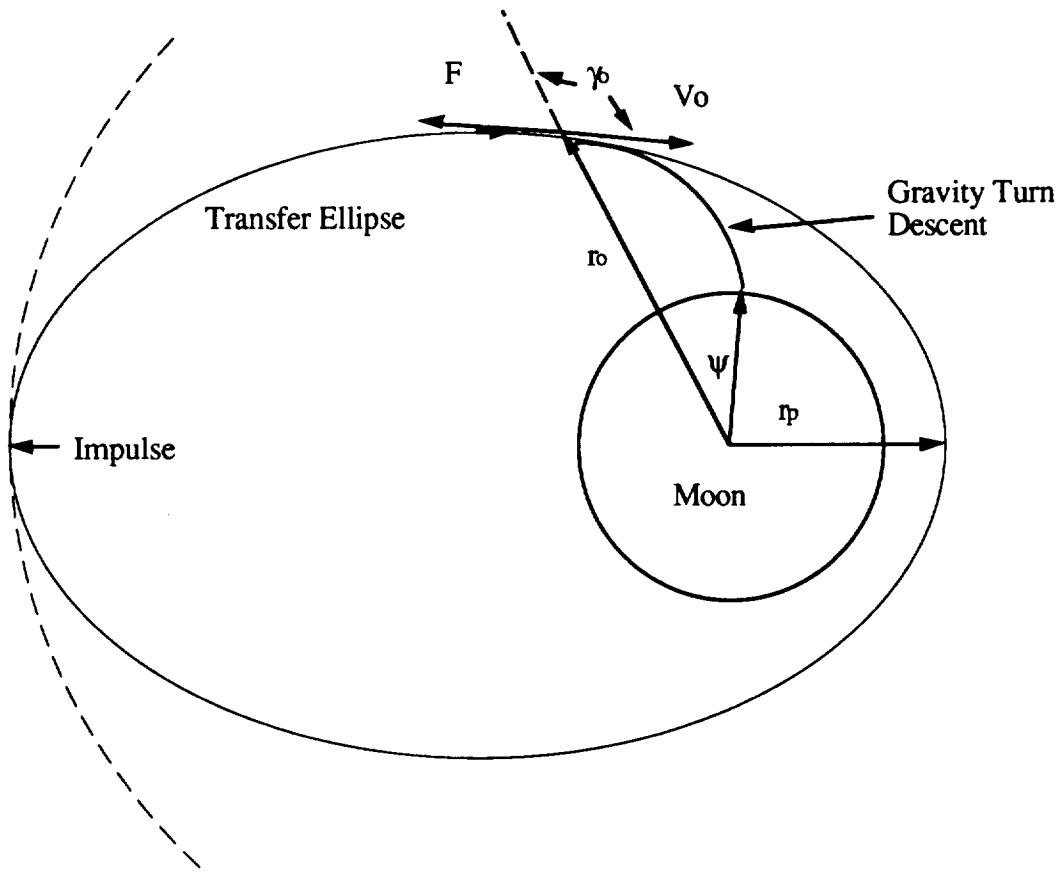


**Figure 5-18**  
**Lunar Descent Profile**

This point,  $r_o$ , is determined by the vehicle's thrust to weight, given the condition of arriving at an altitude of 400 m with a 4m/s vertical velocity. For our landing configuration,  $T/W_o = 0.3$  for two engines at full thrust. This anticipates a single engine out. This gives  $r_o = 1795.4$  km ( $h = 55.4$  km). The true anomaly at this point is 92 degrees, and the flight path angle is  $90.56^\circ$ . Burn time for the LBM during the terminal descent is 379 s, after which it is staged. Staging occurs at an altitude of 2806 m. The velocity of the vehicle at this point is 59 m/s at an angle of  $64^\circ$  down from the horizontal. The LBM will free fall from this point, landing 1270 m downrange of the PLM/ERM landing point. Due to this proximity, it has been decided to thrust the PLM/ERM to the side of the trajectory during part of the descent phase. Accounting for a 15 second staging time, the PLM/ERM will be at an altitude of 2226 m when it fires. Thrust should be set at 114,000 N for 43 seconds to arrive at the 400 m point with a vertical velocity of 4 m/s. Additionally, at the start of this burn, the PLM/ERM should thrust to induce a velocity of 20

m/s perpendicular to the previous descent trajectory. At the 43 second point, this horizontal velocity should be zeroed. This precautionary measure prevents the staged LBM from flying over the habitat, as it will be 860 meters to the side. These results were derived from the following equations of motion by numerical integration [Akridge, 1963]:

$$\dot{V} = \frac{T}{m} - \frac{g_m r_m^2}{r^2} \cos \gamma \quad (5-15)$$

$$V\dot{\gamma} = \left[ \frac{r_m^2 g_m}{r^2} - \frac{V^2}{r} \right] \sin \gamma \quad (5-16)$$

$$\dot{r} = V \cos \gamma \quad (5-17)$$

$$\dot{\psi} = \frac{V \sin \gamma}{r} \quad (5-18)$$

Numerical integration was performed in MATLAB. The code is included in appendix II. From the 400 m altitude point, the lander will continue to the surface at a 4m/s descent rate. The engine must be throttled to exactly counter lunar gravity. Small translational maneuvers may be made during this hover phase with the RCS system, or by throttling and gimbaling the engines. For the given descent rate, the lander will reach the surface in 98 s. This burn requires a  $\Delta V$  of 162 m/s. To achieve the specified final landing descent rate of 0.5 m/s, the engines must provide a larger impulse just before touchdown. This should occur at an altitude of 8 m. The impulse to slow to 0.5 m/s requires an additional  $\Delta V$  of 7 m/s for a thrust to lunar weight ratio of two. Burn time is 2.12 seconds. At this point, the spacecraft's altitude will be 3.24 m above the lunar surface with a 0.5 m/s descent rate. The final descent is done with the engines throttled to cancel gravity. The  $\Delta V$  required until touchdown is 10.7 m/s.

At any time during the descent, an abort can be made by rotating to thrust vertically up. Once a positive rate of climb is achieved, the spacecraft can be guided back to an ascent trajectory discussed in the following section. The actual trajectory depends on the thrust available (dependant upon point of failure), and the point on the abort that the failure occurred.

### **5.3.5 Lunar Ascent**

During this phase, the ERM ignites on the lunar surface and propels itself and the command module into LLO (100 km) where they orbit until the TEI burn. Ascent from the lunar surface will be completed using a gravity turn trajectory just as in the lunar descent. Again, this method, requires a simple steering law, and has small gravity losses (approximately 60 m/s since the ERM has a much higher T/W ratio, although it is not an optimal ascent trajectory. The equations of motion for this trajectory are the same as described in the descent phase (equations 5-15 through 5-18). Considerations for this phase are the T/W ratio of the ERM at liftoff, and the orientation of the lunar orbit desired for return to Earth.

From liftoff, given a perfectly aligned launch, the gravity turn trajectory will follow a straight ascent all the way through burnout. This would leave the spacecraft at some altitude with zero tangential velocity. A small deviation from vertical is necessary to initiate the gravity turn during ascent. This deviation is determined to meet the desired end condition of zero vertical velocity ( $V = V_{llo}$  tangential to the lunar surface) at burnout. This initial angle is critical since deviations of less than one degree, uncorrected, would either loft the spacecraft into an elliptical orbit, or drive it into the lunar surface. Also this initial tilt angle determines the orientation of the achieved lunar orbit. At this time, the initial tiltover angle has not been calculated.

These trajectory calculations are made assuming a constant thrust of 184,000 N (the thrust of two RL-10's). The initial phase for liftoff is a 10 second burn vertically from the lunar surface. This requires a  $\Delta V$  of 42 m/s and places the vehicle at an altitude,  $h$ , of 130 m with a vertical velocity of 26 m/s. At this point, the spacecraft is tilted to the initial ascent tilt and thrust is continuously angled in the direction of the velocity vector. Lunar elliptical orbit is achieved at the specified altitude of 15 km with a total  $\Delta V$  from liftoff of 1798 km/s. This elliptical orbit will be circularized after 57 minutes at its aposelenium of 100 km by a burn of 20 m/s  $\Delta V$ . These steps are illustrated in Figure 5-19. The spacecraft will wait in LLO for the proper time to initiate the TEI burn.

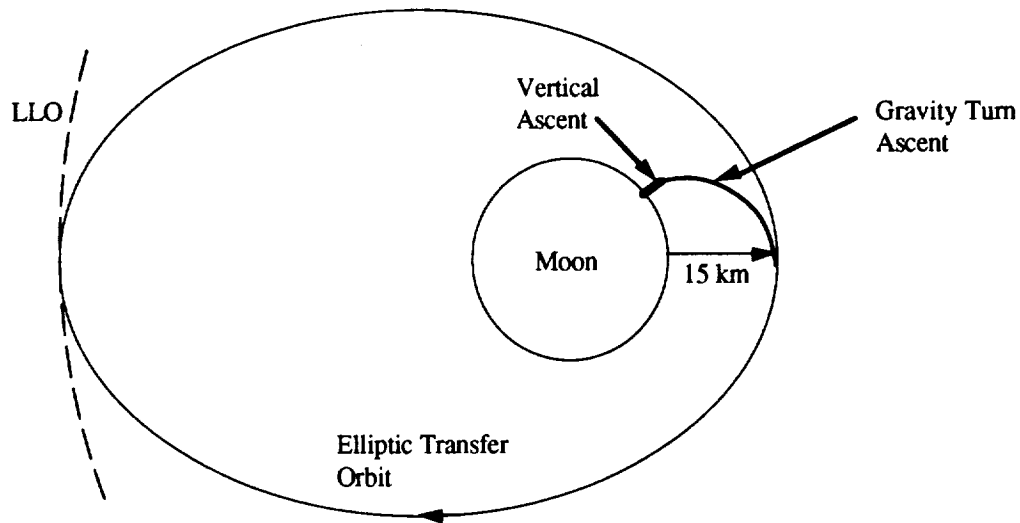


**Figure 5-19**  
**Lunar Ascent Profile**

### **5.3.6 Earth Transfer Orbit**

The Earth transfer orbit is the trajectory which brings the spacecraft from LLO to the Earth for the aerobraking reentry. Accuracy in the arrival point is critical because of the constraints on the reentry window. The Earth transfer orbit is nearly identical to the Lunar transfer orbit. An injection burn places the spacecraft on a coasting trajectory to the Earth. A midcourse correction, similar to the one occurring outbound, will take place. The major difference is that at Earth arrival, no braking maneuver will be made. Instead the spacecraft will enter the atmosphere directly.

Trajectory calculations of the return have not been completed. The numerical integration routine will developed singularities in the close proximity of the moon, so simplex failed to find a reasonable trajectory. The mission is currently designed to implement a return using a  $\Delta V$  of 1060 m/s. This was judged to be reasonable according to the  $\Delta V$  required to brake into lunar orbit when arriving from the Earth. It is expected that a midcourse correction will take place at an appropriate point along the trajectory. The goal of the trajectory is to arrive at the Earth reentry window at the proper angle.

### **5.3.7 Reentry into Earth's Atmosphere**

Trajectory control during the atmospheric reentry phase of the program poses many challenging questions to the design. Reentry into the atmosphere is a difficult process in which the spacecraft is subjected to large heating and aerodynamic loads. The violent and

potentially dangerous nature of reentry drives requirements in aerodynamic design, heatshield composition and structure, and control of the spacecraft. Reentry considerations are also instrumental in determining lunar launch windows and trajectory requirements for Earth return. This section will cover the lunar entry flight phase ( lunar launch windows and trajectory requirements), the entry corridors into the atmosphere, the reentry process, and final descent by the means of parachute operations. The discussions will be on a system level omitting detailed design.

#### 5.3.7.1 Reentry Configuration

The reentry configuration is based upon a biconic design with a lift to drag ratio greater than one. This is known as a lifting reentry body. A lifting reentry body has numerous advantages for a manned mission. The additional lift allows for a shallow descent into the atmosphere, lowering the deceleration loads, lowering heating rates, and providing the ability for maneuvers during reentry. This maneuverability allows the vehicle to land at a predetermined site and produces a landing footprint to which the vehicle can maneuver to. A view of the biconic design is featured in Figure 5-20.

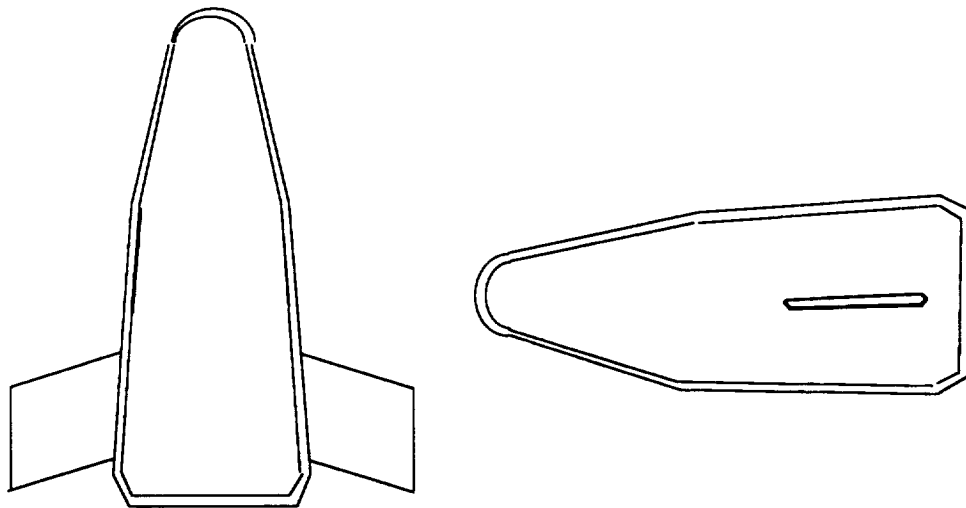


**Figure 5-20**

#### **Biconic Design of the Entry Vehicle**

An interesting feature to note are the horizontal stabilizers. They provide for additional stabilization during reentry and provide a simple mechanism for changing the angle of attack and the bank angle of the vehicle during reentry. The angle of attack allows precise control over the lift to drag ratio, thereby controlling the descent rate of the vehicle.

### 5.3.7.2 Lunar Launch Windows and Trajectories

The considerations for Earth reentry begins on the lunar surface. The lunar launch window and trajectory needs to be carefully tailored to the motion of the Moon, Earth, and the Earth-Moon system. The system is primarily driven by the entry corridor into Earth, see figure 5-21. The entry corridor represents a finite time (entry window) allotment in which the entry vehicle may reach the prescribed landing site. The complexities of determining this window will be discussed in section 5.6.3.1. The system is further complicated by the effects of the motion of the Moon and the Earth's rotation.

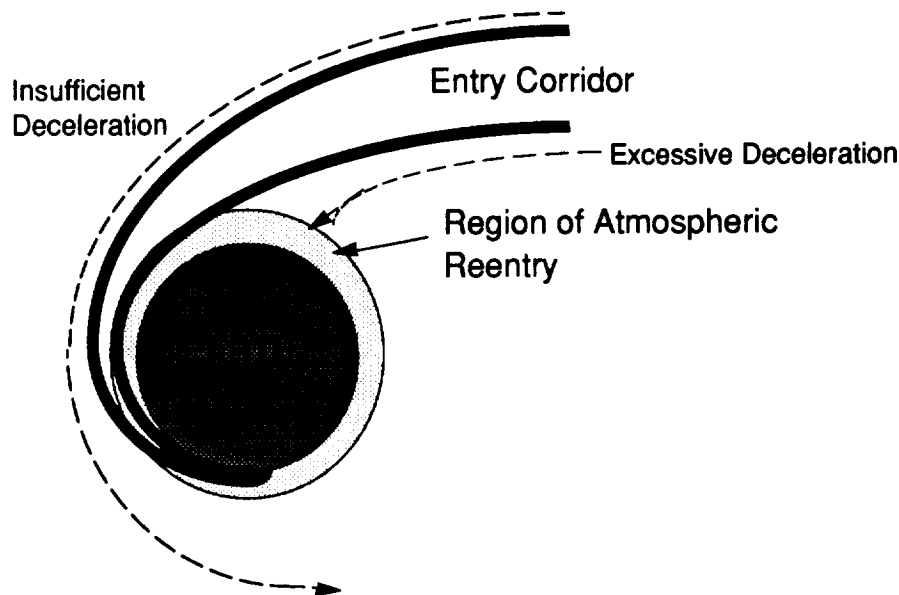


**Figure 5-21**  
**Entry Corridor**

#### 5.3.7.2.1 Entry Corridor

The entry corridor serves as velocity and consequently position boundary conditions for the spacecraft to successfully navigate to the landing site. The upper and lower velocity boundaries represent the overshoot and undershoot criteria. The overshoot criteria is established by examining the maximum allowable range of the spacecraft for landing. This calculation takes into account the range covered during the reentry and parachute phases. The undershoot criteria is established by maximum heating and acceleration limits rather than range requirements. Figure 5-22 gives a graphical representation of the range between overshoot and undershoot.

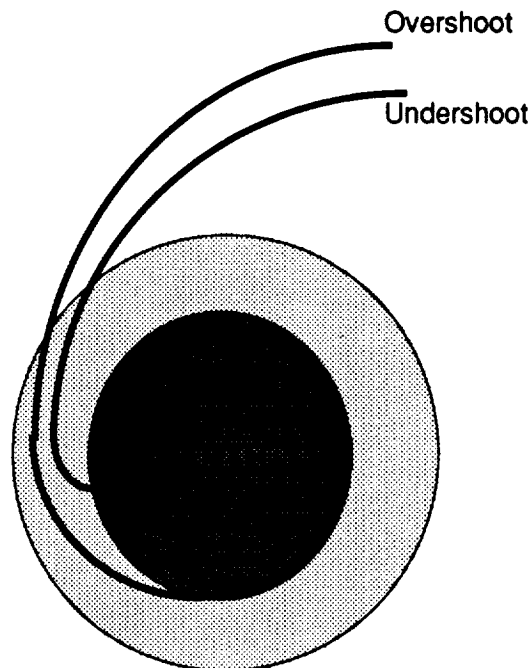


**Figure 5-22**  
**Corridor Sizing**

The reentry corridor also has a finite width. The cross range of the vehicle is controlled by rolling the vehicle during reentry. The current design allows for a maximum cross range of 1540 km. The details of this calculation is discussed in the Appendix.

The final entry corridor is represented by a three dimensional view in figure 5-23. The current injection window has the following dimensions:

Length : 4500 km

width : 1500 km

The consequences of the substantial size of the entry corridor allows for a 1.5 hour margin of error for lunar launch.

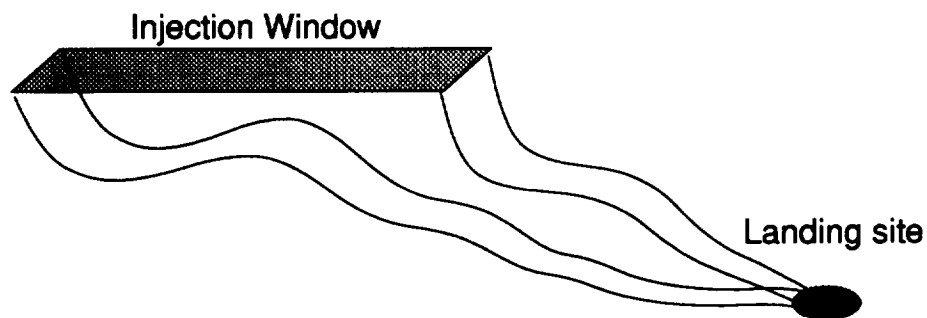


**Figure 5-23**  
**3-D View of the Reentry Window**

#### 5.3.7.2.2 Earth Return Window

The Earth Return Window is a function of time. The injection burn into trans earth orbit must be timed such that the reentry occurs when the entry corridor is in the proper location. A worst case scenario would require the reentry craft to land at an alternate landing site. Although this may be possible, it is not a desirable event. The Moon-Earth transfer trajectory needs to be carefully designed to place the vehicle at the correct location at the correct time.

The Earth return window and return trajectory are dependent on time. The rotational motion of the Moon about the Earth, and the Earth and Moon about their respective axis set the limitations for launch and the trajectory necessary. Section 5.3.2.1 discussed the effects of the orbital inclination of the Moon and Earth system. The conclusion of this discussion was that the return trajectory is dependent on the year, month and day. Figure 5-24 illustrates how the Moon location shifts with respect to the landing site.

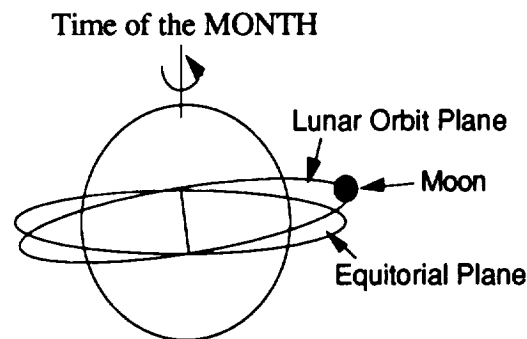


**Figure 5-24**  
**Time-geometry relationship**

The primary effect on the Earth return window is the rotation of the Earth. The landing site rotates  $360^\circ$  a day with respect to the Moon. The entry corridor to the atmosphere for the return trajectory is therefore only available once a day. The length of the reentry corridor allows for a margin of three hours during which the vehicle may successfully land. See Figure 5-25 for a graphical representation of the limitation.



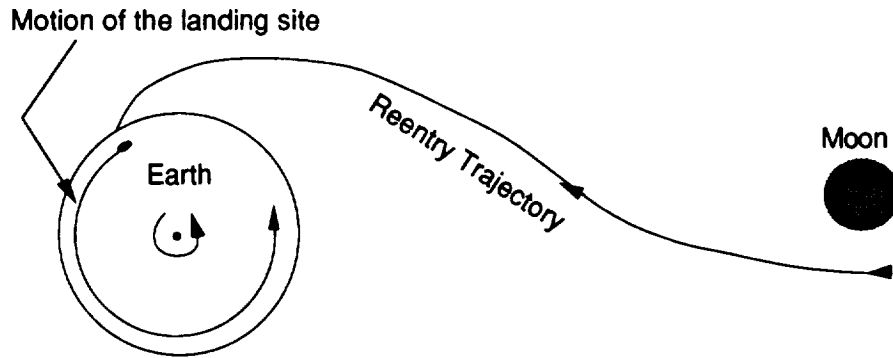


**Figure 5-25**  
**Motion of Landing Site**

In conclusion, the launch window is restricted to once a day with a margin for error of 1.5 hours. The motion of the moon with respect to the earth effects only the return trajectories and the transit time not the actual return window itself.

#### 5.3.7.2.3 Initial Reentry Trajectory

The atmospheric reentry profile will primarily discuss the trajectory from an altitude of approximately 120 km to the drogue parachute opening at an altitude 30 km. The design of this trajectory was carefully controlled to keep the aerodynamic and heating loads below acceptable levels.

The crew capsule will enter the atmosphere at a velocity of approximately 11,000 m/s at an orbital altitude of 120 km. The trans earth trajectory will place the craft within the specified entry corridor at a  $-1^\circ$  entry angle. The maximum angle of entry was calculated to be  $-2.5^\circ$  before the dynamic g-loading exceeded the design limits. The current expected entry angle accuracy is  $.05^\circ$ . The low angle of insertion provides for longer range and lower heating rates and deceleration loads.

#### 5.3.7.2.4 Reentry Trajectory

The reentry trajectory depends on the initial insertion location and angle, the initial velocity, and the maneuver profile of the vehicle. Each insertion location will have an optimum trajectory to the landing site which can be controlled by the bank angle and the angle of attack of the vehicle. The bank angle allows for lateral compensation (cross range), the angle of attack changes the lift to drag ratio thereby extending or shortening the range of the craft. These maneuvers will be performed by the Reaction Control System. The current

trajectory is an approximation of the actual behavior of the craft. During reentry, the craft will have to be continually monitored and the trajectory optimized to the current conditions.

When the spacecraft first enters the atmosphere it will experience oscillations. The first oscillation represents a mission critical phase, where the craft may actually skip back out of the atmosphere. Figure 5-26 displays several different trajectories depending on the initial velocity and angle of entry.

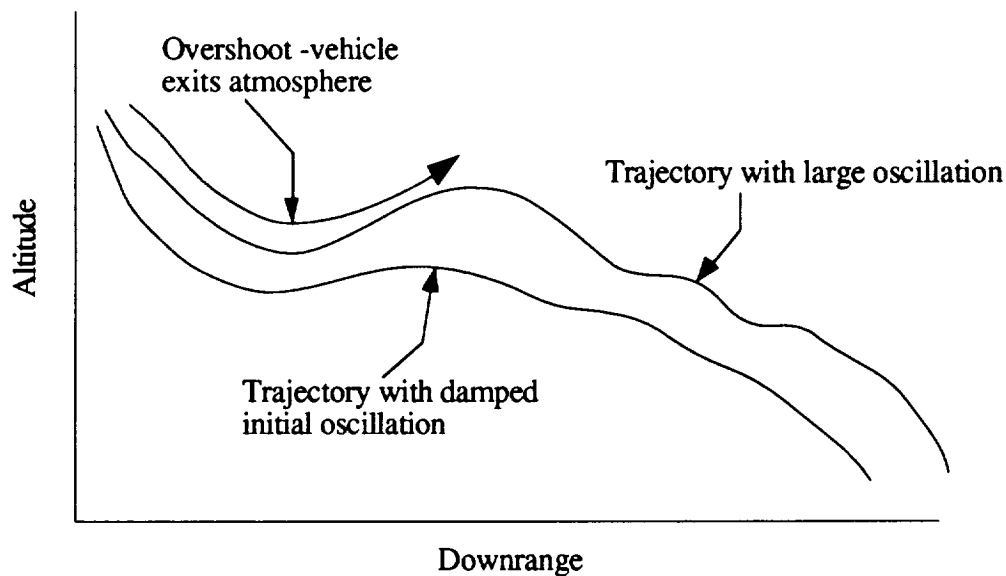


**Figure 5-26**  
**Reentry Trajectories**

To alleviate this problem the following mission profile has been devised. The reentry vehicle will enter the atmosphere at its lowest stable lift over drag angle of attack at about  $64^\circ$  [Minnesota, 1990]. The high drag configuration will aid in alleviating the skip reentry problem. At 70,000 m, the angle of attack will be decreased to its lowest drag configuration of  $24^\circ$ . This maneuver is done to keep the g loading of the craft below the design limits with a safety factor of 1.5.

When the vehicle reaches its lowest point at 55,000 m in its initial plunge the angle of attack will be decreased to its lowest stable lift over drag at  $64^\circ$ . At an altitude of 82,500 m the craft will be rotated  $180^\circ$  so the lift vector points toward the earth. These maneuvers are done to prevent the uncontrolled rebound away from the earth. The resulting maximum altitude is 92,000 m at a velocity of 6,300 m/s.

Slightly after the vehicle reached the highest point in its initial rebound the craft will rotate back and the lift over drag will be increased to its highest value of  $26.5^\circ$ . This maneuver is done to extend the range and to slow the second oscillation drop in altitude. The angle of attack is now kept constant until the parachute system is deployed. Figure 5-27 shows the actual expected trajectory for a  $-1^\circ$  entry angle. Figure 5-28 gives the velocity versus time profile and figure 5-29 shows the loading profile for reentry.

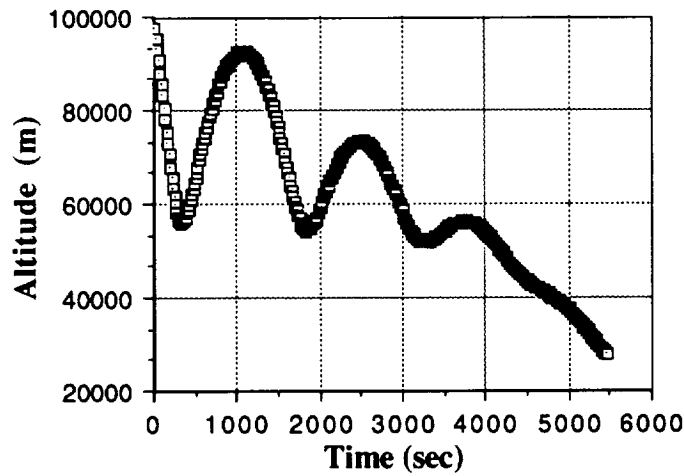


**Figure 5-27**  
**Altitude vs. Time for Reentry Trajectory**

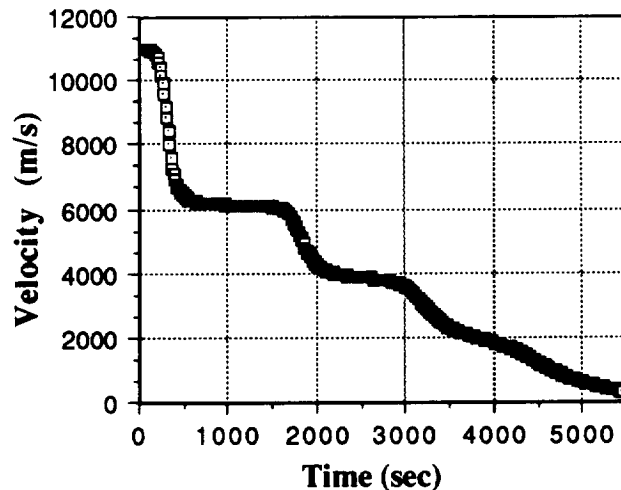


**Figure 5-28**  
**Velocity vs. Time for Reentry Trajectory**

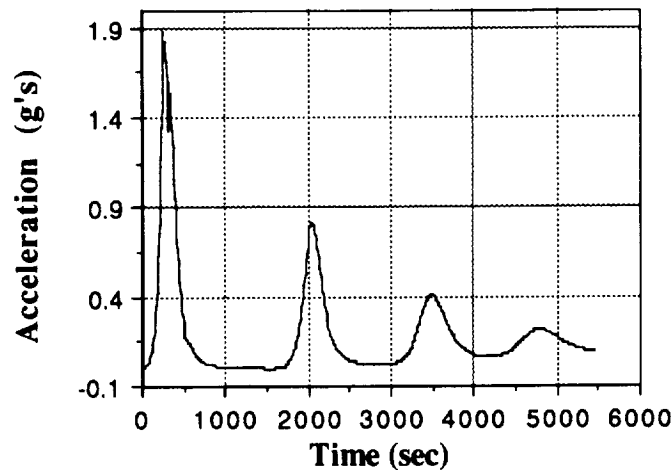


**Figure 5-29**  
**Acceleration vs. Time for Reentry**

#### 5.3.7.2.5 Parachute Operations

The final deceleration and approach to landing is achieved by the deployment of two types of parachutes. The initial deceleration is done by a drogue parachute deployed at about 27 km with an expected velocity of 341 m/s. The Drogue parachute decelerates the craft to 72 m/s at an expected altitude of 3,300 m. A Ram-Air Parafoil is now deployed which deployed resembles a low aspect ratio wing. The parachute provides sufficient control for a runway landing capability. Expected vertical touch down velocity is 2.7 m/s and expected horizontal velocity is 10 m/s. The parachute design allows the reentry vehicle to land similarly to an air plane. This allows for reusability of the craft.

The deployment of the Ram-Air foil will be composed of three stages. The initial deployed airfoil is 22% of the final size. This is done to keep the aerodynamic pressure from damaging the airfoil. Once the velocity is cut in half, lowering the dynamic pressure by three fourths, another 20% of airfoil is disreefed. Disreefing is a process where the existing cells expand to increase the airfoil volume. See Volume 3 for a complete description of this process and the associated hardware. The velocity is now further decreased to 28 m/s where the final 58% of the airfoil is disreefed. The parachute and vehicle combination now enters a full glide to the landing area. Just prior to landing the parachute will perform a flare maneuver to slow the craft to touchdown velocity.

A detailed event profile is contained within Table 5-12. A graphical representation of the events is featured in Figure 5-30 Parachute profile. Please refer to sections 6.2.7.4 and 6.2.7.5 for the detailed discussions of the drogue and parafoil designs.

**Table 5-12: Event Profile**

EVENT	Altitude (m)	Vert. Velocity (M/S)	Hori. Velocity (M/S)	Time (s)
Deploy Drogue	27,000	30	340	0
Deploy Parafoil	3,048	72	0	550
Disreef, 2nd Stage	2,743	36.6	107.8	555.6
Disreef, Completed	2,134	21.3	72.4	576.6
Flap Release	1,829	12.8	43.4	594.5
Full Glide	1,676	7.1	65.2	609.5
Flare Maneuver	30.5	9	25	969.6
Touchdown	0	1.5	20.2	990.5

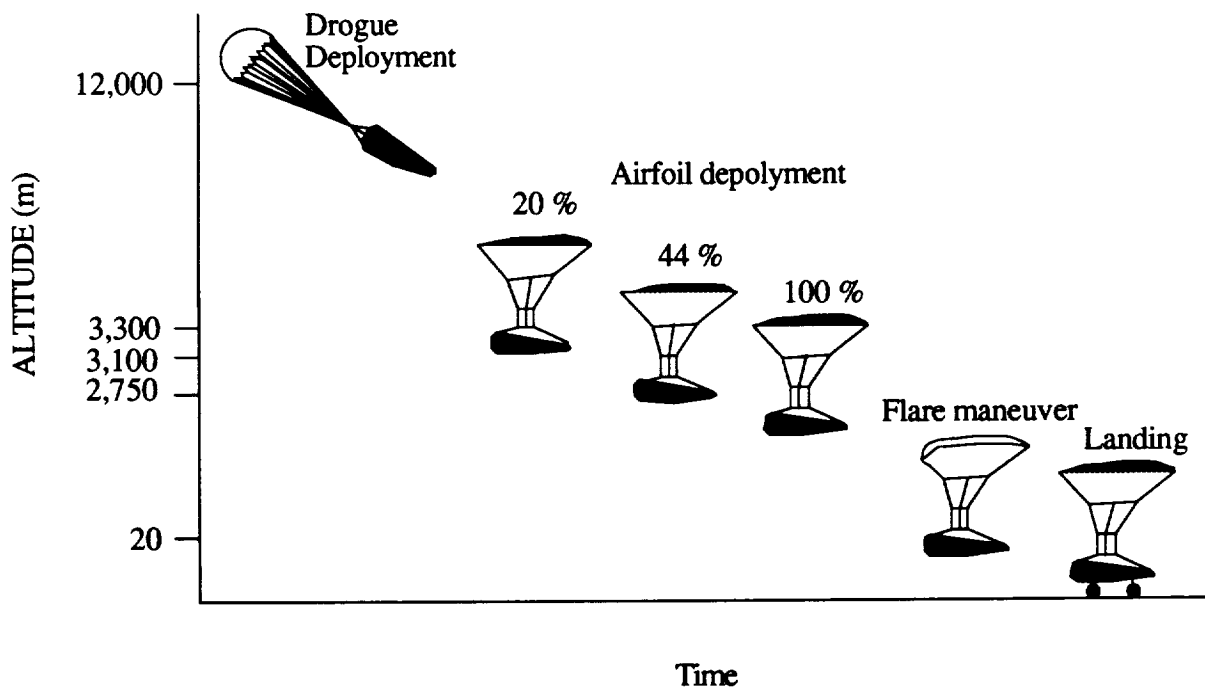


**Figure 5-30**  
**Graphical Representation of the Parachute Profile**

### Definition of Symbols for trajectory section

Symbol	Definition
T	Thrust, N
$g_m$	lunar g 1.655 m/s gravitation acceleration
$g_e$	Earth g 9.8 m/s
h	Altitude, km
m	mass
$r_m$	lunar radius, 1738.3 km
r	radius, km
V	velocity
$\gamma$	flight path angle from vertical, deg
$\psi$	central angle from arbitrary reference
$W_m$	lunar weight ( $m \cdot g_m$ ), N
$W_o$	initial earth weight (in LLO), N
D	Earth-moon distance = 384, 401 km
$\mu_3$	ratio of Moon to Earth mass
$\mu_e$	gravitational parameter of Earth = 3.98601
$\mu_m$	gravitational parameter of Moon =

### Acronyms

MCC	Mid-Course Correction
MEP	Moon-Earth Plane
TEI	Trans- Earth Injection
TLI	Trans-Lunar Injection

## **5.4 Mission Timeline**

This chapter is set up to clarify the order of events that occur for both the piloted and precursor missions of the Columbiad project. Abort sequences are also included for the situations in which the nominal mission event timeline can no longer be followed.

### **5.4.1 Nominal Precursor Mission Event Timeline**

#### **5.4.1.1 Premission Operations**

Map out lunar surface areas to look for a desired landing site  
Send out predeployed beacons for navigational aids

#### 5.4.1.2 Earth Surface Operations

Set up Launch 1 on launch pad 39A

Set up Launch 2 on launch pad 39B

#### 5.4.1.3 Prelaunch Checkout to EOR

Status checks

Launch systems brought to fully operational levels

Countdown

Launch 1 PTLI is Target Vehicle (TV)

Ignite main engines and SRB's	t = 0	h = 0 km
Drop burned out SRB's	t = 123 sec	h = 98 km
Main engine cutoff	t = 416.5 sec	h = 127 km
Ignite second stage	t = 432 sec	h = 131 km
Jettison nose cone and external tank	t = 432 sec	h = 131 km

Separate from LV

Status check of PTLI

Circularization burn t = 967.5 sec h = 200 km

Start 5 PTLI engines

RL-10 firing

Cool down valves

Open 2 inlet valves: 1 H<sub>2</sub>; 1 O<sub>2</sub>

Open 2 propellant management valves

Open shut off valve

Ignite combustion chamber

Shut off 5 PTLI engines

RL-10 shut off

Close 5 valves

Open 2 drainage valves

Higher orbit initial burn h = 200 km

Start 1 PTLI engine (see RL-10 firing)

Shut off 1 PTLI engine (see RL-10 shut off)  $\Delta t = 15$  sec

Higher orbit final burn h = 275 km

Start 1 PTLI engine (see RL-10 firing)

Shut off 1 PTLI engine (see RL-10 shut off)  $\Delta t = 15$  sec

Initiate required thermal control spin for PTLI

Data link with ground control -- low gain antenna	Earth to lunar transit
Status check of PTLI	LEO = 275 km
Orbit and attitude maintenance of PTLI	During wait for EOR
RCS firings	
Open 4 valves: 2 MMH valves; 2 N <sub>2</sub> O <sub>4</sub> valves	
Open shut off valve	
Ignite combustion chamber	
Close 5 valves; Open 2 drainage valves	
Close 2 drainage valves	
Launch 2 Precursor Payload is Chaser Vehicle (CV)	
Ignite main engines and SRB's	t = 0            h = 0 km
Drop burned out SRB's	t = 123 sec     h = 98 km
Main engine cutoff	t = 416.5 sec   h = 127 km
Ignite second stage	t = 432 sec     h = 131 km
Jettison nose cone and external tank	t = 432 sec     h = 131 km
Separate from LV	
Circularization burn	t = 967.5 sec   h = 200 km
Start 3 LBM engine (see RL-10 firing)	
Shut off 3 LBM engine (see RL-10 shut off)	
Higher orbit initial burn	h = 200 km
Start 1 LBM engine (see RL-10 firing)	
Shut off 1 LBM engine (see RL-10 shut off)	$\Delta t = 15$ sec
Higher orbit final burn	h = 275 km
Start 1 LBM engine (see RL-10 firing)	
Shut off 1 LBM engine (see RL-10 shut off)	$\Delta t = 15$ sec
Data link with ground control -- low gain antenna	Earth to lunar transit
High gain antenna deployment	LEO
Deploy any external cameras	LEO
Precursor landing legs deployed on PLM	
Status check of PTLI 1 & Payload Vehicle	LEO
EOR	LEO = 275 km
CV removes any out of plane velocity component	
PLM/BioCan RCS	



Wait phase

CV impulses two times

PLM/BioCan RCS

Despin PTLI

Docking begins

RCS firings (PTLI and PLM/BioCan)

Docking ends

Status check

CV - LV distance = 1000 m

max time ~ 1 hour

#### 5.4.1.4 Trans-Lunar Injection to LLO

Primary Trans-Lunar Injection burn

Launch window to Moon

Start 5 PTLI engines

RL-10 firing

Cool down valves

Open 2 inlet valves: 1 H<sub>2</sub>; 1 O<sub>2</sub>

Open 2 propellant management valves

Open shut off valve

Ignite combustion chamber

Shut off 5 PTLI engines

RL-10 shut off

Close 5 valves

Open 2 drainage valves

Stage PTLI

$\Delta V_{\text{injection 1}} \sim 2414 \text{ m/s}^{**}$

Explosive bolts

Fire staging engines

Secondary Trans-Lunar Injection burn by LBM

$\Delta V_{\text{injection 2}} \sim 726 \text{ m/s}^{**}$

Start 3 LBM engines (see RL-10 firing)

Shut off 3 LBM engines (see RL-10 shut off)

Initiate transit vehicle spin ~1rev/hour

Midcourse Corrections

$\Delta V \sim 120 \text{ m/s allocated}^{**}$

Check out high gain antenna

High and low gain antenna overlap

Switch from low gain to high gain antenna

Lunar braking into LLO

$t \sim 3 \text{ days after launch}$

Restart 3 LBM engines (see RL-10 firing)

Shut off 3 LBM engines (see RL-10 shut off)

$\Delta V_{\text{LLO braking}} \sim 1060 \text{ m/s}^{**}$

#### 5.4.1.5 LLO to Precursor Landing and Deployment

Lunar descent

Window to lunar landing site

Restart 3 LBM engines (see RL-10 firing)

LBM engine throttling

controlled descent

Stage LBM

altitude = 800 m

Shut off 3 LBM engines (see RL-10 shut off)

$\Delta V_{\text{descent}} \sim 1700 \text{ m/s}^{**}$

Explosive bolts to release LBM

Fire staging engines

Lunar hover and land

altitude = 600 m

Start 3 PLM engines (see RL-10 firing)

Shut off 3 PLM engines (see RL-10 shut off)

altitude  $\sim 1 \text{ m}$

Land on 4 landing legs

Deployment of Surface Payloads

touchdown

Deploy 4 support legs

Tip habitat to horizontal position

Fire 3 Star 48/TE-M-236 solid tip-over rockets

$t = 0$

3 solid rocket tip-over motors end firing

$t = 6.5 \text{ sec}$

Stability point is crossed

$t = 6.9 \text{ sec}$

2 throttled XLR-132 liquid rockets brake habitat

maintain tip-over at  $6.9^\circ/\text{sec}$

2 XLR-132 at full thrust -- slows tip-over

$25^\circ$  from horizontal

Habitat is horizontal

tip-over rate reaches  $0^\circ/\text{sec}$

2 landing legs retract -- habitat on 4 support legs

Systems Check on Lunar Surface

#### 5.4.2 Nominal Piloted Mission Event Timeline

##### 5.4.2.1 Earth Surface Operations

Confirmation of Precursor surface payloads status

Set up Launch 3 on launch pad 39A

Set up Launch 4 on launch pad 39B

### 5.4.2.2 Prelaunch Checkout to EOR

Status checks

Launch systems brought to fully operational levels

Countdown

Launch 3 PTLI is Target Vehicle (TV)

Ignite main engines and SRB's	t = 0	h = 0 km
Drop burned out SRB's	t = 123 sec	h = 98 km
Main engine cutoff	t = 416.5 sec	h = 127 km
Ignite second stage	t = 432 sec	h = 131 km
Jettison nose cone and external tank	t = 432 sec	h = 131 km

Separate from LV

Status check of PTLI

Circularization burn	t = 967.5 sec	h = 200 km
----------------------	---------------	------------

Start 5 PTLI engines (see RL-10 firing)

Shut off 5 PTLI engines (see RL-10 shut off)

Higher orbit initial burn

h = 200 km

Start 1 PTLI engine (see RL-10 firing)

Shut off 1 PTLI engine (see RL-10 shut off)

$\Delta t = 15$  sec

Higher orbit final burn

h = 275 km

Start 1 PTLI engine (see RL-10 firing)

Shut off 1 PTLI engine (see RL-10 shut off)

$\Delta t = 15$  sec

Initiate required thermal control spin for PTLI

Data link with ground control -- low gain antenna

Earth to lunar transit

Status check of PTLI

LEO = 275 km

Orbit and attitude maintenance of PTLI

During wait for EOR

RCS firings

Open 4 valves: 2 MMH valves; 2 N<sub>2</sub>O<sub>4</sub> valves

Open shut off valve

Ignite combustion chamber

Close 5 valves; Open 2 drainage valves

Close 2 drainage valves

Launch 4 Piloted Vehicle is Chaser Vehicle (CV)

Ignite main engines and SRB's	t = 0	h = 0 km
-------------------------------	-------	----------

Drop burned out SRB's	t = 123 sec	h = 98 km
-----------------------	-------------	-----------

Main engine cutoff	t = 416.5 sec	h = 127 km
Ignite second stage	t = 432 sec	h = 131 km
Jettison nose cone and external tank	t = 432 sec	h = 131 km
Separate from LV		
Circularization burn	t = 967.5 sec	h = 200 km
Start 3 LBM engine (see RL-10 firing)		
Shut off 3 LBM engine (see RL-10 shut off)		
Higher orbit initial burn		h = 200 km
Start 1 LBM engine (see RL-10 firing)		
Shut off 1 LBM engine (see RL-10 shut off)	$\Delta t = 15$ sec	
Higher orbit final burn		h = 275 km
Start 1 LBM engine (see RL-10 firing)		
Shut off 1 LBM engine (see RL-10 shut off)	$\Delta t = 15$ sec	
Voice and data link with ground control -- low gain antenna	Earth to lunar transit	
High gain antenna deployment	LEO	
Deploy any external cameras	LEO	
Status check of PTLI 1 & Payload Vehicle	LEO	
EOR	LEO = 275 km	
CV removes any out of plane velocity component		
ERM/CM RCS		
Wait phase		
CV impulses two times		
ERM/CM RCS		
Despin PTLI		
Docking begins	CV - LV distance = 1000 m	
RCS firings (PTLI and ERM/CM)		
Docking ends	max time ~ 1 hour	
Status check		

#### 5.4.2.3 Trans-Lunar Injection to LLO

See Section 5.4.1.4

#### 5.4.2.4 LLO to Piloted Vehicle Landing

Use low gain antenna to check status of precursor payload

Lunar descent Window to lunar landing site

Restart 3 LBM engines (see RL-10 firing)

LBM engine throttling controlled descent

Stage LBM altitude = 800 m

Shut off 3 LBM engines (see RL-10 shut off)  $\Delta V_{\text{descent}} \sim 1700 \text{ m/s}^{**}$

Explosive bolts to release LBM

Fire staging engines

Lunar hover and land altitude = 600 m

Start 3 ERM engines (see RL-10 firing)

Shut off 3 ERM engines (see RL-10 shut off) altitude  $\sim 1 \text{ m}$

Touchdown

#### 5.4.2.5 Lunar Surface Operations

Day 1:

CM depressurization

Crew egress

CM repressurization with inert gas

Precursor transmitter shut down

Habitat and SLurPP systems check

Food and supplies transfer from CM to habitat 2 hours x 2 astronauts

Setting up outdoor lighting 2-4 hours x 3 astronauts

Rover deployment

Other cargo (Conveyer, Collector, 2 hours x 2 astronauts

Support Structure etc.) deployment

Day 2 :

Setting up Regolith Support Structure 6-8 hours x 2 astronauts

Assemble Regolith Collector 4 hours x 2 astronauts

Assemble Lunar Conveyer 4 hours x 2 astronauts

Day 3 through Day 8 :

Build regolith protection layer on habitat 80 hours x 2-3 astronauts

Setting up SLurPP 12 hours x 2 astronauts

- Setting up panels
- Setting up cables etc.

Scientific experiments begin

Day 9 onwards :

Scientific experiments

- Lunar Astronomy
- Biological
- Others

Day 15 onwards :

More experiments and exploration -

- Selenology and Selenophysics

#### Average Day (24 hour cycle) on Moon :

Work (IVA / EVA)	8-10 hours
Sleep	6-8 hours
Exercise / Food / Hygiene etc.	4-6 hours
Personal recreation	2-4 hours

At the end of 28 day lunar stay :

Preparation of habitat, power supply, etc for dormancy

Precursor transmitter operational

Prepare ERM and CM for lunar launch

CM depressurization

Crew boarding

CM repressurization

#### 5.4.2.6 Lunar Launch to Return Midcourse Corrections

Lunar Launch to LLO

Launch checkout OK

Restart 3 ERM engines (see RL-10 firing)

Shut off 3 ERM engine (see RL-10 shut off)

Injection for Earth Return

within return launch window

Restart 3 ERM engines (see RL-10 firing)

Shut off 3 ERM engines (see RL-10 shut off)

Switch from high to low gain antenna  
Midcourse Corrections (see RCS firing)

#### **5.4.2.7 Reentry and Landing**

Stage ERM

Explosive bolts

Fire staging engines

ERM burns up

CM reenters Earth's atmosphere safely

Low gain antenna signal transmission

Deploy drogue

Deploy parafoil

Parafoil deployment completed

Flap release

Deploy landing wheels

Full glide

Flare maneuver

Land

Reentry of Earth's atmosphere

as soon as blackout is over

t = 0            h = 27 km

t = 550 sec    h = 3 km

t = 576.6 sec   h = 2.1 km

t = 594.5 sec   h = 1.8 km

t = 609.5 sec   h = 1.7 km

t = 969.6 sec   h = 30 m

t = 990.5 sec

#### **5.4.3 Abort Sequences (Precursor Mission)**

The abort modes available to the precursor mission consist of a subset of the abort modes for the piloted mission (see 5.4.4). The two main goals of the precursor mission abort sequences are 1) range safety, and 2) safing of spacecraft components, where possible. If spacecraft components can be preserved and safely placed on the lunar surface or left in Earth orbit for subsequent usage, the abort mode selected will reflect this decision. For all other circumstances, spacecraft components will be destroyed, deorbited, or placed in a benign trajectory to ensure range safety and/or minimize any orbital debris hazard.

All abort modes non-specific to the piloted mission (i.e., involving a capability to recover the crew) are available to the precursor mission. This includes engine-out capabilities and trajectory modifications.

#### **5.4.4 Abort Sequences (Piloted Mission)**

The abort modes for the piloted phase of Project Columbiad follow two differing philosophical lines depending upon the severity of the emergency. For non-catastrophic failures, an intact abort (i.e., one in which the Crew Module is recovered) will be initiated if feasible. Should this prove unobtainable, as in the case of launch vehicle failure soon after launch, a contingency abort will be initiated. A contingency abort involves abandonment of the spacecraft by the crew. Contingency aborts generally involve the use of the spacecraft ejection seats (an exception is the use of the slidewire escape system while on the launch pad).

The Project Columbiad design maximizes the probability of success and minimizes the chance of catastrophic loss by use of conservative safety factors for all structural components, and by incorporation of high reliability subsystems. Where practical, subsystems are fail-operational, and at least fail-safe.

##### **5.4.4.1 Conditions for Abort**

The abort decision is a complex one which requires weighing the hazards against the desire to continue the mission. The accepted reasons abort include danger to the crew and sufficient malfunction of equipment so that even if the crew is not endangered, the mission will not be a success. More often, aborts occur because of danger to the crew. It is important to layout the different conditions for abort before the mission commences so that ground control and crew have an background against which to make decisions. Since every failure cannot be predicted, it is important to have aborts planned from each phase of the mission and to leave the decision for the abort up to crew and control. The most important goal in an abort or continue decision is that the crew is comfortable with the decision. Crew dissatisfaction, especially about a decision to continue, can have serious consequences.

#### **Critical Mission Phases**

Pre-Launch	Assembly Testing
Launch	Go-No Go Fuel Loading



LEO	Easy Abort Propulsion Check
Lunar Injection Burn	Course Corrections Fuel Margins
Lunar Abort	Easy Abort Power System Check
Descent	Equipment Damage Surface Abort Possibilities with loss of fuel during first 24 hrs
Return	Surface repairs should withstand return voyage

There are two types of abort decisions, those that call for an immediate abort and those which can take a more sit-back-and-wait attitude. Which of these is in effect depends on the level of danger and the phase of the mission.

The first is a conditional danger, in this situation, there is a failure, but there is no immediate danger to the astronauts. This situation requires extensive evaluation, including a possible modification to the mission, but might not lead to an abort. If a failed system can be resuscitated with at least one reliable redundancy or if modifications can be made to the mission profile such that a shortened mission still meets safety criteria. If failure occurs before the TLI burn, abort should be considered for almost any major failure.

The second type is an immediate abort. If there is an imminent and unavoidable disaster, then immediate abort is in order. The implementation of the abort process begins as soon as the danger is identified and confirmed.

#### **5.4.4.2 Redundant-Set-Launch Sequencer Abort**

While the spacecraft is on the launch pad before engine ignition, a slidewire egress system similar to that used by the Space Shuttle is available. In the event of an abort, the crew will cross the egress catwalk and proceed to the opposite side of the launch tower where

multiple slidewire baskets are positioned. These baskets are manually released to transport crewmembers to a recovery area several hundred meters away from the pad. The crewmembers exit the baskets to enter a protected bunker which provides blast protection in the event of an explosion. If needed, an M113 armored personnel carrier parked outside the bunker provides a means of transportation from the site.

#### 5.4.4.3 SRB-Powered Flight Ejection Abort

The spacecraft ejection seats provide the next available abort option from before launch vehicle ignition (should not enough time exist to initiate slidewire abort) until T+82 seconds, when the spacecraft passes through 36 km (120,000 ft.) altitude. In the event of an on-the-pad ejection, however, survivability is crucially dependent upon the nature of the contingency. A full launch vehicle explosion may be sufficiently violent to kill or severely injure the astronauts while still descending underneath their parachute canopies. Ejection following the first 5 seconds of liftoff (after the launch vehicle has cleared the launch tower, initiated the roll maneuver, and gained some horizontal velocity) is considered to be a more survivable abort condition.

#### 5.4.4.4 Capsule Release and Ejection Abort

Following passage of the spacecraft through 36 km altitude, the next abort mode involves separation of the Crew Module from the launch vehicle stack. This is initiated by firing the engines of the Earth Return Module to push the Crew Module away from the launch vehicle. Normal recovery sequences are then followed. In the event of major structural damage or other failure requiring spacecraft abandonment, ejection seat abort can be used once the spacecraft has descended to within the safe operating parameters of the ejection seats.

The CRE abort mode is available beginning at T+117 seconds. Consequently, a window 35 seconds in duration exists in the flight trajectory between the time when ejection seats no longer are available as a means of escape and when capsule abort becomes available. This window is a direct result of the high loading placed on the launch vehicle stack by the attached solid rocket boosters. Abort during this period must be delayed until after the vehicle unloads to below 2.53 g's for adequate separation of the Crew Module from the launch vehicle to occur. Should a catastrophic failure of the launch vehicle stack occur during these 35 seconds, however, a preliminary analysis of the expected breakup loads indicates that the crew module will remain intact following a launch vehicle explosion.

Assuming the crew is not incapacitated, the mission commander can command seat ejection once the crew module has fallen below the 36 km altitude mark. Alternatively, ejection seat activation can be remotely initiated via radio command signal from the Launch Director, or Range Safety Officer.

#### 5.4.4.5 Trans-Atlantic/Abort-Once-Around/Abort-To-Orbit Aborts

Capsule abort may result in landing in one of several possible recovery zones. Abort soon after launch will necessitate a water recovery in the Atlantic Ocean. Abort further along the launch trajectory will result in a Trans-Atlantic (TAL) abort or Abort-Once-Around (AOA) similar to those planned for Space Shuttle contingencies. Primary abort landing sites for TAL/AOA aborts include Banjul, Republic of The Gambia; Dakar, Senegal; and Edwards AFB, California. Emergencies close to final orbital insertion cutoff will be treated as an Abort-To-Orbit (ATO), again similar to standard Space Shuttle criteria.

#### 5.4.4.6 Earth Orbit Abort

A return-to-earth abort any time prior to the Primary Trans-Lunar Injection (PTLI) can be initiated using the propulsion systems of the Earth Return Module. Following separation of the Earth Return Module and Crew Module from the remainder of the spacecraft stack, the primary propulsion system (3 RL-10 engines) fires to deorbit the vehicle for Earth return. In the event of primary propulsion system failure, the ERM reaction control system is capable of deorbiting the vehicle. The Earth Return Module is separated normally following the deorbit burn, and recovery of the Crew Module follows in standard sequence. Potential landing sites for Earth Orbit Abort include those previously mentioned for TAL/AOA aborts, as well as Rota, Spain; Andersen AFB, Guam; Hickam AFB, Hawaii; White Sands Proving Ground, New Mexico; and Kennedy Space Center, Florida.

Remaining elements of the spacecraft stack may be deorbited or left in orbit as dictated by safety criteria or mission requirements.

#### 5.4.4.7 Trans-Lunar Injection Abort

The Primary Trans-Lunar Injection stage possesses a single engine-out capability (4 out of 5 engines operable) for the entire length of the PTLI burn. Similarly, the Lunar Braking Module possesses a single engine-out capability (2 out of 3 engines operable) for its portion of the trans-lunar injection burn.

#### 5.4.4.8 Trans-Lunar Abort

During Trans-Lunar coast, several abort modes are available depending upon the timing, nature, and severity of the emergency. A direct return abort can be initiated at any time during the outbound leg. For this mode, the primary propulsion systems of the LBM or ERM (or both) are used. These stages fire to cancel the forward velocity of the spacecraft and place the vehicle on a return trajectory. A second abort mode (Near Lunar Abort) delays the initiation of an abort propulsive burn until the spacecraft is within the vicinity of the Moon (3 days out from Earth). Near the Moon, while behind the visible face, the primary propulsion system of the LBM or ERM burns to place the spacecraft onto an earth-return trajectory. This abort mode places less demanding requirements upon the spacecraft propulsion and guidance systems, and would be used if the extra transit time needed to complete such an abort were deemed available.

#### 5.4.4.9 Lunar Orbit Insertion Abort

The Lunar Braking Module possesses a single engine-out capability (2 out of 3 engines operable) during the Lunar Orbit Insertion (LOI) burn. In the event of a decision to abort landing operations at this point, the ERM (along with the remaining propulsive capability of the LBM, if needed) injects the spacecraft into an Earth-return trajectory using the Near Lunar Abort mode.

#### 5.4.4.10 Descent Abort

During powered descent, several abort options are available depending upon the nature of the emergency. The LBM is capable of completing its descent propulsion burn with a single engine-out failure, although the fuel reserve available (in the ERM) for final hover is minimized, decreasing the time available to the astronauts for last minute flightpath corrections. The ERM is double engine-out failure tolerant (1 out of 3 engines operable) for landing; however, two engines must be operable to complete an abort to lunar orbit. An abort to lunar orbit (vs. an abort to the lunar surface with degraded performance) will be accomplished when the failure is such that a stay on the lunar surface is not desirable. Aborts to lunar orbit are available at any time during the landing sequence, and are initiated by jettisoning the LBM and igniting the primary propulsion system of the ERM to complete orbital injection. If an abort to lunar orbit is chosen prior to LBM separation, the primary propulsion system of the LBM may be used to assist in this burn (or increase the abort decision-making time available to the crew).

#### **5.4.4.11 Surface Abort**

Following landing on the lunar surface, an immediate abort (i.e., accomplished within a matter of minutes) to lunar orbit can be initiated within the first 3 hours after touchdown. After 3 hours, the vehicle is powered down and 24 hours is required before an abort to lunar orbit can be completed. Aborts to lunar orbit are available at any time during the nominal 28-day mission stay.

#### **5.4.4.12 Ascent Abort**

During the ascent burn, the ERM is single engine-out capable (2 out of 3 engines operable). A double engine-out abort is possible only during the final phase of the insertion burn.

#### **5.4.4.13 Trans-Earth Injection Abort**

The ERM is double engine-out capable (1 out of 3 engines operable) during the Trans-Earth Injection (TEI) burn.

#### **5.4.4.14 Post-Reentry Abort**

Following reentry, the ejection seats are again available for spacecraft abandonment in the event of primary recovery system failure. To operate the ejection system, the spacecraft must be below 36 km altitude and 308 m/s equivalent airspeed.

### **5.5 Loading Profile**

The loading profile is characterized by each mission phase. The mission phases consists of the launch vehicle, each burn during the mission profile, reentry into the Earth's atmosphere, and parachute operations. For the following discussion, each burn during the mission profile is headed by the corresponding propulsion stage responsible for the burn.

#### **5.5.1 Launch Vehicle Loading**

The launch vehicle loading is mainly due to dynamic forces and booster ignition and separation. The large load spikes are mainly due to solid booster ignition and separation. Figure 5-31 shows the launch loading vs. time. The launch loads will be explained in greater detail in Volume 3.

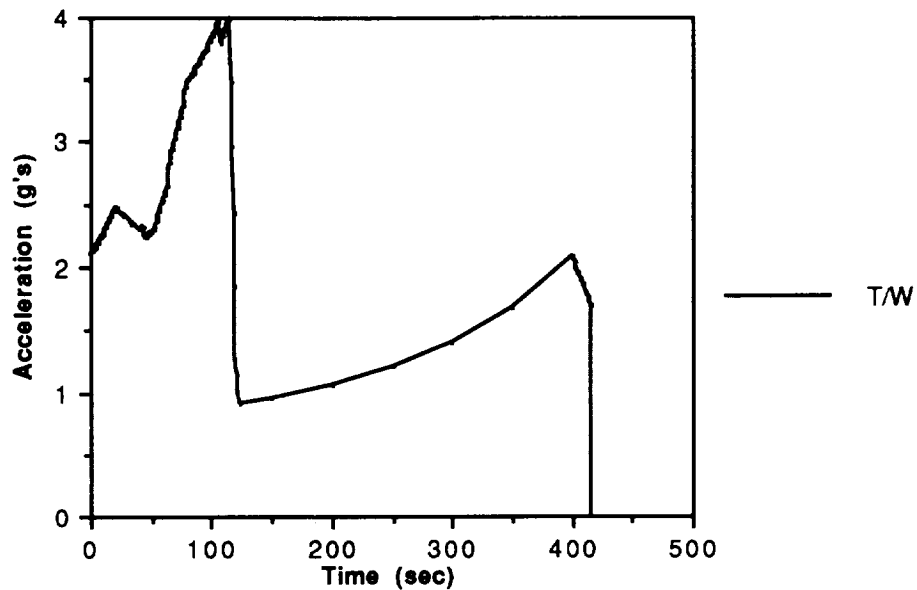


**Figure 5-31**  
**Launch Loading**

### **5.5.2 PTLI Propulsion Stage**

As discussed previously in the time line the PTLI stage performs two burns : orbit circularization and Trans-Lunar injection. The loading is low for both burns mainly due to the amount of mass the stage needs to propel. Figures 5-32 and 5-33 illustrate the g-loading versus time for both phases.

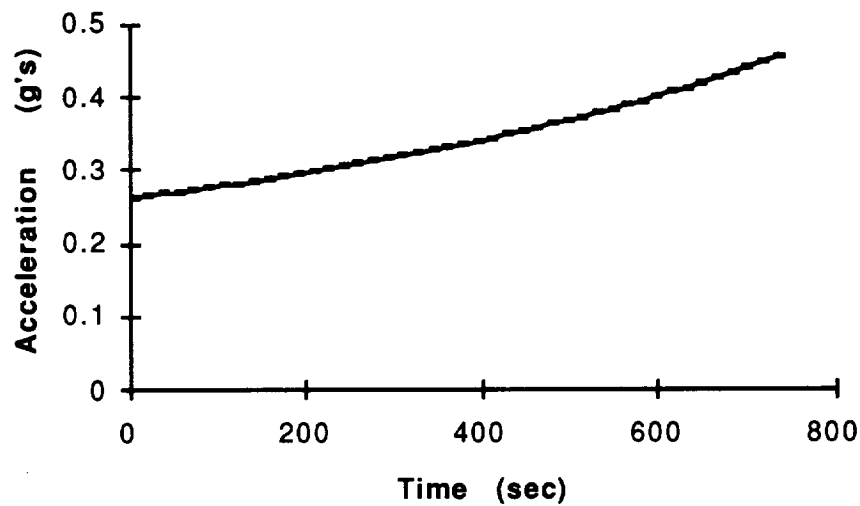


**Figure 5-32**  
**PTLI Loading from Trans-Lunar Injection Burn**

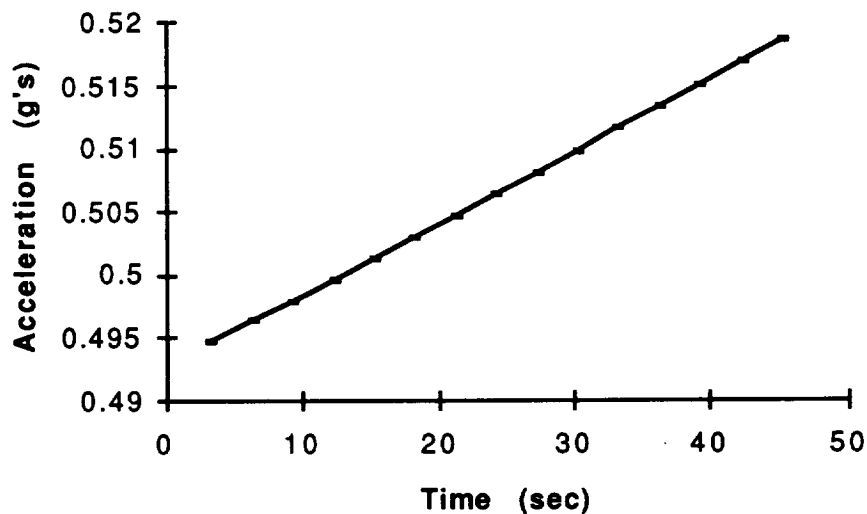


**Figure 5-33**  
**PTLI Loading from Circularizing Burn**

### **5.5.3 The LBM loading profile**

The Lunar Braking Module perform the maneuvers discussed in the mission time line (section 5.4) namely: The orbit circularization, second leg of the TLI burn, midcourse maneuvers, and Lunar orbit breaking and descent. This loading is shown in Figures 5-34, 5-35, 5-36, and 5-37.

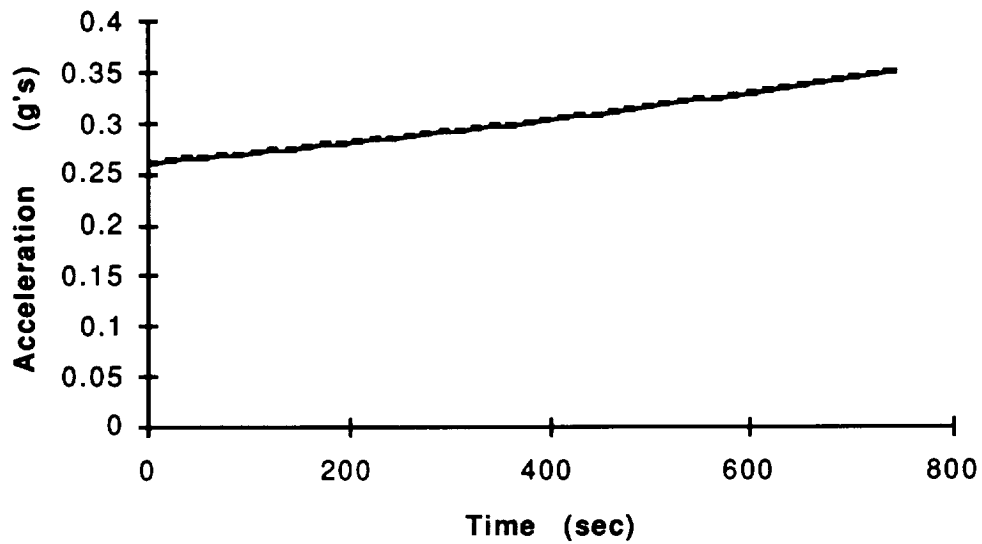


**Figure 5-34**  
**LBM Loading during LEO Circularization**

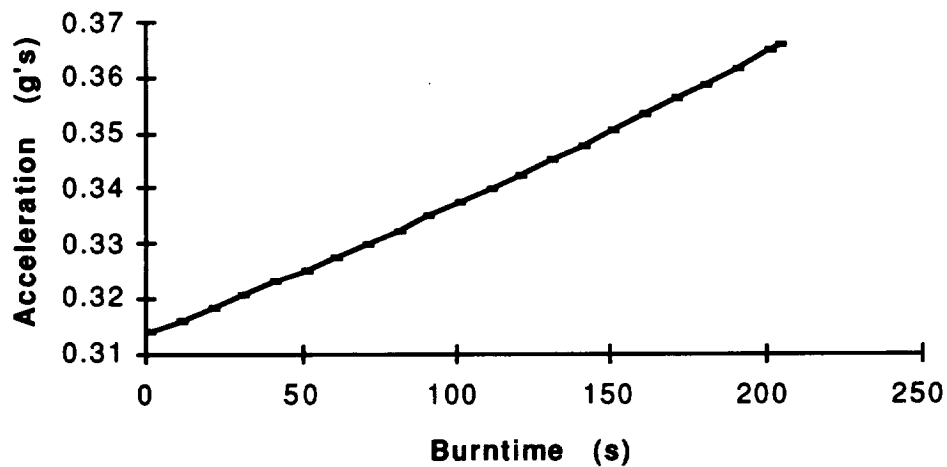


**Figure 5-35**  
**LBM Loading due to the TLI Burn**



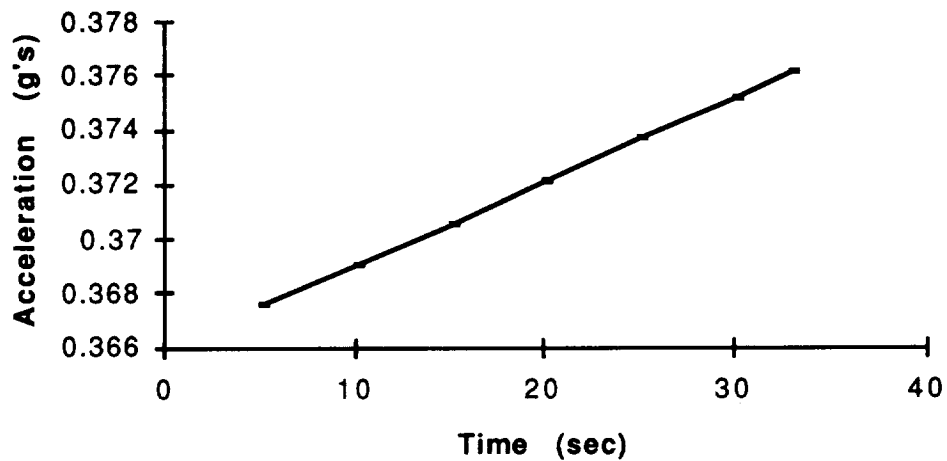


**Figure 5-36**  
**LBM Loading from Midcourse Burn**

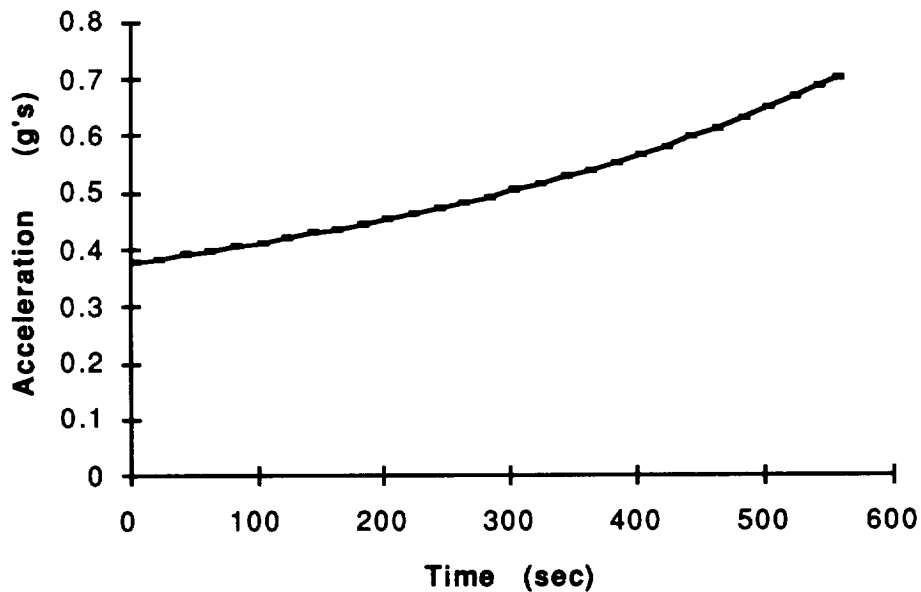


**Figure 5-37**  
**LBM Loading from Lunar Orbit Braking Burn**

#### **5.5.4 ERM Loading Profile**

The Earth Return Module will experience the following expected loads during :  
Lunar hover and landing, Lunar launch burn, Trans-Earth burn, and midcourse correction burns. Figures 5-38 through 5-41 show these loading profiles.

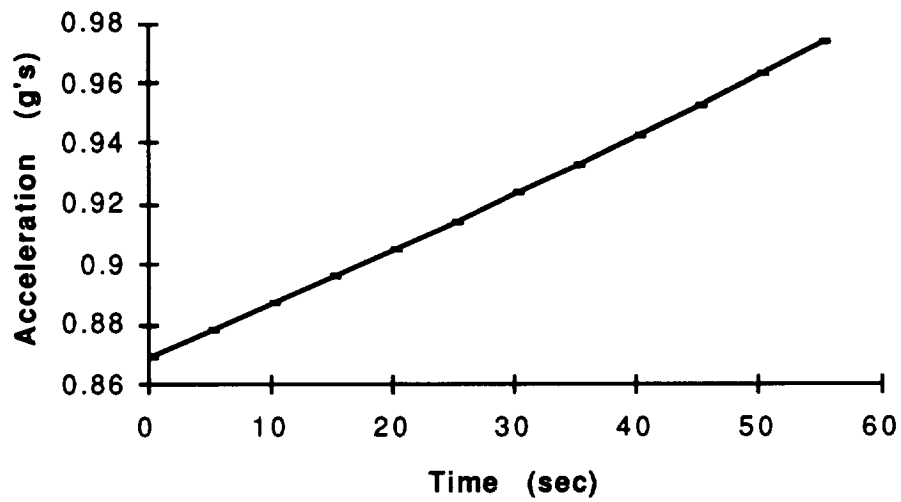


**Figure 5-38**  
**ERM Loading during Lunar Hover**

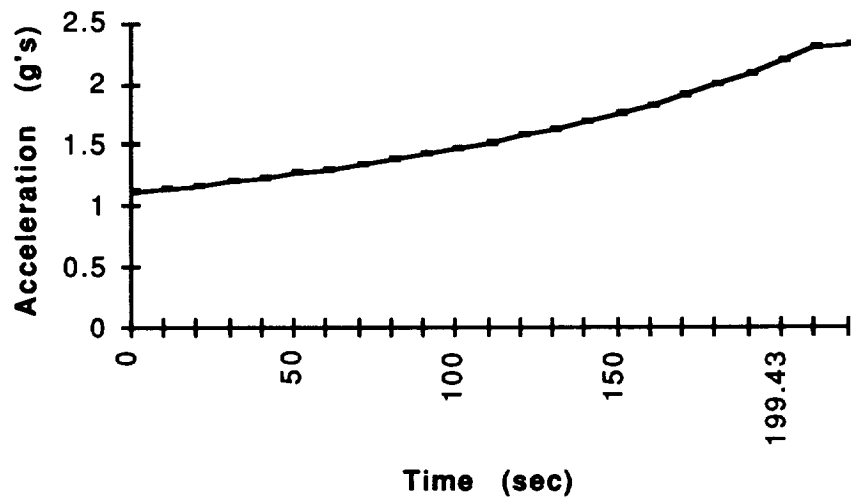


**Figure 5-39**  
**ERM Loading during Lunar Launch**

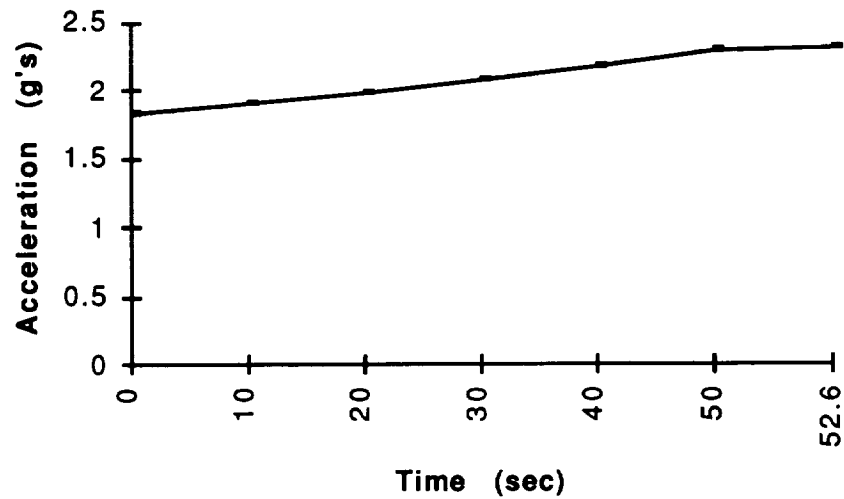


**Figure 5-40**  
**ERM Loading during Trans-Earth Burn**

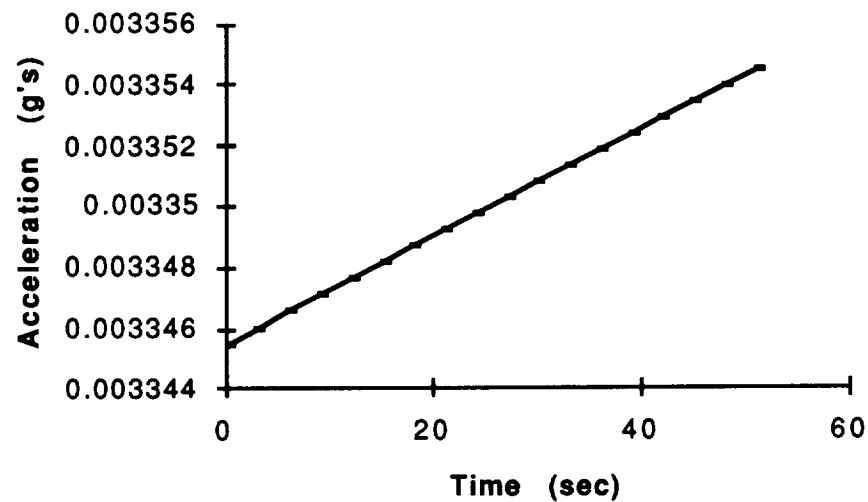


**Figure 5-41**  
**ERM Loading during Midcourse Maneuvers**

#### **5.5.5 Reentry Loading of the Command Module**

The reentry loads are primarily due to areodynamic forces. The peak forces are experienced as the craft dips deeply into the atmosphere. See Figure 5-42.

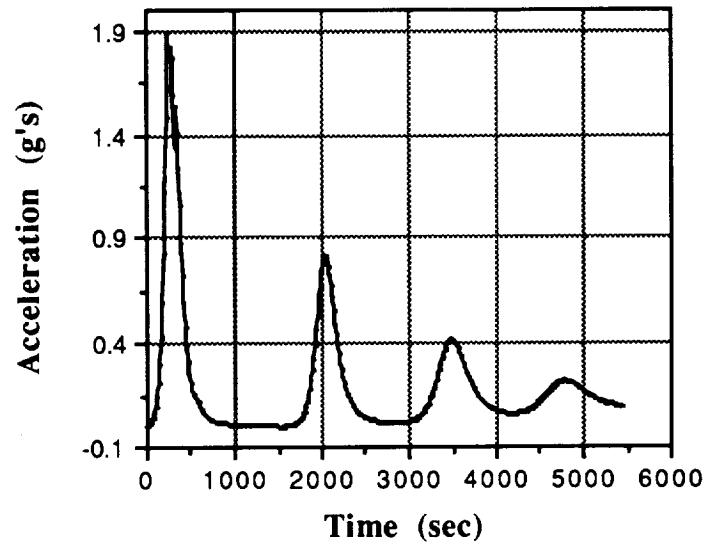


**Figure 5-42**  
**Reentry Loading**

#### **5.5.6 Parachute Loading**

The Parachute loading is primarily due to the opening shock of the parachute. Both the drogue and parafoil chutes will experience variable loading due to the disreefing of the main parachute prior to full deployment.

##### **5.5.6.1 Drogue Parachute**

The drogue parachute experiences a moderate initial loading from the disreefing and the peak loading is experienced during full deployment. Figure 5-43 shows the loading on the drogue parachute.

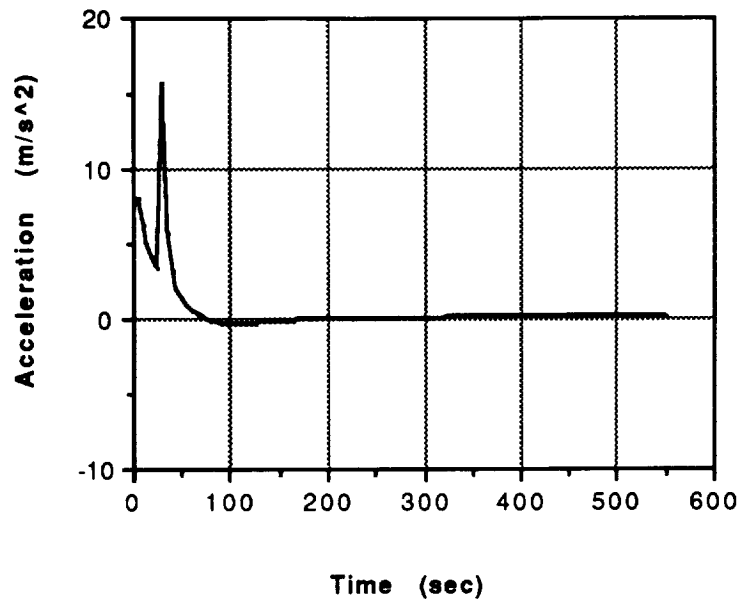


**Figure 5-43**  
**Drogue Parachute Loading**

#### 5.5.6.2 Parafoil Deployment

The loading during the final stage of descent is dominated by the three stage disreefing until final deployment. High loading spikes are expected at these points. The load factor at each one of these points have been calculated and are displayed in Table 5-13 (see section 6.2.7.5).

**Table 5-13: Parafoil Load Factors**

<b>Disreefing percentage</b>	<b>Expected Load (N)</b>	<b>Load factor (g's)</b>
<b>25 %</b>	93741.7	1.28
<b>50 %</b>	42332.6	0.58
<b>100 %</b>	37502.9	0.51

## **5.6 Mission Reliability Analysis**

A reliability analysis was conducted in order to determine how well the Columbiad design meets top level mission success and survivability requirements. As a start, the reliabilities for each component or subsystem were compiled together. Where no reliability numbers were available, appropriate estimates were made. After the initial overall mission success and survivability probabilities were calculated, some minor changes in required component reliabilities and/or redundancy were made to bring the overall reliabilities up to par with the top level requirements. The end result is a list of minimum required reliabilities for components that are to be used in the Columbiad mission.

### **5.6.1 Event Breakdown**

Since there are two missions associated with the Columbiad mission, a precursor and a piloted mission, the number of events to evaluate for mission success and survivability is nearly twofold. The precursor mission was broken up into sixteen distinct events while the piloted mission was broken up into an additional 25 events (totaling 41 distinct events). These 41 events are collections of the more detailed events that can be found in section 5.4. Tables 5-14 and 5-15 show what reliability corresponds to each event and what components and/or subsystems are associated with it.

**Table 5-14: Precursor Mission Event Break-up**

Event #	Event	Components of Event	Reliability
1	L1 to LEO	Launch Vehicle*3 (5 RL10) burns*power*valves	0.99869
2	Maintain orbit until L2	Power*PTLI C3 * GNC Stationkeeping	0.99989
3	L2 to LEO	Launch Vehicle*3 (3 RL10) burns*power*valves	0.99869
4	EOR & Docking	GNC Rendezvous	0.99888
5	LEO operations (antenna depl)	Power*LEO structures depl* C3	0.99979
6	PTLI burn	(5 RL10) burn*valves*power*GNC TLI/MidC Prec	0.99891
7	PTLI staging	staging rel	0.99950
8	STLI burn by LBM	(3 RL10) burn*valves*power*GNC TLI/MidC Prec	0.99891
9	Midcourse corrections	power * GNC TLI/Midc	0.99901
10	High gain antenna operational	power*HG antenna	0.99989
11	Lunar braking burn	(3 RL10) burn*valves*power*GNC LOI/land Prec	0.99809
12	Initial lunar descent burn	(3 RL10) burn*valves*power*GNC LOI/land Prec	0.99809
13	LBM staging	staging rel	0.99950
14	Final descent burn	(3 RL10) burn*valves*power*GNC LOI/land Prec	0.99809
15	PLM hover and land	Precursor Str landing	0.99990
16	Deployment of Surf Payloads	Surf Payl depl	0.98000

**Table 5-15: Piloted Mission Event Break-up**

Event #	Event	Components of Event	Reliability
17	L3 to LEO	Launch Vehicle*3 (5 RL10) burns*power*valves	0.99869
18	Maintain orbit until L4	Power*PTLI C3 * GNC Stationkeeping	0.99989
	<b>Begin Piloted portion</b>		
19	L4 to LEO	Launch Vehicle*3 (3 RL10) burns*power*valves	0.99869
20	EOR & Docking	GNC Rendezvous	0.99888
21	LEO operations (antenna depl)	Power*LEO structures depl* C3	0.99979
22	PTLI burn	(5 RL10) burn*valves*power*GNC TLI/MidC Pil	0.99979
23	PTLI staging	staging rel	0.99950
24	STLI burn by LBM	(3 RL10) burn*valves*power*GNC TLI/MidC Pil	0.99979
25	Midcourse corrections	power * GNC TLI/Midc	0.99901
26	High gain antenna operational	power*HG antenna	0.99989
27	Lunar braking burn	(3 RL10) burn*valves*power*GNC LOI/land Pil	0.99909
28	Initial lunar descent burn	(3 RL10) burn*valves*power*GNC LOI/land Pil	0.99909
29	LBM staging	staging rel	0.99950
30	Final descent burn	(3 RL10) burn*valves*power*GNC LOI/land Pil	0.99909
31	ERM hover and land	Piloted Struc landing	0.99990
32	Lunar surface survivability	Hab env*space suit	0.99947
33	Lunar Launch	(3 RL10) burn*valves*power*GNC LOI/land Pil	0.99909
34	Injection for Earth Return	(3 RL10) burn*valves*power*GNC LOI/land Pil	0.99909
35	Midcourse corrections	power*GNC MidC Pil	0.99989
36	ERM staging	staging	0.99950
37	CM reentry	reentry*CM env (for entire trip)	0.99959
38	Drogue deployment		0.99900
39	Chute deployment		0.99900
40	Landing wheel deployment		0.99900
41	CM Landing		0.99990
	Abort Mode 1	Ejection seats	0.95000
	Abort Mode 2	ERM burn + 36 + 37 + 38 + 39 + 40 + 41	0.99509
	Abort Mode 3	ERM burn + 35 + 36 + 37 + 38 + 39 + 40 + 41	0.99498
	Abort Mode 4	33 + 34 + 35 + 36 + 37 + 38 + 39 + 40 + 41	0.99407
	Abort Mode 5	Ejection seats	0.95000

The abort modes mentioned in Table 5-15 are those that are mentioned in section 5.4.4. There are essentially four different event sequences that can be used at different times during the piloted mission to abort from the nominal mission.

### **5.6.2 Component or Subsystem Break-up**

Each component or subsystem reliability is shown in Table 5-16. The boldface values in the initial reliability column are reliability numbers that were found for a specific component while the plain text initial reliability numbers are good estimates. For components or subsystems that did not have a good initial reliability estimate, a minimum final reliability was set in the fourth column. This would be the final reliability goal of the subsystem when components were tested out and levels of redundancy were determined more solidly.

The level of redundancy is set in the third column. This column is labeled as the number of [component/subsystem] failures intolerance because there are situations in which full redundancy does not exist, but "k-out-of-n" [Wertz, 1991] redundancy does. A good example of this partial redundancy is the single engine out capability in all of the stages. Regardless of whether three or five engines exist in a stage, two engine outs are required before the system is unable to tolerate the lack in performance.

The final reliability for a subsystem or component grouping is determined by the overall layout of the component grouping. The layouts for the component groupings in 5-16 are often combinations of series and parallel component groupings -- not solely one or the other. The subsystem sections in Volumes II and III should explain the layout in more detail.

**Table 5-16: Component/Subsystem Reliabilities**

<b>Subsystem or Component</b>	<b>Initial Reliability</b>	<b># of Failures Intolerance</b>	<b>Final Reliability</b>
Launch Vehicle			0.999
Stage power source			0.99999
5 RL10 ignition	<b>0.99867</b>	2	0.99999999999687
3 RL10 ignition	<b>0.99867</b>	2	0.99999823110000
RL10 valves			0.9999
8 engine RC System		1	0.9995
16 engine RC System		2	0.99999975
Staging			0.9995
Earth sensor	<b>0.998</b>		
Rate gyro 2 sets of 3	<b>0.999</b>	2	0.99999998
GNC Stationkeeping			0.99999975
GPS Receiver	0.99999		



Ground tracking	0.99999		
Docking camera	0.95	3	0.999875
Docking laser radar	0.999		
GNC Rendezvous			0.998875125
INS	0.999		0.99999998
Star Tracker 3	0.99	2	0.9999
Sun sensor electronics	0.999125		
Sun sensor	0.999996		
GNC TLI/MidC Precursor			0.999020822
Transponder Radar	0.98	2	0.9996
Lunar surface beacon	0.98	2	0.9996
Boulder detection			0.999
GNC LB & land Precursor			0.99820071
Pilot sighting			0.9999
GNC TLI/MidC Piloted			0.999899642
Pilot sighting/override			0.9999
GNC LB & land Piloted			0.99919981
Stability wings			0.99
GNC reentry			0.999995
Structural LEO Depl			0.9999
Precursor Str Landing			0.9999
Piloted Str Landing			0.9999
C3 HG Antenna			0.9999
Surf Payload Depl			0.98
Data processor	0.99	3	0.999999
Other PTLI C3			0.9999
C3 PTLI			0.999899
HP GaAs Computer	0.99	3	0.999999
Other CM & ERM C3			0.9999
C3 CM & ERM			0.999899
C3 Habitat			0.999899
Data Processor	0.99		0.99
Solid State Memory	0.95		0.95
Other Rover C3			0.99
C3 Rover			0.931095

O2 tank	0.99	3	0.999999
N2 tank	0.99	3	0.999999
H2O tank	0.999	6	1
Wash water recovery	0.95	3	0.999875
CO2 molecular sieve	0.95	2	0.9975
LiOH system	0.9995	1	0.9995
Thermal control	0.9999	1	0.9999
Humidity control	0.9999	1	0.9999
Fire prevention	0.9999	1	0.9999
Habitat environment			0.999573065
Space suit			0.9999
O2 tank	0.99	3	0.999999
N2 tank	0.99	3	0.999999
H2O tank	0.999	2	0.999999
LiOH system	0.9999	1	0.9999
Thermal control	0.9999	1	0.9999
Humidity control	0.9999	1	0.9999
Fire prevention	0.9999	1	0.9999
CM environment			0.999597061

### **5.6.3 Reliability Analysis Summary**

At the end of the analysis, the total mission success probability was 95.095% while the mission survivability was 99.693%. The mission success probability meets the overall Columbiad mission success goal of 95%. The mission survivability, however, falls slightly under the Columbiad mission survivability target of 99.9%. Tables 5-17 and 5-18a and b show how these final probabilities were calculated.

The inherent reliability of a step is the value calculated in Tables 5-14 and 5-15 while the probability of reaching the step is the probability of reaching the previous step multiplied by the inherent reliability of the previous step. The probability of reaching the first step in both the precursor and piloted mission is 1. In other words, the analysis is based upon the assumption that the first launch of each mission will occur. The probability of completing the last step in each mission is the mission success probability. The total mission success probability is then the product of the two individual mission success probabilities.

For the case of the piloted mission 5-18b details the abort failure probability. The probability that an abort will be required is the inherent reliability value subtracted from one. The abort reliability is the reliability calculated in Table 5-15. The abort unreliability

is this abort reliability subtracted from one. The abort safety failure probability is then the product of the probability of reaching the step, the abort probability, and the abort unreliability. This is the probability that the crew will perish at this step. The crew nonsurvivability probability is the sum of these abort failure probabilities. The survivability, or crew safety, is then this value subtracted from one.

Despite the fact that the crew survivability goal falls slightly below the top level survivability goal, it is still very high. There are numerous places in which small reliability improvements can be made in order to increase the crew safety probability to this desired level. However, for the level of reliability analysis that was conducted, the changes that could be made at this point would not be very meaningful in the overall end design. Hence the reliability requirements were left at the already high values that exist in this analysis with the understanding that a much more complete analysis would be conducted at a later step in the design process.

**Table 5-17: Precursor Mission Success Probability**

Event #	PRECURSOR EVENTS	Inherent reliability	Probability of reaching step
1	L1 to LEO	0.9987	1.00000
2	Maintain orbit until L2	0.9999	0.99869
3	L2 to LEO	0.9987	0.99858
4	EOR & Docking	0.9989	0.99727
5	LEO operations (antenna depl)	0.9998	0.99614
6	PTLI burn	0.9989	0.99594
7	PTLI staging	0.9995	0.99485
8	STLI burn by LBM	0.9989	0.99435
9	Midcourse corrections	0.9990	0.99327
10	High gain antenna operational	0.9999	0.99229
11	Lunar braking burn	0.9981	0.99218
12	Initial lunar descent burn	0.9981	0.99028
13	LBM staging	0.9995	0.98839
14	Final descent burn	0.9981	0.98789
15	PLM hover and land	0.9999	0.98601
16	Deployment of Surf Payloads	0.9800	0.98591
	<b>Precursor Mission Success</b>	<b>0.96619</b>	

**Table 5-18a: Probability of Piloted Mission Success and Survivability**

Event #	PILOTED MISSION EVENTS	Inherent reliability	Probability of reaching step
17	L3 to LEO	0.9987	1.00000
18	Maintain orbit until L4	0.9999	0.99869
	<b>Begin Piloted portion</b>		
19	L4 to LEO	0.9987	0.99858
20	EOR & Docking	0.9989	0.99727
21	LEO operations (antenna depl)	0.9998	0.99614
22	PTLI burn	0.9998	0.99594
23	PTLI staging	0.9995	0.99573
24	STLI burn by LBM	0.9998	0.99523
25	Midcourse corrections	0.9990	0.99502
26	High gain antenna operational	0.9999	0.99403
27	Lunar braking burn	0.9991	0.99392
28	Initial lunar descent burn	0.9991	0.99302
29	LBM staging	0.9995	0.99211
30	Final descent burn	0.9991	0.99162
31	ERM hover and land	0.9999	0.99071
32	Lunar surface operations success	0.9995	0.99061
33	Lunar Launch	0.9991	0.99009
34	Injection for Earth Return	0.9991	0.98919
35	Midcourse corrections	0.9999	0.98829
36	ERM staging	0.9995	0.98818
37	CM reentry	0.9996	0.98768
38	Drogue deployment	0.9990	0.98728
39	Chute deployment	0.9990	0.98629
40	Landing wheel deployment	0.9990	0.98531
41	CM Landing	0.9999	0.98432
	<b>Piloted Mission Success</b>	<b>0.98422</b>	
	<b>Precursor Mission Success</b>	<b>0.96619</b>	
	<b>Total Mission Success</b>	<b>0.95095</b>	
	<b>Crew Safety</b>	<b>0.99693</b>	

**Table 5-18b: Probability of Piloted Mission Success and Survivability**

Event #	Abort probability	Abort reliability	Abort unreliability	Abort safety failure probability
17				
18				
19	0.00131	0.95000	0.05	6.56544E-05
20	0.00112	0.99509	0.004909842	5.50786E-06
21	0.00021	0.99509	0.004909842	1.02703E-06
22	0.00021	0.99498	0.005019657	1.05157E-06
23	0.00050	0.99498	0.005019657	2.4991E-06
24	0.00021	0.99498	0.005019657	1.05966E-06
25	0.00099	0.99498	0.005019657	4.94054E-06
26	0.00011	0.99498	0.005019657	5.48862E-07
27	0.00091	0.99498	0.005019657	4.54945E-06
28	0.00091	0.99498	0.005019657	4.5453E-06
29	0.00050	0.99498	0.005019657	2.49003E-06
30	0.00091	0.99498	0.005019657	4.53889E-06
31	0.00010	0.99498	0.005019657	4.97303E-07
32	0.00053	0.99407	0.005926948	3.09354E-06
33	0.00091		1	0.000902831
34	0.00091		1	0.000902008
35	0.00011		1	0.000109064
36	0.00050		1	0.000494088
37	0.00041		1	0.000402912
38	0.00100	0.95000	0.05	4.9364E-05
39	0.00100	0.95000	0.05	4.93146E-05
40	0.00100	0.95000	0.05	4.92653E-05
41	0.00010	0.95000	0.05	4.9216E-06
			<b>Crew Safety</b>	<b>0.996934228</b>

## REFERENCES:

- AEM 5331 Class of 1990, "Biconic Cargo Return Vehicle with an Advanced Recovery System," University of Minnesota, N90-26052, p 142.
- Akridge, Charles M. and Harlin, Sam H., "Parametric Performance Analysis of Lunar Missions, Lunar Descent," George Marshall Space Flight Center, 1963.
- Cole, E.G., "Entry Guidance and Control," *Lunar Missions and Exploration*, Johan Wiley & Sons, Inc. New York, London, Sydney, 1964, p548-587.
- Compton, William D., *Where No Man Has Gone Before*. The NASA History Series, Washington, D.C., 1989.
- Furhmann, H., Weekly Report by Henry Furhmann. Department of Aeronautics and Astronautics, MIT, March 1992.
- Griffin, M. D., and French, J. R., *Space Vehicle Design*, American Institute of Aeronautics and Astronautics, Inc., Washington D.C., 1991.
- Griffen, M.D., Letter from the Associate Administrator for Exploration. National Aeronautics and Space Administration, Washington, D.C., December 1991.
- Larson, W. J., and Wertz, J. R., *Space Mission Analysis and Design*, Kluwer Academic Publishers, 1991.
- "Manned Lunar Landing Program Mode Comparison," Office of Manned Space Flights, July 1962.
- Newman, A., Weekly Report by Aaron Newman. Department of Aeronautics and Astronautics, MIT, March 1992.
- Ruppe, Harry O., *Introduction to Astrodynamics*, Academic Press, New York, 1968.
- Strizzi, J., Weekly Report by Jon Strizzi. Department of Aeronautics and Astronautics, MIT, March 1992.
- Wiesel, W. E., *Spaceflight Dynamics*, McGraw-Hill Publishing Co., 1989.

## **APPENDIX I**

**MATLAB file optim.m: conducts a search for a planar lunar orbit:**

```
V = [-4, 10, 0.1, 1];
q = fmins('ntrajcost', V, 1)

g = input('Plot and show stats?');

%q = Vx, Vy, Vz, phi, alpha

if g ~= 1,
phi = q(4);
alpha = 0;
rleo = 6655;
d = 384401;
phi_rad = phi*pi/180;
alpha_rad = alpha*pi/180;

tx = .01213 + (rleo/d) * cos(phi_rad)*cos(alpha_rad);
y = (rleo/d) * sin(phi_rad)*cos(alpha_rad);
z = (rleo/d) * sin(alpha_rad)*cos(phi_rad);

x0(1) = q(1);
x0(2) = tx;
x0(3) = q(2);
x0(4) = y;
x0(5) = q(3);
x0(6) = z;

x0 = x0';

t0 = 0;
tfinal = 0.7;
tol = 0.0001;

[t, x] = ode23('three_body', t0, tfinal, x0, tol, 0);

subplot(211)
plot(x(:,2), x(:,4))
hold on
plot(-0.9879, 0, '+')
plot(0.01213,0,'+')
hold off

V0 = sqrt(x0(1)^2 + x0(3)^2 + x0(5)^2)
deltaV = V0 - 7.7392

r0 = sqrt((x0(2)-.01213)^2 + x0(4)^2 + x0(6)^2)*d

radius = (sqrt((x(:,2)+.9879).^2 + x(:,4).^2 + x(:,6).^2));
[rm, i] = min(radius);
T = (t(i)/(2*pi))*28
```

```

rm*d

top = max(size(x));
time =(t./(2*pi))*28;

V = sqrt(x(:,1).^2 + x(:,3).^2 + x(:,5).^2);

index = 1:1:top;
index = index';

pause
plot(x(:,2), x(:,6))
hold on
plot(-0.9879, 0, '+')
plot(0.01213,0,'+')
hold off
end

```



**MATLAB File: op3.m conducts a search for a polar lunar orbit:**

```
% this thing takes orb from the nice planar one and tries too shoot off from it
% orb = [x, y, z, Vx, Vy, Vz]
% V = [Vx, Vy, Vz, time]

V = [0, 0, 0.1, 30];

neb = fmins('J3', V, 1)

g = input('Plot and show stats?');

%q = Vx,x,Vy,y,Vz,z

if g ~= 1,

p = neb(4);

q = stuff(p,:);
% stuff is a matrix of the points calculated along the planar trajectory.

x0(1) = neb(1) + q(1);
x0(2) = q(2);
x0(3) = neb(2) + q(3);
x0(4) = q(4);
x0(5) = neb(3) + q(5);
x0(6) = q(6);

d = 384401;

x0 = x0';
t0 = 0;
tfinal = 0.8 - q(7);
tol = 0.0001;

[t, x] = ode23('three_body', t0, tfinal, x0, tol, 0);

deltaV = sqrt(neb(1)^2 + neb(2)^2 + neb(3)^2)

radius = (sqrt((x(:,2)+.9879).^2 + x(:,4).^2 + x(:,6).^2));
[rm, i] = min(radius);
erm = (radius(i) - 0.00474867);

subplot(211)
plot(x(:,2), x(:,4))
hold on
plot(-0.9879, 0, '+')
plot(0.01213,0,'+')
hold off

T = (t(i)/(2*pi))*28
rm*d
```

```
top = max(size(x));  
time =(t./(2*pi))*28;  
  
pause  
plot(x(:,2), x(:,6))  
hold on  
plot(-0.9879, 0, '+')  
plot(0.01213,0,'+')  
hold off  
  
end
```

**MATLAB File: ntrajcost.m calculates the cost function for a planar lunar orbit:**

```
function cost = ntrajcost(V);

% stuff that numerically integrates the equations of motion for the
% three body problem
% x(1) = Vx
% x(2) = x
% x(3) = Vy
% x(4) = y
% x(5) = Vz
% x(6) = z

% d is earth-moon dist
d = 384401;

% ***** angles
phi = V(4);
alpha = 0;
rleo = 6655;
d = 384401;
phi_rad = phi*pi/180;
alpha_rad = alpha*pi/180;

x = .01213 + (rleo/d) * cos(phi_rad)*cos(alpha_rad);
y = (rleo/d) * sin(phi_rad)*cos(alpha_rad);
z = (rleo/d) * sin(alpha_rad)*cos(phi_rad);
% *****

x0(1) = V(1);
x0(2) = x;
x0(3) = V(2);
x0(4) = y;
x0(5) = V(3);
x0(6) = z;

x0 = x0';
t0 = 0;
tfinal = 0.7;
tol = 0.01;

[t, x] = ode23('three_body', t0, tfinal, x0, tol, 0);

V0 = sqrt(x0(1)^2 + x0(3)^2 + x0(5)^2);

% approximate deltaV
deltaV = V0 - 7.7392;
radius = (sqrt((x(:,2)+.9879).^2 + x(:,4).^2 + x(:,6).^2));
[rm, i] = min(radius);
erm = (radius(i) - 0.00474867);

cost = 0.35*abs(deltaV) + 100*erm^2 + 50*x(i,6)^2 + x(i,5)^2;
```

**MATLAB File: J3.m calculates the cost function for a polar lunar orbit:**

```
function cost = J3(V);

% stuff that numerically integrates the equations of motion for the
% three body problem
% x(1) = Vx
% x(2) = x
% x(3) = Vy
% x(4) = y
% x(5) = Vz
% x(6) = z

p = V(4);

stuff = [ an array of numbers describing the planar Earth-Moon trajectory
          These can be calculated from optim.m ];

q = stuff(p,:);

x0(1) = V(1) + q(1);
x0(2) = q(2);
x0(3) = V(2) + q(3);
x0(4) = q(4);
x0(5) = V(3) + q(5);
x0(6) = q(6);

x0 = x0';
t0 = 0;
tfinal = 0.8 - q(7);
tol = 0.001;

[t, x] = ode23('three_body', t0, tfinal, x0, tol, 0);

deltaV = sqrt(V(1)^2 + V(2)^2 + V(3)^2);

radius = (sqrt((x(:,2)+.9879).^2 + x(:,4).^2 + x(:,6).^2));
[rm, i] = min(radius);

erm = (radius(i) - 0.00474867);

cost = 0.04*abs(deltaV) + 500*erm^2 + 200*x(i,4)^2 + 0.05*x(i,1)^2 + 0.1*x(i,3)^2;
```

**MATLAB FILE: three\_body.m used by ode23 to numerically integrate the equations of motion for the three body problem:**

```
function xprime = three_body(t,x);

% This calculates the 6 degree derivative of the 3 DOF three body problem

% Constants
mew = 0.01213;
mn = 1 - mew;

% Calculations xprime
% x1 = xdot
% x2 = x
% x3 = ydot
% x4 = y
% x5 = zdot
% x6 = z

r1 = ((x(2) - mew)^2 + x(4)^2 + x(6)^2)^(3/2);
r2 = ((x(2) + mn)^2 + x(4)^2 + x(6)^2)^(3/2);

xprime = [ (2*x(3) + x(2) - (mn*(x(2) - mew))/r1 - (mew*(x(2) + mn))/r2) ;
           x(1) ;
           ((-mn*x(4))/r1 - (mew*x(4))/r2 + x(4) - 2*x(1)) ;
           x(3) ;
           ((-x(6)*mn)/r1 - (mew*x(6))/r2) ;
           x(5) ];
```

**MATLAB FILE: turn.m** uses the equations of motion of the gravity turn descent described in `grav_turn.m` to calculate the lunar descent.

```
% x0 are the initial conditions
% x0 = (downrange distance, altitude, velocity, vehicle mass, flight path angle)
% This x0 describes the beginning of the terminal descent phase
x0 = [ 0 , 1795400, -1611, 60600, 0.0098 ];
t0 = 0;
tfinal = 379;
tol = 0.00001;

% Here is the actual numerical integration command
[t, x] = ode23('grav_turn', t0, tfinal, x0, tol, 1);

plot(t,x(:,2))
pause
plot(t,x(:,3))
pause
plot(t,x(:,1))
```

**MATLAB FILE: grav\_turn.m** expresses the equations of motion for the gravity turn descent

```
function xprime = grav_turn(t,x);

% x1 = x
% x2 = h
% x3 = V
% x4 = m
% x5 = gamma (in radians)
% T = thrust

T = 184000;
g = 9.81/6;
R = 1740000;

xprime = [ x(3)*cos(x(5)) ;
           x(3)*sin(x(5)) ;
           ((T/x(4)) - (g - ((x(3)*cos(x(5)))^2)/(R + x(2)))*sin(x(5))) ;
           -T/(9.8*449) ;
           ((-g - ((x(3)*cos(x(5)))^2)/(R+x(2)))*cos(x(5)))/x(3) ; ];
```

## **APPENDIX II : Human Limitations of Multiple G**

Adverse effects of multiple g acceleration on the human physiology provide a major limitation in the development of propulsion stages in the piloted mission. The direction, magnitude and duration of multiple g forces factor simultaneously in determining the acceptability of each flight stage with regard to crew health. The "NASA-STD-3000 Man-Systems Integration Standards " provide a summary of human responses to both linear (G) and rotational (R) accelerations. The coordinate system used in defining the direction of accelerations encountered by the astronaut is shown in Figure II-1 below. The +1  $G_z$  vector represents everyday terrestrial gravity.

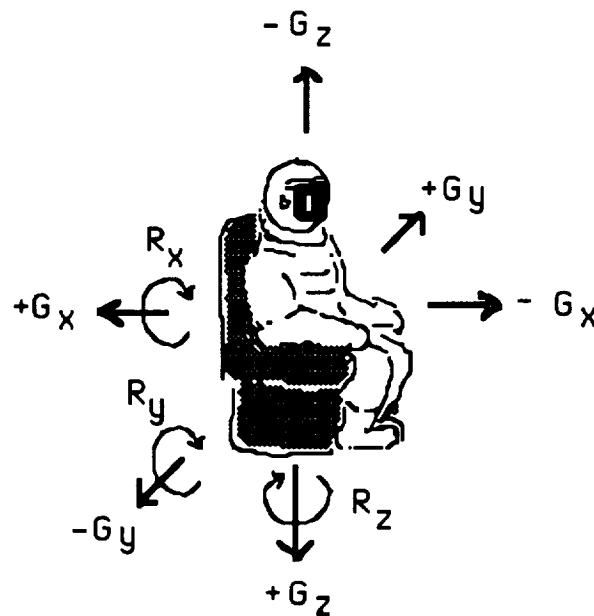


**Figure II-1**  
**Acceleration Vector Convention**

For each of the vector directions, Table II-1 summarizes the acceleration magnitudes and durations which may result in personal injury. Lower magnitudes can be sustained for longer durations while higher magnitudes may be acceptable if encountered for a much shorter period of time.

**Table II-1: Human Limitations of Multiple Acceleration**

Vector	Magnitude	Duration of Toleration	Dangers
+/- G x	4 G	60 min	Progressive chest pain; loss of peripheral vision; difficulty in breathing and speaking; blurring of vision
+/- G y	3 G	10 sec	Pressure on restraint system--stress on clavicle and <i>dependent</i> elbow, inertial movement of hips and legs, rotation of head toward shoulder
+ G z	3 - 4 G	10 sec	Progressive dimming of vision after 3 to 4 seconds; Progressive blackout possible at levels of 4.5 G
- G z	2 - 3 G	5 sec	Severe facial congestion; throbbing headache; blurring of vision; possible hemorrhaging
R x	12 rpm	30 sec	Nausea; disorientation
R y	80 rpm	3 sec	(same symptoms as - G x)
R z	60 rpm	4 min	Nausea; disorientation; headache

Consideration of these human responses to acceleration has set the maximum g-load requirements as follows:

- *Axial*            + G<sub>z</sub> = 3.5 g  
                         - G<sub>z</sub> = 2.0 g
- *Lateral*           +/- G<sub>x</sub> = 3.0 g  
                         +/- G<sub>y</sub> = 3.0 g
- *Rotational*       (As listed in table)

**Abort modes** will allow short duration, sustained emergency gravitational loads as high as 7.0 g. Ejection seat abort will result in an instantaneous loading close to 20 g. The +G<sub>z</sub> impulse encountered during this procedure will require adequate head restraints but should not result in severe injury.



## **APPENDIX III**

### **The Reentry Problem**

The reentry guidance problem is a complex problem requiring careful study. For an accurate analysis of a trajectory, one must consider many factors. These include vehicle characteristics ( drag, lift, heating rates, stability), atmospheric entry angle, variation of density with altitude, wind, earth rotation, and gravity. This section will attempt to explain the major issues concerning reentry and the equations governing these phenomena.

### **Equations of Motion**

The motion of the vehicle is mainly determined by aerodynamic forces associated with reentry and the pull of gravity. The relationship of lift and drag is especially important for lifting reentry bodies such as the biconic design featured in the Columbiad project. The variable lift allows certain amount of control of the reentry path allowing for down and cross ranges of the vehicle.

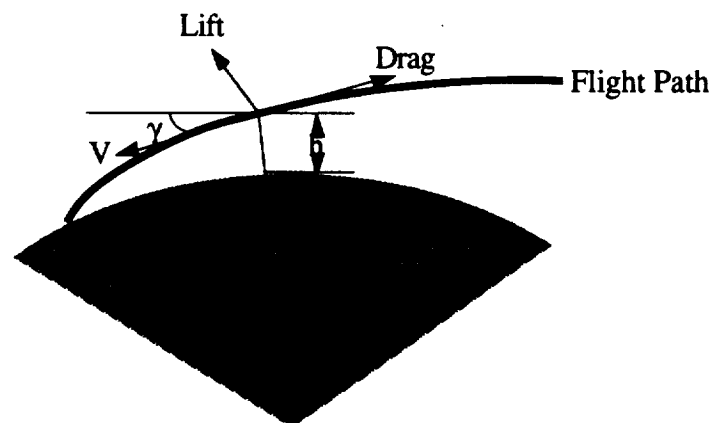


**Figure III-1**  
**Geometry of Reentry**

The basic equations of motion are derived with the coordinate frame established in figure III-1.

$$m\dot{V} = -D - mg\cos\theta \quad (\text{III-1})$$

$$mV(\dot{\phi}) = -L + mg\sin\theta \quad (\text{III-2})$$

$$\dot{h} = V\sin\theta \quad (\text{III-3})$$

where

$$g = g_0 \left( \frac{R}{R+h} \right)^2 \quad (\text{III-4})$$

$$\rho = \rho_0 e^{-\beta h} \quad (\text{III-5})$$

$$D = \frac{1}{2} C_D \rho V^2 S \quad (\text{III-6})$$

$$L = \frac{1}{2} C_L \rho V^2 S \quad (\text{III-7})$$

$$g_0 = 9.815 \text{ m/s}^2$$

$$\rho_0 = .0027 \text{ slugs/ft}^3$$

$$C_D = \text{set by geometry}$$

$$C_L = \text{set by geometry}$$

$$S = \text{incident surface area}$$

$$\beta = 1.42 \text{E-}5 \text{ m}^{-1}$$

$$\theta = \text{Entry Angle}$$

These equations need to be solved to determine the flight trajectories. Furthermore, the cross and down range can also be determined.[Minnesota,1990]

$$\text{Crossrange} = R_e \left( \frac{(L/D)^2 \Pi^2 \sin^2 \phi}{48} \right) * \left[ 1 - \frac{3(L/D)^2 \cos^2 \phi}{2 \Pi^2} \sum_{n=1}^{\infty} \left( \frac{1}{n^2 (n^2 + \frac{1}{4} ((L/D) \cos \phi)^2)} \right) \right] \quad (\text{III-8})$$

$$\text{Downrange} = \frac{1}{2} R_e \frac{L}{D} \ln \left[ \frac{1}{1 - \left( \frac{V_e^2}{g R_e} \right)} \right] \quad (\text{III-9})$$

$$R_e = \text{Earth radius}$$

$$g = \text{Gravitational acceleration}$$

$$\phi = \text{Bank angle}$$

$$V_e = \text{Entry velocity}$$

### Deceleration

The deceleration profile is of particular interest during reentry. Large deceleration spikes may injure the crew and damage the structural integrity of the craft. Due to the shallow angle of entry of the craft into the atmosphere the main component contributing to the loading is Lift and the Drag. The dimensionless aerodynamic acceleration  $a$  is defined as

$$a = \frac{\sqrt{L^2 + D^2}}{mg_0} \quad (\text{III-10})$$

Once the proper velocity profile has been determined, a graph of acceleration versus time will be generated. The graph is expected to like figure III-2 . [Minnesota, 1990] As can be seen by the graph small accelerations in the order of 1 g is expected.

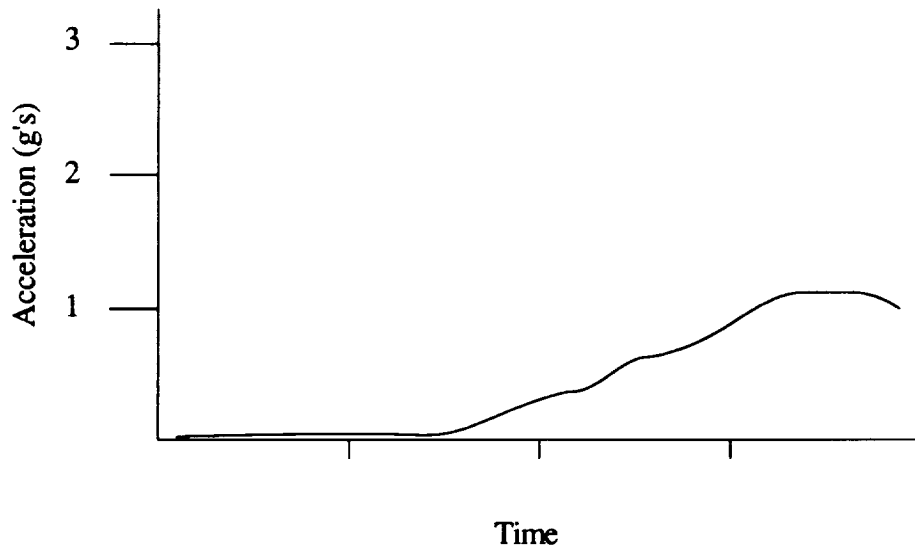


**Figure III-2**  
**Acceleration Profile during Reentry**

### Surface Heating

During atmospheric penetration, the aerodynamic drag transforms KE into thermal energy heating the air surrounding the vehicle. Part of this thermal energy is transferred to the vehicle while most of the energy is transported by the air away from the body. The energy absorbed by the vehicle depends primarily upon the vehicle shape, velocity, and atmospheric density (altitude).

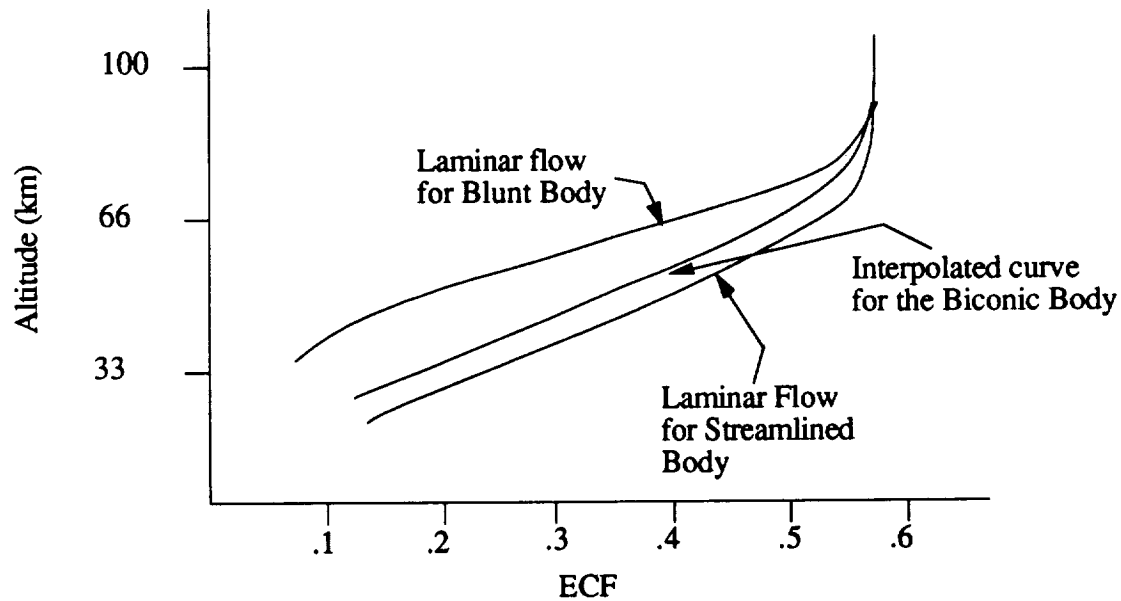
The atmospheric heating rate can be calculated through change in Kinetic energy with respect to time yielding the following result. [Unknown] The result is a simplistic relation for the heating rate that does not consider the actual heating rate of the body.

$$\frac{dQ}{dt} = \frac{\rho V^3}{2} (C_D A) \quad (\text{III-11})$$

The surface heating rate is governed by the amount of energy transferred to the body by the atmosphere. An energy conversion factor (ECF) can be defined which is the fraction of the converted kinetic energy that enters the vehicle as heat. This heat input will then determine the type of insulation necessary for vehicle protection. The ECF is primarily a function of vehicle shape, velocity and altitude (density of atmosphere).

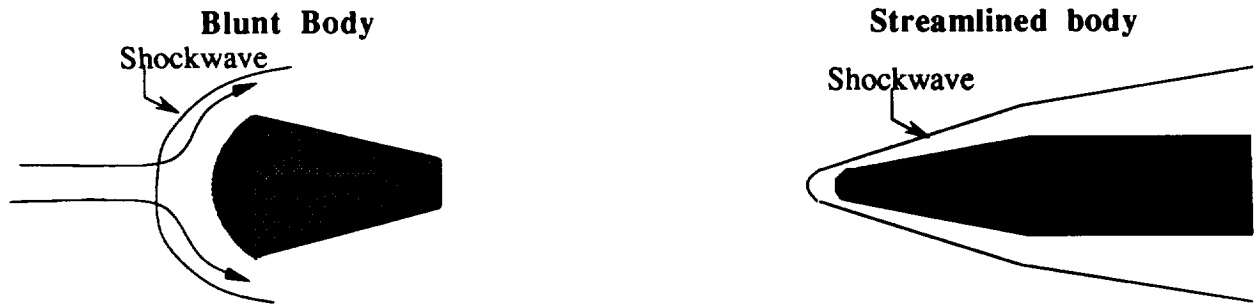
$$\frac{\text{Heat absorbed by vehicle}}{\text{Total heat generated}} = \text{ECF} \quad (\text{III-12})$$

Figure III-3 shows the relationship of ECF with altitude for different reentry vehicles, blunt body and streamlined body. The behavior of the biconic reentry vehicle was determined to be a combination of the two vehicles. The ECF curve therefore lies in between the two bodies.



**Figure III-3**  
**Energy Conversion Factor with respect to Altitude**

Figure III-4 illustrates the flow field around the blunt body and the streamlined body. The geometry of the biconic reentry vehicle is in between these two configurations.



**Figure III-4**  
**Flow Field around Blunt Body and Streamlined Body**

The heating rate that the body experiences is therefore:

$$\frac{dQ}{dt} = \frac{\rho V^3}{2} (C_D A) (ECF) \quad (III-13)$$

It is important to note that ECF is a function of altitude.

#### REFERENCES:

- AEM 5331 Class of 1990, "Biconic Cargo Return Vehicle with an Advanced Recovery System," University of Minnesota, N90-26052, p 142.
- Akridge, Charles M. and Harlin, Sam H., "Parametric Performance Analysis of Lunar Missions, Lunar Descent," George Marshall Space Flight Center, 1963.
- E.G. Cole, "Entry Guidance and Control," *Lunar Missions and Exploration*, Johan Wiley & Sons, Inc. New York, London, Sydney, 1964, p548-587.
- Griffin, M. D., and French, J. R., *Space Vehicle Design*, American Institute of Aeronautics and Astronautics, Inc., Washington D.C., 1991.
- Kaplan, Marshall H., *Space Shuttle: America's Wings to the Future*, Aero Publishers Inc., 1978.
- Larson, W. J., and Wertz, J. R., *Space Mission Analysis and Design*, Kluwer Academic Publishers, 1991.
- National Aeronautics and Space Administration (NASA), "Space Transportation System", N82-75205, 1982.
- Ruppe, Harry O., *Introduction to Astrodynamics*, Academic Press, New York, 1968.
- Suit, William and Foernsler, Linda. Personal Communication with staff at NASA Langley Research Center, March 1992.
- Wiesel, W. E., *Spaceflight Dynamics*, McGraw-Hill, 1989.

**VOLUME II**  
**Subsystem Trade Studies and Selection**

## Table of Contents

<b>1 Overview</b>	<b>1</b>
1.1 Top Level Requirements	1
1.1.1 Structures and Thermal Protection	1
1.1.2 Propulsion	1
1.1.3 Command, Communications, and Control	1
1.1.4 Guidance, Navigation, and Control	2
1.1.5 Power and Thermal Protection	2
1.1.6 Crew Systems	2
1.1.7 Status and Monitoring	2
1.2 Trade Studies and Design Selection	2
<b>2 Structural Manifesto</b>	<b>4</b>
2.1 Structural Design Methods	4
2.1.1 STP Basic Principles	4
2.1.2 Beam Statics	5
2.1.2.1 Buckling	6
2.1.3 Structural Configuration Comparison	7
2.1.3.1 Description of Monocoque Structures	7
2.1.3.2 Description of Sandwich Panels	8
2.1.3.3 Description of Semi-Monocoque Structures	10
2.1.3.4 Test Case 1 – Solid Monocoque	10
2.1.3.5 Test Case 2 – Sandwich Monocoque	12
2.1.3.6 Test Case 3 – Solid Semi-Monocoque	14
2.1.3.7 Test Case 4 – Sandwich Semi-Monocoque	14
2.1.3.8 Structural Configuration Summary	16
2.1.4 Rocket Stage Casing Design	17
2.1.4.1 Stringers	22
2.1.4.2 Frames	23
2.1.4.3 Skin	27
2.1.4.4 Frequency Analysis	30
2.1.5 Pressure Vessels	31
2.1.5.1 End Caps	32
2.1.5.2 Cylindrical Body	34
2.1.6 Materials	36
2.2 Stage Designs	37
2.2.1 PTLI Stage Design	37
2.2.1.1 Five Engine Rocket Support Truss	37
2.2.1.2 Stage Casing	41
2.2.1.3 Oxygen and Fuel Tanks	45
2.2.1.4 Summary	48
2.2.2. LBM Stage Design	49
2.2.2.1. Three Engine Rocket Support Truss	50
2.2.2.2. Stage Casing	53
2.2.2.3. Oxygen and Fuel Tanks	56
2.2.2.4 Summary	57
2.2.3. ERM Stage Design	59
2.2.3.1. Three Engine Rocket Support Truss	59
2.2.3.2. Stage Casing	60
2.2.3.3. Oxygen and Fuel Tanks	62
2.2.3.4 Summary	64
2.2.4. Crew Capsule Design	66
2.2.4.1 Aerodynamic Design	67

2.2.4.1.1 Stability .....	68
2.2.4.1.2 Wing .....	71
2.2.4.1.3 Parafoil Airfoil .....	72
2.2.4.2 Sizing and Configuration.....	74
2.2.4.3. Structural Design and Loading .....	79
2.2.4.4. Re-entry Heating .....	84
2.2.4.5. Thermal Protection & Heat Shield Design.....	85
2.2.5 Precursor Mission Structures .....	87
2.2.5.2 Ground Support.....	92
2.2.5.2.1 Landing Legs.....	92
2.2.5.2.2 Support Legs.....	97
2.2.5.3 Propulsion Section.....	98
2.2.5.4 Cargo Bay.....	100
2.2.5.4.1 Hatch.....	100
2.2.5.4.2 Gangway .....	101
2.2.5.5 BioCan Lunar Habitat .....	101
2.2.5.6 Regolith Support Structure.....	104
2.2.5.6.1 Side Ramps.....	104
2.2.5.6.2 Canopy.....	107
2.2.5.7 PLM Stage Specifications Summary.....	108
<b>3 Propulsion Systems Design .....</b>	<b>109</b>
3.1 Introduction .....	109
3.2 System Drivers and Requirements .....	109
3.2.1 Safety Considerations .....	109
3.2.2 Cost Considerations .....	111
3.2.3 Performance Considerations.....	111
3.2.4 Other Considerations .....	112
3.2.5 Mission Requirements.....	113
3.3 Design Approach.....	114
3.3.1 Propellant selection .....	114
3.3.1.1 Thermochemical Assessment .....	116
3.3.2 Engine Cycle Selection.....	118
3.3.3 Selection of Structural Materials .....	120
3.4 Component Selection And Sizing .....	122
3.4.1 Primary Propulsion Engines.....	122
3.4.2 Attitude Control Thrusters.....	126
3.4.3 Precursor Payload Deployment Engines .....	128
3.4.4 Propellant Tanks .....	129
3.4.4.1 Structural Requirements .....	129
3.4.4.2 Insulation Requirements.....	129
3.4.4.3 Propellant Expulsion Mechanism.....	129
3.4.5 Pressurization Schemes.....	131
3.4.6 Propellant Lines and Valves .....	132
3.4.7 Control and Monitoring Equipment.....	134
3.4.8 Burn Times and Engine Configurations.....	135
3.5 Launch Escape System Selection.....	138
3.5.1 Characteristics of Launch Phase .....	139
3.5.2 Historical Perspective on Launch Escape System Selection .....	139
3.5.3 Results of Project Columbiad Escape System Trade Study.....	140
3.5.4 Decision on Launch Abort System Selection .....	142
<b>4 Command, Control and Communications Selection.....</b>	<b>143</b>
4.1 Requirements for Command, Control and Communications .....	143
4.2 Overview of Proposed C3 Systems.....	145
4.2.1 Primary Trans-Lunar Injection and Earth.....	148



4.2.2	Precursor and Earth.....	149
4.2.3	Earth Return Module and Earth .....	150
4.2.4	Crew Module and Earth.....	151
4.2.5	Crew Module and Precursor.....	151
4.2.6	Lunar Rover and Earth .....	151
4.3	Design of Communications Systems.....	152
4.3.1	Design of the Receiver Systems .....	154
4.3.2	Design of the Transmitter Systems .....	156
4.3.3	Antenna Design .....	158
4.3.3.1	Low-gain Antennae .....	158
4.3.3.2	High-gain Transmitting Antennae .....	159
4.3.3.3	High-gain Receiving Antennae .....	164
4.3.4	Descriptions of Communications Links.....	165
4.3.4.1	Earth to Low Earth Orbit. ....	166
4.3.4.2	Low Earth Orbit to Lunar Vicinity.....	166
4.3.4.3	Lunar Landing.....	167
4.3.4.4	Lunar Surface Operations .....	167
4.3.4.4.1	Habitat.....	167
4.3.4.4.2	Lunar Rover .....	168
4.3.4.5	Reentry .....	168
4.3.5	Backup Mechanisms for Communications Equipment.....	168
4.4	Design of Onboard Computer Systems.....	169
4.4.1	Computer Architecture .....	170
4.4.2	Computer Fault Tolerance .....	173
4.4.3	Data Bus Fault Tolerance .....	175
4.4.4	Processor Sizing.....	177
4.4.4.1	Data Rate Estimates .....	177
4.4.4.2	Crew Module Throughput Estimates.....	177
4.4.4.3	Earth Return Module Throughput Estimates .....	180
4.4.4.4	Habitat Throughput Estimates .....	180
4.4.4.5	Primary Trans-Lunar Injection Estimates.....	182
4.4.5	Data Storage Equipment.....	183
4.5	Modulation and coding .....	184
4.5.1	Why digital ? .....	184
4.5.2	Modulation.....	185
4.5.2.1	The effect of thermal noise .....	186
4.5.2.2	Spectra.....	187
4.5.2.3	Adjacent channel interference .....	188
4.5.2.4	Co-channel interference.....	188
4.5.2.5	Phase noise.....	188
4.5.2.6	Band limitation and delay distortion .....	189
4.5.2.7	Modulation circuitry for FFSK.....	189
4.5.2.8	Demodulation Circuitry for FFSK .....	189
4.5.3	Coding.....	191
4.5.3.1	Shannon limit.....	191
4.5.3.2	Error correction.....	192
4.5.3.3	Code selection .....	193
4.5.4	Video Compression .....	198
4.6	Power, Size and Weight for Communications Equipment .....	198
4.6.1	Crew Module.....	199
4.6.2	Earth Return Module .....	200
4.6.3	Habitat.....	200
4.6.4	Primary Trans-Lunar Injection Stage.....	201

<b>5 Guidance, Navigation and Control Selection .....</b>	<b>203</b>
5.1 Introduction.....	203
5.2 Trade Studies and Instrument Selection.....	203
5.2.1 Attitude Determination and Control.....	203
5.2.2 Coordinate Systems .....	204
5.2.3 Onboard vs. Ground-based ADCS .....	204
5.2.3.1 Stabilization .....	205
5.2.4 Reaction Control System.....	205
5.2.4.1 Reaction Wheels.....	206
5.2.4.2 Momentum Wheels.....	206
5.2.4.3 Magnetic Torquers .....	206
5.2.4.4 Control Moment Gyros.....	206
5.2.4.5 Gas Jets.....	207
5.2.4.6 Choosing a Reaction Control System.....	207
5.2.4.7 Design Choice for RCS.....	208
5.2.4.7.1 Theory of Gas Jet Attitude Maneuvers .....	208
5.2.4.7.2 RCS Thruster Locations .....	208
5.2.5 Attitude Determination System .....	209
5.2.5.1 Horizon Sensors.....	209
5.2.5.2 Sun Sensors.....	210
5.2.5.3 Star Trackers.....	210
5.2.5.4 Magnetometers.....	211
5.2.5.5 Optical Sensor Choice .....	211
5.2.6 Gyroscopes.....	211
5.2.6.1 G-sensitive Errors in Gyroscopes.....	212
5.2.6.2 Cost and Reliability of Gyros.....	213
5.2.6.3 Theory of Laser Gyroscopes.....	214
5.2.7 Attitude Determination and Control Final Design .....	214
5.2.8 Accelerometers .....	214
5.2.8.1 Theory of Solid State Accelerometers.....	215
5.2.9 Inertial Measurement Unit .....	216
5.2.9.1 Orientation of IMU Components .....	216
5.2.9.2 Component to Spacecraft Coordinates.....	217
5.2.9.3 Spacecraft to Inertial Coordinates .....	218
5.2.10 Operation of Attitude Determination and Control System .....	218
5.2.11 Inertial Navigation.....	219
5.2.12 Radar Systems.....	220
5.2.12.1 LADAR v. Microwave.....	221
5.2.13 Docking Radar.....	222
5.2.14 Laser Retro-Reflectors.....	222
5.2.15 Visual Targets.....	222
5.2.16 Video Cameras.....	223
5.2.17 CRT Displays.....	223
5.2.18 LCD Displays.....	223
5.2.19 External Spacecraft Tracking.....	223
5.2.19.1 The Global Positioning System.....	224
5.2.19.2 Ground Tracking.....	224
5.2.19.3 Pre-Deployed Navigation Aids.....	224
5.3 Precursor Mission.....	228
5.3.1 Launch .....	228
5.3.2 PTLI Stationkeeping.....	228
5.3.2.1 PLTI Attitude Determination.....	228
5.3.2.2 PLTI Translational Navigation .....	228
5.3.2.3 PLTI Guidance and Control .....	229

5.3.2.3.1	Bang-Bang Control.....	229
5.3.2.3.2	Emergency Attitude Acquisition .....	230
5.3.3	Earth Orbit Rendezvous.....	231
5.3.3.1	Docking .....	231
5.3.3.1.1	Docking Zones.....	231
5.3.3.1.2	Docking Accuracies.....	231
5.3.3.1.3	The 0.1% Rule.....	232
5.3.3.1.4	Docking System.....	232
5.3.4	Trans-Lunar Injection .....	234
5.3.4.1	Trans-Lunar Injection Navigation.....	234
5.3.4.2	Trans-Lunar Injection Guidance.....	234
5.3.4.2.1	Present Velocity Required Guidance .....	234
5.3.4.3	Trans-Lunar Injection Control.....	235
5.3.5	Lunar Transfer Orbit.....	235
5.3.5.1	Lunar Transfer Orbit Navigation .....	235
5.3.5.2	Lunar Transfer Orbit Guidance and Control .....	236
5.3.6	Lunar Orbit Injection .....	236
5.3.6.1	Lunar Orbit Injection Navigation.....	236
5.3.6.2	Lunar Orbit Injection Guidance and Control.....	237
5.3.7	Lunar Descent.....	237
5.3.7.1	Lunar Landing Navigation .....	237
5.3.7.2	Lunar Landing Guidance .....	237
5.3.7.2.1	Position Constrained Guidance .....	237
5.3.7.3	Lunar Descent Control.....	238
5.4	Piloted Mission.....	238
5.4.1	Mission Similarities.....	238
5.4.2	Lunar Landing.....	238
5.4.3	Lunar Launch.....	238
5.4.3.1	Lunar Launch Navigation .....	238
5.4.3.2	Lunar Launch Guidance and Control .....	238
5.4.4	Trans Earth Injection .....	239
5.4.4.1	Trans-Earth Injection Navigation.....	239
5.4.4.2	Trans-Earth Injection Guidance .....	239
5.4.5	Earth Transfer Orbit .....	239
5.4.5.1	ETO Navigation .....	239
5.4.5.2	ETO Guidance and Control .....	239
5.4.6	Reentry Navigation, Guidance and Control .....	239
5.4.6.1	Reentry Navigation .....	239
5.4.6.2	Reentry Guidance and Control .....	240
5.4.6.2.1	Pre-Entry.....	240
5.4.6.2.2	Initial Pull-up.....	240
5.4.6.2.3	Controlled Climb.....	240
5.4.6.2.4	Ballistic Skip / High Altitude Cruise.....	241
5.4.6.2.5	Final Glide.....	241
5.5	Lunar Operations .....	241
6	<b>Power and Thermal Control Hardware Selection .....</b>	<b>243</b>
6.1	General Power Hardware Selection, Issues, and Trade Studies.....	243
6.1.1	Choice of Conductor .....	243
6.1.2	Power Conversion .....	244
6.1.3	Electrical Storage Survey and Selection.....	244
6.1.4	Bus Voltage Selection .....	245
6.1.5	Power Distribution Characteristics.....	246
6.1.6	Power Systems Safety Factor Definition.....	246

6.2	Lunar Surface Power Plant Selection.....	246
6.2.1	Introduction.....	246
6.2.2	Scale of Lunar Surface Power Plant.....	247
6.2.3	Trade Study	
	Type of Power Plant.....	248
	6.2.3.1 Power Plant System Mass Comparison .....	248
	6.2.3.2 Additional Comparative Considerations of Power	
	Plant Choice .....	250
6.3	Spacecraft Power Hardware Selection and Trade Studies.....	251
6.3.1	Power Supply Placement on Vehicle Stages.....	251
6.3.2	Wraparound Solar Array on Primary Vehicle Power Stages .....	252
6.3.3	Integration of Lunar Power Plant with Payload Landing	
	Module .....	254
6.3.4	Integration of Fuel Cell Reactant Tanks with Propellant	
	Tanks.....	254
6.3.5	Power Dependency of ERM/CM on Solar Lunar Power Plant....	255
6.4	Cryogenic Storage.....	255
6.4.1	Storage Options .....	256
	6.4.1.1 Passive Control.....	257
	6.4.1.2 Refrigeration System.....	257
	6.4.1.3 Partial Reliquefaction .....	257
	6.4.1.5 Total Reliquefaction.....	257
6.4.2	Calculations.....	258
	6.4.2.1 Boundary Conditions.....	258
	6.4.2.1.1 Heat flux.....	258
	6.4.2.1.2 Spacecraft Surface Temperature.....	259
	6.4.2.1.3 Fuel Boiling Points and Heats of	
	Vaporization.....	259
	6.4.2.2 MultiLayer Insulation Design .....	260
	6.4.2.2.1 Primary Design Considerations .....	260
	6.4.2.2.2 Secondary Design Considerations .....	263
	6.4.2.3 Trade Studies .....	263
	6.4.2.3.1 Assumptions.....	263
	6.4.2.3.2 Trade Study of Selected Materials .....	264
	6.4.2.3.3 Trade Study of ERM Stage .....	265
	6.4.2.3.4 Trade Study for LBM and TLI Stages.....	266
6.4.3	Conclusions .....	267
7	Crew Systems Selection.....	268
7.1	Crew Provisions.....	268
7.2	Environmental Control.....	269
7.2.1	Atmosphere.....	270
	7.2.1.1 Requirements .....	271
	7.2.1.1.1 Pressurization .....	271
	7.2.1.1.2 Gas Content.....	272
	7.2.1.1.3 Temperature and Humidity .....	278
	7.2.1.2 Selection of Cabin and Lunar Habitat Atmosphere .....	279
	7.2.1.3 Carbon Dioxide Removal.....	280
	7.2.1.4 Oxygen Reclamation .....	281
	7.2.1.5 Oxygen and Nitrogen Tank Design .....	283
	7.2.1.6 Other Atmospheric Control Aspects.....	286
7.2.2	Water Management .....	286
	7.2.2.1 Wash Water Reclamation.....	287
	7.2.2.2 Water Tank Design.....	287
7.2.3	Waste Management .....	288

7.3 Radiation Requirements .....	290
7.3.1 Human Radiation Tolerance .....	290
7.3.2 Types of Radiation .....	291
7.3.3 Capsule Radiation Design Considerations .....	292
7.3.4 Habitat Radiation Design Considerations .....	292
7.4 Spacesuits and Other Garments .....	292
7.4.1 Crew Capsule Garments .....	293
7.4.1.1 IVA Undergarments.....	293
7.4.1.2 IVA Spacesuit.....	293
7.4.1.3 Habitat-Capsule Transfer.....	294
7.4.2 Habitat Garments .....	294
7.4.2.1 IVA Garments .....	294
7.4.2.2 EVA Spacesuits.....	295
7.4.2.2.1 Metabolic Requirements.....	296
7.4.2.2.2 Medical Monitoring.....	298
7.4.3 Personal Rescue Spheres .....	300
7.5 Medical Monitoring in the Crew Module .....	300
7.5.1 Cardiovascular Effects of Rapid "G"-Variations .....	301
7.5.1.1 Detection of Cardiac Irregularities.....	301
7.5.1.2 Prevention of Orthostatic Hypotension .....	301
7.5.2 Musculoskeletal Effects of Microgravity.....	302
7.5.3 Inflight Medical Support.....	303
7.6 Medical Monitoring on the Lunar Habitat .....	304
7.6.1 Monitoring Cardiovascular Deconditioning.....	305
7.6.2 Monitoring Musculoskeletal Atrophy.....	305
7.6.3 Habitat Medical Support .....	307
7.7 Additional Crew System Concerns .....	308
7.7.1 Mass of Cabin Air .....	308
7.7.2 Other Equipment.....	309
7.7.2.1 Spacesuit Checkout and Recharge System .....	310
<b>8 The Status Group .....</b>	<b>311</b>
8.1 Testing.....	311
8.1.1 Ground Testing.....	312
8.1.2 Ground Test Philosophy.....	312
8.1.3 Countdown Demonstration Test .....	313
8.1.4 Astronaut's Role in Testing.....	314
8.1.5 Pre-launch Testing.....	314
8.1.6 Integrated Systems Tests.....	315
8.2 Sensors.....	317
8.3 Importance of Documentation.....	318
8.4 Failure Studies.....	319
8.4.1 Handling of Failure Data.....	320
8.4.2 Failure Mode Analysis .....	321
8.4.2.1 Ranking Failure Modes.....	322
8.5 Efficient Maintenance Techniques.....	323
8.5.1 Definitions .....	324
8.5.2 Program.....	324
8.6 Industry Streamlining Efforts.....	325
8.6.1 Advanced Technologies.....	327
<b>REFERENCES .....</b>	<b>329</b>
<b>APPENDIX I Spacecraft Propulsion Theory.....</b>	<b>335</b>
<b>APPENDIX II Communications Theory and Background.....</b>	<b>339</b>
<b>APPENDIX III Status and Monitoring Methods and Definitions .....</b>	<b>358</b>

## List of Figures

Figure 2-1 Construction of a Sandwich Structure.....	8
Figure 2-2 Sandwich Construction Comparison .....	9
Figure 2-3 Semi-Monocoque Structure Construction.....	10
Figure 2-4 Typical Plate Deflection .....	11
Figure 2-5 Representative Results for a Solid Monocoque Panel .....	12
Figure 2-6 Representative Results for a Sandwich Monocoque Panel.....	13
Figure 2-7 Representative Results for a Solid Semi-Monocoque Panel .....	15
Figure 2-8 Representative Results for a Sandwich Semi-Monocoque Panel.....	16
Figure 2-9 Function Definitions for Rocket Casing Calculations .....	19
Figure 2-10 Equations for Determining Shear and Bending Moments.....	22
Figure 2-11 Equations for Determining Stringer Geometry.....	23
Figure 2-12 Representative Frame FEM Results.....	24
Figure 2-13 Frame Bending First Mode.....	25
Figure 2-14 Panel Instability in Semi-Monocoque Structures .....	26
Figure 2-15 General Instability in Semi-Monocoque Structures .....	26
Figure 2-16 Equations for Determining Longerons Geometry.....	27
Figure 2-17 Axial Compressive Buckling Coefficients for Curved Plates .....	28
Figure 2-18 Shear Buckling Coefficients for Clamped Curved Plates.....	29
Figure 2-19 Equations for Determining the First Mode Frequency of the Structure .....	30
Figure 2-20 Intentionally Left Out	
Figure 2-21 Construction of Oxygen and Fuel Tanks .....	31
Figure 2-22 Non-dimensional Meridional Stress Coefficient for 2:1 Ellipses .....	33
Figure 2-23 Non-dimensional Tangential Stress Coefficient for 2:1 Ellipses.....	34
Figure 2-24 Critical Buckling Stress for Solid Cylinder vs. Skin Thickness.....	35
Figure 2-25 Curve Fit of Critical Buckling Stress for Solid Cylinder of 3m Radius .....	35
Figure 2-26 PTLI Finite-Element Model .....	37
Figure 2-27 Five-Engine Truss - Top View .....	38
Figure 2-28 Five-Engine Truss - Oblique View.....	39
Figure 2-29 Typical Deflections and Stresses for Five-Engine Rocket Truss .....	40
Figure 2-30 PTLI Shear Stress vs. Stage Height .....	41
Figure 2-31 PTLI Bending Moment vs. Stage Height.....	42
Figure 2-32 PTLI Axial Stress vs. Total Stage Area.....	42
Figure 2-33 PTLI Axial Stress vs. Stage Height for a Set Stage Area.....	43
Figure 2-34 PTLI Required Stringer Area vs. Number of Stringers.....	43
Figure 2-35 PTLI Stringer Inertia vs. Stringer Outer Diameter.....	44
Figure 2-36 PTLI Stringer Buckling Stress vs. Stringer Length.....	45
Figure 2-37 PTLI Hydrogen Tank Design Parameters .....	46
Figure 2-38 PTLI Oxygen Tank Design Parameters.....	47
Figure 2-39 PTLI Stage Design Inputs.....	48
Figure 2-40 PTLI Configuration Summary.....	49
Figure 2-41 LBM Finite-Element Model .....	50
Figure 2-42 Three-Engine Truss - Top View.....	51
Figure 2-43 Three-Engine Truss - Oblique View .....	52
Figure 2-44 Typical Deflections and Stresses for Three-Engine Rocket Truss.....	53
Figure 2-45 LBM Shear Stress vs. Stage Height .....	54
Figure 2-46 LBM Bending Moment vs. Stage Height.....	54
Figure 2-47 LBM Axial Stress vs. Total Stage Area.....	55
Figure 2-48 LBM Stringer Buckling Stress vs. Stringer Length.....	55
Figure 2-49 LBM Hydrogen Tank Design Parameters .....	56
Figure 2-50 LBM Oxygen Tank Design Parameters.....	57

Figure 2-51 LBM Stage Design Inputs.....	58
Figure 2-52 LBM Configuration Summary.....	59
Figure 2-53 ERM Shear Stress vs. Stage Height .....	60
Figure 2-54 ERM Bending Moment vs. Stage Height.....	60
Figure 2-55 ERM Axial Stress vs. Total Stage Area.....	61
Figure 2-56 ERM Stringer Buckling Stress vs. Stringer Length .....	61
Figure 2-57 ERM Hydrogen Tank Design Parameters .....	63
Figure 2-58 ERM Oxygen Tank Design Parameters.....	64
Figure 2-59 ERM Stage Design Inputs.....	65
Figure 2-60 ERM Configuration Summary.....	66
Figure 2-61 Biconic Re-entry Vehicle - Crew Capsule.....	67
Figure 2-62 L/D of Biconic Re-entry Vehicle vs. AOA .....	67
Figure 2-63 Crew Capsule Pitching Moment vs. AOA.....	69
Figure 2-64 Crew Capsule Top View with Wings.....	70
Figure 2-65 Biconic Re-entry Vehicle Yawing Moment vs. AOA .....	71
Figure 2-66 NACA 0505 at AOA of 0°.....	72
Figure 2-67 NACA 0505 at AOA of 2°.....	72
Figure 2-68 NACA 2210 at AOA of 0°.....	73
Figure 2-69 NACA 2210 at AOA of 2°.....	73
Figure 2-70 Crew Capsule - Side View - Dimensioned .....	74
Figure 2-71 Crew Capsule - Top View - Dimensioned.....	74
Figure 2-72 Sample Case for Determining Vehicle Geometry Ratios.....	76
Figure 2-73 Derivation of Formulas for an Oblique Tapered Cylinder .....	78
Figure 2-74 Inside Volume vs. Maximum Diameter .....	79
Figure 2-75 Finite-element Model of Crew Capsule.....	80
Figure 2-76 Velocity and Pressure Trajectories .....	81
Figure 2-77 Typical Deflections and Stress for Crew Capsule Loading.....	82
Figure 2-78 Crew Capsule Weight vs. Inside Volume .....	83
Figure 2-79 PLM Stage - Cutaway View (landing).....	87
Figure 2-80 PLM Stage - Cutaway View (deployed).....	88
Figure 2-81 PLM Stage - Internal Structures .....	88
Figure 2-82 PLM stage - Framework.....	89
Figure 2-83 PLM stage - Skin Panels .....	90
Figure 2-84 Effective Base Radius Comparison for 3-leg and 4-leg Cases.....	92
Figure 2-85 Landing Gear Configuration .....	93
Figure 2-86 Landing Gear Deployment .....	94
Figure 2-87 Landing Gear Structure - Axial Load Diagram.....	95
Figure 2-88 Landing Gear Structure - Moment Diagram.....	96
Figure 2-89 Support Leg Configuration.....	97
Figure 2-90 PLM Propellant Tanks.....	99
Figure 2-91 BioCan Configuration .....	102
Figure 2-92 Regolith Support Structure Configuration.....	104
Figure 2-93 Regolith Support Panel Assembly.....	105
Figure 2-94 Finite Element Model - Undeformed and Deformed Views .....	106
Figure 3-1 Turbopump Feed System Cycles for Liquid Propellant Rocket Engines.....	120
Figure 3-2 The RL10A-4 Engine.....	124
Figure 3-3 RL10A-4 Propellant Flow Schematic .....	124
Figure 3-4 The R4-D Engine .....	127
Figure 3-5 Available Options for Positive Expulsion Tanks.....	130
Figure 4-1 Communication Links on Launch.....	145
Figure 4-2 Communication Links of Precursor in LEO and LTO.....	146
Figure 4-3 Communication Links on Piloted Mission in LEO and LTO .....	147

Figure 4-4	Communication Links on Lunar Surface.....	148
Figure 4-5	Communications System on PTLI Stages .....	149
Figure 4-6	Communications System on Habitat.....	150
Figure 4-7	Communications System on Crew Module and Earth Return Module .....	151
Figure 4-8	Communications System on Lunar Rover .....	152
Figure 4-9	Receiver System Block Diagram.....	155
Figure 4-10	Transmitter System Block Diagram .....	157
Figure 4-11	Linear Phased Array .....	159
Figure 4-12	Visible Range for $k_d = \pi$ and for $k_d = 8\pi/5$ .....	160
Figure 4-13	Weight and Power Requirements as a Function of Frequency.....	161
Figure 4-14	Single and Multiple Reflector Systems .....	162
Figure 4-15	Comparison of Offset and Symmetric Reflector Performance .....	163
Figure 4-16	System Configuration Selected for Columbiad High-gain Antennae.....	165
Figure 4-17	Architecture of Columbiad's Computing System.....	170
Figure 4-18	Common Computer Architectures.....	172
Figure 4-19	Voting Fault Tolerance.....	174
Figure 4-20	Quizzing Fault Tolerance .....	174
Figure 4-21	Pair of Pairs Fault Tolerance.....	175
Figure 4-22	Optical Databus Multi-node Fault Tolerant Topology .....	176
Figure 4-23	FFSK Modulation Structure .....	189
Figure 4-24	Modulation Circuitry for FFSK .....	190
Figure 4-25	Clock Recovery.....	191
Figure 4-26	Elias Bound.....	124
Figure 4-27	Encoding Block Diagram.....	195
Figure 4-28	Error Detection Block Diagram .....	196
Figure 4-29	Modem/codec Structure.....	197
Figure 4-30	Reliability Schematic.....	198
Figure 5-1	Attitude Determination and Control Feedback Loop .....	204
Figure 5-2	RCS Thruster Locations .....	209
Figure 5-3	Schematic of a Solid-state Accelerometer .....	216
Figure 5-4	Schematic of Attitude Determination and Control System .....	219
Figure 5-5	Schematic of Inertial Navigation System.....	220
Figure 5-6	Visual Target Surrounding Docking Interface.....	223
Figure 5-7	Optimal Transponder Beacon Orientation.....	226
Figure 5-8	Optimal Beacon Configuration .....	226
Figure 5-9	Bang-Bang Controller.....	230
Figure 5-10	Instrumentation Layout.....	233
Figure 6-1	Evaluation of Storage Methods.....	256
Figure 6-1	Expected Sources of Heat Flux .....	258
Figure 6-2	The Innermost Layers .....	260
Figure 6-3	Subsequent Layers.....	262
Figure 7-1	Habitat Semi-Renegenerative Environment System .....	270
Figure 7-2	Approximate Time of Appearance of Hyperoxic Symptoms .....	274
Figure 7-3	Oxygen Requirement Per Total Atmospheric Pressure.....	275
Figure 7-4	Toxicity Limits of Potential Diluents .....	277
Figure 7-5	Thermal Environment Requirements for Human Comfort.....	279
Figure 7-6	Oxygen Reclamation System .....	282
Figure 7-7	Biobelt Assembly for EVA Medical Monitoring .....	299
Figure 7-8	Biobelt Assembly Electrode Placement.....	299
Figure 7-9	MK-I Exercise Positions.....	303
Figure 7-10	The Angled Lunar Habitat Treadmill.....	306
Figure II-1	Parameters of Source Radiation Problem.....	343



Figure II-2 Parameters for Radiating Source in the Far Field.....	344
Figure II-3 Near- and Far-field Regions of a Large ( $D \gg 1$ ) Antenna .....	345
Figure II-4 Wave Polarizations.....	347
Figure II-5 Wave Propagation.....	348
Figure II-6 Sky Temperature vs. Frequency.....	350
Figure II-7 Atmospheric Absorption vs. Frequency.....	351
Figure II-8 Absorptive Losses due to Rain vs. Frequency.....	351
Figure II-9 Absorptive Losses due to Fog and Clouds vs. Frequency .....	352
Figure II-10 Coax Cable Attenuation vs. Frequency and Cable Type.....	357

## List of Tables

Table 2-1: Relative Properties of Sandwich Structures.....	9
Table 2-2: Structural Configuration Comparison and Conversion Factors.....	17
Table 2-3: Maximum Accelerations for Launch and Burns .....	21
Table 2-4: Maximum Stage Loading for PTLI, LBM, and ERM.....	21
Table 2-5: Summary of Selected Material Properties .....	36
Table 2-6: Summary of Wing Dimensions.....	71
Table 2-7: Summary of Geometric Configuration.....	75
Table 2-8: Constants for Geometric Configuration .....	77
Table 2-9: Skin Thickness and Weight for a Solid Monocoque Al Structure .....	83
Table 2-10: Insulation Materials.....	85
Table 2-11: Calculation of Heat Shield Coverage and Weights.....	86
Table 2-12: PLM Primary Hull Specifications.....	91
Table 2-13: Landing Gear Geometry & Mass Estimate.....	96
Table 2-14: Support Leg Geometry & Mass Estimate .....	98
Table 2-15: PLM Propellant Section Specifications.....	100
Table 2-16: BioCan Geometry and Mass Estimate.....	103
Table 2-17: Regolith Support Structure Geometry and Mass Estimates.....	107
Table 2-18: PLM Specifications Summary.....	108
Table 3-1: Ranges of Typical Performance Parameters for Rocket Engines .....	112
Table 3-2: Spacecraft Propulsion Functions for Project Columbiad .....	114
Table 3-3: Comparative Performance of Several Spacecraft Propellants .....	115
Table 3-4: Some Physical Properties of Selected Propellants.....	118
Table 3-5: Properties of Selected Propulsion System Structural Materials.....	122
Table 3-6: Mass Breakdown of the RL10A-4 Engine .....	125
Table 3-7: RL10A-4 Component Details .....	125
Table 3-8: R4-D Engine Qualification Test Summary .....	127
Table 3-9: Main Features of the XLR-132 Engine .....	128
Table 3-10: Attributes of Different Positive Expulsion Tank Designs .....	131
Table 3-11: Valve Symbols and Nomenclature for Propulsion System Schematics .....	134
Table 3-12: Number of Engines and Total Burn Times for Each Propulsion Stage.....	127
Table 4-1: Projected Operational Parameters for DSN.....	153
Table 4-2: Antenna Distribution .....	154
Table 4-3: Crew Module and Earth Return Module Throughput Estimates .....	178
Table 4-4: Habitat Throughput Estimates .....	180
Table 4-5: PTLI Throughput Estimates.....	182
Table 4-6: Adjacent Channel Power .....	188
Table 4-7: Communications General Power, Weight and Size Estimates .....	199
Table 4-8: Communications Equipment on CM Power, Size and Weight Estimates.....	200
Table 4-9 Power, Weight and Size Estimates for Earth Return Module.....	200
Table 4-10: Communications on Habitat and PLM Power, Size and Weight.....	201
Table 4-11: Communications Equipment for PTLI Power, Size and Weight.....	202
Table 5-1: Typical Characteristics of Actuation Devices.....	207
Table 5-2: Characteristics of Adcole Sun Sensors .....	210
Table 5-3: Attitude Determination Gyroscope Assembly.....	212
Table 5-4: Component Orientation in IMU.....	217
Table 5-5: GNC Instrumentation Breakdown .....	227
Table 5-6: Docking Requirements/Accuracies .....	232
Table 6-1: Conductor Properties .....	243
Table 6-2: Electrical Storage Devices .....	244
Table 6-3: Power Plant Performance Parameters.....	248

Table 6-4: Preliminary Power Plant Mass Breakdowns.....	249
Table 6-5: Vehicle Stages .....	252
Table 6-5: Boiling Points and Specific Heats of Vaporization of Fuels .....	259
Table 6-6: Properties of Selected Materials .....	264
Table 6-7: Material Trade Study Results .....	265
Table 6-8: Results of ERM Stage Trade Study .....	266
Table 6-8: Results of LBM and TLI Trade Study.....	266
Table 7-1: Effects of Insufficient Oxygen.....	273
Table 7-2: Physical Properties of Potential Diluents .....	276
Table 7-3: The Cabin and Lunar Habitat Atmospheres .....	280
Table 7-4: Suppliers/Contractors for Environmental Control Systems.....	286
Table 7-5: Radiation Exposure Limits Recommended for SpaceFlight Crews .....	291
Table 7-6: Columbiad Spacesuits and Crew Garments.....	292
Table 7-7: Crew Metabolic Rates During Apollo 11 Surface EVAs.....	297
Table 7-8: Inflight Medical Support.....	304
Table 7-9: Minimum Exercise Requirements on the Lunar Habitat .....	307
Table 7-10: Habitat Medical Support .....	308
Table 7-11: Additional Equipment for the Crew Module.....	309
Table 7-12: Additional Equipment for the Habitat.....	309
Table 8-1: Sensor Characteristics .....	317

# **1 Overview**

Volume II of the Columbiad Program Final Report is a look at the subsystem requirements and trade studies. The following subsystems each have a chapter: Structures and Thermal Protection; Propulsion; Command, Communications, and Control; Guidance, Navigation, and Control; Power and Thermal Control; Crew Systems; and Status and Monitoring. Each subsystem, given requirements by Systems Engineering and the Project Groups, designed a system that minimized cost, mass, and production time. One of the mission level requirements was to use as much existing technology as possible, in order to reduce development costs and time. The subsystem groups designed their systems with this in mind, keeping the use of undeveloped technology to a minimum.

## **1.1 Top Level Requirements**

There are certain common top level requirements for the entire project, including all subsystems. These requirements are to insure crew safety, minimize cost, minimize production and development time, minimize mass, and maximize performance. In addition, each subsystem has specific requirements to fulfill.

### **1.1.1 Structures and Thermal Protection**

STP is required to design structures for Project Columbiad that will withstand the environment of the mission without deforming or failing. The outer structure of the following modules must be designed: The PTLI, the LBM, the ERM, the PLM, the BioCan and precursor payload, and the Crew Module. In addition, the tanks that hold propellant and oxydizer for the engines must be designed to fulfill a "leak before burst" criteria.

### **1.1.2 Propulsion**

The Propulsion subsystem is responsible for determining the best method of propulsion for the Columbiad Mission. Once the method is determined, the specific design of the propulsion system for each of the stages is designed, including all associated hardware. The methods of abort during all stages of the mission are also the responsibility of this group.

### **1.1.3 Command, Communications, and Control**

The Command, Communications, and Control (C3) subsystem is responsible for providing communications with the Earth and between the astronauts during the mission. In addition,

C3 designs the necessary computing and information storage systems for the mission, as well as the software needed to insure the mission runs smoothly.

#### **1.1.4 Guidance, Navigation, and Control**

The purpose of the GNC group is to determine where the vehicle is, where it needs to be, and how it is to get there. GNC designs the position determining system of the mission, interfaces with the computing facilities of C3 to determine how to get where the vehicle needs to be, and interfaces with the Propulsion system in order to get the vehicle there.

#### **1.1.5 Power and Thermal Protection**

The primary responsibility of PTC is to provide sufficient power during every phase of the mission. This includes the month-long surface operations, as well as the trips to and from the Moon. An additional responsibility of the PTC group is to design the method by which temperatures in the different parts of the modules remain within specified bounds. Specifically, the insulation for the cryogenic storage tanks is designed by PTC.

#### **1.1.6 Crew Systems**

The purpose of Crew Systems is to insure the health and safety of the crew during the stay on the Moon, and the trip to and from the Moon. They determine what provisions need to be taken along, and what systems are needed to provide a comfortable living environment for the crew.

#### **1.1.7 Status and Monitoring**

There are two main responsibilities of the Status subsystem. Status is responsible for testing the flight hardware. This includes specification testing, acceptance testing, and status testing prior to launch. During the mission, the purpose of the Status subsystem is to monitor the state of the vehicle, to determine if all the components are operating properly and within their design parameters.

### **1.2 Trade Studies and Design Selection**

The following chapters describe the trade studies performed by each subsystem to determine the best way to fulfill the requirements of their system. A design is selected based on the outcome of the trade studies. The final design of each system is not presented here, however. The detailed design of each mission module (PTLI, LBM, PLM, ERM, CM, BioCan, and surface payloads) is presented in Volume III. The final subsystem designs are presented in Volume III as well, in the Chapter corresponding with the physical

location of the subsystem. For example, the final design for the power subsystem on the PTLI stage is located in Volume III, Chapter 3: Primary Translunar Injection Stage. However, the final design of the power system for the lunar surface operations is presented in Volume III, Chapter 8: Surface Payloads Description.

## **2 Structural Manifesto**

### **2.1 Structural Design Methods**

“...the only way to predict the future is to invent it!”

The following section contains the basic principles, equations, and methods that are employed by the STP subsystem group. These form the foundation for all of our designs and allow us to determine the design parameters described in section 2.2. In appropriate cases the relation between the methods and the actual design calculations will be made evident and demonstrated.

#### **2.1.1 STP Basic Principles**

In order to design any type of flight vehicle structure, where weight is a critical link between performance and safety, it is necessary to quantify the balance. This is implemented with the structural factor of safety. The maximum loads are determined, and then the design is carried out for loads a factor of safety above that of maximum. For all of Project Columbiad, this factor is 1.4.

In order to carry out the rapid design required by Project Columbiad it become necessary to use analytic and approximate methods where ever possible. Only during final designs and as verification were finite-element models developed and tested using the matrix method of structural analysis. While the matrix methods offer superior accuracy and precision, the development and computational times required would damp the design process if used exclusively.

Lastly, the structural design of Project Columbiad has emphasized the utilization of advanced technology. Unlike other subsystems, the vehicle structure will be wholly new for Project Columbiad. There is no possible way to use off-the-self hardware for a custom designed vehicle structure. We were therefore free to use the latest techniques and processes, especially those employing composites. As you will notice, a great deal of the structural design abandons conventional isotropic metals in favor of refractory fibrous composites. While the computational burdens are increased by this choice, composites' substantial weight savings justify the expenditure.

### 2.1.2 Beam Statics

There is no room or desire to summarize the theory of elasticity or the basics of beam analysis. However, to understand the structural design it is important that the reader have a grasp of some key concepts. These are summarized below. For a more complete discussion see the references at the end of the chapter.

The shear and bending moment can be derived for the applied load distribution. Two arbitrary constants will be introduced that will be supplied from the structural boundary conditions. See equations 2-1 and 2-2.

$$\frac{\partial S(x)}{\partial x} = P(x) \quad (2-1)$$

$$\frac{\partial M(x)}{\partial x} = S(x) \quad (2-2)$$

The axial stress can be derived from an axial applied load by equation 2-3 show below. If the load is applied laterally, the induced axial stress from bending is given by equation 2-4.

$$\sigma_{xx_{axial}} = \frac{P}{A} \quad (2-3)$$

$$\sigma_{xx_{bending}} = \frac{-M(x)y}{I} \quad (2-4)$$

If it is necessary to determine the deflection of the beam, equation 2-5 will provide the answer after solving a usually involved double integration.

$$v(x) = \iint_{area} \frac{M(x)}{EI} dx \quad (2-5)$$

In all the above equations, the area moment of inertia plays a central role. The area moment of inertia is defined by the equation given in 2-6.

$$I_{axis} = \int_{area} y^2 da \quad (2-6)$$



For a circular cross-section  $I$  is defined as described in equation 2-7. The area moment of inertia of a hollow circular cross-section can be found by subtracting the  $I$  of circle of a radius equal to that of the inner diameter.

$$I_{circle} = \frac{\pi R^4}{4} \quad (2-7)$$

Finally, the stress in the skin is defined by the stress state of the attached stringers. The axial and shear stress is given in equations 2-8 and 2-9. These are almost always computed numerically, and rarely are provided in an analytic manner.

$$\sigma_{x_{skin}}(x) = \sigma_{xa}(x) - \sigma_{xb}(x) \quad (2-8)$$

$$\sigma_{xy_{skin}}(x) = \int [\sigma_{xa}(x) - \sigma_{xb}(x)] dx \quad (2-9)$$

### 2.1.2.1 Buckling

In addition to the failure modes described above in which the beam fails when the materials yield and ultimate stresses are exceeded, it is possible for a beam to fail under a lesser load if under compression. The critical buckling stress is given in equation 2-10. This is critical in the design of the rocket support truss and the casing stringers, both of which use beam members in compression. The effective length depends on the end point constraints. For the rocket support truss and the stringers we have assumed an effective length factor of (2/3) to account for the no rotation of the end points.

$$P_{cr_{buckling}} = \frac{\pi^2 EI}{(L')^2} \quad (2-10)$$

### **2.1.3 Structural Configuration Comparison**

The analysis and design of space structures represents an enormous task for even the most dedicated and brilliant engineers. While we possess large quantities of the former, it is our distinct lack of the latter that required us to develop methods of quickly and accurately computing structural loads and masses. The necessity for rapid design estimates and prototyping dictated that we use monocoque structures. Even complex structures can be reduced without large expenditures of effort to a reasonable finite-element model employing a monocoque structure. While monocoque structures provide the desired ease of computation, they are structurally inefficient and therefore unacceptable for a weight critical vehicle. Clearly we need the ease of monocoque calculations with the structural efficiency of semi-monocoque structures.

An experiment was performed to determine the masses of different structural configurations that all provided the same structural performance. With this, we could determine mass conversion factors for the different structural constructions. You could then design for any structural configuration (most likely monocoque) and simply convert to the one of choice when finished.

These conversion factors would only be valid if the structural samples are matched physically. This meant that the masses would have to come from structural constructions that were stressed and deflected the same amount. Without this, we could not simply replace a semi-monocoque construction for a monocoque one, without changing the structural state of the body. In the end, this provided us a way converting from a monocoque structure with acceptable stresses and strains (determined by the wall thickness largely), but physically beyond acceptable mass limits. By employing the conversion factors derived in this section, the result would be a semi-monocoque structure with acceptable stress and strain (they would be exactly the same as the monocoque structure), with a reduced mass that derives from semi-monocoque efficiency.

Following is a discussion of the different constructions. Following this is the experimental samples and results followed by a summary of the construction conversion factors.

#### **2.1.3.1 Description of Monocoque Structures**

The construction of a monocoque structure is the simplest to conceptualize and analyze (though ironically due to manufacturing problems it is nearly impossible to realize – lucky it is so inefficient). The interior of the structure is void of any load bearing members or

supports. All of the loads (pressure, shear, and bending) are carried in the skin. This requires that the skin be excessively thick and hence its mass is larger than necessary. A monocoque structure can be easily modeled and analyzed with the use of a finite-element analysis program.

#### 2.1.3.2 Description of Sandwich Panels

Since the area moment of inertia is critical in determining the bending stresses in a body, the method of sandwich construction was developed to help increase the area moment of inertia of monocoque structures. The area moment of inertia is maximized by locating the mass as far from the neutral axis as possible. This is the same reasoning that underlies the design of I-beams over solid ones.

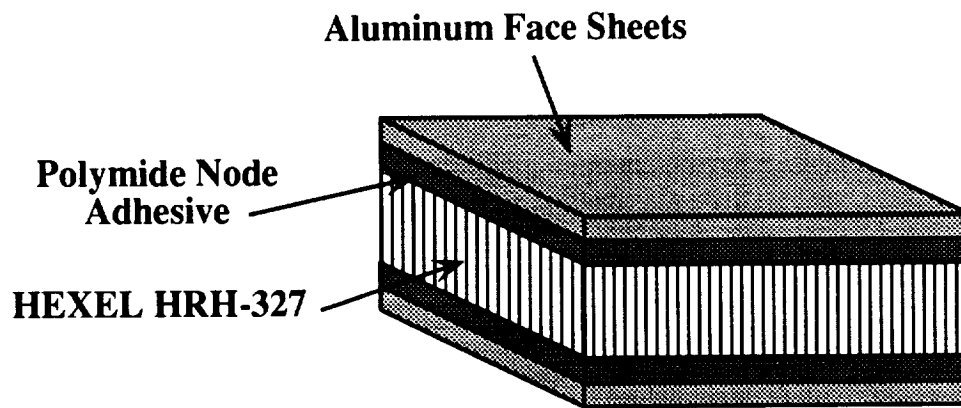


**Figure 2-1**  
**Construction of a Sandwich Structure**

Sandwich construction is used because it provides more strength and much more stiffness for a given weight. A panel is constructed by placing a filler material between two face sheets. The filler material is HEXEL HRH-327 honeycomb. HRH-327 is a polymide node structure dipped in a resin for rigidity. The face sheets are bonded to the honeycomb with a resin adhesive. Typically the face sheets will be aluminum sheet or composite panels. See Figure 2-1.

This construction has two effects. First, the stiffness of the panel is increased since it scales with  $EI$ , and we have purposefully increased  $I$ . Second, the strength of the panel is increased because the stress in the face sheets are less because they are deflected less (due

to the increased stiffness). The filler material carries very little stress loads since it is close to the neutral axis.

Various honeycomb constructions are shown in Figure 2-2. In all three case the same amount of face sheet is used per  $m^2$ . Therefore, for practical purposes the weight of the three modes are the same, since the density of the honeycomb material is very small compared to that of the face sheets. A summary of structural properties for sandwich constructions are shown in Table 2-1.

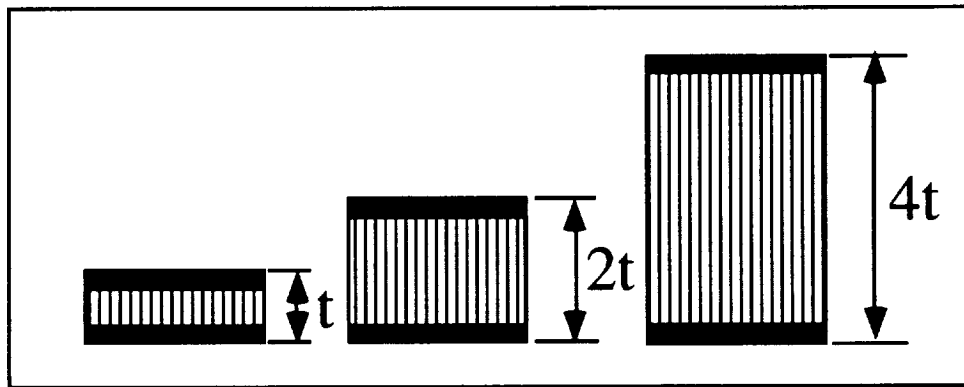


**Figure 2-2**  
**Sandwich Construction Comparison**

It is obvious the there is significant advantage to using a sandwich structure. For nearly the same weight we can achieve a 37x specific stiffness and also 9x higher specific strength. This combination is very beneficial for reducing weight since a smaller thickness of the face sheets can achieve what would have required a much thicker solid structure.

**Table 2-1: Relative Properties of Sandwich Structures**

	$t$	$2t$	$4t$
<b>Relative Stiffness</b>	1	7	37
<b>Relative Strength</b>	1	3.5	9.25
<b>Relative Weight</b>	1	1.03	1.06

It is important to realize that the honeycomb can not be made to exceed very large ratios of the face sheets. If this happens, our assumption of no shear stress in the honeycomb will

no longer be valid, and the it will eventually buckle. A ratio of 4x is used for all panel structures for Project Columbiad.

#### **2.1.3.3 Description of Semi-Monocoque Structures**

If instead of relying completely on the skin to carry the loads, we replace the skin with stringers (axial), longerons (lateral), and a much thinner skin, we can design a structure with the same performance, but much less weight. A sample of a monocoque structure is shown in Figure 2-3.

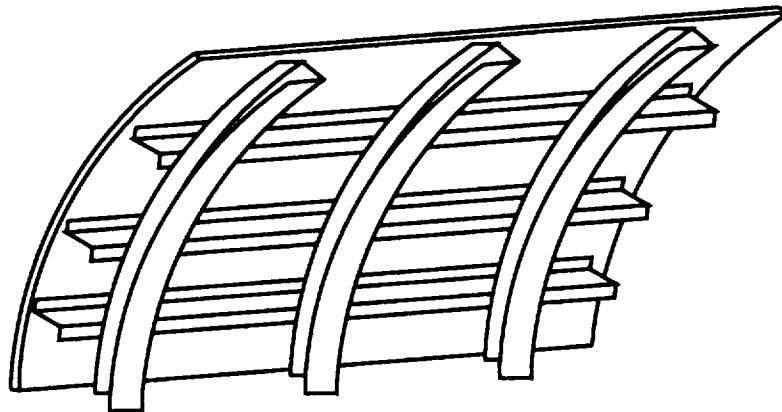


**Figure 2-3**  
**Semi-Monocoque Structure Construction**

The skin is maintained in a semi-monocoque structure for two purposes. First, it carries all of the torsional loads. An unskinned Semi-Monocoque structure has a very low torsional constant, and without the skin there could possibly be unacceptable deflections. Second, it is used to provide an aerodynamic shape, and transfer the aerodynamic loads ( $q$ , dynamic pressure) to the longerons and stiffeners. Therefore, the skin must be designed to carry aerodynamic loads without failing.

#### **2.1.3.4 Test Case 1 – Solid Monocoque**

To carry out the experiment, a 4x4m flat plate was generated using a finite-element analysis program. The first case was a solid monocoque plate. An arbitrary thickness of 4cm was chosen. The entire plate is made of aluminum. This plate has a mass of 1770kg.

The plate was pinned at the four corners and load with an arbitrary 20,000 Pa pressure over the whole surface. No acceleration, gravity, or point loads were applied during the test to help minimize computational times.

A typical deflection pattern is shown in Figure 2-4. The four corners have zero translation, but are free to rotate. The pressure deflects the plate in a parabolic shape.

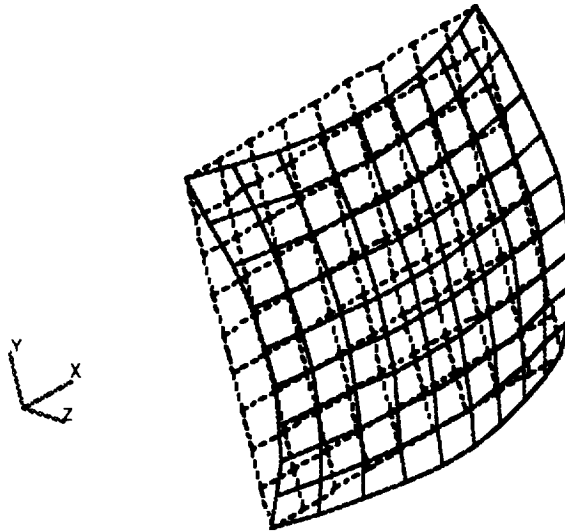


**Figure 2-4**  
**Typical Plate Deflection**

The results from the analysis show that the maximum deflections are on the order of 25 to 30 cm. This is high, but not excessive since the plate is 4m across. The aluminum is stressed to approximately  $1.5 \times 10^8$ , which about 35% of its yield stress. Representative values are shown in Figure 2-5.

To determine our conversion factors for other types of construction, we generate a finite-element model of each and change its geometry until it is stressed and deflects approximately the same amount as the solid monocoque structure described above. Then by comparing mass of these other constructions, we can determine a ratio of the masses between types of structural configuration.

DISPLACEMENTS						
NODE	X TRANS	Y TRANS	Z TRANS	X ROT	Y ROT	Z ROT
33	0.0000E+00	0.0000E+00	2.5310E-01	5.2860E-02	-6.5764E-02	0.0000E+00
34	0.0000E+00	0.0000E+00	2.7816E-01	4.4412E-02	-4.4412E-02	0.0000E+00
35	0.0000E+00	0.0000E+00	2.9179E-01	4.0148E-02	-1.5635E-02	0.0000E+00

MAXIMUM STRESSES FOR QUAD ELEMENT					VON MISES CRITERION	
ELEMENT	NODE	MAJOR	MINOR	SHEAR	STRESS	% YIELD
44	0	1.539E+08	-1.539E+08	4.227E+07	1.335E+08	32.3
44	48	1.469E+08	-1.469E+08	2.862E+07	1.282E+08	31.0
44	49	1.610E+08	-1.610E+08	5.591E+07	1.429E+08	34.6
44	59	1.610E+08	-1.610E+08	5.591E+07	1.429E+08	34.6
44	58	1.469E+08	-1.469E+08	2.862E+07	1.282E+08	31.0

MAXIMUM STRESSES FOR SURFACE/SOLID ELEMENTS				VON MISES
NODE	MAJOR	MINOR	SHEAR	STRESS CRITERION
41	1.804E+08	-1.804E+08	9.163E+07	1.818E+08
42	1.632E+08	-1.632E+08	5.818E+07	1.456E+08
43	1.493E+08	-1.493E+08	3.103E+07	1.300E+08

**Figure 2-5**  
**Representative Results for a Solid Monocoque Panel**

#### **2.1.3.5 Test Case 2 – Sandwich Monocoque**

The second construction sample was also a monocoque structure, but the solid aluminum sheet was replaced by a sandwich assembly. By changing the thickness of the aluminum face sheets, it was possible to match the structural state of test case 1. Representative values are shown in Figure 2-6. In this analysis it is assumed that the thickness of the honeycomb core is scaled with the face sheets so that it maintains a 4x ratio.

DISPLACEMENTS						
NODE	X TRANS	Y TRANS	Z TRANS	X ROT	Y ROT	Z ROT
40	0.0000E+00	0.0000E+00	4.1378E-02	1.7762E-02	1.4152E-02	0.0000E+00
41	0.0000E+00	0.0000E+00	4.6728E-02	6.0850E-03	-1.1657E-02	0.0000E+00
42	0.0000E+00	0.0000E+00	5.2619E-02	4.9292E-03	-1.3820E-02	0.0000E+00
43	0.0000E+00	0.0000E+00	5.8653E-02	4.0038E-03	-1.2509E-02	0.0000E+00
MAXIMUM STRESSES FOR QUAD ELEMENT						
ELEMENT	NODE	MAJOR	MINOR	SHEAR	STRESS	% YIELD
44	0	6.149E+08	-6.149E+08	1.676E+08	5.332E+08	14.4
44	48	5.875E+08	-5.875E+08	1.134E+08	5.132E+08	13.9
44	49	6.422E+08	-6.422E+08	2.219E+08	5.695E+08	15.4
44	59	6.422E+08	-6.422E+08	2.219E+08	5.695E+08	15.4
44	58	5.875E+08	-5.875E+08	1.134E+08	5.132E+08	13.9
MAXIMUM STRESSES FOR SURFACE/SOLID ELEMENTS						
NODE	MAJOR	MINOR	SHEAR	VON MISES STRESS CRITERION		
40	6.901E+08	-6.901E+08	3.670E+08	7.132E+08		
41	7.176E+08	-7.176E+08	3.646E+08	7.235E+08		
42	6.511E+08	-6.511E+08	2.311E+08	5.803E+08		
43	5.974E+08	-5.974E+08	1.232E+08	5.202E+08		

**Figure 2-6**  
**Representative Results for a Sandwich Monocoque Panel**

The structural state shown in Figure 2-6 was achieved with 0.7cm thick face sheets. This gives a total thickness (including honeycomb) of 7cm. The weight of the entire structure is approximately 939kg. This immediately indicates the benefit of sandwich construction. The monocoque structure required 4cm thickness to perform the same load carry ability, and nearly 1800kg.



#### **2.1.3.6 Test Case 3 – Solid Semi-Monocoque**

Test case 3 involves a semi-monocoque construction with a solid skin covering. The semi-monocoque structural sample consists of evenly spaced stiffeners 0.66m apart starting from the edges. Therefore, there are 7 stiffeners in each direction. The stiffeners are rectangular beams with the axis normal to surface of the skin significantly larger than the width. This is to increase the area moment of inertia of the beam (I). Both the skin thickness and the dimensions of the beams were the independent variables that could be chosen to attempt to match the structural state of test case 1.

For the case of 14x1cm bars and a skin thickness of 1cm the values shown in Figure 2-7 are representative. The beams and the plate are stressed to the same yield % as the plate in the solid Monocoque case. The weight of this semi-monocoque structure is 1203kg. This is approximately 500kg lighter than a solid monocoque construction.

#### **2.1.3.7 Test Case 4 – Sandwich Semi-Monocoque**

The final case is very similar to test case 3, except that a sandwich panel replaces the solid panel for the skin. The configuration of the stiffeners remained the same. Since the skin thickness of the semi-monocoque structure is test case 3 is already very thin, it was clear that we were not going to be able to realize a significant mass decrease. For the values shown in Figure 2-8 below, a 3mm face sheet thickness was used along with the 14x1cm bars described in case 3. The mass of this sample is 800kg.

NODE	X TRANS	Y TRANS	Z TRANS	X ROT	Y ROT	Z ROT
41	0.0000E+00	0.0000E+00	3.9104E-01	3.2218E-04	-6.0641E-02	0.0000E+00
42	0.0000E+00	0.0000E+00	4.1089E-01	5.1549E-04	-5.8566E-02	0.0000E+00
43	0.0000E+00	0.0000E+00	4.2939E-01	5.7982E-04	-5.2980E-02	0.0000E+00

MAXIMUM STRESSES FOR QUAD ELEMENT					VON MISES CRITERION	
ELEMENT	NODE	MAJOR	MINOR	SHEAR	STRESS	% YIELD
44	0	6.720E+07	-6.720E+07	2.171E+07	5.902E+07	14.3
44	48	5.156E+07	-5.156E+07	3.012E+07	5.641E+07	13.7
44	49	9.039E+07	-9.039E+07	1.743E+07	7.896E+07	19.1
44	59	8.089E+07	-8.089E+07	1.467E+07	7.092E+07	17.2
44	58	4.767E+07	-4.767E+07	2.631E+07	5.033E+07	12.2

MAXIMUM STRESSES FOR BEAM				VON MISES CRITERION				
ELEMENT	MAJOR	MINOR	SHEAR	STRESS	% YIELD	@NODE	CONNECTIVITY	
110	1.123E+08	-1.123E+08	5.617E+07	1.123E+08	27.2	25	15 25	
111	2.135E+08	-2.135E+08	1.068E+08	2.135E+08	51.7	35	25 35	
112	2.603E+08	-2.603E+08	1.301E+08	2.603E+08	63.0	45	35 45	

MAXIMUM STRESSES FOR SURFACE/SOLID ELEMENTS				VON MISES
NODE	MAJOR	MINOR	SHEAR	STRESS CRITERION
44	3.334E+07	-3.334E+07	7.838E+06	3.020E+07
45	2.389E+07	-2.389E+07	3.306E+06	2.137E+07
46	3.240E+07	-3.240E+07	8.905E+06	3.041E+07

**Figure 2-7**  
**Representative Results for a Solid Semi-Monocoque Panel**

NODE	X TRANS	Y TRANS	Z TRANS	X ROT	Y ROT	Z ROT
43	0.0000E+00	0.0000E+00	1.4675E-01	-2.7301E-04	-1.6279E-02	0.0000E+00
44	0.0000E+00	0.0000E+00	1.5567E-01	-2.7795E-04	-9.6075E-03	0.0000E+00
45	0.0000E+00	0.0000E+00	1.5888E-01	-3.4418E-04	3.4418E-04	0.0000E+00

MAXIMUM STRESSES FOR QUAD ELEMENT					VON MISES CRITERION	
ELEMENT	NODE	MAJOR	MINOR	SHEAR	STRESS	% YIELD
44	0	3.175E+06	-3.175E+06	1.473E+06	3.068E+06	0.1
44	48	2.846E+06	-2.846E+06	2.085E+06	3.690E+06	0.1
44	49	3.939E+06	-3.939E+06	1.147E+06	3.426E+06	0.1
44	59	3.511E+06	-3.511E+06	9.760E+05	3.047E+06	0.1
44	58	2.538E+06	-2.538E+06	1.817E+06	3.229E+06	0.1

MAXIMUM STRESSES FOR BEAM				VON MISES CRITERION				
ELEMENT	MAJOR	MINOR	SHEAR	STRESS	% YIELD	@NODE	CONNECTIVITY	
93	3.108E+08	-3.108E+08	1.555E+08	3.108E+08	75.3	33	23	33
94	3.541E+08	-3.541E+08	1.771E+08	3.542E+08	85.8	43	33	43
95	3.541E+08	-3.541E+08	1.771E+08	3.542E+08	85.8	43	43	53

MAXIMUM STRESSES FOR SURFACE/SOLID ELEMENTS				VON MISES	
NODE	MAJOR	MINOR	SHEAR	STRESS	CRITERION
41	4.773E+06	-4.773E+06	1.574E+06	4.203E+06	
42	3.842E+06	-3.842E+06	1.892E+06	4.077E+06	
43	2.879E+06	-2.879E+06	1.581E+06	3.176E+06	

**Figure 2-8**  
**Representative Results for a Sandwich Semi-Monocoque Panel**

### **2.1.3.8 Structural Configuration Summary**

A summary of the weights for the four structural samples is shown in Table 2-2. If we non-dimensionalize the mass by the mass of the solid monocoque structure we can determine what advantage the other structural construction techniques offer.

**Table 2-2: Structural Configuration Comparison and Conversion Factors**

	Weight (kg)	Relative Weight
<b>Solid Monocoque</b>	1772	100%
<b>Sandwich Monocoque</b>	939	53%
<b>Solid Semi-Monocoque</b>	1203	68%
<b>Sandwich Semi-Monocoque</b>	849	48%

A sandwich panel on a semi-monocoque structure is evidently the most structurally efficient. While a sandwich monocoque structure has only a 5% higher relative mass, the complexity of manufacture and assembly a monocoque structure clearly diminishes its advantage.

These non-dimensionalized relative mass figures serve as the structural conversion factors. If, for example, a design of a solid monocoque structure is 400kg, it is possible to construct a sandwich semi-monocoque structure for:

$$48\% \cdot 400\text{kg} = 192\text{kg}$$

This would then equal the mass of the designed semi-monocoque structure.

#### **2.1.4 Rocket Stage Casing Design**

Since the rocket stages for Project Columbiad were all designed with a common geometry, it was highly desirable to develop a generalized structural design procedure that would work for all of them. The methods described in this section were employed for the design of the PTLI, the LBM, and the ERM. The procedure will be described in this section and only the highlights of the calculation will be described in each stages design section in Volume III.

The typical rocket stage consists of a semi-monocoque outer casing. The casing consists of axial stringers designed to take the axial and bending loads of the vehicle. Lateral longerons (or frames in the aircraft sense) provide the structure to resist the normal lateral loads and the resistance to prevent stringer buckling. The structure is covered on the outside with a skin to resist torsional loads and aerodynamic pressure.

At the bottom of the casing is the rocket support truss. This truss is designed to distribute the force of the engines to the structural casing. Depending on the stage it is either a three or five engine truss. The truss will be discussed in section 2.2.

The main bulk of the interior of the casing is oxidizer and fuel propellant tanks. The tanks are made to fill the inside diameter, allowing for cryogenic insulation. The tanks are cylindrical with 2:1 elliptical end caps.

Each stage was design on the basis of a small number of parameters. These include propellant weight, number of engines, and spacing requirements.

The functions described in Figure 2-9 were written to generalize some of the more common tasks. These will be used in later sections and are provided here as a reference for the reader and future students. The inputs to the procedure are include between [...]’s. the output is the quantity of the left, and most of the variables are quite explicit.

```

FindStringerMass[stringerArea_, stageHeight_, materialDensity_] :=
    stringerArea stageHeight materialDensity

FindMassFraction[structureMass_, fuelMass_] :=
    (structureMass / (fuelMass + structureMass)) 100;

FindMinimumRadius[area_] := Sqrt[area / Pi];

FindMinimumDiameter[area_] := 2 FindMinimumRadius[area];

FindStageInertia[numStringers_, stageRadius_, outerDiameter_, thickness_] :=
    Sum[FindStringerInertia[outerDiameter, thickness] +
        FindStringerArea[outerDiameter, thickness] (stageRadius Sin[theta Degree])^2,
        {theta, 0, 360 (1 - 1/numStringers), 360 / numStringers}]

FindApproximateStageInertia[stageArea_, numStringers_, stageRadius_] :=
    Sum[(stageArea / numStringers) (stageRadius Sin[theta Degree])^2,
        {theta, 0, 360 (1 - 1/numStringers), 360 / numStringers}]

FindStringerInertia[outerDiameter_, thickness_] :=
    (Pi/4) ((outerDiameter/2)^4 - ((outerDiameter/2) - thickness)^4)

FindStringerArea[outerDiameter_, thickness_] :=
    Pi ((outerDiameter/2)^2 - ((outerDiameter/2) - thickness)^2)

FindStringerThickness[outerDiameter_, stringerArea_] :=
    (outerDiameter/2) - Sqrt[(outerDiameter/2)^2 - stringerArea / Pi]

FindOuterDiameter[stringerArea_, thickness_] :=
    (stringerArea / (Pi * thickness) + thickness)

FindLongeronMass[longeronThickness_, longeronWidth_, stageRadius_,
    materialDensity_] :=
    Pi (stageRadius^2 - (stageRadius - longeronWidth)^2) *

```

```

longeronThickness * compositeDensity //N

FindBucklingStress(materialModulus_,beamInertia_,beamlength_,
    beamArea_,effectiveLengthFactor_):=
    (Pi^2 materialModulus beamInertia / (effectiveLengthFactor beamlength)) /
    beamArea

FindMaximumStringerLength(materialModulus_,bodyInertia_,
    materialYieldStress_,stringerArea_,effectiveLengthFactor_):=
    Pi^2 materialModulus bodyInertia /
    (materialYieldStress stringerArea effectiveLengthFactor)

```

**Figure 2-9**  
**Function Definitions for Rocket Casing Calculations**

Each stage is operated in two distinct regimes. The first is during launch, when the PTLI stage has no payload, and the second is during the space burn, when it has the full payload. It is necessary to determine the regime in which it will experience the greatest loads, since these will be the driving factors in the structural configuration.

The maximum accelerations are shown in Table 2-3. As can be seen in Table 2-4, even though during the space burn the PTLI stage has a much greater mass to thrust ratio, the lower accelerations actually make the loads less than that of launch where it experiences the full 3.5 g's of its own weight. Obviously the LBM and ERM experience their maximum loads during launch, where they experience the full 3.5 g's axially and also carry their payload.

**Table 2-3: Maximum Accelerations for Launch and Burns**

<b>Stage Loading Inputs</b>	
Earth Acceleration	9.8
Factor of Safety	1.4
Space Axial Acceleration	1.5
Space Lateral Acceleration	1
Launch Axial Acceleration	3.5
Launch Lateral Acceleration	2.5

**Table 2-4: Maximum Stage Loading for PTLI, LBM, and ERM**

	<b>PTLI</b>	<b>LBM</b>	<b>ERM</b>
Stage Fuel	85000	55600	17700
Stage Mass	94881	62050	23121
Structural Mass	6550	4150	4097
Stage Radius	3	3	3
Stage Height	16.46	13.2	8.97
Stage Payload	90871	28821	5700
Space Axial Loading	3,822,776	1,870,125	593,136
Space Lateral Loading	13,982,866	5,485,701	1,182,318
Space Effective Loading	17,805,642	7,355,826	1,775,454
Launch Axial Loading	4,556,186	2,979,641	1,110,270
Launch Lateral Loading	17,855,908	9,364,586	2,371,220
Launch Effective Loading	22,412,094	12,344,227	3,481,491
Maximum Loading	22,412,094	12,344,227	3,481,491
Regime	Launch	Launch	Launch

Once the loads are determined, shown in Table 2–4, it is possible to derive the shear and bending moments of the stage. These are required to determine the stress state in the structure. This is basic structural methodology and will not be summarized here. However, Figure 2–10 shows the equations for computation.



```

lateralLoad = launchLateralAcceleration stageMass factorOfSafety earthAcceleration

axialLoad = stageMass launchAxialAcceleration factorOfSafety earthAcceleration

lateralLoadDensity = lateralLoad/stageHeight

axialLoadDensity = axialLoad/stageHeight

shearStress = lateralLoad - Integrate[lateralLoadDensity,x]

bendingMoment = lateralLoad stageHeight/2 - Integrate[shearStress, x]

```

**Figure 2-10**  
**Equations for Determining Shear and Bending Moments**

To repeat for clarity, these steps will be performed for each stage. This is simply a presentation of the methods that were employed in a generalized rocket stage design. See section 2.2 for more detailed analysis of the individual stage design.

#### 2.1.4.1 Stringers

The stringers carry the axial and bending loads the vehicle. The stringers were assumed to have a circular cross section, with a hollow core. Once the inertia of the stage is calculated (almost completely independent of the area of the stringers), the axial stress can be determined as a function of the total stage area. An area is chosen so that the material of choice does not fail, and subsequently the area of the individual stringers can be calculated. To then maximize the inertia of the stringers, which is critical for the buckling loads, a minimum thickness is chosen, and the outer diameter is calculated so that the stringer will have the requisite area. At this point the stringer geometry is set. These equations are summarized in Figure 2-11.

```

approximateStageInertia =
    FindApproximateStageInertia[stageArea,numberStringers, stageRadius] //N

axialStress =
    axialLoad/stageArea + bendingMoment stageRadius/approximateStageInertia

stageArea = stageArea /. FindRoot[(axialStress /. x->0) == compositeYieldStress,
    {stageArea, 0.005}]

stringerArea = stageArea/numberStringers

stringerMass = FindStringerMass[stringerArea, stageHeight, compositeDensity]

totalStringerMass = stringerMass numberStringers

minimumThickness = 0.004;

outerDiameter = FindOuterDiameter[stringerArea, minimumThickness] //N

stringerThickness = N[FindStringerThickness[outerDiameter, stringerArea]]

stringerInertia = N[FindStringerInertia[outerDiameter, stringerThickness]]

stageInertia =
    FindStageInertia[numberStringers,stageRadius,outerDiameter,stringerThickness]

```

**Figure 2-11**  
**Equations for Determining Stringer Geometry**

#### 2.1.4.2 Frames

The frames are design to carry the lateral acceleration and to prevent the stringers from buckling. The frame is first designed to carry the lateral loads, and then is spaced just under

the buckling length of the stringers. So, in essence, the lateral load determines the size and geometry of the frames, and stringer buckling sets the longeron spacing.

To determine the size of the frames a finite-element model was generated and loaded with the lateral loads (accelerations times the stage mass) divided by the number of frames. This load was then distributed over one side of the longeron in the plane of the frame. The cross section of the frame is rectangular with the axial distance much longer than the thickness.

DISPLACEMENTS						
NODE	X TRANS	Y TRANS	Z TRANS	X ROT	Y ROT	Z ROT
5	-1.5698E-01	-2.4396E-01	0.0000E+00	0.0000E+00	0.0000E+00	-5.9892E-01
6	-5.4741E-01	1.4659E-01	0.0000E+00	0.0000E+00	0.0000E+00	1.5671E-01
8	-5.4741E-01	-1.4659E-01	0.0000E+00	0.0000E+00	0.0000E+00	-1.5671E-01

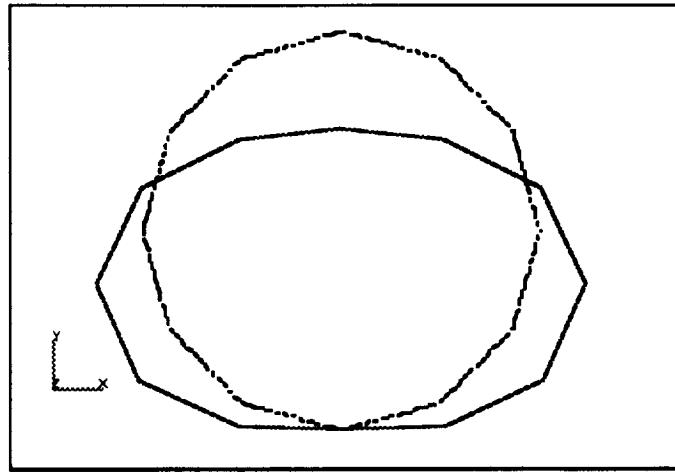
  

MAXIMUM STRESSES FOR BEAM				VON MISES CRITERION				
ELEMENT	MAJOR	MINOR	SHEAR	STRESS	% YIELD	@NODE	CONNECTIVITY	
5	9.792E+08	-9.962E+08	4.981E+08	9.962E+08	74.5	6	5	6
6	1.178E+09	-1.194E+09	5.969E+08	1.194E+09	89.3	7	6	7
7	1.178E+09	-1.194E+09	5.969E+08	1.194E+09	89.3	7	7	8
8	9.792E+08	-9.962E+08	4.981E+08	9.962E+08	74.5	8	8	9

**Figure 2-12**  
**Representative Frame FEM Results**

The finite-element model determined that frames that could withstand the requisite loads had a 1.3x10cm cross section. Figure 2-12 shows the stresses and deflections for this size frame using the PTLI lateral loads. The same frame was used on all of the stages, since it would have required far too much effort to resize the frame for each stage. This simply means that the frames for the LBM and ERM are larger than required (this is because the frames were calculated with the PTLI lateral loads since they were the largest).

The Figure 2-13 shows the bending mode of a typical frame due to the lateral loads. The scales are exaggerated in order to be able to see the deflections.



**Figure 2-13**  
**Frame Bending First Mode**

There are two possible ways that the stringers could fail. These are shown in Figure 2-14 and 2-15. The first, called panel instability, occurs when the stringers buckle. To prevent this from occurring it is necessary to space the longerons, which act as support,, a distance that causes the stringer buckling stress to be above or at the material yield stress. This is a simple calculation and the equations are shown in Figure 2-16.

The second mode of failure is referred to as general instability. This occurs when the frames are not sufficient to resist the first buckling mode of the stringers and the frame fails. The frames that were designed above have more than adequate strength to resist a general instability failure as long as the maximum lateral accelerations are not exceeded.

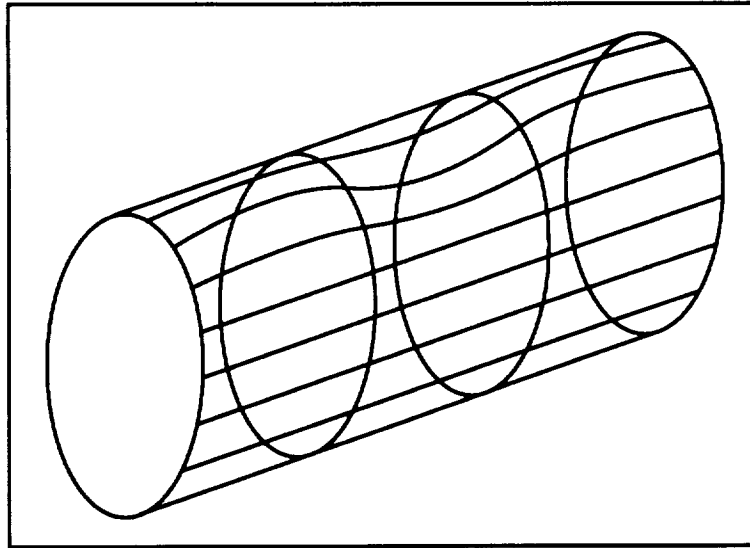


**Figure 2-14**  
**Panel Instability in Semi-Monocoque Structures**

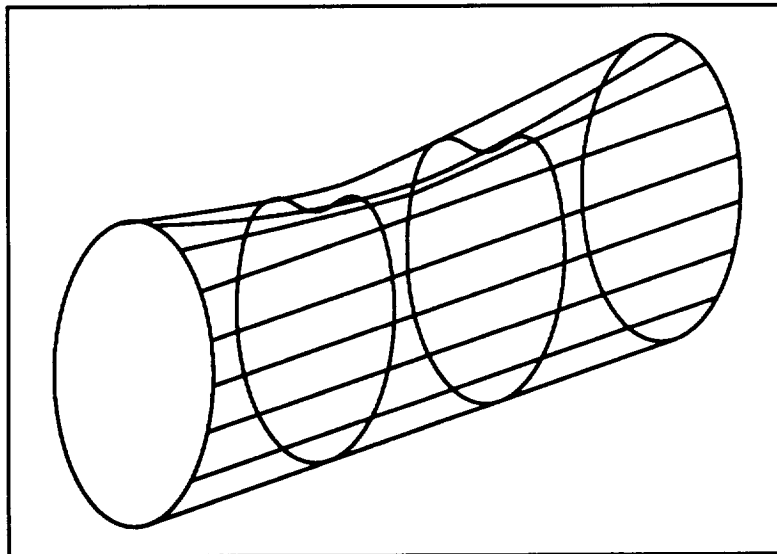


**Figure 2-15**  
**General Instability in Semi-Monocoque Structures**

The equations that are shown in Figure 2-16 determine the number of longerons that are required for each stage, and then, using the designed frame geometry described above, the total mass is calculated.

```

stringerLength = N[FindMaximumStringerLength[compositeModulus, stringerInertia,
    compositeYieldStress, stringerArea, (2/3)]]

numberLongerons = Ceiling[stageHeight/stringerLength]

longeronSpacing = N[stageHeight/numberLongerons]

longeronThickness = 0.013;

longeronWidth = 0.10;

longeronMass = FindLongeronMass[longeronThickness, longeronWidth, stageRadius,
    compositeDensity]

totalLongeronMass = longeronMass numberLongerons

```

**Figure 2-16**  
**Equations for Determining Longerons Geometry**

#### 2.1.4.3 Skin

The axial and shear stress in the skin is determined from the equations described in section 2.1.2. These are needed to correctly size the skin for the crushing failure mode. However, with long thin curved panels, there is a very high likelihood that the panel will buckle before it ever reaches the design limit stress. Therefore it is necessary to determine the forces the will buckle a curved skin panel and compare this with the loads applied to the skin. The load that will buckle the skin is given in equation 2-11. The arbitrary constant  $K_c$  can be found from the chart given in Figure 2-17. The independent axis is a function of  $Z$  which is given in equation 2-12. Notice that  $Z$  is dependent only on the width of the panel, and the thickness (the radius and Poisson's ratio are set by the design geometry and material and therefore are not independent).

$$F_{CF\text{ compression}} = \frac{K_c \pi^2 E}{12(1 - \nu_c^2)} \left( \frac{t}{b} \right)^2 \quad (2-11)$$

$$Z = \frac{b^2}{rt} \sqrt{1 - \nu_e^2} \quad (2-12)$$

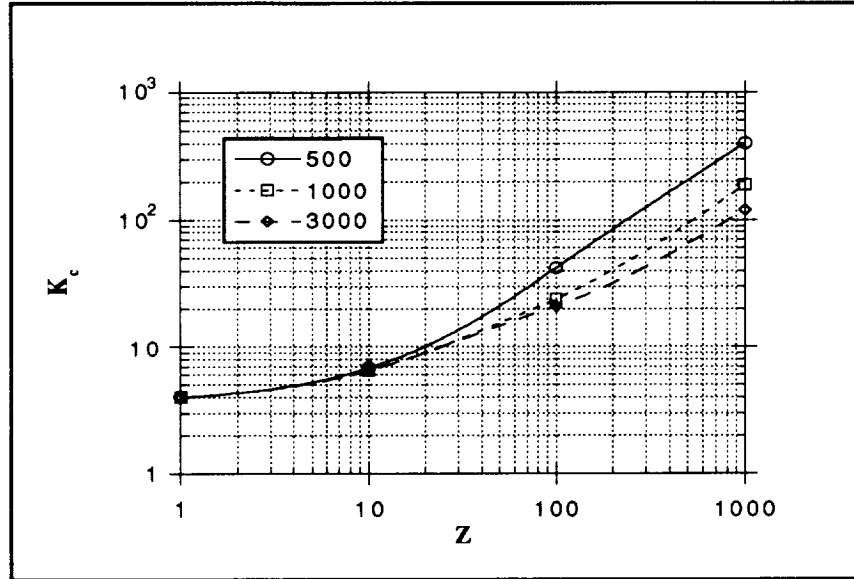


**Figure 2-17**  
**Axial Compressive Buckling Coefficients for Curved Plates**

We can therefore size the skin panels so that the axial buckling stress is equal to the material buckling stress by changing the width of the panel and the thickness of the skin. However, as is clearly evident, increasing the skin thickness to increase the critical buckling stress also raises the weight of the skin.

In a similar manner, the critical buckling load for shear failure is given by equation 2-13. The variable is the same, however,  $K_s$  is given in Figure 2-18.

$$F_{cr, shear} = \frac{K_s \pi^2 E}{12(1 - \nu_e^2)} \left( \frac{t}{b} \right)^2 \quad (2-13)$$

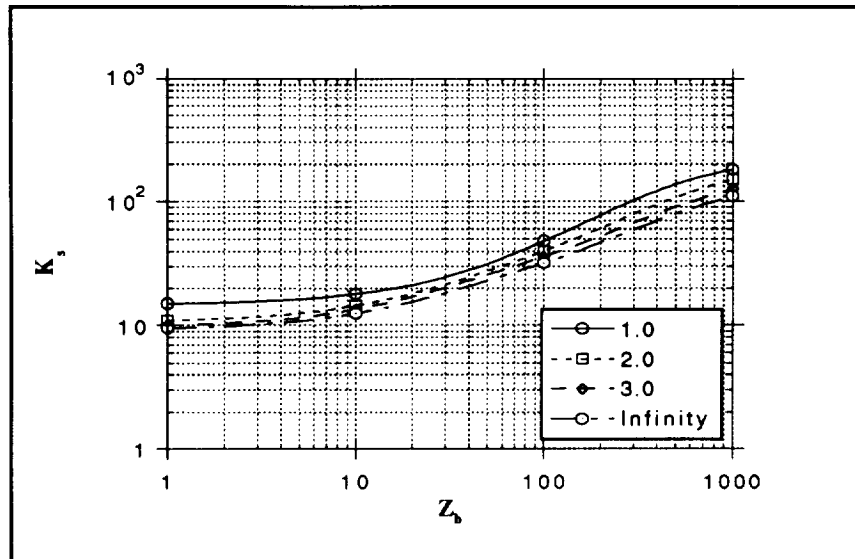


**Figure 2-18**  
**Shear Buckling Coefficients for Clamped Curved Plates**

For the rocket casing, the required thickness to prevent buckling in the skin was enormous, on the order of 10cm. This would mean a weight of several thousand kilograms. It was therefore desirable to allow the skin panels to buckle and design them simply to withstand the aerodynamic loads during launch.

This is a valid structural design because even with the skin failed, the structural integrity of the vehicle is still intact as long as the support frame (stringers and longerons) have not failed. When we design the skin to buckle, the skin is not designed to carry any of the structural loads.

This design had two repercussions. First, the design of integral fuel tanks was not possible. Originally the fuel tanks were designed to be part of the outside structure with skirts between the tanks and the truss and tanks. This would have required that the skin not buckle, since the skin would be functioning as a pressure vessel for the propellants. So, instead the tanks were designed to be completely within the outside casing of the stage. The second outcome is that the skin could be made very thin since it was required only to withstand a maximum 8000 Pa aerodynamic pressure.



#### 2.1.4.4 Frequency Analysis

The structural analysis in the frequency domain represents a complex and difficult task at best. Since the frequency environment of the NLS launch vehicle was not available, STP was not able to design the first axial mode of the vehicle above that of the launch vehicle. As an interim analysis, we simply calculated the first mode of the vehicle, to provide some reference for the future.

The frequency of a vehicle mode composed of a structural casing is given by equation 2-14, where  $i$  is the mode number, and  $m$  is the mass per unit length.

$$f_{lateral,i} = \left( \frac{\lambda_i}{2\pi L} \right)^2 \sqrt{\frac{EI}{m}} \quad i = 1, 2, 3, \dots \quad (2-14)$$

The parameter  $\lambda$  is determined experimentally and is given in equation 2-15 for the  $i$ 'th mode of the vehicle.

$$\lambda_i = 1.875, 4.694, 7.854, \dots, (2i-1)\frac{\pi}{2} \quad (2-15)$$

The axial frequency for the first mode is given by equation 2-16.

$$f_{axial,i} = 0.25 \sqrt{\frac{AE}{M_{total}L}} \quad (2-16)$$

The equations shown in Figure 2-19 were used during the design process for determining the frequency modes of the vehicle stage.

```
lambda = 1.875

massPerLength = structureMass/stageHeight

lateralFrequency = lambda^2 Sqrt[compositeModulus stageInertia/massPerLength]/
(2 Pi stageHeight^2)
```

$$\text{axialFrequency} = 0.250 \sqrt{\text{stageArea} \cdot \text{compositeModulus} / (\text{structureMass} \cdot \text{stageHeight})}$$

**Figure 2-19**

### **Equations for Determining the First Mode Frequency of the Structure**

#### **2.1.5 Pressure Vessels**

All the rocket stages have two major pressure vessels for the oxidizer and fuel propellants. The construction of a tank consists of a fibrous composite wound around a solid core of non-reactive material (assumed to be steel for the design process). The entire outside of the tank is surrounded by a 20cm thick layer of cryogenic insulation. The composite is designed to carry all of the loads experienced by the structure. This consists not only of the internal pressure, but also the inertia loads of the propellants and insulation during launch. The internal core is simply to prevent oxidation or degradation of the composite structure. It is assumed to be non-reactive with both the oxidizer and fuel. The construction is shown in Figure 2-21.

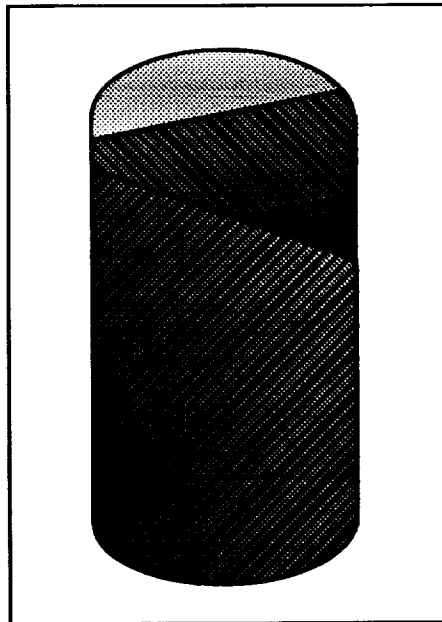


**Figure 2-21**

### **Construction of Oxygen and Fuel Tanks**

The assumed tank geometry consists of a cylindrical body with 2:1 elliptical end caps. The structural analysis of the tanks requires looking at two specific parts of the structure. First,

the meridional stresses in the lower end cap. This is where the highest stresses will be found. This thickness will then be used for the entire tank. However, in the cylindrical side walls it is important to determine that the stress does not exceed the critical buckling stress for a solid monocoque cylinder. If this is the case, the tank will not fail during the launch loads.

#### 2.1.5.1 End Caps

Structurally, the most efficient form of pressure vessel is one in which the lateral pressures are supported by tensile stresses alone in the curved walls of the vessel. While hemispherical bulkheads are highly desirable from a stress standpoint, such forms are uneconomical as regards to space utilization. On the other hand, a flat bulkhead, while providing far more useful volume, cannot resist the pressure loading by membrane stresses requiring additional support and hence is structurally inefficient.

Another form of bulkhead used to close a circular pressure cylinder is elliptical. Such a bulkhead shape provides tangential meridional forces at the seam (requiring no reinforcing ring) and yet is reasonably efficient as regards space utilization. This was the geometry chosen for the tanks used in Project Columbiad.

The stress in the walls is given by equation 2-17. The stress is proportional to the skin thickness by the stress coefficient. The tangential and meridional stress coefficients are given in equations 2-18 and 2-19. Both of these are a function of the x and y coordinates that define the ellipse. The semi-major axis of the ellipse (which is equal to the radius of the cylindrical section) is designated by a, and the semi-minor axis by b (0.5a).

$$\sigma = \frac{N}{t} \quad (2-17)$$

$$N_m = \frac{pR_t}{2} = \frac{p}{2} \frac{\sqrt{a^4 y^2 + b^4 x^2}}{b^2} \quad (2-18)$$

$$N_t = p \frac{\sqrt{a^4 y^2 + b^4 x^2}}{b^2} \left[ 1 - \frac{a^4 b^2}{2(a^4 y^2 + b^4 x^2)} \right] \quad (2-19)$$

Both stress coefficients are also a function of the applied pressure loads. The variable  $p$  can be a constant or a function of either  $x$  or  $y$  or both. The stress in the walls is then a function of  $x$  and  $y$ , but is constant radially around the tank.

According to the chart in Figure 2-22, it is clear that the maximum meridional stress occurs not at the seam of the cylindrical body and the elliptical end cap, which seems to be intuitive, but at the very bottom of the tank. This is where the required skin thickness will be calculated.

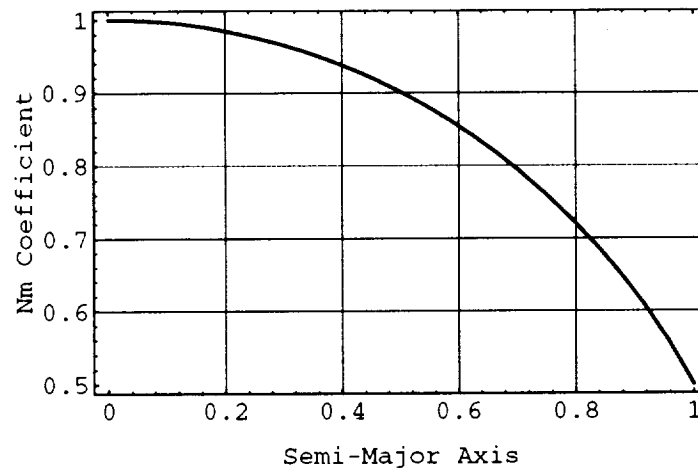


**Figure 2-22**  
**Non-dimensional Meridional Stress Coefficient for 2:1 Ellipses**

The tangential stress is compressive at the bottom of the tank where the maximum meridional stress occurs, so there will be large shear stresses at this location. An interesting note about the tangential stress is that it is compressive at the seam of the tank. therefore the seam will be strained inwards somewhat like a noose.

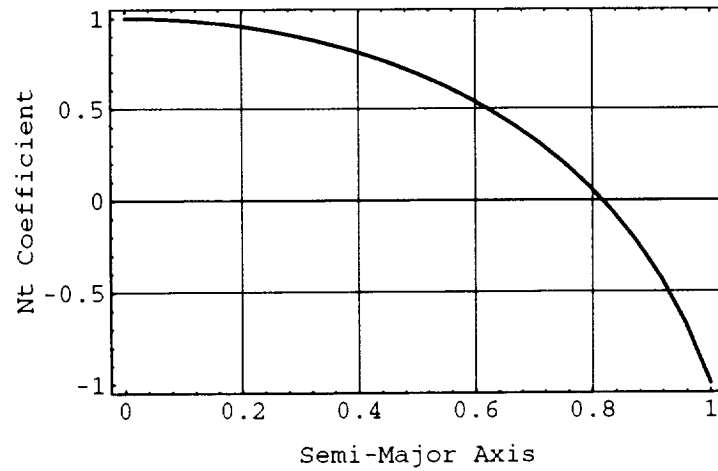


**Figure 2-23**  
**Non-dimensional Tangential Stress Coefficient for 2:1 Ellipses**

#### 2.1.5.2 Cylindrical Body

The cylindrical body of the tank must not buckle under the loads from launch. Since it is a solid monocoque structure the stress is given by equations 2-20 through 2-22. These are complex non-linear coupled equations. The critical stress versus the skin thickness for an assumed radius of 3m is given in Figure 2-24.

$$\sigma_{cr} = 0.6\gamma \frac{Et}{R} \quad (2-20)$$

$$\varphi = \frac{1}{16} \sqrt{\frac{R}{t}} \quad (2-21)$$

$$\gamma = 1.0 - 0.901(1.0 - e^{-\varphi}) \quad (2-22)$$

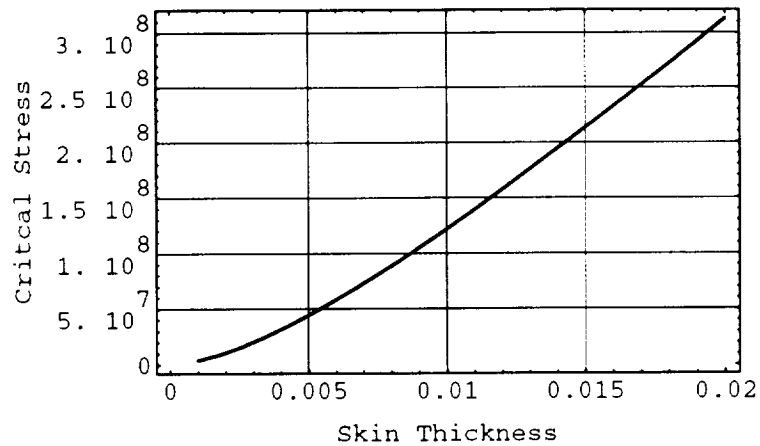


**Figure 2-24**  
**Critical Buckling Stress for Solid Cylinder of 3m Radius versus Skin Thickness**

To speed the analysis of the tanks, a linear curve fit of the curve was done around the point of skin thickness equal to 1cm. The equation for the critical stress is then given by equation 2-23 as a function of the skin thickness alone.

$$\sigma = -3.38 \cdot 10^7 + 1.66 \cdot 10^{10} \tau_{skin} \quad (2-23)$$

The chart in Figure 2-25 shows a comparison of the linear curve fit and the actual critical stress for skin thickness values ranging from 1mm to 2cm.

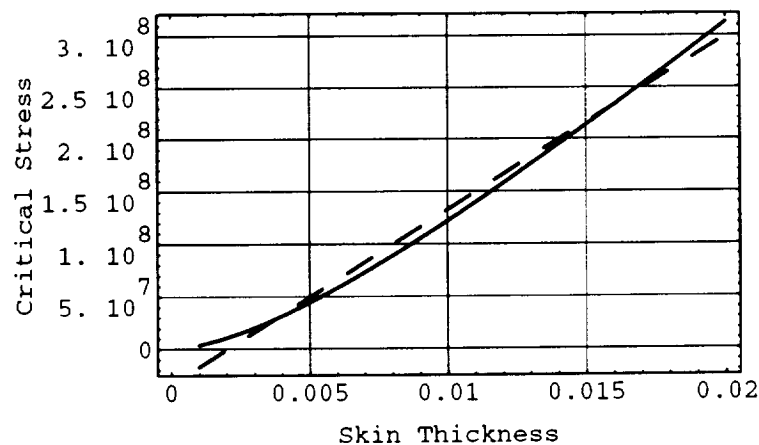


**Figure 2-25**  
**Curve Fit of Critical Buckling Stress for Solid Cylinder of 3m Radius**

Since the design process has the critical stress as an input, it would be ideal if it equaled the material yield stress since it would buckle and crush at the same time. The linear equation was solved for the variable skin thickness. This is given in equation 2-24. It is not trivial to calculate the required skin thickness for a given critical stress in cylindrical body.

$$\tau_{skin} = 6 \cdot 10^{-11} (3.3779 \cdot 10^7 + \sigma_{cr}) \quad (2-24)$$

### 2.1.6 Materials

The choice of materials for Project Columbiad's structures involves a trade-off between the cost of the material, its strength, stiffness, and density. For most structures, HTS 101 composite has been used. This is to make the maximum use of advancing technology and increase the performance of our structures. Composites have very high stiffness and strength and a very low density to make it ideal for aerospace structures. Even its high manufacture cost is outweighed by its superior performance. For designs where a higher shear stress is required HTS 102 $\pm$ 451 is used. For non-critical items, aluminum is the material of choice for its ease of manufacture and low cost. For some high performance areas, such as landing legs and truss joints where an isotropic material is required, either beryllium or titanium has been employed. A summary of all the materials used for Project Columbiad by the STP group is given in Table 2-5.

**Table 2-5: Summary of Selected Material Properties**

	Material Form	Density	Ultimate Strength (E6)	Yield Strength (E6)	Young's Modulus (E9)	Shear Modulus (E9)
<b>Aluminum</b>	2024-T36	2770	482	413	72	28
	7075-T6	2800	523	448	71	27
<b>Composite</b>	HTS 101	1490	1,337	66	151	6
	HTS 102/ $\pm$ 451	1490	641	289	82	
<b>Titanium</b>	A1-4 Sheet	4430	1,103	999	110	43
	A1-4 Bar	4430	1,034	965	110	42
<b>Beryllium</b>	Extrusion	1850	620	413	293	138
	Sheet	1850	448	289	293	138

## **2.2 Stage Designs**

### **2.2.1 PTLI Stage Design**

The PTLI, following the description of the general stage geometry given in section 2.1.4, is designed with three major components. These are the rocket support truss, the casing, and the propellant tanks. All three represent their own special technical difficulties and will be discussed in detail below. It is nonetheless important that the reader be familiar with section 2.1.4 since it is there that much of the ground work for this design is laid out and explained.

Shown in Figure 2-26 is a represented rendering of the vehicle stage. This is actually the finite-element model that was used to proof the results in the casing section, especially the frequency analysis.

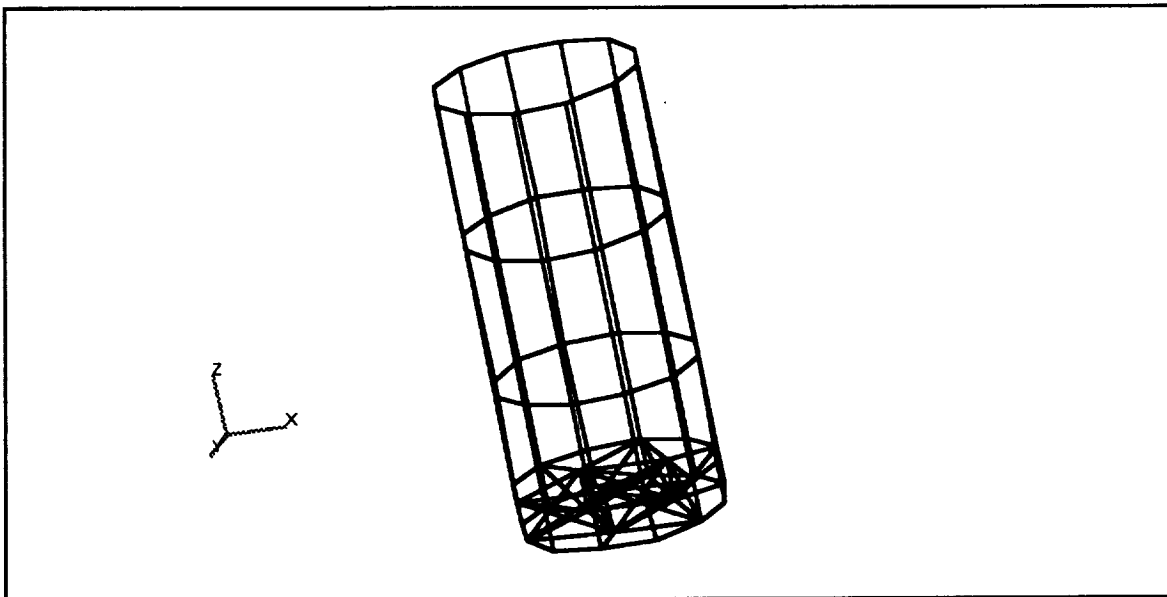


**Figure 2-26**  
**PTLI Finite-Element Model**

#### **2.2.1.1 Five Engine Rocket Support Truss**

In order to distribute the thrust loads from the engines to the rocket casing, it is necessary to include a structure across the diameter of the stage casing. To save weight as much as possible a truss design was chosen. The TLI stage has five engines arranged as seen on a die. There were two main drivers. The first, obviously, was to minimize weight. This



could be done by eliminating unstressed bars, using materials other than aluminum, and changing the cross-sectional geometry of the beam members. It was decided to use Graphite/Epoxy HTS [0°] as the material for construction of the truss members. This material has a modulus of  $1337 \times 10^9$  and a density of  $1490 \text{ kg/m}^3$ . See section 2.1.6 for a complete discuss of material properties.

The bars were chosen to be hollow cylindrical tubes since it is a reasonable compromise between structural efficiency and computability. Hollow tubes provide a much higher area moment of inertia for a given amount of material than a solid cylindrical beam. The inside and outside diameters were sized iteratively using a finite-element model. See figure 2-27 and 2-28 below. In addition, during the finite-element calculations, any bars that were seen to be unstressed or adding little to the structural integrity of the truss were removed from the final design.

The height of the truss is 1m, to provide rigidity against the engine thrusting forces. However, the space is largely empty and is being utilized by components that can withstand the environment that close to the engines

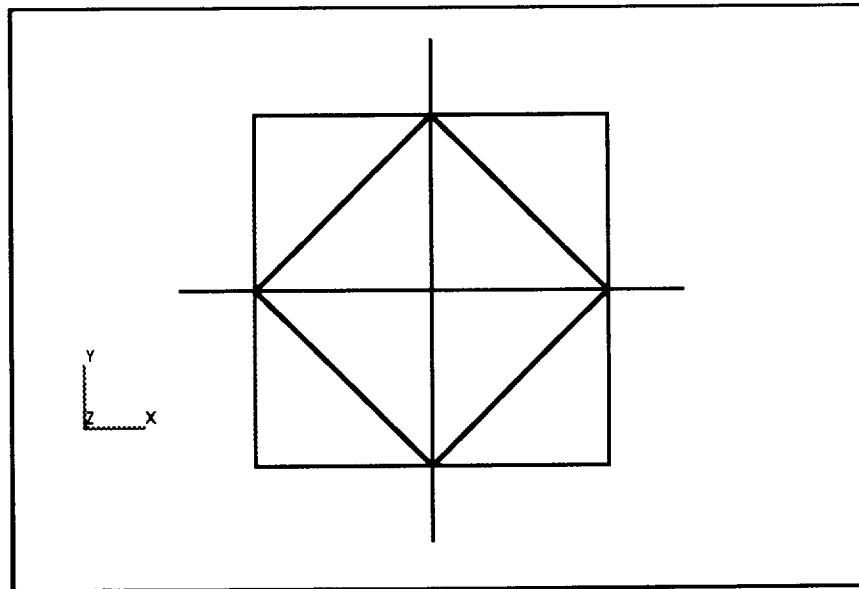


**Figure 2-27**  
**Five-Engine Truss - Top View**

It was determined that the weight of the PTLI multiplied by the launch accelerations and factor of safety gave a maximum thrust produced by the engines of 4.3 million Newtons. This force distributed over the five engines gave a thrust of 864,000 N at each of the engine point nodal locations. This is how the truss was loaded to determine the size of the truss members.

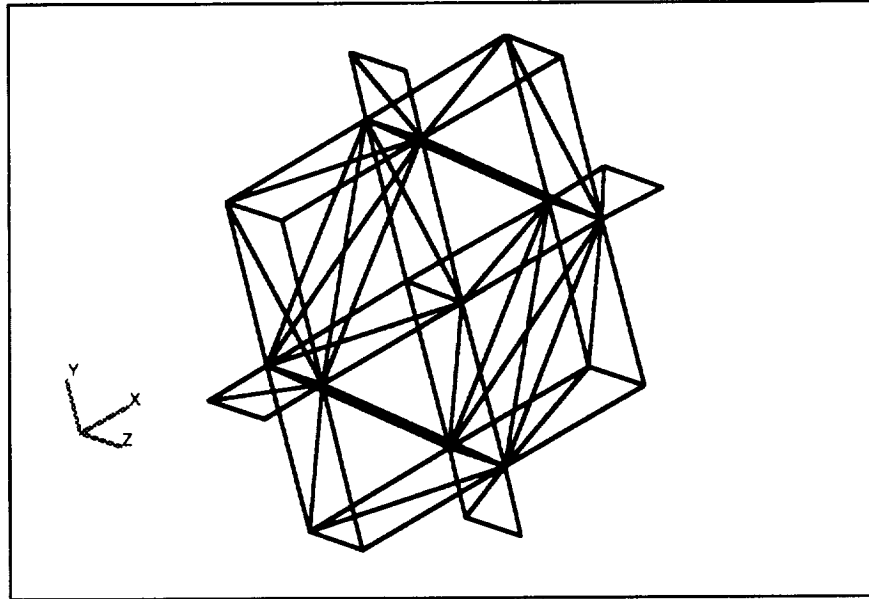


**Figure 2-28**  
**Five-Engine Truss - Oblique View**

After several iterations, truss members that had a 16cm outer diameter and 1cm thickness produced results shown in figure 2-29. The members are reasonably stressed with a full 60% margin of their ultimate failure strength, and deflections on the order of 1-2cm in the axial direction. This is clearly acceptable. The weight of this rocket truss, calculated exactly by the finite-element program, is 557kg.

#### APPLIED FORCES

NODE	DIR	VALUE	NODE	DIR	VALUE	NODE	DIR	VALUE
1	Z T	8.640E+05	3	Z T	8.640E+05	5	Z T	8.640E+05
6	Z T	8.640E+05	8	Z T	8.640E+05			

#### EXTERNAL FORCES

NODE	DIR	VALUE	NODE	DIR	VALUE	NODE	DIR	VALUE
10	X T	-5.691E-12	10	Y T	7.693E+05	10	Z T	-7.264E+05
10	X R	3.255E+04	10	Y R	-1.169E-12	10	Z R	-1.474E-12
11	X T	7.693E+05	11	Y T	4.289E-12	11	Z T	-7.264E+05
11	X R	-1.214E-12	11	Y R	-3.255E+04	11	Z R	-6.731E-13
12	X T	4.032E-12	12	Y T	-7.693E+05	12	Z T	-7.264E+05
12	X R	-3.255E+04	12	Y R	1.008E-12	12	Z R	-1.459E-12

#### DISPLACEMENTS

NODE	X TRANS	Y TRANS	Z TRANS	X ROT	Y ROT	Z ROT
6	-4.2579E-04	1.5394E-19	7.7078E-03	6.0291E-19	4.3939E-03	-7.9819E-20
8	-1.3995E-19	4.2579E-04	7.7078E-03	4.3939E-03	1.0070E-18	6.9447E-19
21	-1.7528E-19	1.1117E-21	1.5641E-02	-6.7240E-18	-7.3302E-18	-1.1425E-20
23	-3.7636E-20	8.3296E-04	5.0819E-03	-3.7555E-03	-3.4504E-18	1.7050E-19

#### ELEMENT RECOVERY

ELEMENT	MAXIMUM STRESSES FOR BEAM			VON MISES CRITERION				
	MAJOR	MINOR	SHEAR	STRESS	% YIELD	@NODE	CONNECTIVITY	
47	0.000E+00	-5.017E+08	2.508E+08	5.017E+08	37.5	6	6 26	
48	4.416E+08	0.000E+00	2.208E+08	4.416E+08	33.0	11	26 11	
51	4.416E+08	0.000E+00	2.208E+08	4.416E+08	33.0	10	10 23	
52	0.000E+00	-5.017E+08	2.508E+08	5.017E+08	37.5	3	23 3	

**Figure 2-29**  
**Typical Deflections and Stresses for Five-Engine Rocket Truss**

### 2.2.1.2 Stage Casing

The rocket casing is by far the most complex and involved structural calculation performed for Project Columbiad. It involved a great deal of effort just to develop and proof the algorithms. Most of the calculations utilize the formulas and methods described in section 2.1.4. For efficiency's sake, I will simply summarize periodically the results of the equations described in Figures 2-9 through 2-19. It is very important for the reader to be familiar with these to appreciate the depth of the results provided in this section.

With the PTLI stage propellant mass of 85000kg and the launch accelerations, the shear and bending moment diagrams were calculated for the PTLI length of 16.46m. These are shown in figure 2-30 and 2-31.

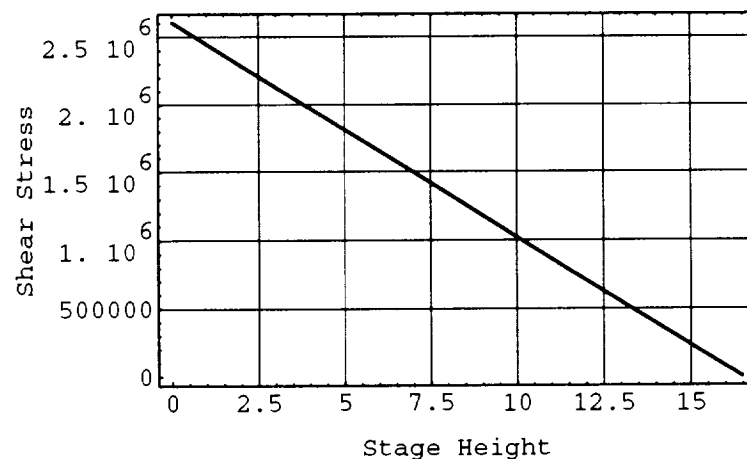


**Figure 2-30**  
**PTLI Shear Stress versus Stage Height**

It is clear that the maximum shear and bending moment occur at the bottom of the stage. This is defined as zero in the x axis (axial axis). What was not appreciated at the time was the extent that the weight of the vehicle grew with increases in length. As can be seen from the bending moment diagram in figure 2-31, a steep rise occurs in the bottom few meters alone. The rocket casings for Project Columbiad are not employing a stepped casing. The thickness is calculated from the stress at  $x=0$ , and that is used for the entire stage. Further design refinement would have the casing thickness change with the axial height to save weight.

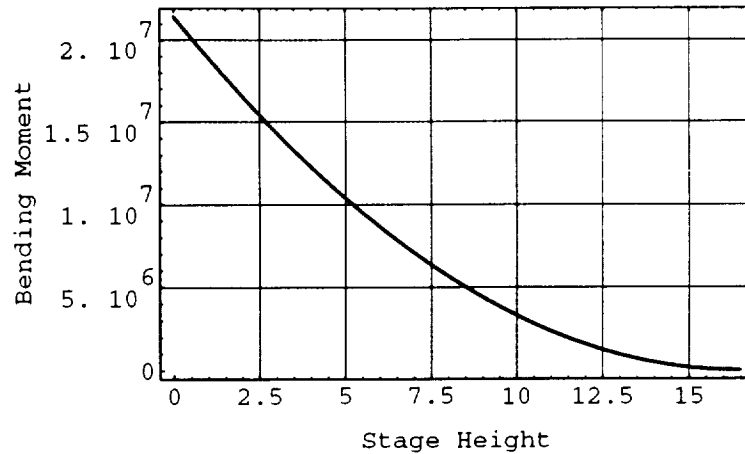


**Figure 2-31**  
**PTLI Bending Moment versus Stage Height**

The axial stress is dependent on both the axial applied loads and the lateral bending moments as shown in figure 2-31. The axial stress is a function of the total stage area (the sum of the cross-sectional area of the stringers) and the axial distance. If we look at  $x=0$ , we determine the axial stress as a function of the stage area. This is shown in figure 2-32 along with the material yield stress of composite. According to the chart, the PTLI requires a total of 0.0088 in order to avoid failure during launch.

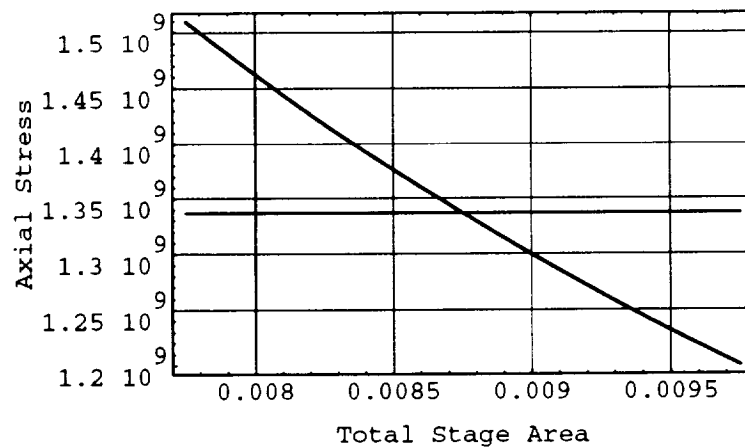


**Figure 2-32**  
**PTLI Axial Stress versus Total Stage Area**

With this for the stage area, we can also plot the axial stress as a function of the axial distance. this is shown in figure 2-33

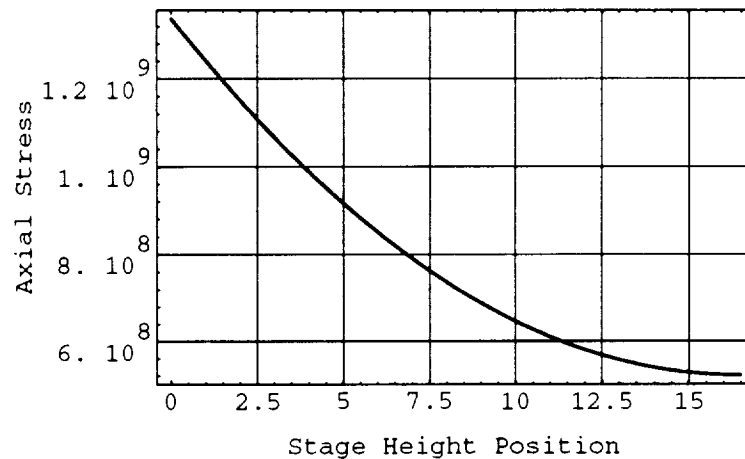


**Figure 2-33**  
**PTLI Axial Stress versus Stage Height for a Set Stage Area**

The stringer area can be determined once we decide on how many to use. Figure 2-34 shows how the stringer area varies as the number of stringers is increased. Around 8-15 stringers the curve levels off and there is little gain in having many more stringers. A total of 12 stringers were chosen because of the chart in figure 2-34 and the symmetrical pattern it makes with  $30^\circ$  spacing around the circumference of the stage.

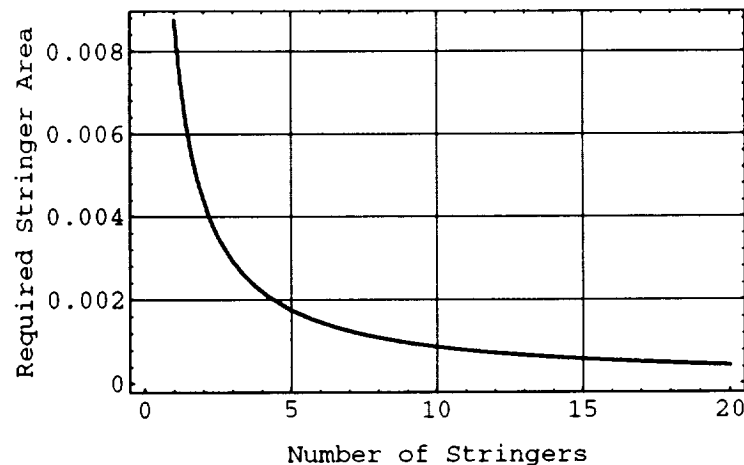


**Figure 2-34**  
**PTLI Required Stringer Area versus number of stringers**

To make the stringers as defensible to buckling as possible it is desirable to maximize their area moment of inertia. This can be done by making the hollow cylindrical cells as large as possible. This can be seen in figure 2-35, which plots the area moment of inertia for a hollow circular beam as the outer diameter increases. This is also imposing the constraint that the area remain constant, since our stringer area has already been set above.

A minimum manufacturable thickness of 4mm was chosen, and the outer diameter was sized from that. The stringers have an outside diameter of 6cm and a thickness of 4mm.

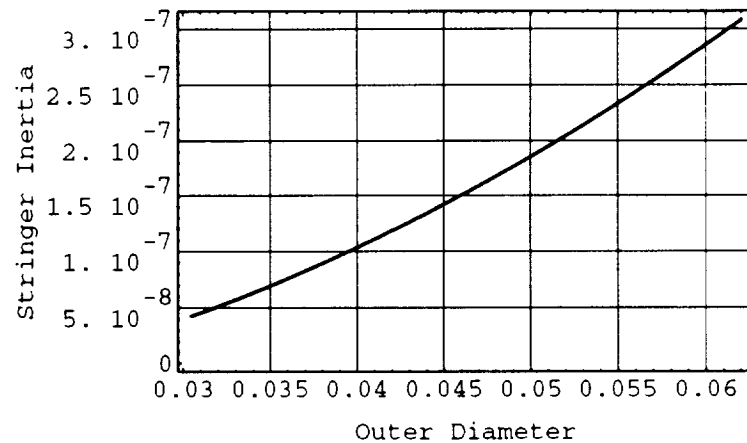


**Figure 2-35**  
**PTLI Stringer Inertia versus Stringer Outer Diameter**

The next structural members that need to be designed are the frames and the frame spacing. As discussed in section 2.1.4.2, the frame geometry was designed using a finite-element program, and is used on every stage the exact same way. Thus, the frames are assured of avoiding general instability. The frame spacing, however, still needs to be calculated to prevent the stringers from buckling and cause panel instability.

The chart in Figure 2-36 shows the buckling stress of the stringers as a function of their length. Also shown on the chart is the yield stress of HTS composite. The length which yields the composite yield strength is the maximum allowed for the longeron spacing. If the frames are spaced any further apart, the stringers will buckle before they crush. This would be unacceptable. Therefore, a longeron spacing of 0.64m was chose which indicates that a total of 25 longerons are required. Each frame weighs 72kg.

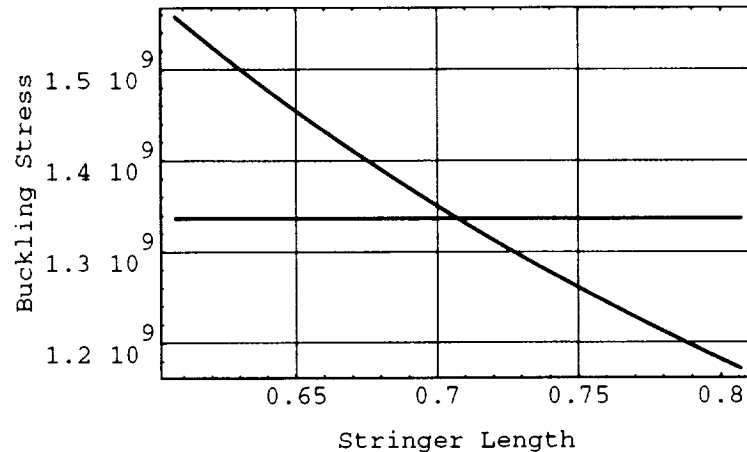


**Figure 2-36**  
**PTLI Stringer Buckling Stress versus Stringer Length**

The skin, which is allowed to buckle as discussed in section 2.1.4.3, was sized to withstand an aerodynamic pressure load of 8000Pa. With the simple finite-element model it was determined that a thickness of 2cm is more than adequate to support that load. This was then the design skin thickness for all three rocket stages.

The rocket casing mass came to a total of 3835kg. This was broken down into 1822kg for longerons, 1800kg for skin, and 203kg for the stringers.

From the equations described in section 2.1.4.4, the first axial and lateral vibrational modes of the structure were calculated. The results were 19 Hz laterally and 32 Hz axially. This is well above the recommended values in Wertz and Larson of 10 Hz and 25 Hz respectively.

### 2.2.1.3 Oxygen and Fuel Tanks

The propellant tanks are required to carry a total of 85,000 kg. The oxidizer to fuel ratio is 5.5. Most of the inputs for the tank calculations are summarized in Figure 2-39. The Figures 2-37 and 2-38 show the design values for the two tanks.

The procedure for the tank calculation is as follows. Once the required volume is determined from the mass, the volume that will be enclosed in the end caps are calculated and subtracted from the total volume of the propellants. The end caps are 2:1 ellipses, however, the tank radius is not equal to the stage radius. The maximum size of the tank radius would be the stage radius minus the insulation thickness (typically 20cm). The



height of the cylindrical body is then determined so that the its volume will enclose the remainder.

<b>Hydrogen Tank</b>	
Hydrogen Mass	13076.92
Hydrogen Volume	184.18
Hydrogen Tank Volume	193.39
Hydrogen Tank Radius	2.80
Hydrogen Tank Cap Radius	1.40
Hydrogen Tank Cap Volume	45.98
Hydrogen Tank Main Volume	147.41
Hydrogen Tank Main Height	5.99
Hydrogen Tank Cap Eccentricity	0.87
Hydrogen Tank Cap Area	57.39
Hydrogen Tank Body Area	105.30
Hydrogen Tank Area	162.69
Hydrogen Tank Wall Thickness	0.0011
Hydrogen Tank Structure Mass	257.12
<i>Hydrogen Tank Coating Thickness</i>	0.0010
Hydrogen Tank Coating Mass	1236.44
Hydrogen Tank Height	8.79
Hydrogen Tank Insulation Mass	1757.05
Hydrogen Tank Mass	1493.56

**Figure 2-37**  
**PTLI Hydrogen Tank Design Parameters**

The area of the tanks are then calculated including the body and endcaps. The wall thickness is then determined by the procedures discussed in section 2.1.6. The cylindrical walls are checked for buckling, and if necessary the thickness of the wall is increased to prevent that failure mode.

The mass of the tank structure is calculated. In addition, the weight of the non-reactive lining and the insulation covering is also calculated and tabulated for determining overall structural mass of the stage. It is important to notice two things. First, a support mechanism for the tanks has not been designed. It was beyond the scope of the preliminary

design process and would have had a very small mass contribution to the stage. Secondly, the insulation is a very significant portion of the total tank weight. This may be an area to be addressed during the detailed design phase of the project.

In the same fashion as the hydrogen tank, the oxygen tank geometry and mass properties are calculated and tabulated in figure 2–38. The oxygen tank, still using the maximum allowable radius is very flat with only 0.63m of cylindrical body height. This odd structural design was not chosen for its structural properties since it requires much more mass, but to limit the height of the PTLI stage. If the stage height ceases to be a problem, the mass of the oxygen tanks could be reduced by modifying the oxygen tank geometry.

<b>Oxygen Tank</b>	
Oxygen Mass	71923.08
Oxygen Volume	58.47
Oxygen Tank Volume	61.40
Oxygen Tank Radius	2.80
Oxygen Tank Cap Radius	1.40
Oxygen Tank Cap Volume	45.98
Oxygen Tank Main Volume	15.42
Oxygen Tank Main Height	0.63
Oxygen Tank Cap Eccentricity	0.87
Oxygen Tank Cap Area	57.39
Oxygen Tank Body Area	11.02
Oxygen Tank Area	68.41
Oxygen Tank Wall Thickness	0.0014
Oxygen Tank Structure Mass	144.92
<i>Oxygen Tank Coating Thickness</i>	0.0010
Oxygen Tank Coating Mass	519.91
Oxygen Tank Height	3.43
Oxygen Tank Insulation Mass	738.81
Oxygen Tank Mass	664.82

**Figure 2–38**  
**PTLI Oxygen Tank Design Parameters**

#### 2.2.1.4 Summary

The design of the PTLI is based on a large number of design parameters, most of which are summarized in Figure 2–39. Nearly all of them are self explanatory, but I will highlight some of the more obscure ones. The utilization volume is the increase in required tank volume over and above that to store the fuel itself. This is for pressurization air and top-off waste. The payload for the stage is the amount of mass that sits on top of the stage during the space burn. For the PTLI this would be the sum of the wet weights for the LBM, ERM, and crew capsule. The electronics height is a reserved space at the top of the truss in which all the C<sup>3</sup> and GNC electronics and computers will be located. The truss height is the physical size of the truss. This will be 1m for all of the stages, since both the five and three engine truss are 1m in depth. The truss spacing is the amount of spacing between the top of the truss and the oxygen tank.

<b>Stage Parameters</b>	
<i>Factor of Safety</i>	1.4
<i>Desired Mass Fraction</i>	10%
<i>Stage Diameter</i>	6
<i>Payload for Stage</i>	86,330
<i>Electronics Height</i>	0.5
<i>Number of Engines</i>	5
<i>Engine Height</i>	2.25
<i>Engine Weight</i>	167
<i>Propellant Mass</i>	85000
<i>LOX/LH Ratio</i>	5.5
<i>Utilization Volume</i>	5%
<i>Oxygen Pressure</i>	340000
<i>Hydrogen Pressure</i>	340000
<i>Insulation Thickness</i>	0.2
<i>Cryogenic Insulation Density</i>	54
<i>Rocket Truss Mass</i>	557
<i>Rocket Truss Height</i>	1
<i>Rocket Truss Spacing</i>	0.5
<i>Launch Axial Acceleration</i>	3.5
<i>Launch Lateral Acceleration</i>	2.2

**Figure 2–39**  
**PTLI Stage Design Inputs**

The structural configuration of the PTLI stage is summarized in the Figure 2–40. The stage is 16.46m from the bottom of the truss to the top of the stage. The engines extend 2.25m from the bottom of the truss. The adapter for the NLS launch system will be attached to the bottom of the rocket truss, and thereby the PTLI engines will be enclosed within the NLS adapter.

The total mass of the cryogenic insulation is 2500kg. The total structural is 6550kg, which yields a mass fraction of 7% and a structure-fuel fraction of 7.8%. This is well within the design goals and is a very acceptable design.

<b>Configuration</b>	
Stage Radius	3
Total Height	16.46
Insulation Mass	2496
<i>Casing Mass</i>	3835
<i>Rocket Truss Mass</i>	557
Tank Mass	2158
Structural Mass	6550
Engine Mass	835
Stage Dry Mass	9881
Stage Wet Mass	94881
Vehicle Wet Mass	181211
Structural Mass Fraction	7%
Structural Fuel Fraction	7.7%

**Figure 2-40**  
**PTLI Configuration Summary**

### **2.2.2. LBM Stage Design**

The LBM is an identical clone of the PTLI geometrical shape, with simply different numbers for the structural members. This means that the exact same design methods that were used for the PTLI are employed in duplicate in this section. For this reason, there will be almost no design discussion in this section. If you wish to understand the design methodology better, see section 2.2.1 or 2.1.4. where the rocket stage design is discussed in much greater detail.

Shown below in Figure 2-41 is a model of the LBM vehicle stage. It is similar to that of the PTLI except that a different truss has replaced the five-engine truss used in the PTLI. The LBM, ERM and PLM all have three engines instead of five. A new truss was designed for these stages because the five-engine truss does not allow symmetrical placement of three engines. The model shown in figure 2-41 is the finite-element model that was used to proof the results in the casing design.

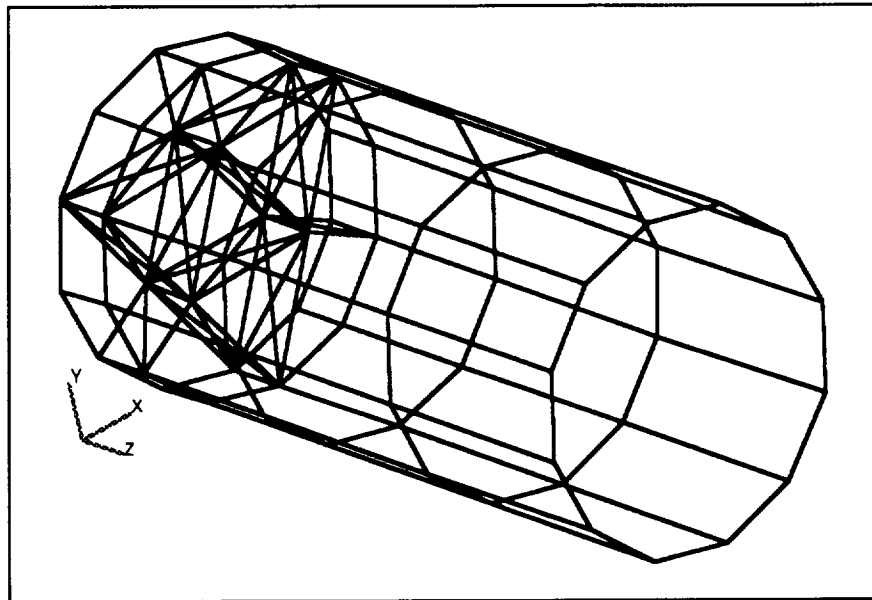


**Figure 2-41**  
**LBM Finite-Element Model**

#### 2.2.2.1. Three Engine Rocket Support Truss

Finite-element calculations on several possible three point truss designs revealed that the one shown in Figure 2-42, to be the most structurally efficient. The engines are placed at the three center nodes. The entire truss is connected to six locations to the outside casing, and each engine is connected to the casing by three members. The nine elements that connect to the casing are the most critical members, and are stressed and deflected the most. See figure 2-44 for representative values.

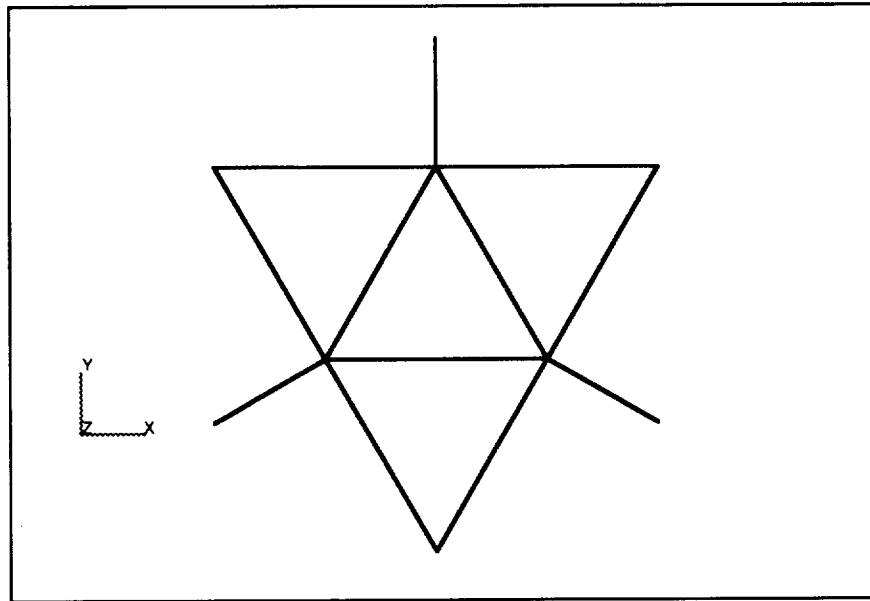


**Figure 2-42**  
**Three-Engine Truss - Top View**

This design initially had a very high tendency to warp axially about the symmetric axis of the truss. While maximum rotations never exceed 1 radian, it was decided to increase the rigidity of the truss to eliminate complications to the engine or guidance control systems that would have had to compensate for this truss rotation. The additional rigidity, achieved by adding the full complement of X-diagonal members to the inter-truss system (see Figure 2-43 for the inter-truss system), means about a 10-20% increase in truss weight. However, the three perpendicular members are only forced in a single direction, and as such only need a single cross member in the negative symmetric direction. See Figure 2-43 for the layout of the cross elements in the truss.

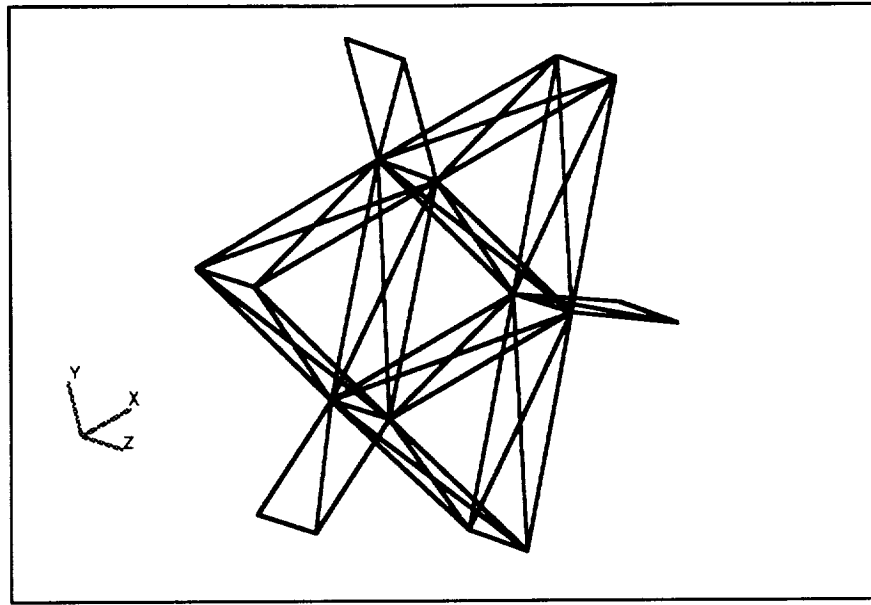


**Figure 2-43**  
**Three-Engine Truss - Oblique View**

To test the truss and correctly size the beam elements, a finite-element model was created of the truss. The maximum load a three-engine truss would see is during the LBM burn. At this point in the mission, the entire vehicle weighs 72,000kg. The maximum axial acceleration of the vehicle is 2g's with the appropriate factor-of-safety this leads to a total 2 million Newton's of thrust produced during this burn. Spread among three engines, each one produces 690,000N. This is the load that is applied to the central node locations.

With a cylindrical beam 10cm outer-diameter (OD) and a 9cm inner-diameter (ID) the truss is well within limits of our design. The truss will deflect on the order of 0.2-0.3mm in the axial direction of the thrust. Side deflections are 1/100th of millimeters. Axial rotation warping is held to negligible amounts. The elements are stressed in the 15-5% of their yield strength. These results are summarized in Figure 2-44 below.

Assuming the cylindrical bar described above, and the density of HTS 101 of 1490kg, the truss weighs 287kg. However, this is the weight of just the members. If we allow a 5% increase for joints and casing connections our weight will be 300kg. However, since the joints and connections will probably be made of beryllium or titanium a 10% increase in the weight of the composite truss is probably more accurate. In this case our weight will probably be closer to 315kg.

DISPLACEMENTS						
NODE	X TRANS	Y TRANS	Z TRANS	X ROT	Y ROT	Z ROT
7	2.5062E-19	-7.5732E-04	7.9297E-03	-2.9374E-03	-4.4523E-18	1.4763E-18
8	-6.5586E-04	3.7866E-04	7.9297E-03	1.4687E-03	2.5439E-03	5.7565E-18
9	6.5586E-04	3.7866E-04	7.9297E-03	1.4687E-03	-2.5439E-03	-1.4271E-18
17	-2.9720E-19	2.1290E-04	7.3746E-03	-2.2594E-03	-3.0422E-18	-3.0463E-18
18	1.8437E-04	-1.0645E-04	7.3746E-03	1.1297E-03	1.9567E-03	4.6049E-19
19	-1.8437E-04	-1.0645E-04	7.3746E-03	1.1297E-03	-1.9567E-03	2.0043E-18

ELEMENT RECOVERY						
MAXIMUM STRESSES FOR BEAM				VON MISES CRITERION		
ELEMENT	MAJOR	MINOR	SHEAR	STRESS	% YIELD	@NODE CONNECTIVITY
40	1.819E+08	-4.733E+02	9.094E+07	1.819E+08	13.6	4 19 4
41	1.819E+08	-4.733E+02	9.094E+07	1.819E+08	13.6	18 4 18
42	7.440E+02	-1.956E+08	9.779E+07	1.956E+08	14.6	8 14 8
43	7.440E+02	-1.956E+08	9.779E+07	1.956E+08	14.6	8 8 12
44	1.819E+08	-4.733E+02	9.094E+07	1.819E+08	13.6	18 18 2
45	1.819E+08	-4.733E+02	9.094E+07	1.819E+08	13.6	17 2 17
46	7.440E+02	-1.956E+08	9.779E+07	1.956E+08	14.6	7 12 7

**Figure 2-44**  
**Typical Deflections and Stresses for Three-Engine Rocket Truss**

#### 2.2.2.2. Stage Casing

Using the LBM stage propellant mass of 55000kg and the launch accelerations, the shear and bending moment diagrams were calculated for the LBM length of 13.2m. These are shown in Figure 2-45 and 2-46. For details on the methods used to calculate these values see section 2.1.4.



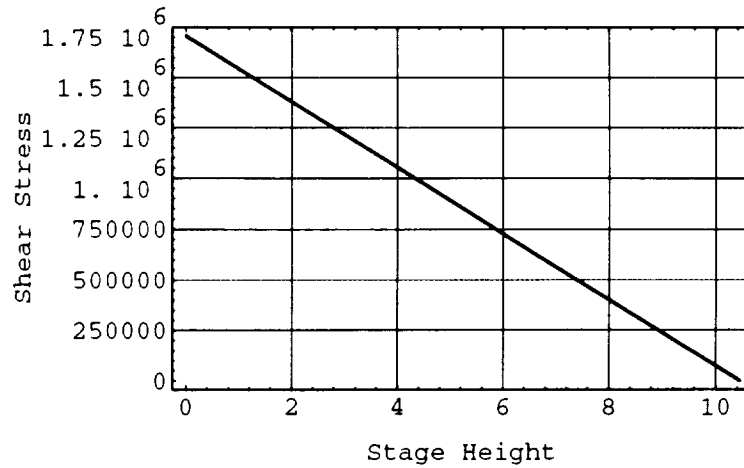


**Figure 2-45**  
**LBM Shear Stress versus Stage Height**

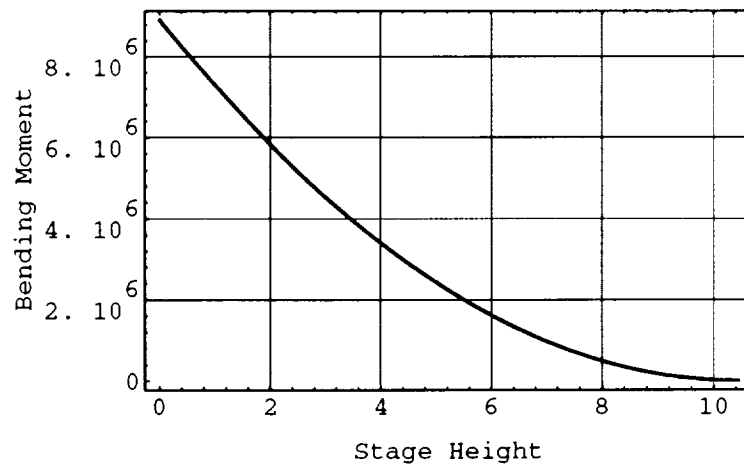


**Figure 2-46**  
**LBM Bending Moment versus Stage Height**

The same reasoning that applied to the PTLI stage is true here. The maximum loading occurs at  $x=0$  in the axial direction (hence, at the bottom). The total stage area is sized from the plot shown in Figure 2-47, which shows the axial stress at  $x=0$  as a function of the stage area. Also shown on the plot is the yield stress of the composite material. The crossing yields a stage area of  $0.004\text{m}^2$ . From this the stringer area can be determined.

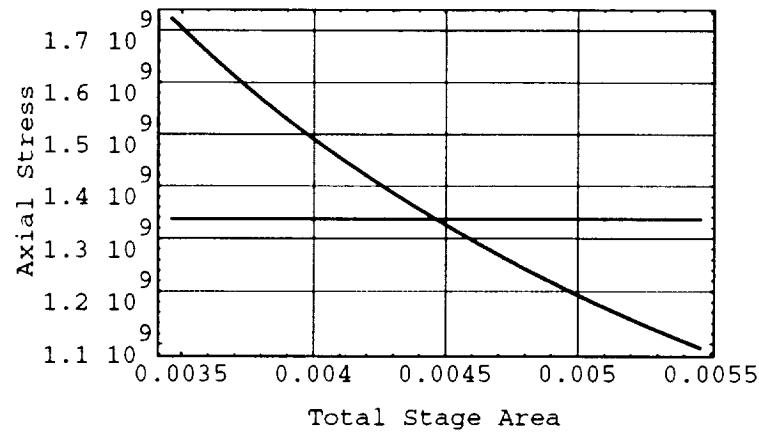


**Figure 2-47**  
**LBM Axial Stress versus Total Stage Area**

Maximizing the stringer inertia by using the minimum thickness, yields an outer diameter of 6.1cm with a thickness of 2mm. The stringers weigh 70kg.

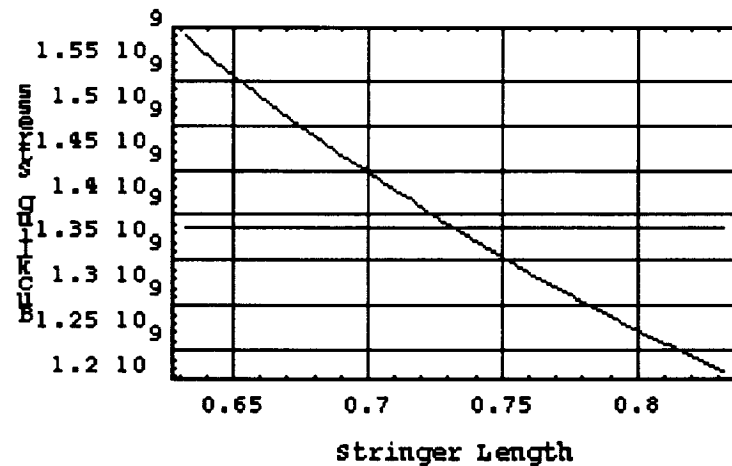


**Figure 2-48**  
**LBM Stringer Buckling Stress versus Stringer Length**

With the stringer geometry defined, we can determine the longeron spacing from Figure 2-48. Matching the critical buckling stress with the composite yield stress gives spacing of 0.7m. This means there will be 15 longerons on the LBM stage. The frames are identical to those on the PTLI, namely a 1.3x10cm cross section weighing 72kg. The total weight

of the frames are 1093kg. The skin on the LBM is identical to the PTLI thickness of 2cm and weighs in at 1181kg. This gives the structural weight of the casing as 2345kg.

By the methods in 2.1.4.4, the first axial mode of the casing is 41 Hz and the first lateral mode of the casing is 37 Hz. These are well above the limits recommended by Wertz and Larson.

### 2.2.2.3. Oxygen and Fuel Tanks

The method for the tank calculation is the very same as the PTLI. Therefore, for a walk-through of the method see section 2.2.1.3. The results will simply be summarized here. See Figures 2–49 and 2–50 for details.

<b>Hydrogen Tank</b>	
Hydrogen Mass	8553.85
Hydrogen Volume	120.48
Hydrogen Tank Volume	126.50
Hydrogen Tank Radius	2.80
Hydrogen Tank Cap Radius	1.40
Hydrogen Tank Cap Volume	45.98
Hydrogen Tank Main Volume	80.52
Hydrogen Tank Main Height	3.27
Hydrogen Tank Cap Eccentricity	0.87
Hydrogen Tank Cap Area	57.39
Hydrogen Tank Body Area	57.52
Hydrogen Tank Area	114.91
Hydrogen Tank Wall Thickness	0.0010
Hydrogen Tank Structure Mass	178.29
<i>Hydrogen Tank Coating Thickness</i>	0.0010
Hydrogen Tank Coating Mass	873.32
Hydrogen Tank Height	6.07
Hydrogen Tank Insulation Mass	1241.04
Hydrogen Tank Mass	1051.61

**Figure 2–49**  
**LBM Hydrogen Tank Design Parameters**

<b>Oxygen Tank</b>	
Oxygen Mass	47046.15
Oxygen Volume	38.25
Oxygen Tank Volume	40.16
<i>Oxygen Tank Radius</i>	2.50
Oxygen Tank Cap Radius	1.25
Oxygen Tank Cap Volume	32.72
Oxygen Tank Main Volume	7.44
Oxygen Tank Main Height	0.38
Oxygen Tank Cap Eccentricity	0.87
Oxygen Tank Cap Area	45.75
Oxygen Tank Body Area	5.95
Oxygen Tank Area	51.70
Oxygen Tank Wall Thickness	0.0012
Oxygen Tank Structure Mass	93.13
<i>Oxygen Tank Coating Thickness</i>	0.0010
Oxygen Tank Coating Mass	392.94
Oxygen Tank Height	2.88
Oxygen Tank Insulation Mass	558.39
Oxygen Tank Mass	486.08

**Figure 2-50**  
**LBM Oxygen Tank Design Parameters**

#### 2.2.2.4 Summary

The design of the LBM is based on a large number of design parameters, most of which are summarized in Figure 2-51. Nearly all of them are self evident, and the obscure ones are defined in section 2.2.1. The only difference is the definition of payload for the LBM stage. It is the amount of mass that sits on top of the stage during the space burn. For the LBM this would be the sum of the wet weights for the ERM and Crew Module.

<b>Stage Parameters</b>	
<i>Factor of Safety</i>	1.4
<i>Desired Mass Fraction</i>	10%
<i>Stage Diameter</i>	6
<i>Payload for Stage</i>	28,821
<i>Electronics Height</i>	0.5
<i>Number of Engines</i>	3
<i>Engine Height</i>	2.25
<i>Engine Weight</i>	167
<i>Propellant Mass</i>	55600
<i>LOX/LH Ratio</i>	5.5
<i>Utilization Volume</i>	5%
<i>Oxygen Pressure</i>	340000
<i>Hydrogen Pressure</i>	340000
<i>Insulation Thickness</i>	0.2
<i>Cryogenic Insulation Density</i>	54
<i>Rocket Truss Mass</i>	267
<i>Rocket Truss Height</i>	1
<i>Rocket Truss Spacing</i>	0.5
<i>Launch Axial Acceleration</i>	3.5
<i>Launch Lateral Acceleration</i>	2

**Figure 2-51**  
**LBM Stage Design Inputs**

The structural configuration of the PTLI stage is summarized in the Figure 2-52. The stage is 13.2m from the bottom of the truss to the top of the stage. The engines extend 2.25m from the bottom of the truss. The adapter for the NLS launch system will be attached to the bottom of the rocket truss, and therefore the LBM engines will be enclosed within the NLS adapter during the second launch.

The total mass of the cryogenic insulation is 1800kg. The total structural is 4150kg, which yields a mass fraction of 7% and a structure-fuel fraction of 7.5%. This is well within the design goals and is a very acceptable design, and is also precisely the same as the PTLI fractions.

<b>Configuration</b>	
Stage Radius	3
Total Height	13.20
Casing Height	10.95
Insulation Mass	1799
<i>Casing Mass</i>	2345
Rocket Truss Mass	267
Tank Mass	1538
Structural Mass	4150
Engine Mass	501
Stage Dry Mass	6450
Stage Wet Mass	62050
Vehicle Wet Mass	90871
Structural Mass Fraction	7%
Structural Fuel Fraction	7.5%

**Figure 2-52**  
**LBM Configuration Summary**

### **2.2.3. ERM Stage Design**

The ERM is an identical clone of the PTLI and LBM geometrical shape, with simply different numbers for the structural members. This means that the exact same design methods that were used for the PTLI and LBM are employed in triplicate in this section. For this reason, there will be almost no design discussion in this section. If you wish to understand the design methodology better, see section 2.2.1 or 2.1.4. where the rocket stage design is discussed in much greater detail.

#### **2.2.3.1. Three Engine Rocket Support Truss**

The exact three-engine truss that is on the LBM is used for the ERM. This was for two reasons. The first, was that the commonalty of the design makes it evident that a cost savings can be had by building more of the same truss, even if each individual stage is custom tailored. The second is that both stages had three engines; it was not worth the effort that would have been required to re-size the members for the ERM stage. So in the end, the ERM is using the LBM truss, and it will be over designed from the ERM's point of view. In sum, the truss weighs 287kg.

### 2.2.3.2. Stage Casing

With the ERM stage propellant mass of 17000kg and the given launch accelerations, the shear and bending moment diagrams were calculated for the ERM length of 8.97m. These are shown in Figures 2-53 and 2-54. For details on the methods used to calculate these values see section 2.1.4.

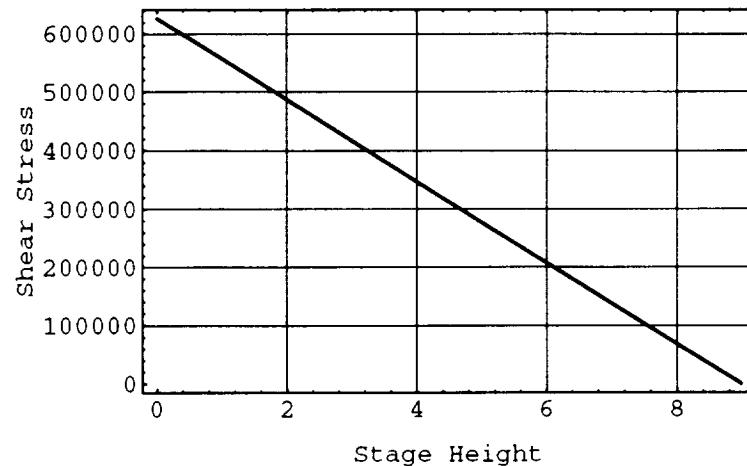


**Figure 2-53**  
**ERM Shear Stress versus Stage Height**

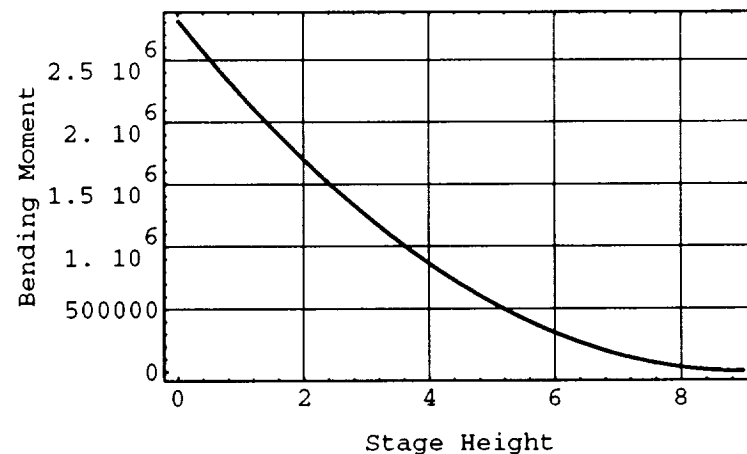


**Figure 2-54**  
**ERM Bending Moment versus Stage Height**

For the ERM stage, it turned out that using the minimum stringer area was not the optimal design for the casing. With the minimum area stringers, the area moment of inertia was

small enough that frames were required every 10cm to prevent buckling. This was unacceptable because the weight of each frame is 72kg. So, the stringers from the LBM were adopted and the casing was designed around them. It is clear then from the chart in Figure 2-55, that the stringers are not even close to being stressed to the yield point.

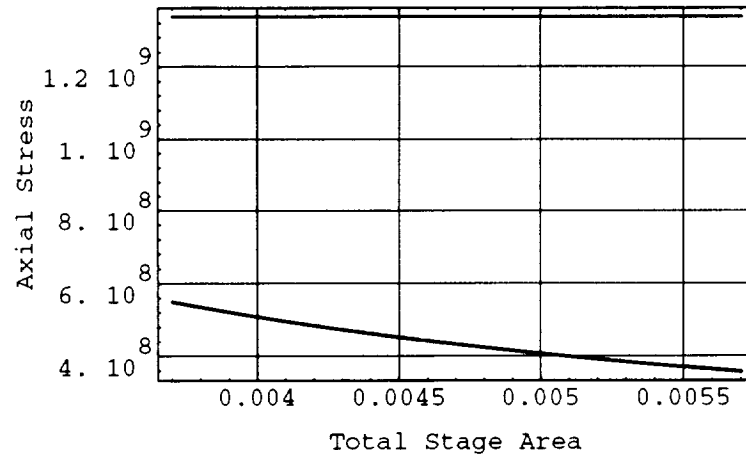


**Figure 2-55**  
**ERM Axial Stress versus Total Stage Area**

The stringers have an outer diameter of 6.1cm and a thickness of 2mm. The stringers weigh a total of 54kg.

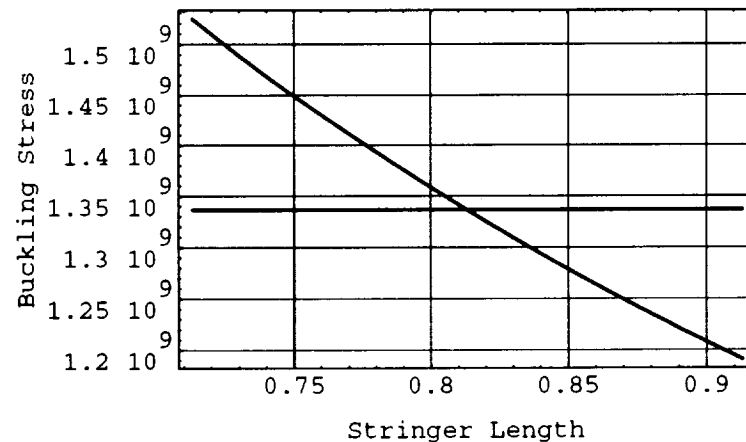


**Figure 2-56**  
**ERM Stringer Buckling Stress versus Stringer Length**



With the stringer geometry defined, we can determine the longeron spacing from figure 2–56. Matching the critical buckling stress with the composite yield stress gives spacing of 0.78m. This means there will be 10 longerons on the ERM stage. The frames are identical to those on the PTLI and LBM, namely a 1.3x10cm cross section weighing 72kg. The total weight of the frames are 729kg. The skin on the LBM is identical to the PTLI thickness of 2cm and weighs in at 882kg. This gives the structural weight of the casing as 1952kg.

By the methods in 2.1.4.4, the first axial mode of the casing is 58 Hz and the first lateral mode of the casing is 71 Hz. This is well above the limits recommended by Wertz and Larson.

#### 2.2.3.3. Oxygen and Fuel Tanks

The method for the tank calculation is the very same as the PTLI and LBM. Therefore, for a walk-through of the method see section 2.2.1.3. The results will simply be summarized here. See Figure 2–57 and 2–58 for details.

<b>Hydrogen Tank</b>	
Hydrogen Mass	2723.08
Hydrogen Volume	38.35
Hydrogen Tank Volume	40.27
<i>Hydrogen Tank Radius</i>	2.50
Hydrogen Tank Cap Radius	1.25
Hydrogen Tank Cap Volume	32.72
Hydrogen Tank Main Volume	7.55
Hydrogen Tank Main Height	0.38
Hydrogen Tank Cap Eccentricity	0.87
Hydrogen Tank Cap Area	45.75
Hydrogen Tank Body Area	6.04
Hydrogen Tank Area	51.79
Hydrogen Tank Wall Thickness	0.0009
Hydrogen Tank Structure Mass	70.18
<i>Hydrogen Tank Coating Thickness</i>	0.0010
Hydrogen Tank Coating Mass	393.61
Hydrogen Tank Height	2.88
Hydrogen Tank Insulation Mass	559.34
Hydrogen Tank Mass	463.78

**Figure 2-57**  
**ERM Hydrogen Tank Design Parameters**

<b>Oxygen Tank</b>	
Oxygen Mass	14976.92
Oxygen Volume	12.18
Oxygen Tank Volume	12.79
<i>Oxygen Tank Radius</i>	1.82
Oxygen Tank Cap Radius	0.91
Oxygen Tank Cap Volume	12.63
Oxygen Tank Main Volume	0.16
Oxygen Tank Main Height	0.02
Oxygen Tank Cap Eccentricity	0.87
Oxygen Tank Cap Area	24.25
Oxygen Tank Body Area	0.17
Oxygen Tank Area	24.42
Oxygen Tank Wall Thickness	0.0008
Oxygen Tank Structure Mass	28.98
<i>Oxygen Tank Coating Thickness</i>	0.0010
Oxygen Tank Coating Mass	185.62
Oxygen Tank Height	1.84
Oxygen Tank Insulation Mass	263.77
Oxygen Tank Mass	214.59

**Figure 2–58**  
**ERM Oxygen Tank Design Parameters**

#### 2.2.3.4 Summary

The design of the ERM is based on a large number of design parameters, most of which are summarized in Figure 2–59. Nearly all of them are self evident, and the obscure ones are defined in section 2.2.1. The payload for the ERM stage is the amount of mass that sits on top of the stage during the space burn. This is simply the wet weight of the Crew capsule.

<b>Stage Parameters</b>	
<i>Factor of Safety</i>	1.4
<i>Desired Mass Fraction</i>	10%
<i>Stage Diameter</i>	6
<i>Payload for Stage</i>	5,700
<i>Electronics Height</i>	0.5
<i>Number of Engines</i>	3
<i>Engine Height</i>	2.25
<i>Engine Weight</i>	167
<i>Propellant Mass</i>	17700
<i>LOX/LH Ratio</i>	5.5
<i>Utilization Volume</i>	5%
<i>Oxygen Pressure</i>	340000
<i>Hydrogen Pressure</i>	340000
<i>Insulation Thickness</i>	0.2
<i>Cryogenic Insulation Density</i>	54
<i>Rocket Truss Mass</i>	267
<i>Rocket Truss Height</i>	1
<i>Rocket Truss Spacing</i>	0.5
<i>Landing Leg Weight</i>	400
<i>Number of Landing Legs</i>	3
<i>Launch Axial Acceleration</i>	3.5
<i>Launch Lateral Acceleration</i>	2

**Figure 2–59**  
**ERM Stage Design Inputs**

The structural configuration of the ERM stage is summarized in the Figure 2–60. The stage is 8.97m from the bottom of the engines (2.25m below the bottom of the truss) to the top of the stage.

The total mass of the cryogenic insulation is 823kg. The total structural is 40970kg, which yields a mass fraction of 18% and a structure-fuel fraction of 23.1%. The addition of landing legs to the structure, for sitting on the moon, is what causes the mass fraction to be so high. See section 2.2.5 for a description of the landing leg design. However, this design is acceptable.

<b>Configuration</b>	
Stage Radius	3
Total Height	8.97
Insulation Mass	823
<i>Casing Mass</i>	1952
Rocket Truss Mass	267
Tank Mass	678
Landing Legs	1200
Structural Mass	4097
Engine Mass	501
Stage Dry Mass	5421
Stage Wet Mass	23121
Vehicle Wet Mass	28821
Structural Mass Fraction	18%
Structural Fuel Fraction	23.1%

**Figure 2–60**  
**ERM Configuration Summary**

#### **2.2.4. Crew Capsule Design**

A biconic re-entry vehicle was chosen for the basic shape of the crew capsule to provide a higher L/D ratio. This ratio determines a great deal. With a L/D of approximately 1, it is possible to control the downrange and cross range landing distances enough so that it becomes practical to land on land and not water. This eliminates the great expense of having to deploy the navy for a crew rescue mission at the end of each flight, a costly notion to say the least. Secondly, it minimizes the total heat flux into the vehicle. With a lower flux it is possible to use radiative cooling instead of ablative techniques. This allows the vehicle to be reusable since the heat shield is not destroyed during re-entry, which also reduces the cost. However, there is a slight weight penalty since the vehicle must carry a set of wings (explained later) and landing gear for the landing. However, in the long term, these issues are amortized with reduced operating expenses. Figure 2–61 shows a side view of the Crew Capsule.

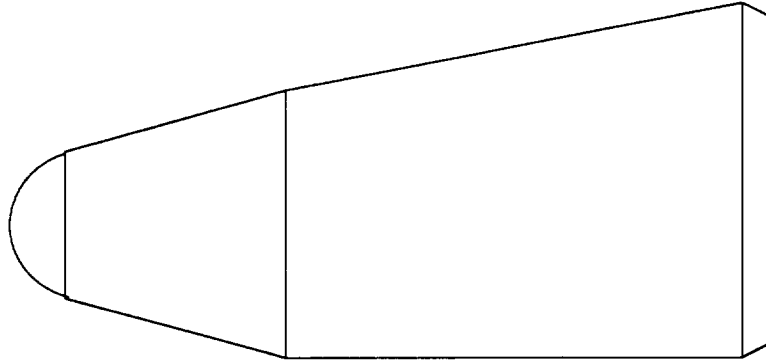


**Figure 2-61**  
**Biconic Re-entry Vehicle – Crew Capsule**

#### 2.2.4.1 Aerodynamic Design

The basic shape of the Crew Capsule was originally designed by the University of Minnesota as a Cargo Return Vehicle (CRV). Since the use of their Hypersonic Arbitrary Body Program was not available to us, we have used their design as a starting point. Since our Crew Capsule will be entering the atmosphere at a higher speed than the design point of the CRV, it was necessary to modify the break angles of the conics slightly. The CRV enters at approximately 8,000m/s (from a Space Station Freedom orbit) compared with our 11,000m/s from the lunar trajectory. The modification was done using simple Newton Hypersonic Flow Theory, and is not presented here for brevity. The geometric results, however, are presented in section 2.2.4.2, and final configuration L/D is presented below in Figure 2-62.

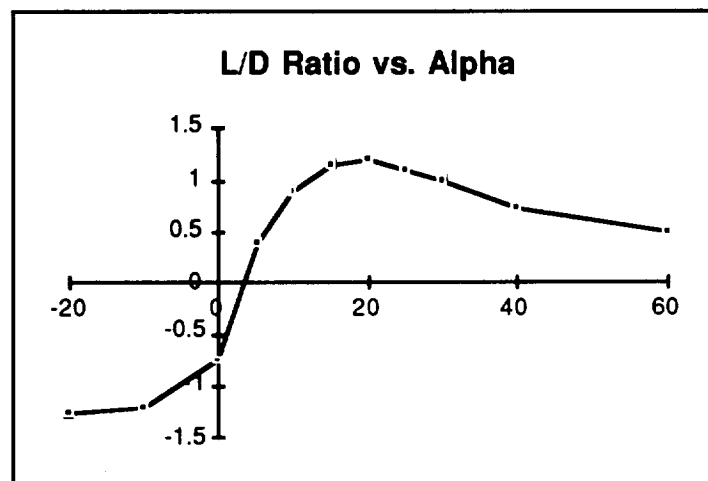


**Figure 2-62**  
**L/D of Biconic Re-entry Vehicle versus AOA**

Since we are aiming for a gliding trajectory, we would like to maximize our L/D ratio. This not only gives us greater control over the trajectory than a vehicle with a higher ballistic coefficient would, but it also reduces our maximum heating rate, which allows a weight savings on the heat shield. The high L/D also allows us to land horizontally (to an extent) on land. We thus eliminate the large sea rescues characteristic of the Apollo landings. To maximize our L/D it is clear according to figure 2-62 that we need to maintain a  $20^\circ$  angle-of-attack. This is  $20^\circ$  above the velocity vector. Since the glide slope is approximately equal to the L/D ratio, the Crew Capsule will have a  $-45^\circ$  glide slope. The  $20^\circ$  angle of attack is above this angle. Therefore, the nose will in fact be pitched  $-25^\circ$  from the horizontal, but still maintain a positive angle of attack.

#### 2.2.4.1.1 Stability

The geometric configuration given in the section 2.2.4.2, allows us to estimate the aerodynamic stability derivatives of the vehicle. These are of critical importance, along with the lift-to-drag plot given in Figure 2-62, for determining the stability of the capsule. The pitching moment shown in Figure 2-63 shows the crew capsule's stability during atmospheric re-entry. To be laterally stable the plot must have a negative slope. This parameter, known as the pitching moment stability derivative and designated  $C_{mb}$ , must be negative. The chart indicates that the crew capsule is only laterally stable if it is pitched to about a 40 degree angle of attack. However, earlier when we discussed the lift-to-drag curve, we determined that the maximum occurred at around 20 degrees. This is where we would like to operate the vehicle. But the vehicle is clearly pitch unstable around 20 degrees. To compensate, we are required to move the center of pressure aft. By introducing wings in the aft section of the crew capsule, we can significantly change the center of pressure. The modified pitching moment curve is shown in Figure 2-63. The  $C_{mb}$  derivative turns zero around 20 degrees and negative at higher angle of attack. This is sufficient to trim the crew capsule to stability.

C-4

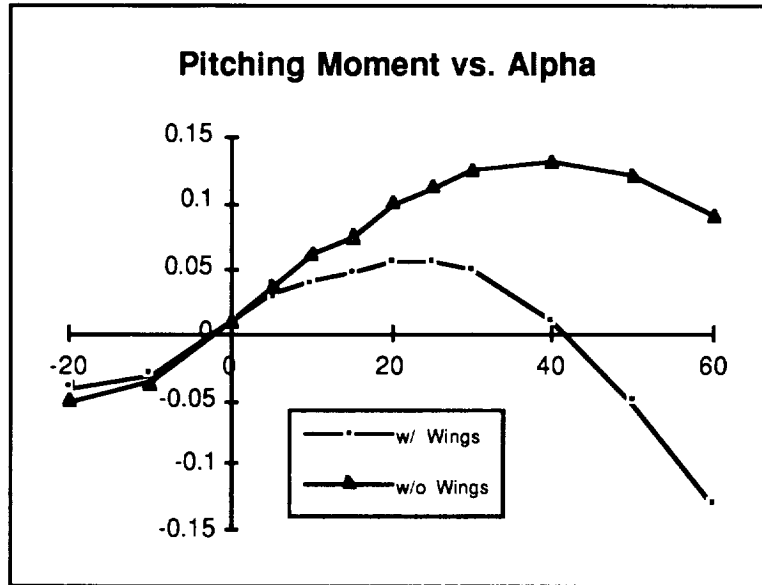


**Figure 2-63**  
**Crew Capsule Pitching Moment versus AOA**

The placement of the wings to achieve the desired pitching moment is shown in Figure 2–64, and are discussed in section 2.2.4.1.2. Since it is necessary to limit the maximum outside diameter during launch and lunar phases of the mission, the wings will be deployable. Only during re-entry, when the wings are needed, will the wings will be deployed.



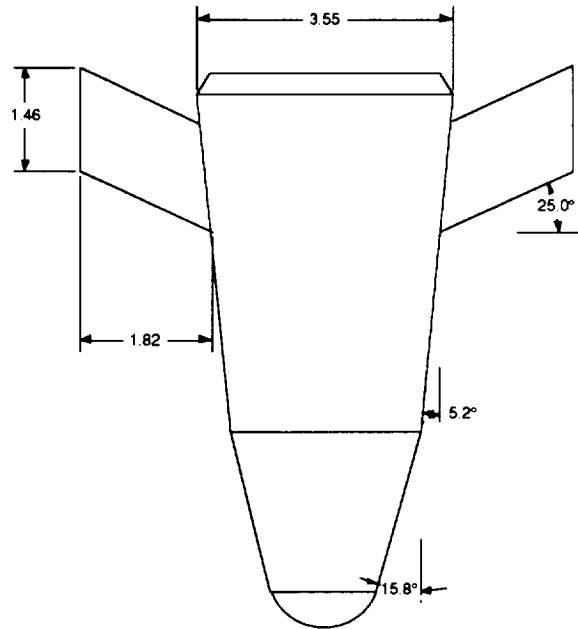


**Figure 2-64**  
**Crew Capsule Top View with Wings**

It needs to be emphasized that the wings are not lifting surfaces. They contribute negligibly to the total lift-to-drag ratio of the vehicle. They work simple as stability augmentors to stabilize the lateral moments. The majority of the lift is generated from flow around the body of the vehicle. It is the Biconic shape (not the wings) that generate the 1.1 L/D.

The longitudinal dynamics are described in Figure 2-65. The crew capsule is stable only when  $C_{nb}$  (the slope of the Yawing Moment curve) is positive. This occurs around  $40^\circ$  AOA. Therefore, at the vehicle trim condition of  $20^\circ$ , the Crew Capsule is longitudinally unstable. This can be corrected by adding a tail surface. This increases the weather-cock stability by changing the slope of the yawing moment more positive. However, there is a drag penalty, and hence a L/D reduction. Instead, I believe that the RCS system, typically not used below 216,000ft can be employed to actively stabilize the longitudinal dynamics. This could be done either with roll or yaw jets since the dynamics of the two modes are closely coupled.

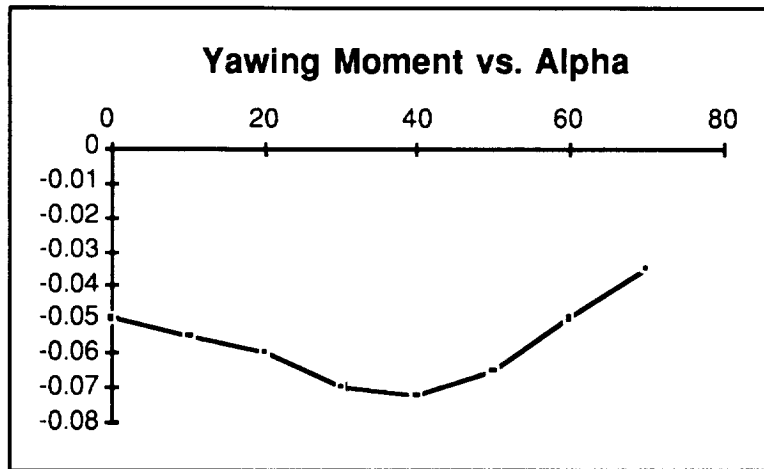


**Figure 2-65**  
**Biconic Re-entry vehicle Yawing Moment versus AOA**

#### 2.2.4.1.2 Wing

The geometry of the wings are summarized in Table 2-6. To be able to trim the vehicle it will be necessary to include flaperons (combination control surfaces of ailerons and flaps) on the trailing edges of the wing. The control surface were design to use 25% of the trailing edge of the chord.

**Table 2-6: Summary of Wing Dimensions**

<b>Wings</b>	
Wing Span	1.8204
Wing Chord	1.4555
Wing Thickness	0.0728
Airfoil Area	0.0741
Airfoil Circumference	3.2749
Wing Volume	0.1350
Wing Area	6.0359

A NACA 0505 was chosen for the wing and its characteristics are shown in Figures 2–66 and 2–67 for 0° and 2° angle of attack respectively. The designation indicates that there is 0% chamber and 5% maximum thickness. These figures provide the two-dimensional L/D ratio for the airfoils.

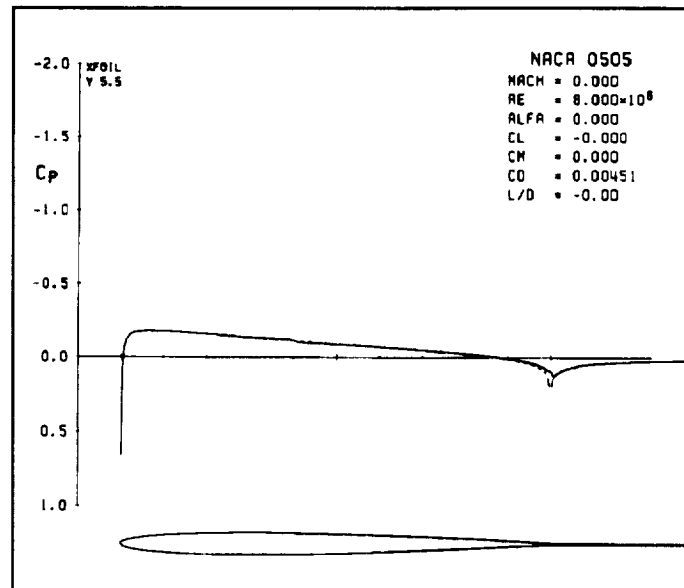


**Figure 2-66**  
**NACA 0505 at AOA of 0°**

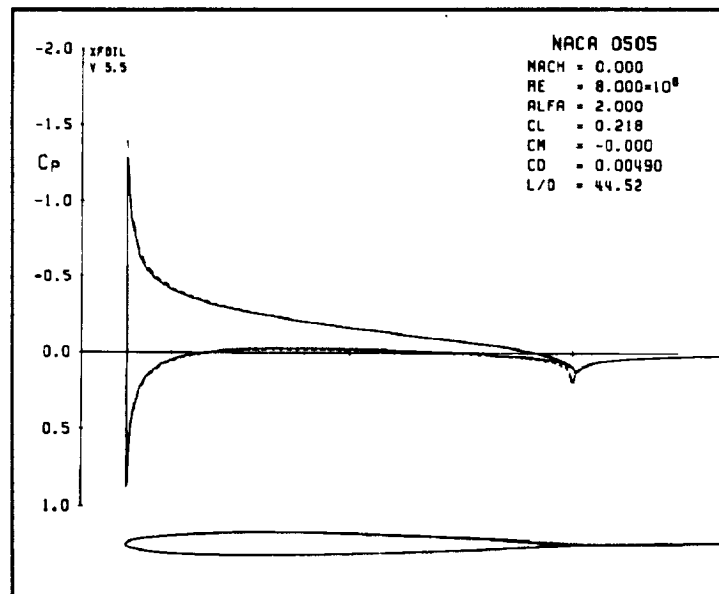


**Figure 2-67**  
**NACA 0505 at AOA of 2°**

#### 2.2.4.1.3 Parafoil Airfoil

The parafoil is used to increase the L/D at low speeds to allow maximum control of the cross range and downrange landing targets. The airfoil cross-section is chosen as a NACA

2210 and is shown in Figures 2-68 and 2-69 for 0° and 2° angle-of-attack respectively. The airfoil has a maximum 2% camber located 20% of the chord from the leading edge. It also has a maximum thickness of 10%. See Chapter 6 of Volume III for a more thorough discussion of the parafoil system.

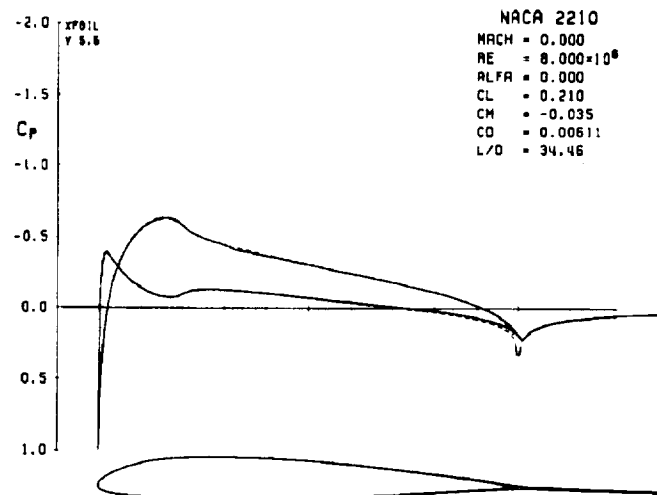


**Figure 2-68**  
**NACA 2210 at AOA of 0°**

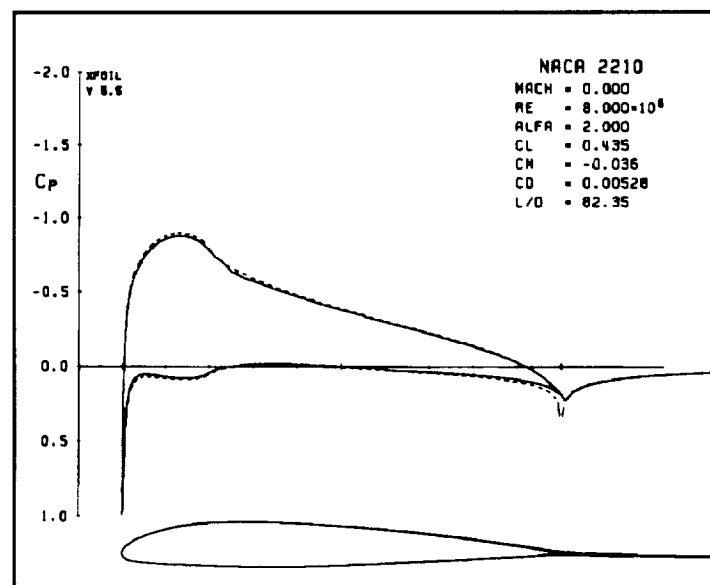


**Figure 2-69**  
**NACA 2210 at AOA of 2°**

#### 2.2.4.2 Sizing and Configuration

The final geometrical configuration of the crew capsule is shown in Figures 2–70 and 2–71. The Table 2–7 summarizes the dimensions and volumes for a crew capsule of 45 m<sup>3</sup> inside volume.

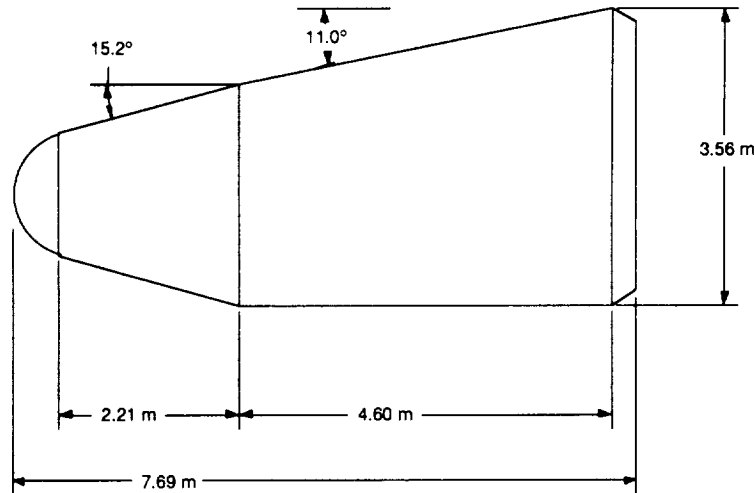


**Figure 2-70**  
**Crew Capsule - Side View - Dimensioned**

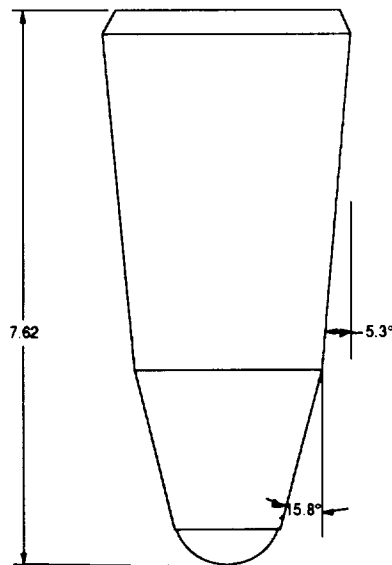


**Figure 2-71**  
**Crew Capsule - Top View - Dimensioned**

**Table 2-7: Summary of Geometric Configuration**

<b>Geometric Configuration</b>	
<i>Maximum Diameter</i>	3.55
Total Area	86.89
Total Volume	46.22
Extended Width	7.19
Total Length	7.85

I will now present the methods for calculating the crew capsule geometrical parameters. This section can be skipped by the reader without loss of continuity.

To determine the volume, and to be able to re-size the vehicle easily with varying parameters, the entire vehicle was non-dimensionalized. The ratios of the geometrical parameters were found with an arbitrary case. This calculation is shown in Figure 2-72. With a given maximum diameter, the length of the frontal and main cone, along with the boattail, nose, and break diameter can be calculated from the set of equations. Using these values we can find ratios of these quantities to the input maximum diameter. This is then the value from which the entire vehicle geometry depends.

```

(* These are some Calculations for the Biconic Sizing
   by Charles Bruen - STP *)

(* d = Maximum Diameter *)

d = 4,

(* b = break diameter/max. diameter *)

b = 0.75,

(* r = radius of nose *)

r = 0.82,

(* a = first conic length/ total length *)

a = 0.4,

(* h = break point diameter *)

h = b d,

FindRoot[{(a-1) x + a y + a r == 0,
           x + y + r == 2.5 d,
           Tan[alpha] y + h == d,
           (h - r) == 2 x Tan[theta]},
          {x, 2}, {y, 7}, {theta, .17}, {alpha, .15}]

{x -> 4., y -> 5.18, theta -> 0.26604, alpha -> 0.190704}

(*      x = First Conic length
        y = second conic length
        theta = second conic dip angle
        alpha = first conic taper angle *)

```

**Figure 2-72**  
**Sample Case for Determining Vehicle Geometry Ratios**

A table of geometric constants was derived for the Crew Capsule and is summarized in Table 2-8. These were calculated from the ratios for the test case described above. As can

be seen, almost every length quantity is non-dimensionalized to the maximum diameter. This is the diameter of the main cone trailing edge. It is the widest point on the vehicle.

**Table 2-8: Constants for Geometric Configuration**

Constants	
<i>Pi</i>	3.14159
<i>Nose Radius/Max Diameter</i>	0.205
<i>Break Diameter/Max Diameter</i>	0.7500
<i>FC Length/Total Length</i>	0.4000
<i>Trailing Diameter/Max Diameter</i>	0.9000
<i>Alpha</i>	0.1907
<i>Alpha in Degrees</i>	10.9265
<i>Theta</i>	0.2660
<i>Theta in Degrees</i>	15.2430
<i>Phi</i>	0.5236
<i>Phi in Degrees</i>	30.0001
<i>Wing Sweep</i>	0.4363
<i>Wing Sweep in Degrees</i>	25.0000
<i>Wing Span/Maximum Diameter</i>	0.5128
<i>Wing Chord/Maximum Diameter</i>	0.4100
<i>Airfoil Shape</i>	NACA 0505
<i>Aspect Ratio</i>	1.2500
<i>Airfoil Maximum Thickness</i>	5%
<i>Beryllium Density</i>	1850
<i>Aluminum Density</i>	2770

Once the maximum diameter has been set., the inside volume and area of the vehicle needs to be calculated. During first iterations a blunt cone approximation was used. However, as the design progressed a more accurate calculation was required. The nose, frontal cone, and boat tail can easily be calculated from the given parameters since they are standard geometrical shapes. However, the main cone is an oblique tapered cone, and a rather complicated formula is required find the volume and area. The formula had to be derived and is shown in figure 2-73. The calculation involves integrating a body of revolution about a variable axis of symmetry.



```
(* These formulas are for calculating an Oblique Tapering
cylinder.

These are used in the Biconic calculations.

Developed by Charles Bruen - STP *)
```

```
r[x_] := Tan[theta] x / 2 + r0
```

```
(* Volume *)
```

```
Integrate[Pi * r[x]^2, {x,0,L}]
```

$$L \text{ Pi } r_0 + \frac{L^3 \text{ Pi } r_0^2 \text{ Tan}^2[\theta]}{2} + \frac{L^3 \text{ Pi } \text{Tan}^3[\theta]}{12}$$

```
(* Area *)
```

```
Integrate[2 Pi r[x], {x,0,L}]
```

$$2 L \text{ Pi } r_0 + \frac{L^2 \text{ Pi } \text{Tan}^2[\theta]}{2}$$

**Figure 2-73**

### **Derivation of Formulas for an Oblique Tapered Cylinder**

It was then easy to determine the inside volume and structural weight (see section 2.2.4.2) by varying the maximum diameter. Figure 2-74, shows how the inside volume varies with the maximum diameter. The Crew Capsule project team has indicated that they require a

45m<sup>3</sup> inside volume. From Figure 2–74, this indicates approximately a 3.5m maximum diameter.

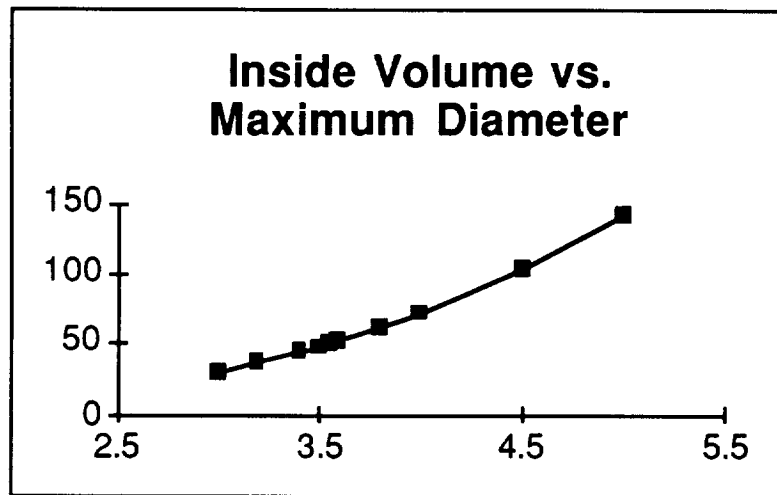


**Figure 2–74**  
**Inside Volume vs. Maximum Diameter**

From a spreadsheet calculation, it is easy to determine the remaining geometric parameters. Table 2–7 at the beginning of the section, is a summary of the most critical ones.

#### 2.2.4.3. Structural Design and Loading

The structural design of the Crew Capsule is a complicated calculation that is only really possible using the finite-element method. A model was developed and is shown in figure 2–75. By using the process described in 2.1.3, we can design the vehicle using a solid monocoque structure, and use the conversion factors for determining the mass of a semi-monocoque design with the same structural state values.

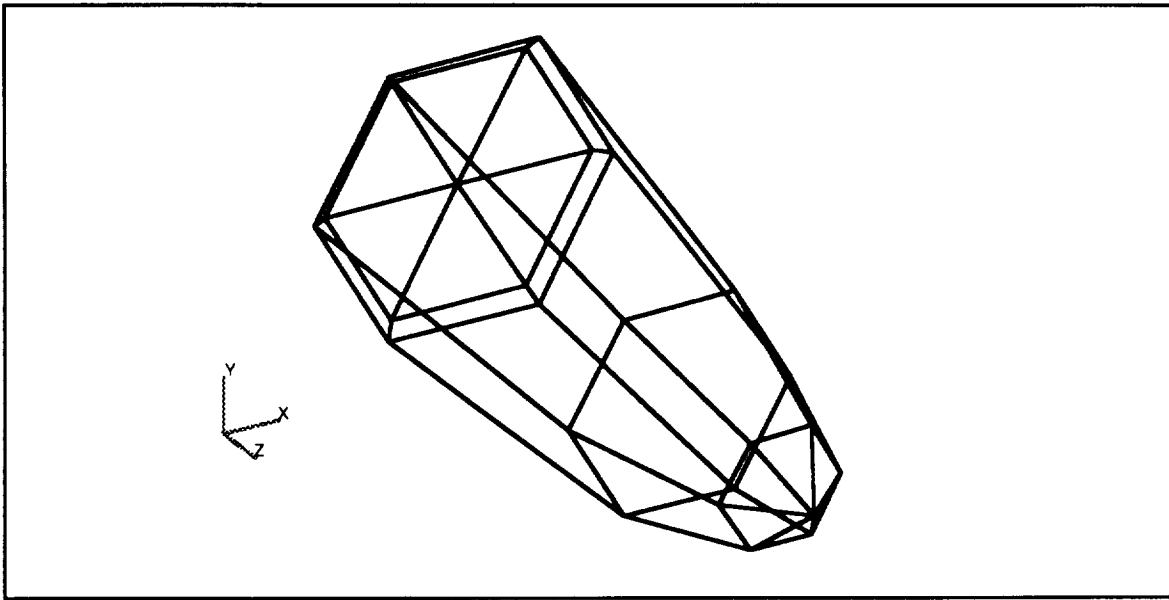


**Figure 2-75**  
**Finite-element model of Crew Capsule**

In order to use the Finite-Element model we need to determine the maximum loads experienced for the vehicle. Since during launch it is enclosed in an aerodynamic fairing, it experiences only the 3.5g's acceleration and no aerodynamic loads. However, during reentry it experiences 1g acceleration plus the aerodynamic pressure. According to Figure 2-76 the maximum dynamic pressure is about 8,000 Pa. The dynamic pressure and the 3.5g acceleration load experienced during launch are the design loads for the Crew Module.

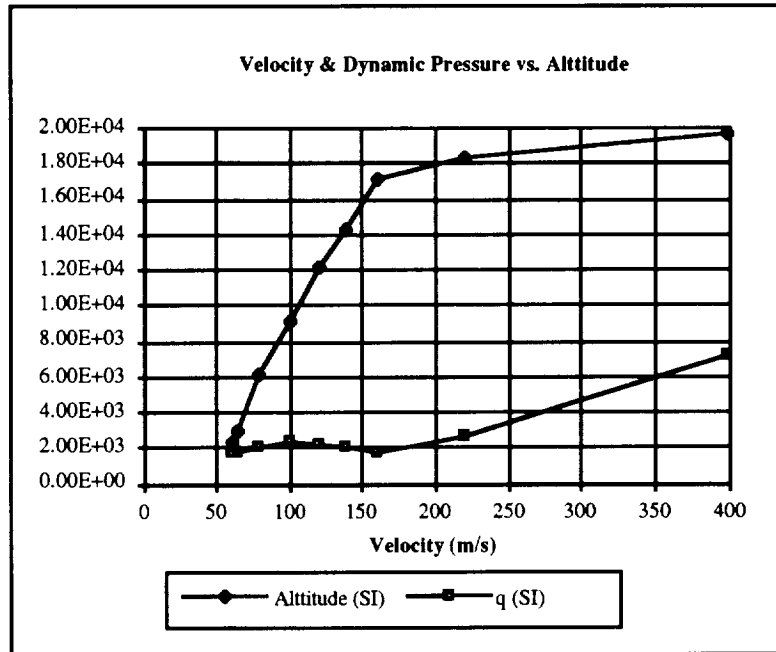


**Figure 2-76**  
**Velocity and Pressure Trajectories**

After several design iterations, a 1.5cm solid aluminum structure resulted in the stresses and deflections show in Figure 2-77 below. This configuration is very capable of carrying the applied loads. It is under stressed to allow for increases in the un-modeled internal mass of the crew capsule.

CREW CAPSULE VEHICLE

NODE	X TRANS	Y TRANS	Z TRANS	X ROT	Y ROT	Z ROT
14	-2.2932E-06	2.3533E-05	1.9645E-05	-1.3273E-03	-7.9606E-04	-1.7440E-03
16	7.8082E-05	4.9446E-05	1.1026E-05	5.8846E-04	-8.7915E-04	-1.3884E-03
19	-7.8082E-05	4.9446E-05	1.1026E-05	5.8846E-04	8.7915E-04	1.3884E-03
20	-1.8727E-06	9.3701E-05	2.6374E-06	2.9811E-03	-1.0261E-03	6.6982E-04

MAXIMUM STRESSES FOR QUAD ELEMENT VON MISES CRITERION

ELEMENT	NODE	MAJOR	MINOR	SHEAR	STRESS	% YIELD
13	0	5.792E+05	-4.705E+05	4.189E+05	7.273E+05	0.2
13	16	2.004E+06	-2.089E+06	1.993E+06	3.454E+06	0.8
13	17	9.375E+05	-1.066E+06	5.044E+05	9.751E+05	0.2
13	24	9.446E+05	-1.626E+06	7.245E+05	1.545E+06	0.4
13	23	2.384E+06	-1.620E+06	7.351E+05	2.083E+06	0.5

MAXIMUM STRESSES FOR TRIANGLE CENTER VON MISES CRITERION

ELEMENT	MAJOR	MINOR	SHEAR	STRESS	% YIELD	CONNECTIVITY
23	6.742E+05	-5.060E+04	3.624E+05	7.008E+05	0.2	1 6 7
24	3.187E+05	6.143E+04	1.286E+05	2.929E+05	0.1	1 7 2
25	4.461E+05	-7.853E+05	6.157E+05	1.080E+06	0.3	29 23 24
26	-1.092E+05	-3.587E+05	1.248E+05	3.185E+05	0.1	29 24 25

MAXIMUM STRESSES FOR SURFACE/SOLID ELEMENTS VON MISES

NODE	MAJOR	MINOR	SHEAR	STRESS CRITERION
13	1.144E+07	-1.152E+07	3.778E+06	1.029E+07
14	1.144E+07	-1.152E+07	3.778E+06	1.029E+07
16	3.212E+06	-3.229E+06	1.435E+06	3.295E+06
17	1.004E+06	-9.352E+05	4.068E+05	9.741E+05

**Figure 2-77**  
**Typical Deflections and Stress for Crew Capsule Loading**

The 1.5cm aluminum skin thickness produces about a 3600kg total structure weight. This is shown in Table 2-9.

**Table 2-9: Skin Thickness and Weight for a Solid Monocoque Aluminum Structure**

<b>Solid Aluminum Weight</b>	
<i>Skin Thickness</i>	0.015
Aluminum Total Weight	3610.23

In order to trade-off the weight versus the inside volume it was necessary to find the weight sensitivity to the volume parameter. As shown in Figure 2-78, initial increases in the volume produce significant increases in weight. However, above 100m<sup>3</sup> the weight increases vary linearly with the inside volume.

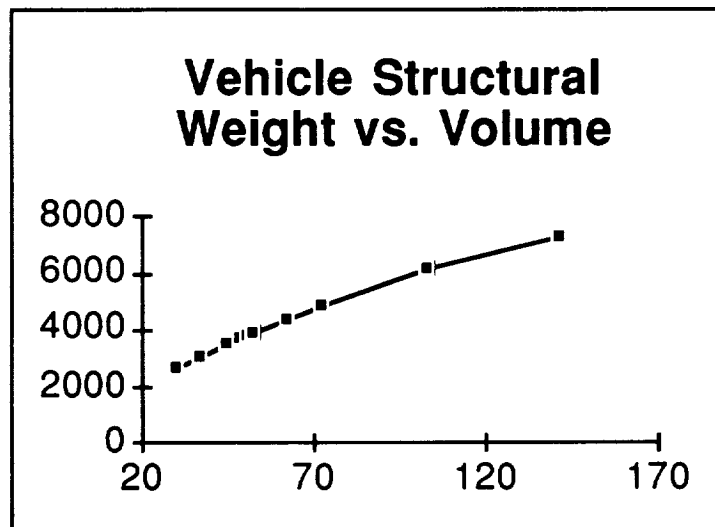


**Figure 2-78**  
**Crew Capsule Weight versus Inside Volume**  
**(Aluminum Solid Monocoque Construction)**

As was shown in section 2.1.3, the weight of a semi-monocoque structure that induces the same stresses and deflections as a solid monocoque one, is about 50% of the weight and about 2.5x as thick as the monocoque structure. If the Crew Module weight based on a solid aluminum structure is 3600kg, our semi-monocoque structure will weigh

approximately 1800kg. With the weight of the wings and wing deployment system, the final structural weight is 2000kg.

#### 2.2.4.4. Re-entry Heating

In order to properly size the heat shield, a rough estimate of the heating rate and the total heat flux experienced during re-entry needs to be calculated. According to Equation 2-25, the total heat flux is proportional to the dynamic pressure ( $1/2\rho V^2$ ) times the coefficient of friction.

$$Q = \rho V^3 S_w C_F / 4 \quad (2-25)$$

The vehicle  $C_F$  is determined by integrating the local  $C_f$  over the surface of the body normalized to the local pressure. This is shown in equation 2-26.

$$C_F = (1/S_w) \int C_f [(\rho V)_{oe} / \rho V] ds \quad (2-26)$$

To simplify expression 2-26, we make an assumption that  $C_f$  is proportional to the heat gradient over the local dynamic pressure. This is shown in equation 2-27. This assumption will break down at very high heat rates. But with our gliding trajectory (a product of the high L/D), we will be able to limit the heating rate and hopefully maintain this as a good assumption.

$$C_f = 2 \tau_w / (\rho V^2)_{oe} \quad (2-27)$$

$$\tau_w = \mu (\partial V / \partial y)_w \quad (2-28)$$

By using the boundary layer approximations this can be reduced to an approximation for  $C_F$  based entirely on the Reynolds Number. The  $C_F$  is proportional to the inverse of the square-root of the Re, given by equation 2-29.

$$C_F = 1.328 / \text{Re}^{1/2} L \quad (2-29)$$

With a Reynolds number of 8 million this gives us a  $C_F$  equal to  $4.69 \times 10^{-4}$ .

We would also like to determine the maximum heating rate. For an equilibrium gliding re-entry, equations 2–30 through 2–32 describe the key parameters [Griffin, 1991].

$$q_{avg_{max}} = (g^3 R / 27)^{1/2} (m / SC_D) / (L/D) \quad (2-30)$$

$$\rho_{crit} = (4/R)(m/SC_D)/(L/D) \quad (2-31)$$

$$V_{crit} = (gR/3)^{1/2} \quad (2-32)$$

#### 2.2.4.5. Thermal Protection & Heat Shield Design

Three types of radiative insulation are available. They are summarized in Table 2-10. Each can be used in a different temperature regime, and they are listed in order of descending tolerance to heat. Also listed in Table 2–10 is the required thickness of insulation for each of the heat regimes based on equation 2–30.

**Table 2–10: Insulation Materials**

<b>Material</b>	<b>Abbreviation</b>	<b>Density</b>	<b>Thickness</b>
Lockheed Insulation	LI-2200	353	0.063
Fibrous Refractory Composite Insulation	FRCI	388	0.058
Tailorable Advanced Blanket Insulation	TABI	258	0.0127

Table 2–11 summarizes the insulation covering of the crew capsule. The heat shield is broken down by area, and is listed according to the amount of insulation covering each section. For instance the entire nose needs to be covered with LI-2200 since it experiences the maximum heating and LI-2200 is the only insulation that can withstand that environment. On the other hand, only 25% of the frontal cone needs the FRCI insulation and the rest (mostly on top) can be the lighter and cheaper TABI insulation.



**Table 2-11: Calculation of Heat Shield Coverage and Weights**

<b>Location</b>	<b>Area</b>	<b>Material</b>	<b>Weight</b>
Nose Surface	3.3277	LI-2200	74.00
Wing % Heat Shield		0.25	
Wing Leading Edge	1.5090	LI-2200	33.56
Wing Surface	4.5269	FRCI	101.87
Frontal Cone % Heat Shield		0.25	
Frontal Cone Lower Surface	3.7120	FRCI	83.54
Frontal Cone Upper Surface	11.1361	TABI	36.49
Main Cone % Heat Shield		0.2	
Main Cone Lower Surface	8.9725	FRCI	201.92
Main Cone Upper Surface	35.8901	TABI	117.60
Boat Tail % Heat Shield		0.2	
Boat Tail Lower Surface	2.3557	FRCI	53.01
Boat Tail Upper Surface	9.4229	TABI	30.87
Removable Material Weight			412.47
Support Structure Weight			254.40
Attachment Mechanism Weight			25.44
Removable Shield Weight			692.31
Weight Remaining w/Vehicle			320.39
<b>Total Weight of Removable</b>			<b>1012.70</b>
<b>Total Integrated Shield Weight</b>			<b>732.86</b>

It was decided that the heat shield would remain permanently attached to the crew capsule. Therefore, its total weight is 732kg. This is in addition to the 2000kg weight for structure.

### **2.2.5 Precursor Mission Structures**

The Precursor Landing Module, or PLM, will take the lunar habitat and all necessary set-up equipment down to the lunar surface after the LBM is ejected (Figure 2-79). The main body of the PLM itself is a semi-monocoque cylinder. This Primary Hull is designed to take the brunt of the axial and lateral launch accelerations, as well as the bending stresses after the structure is deployed horizontally.

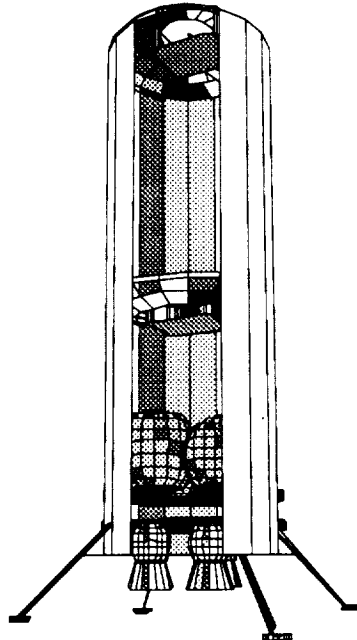


**Figure 2-79**  
**PLM Stage—Cutaway View (landing)**

The PLM has two sets of support structures to buffer it from the lunar surface. The landing gear is composed of 4 landing legs which deploy just before LBM separation. These legs provide stability and cushion the impact at touchdown. After the PLM has landed, it will tilt to a horizontal position (Figure 2-80). In this deployed state, the vehicle will rest on four support legs, which will serve as a permanent supports for the lifetime of the lunar base.

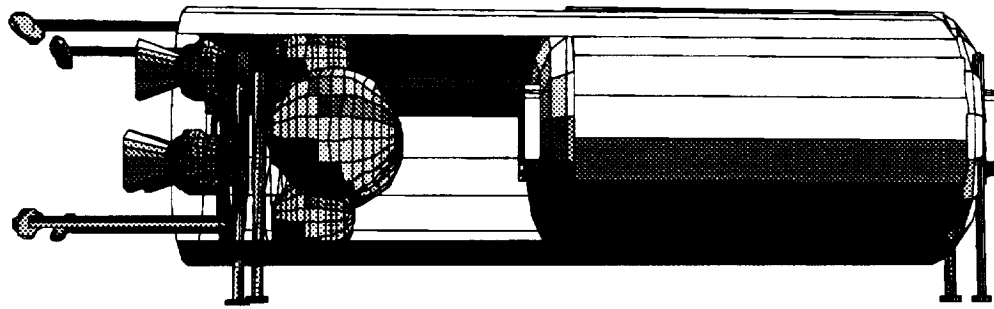


**Figure 2-80**  
**PLM Stage—Cutaway View (deployed)**

The remainder of the PLM stage structures are internal and are grouped into three sections for analysis (Figure 2-81). At the base of the PLM is the Propulsion Section where the rocket motors and propellant tanks are attached to the Rocket Truss. Above this section is the cargo bay used for storing the solar arrays, lunar rover, regolith support structure, and various other supplies and machines necessary for set-up of the lunar base. At the top of the PLM rests the BioCan lunar habitat, where the crew will live for the 28-day mission.

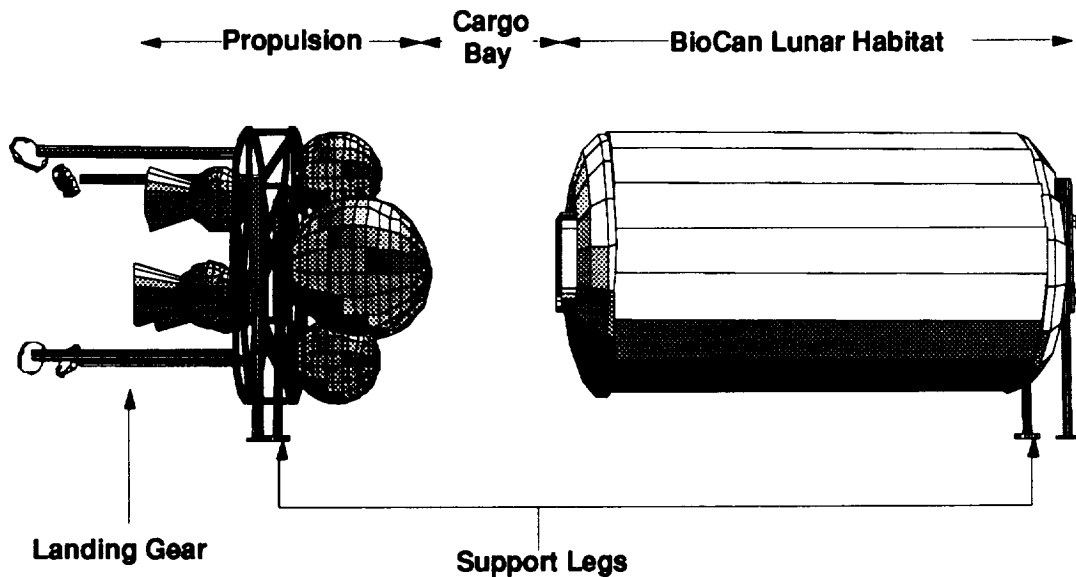


**Figure 2-81**  
**PLM Stage—Internal Structures**

The last and most time-consuming task of setup for the lunar base is assembly of the Regolith Support Structure and covering it with regolith to protect the crew from solar flare radiation. This structure will be assembled by the crew once they arrive via the piloted mission.

#### 2.2.5.1 PLM Primary Hull

##### **Load Criteria**

The PLM stage is expected to withstand launch accelerations of up to 3.5 g's axially and 2.5 laterally. In its horizontal position after deployment, the stage must endure the bending loads due to its own weight as well as the regolith shielding which will cover it.

##### **Configuration**

The main body of the PLM itself is a semi-monocoque cylinder of radius 6m and length 19m. This Primary Hull is designed to take the brunt of the axial and lateral launch accelerations, as well as the long-term bending stresses once the structure is deployed horizontally. There are 12 stringers and 18 frames in the design (Figure 2-82). The frames make up the largest portion of the total framework mass, due to the large stresses induced by lateral accelerations and regolith shielding. Specifications are given in Table 2-12.

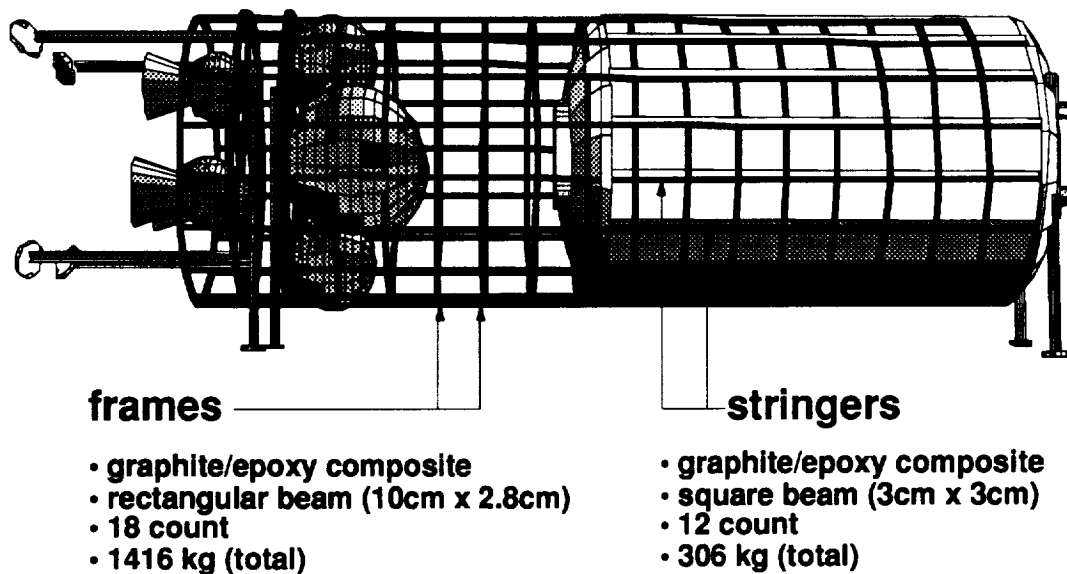
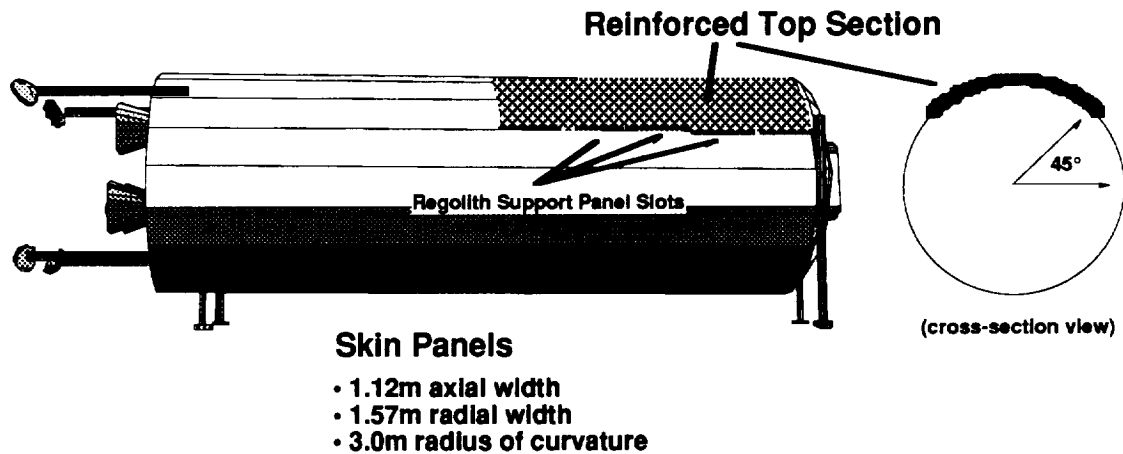


**Figure 2-82**  
**PLM stage—Framework**

The framework is covered with thin, curved skin panels. These bolt-on panels are removable to allow access to the BioCan pressure vessel and other internal structures for

inspection and repair. The major portion of the skin is composed of 0.5 mm composite panels. The primary forces on these panels are aerodynamic. The portion of the skin which will support regolith above the BioCan is composed of reinforced aluminum panels, 2mm thick (Figure 2-83). Along the bottom edge of this reinforced section are several horizontal slots. These slots are important in the assembly of the Regolith Support Structure, to be discussed later in this chapter. Table 2-12 at the end of this section contains a summary of the Primary Hull statistics.



	Material	Thickness	Count	Weight
Normal	graphite/epoxy composite	0.5 mm	177	232 kg
Reinforced	aluminum	2.0 mm	27	263 kg
Total			204	495 kg

**Figure 83**  
**PLM stage—Skin Panels**

### Structural Analysis

The Primary Hull is designed to take the most of the axial, lateral, and bending moment loads that will be seen by the PLM. The axial stress is concentrated at the bottom during launch, since the weight of the entire structure presses on this section. By totaling the mass estimates for all parts of the PLM stage, the resulting axial stress is compared to the critical buckling stress of a stringer section. The stringer section is considered a pinned-pinned beam of the same length as the frame spacing. The stress in the stringers is also determined for the bending moment introduced upon horizontal deployment. For this case, the PLM is modeled as a uniformly loaded beam, as if it were entirely covered by regolith—not just on the BioCan section. Bending beam stress equations are used for the analysis. The frames are considered to take all the lateral loads, including the additional load of the regolith radiation shield. The frame cross-sections are determined first by rough estimate using

beam theory and then testing a finite-element model using pressure loads similar to those expected from the lateral accelerations and regolith covering.

## Summary Specifications

**Table 2-12: PLM Primary Hull Specifications**

<b>PLM Body:</b>			
Body Diameter	6.0 m	<b>Stringers:</b> (graphite/epoxy composite HTS [0])	
Body Radius	3.0 m	Stringer Cross Section Type	square
Propellant Section Height	5.69 m	Stringer outer radius	0.030 m
Cargo Bay Height	2.50 m	Stringer inner radius	0.030 m
BioCan Height	11.00 m	Number of Stringers	12
Total Body Length	19.03 m		
<b>Panels:</b>		<b>Frames:</b> (graphite/epoxy composite HTS [0])	
Panel axial width	1.119 m	Frame Cross Section Type	rectangular
Panel radial width	1.571 m	Frame height	0.10 m
Panel radius of curvature	3.0 m	Frame width	0.028 m
		Frame Spacing	1.12 m
Normal Panels (graphite/epoxy composite [0] HTS)		Number of Frames	18
Number of Normal Panels	177		
Normal Panel Thickness	0.0005 m		
Reinforced Panels (aluminum 2024-T36)			
Number of Reinforced Panels	27		
Reinforced Panels Thickness	0.002 m		
Total Number of Panels	204		
<b>MASS ESTIMATES</b>			
Mass of Stringers	294 kg		
Mass of Frames	1,429 kg		
Mass of Panels	495 kg		
Lander Body Mass Subtotal	1,968 kg		
Joints & fittings allowance	25%		
<b>Primary Hull Mass (empty)</b>	2,460 kg		

## 2.2.5.2 Ground Support

### 2.2.5.2.1 Landing Legs

#### **Load Criteria**

The landing gear for both the Precursor and Piloted landing vehicles is identical. The legs are required to support the entire weight of the vehicle (about 26 metric tons) under a landing shock of 0.6 g. The horizontal velocity component is expected to be negligible at touchdown. The craft is expected to be reasonably stable, yet for the case of the Precursor mission, it is desired to topple the PLM by a set of solid rocket motors at deployment time. Therefore, two of the landing legs are expected to support the entire weight of the vehicle for a brief period during deployment. In addition, the soft, uncertain lunar regolith necessitates some sort of landing feet to prevent excessive sinking of the legs into the surface.

#### **Configuration**

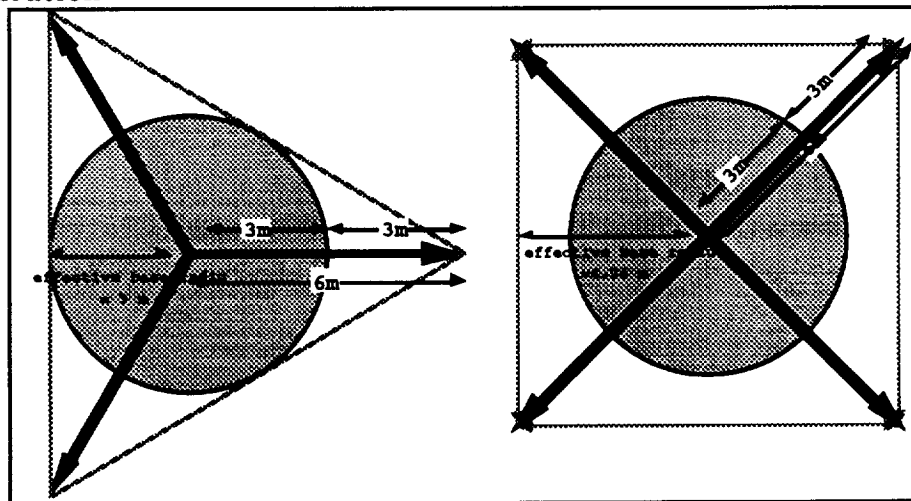


**Figure 2-84**

#### **Effective Base Radius Comparison for 3-leg and 4-leg Cases**

The stability of a landing gear configuration with a circular spread can be expressed by its effective base radius, or the length of the moment arm generated by the landing legs in the direction most susceptible to toppling (Figure 2-84). The effective base radius is determined by the number, length, and angle of the landing legs. The tripod and four-leg configuration were considered most seriously for this project. The four-leg configuration was chosen over the tripod because of its favorable mass to effective base radius ratio.

Each landing leg makes an angle of  $45^\circ$  to the surface. The angle was chosen as a trade-off between the larger angles with large bending moments and smaller angles with less stability.

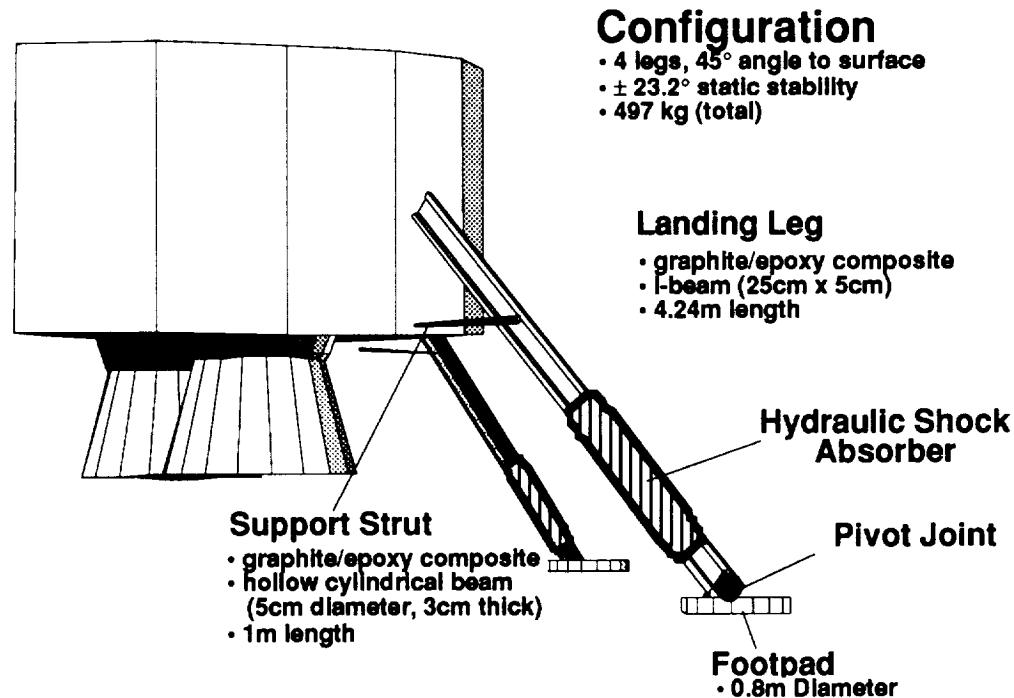


**Figure 2-85**  
**Landing Gear Configuration**

Each landing leg consists of a main beam, support strut, and footpad (Figure 2-85). The main beam is a composite I-beam, equipped with a hydraulic shock absorber to cushion impact at touchdown. The I-beam configuration was chosen to more efficiently react the large bending moments in the vertical direction. The hydraulic shock absorber was chosen over a crushable balsa shock absorber used in the Apollo moon missions due to its reusability. If the initial landing site proves unsatisfactory for some reason, it may be possible to use the remaining fuel on board to relocate. The footpad is attached to the main beam via a pivot joint, which allows the footpad to accept any surface angle upon landing. This pivoting is also necessary to accommodate the toppling motion of the PLM during deployment. The joint is spring-centered to prevent awkward footpad angles upon initial contact with the surface. The support strut acts to reduce the moment arm of the main beam at its connection with the Rocket Truss. Its construction is a hollow cylindrical composite beam. A screw-action motor pushes the support strut outwards to deploy the landing leg (Figure 2-86). The support strut is much smaller and lighter than the main beam since it is



not expected to see large moments, but only axial loads. The sizes and masses of the various components are given in Table 2-13 at the end of this section.

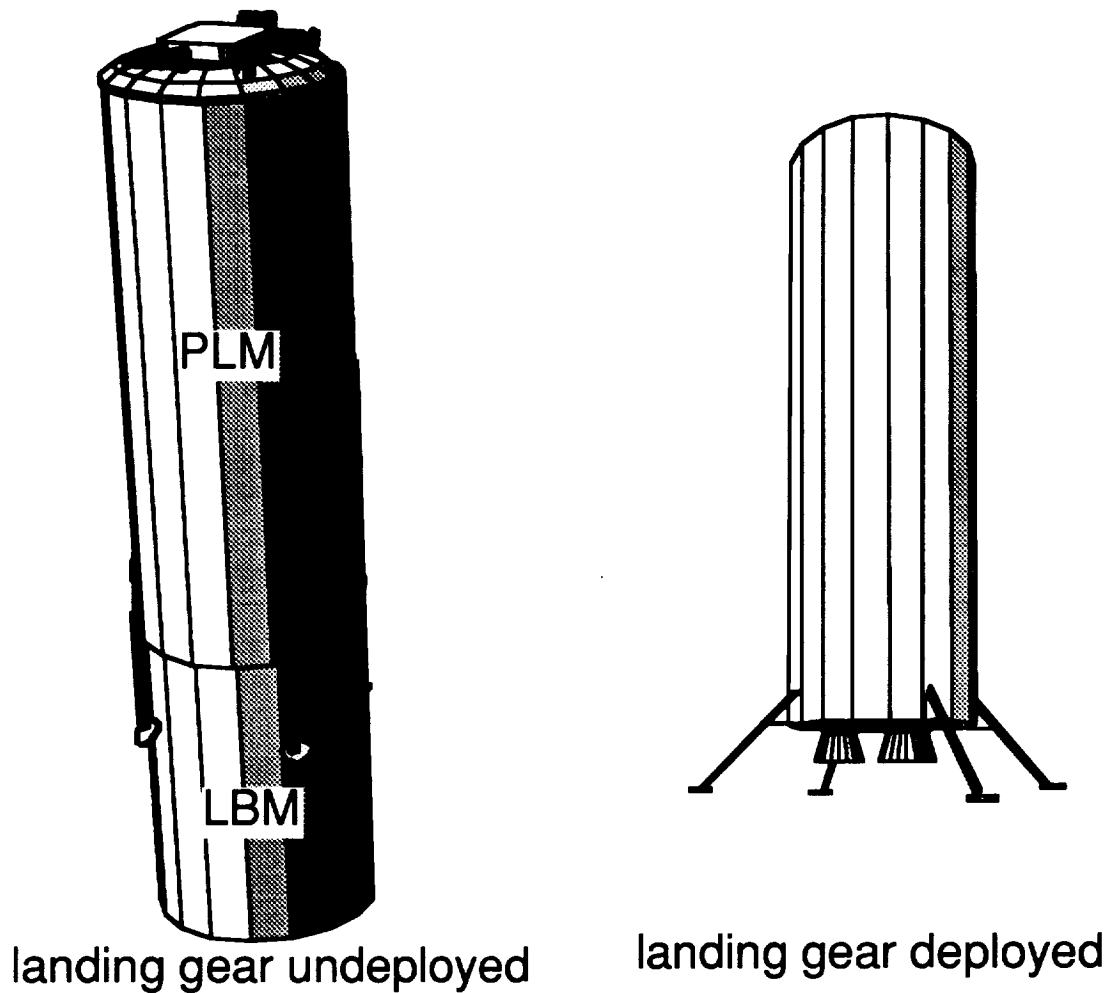


**Figure 2-86**  
**Landing Gear Deployment**

### **Structural Analysis**

The landing gear is analyzed using standard beam theory for buckling and bending of beams. Figure 2-87 is a force diagram of the axial loads present in each part of the leg structure.

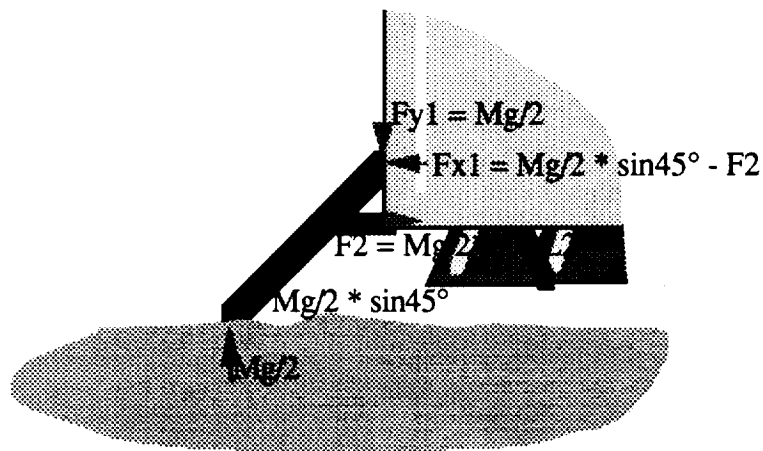


**Figure 2-87**  
**Landing Gear Structure—Axial Load Diagram**

Because the axial forces are different in each part of the landing gear structure, the axial loads are tested separately against the critical buckling load for the main beam upper section, main beam lower section, and support bar. The bending stresses are calculated using the moment diagram in Figure 2-88. From the moment diagram, the bending stress in the beams is computed and compared to the yield stress of the material to check for failure.

### **Stability Analysis**

In order to calculate the static stability of the vehicle on a sloped surface, the center of mass is calculated using the mass estimates for each part of the lander—the BioCan, cargo bay, PLM propellant section, and landing gear. In the center of mass calculations, it is assumed that the mass allocated for each section is evenly distributed within that particular section. Using the effective base radius of the vehicle (as previously described in the Configuration subsection) and this rough idea of center of mass, a maximum tilt angle of 23.2° is computed (Table 2-13).

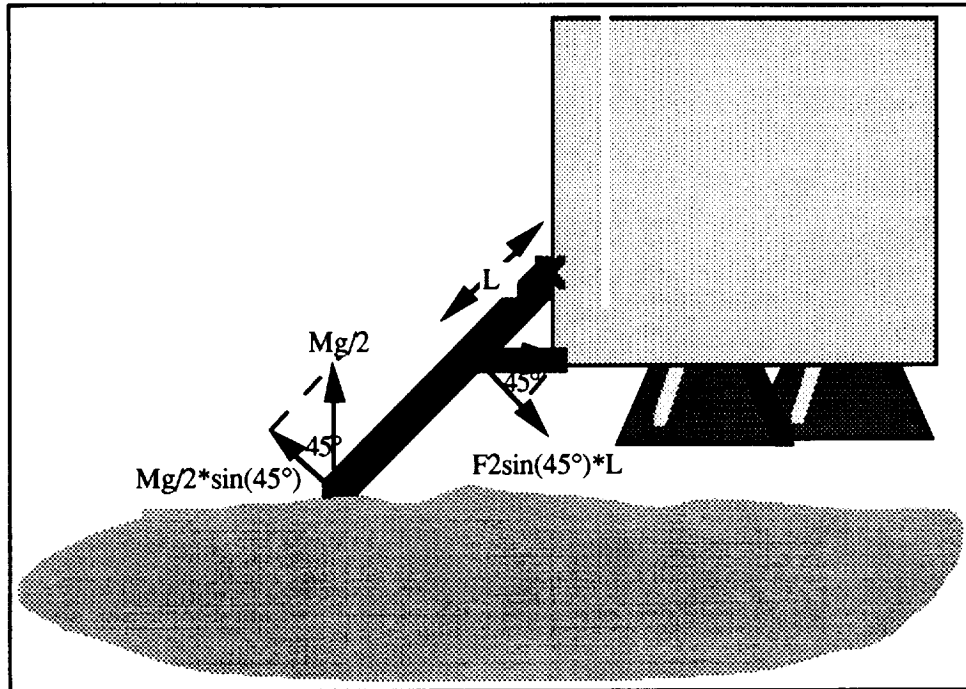


**Figure 2-88**  
**Landing Gear Structure—Moment Diagram**

### Summary Specifications

**Table 2-13: Landing Gear Geometry & Mass Estimate**

<b>GEOMETRY</b>		<b>MASS ESTIMATE</b>	
<b>Leg Length</b>	<b>4.24 m</b>	Footpad mass	22.5 kg
<b>Leg Angle</b>	<b>45°</b>	Support bar mass	0.7 kg
<b>Ground Clearance</b>	<b>2.00 m</b>	Mass of Main beam	45.8 kg
<b>Support Bar length</b>	<b>1.00 m</b>	Joints & Fittings	35%
<b>Stage radius</b>	<b>3.00 m</b>	Motors & Misc	100 kg
<b>Effective base radius</b>	<b>4.24 m</b>		
<b>Footpad thickness</b>	<b>0.03 m</b>	<b>Total Landing Gear Mass</b>	<b>497 kg</b>
<b>Footpad radius</b>	<b>0.40 m</b>		
<b>Number of Legs</b>	<b>4</b>	<b>STABILITY</b>	
		Center of Mass	9.9m above surface
		<b>Stable Angle (deg)</b>	<b>23.2°</b>

### 2.2.5.2.2 Support Legs

#### **Load Criteria**

The Support legs keep the entire PLM structure from touching the lunar surface in order to prevent thermal conduction and also to level the structure and provide a comfortable living environment for the crew. During the deployment procedure, these legs must carry the entire weight of the PLM through the landing shock experienced after toppling. For the lifetime of the habitat, these legs must carry not only the weight of the entire stage, but also the weight of the lunar regolith shielding which will cover the habitat. These items will be discussed in more detail in the next section, *Regolith Support Structure*.

#### **Configuration**

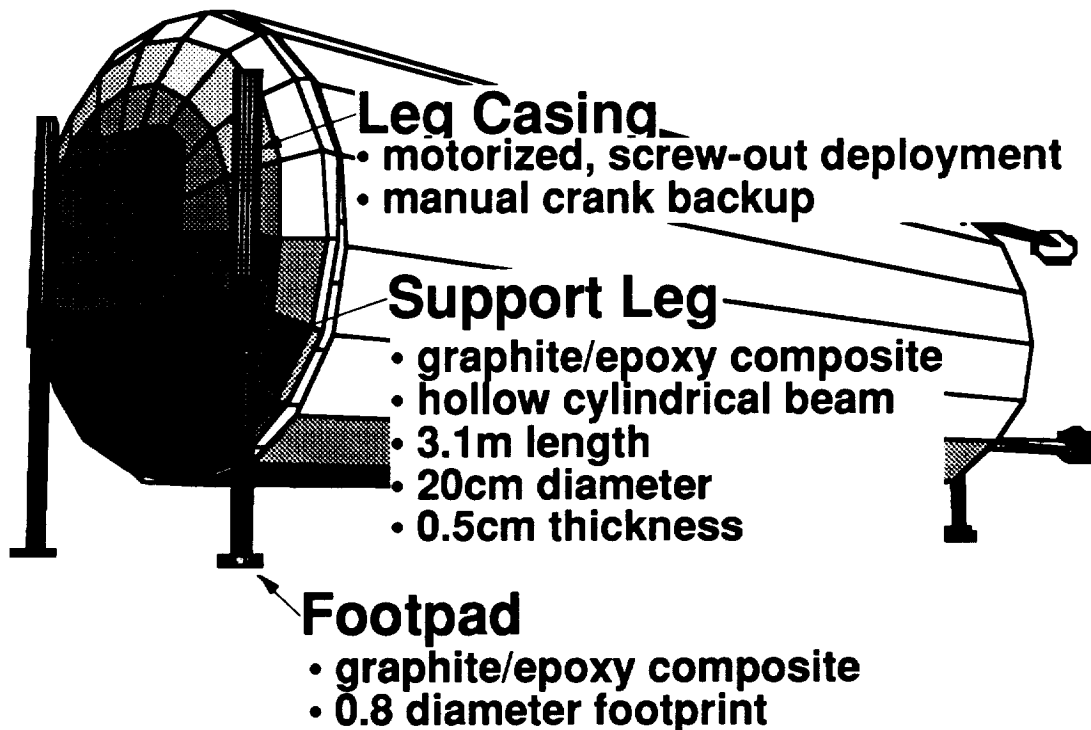


**Figure 2-89**  
**Support Leg Configuration**

There are four support legs on the PLM stage (Figure 2-89). Each is a hollow, cylindrical beam made of graphite/epoxy composite. These four legs extend out of their casings by mechanical screw-action motors to full length shortly before toppling deployment. Each leg

can also be deployed by manual cranking as a redundant backup in case of motor failure. At maximum extension, the ground clearance on a hard surface is one meter. At the end of each leg is composite footpad with a 0.8m diameter footprint. After making sure that the hull will not be breached by underlying rocks, the PLM will be slightly lowered to make crew access and regolith shield construction easier.

### Structural Analysis

Because the support legs are not expected to see much bending moment, the primary failure mode is buckling. The analysis is a simple comparison of the buckling load of a cylindrical column and the total load divided by the number of legs. This assumes that the loading is uniform along the long of the PLM. Due to the regolith covering of only the BioCan section, the loading is not uniform. However, the lack of moments on the legs allows them to support much more weight than would be possible for angled legs of comparable weight (the landing legs, for example). Because of the critical nature of the support legs, and because of uncertainty as to the dynamics of the toppling deployment, each of the four support legs is designed to be capable of holding the entire weight of the PLM. The specifications for the support legs are presented in Table 2-14.

### Summary Specifications

**Table 2-14: Support Leg Geometry & Mass Estimate**

GEOMETRY		number of legs		MASS ESTIMATE	
body radius	3.00	Leg outer	0.100	Single leg mass	14.23
	m	radius	m		kg
distance from	2.87	Leg inner	0.095	Foot mass	14.98
center	m	radius	m		kg
distance from	2.12	Foot Radius	0.4 m	Leg mass subtotal	117 kg
bottom	m			(4 legs)	
in-case allowance	0.50	Foot Thickness	0.02 m	Casing/Extension	150*
	m			Motor Allowance	
ground clearance	1.00				
	m				
Leg length	3.12			Total Support Leg	292 kg
	m			Mass	

#### 2.2.5.3 Propulsion Section

##### Load Criteria

The propulsion section must transfer the thrust from the three RL-10 rocket engines to the rest of the vehicle and store the liquid hydrogen and liquid oxygen propellants to be used in

the engines. In addition, the propellant tanks will be used to store the fuel for the fuel cells which will power the lunar base while the solar cells are ineffective during the 14-day lunar night. The propellant tanks will be under 340,000 Pa of internal pressure in addition to the dynamic pressure of the contents during launch acceleration.

### Configuration

The propellant tanks are mounted on the top of the Rocket Truss. The two hydrogen tanks and two oxygen tanks are mounted side by side. The configuration of 4 spherical tanks side-by-side was chosen to reduce the height of the vehicle. The hydrogen tanks decide the height of this propellant section because of their greater size (Figure 2-90 & Table 2-15). Each tank is a graphite/epoxy composite pressure vessel with a wall thickness of 0.5 mm. The tanks are covered externally with insulation for the cryogenic contents. This thickness is 16.3 cm for the hydrogen tanks and 10 cm for the oxygen tanks. A half millimeter of steel lining on the interior of the tanks prevents the cryogenic contents from reacting adversely with the composite tank walls.

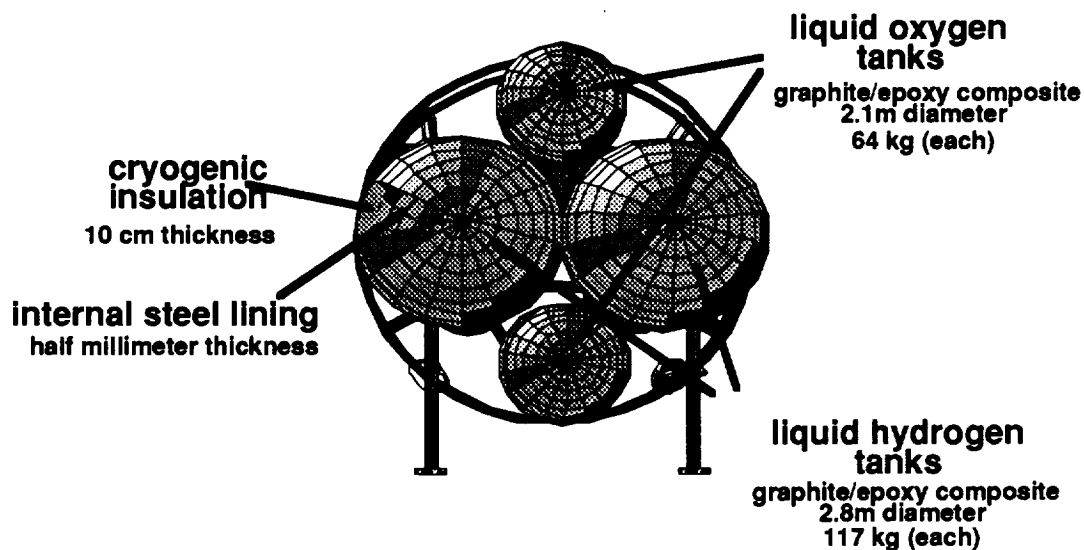


**Figure 2-90**  
**PLM Propellant Tanks**

### Structural Analysis

The volume of the propellant tanks was calculated from the propellant masses needed for descent to the lunar surface and fuel for the fuel cells during the lunar night. A 5% extra fill space is added to this volume to allow for less than total fillage of the tanks. The

pressure is the same for both hydrogen and oxygen tanks—340000 Pa. In addition to the static internal pressure, dynamic pressure of the contents during launch accelerations must be taken into account. Hoop stress equations are used to determine the stress in the tank walls, and this is compared to the yield stress of the material to detect failure.

## Summary Specifications

**Table 2-15: PLM Propellant Section Specifications**

Configuration		Oxygen Tanks		Hydrogen Tanks	
Truss Mass	250 kg	Oxygen Mass	8780	Hydrogen Mass	1270
Tank Mass	362 kg	Oxygen Volume	7.4951	Hydrogen Volume	18.7817
Tank Truss, Piping, Fittings	350 kg	Oxygen Tank Geometry	spherical	Hydrogen Tank Geometry	spherical
Insulation Mass	458 kg	Number of Oxygen Tanks	2	Number of Hydrogen Tanks	2.0000
Engine Mass	501 kg	Oxygen Tank Radius	0.9636	Hydrogen Tank Radius	1.3088
<b>Section Dry Mass</b>	<b>1921 kg</b>				
		Oxygen Tank Wall Thickness	0.0005 m	Hydrogen Tank Wall Thickness	0.0005 m
<b>Total Section Height</b>	<b>5.70</b>	Oxygen Tank Insulation Thickness	0.10 m	Hydrogen Tank Insulation Thickness	0.163 m
		Oxygen Steel Lining Thickness	0.0005 m	Hydrogen Steel Lining Thickness	0.0005 m
		Oxygen Tank Mass w/fittings	64 kg	Hydrogen Tank Mass w/fittings	117 kg
		Oxygen Tank Insulation Mass	57 kg	Hydrogen Tank Insulation Mass	172 kg
		Oxygen Tank Mass w/fittings & insulation	121 kg	Hydrogen Tank Mass w/fittings & insulation	289 kg

### 2.2.5.4 Cargo Bay

The cargo bay is located between the BioCan pressure vessel and the propellant tanks. The structural components of this section consist mainly of fittings and shelves to store the solar panels, regolith support structure, lunar rover, and construction machinery during the flight. No new calculations are performed specifically for this section, but two features need to be mentioned briefly—the access hatch and the gangplank.

#### 2.2.5.4.1 Hatch

An access hatch exists on the side of the PLM stage to facilitate unloading of the cargo bay. This section is not pressurized, so the hatch need not be airtight. However, once deployed

in the horizontal position, stress concentrationd can arise in the primary hull near the hatch when it is opened. This necessitates a “beefing up” of the frame surrounding the hatch to compensate.

The hatch for the cargo bay is shaped identically to the wall section that it replaces. The hatch opens by sliding up and away on two side rails, much like a typical garage door.

#### 2.2.5.4.2 Gangway

The crew will need a convenient way to get large, heavy objects in and out of the cargo bay. A gangplank has been chosen for this purpose. The lunar rover will drive down the gangplank, and the solar arrays and regolith support structure will also be carried across it. In the interests of modularity, and because the expected loads are about the same order of magnitude, this gangplank is identical to one of the regolith support structure panels discussed in Section 2.2.5.6, *Regolith Support Structure*. The gangplank must be located at an easily accessible location from the outside of the PLM, since the internal airlock of the BioCan may not be openable until the cargo bay is sufficiently unloaded to allow the airlock door to swing outward into the cargo bay. The gangplank slides out from the side of the PLM hull just under the cargo bay hatch.

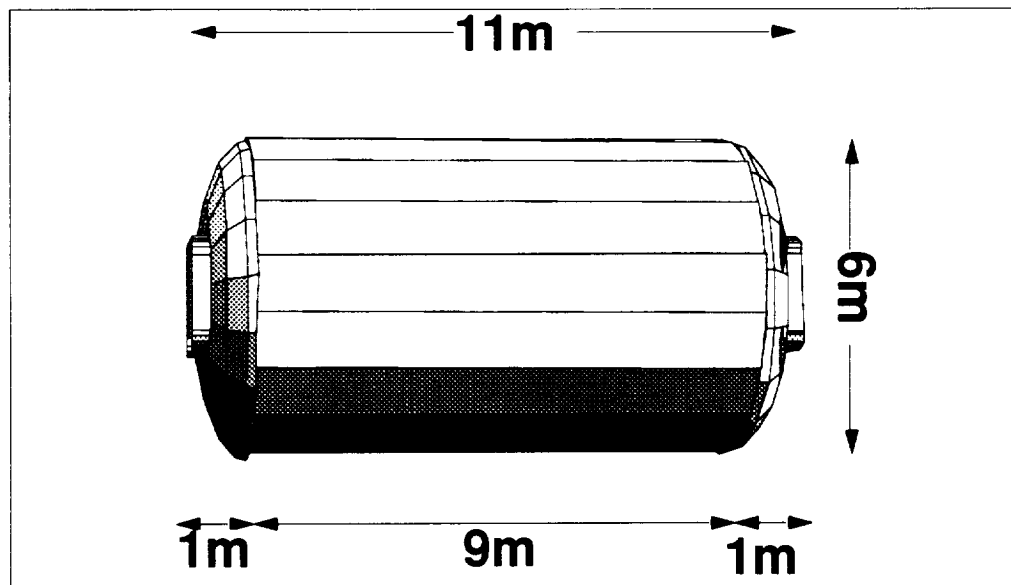
#### 2.2.5.5 BioCan Lunar Habitat

##### **Load Criteria**

The structure for the BioCan lunar habitat is expected to endure a 35000 Pa internal atmospheric pressure. It is also expected to endure the axial loads and lateral accelerations of launch on its walls and internal structures. It is not expected to experience the bending stresses present after deployment to the horizontal position, since most of these forces are taken by the PLM Primary Hull. The need for a certain degree of thermal protection was also evident, in order to protect the habitat from the extremes of the lunar environment.



## Configuration



## BioCan Lunar Habitat

- 35,000 Pa cylindrical pressure vessel
- Aluminum
- 3:1 elliptical endcaps
- dual airlocks
- vacuum cavity insulated

**Figure 2-91**  
**BioCan Configuration**

A configuration having at least two exit hatches is necessary in case of fire or other emergency. The cylindrical payload area of the launch vehicle puts constraints on the shape and size of the structure. A cylindrical configuration was chosen for the habitat section of the PLM stage (Figure 2-91). The cylindrical body has a radius of 2.9 m and attaches to the inside of the frames of the Primary Hull. The BioCan itself is primarily an aluminum pressure vessel with wall thickness of 2mm. The elliptical endcaps have a 3:1 ratio, and extend another meter past the nine meter cylindrical body on each side. From the end of each endcap, the total length of the BioCan is 11 meters. A rectangular airlock exists on each side, situated in the endcaps. Table 2-16 at the end of this section shows the geometry and mass estimate for the BioCan pressure vessel.

## Structural Analysis

The primary failure modes examined for the BioCan include pressure-induced stress, axial stress, and resonance at the natural frequency.

The peak pressure induced stress was analyzed for the elliptical endcaps using meridional stress equations. The skin thickness required at this critical point was made uniform throughout the rest of the cylinder.

The primary axial stress occurs during launch. The BioCan is loaded by its own weight and its internal structures under accelerations up to 3.5 g. The resulting axial stress in the sides are compared with the theoretical cylinder buckling stress and the material's yield stress to test for buckling and crushing failure.

Finally, a simple analysis of the cylinder is made to insure that the natural frequency is high enough to prevent resonance in the acoustics of the launch environment. A simple beam model is used, and the minimum requirements are 25 Hz axial frequency and 10 Hz lateral frequency.

## Summary Specifications

**Table 2-16: BioCan Geometry and Mass Estimate**

<b>GEOMETRY</b>		<b>MASS ESTIMATE</b>	
Cylinder Diameter	5.8 m	Material	Aluminum
Cylinder Radius	2.9 m	Mass of Internal Structures	6669 kg
Cylinder Length	9 m	Basic Structure Mass	1245 kg
End Cap Ellipse Ratio	3:1	Airlock & Hatch Allowance	800 kg
End Cap semi-minor axis	1 m	Joints & Fittings	35%
		<b>Total BioCan Structural Mass</b>	<b>2760 kg</b>
Total BioCan length	11 m	Total BioCan Mass (full)	9429 kg
Skin Thickness	0.002 m		

## 2.2.5.6 Regolith Support Structure

### 2.2.5.6.1 Side Ramps

#### **Load Criteria**

The Regolith Support Structure is the base framework for the lunar regolith, or dirt, which covers the BioCan lunar habitat and protects it from radiation. The density of lunar regolith is approximately 1200 kg/m<sup>3</sup>, and a 50 cm layer is to be deposited. However, the structure is designed to handle 80 cm of coverage as a safety factor. In addition, the load of any machinery that must climb onto the shield during the construction process must be taken into account. A conveyor belt machine has been chosen as the primary construction vehicle, and its load on the shield is assumed not to exceed 800 kg/m<sup>2</sup> in the following calculations. The structure is also loaded by its own weight, which for this case turns out to be minimal compared to the other loads.

#### **Configuration**

The latitude of the landing site dictates the path of the sun as seen by the lunar habitat during the 28-day stay. The BioCan will be positioned with the ends of the cylinder pointing perpendicular to the morning sun. At an equatorial landing site, the sun would pass directly overhead, and the radiation shield would only need to cover the sides of the BioCan cylinder. However, at higher latitudes, the Sun's arc is inclined, and some protection must be afforded the end of the BioCan facing the Sun at high noon.

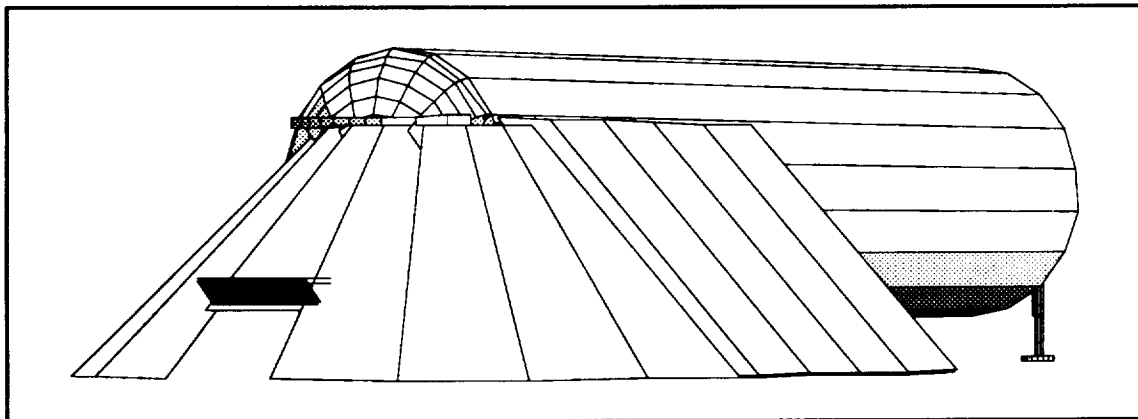


**Figure 2-92**  
**Regolith Support Structure Configuration**

A configuration was chosen which consists of side ramps which lean against the side of the habitat, and a conical-shaped canopy which covers the end of the BioCan (Figure 2-92). This

arrangement provides excellent coverage for most latitudes. A landing site at the pole, however, would see a sun which travels all the 360° around the habitat, making total coverage necessary. For this case, additional shielding would need to be designed which is not included in this report.

Easy setup and compact packaging were also desirable, so a configuration was chosen which consists of many smaller sections which are disassembled and stacked in the cargo bay during the journey. Assembly and installation will take place upon arrival of the crew. Each panel section is assembled as shown in Figure 2-93. There are 5 sections in each of the two side ramps, and 9 sections in the canopy. Each of these sections consists of three plates stacked end to end vertically. A hollow cylindrical beam fits through a slot on each vertical side of the plates, such that two of these beams connect all three plates together. Crossbars are built into the plates and help support the skin laterally. A locking mechanism is present on the side of each plate. This lock is engaged after the beam is inserted into the plate slot to insure that it does not slip in the slot.

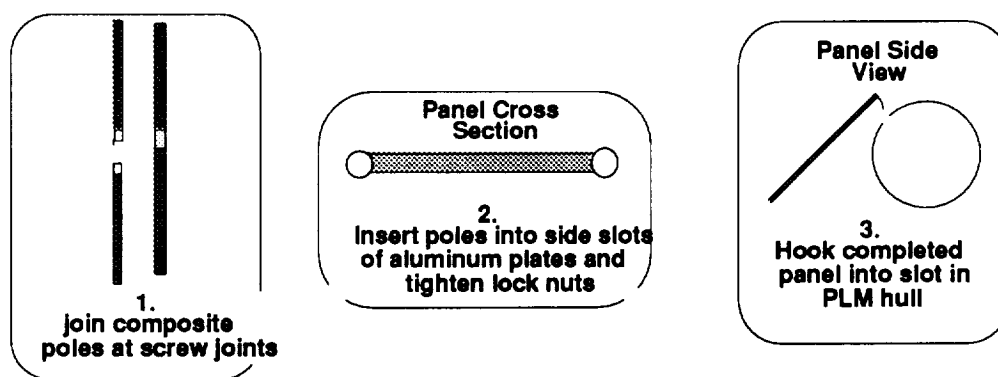


**Figure 2-93**  
**Regolith Support Panel Assembly**

Each panel section of the Regolith Support Structure is basically a skin suspended on a beam frame. At design time, specifications were not available on the material properties of cloth mesh materials, such as those of graphite or nylon fibers. Aluminum was chosen as the skin material in this design. However, a design utilizing a mesh skin would probably result in weight savings over the aluminum skin implementation. The poles are constructed of graphite/epoxy composite [0] HTS.

## Structural Analysis

The primary methods used for analysis of the Regolith Support Structure are bending beam stress equations and finite element computation.

The loading of the support beams is a summation of the regolith, construction machinery, and self-loading of the panel section under its own weight. The load is distributed between the two support beams on each panel. A support beam is modeled as horizontal beam pinned on both ends and subjected to a uniform vertical load. The diameter and thickness of the cylindrical support beam is iterated to produce a structure which yields at the expected load scaled by a 1.4 safety factor.

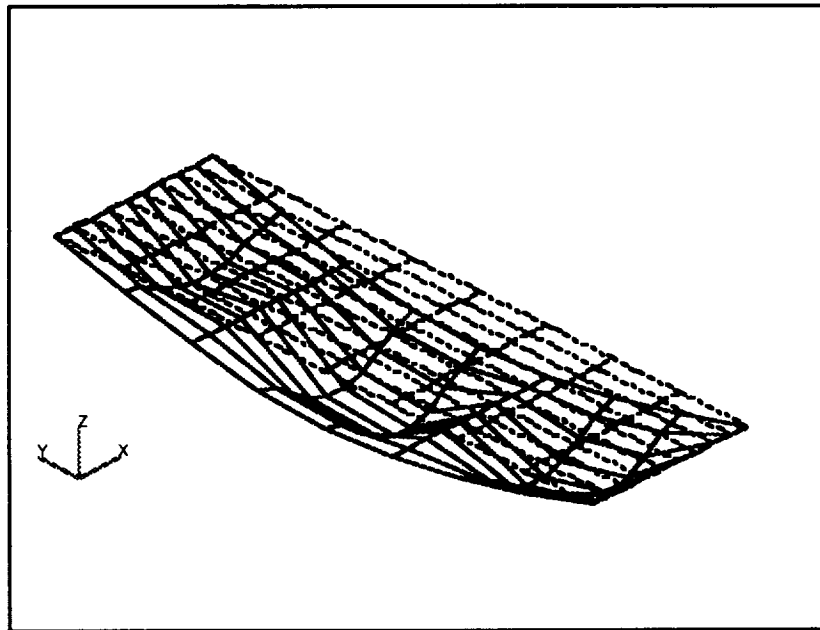


**Figure 2-94**

### **Finite Element Model—Undeformed and Deformed Views**

The aluminum skin is analyzed using finite element methods. The model consists of a beam frame with two support beams and 4 crossbars (Figure 2-94). The crossbars are of the same cross-section as the support bars. An aluminum skin is attached to this framework, and the entire panel is subjected to a uniform pressure load. The four corners are under pinned conditions. The results of the computation insure that the skin will not yield under the prescribed load. Iteration produces an efficient skin thickness for the design.

## Summary Specifications

**Table 2-17: Regolith Support Structure Geometry and Mass Estimates**

<b>MASS ESTIMATE</b>		<b>GEOMETRY</b>	
Single Support Beam mass	19.9 kg	ramp angle	45°
Crossmember mass	4.7 kg	height of ramp	4.9 m
beam mass per panel	58.5 kg	length of ramp	6.90 m
Beam subtotal	1111.7 kg	number of sections per side	5.00
		number of sections in canopy	9.00
Skin mass per panel	88.7 kg	total number of sections	19.00
skin subtotal	1684 kg		
		number of beams per section	2
		number of crossmembers per section	4
		panel length	2.30 m
regolith support subtotal	2796.2 kg	panel width	2.00 m
Joints & Fittings	10%	panel thickness	0.0035 m
		beam type	cylindrical
regolith support structure mass	3075.8 kg	beam outer radius	0.030 m
mass per panel	161.9 kg	beam inner radius	0.020 m

### 2.2.5.6.2 Canopy

The canopy section of the Regolith Support Structure is very similar in construction to the side ramps. All sections are designed with the same cross-section for beams and thickness for skin, but the dimensions are slightly different to account for the curving attachment surface on the elliptical end cap. The method of attachment is the same for the canopy panels as the side panels—an attachment bar runs along the face of the endcap, and the hooked ends of the panels slide in from the top. The middle section of the canopy has open space for an accessway. Above this accessway is a small lip which keeps the regolith above from sliding down over the opening.

### 2.2.5.7 PLM Stage Specifications Summary

Table 2-18 summarizes the information provided in this section on the PLM structure.

**Table 2-18: PLM Specifications Summary**

<b>GEOMETRY</b>		
Ground Clearance	2.00	m
Propulsion Section Height	5.53	m
Cargo Bay Height	2.50	m
Biocan Height	11.00	m
<b>Total PLM Height w/out legs</b>	<b>19.03</b>	<b>m</b>
<b>Total PLM Height w/legs</b>	<b>21.03</b>	<b>m</b>

<b>MASS ESTIMATES</b>		
Primary Hull	2549	kg
Landing Gear Mass	497	kg
Support Leg Mass	292	kg
Propulsion Section Mass (dry weight)	1921	kg
Biocan Mass (unfurnished)	2729	kg
<b>Total PLM Structural Mass</b>	<b>7987</b>	<b>kg</b>

## **3 Propulsion Systems Design**

### **3.1 Introduction**

This chapter describes the procedure followed in the design of all Project Columbiad propulsion systems, excluding those used on the launch vehicles for initial placement of the payload into LEO. Three different systems are described herein, classified according to their particular function within the mission. *Primary propulsion systems* will provide the necessary thrust for major impulsive trajectory changes. *Secondary propulsion systems* or *reaction control systems* (RCS) will generate stabilizing torques for attitude control, orbit maintenance and minor trajectory corrections. Finally, *abort systems* will provide a rapid and safe means of escape for the human crew in the event of a mission abort. The opening section of this chapter is a brief discussion of the main priorities and driving requirements which govern the design. This is followed by a summary of the trade studies performed and the results obtained. Component selection and/or sizing is then addressed, with a separate section devoted to launch escape system selection. All parameters mentioned in this chapter which are used to quantify propulsion system performance, as well as the symbols used throughout this chapter, are listed, defined and discussed in detail in Appendix I.

### **3.2 System Drivers and Requirements**

The main priorities in the design of project Columbiad propulsion systems are, in order of importance: overall safety, a low cost, and the highest possible system performance. The safety of all personnel involved with the mission is enhanced by utilizing well-developed technology, and by the selection of propellants which harbor the least possible health hazards during storage and operation. The cost factor is linked to the mass and materials of the system components, the amount and type of propellant used for each propulsion stage, and the level of technological development of the propulsion system. System performance is a generally a function of the chemical composition of the propellants and the geometry of the rocket combustion chamber and nozzle. This section will identify the main trade studies which arise from these considerations.

#### **3.2.1 Safety Considerations**

Conventional propulsion systems rely on the controlled combustion of harmful and explosive chemicals in close proximity to the crew. Thus, issues of safety by far outweigh considerations of system performance. While no piloted space mission is entirely safe, the risk of fatal accidents may be greatly reduced by enhancing propulsion system safety. This



may be accomplished with an adequate selection of propellants and mature propulsion technology.

Propellant selection plays an important role in the safety of the propulsion system. Thorough chemical analysis of the combustion process should ensure that there is a minimum amount of harmful substances in the exhaust gases. In addition, the manufacture and storage of the propellants must not pose any health hazards to responsible personnel. It is for these reasons that several advanced high-energy propellants were not considered for use in Project Columbiad. For example, a beryllium hydride grain in place of the more common aluminum perchlorate can raise the specific impulse for solid boosters from the usual 200-300 s range up to 340-380 s, but the high toxicity of beryllium makes this fuel option unacceptable. Similarly, liquid fluorine offers higher values of performance and specific gravity for liquid thrusters than liquid oxygen, but is plagued with extreme toxicity, corrosiveness, and reactivity; it will spontaneously react with many common materials and metals.

Safety considerations are closely linked to system reliability, since a propulsion system failure can have catastrophic consequences. Valve leakage can lead to fume inhalation, combustion instabilities may result in an unwanted explosion, and a failed burn or mechanical failure could leave the crew stranded on the moon or set the command module on a never-returning trajectory. For this reason, Project Columbiad will utilize well-developed propulsion technology rather than push the limits of the "state of the art". This decision precludes the use of more advanced but experimental nuclear or electric propulsion devices in favor of conventional chemical rocket engines. In addition, three basic measures will be taken to increase propulsion system reliability: *simplification* of the system in order to reduce the number of components that contribute to failure probability, *fault avoidance* by selecting components with low failure rates, and *fault tolerance* by introducing additional redundancy into the system. Thus, a simpler system with multiple levels of redundancy in its key components provides for greater reliability and ease of repair. Finally, an additional increase in reliability is provided by the selection of propellants which are stable enough to reduce the possibility of unwanted spontaneous combustion, and which suffer negligible deterioration of their fuel properties with long term storage.

Past experience has shown most spacecraft propulsion systems to be remarkably reliable. A study conducted by Hecht and Hecht in 1985 shows that an average of four subsystem failures occur during the first year of operation of a spacecraft, and that the failure rate decreases markedly with increasing mission time. Furthermore, the study shows that

propulsion system failures account for only 3.7% of the causes of spacecraft failures which occurred between 1962 and 1983.

### **3.2.2 Cost Considerations**

The cost of Project Columbiad will be strongly affected by the mass of the spacecraft which is launched into space; a heavier spacecraft will require greater launch vehicle capability which in turn will imply a more expensive mission. The propellant mass ( $M_p$ ) which a spacecraft must carry is usually several times greater than the dry mass of the spacecraft itself, so it is desirable for a spacecraft to be able to transport the maximum amount of useful payload mass ( $M_{pl}$ ) using the least amount of fuel and structural mass ( $M_s$ ) possible. Since  $M_{pl}$  and total allowable initial mass ( $M_0$ ) are usually prescribed quantities, an optimum propulsion system design maximizes the ratio  $M_{pl}/M_0$  or minimizes the ratio  $M_s/M_0$ . Thus, the overall cost of the mission is influenced by the performance of the propulsion systems used.

The total cost of a propulsion system itself is influenced by several factors. The most critical ones are the availability and manufacturing ease of the structural materials, the availability and required maintenance of the propellants, the level of development of the propulsion technology, and the amount of power required for effective operation. The mass of the propulsion system is also an important factor which drives its cost, and is in turn dependent on the mass of the spacecraft which it is expected to transport. The financial expense incurred in the development of appropriate propulsion systems is further reduced by using commercially available hardware, which may be slightly modified to meet mission requirements. For this purpose, Project Columbiad will employ existing engines and components wherever possible. Component selection and sizing is discussed in section 3.4.

### **3.2.3 Performance Considerations**

The performance of a spacecraft propulsion system is a broad term which hinges upon several physical factors, and is generally assessed with a quantity known as *specific impulse*, which is measured in seconds and is denoted by the symbol  $I_{sp}$ . Typical specific impulse ranges are between 200-300 s for solid propellant rockets and 300-480 s for liquid propellant rockets. The specific impulse of an engine is a function of engine exhaust velocity, which is in turn proportional to the square root of the ratio of the combustion temperature to the mean molecular mass of the combustion products. Thus, increasing the combustion temperature, or decreasing the average molecular mass of the exhaust gases is one way of increasing the specific impulse of a propulsion system. The maximum

allowable temperature is limited by the choice of structural material, so a usual approach is to use hydrogen-rich propellants which have a low molecular mass.

The specific impulse for a given spacecraft velocity increment  $\Delta v$  is related directly to propellant mass through the *rocket equation* (see appendix I). Since the total weight of a rocket is strongly dependent upon the amount of propellant it must carry, and the propellant exhaust velocity determines the level of thrust an engine can produce, an increase in the propellant exhaust velocity, and hence specific impulse, decreases the amount of propellant mass required to achieve a given  $\Delta v$ . Hence, rocket engine design is always pushed towards the achievement of the highest possible specific impulse. In attempting to maximize this parameter, however, it is useful to remember that rocket engines with higher specific impulses tend to be heavier and more complex.

Several parameters other than  $I_{sp}$  are used to quantify rocket performance. The most important ones are thrust-to-weight ratio  $T/W$ , and specific power, i.e. the kinetic energy per unit exhaust flow. Table 3-1 lists approximate ranges for these performance parameters for chemical rockets. Other performance parameters, such as characteristic velocity and thrust coefficient, are defined in Appendix I.

**Table 3-1: Ranges of Typical Performance Parameters for Different Rocket Engines**

Engine Type	$I_{sp}$ [s]	$T/W$	Specific Power [kW/kg]
Solid	200-300	0.01 to 10	0.1 to 100
Liquid Monopropellant	180-240	0.01 to 0.1	0.02 to 200
Liquid Bipropellant	300-480	10 to 100	100 to 1000

#### **3.2.4 Other Considerations**

There are several other factors which must be taken into consideration when designing spacecraft propulsion systems. The most prominent of these are power requirements and mass and volumetric constraints. Electric power is needed for valve actuation and ignition, and for operation of the turbopumps in smaller liquid systems. Higher power requirements generally imply heavier power plants, increasing overall weight and cost. The payload capability of the chosen launch vehicle limits the mass and volume of the command and service modules, and therefore the mass of the propulsion systems, the maximum exit diameter of the thrusters, and the volume of the propellant to be carried on board. Thus, in

order to accommodate a large mass of propellant in a given vehicle tank space, a dense propellant is required. It permits a small tankage which leads to relatively low structural weight and low aerodynamic drag. Other selection criteria that may be involved in the design trades include restrictions on operational use, control capabilities, response time, maneuvering accuracy and subsystem interface considerations.

### **3.2.5 Mission Requirements**

As mentioned in section 3.1, Project Columbiad propulsion systems will perform a variety of tasks throughout the mission. These functions are summarized in Table 3-2, along with the corresponding velocity increments and thrust levels required for the given payload masses. In view of the considerations mentioned in the previous chapter, the mission requirements imposed upon Project Coulmbiad propulsion systems are as follows:

- (1) The highest possible specific impulse to maximize engine efficiency and reduce overall system weight. At the very minimum, primary propulsion engines will be required to deliver a specific impulse of at least 435 seconds.
- (2) Thrust levels high enough to minimize gravity losses but low enough to limit acceleration loading to 3 g's for the piloted mission or 5 g's for the precursor mission.
- (3) Multiple levels of redundancy to enhance reliability. Overall system reliability must be in excess of 0.99.
- (4) For the primary propulsion system, a multiple restart capability and the ability to control thrust level and thrust vectoring.

**Table 3-2: Spacecraft Propulsion Functions for Project Columbiad**

Propulsive Function	Velocity Increment ( $\Delta v$ ) [m/s]	Thrust Level [kN]
Orbit circularization	177	300 - 400
Trans-lunar injection	3140	450 - 500
Break Into Lunar Orbit	1060	250 - 300
Lunar de-orbit	1700	250 - 300
Hover and Land on Lunar Surface	500	Variable from 300 to 10 kN
Precursor Mission Payload Deployment	0	Variable from 30 to 1 kN
Launch From Lunar Surface	2100	250 - 300
Trans-Earth Injection	1060	250 - 300
Attitude control		
(Low total impulse, several short pulses. Thrust ranges from 20 Ns impulse bits to 1 kN, depending on pulse duration.)		
Midcourse corrections	120	1 K to 10 K pulses
Control during $\Delta v$ thrusting	150	10 K to 100 K pulses
Attitude control during reentry	150	10 K to 100 K pulses

### **3.3 Design Approach**

It is necessary to trade propulsion system attributes against mission requirements in order to select the best design approach for a particular mission. This section will discuss the results of several studies which were performed to determine, for both primary and secondary propulsion systems, (1) the optimum combination of propellants, (2) the most efficient engine cycle, and (3) the strongest and lightest structural materials for propulsion system components.

#### **3.3.1 Propellant selection**

The required levels of thrust and performance for both primary and secondary propulsion systems play a decisive role in the selection of appropriate propellants. Liquid propellants offer higher performance than solid grains, but this advantage is obtained at the expense of system reliability due to the added complexities of plumbing, management devices and turbomachinery required for the liquid systems. However, the only engines presently capable of meeting the required specific impulse of 435 seconds for the primary propulsion system are those which run on cryogenic propellants. Thus, the physical properties of several cryogenic propellant combinations must be compared in search of an optimum

combination of desirable attributes, most importantly low molecular weight, freezing point, and vapor pressure, and high specific gravity, specific heat, and chemical stability.

Cryogenic propellants are not necessary for an effective reaction control system where low thrust levels and short burn times allow the designer to dispense of higher performance in favor of a lighter and less complex system. Smaller, pressure-fed thrusters which operate on earth-storable propellants may be used, either in monopropellant or bipropellant configurations, to provide an acceptable level of thrust and performance. Properties of selected propellants for Project Columbiad are listed in Table 3-4.

Diatomic hydrogen ( $H_2$ ) provides the smallest molecular weight possible of any propellant, with the exception of dissociated H, and is the choice fuel to be used in Project Columbiad primary propulsion systems. The challenge is then to develop a propulsion method that heats the propellant to the high temperatures necessary to achieve large values of  $I_{sp}$ . The results of a theoretical analysis of several pure gases in monopropellant configurations, assuming a 3500 K combustion temperature and no dissociation of the fluid, are shown in Table 3-3, demonstrating how various other propellants provide significantly degraded performance in comparison to hydrogen.

**Table 3-3: Comparative Performance of Several Spacecraft Propellants**

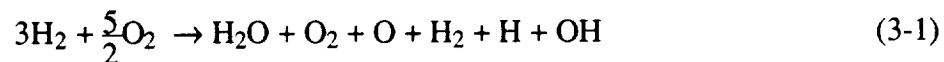
Propellant	Molecular Mass [kg/mol]	$C_p$ [J/Kg/K]	Ideal $I_{sp}$ [s]
$H_2$	0.002	14209	1018
He	0.004	5139	615
$CH_4$	0.016	2254	405
$CO_2$	0.044	842	248

For the secondary propulsion systems, the propellant options are cold pressurized gas and storable liquids. Liquid systems provide higher thrust, performance and control than their cold gas counterparts, and are therefore the selection for Project Columbiad. The most extensively used liquid propellant for attitude control thrusters is hydrazine ( $N_2H_4$ ), a colorless liquid with properties similar to those of water, which provides thrust either through catalytic decomposition as a monopropellant, or through combustion with nitrogen tetroxide ( $N_2O_4$ ) in a hypergolic bipropellant configuration. Both options are discussed in the following section.

The *mixture ratio*, O/F, of the propellants is defined as the ratio of the oxidizer mass to the fuel mass injected into the combustion chamber, and is usually selected to enhance the performance of the propulsion system. Engine start-up mixture ratios near stoichiometric proportions have a high heat release per unit of propellant and therefore permit bringing the chamber and the gases up to equilibrium faster than what would be possible with other mixtures. The operating mixture ratio is usually fuel rich and is selected for optimum specific impulse.

### 3.3.1.1 Thermochemical Assessment

The combination of liquid hydrogen and liquid oxygen is a standard bipropellant configuration in widespread use today. Water is the main product in the combustion of hydrogen with oxygen, accounting for over 60% of all exhaust products. Subsequent dissociation reactions produce diatomic hydrogen, diatomic oxygen, hydroxyl, monatomic oxygen, and monatomic hydrogen making a total of six combustion products. In this case all the reactants and products are gaseous. Theoretically, there could be two additional products: ozone (O<sub>3</sub>) and hydrogen peroxide (H<sub>2</sub>O<sub>2</sub>); however, these are unstable materials that do not readily exist in high temperature, and which may therefore be ignored. In chemical notation the oxygen/hydrogen combustion reaction may be stated by equation 3-1.



There are several advantages to using the oxygen/hydrogen combination. Propulsion technology which utilizes these propellants is very efficient and highly developed. The combustion reaction results in high combustion temperatures, typically above 3000 K depending on the O/F ratio. With an O/F ratio around 5:1, the expanding effluent is capable of providing specific impulses as high as 460 s. Engine T/W ratios are generally high, in the range of 50. None of the exhaust products are toxic.

As mentioned before, hydrazine may be used in rocket engines in two different configurations. As a monopropellant, hydrazine decomposes into ammonia, nitrogen and hydrogen in various phases of catalytic decomposition. The decomposition process may be approximated by the reaction shown in equation 3-2



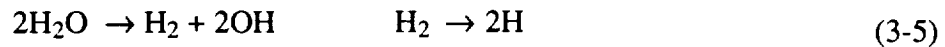
and the dissociation reaction in equation 3-3.



In a bipropellant configuration with nitrogen tetroxide ( $\text{N}_2\text{O}_4$ ) as an oxidizer, the combustion reaction proceeds as in equation 3-4



with the dissociation reactions as in equation 3-5.



Thermodynamic analysis of the two combustion reactions, assuming a combustion pressure of 30 atm and an initial propellant temperature of 293 K, yields an adiabatic flame temperature of 2064 K and an upper-limit  $I_{sp}$  of 296 s for the monopropellant decomposition, while the bipropellant reaction is found to proceed at an adiabatic flame temperature of 4127 K and an ideal  $I_{sp}$  of 431 s. Actual hydrazine monopropellant thrusters deliver specific impulses around 240 s, while bipropellants demonstrate a maximum of about 340 s. Performance may be improved by substituting monomethylhydrazine ( $\text{CH}_3\text{NHNH}_2$ ) for hydrazine in the bipropellant configuration.

The system simplicity which results from using hydrazine as a monopropellant is thus countered by a pitifully low performance. The electrical post-heating of the reaction gases from hydrazine catalysis results in an increase of specific impulse to only about 290-300 s at most. Another problem of using hydrazine as a monopropellant lies in the design of the catalyst bed necessary to accomplish monopropellant decomposition. Virtually all hydrazine monopropellant rockets use finely dispersed iridium deposited on porous ceramic (aluminum oxide) substrate pellets 1.5 to 3 mm in diameter as a catalyst. Design and development of the catalyst bed are the most complex and least understood aspects of hydrazine rockets. Mechanical, thermal, and chemical problems arise in designing a catalyst bed for igniting hydrazine, the more important of which are catalytic attrition and catalyst poisoning. Catalytic attrition stems from motion and abrasion of the pellets with loss of very fine particles. Crushing of pellets can occur because of thermal expansion and momentary overpressure spikes. Catalyst activity can also decline because of poisoning by trace quantities of contaminants present in the hydrazine. Catalyst degradation, regardless of cause, produces ignition delays and overpressures which result in undesirable performance.



The bipropellant combination of hydrazine or monomethylhydrazine fuel and nitrogen tetroxide oxidizer is therefore the choice of propellants for Project Columbiad secondary propulsion systems. This selection will imply greater system complexity and the danger of spontaneous hypergolic combustion. However, the technology is available to minimize or eliminate these problems, and the enhanced performance is well worth the technical difficulties incurred in the system's realization. At the slight expense of specific impulse the added convenience of equally sized oxidizer and fuel tanks may be achieved by selecting an O/F ratio of 1.64 .

**Table 3-4: Some Physical Properties of Selected Propellants**

Propellant	Liquid Oxygen	Liquid Hydrogen	Nitrogen Tetroxide	Monomethyl Hydrazine
Chemical formula	O <sub>2</sub>	H <sub>2</sub>	N <sub>2</sub> O <sub>4</sub>	CH <sub>3</sub> NHNH <sub>2</sub>
Molecular mass [kg/kmol]	32.00	2.016	92.016	46.08
Density [kg/m <sup>3</sup> ]	1140 (90.4 K)	71 (20.4 K)	1447 (293 K)	87.88 (293 K)
Freezing point [K]	54.4	14.0	261.5	220.7
Boiling point [K]	90.0	20.4	294.3	360.6
Heat of vaporization [kJ/kg]	213	446	413 <sup>a</sup>	790 <sup>a</sup>
Specific heat [cal/kg•K]	0.4 (65.15 K)	1.75 (20.4 K)	0.367 (290 K)	0.688 (293 K)
Viscosity [centipoise]	0.19 (90.4 K)	0.013 (20.4 K)	0.423 (293 K)	0.855 (293 K)
Vapor pressure [MPa]	0.0052 (88.7 K)	0.0083 (13.7 K)	0.0958 (293 K)	0.0069 (300 K)

<sup>a</sup> At boiling point

### **3.3.2 Engine Cycle Selection**

In a liquid bipropellant system, fuel and oxidizer are fed upon demand to the combustion chamber by way of gas pressurization or a turbopump (see section 3.4.4). A pressure-fed scheme is the optimal selection for low thrust levels and short burn times such as those required for the secondary propulsion system. For the greater thrust levels and burn times of primary propulsion, turbopump-fed engines provide better performance and less overall system weight.

There are two classes of turbopump-fed rocket engine cycles, *open cycles* and *closed cycles*. In an open cycle, the working fluid exhausting from the turbine is discharged overboard, after having been expanded in a nozzle of its own, or discharged into the engine nozzle at a point in the expanding section downstream of the main thrust chamber nozzle. In a closed or topping cycle, all working fluid from the turbine is injected into the engine combustion chamber to make the most efficient use of its remaining energy. Closed cycles deliver higher performance than open cycles, due to the characteristically larger pump discharge pressures, and because turbine exhaust gases are expanded through the full pressure ratio of the main thrust chamber, as opposed to the open cycle, where the exhaust gases only expand through a relatively small pressure ratio.

The closed cycle was selected on the basis of its slightly superior performance, which in turn augments the engine specific impulse by several seconds. This decision narrowed the choice of engine cycles down to two alternatives: the *expander cycle* and the *staged combustion cycle*. Both cycles are schematically illustrated in Figure 3-1. In the expander cycle, most of the engine coolant (usually hydrogen fuel) is fed to low pressure-ratio turbines after having passed through the cooling jacket where it has picked up energy. Part of the coolant, perhaps 5 to 15%, bypasses the turbine and rejoins the turbine exhaust flow before the entire coolant flow is injected in the chamber where it mixes with the oxidizer. In the staged combustion cycle, the coolant flow path through the cooling jacket is the same as that of the expander cycle. However, a high pressure precombustor (gas generator) burns all the fuel with part of the oxidizer to provide high energy gas to the turbines. The total turbine exhaust gas flow is injected into the main combustion chamber where it burns with the remaining oxidizer.

Close examination of the traits of both options led to the selection of the expander cycle over the staged combustion cycle. The primary advantages of the expander cycle are good specific impulse, engine simplicity, and relatively low weight. In the expander cycle all the propellants are fully burned and expanded efficiently in the engine exhaust nozzle. For high chamber pressure, however, the energy required for driving the turbine is larger than can be supplied by the vaporized fuel; this cycle is not practical above chamber pressures greater than 7.58 MPa. The precombustor of the staged combustion cycle allows higher chamber pressure operation and therefore a smaller thrust chamber size. However, the extra pressure drop in the precombustor and turbines causes the pump discharge pressures of both fuel and oxidizer to be much higher than in the expander cycle, requiring heavier and more complex pumps, turbines, and piping. This cycle is capable of providing the

highest specific impulse for a given propellant combination, but it was decided that the advantage of simplicity offered by the expander cycle by far outweighed the higher performance of staged combustion.

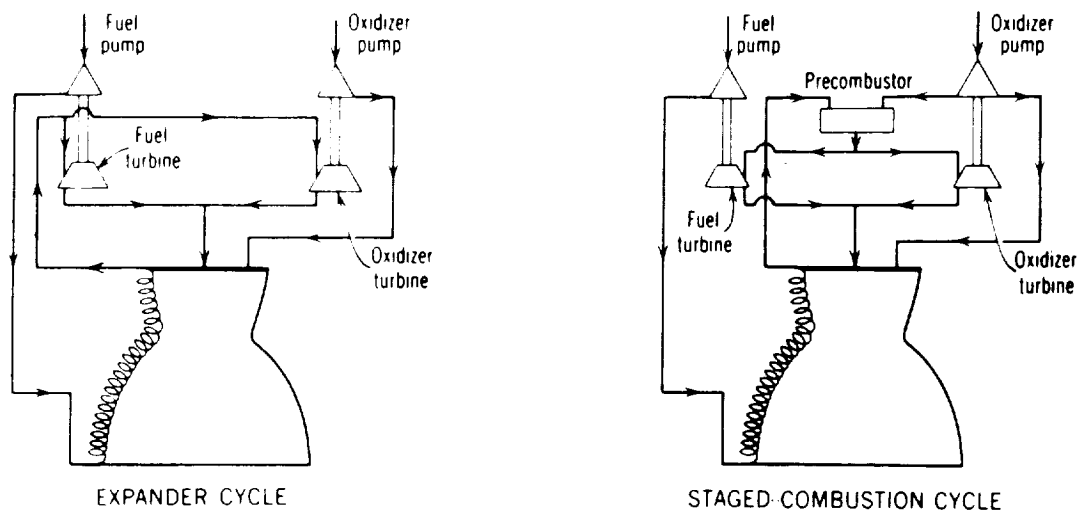


**Figure 3-1**  
**Turbopump Feed System Cycles for Liquid Propellant Rocket Engines**  
 (From Sutton, *Rocket Propulsion Elements*, 1989)

### 3.3.3 Selection of Structural Materials

Propulsion system components are subjected to extremes of temperature and pressure, in addition to several other loads during the powered thrust phases of the mission. Detailed stress analysis of each individual unit is necessary to determine necessary wall strengths and, consequently, the lightest materials which will withstand the loads to which the system will be exposed. Of major concern are the liquid propellant thrust chambers, which are subjected to radial and axial pressure loads, the reaction forces of the mounting device, acceleration loads, vibration loads, and thermal expansion stresses. These loads are different for almost every design, but may be assessed by using a few simple approximations. The radial stress  $\sigma_R$  can be estimated by using the simple hoop stress approximations, provided that the thickness of the chamber walls is much smaller than the chamber radius. See equation 3-6.

$$\sigma_R = \frac{p r}{2 t} \quad (\text{spherical chamber}) \quad \sigma_R = \frac{p r}{t} \quad (\text{cylindrical chamber}) \quad (3-6)$$

Here,  $p$  is the combustion chamber pressure, usually between 30 and 50 atm, and  $t$  is the thickness of the chamber walls, usually on the order of a few millimeters with an added factor of safety.

Combustion temperature is a major performance parameter which is limited by the choice of materials of the combustion chamber. A temperature differential introduces a compressive stress on the inside and a tensile stress on the outside of an inner wall. The thermal stress  $\sigma_T$  can be calculated for cylindrical chamber walls that are thin in relation to their radius with equation 3-7.

$$\sigma_T = \frac{2 \lambda E \Delta T}{1 - \nu} \quad (3-7)$$

$\lambda$  is the coefficient of thermal expansion of the wall material,  $E$  is the modulus of elasticity of the wall material,  $\Delta T$  is the temperature drop across the wall, and  $\nu$  is the Poisson ratio of the wall material. Temperature stresses in rocket engines frequently exceed the yield point, and the materials experience a change in the yield strength and their modulus of elasticity with temperature. This yielding of rocket thrust chamber wall materials can be observed by the small and gradual contraction of the throat diameter after each operation, and the formation of progressive cracks of the inside wall surface of the chamber and throat after successive runs. These phenomena limit the useful life and the number of starts of a thrust chamber.

The structural design of the rocket engines is not of concern to project Columbiad, since all engines will be purchased as finished products. However, the stress relationships presented above apply to the design of the propellant tanks and piping required in the complete propulsion system. Detailed stress considerations for all components are omitted from this discussion because stresses for irregular shapes are beyond the scope of this chapter, and because other loads besides internal pressure and temperature loads should be taken into consideration. Selection of structural materials has been made on the basis of previous designs, with the intention of providing maximum strength at the lowest possible weight. A breakdown of suggested materials to be used in the construction of Project Columbiad propulsion systems is given in Table 3-5.

**Table 3-5: Properties of Selected Propulsion System Structural Materials**

Material	Aluminum 7075-T6	Steel PH15-7 MO	Graphite Composite HTS IOI
Component application	Valves	Engines Pipelines	Propellant Tanks Pressurant Tanks
Density [kg/m <sup>3</sup> ]	2800	7600	1490
Longitudinal Ultimate Tensile Strength [MPa]	523	1309	1337
Longitudinal Tensile Yield Strength [MPa]	448	1171	- - -
Young's Modulus [GPa]	71	200	151
Specific Heat [J/kg·K]	837	- - -	- - -
Thermal Expansion [10 <sup>-6</sup> / K]	28.9	11.0	-0.36
Thermal Conductivity [W/m·K]	134	15.4	- - -
Melting Temperature [K]	933	1810	340

Materials other than those listed in Table 3-5 may be used depending on particular applications. Liquid propellant feedlines, for example, have been most commonly made of stainless steels of the 18-percent-chromium, 8-percent-nickel family which are known as 18-8 corrosion-resistant steel (18-8 CRES). However, recent developments in space technology which demand longer low- and high-cycle fatigue lives, improved long-term corrosion resistance, and greater number of gimballing cycles for articulating ducts, have driven pipeline material selection towards stronger nickel-base alloys such as Inconel 600, 625 and 718.

### **3.4 Component Selection And Sizing**

A complete spacecraft propulsion system consists of the engines or thrusters, tankage to hold the propellants, propellant lines and valves, and appropriate controls to monitor and regulate the performance of the system. This section describes the selection and sizing of these individual components, as well as necessary modifications or additions that will have to be made to those components which are commercially manufactured.

#### **3.4.1 Primary Propulsion Engines**

The engines responsible for providing the thrust for the major trajectory changes of Project Columbiad must deliver very high levels of performance in order to minimize the amount of propellant and time needed to achieve the required velocity increments. Thus, the highest

possible specific impulse and T/W ratio are primary requirements in the selection of primary propulsion engines. Furthermore, the engines must be throttlable and also possess some means of thrust vector control to allow for high maneuvering accuracy, particularly during the lunar landing phase. Extensive restart capability and a maximum single burn time on the order of 900 seconds is also required, as well as a long-term storage life for extended stays on the moon.

The high levels of performance within the thrust ranges specified in section 3.2.5 severely limited the range of engine options available for Project Columbiad's primary propulsion system. A survey of commercially available cryogenic engines immediately pointed towards the Pratt & Whitney RL10A-4 as the sole candidate engine. This formidable machine (Figure 3-2) is the most recent version of Pratt & Whitney's classic RL10 model, which has been in production since 1960. The new engine, in production since 1991, was developed to provide additional payload capability to the Atlas IIA and Atlas IIAS vehicles, and represents a considerable improvement over its immediate predecessor, the RL10A-3A. The RL10A-4 can produce 92,518 N of thrust at a chamber pressure of 38.13 atm and a combustion temperature of 3360 K. With a specific impulse of 449 s, it delivers the highest performance of any cryogenic motor on the market today, with the exception of the Space Shuttle Main Engines.

The RL10A-4 engine possesses several other features which make it attractive to Project Columbiad. It is gimbal mounted, providing thrust vector control capability in a square pattern  $\pm 4^\circ$  from the engine centerline (actuators are not supplied as part of the engine). The single turbopump-fed thrust chamber is regeneratively cooled by the incoming hydrogen fuel, and the heat rejected by the thrust chamber is used to drive the propellant turbopumps (Figure 3-3). Hydrogen, after passing through a two-stage centrifugal pump and thrust chamber wall, is expanded in a turbine before being injected into the combustion chamber. The heat absorbed in the cooling jacket provides sufficient energy to drive the turbopumps at a turbine inlet temperature of less than 222K. The engine is designed to start and operate at altitudes of 12,192 m and above and has a multiple start capability. The engine is not throttlable in its present configuration, but the addition of appropriate control valves allows throttling down to 25% of its full rated thrust without requiring any changes to the injection system. The manufacturer's quoted price is approximately \$2 million per engine, with a predicted reliability of 0.99867. Tables 3-6 and 3-7 summarize some of the main features of the RL10A-4.



**Table 3-6: Mass Breakdown of the RL10A-4 Engine**

Chamber and injector	54.9 kg
Turbopump assembly	34.7 kg
Propellant lines, valves	36.5 kg
Nozzle extension and hardware	29.2 kg
Engine mount and turbopump	5.4 kg
Igniter assembly	3.3 kg
Instrumentation	4.0 kg
<b>TOTAL ENGINE DRY WEIGHT</b>	<b>167.8 kg</b>

**Table 3-7 : RL10A-4 Component Details**

Thrust Chamber length (injector face to end of exhaust skirt)	1.151m
<b>Nozzle (including nozzle extension):</b>	
Length, throat to exit	1.68 m
Throat diameter	0.126 m
Throat area	0.0125 m <sup>2</sup>
Exit diameter	1.173 m
Exit Area	1.0815 m <sup>2</sup>
Expansion Ratio	84:1
Construction material	stainless steel
<b>Combustion Chamber</b>	
Inner diameter	0.950 m
Inner surface area	0.259 m <sup>2</sup>
Chamber temperature	3360 K
Chamber pressure	38 kPa
<b>Injector</b>	
216 elements in 8 equally spaced concentric circles; each element has a LOX orifice with concentric fuel annulus.	
<b>Ignition System</b>	
Rigid, radio-shielded, high tension lead, single spark igniter and exciter assembly.	
<b>Turbopumps</b>	
Type	Centrifugal
Speed	14,300 rpm
No. of Stages	1
Temperature in	97.5 K
Pressure in	300 kPa
Pressure out	5530 kPa
<b>Oxidizer</b>	
Type	Centrifugal
Speed	35,750 rpm
No. of Stages	2
Temperature in	21.7 K
Pressure in	196.5kPa
Pressure out	9073.6 kPa
<b>Fuel</b>	
Type	Centrifugal
Speed	35,750 rpm
No. of Stages	2
Temperature in	21.7 K
Pressure in	196.5kPa
Pressure out	9073.6 kPa



### **3.4.2 Attitude Control Thrusters**

The selection of appropriate rockets for the secondary propulsion systems of Project Columbiad is based on several requirements which ensure successful attitude control. Foremost is the capability to apply the thrust levels specified in section 3.2.5 with burn times ranging from a steady state duration of several minutes down to small impulse bits (rapid thrust rise and a sharp cutoff) with high reproducibility of the thrust pulses. Second is an extensive restart capability for repeated use, and long term storage life for extended stays on the moon. As always, an optimum balance between highest possible performance and the least weight is required as well.

Small liquid monopropellant and bipropellant units are common in current auxiliary rocket systems for thrust levels typically above 2 N and total impulse values above 3000 N-s. As mentioned in section 3.3.1, a pressure-fed bipropellant system delivers superior performance while minimizing overall system weight, and is the configuration of choice for this mission. Throughout space exploration history, bipropellant attitude control thrusters have varied from 5 to 4000 N of thrust, depending on the size of the spacecraft. All use basically pressurized feed systems with multiple thrust chambers equipped with fast-acting positive-closing precision valves. Many systems use small, uncooled, metal constructed supersonic nozzles which are strategically located on the periphery of the spacecraft.

After surveying several commercially available engines, the Marquardt model R4-D bipropellant engine shown in Figure 3-4 was selected for use in Project Columbiad. It is a bipropellant engine, specifically designed to provide the propulsion for the apogee and/or orbit change maneuvers using nitrogen tetroxide oxidizer and monomethylhydrazine fuel. It also has a proven track record, beginning with its initial qualification for the Lunar Orbiter and Apollo Lunar Module and Service Module. Subsequently, the thruster has been used for the manned orbiting laboratory and Lockheed P-50 programs, and is currently in use on several commercial satellites, including INSAT, ARABSAT, AUSSAT, and IABS.

The engine's impressive qualifications are summarized in Table 3-8. A high nominal specific impulse of 312 seconds and the capability to operate from discrete operating durations of 0.010 seconds up to continuous firings in excess of one hour provide control capabilities in excess of those required for Project Columbiad. System feed pressures up to 2.76 MPa can be used, with a minimum propellant feed pressure of 1.52 MPa required at the 490 N thrust level. Calibration for the desired thrust level, based on feed pressure, is made at the engine level using trim orifices. The thruster is radiation and fuel film cooled

and can be located inside the spacecraft by providing a heat shield cone to protect the internal systems from excessive heating. High steady state performance is obtained using a multiple inlet doublet injector and a columbium/titanium material system. The highly responsive solenoid valves utilize a Teflon sealing interface and have a demonstrated capability in excess of 1,000,000 cycles. Qualification test of this thruster included a demonstration of greater than 11 hours of firing time, random vibration test levels of 17 GRMS; and complete gas ingestion/propellant depletion. The manufacturers quoted price is \$200,000 per engine.

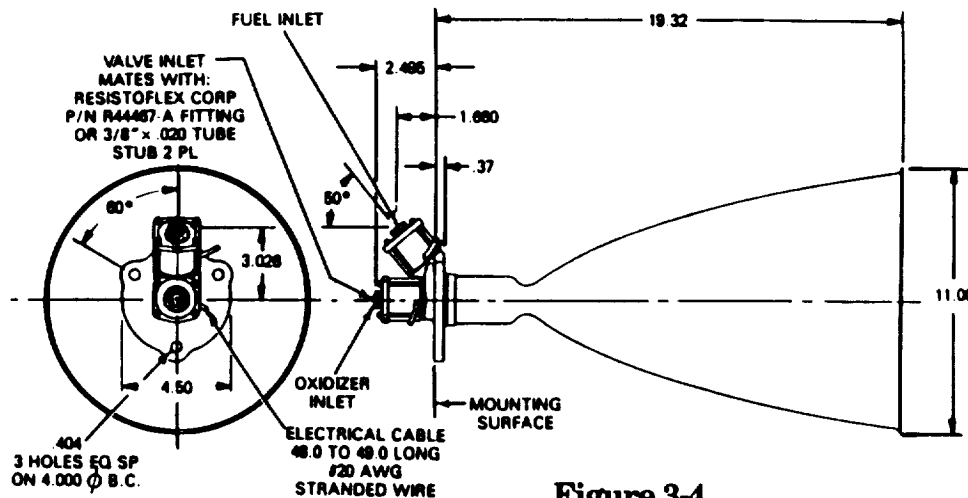


**Figure 3-4**

**NOTE: DIMENSIONS ARE INCHES**

**The R4-D Engine (Courtesy of the Kaiser Marquardt Corporation)**

**Table 3-8: R4-D Engine Qualification Test Summary**

Nominal Thrust	445 - 512 N @ 1517 kPa
Thrust Range	231 - 680 N
Minimum impulse bit	36 Ns
Specific Impulse	312 s
Maximum burn time	40,781 s
Maximum single burn	7600 s
Number of starts	20,781
Propellant temperature	-6° to 71° C
Helium gas ingestion	
Start/midrun	164 cm <sup>3</sup> @ 1517 kPa
continuous	Up to 50 % by volume
Valve Voltage	18-50 Volts
Power Consumption	1-4 amps @ 28 VDC
Vibration, random	17 GRMS
sine	20 G's (30-70 Hz)
	5 G's (70-2000 Hz)
Weight	3.75 kg

### **3.4.3 Precursor Payload Deployment Engines**

The selection of appropriate engines to be used for precursor payload deployment was driven by the requirement of overall system simplicity, compactness, and the ability to provide a controllable thrust profile to ensure the soft landing of the payload stack. In view of the relatively low thrust levels required for deployment, it was decided to dispense of the complexities of a cryogenic propulsion system in favor of the reliability offered by hypergolic storable propellants and solid rockets.

The two engines selected for precursor payload deployment are the Rocketdyne XLR-132 and the Morton Thiokol TE-M-236. The TE-M-236 is a solid rocket which has been used in the SARV satellite as a retrograde motor. It uses an internal burning case-bonded grain weighing 18.3 kg in a case of 4130 steel, with a reentrant conical rear closure to keep the total length at 324 mm. It is one of Morton Thiokol's smaller boosters, producing an average thrust of 5.6 kN over a burn time of 7.5 s. The XLR-132, whose features are summarized in table 3-9, is a compact, high pressure pump-fed engine which was developed by Rocketdyne under USAF contract as a shuttle payload engine and, potentially, for propelling a space transfer vehicle. It can produce a maximum thrust of 16.68 kN in a vacuum, and with a minimum specific impulse of 340 s it produces the highest performance known for the MMH/N<sub>2</sub>O<sub>4</sub> bipropellant combination. A cluster of TE-M-236 rockets will provide the initial impetus which will tip over the payload stack past its stability point, after which a modified throttlable version of the XLR-132 will be employed to control the angular velocity of the falling stack.

**Table 3-9: Main Features of the XLR-132 Engine**

dry mass	54 kg
Length	120 cm
Maximum diameter	60 cm
Engine cycle	Gas generator
Propellants	Nitrogen Tetroxide/Monomethyl Hydrazine
Thrust	16.68 kN vacuum
Specific Impulse	340 s vacuum
Expansion Ratio	400:1
Thrust Chamber	
Materials	columbium
cooling	radiative
Combustion Chamber	
Pressure	102 atm at injector end
Cooling	Regenerative by fuel
Ignition	Hypergolic
Burn Time	4000 s in 10 starts

### **3.4.4 Propellant Tanks**

#### **3.4.4.1 Structural Requirements**

Project Columbiad will require the long term storage of the liquid propellants at the inlet pressures required by the engines. Because the tanks must fly, their weight is at a premium and tank material is therefore highly stressed. Pressurized tank walls are considerably thick, so care must be taken to select a material which is as light and strong as possible. An extra 20 to 30 percent of the overall tank weight must be added to account for mounting hardware and propellant management devices. The design of Project Columbiad tanks makes use of a wound graphite composite shell to provide high strength at low densities and an thin inner lining constructed of a non-reactive metal. Tank sizes were calculated based upon the required propellant volumes, allowing an extra 5% for ullage. Detailed structural design and sizing of propellant tanks is discussed in Volume II, section 2.1.6.

#### **3.4.4.2 Insulation Requirements**

The propellants to be employed in the secondary propulsion system remain in the liquid state at normal temperatures, and therefore will not require special thermal protection during storage. However, this is not the case with the propellants used in the primary propulsion system, which are liquids only at cryogenic temperatures. The comparatively low technical risk of developing LOX/LH engines is at least partially offset by the difficulty of storing cryogenic propellants for extended periods of time before use. During earth storage, cryogenic propellants cool the tank wall temperatures far below ambient air temperature; with LH it is possible to liquefy or solidify the ambient air on the outside of the tank. This causes condensation of moisture on the outside of the tank and usually also formation of ice during the period prior to launch. Ice is undesirable because it increases vehicle inert weight and can cause valves to malfunction. Thus, it is necessary for cryogenic storage tanks to be thermally insulated. Another problem presented by the storage of cryogenics is the high storage pressures required to prevent "boil off"; even with heavy insulation and low thermal conductivity structural tank supports, it is not possible to prevent the continuous evaporation of the cryogenic fluid. Therefore the tank design must include vents or other pressure relief provisions to prevent self-over-pressurization. The detailed design of cryogenic storage facilities is addressed in section 6.3.

#### **3.4.4.3 Propellant Expulsion Mechanism**

The design of liquid storage systems must also provide a means of managing the liquid propellants under zero g to ensure that liquid, rather than gas or vapor, is expelled from the tank during engine operation. For this purpose, several propellant expulsion devices were

examined for possible use in Project Columbiad propellant tanks. The alternatives were *positive expulsion*, *surface tension* systems, and *artificial gravity*. Positive expulsion systems use an active element (a bladder diaphragm, piston or bellows) to separate a pressurant gas from the liquid propellants under all dynamic conditions and to force the liquid from the tank into the feed lines on demand. Liquid is forced to flow by the slightly higher differential gas pressure acting on the expulsion device. The relative merits of the available positive expansion devices are shown in Table 3-10. Surface tension systems passively manage propellants in a near zero-gravity environment by using vanes, screens or sponges to wick the propellant into the propellant tank outlets. In this manner the pressurizing gas bubble is always maintained in the center of the tank. All of these devices rely on surface tension forces to separate liquids from gases. Propellant expulsion may also be achieved by inducing artificial gravity with a spinning spacecraft or a small acceleration produced by another rocket.

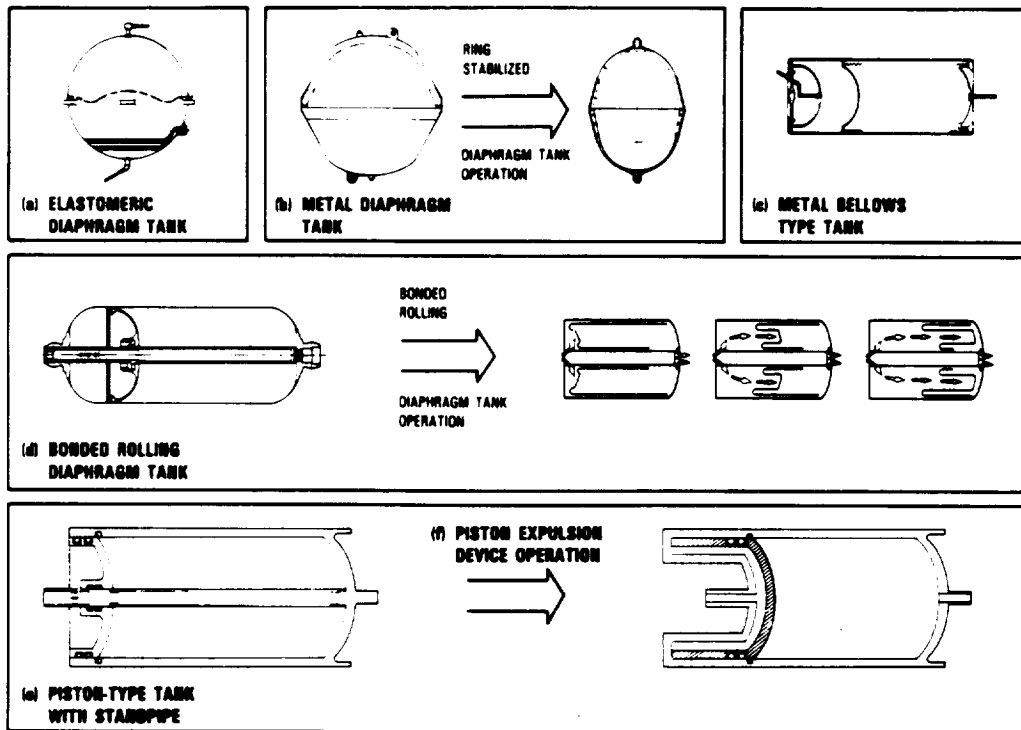


**Figure 3-5**

**Available Options For Positive Expulsion Tanks**

**(from Wertz & Larson, *Space Mission Analysis and Design*, 1991)**

**Table 3-10: Attributes of Different Positive Expulsion Tank Designs**

Expulsion Scheme	Advantages	Disadvantages
Metal Diaphragm Tank	High volume efficiency Good center of gravity control No ullage volume Proven design	High weight High cost High expulsion $\Delta p$ Optimizes only for special envelope
Rolling Diaphragm Tank	Light weight Low cost Low $\Delta p$ during expulsion	Inspection of internal welds
Piston Tank	Extensive data base Low $\Delta p$ during expulsion Design adapts easily to growth	High cost Low volumetric efficiency Critical tolerance on shell Sliding seals; possible blowby
Rubber Diaphragm Tank	Extensive data base Low $\Delta p$ during expulsion Not cycle-limited Proven design High expulsion efficiency	Compatibility limits on propellants
Metal Bellows Tank	No sliding seals Good center of gravity control Proven design Good compatibility Hermetically sealed	High weight High cost Limited cycle capability Low volumetric efficiency

$\Delta p$  = pressure differences

The high efficiency and relatively low cost of the elastomeric positive expulsion device compared to the surface tension schemes and the other positive expulsion devices makes it a prime candidate for our systems. However, it can only be used for the secondary propulsion system, since the Teflon rubber generally used in such devices cannot withstand cryogenic temperatures. For the primary propulsion systems, it will be necessary to use the artificial gravity option, employing the secondary thrusters to provide a small "kick" immediately preceding ignition of the cryogenic engines.

### **3.4.5 Pressurization Schemes**

There are two standard measures for pressurizing propellant tanks: gas pressurization, in which a high pressure gas such as nitrogen or helium displaces the propellant and forces it

into the combustion chamber, and turbomachinery, which raises the propellant from its low tank pressure to a value above the engine's chamber pressure. Gas pressurization is exceedingly simple and reliable, requiring none of the complicated mechanisms necessary to implement turbopumping. The mass ( $m$ ) of the compressed gas needed to evacuate a propellant tank can be determined from equation 3-8.

$$m = \frac{pV}{R_s T_o} \left( \frac{\gamma}{1 - \frac{p}{p_o}} \right) \quad (3-8)$$

Here,  $p$  and  $V$  are the pressure and volume of the cryogenic tank,  $p_o$  and  $T_o$  are the gas tank pressure and temperature, respectively, and  $\gamma$  and  $R_s$  are functions of the pressurant gas. The pressure in the propellant tanks must be higher than the chamber pressure in order for transport to take place.  $T_o$  is assumed to be constant, although the pressurizing gas temperature will drop appreciably as the pressure drops within the storage tank. A constant  $T_o$  will give a lower than actual total gas mass.

Gas pressurization is only suitable for short duration or low thrust burns, and will therefore only be used for Project Columbiad's secondary propulsion system. A gas pressurization system's weight increases rapidly with firing duration due to the proportional increase in weight and volume of the propellant which in turn increases the required amount of gas and the weight of the gas tanks. The weight becomes prohibitive for durations longer than 30 or 60 seconds. Thus, for the larger and more powerful primary propulsion systems, turbomachinery is required to reduce overall pressurization system mass. Turbopump and turbine assemblies suffer from greater complexity and thus lower reliability than their gas pressurization counterparts, and are considered questionable in zero-g applications due to a lack of data and experience regarding the use of these systems in space. However, despite these possible problems, the low mass of turbopumping systems makes them very attractive for use in Project Columbiad primary propulsion. Turbopump design is not required, since the RL10A-4 engines are equipped with the necessary turbomachinery.

#### **3.4.6 Propellant Lines and Valves**

The selection of liquid propellants requires the design of a plumbing system which will effectively manage the propellants during engine operation. Like the propellant tanks, propellant lines must be protected from freezing if cryogenic propellants are to be used; this may be accomplished with thermostatically controlled guard heaters or by using insulating layers of foam or aluminized plastic. Power for the heaters should be accounted for when

designing the thermal subsystem. In addition, propellant lines should be as wide and as short as possible to minimize pressure losses occurring during propellant flow; if the lines are modeled as hydraulic pipes the friction losses can be calculated with equation 3-9

$$\frac{\Delta p}{\rho} = f \frac{v^2}{2} \left( \frac{L}{D} \right) \quad (3-9)$$

$\Delta p$  is the friction pressure loss,  $\rho$  is the fluid mass density,  $L$  is the length of the passage,  $D$  is the equivalent diameter,  $v$  is the velocity of the fluid in the pipe and  $f$  is the friction loss coefficient, which is a function of Reynold's number, and has values between 0.02 and 0.05. A typical pressure loss for a cooling jacket, for example, is between 5 and 25% of the chamber pressure. A large portion of the pressure drop in propellant lines usually occurs in those locations where the flow direction or the flow passage cross section is changed; here the sudden expansion or contraction causes a loss.













The structural design of propellant feedlines requires detailed stress analysis which considers flow-induced vibrations as well as the pressure losses just described. In addition, provisions must be made to accommodate engine gimbaling if required; this may be accomplished by strategic placement of bellows joints or by using braided metal flexible hoses in place of rigid pipes. Eventually, the inner diameter of propellant lines is a compromise among tolerable system pressure drop, available space, weight, spring rate and pressure thrust reaction of the bellows used, system dynamic considerations, and cost. However, for the purposes of preliminary propellant line mass estimation, all propellant lines used in project Columbiad have been assumed to have an inner diameter of five centimeters, with a wall thickness of one millimeter. Masses were computed assuming a total piping length of 20 m for the primary propulsion systems and 50 m for the secondary propulsion systems, and 18-8 CRES as the structural material, including an additional 30% for thermally insulated pipes. A more rigorous discussion on the design of plumbing systems for liquid rockets may be found in NASA technical publication SP-8123.

In addition to propellant lines, a considerable number of valves, filters and regulators are required for efficient propellant management. Some of the more important ones are check valves to insure that the flow is going in the right direction, manual valves to fill and drain the propellant tanks, and control valves to regulate propellant flow. Particular requirements regarding operating pressure and temperature, flow range, and power requirements for actuation vary according to system design, but the general requirement is that the valves be



foolproof, for any leakage or valve failure can cause failure of the rocket unit itself. Likewise, valve masses vary according to particular application and manufacturer, but generally won't exceed 1.5 kg for Project Columbiad applications. The locations of valves, filters and regulators are indicated in the propulsion system schematics of sections 3.3.2, 4.3.2, 5.3.2 and 7.3.2 of Volume III, and the symbols and nomenclature used for identifying them are given in Table 3-11 below. A more detailed discussion of valve functions and characteristics may be found in NASA technical publication SP-8112.

**Table 3-11 : Valve Symbols and Nomenclature Used in Propulsion System Schematics**

SYMBOL	COMPONENT
	Manual Fill/Drain Valve
	Check Valve
	Squib Valve
	Pyro Isolation Valve
	Filter
	Burst Disk
	Engine Inlet Valve /Prevalve
	Trim Orifice
	Pressure Regulator
	Relief Valve
	Pressure Transducer
	Temperature Transducer

#### **3.4.7 Control and Monitoring Equipment**

All liquid propellant rockets require controls to accomplish the following tasks:

- Start, shutdown and restart.
- Maintenance of programmed operation, including a predetermined constant or varied thrust, preset propellant mixture ratio or flow.

- Emergency shutdown when safety devices sense a malfunction or a critical condition of the vehicle or the engine.
- Checking of proper functioning of critical components or a group of components without actual hot operation before flight.

The start and stop of the engine is critical to the success of the spacecraft maneuvers, and requires precise timing, valve sequencing, and smooth transient characteristics. A good control system is required to avoid undesirable transient operation caused by ignition delays, and thrust-level overshoots. In addition, close control of the propellant flow, pressure and mixture ratio is necessary throughout engine operation to obtain reliable and repeatable rocket performance. A propellant utilization system is also required, in which the mixture ratio is automatically varied to insure simultaneously emptying the oxidizer and fuel tanks. In that way no undue propellant residue remains to increase the empty weight of the vehicle, which in turn would detrimentally decrease the vehicle mass ratio and the flight performance.

Status monitoring of Project Columbiad propulsion systems is discussed in Chapter 8 and in section 3.3.6 of Volume III. The locations of appropriate monitoring equipment within the propulsion system are indicated in the propulsion system schematics of Chapters 3, 4, 5 and 7 of Volume III.

#### **3.4.8 Burn Times and Engine Configurations**

The amount of  $\Delta v$  that an engine can produce, and the time it takes to produce the required increment, are critical parameters in engine design. Vehicle maneuvers are generally treated as if they were instantaneous; this is a good approximation if the overall vehicle T/W ratio is high and the burn times are negligible compared to the total trip time. A truly instantaneous maneuver would occur over essentially zero time, but since all propulsion systems require a finite burn time to achieve a given  $\Delta v$ , there is always a performance penalty incurred during the execution of a "near impulsive" burn due to gravity losses associated with the proximity of a large planetary mass. This performance penalty is the increased velocity increment which is required to overcome the gravity losses, and is approximated [H. Robbins, 1966] by equation 3-10.

$$\Delta v_p = \frac{g I_{sp}}{4} (\omega_s t)^2 \left[ \frac{-2 g I_{sp}}{\Delta v_I} + \coth\left(\frac{\Delta v_I}{2 g I_{sp}}\right) \right] \quad (3-10)$$

$\Delta v_p$  is the performance penalty associated with a specific burn, while  $\Delta v_I$  represents the ideal impulsive  $\Delta v$ . The variable  $t$  denotes the burn time, and  $\omega_s$  is the *Schuler frequency*, defined by equation 3-11.

$$\omega_s = \sqrt{\frac{G M_c}{r^3}} \quad (3-11)$$

$G$  is the gravitational constant,  $r$  represents the radius of the circular orbit, and  $M_c$  represents the central planetary mass about which the maneuver is being done. The approximation given by equation 3-10 breaks down rapidly when the product  $\omega_s t$  exceeds one although it is quite accurate up to that point. Beyond this limit, it is necessary to numerically integrate the equations of motion, as there is no closed-form solution to the problem. Since the Schuler frequency can be calculated for a specific orbit, a threshold  $t$  can be found beyond which the approximation of equation 3-10 will not hold.

Taking the maximum allowable burn time into consideration, it is possible to calculate the average thrust required to perform a near impulsive burn for a given mission and engine type. If the total impulse  $I$  is known, then the average thrust  $\overline{F_T}$  is given by equation 3-12.

$$\overline{F_T} = \frac{I}{t} \quad (3-12)$$

Finally, the number of engines required to boost a given initial mass nearly impulsively is obtained by dividing the average thrust of equation 3-12 by the thrust produced by each engine. Thus, the number of engines required for primary propulsion is determined by two factors:

- (1) The impulsive thrust required; the near impulsive approximation of equation 3-10 that limits LEO burns to 885 seconds imposes a minimum thrust of ~500kN for a transfer to the moon.
- (2) Whether or not the engines in the propulsion system are capable of gimbaled motion. The need for an engine-out capability (in the event of a single engine failure, the vehicle should still be able to perform the mission) coupled with

fixed vector engines, would lead to a four engine cluster as a minimum, due to symmetry. If the engines are gimbaled, the minimum number of engines will be two.

Fixed engines could be used for the mission; eliminating moving parts in the severe thermal and radiation environment of space would simplify the engineering and eliminate concerns about possible damage of the gimbals. A square four-engine cluster contains the smallest number of engines that allows fixed (non-gimbaled) thrusting; in the case of a single engine failure, a second engine diametrically opposite the failed engine could be shut down and the burn continued. If the engines are gimbaled, however, it is possible to use only two engines to satisfy the engine-out capability requirement; if one fails, the remaining engine may angle its thrust to make sure the thrust vector is pointing in the right direction, provided that the engines are not too far from the vehicle centerline or from each other.

Given the near-impulsive approximation and the achievable thrust levels and gimbaling capability of the RL10A-4 and R4-D engines, appropriate engine configurations and burn times were designed for Project Columbiad. The selected number of primary propulsion engines for each stage is in excess of the required minimum described above, yet is small enough to produce comfortable levels of acceleration for the payload and crew without offsetting the impulsive trajectory change approximation. Engine configurations and burn times are listed in Table 3-12.

**Table 3-12: Number Of Engines And Total Burn Times For Each Propulsion Stage**

Stage	Number of Engines		Total burn time [s]	
	RL10A-4	R-4D	Velocity Correction	Attitude Control
PTLI	5	16	793	200
LBM	3	16	882	200
ERM	3	16	280	200
PLM	3	16	57	200
(PLM Deployment system employs three modified TE-M-236 rockets which burn for 6.5 s each, and two modified XLR-132 engines which burn for 16.7 s each. )				
CM	- -	8	- -	400

### **3.5 Launch Escape System Selection**

A survey of available literature on crew launch escape systems was conducted to assess the needs of Project Columbiad. The top-level requirement was that abort options be available for the crew from the moment they enter the vehicle for liftoff until Crew Module touchdown following the completion of the mission. This requirement dictated all other decisions regarding potential abort systems.

The Project Columbiad safety policy is based upon the principle that the preservation of human life has precedence over the loss of ground and space systems, public and private property [Baccini, 1988]. Human life must be protected during all phases of the precursor and piloted missions. This can be achieved by a systematic risk management approach. We will classify *catastrophic* all hazards resulting in loss of life, life threatening or permanently disabling injury or occupational illness, whereas all others are ranked critical, marginal, or negligible in decreasing severity order. The implementation of this policy requires the definition of safety requirements. Our failure tolerance requirements are the following:

No single failure or single human error shall result in a catastrophic or critical hazard, and no combination of both shall result in a critical hazard.

Multiple failures resulting from common cause failure mechanisms shall be considered as single failures.

Failures shall be considered to originate within hardware, software, firmware or procedures as the result of design error or random failure, or to be caused by natural or induced environmental effects.

and we define the following potentially hazardous situations:

**Emergency:** immediate and preplanned "safing" action is mandatory following an occurrence

**Warning:** the event is imminent and predetermined safing action is required within a limited time

**Caution:** the event may occur and correction measures are required

### **3.5.1 Characteristics of Launch Phase**

This mission phase is particularly critical. The release of such a large amount of energy in such a short period of time can result in the occurrence of serious incidents which can lead to potentially catastrophic accidents.

The following catastrophic hazards are liable to occur on a launch vehicle during the launch phase. As the National Launch System vehicle incorporates both liquid-fuel (LO<sub>2</sub>/LH<sub>2</sub> core stage) and solid-fuel (Solid Rocket Motors) elements, these hazards cover both types of systems. Potentially, several of these hazards can appear in a few milliseconds or in a few seconds:

- Hot spot on booster
- Untimely release
- Cracking of powder segment (solid-fuel component)
- Fire resulting in explosion
- Non-ignition of a booster
- Loss of control
- Overpressure
- Turbopump blockage (liquid-fuel component)
- Line breakages
- etc.

During the launch phase, several main events occur:

- Liftoff of launcher with launch pad facilities in close proximity
- Atmospheric phase with maximum dynamic pressure
- Passing through the maximum acceleration of the launcher

### **3.5.2 Historical Perspective on Launch Escape System Selection**

The following launch escape systems have been previously used by manned spacecraft of the U.S. and the Soviet Union:

**Mercury** - launch escape tower

**Gemini** - ejection seats

**Apollo** - launch escape tower

**Space Shuttle:**

**STS 1-4** - ejection seats (limited capability)

**STS 5-51L** - none

**STS 26-present** - escape pole (limited capability)

**Vostok** - ejection seats

**Voskhod** - none

**Soyuz** - launch escape tower

**Buran** - ejection seats

### **3.5.3 Results of Project Columbiad Escape System Trade Study**

Our Launch Escape System study rejected the following methods of launch abort: Yankee Extraction System, escape pole, and assisted seat-catapult. None of these systems met the required criteria of providing an acceptable method of escape for all portions of the launch envelope. A fourth method, ejectable capsule, was considered in the context of launch escape tower systems.

Both ejection seats and a launch escape tower system are viable options for launch escape. A clear-cut choice between the two systems was not immediately apparent, and depended upon the choice of spacecraft layout chosen (which had not yet been finalized when this study was initiated). To ensure crew survival in the case of an on-the-pad explosion, either system must be capable of transporting individuals to a minimum survivable distance from the launch vehicle within a few seconds. Both modern ejection seats and escape tower systems are capable of providing this performance.

A "generic" ejection seat system capable of supporting 4 crewmembers weighs approximately 365 kilograms. This includes the entire mass of the seats, support rails, support equipment, pyrotechnics, etc., but does not include the mass of the hatches which must be built into the side of the spacecraft. With minimum modifications, current military ejection seats (NACES, ACES II, Martin-Baker 10/12/14, or Stencel SIIS) can provide safe bailout from on-the-pad (zero-zero, nonoptimum ejection attitude conditions) to 15 km altitude (50,000 ft.) and 300 m/s (600 knots) equivalent airspeed. With astronauts suited in full pressure suits (and with minor modifications to the seats) ejection from altitudes as high as 36 km (120,000 ft.) is possible. The total volume taken up by all 4 ejection seats (along with the volume of the astronauts) is 2.28 m<sup>3</sup>. The dimensions of an individual ejection seat is 140 cm tall x 51 cm wide x 80 cm deep. The approximate cost of installation for this system is \$500,000 complete. This does not, however, include the cost of life-support equipment (pressure suits) for the crew.

A launch escape tower also may be used for escape from on-the-pad to 120,000 ft. altitude. The maximum altitude is determined from the need to achieve aerodynamic control surface deflection during the abort sequence. Currently, the only launch escape tower in production is the Russian Soyuz launch escape tower. No specifications are available for

this system. During the Apollo program, a 3800 kg escape tower ensured that the 5500 kg Command Module could be pulled away from the launcher stack. A 1987 British Aerospace study concluded that a launch escape tower weighing only 950 kg could be used in conjunction with a 7000 kg ballistic capsule. Developmental costs for such a system are not known, but can be reliably assumed to be well over several million dollars.

The following is a summary of advantages and disadvantages for both ejection seat and launch tower escape systems.

### **Ejection Seats**

#### **Advantages**

- low cost
- high reliability / proven system with much operational experience
- no new developmental items - low risk
- escape possible following reentry should primary recovery system fail
- can be used if spacecraft is contained in launch shroud (blow-out side panels)
- personnel capsule is not constrained to the top of the stack for launch configuration
- lower initial weight than escape tower
- reusable
- low maintenance

#### **Disadvantages**

- crew becomes separated during abort sequence (increases difficulty of SAR)
- less physical protection during post-abort flight / landing / earth survival
- pyrotechnics are located inside crew compartment
- weight of system must be carried all the way to moon and back  
(ejection seats weigh approximately 190% more than standard crew couches)
- alternate method of escape involving physical separation of personnel capsule must be used from above 120,000 ft. to orbital injection
- difficulties in capsule integration - provisions must be made for multiple hatches in side of vehicle, or one very large hatch must be made with resultant loss of confidence in structural integrity. If a conical personnel capsule is used, difficulty in arranging ejection seats to obtain adequate display panel accessibility or minimize spacecraft width. Biconic capsule design presents less integration difficulties.



## **Launch Escape Tower**

### **Advantages**

- crew remains intact throughout entire abort sequence
- personnel capsule provides physical protection during post-abort flight / landing / earth survival
- associated pyrotechnics located outside personnel capsule and jettisoned following launch phase
- weight of system is not carried into orbit
- escape between 120,000 ft. and orbital insertion is simplified
- ease of capsule integration (conical capsule design only)

### **Disadvantages**

- high cost
- new developmental item - increased risk
- higher initial weight than ejection seats
- no escape possible should primary recovery system fail
- cannot be used if spacecraft is contained in launch shroud (or shroud must be modified to separate before launch tower fires - increased complexity and/or reduced payload volume within shroud)
- personnel capsule constrained to top of the stack for launch configuration
- exceedingly difficult to integrate if biconic capsule design chosen (c.g. requirements, attach points must not interfere with heat shield, etc.)
- nonreusable

### **3.5.4 Decision on Launch Abort System Selection**

Ejection seats were eventually chosen over the launch tower system for use in the Project Columbiad Crew Module. The primary factors which motivated this decision included the choice of a biconic capsule design, low development cost of ejection seats, and the approach & landing abort capability available with ejection seats following reentry or an intact-capsule abort resulting in ocean splashdown. The detailed design of the ejection seat subsystem is presented elsewhere in this chapter.

## **4 Command, Control and Communications Selection**

This chapter will first discuss the requirements on the command, control and communications systems and then give an overview of the proposed command, control and communications system. Following the overview is a discussion of the design considerations that led to the choice of this system over other systems. Finally, the chapter concludes with a summary of the power, size and weight estimates of the communications equipment distributed over each of Project Columbiad's stages.

### **4.1 Requirements for Command, Control and Communications**

The command, control and communication's (C3) primary responsibility is to provide near continuous communication between each of the Project Columbiad vehicles and the Earth. Communication refers to sending data, voice and video information. The requirement for near continuous communication, as opposed to continuous communication, takes into account that there will be a communications blackout when a vehicle travels around the back side of the Moon and when the crew module is surrounded with a plasma layer upon reentry.

The communications blackout on the back side of the Moon constrains the landing sight of the vehicles to the side of the Moon facing the Earth. This requirement could be eliminated if a communication satellite were located around the Moon such that the satellite could relay signals from the back side of the Moon to the Earth. In designing the communications system for the Project Columbiad, only presently existing communication networks were considered.

Another requirement evolving from the near continuous communication requirement is that the receivers of the communication links on vehicles in use will be left on at all times so that ground control may issue override commands at any time.

C3 is also responsible for the coordination of instructions and data to the various systems of the vehicles and for relaying necessary information to the Earth for monitoring. A processor will distinguish data from commands and prioritize the information so that the ground maintains control over the vehicles via override commands in case of emergency. On-board computational capability will be provided for those systems such as guidance and navigation which require autonomy during some mission phases. C3 will also provide on-

board information storage for holding information that is not used immediately or cannot be transmitted to Earth immediately.

C3 will provide the sampling of parameters and the information processing that the Status subsystem requires for an on-board vehicle status monitoring system. C3 will also provide read-only-memory storage (ROM) for storing the operating parameters for equipment as well as the necessary corrective actions. The requirement for ROM comes from the fact that ROM is more reliable than random-access-memory (RAM) because it cannot be changed after launch. RAM may be changed by radiation particles and by a malfunctioning computer. Since the operating parameter limits of equipment do not change, they are safer stored in ROM memory.

C3 will provide memory and throughput of the computer system to run the Guidance, Navigation and Control (GNC) subsystem's algorithms. In addition, C3 will provide some telemetry for GNC via the GPS system. C3 will also provide a communication link between the Earth and the crew module and the Earth and the habitat that is capable of handling video information for docking with the PTLI stage and landing on the lunar surface.

C3 also imposes requirements upon other subsystems. Structures must locate all antennas so that the vehicle will not block communications with the Earth. Any such occultation by the vehicle can cause loss of signal and unnecessarily break communications between the vehicle and Earth. This would be disastrous for any systems which require ground commands. The antenna should be placed so that it will be on the topside of the precursor vehicle once it has landed on the lunar surface. The high gain antenna needs to be shielded from aerodynamic forces during launch. This means placing the high-gain parabolic antenna inside the structure and deploying it after leaving the Earth's atmosphere.

C3 needs the Power and Thermal Control subsystem to dissipate heat from the electronics, to provide steady and surge protected power for operating the computing system, and to provide power to operate the antennas, transmitters, and receivers.

The transmitters and receivers must be located as close as possible to the antennas to minimize transmission line loss.

C3 requires that communications equipment must be space rated and radiation hardened equipment. Processors used in C3 design must be able to support at the very minimum Ada software, and support of C software would be desirable. This is because much avionics software already developed for the military and international agencies has been written in Ada.

#### **4.2 Overview of Proposed C3 Systems**

During each of the four launches of Project Columbiad, the launch site and mission control need to communicate with the vehicle from pre-flight checkout through launch up to LEO. Figure 4-1 shows the four links with each of the launches.

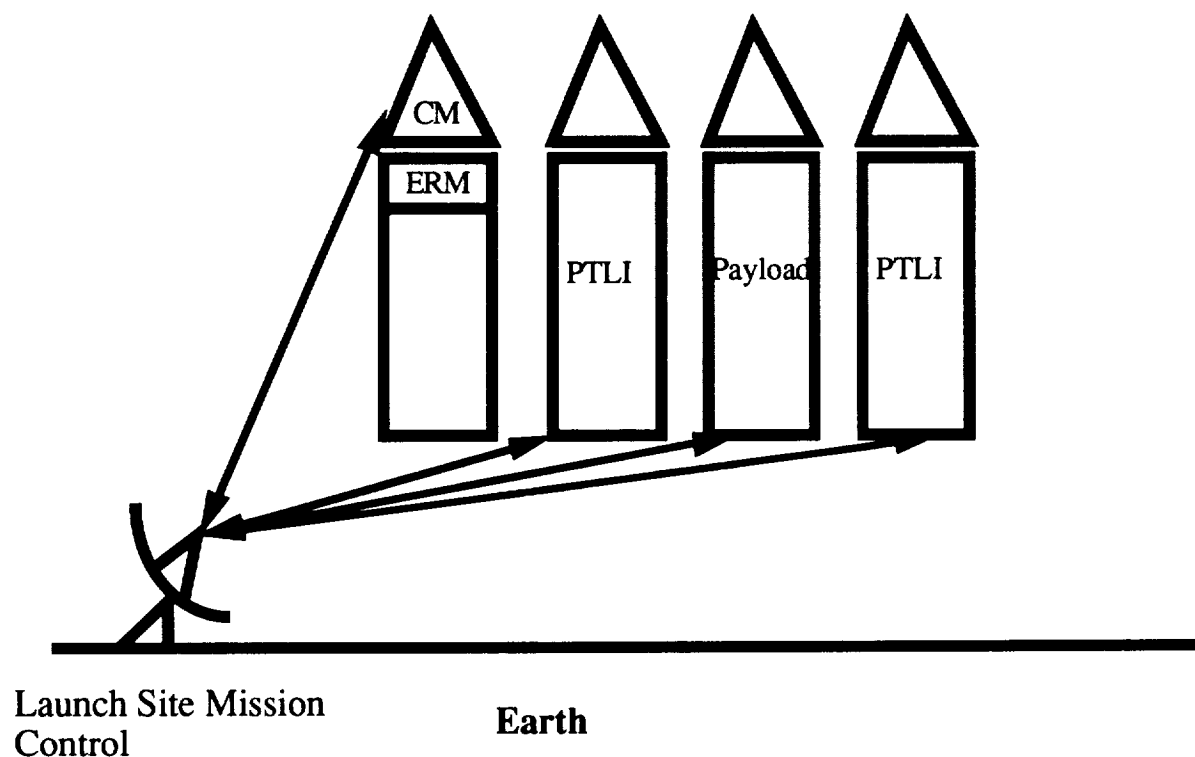


**Figure 4-1**  
**Communication Links on Launch**

During the first and third launches, the ground will maintain communications via low gain antennas and communications equipment found on the PTLI stages. During the fourth launch, the ground will maintain a link with the low gain antennas on the Crew Module. The status of the entire vehicle will be relayed through the data bus up to the Crew Module where the information will be transmitted to ground. Similarly, ground will maintain

communications via a low gain antenna located on the habitat of the payload vehicle. Again, the status of the payload vehicle will be relayed via the data bus to the habitat and transmitted to ground.

Once in LEO, each vehicle will be monitored by the Deep Space Network (DSN). During the precursor mission, video information will be relayed to ground for docking the precursor with its PTLI stage. Figure 4-2 shows that the link with the PTLI and the habitat will be maintained at least until the vehicles are docked. The habitat will also deploy its high gain antennas which will maintain the habitat-Earth link throughout the rest of the lifetime of the habitat.

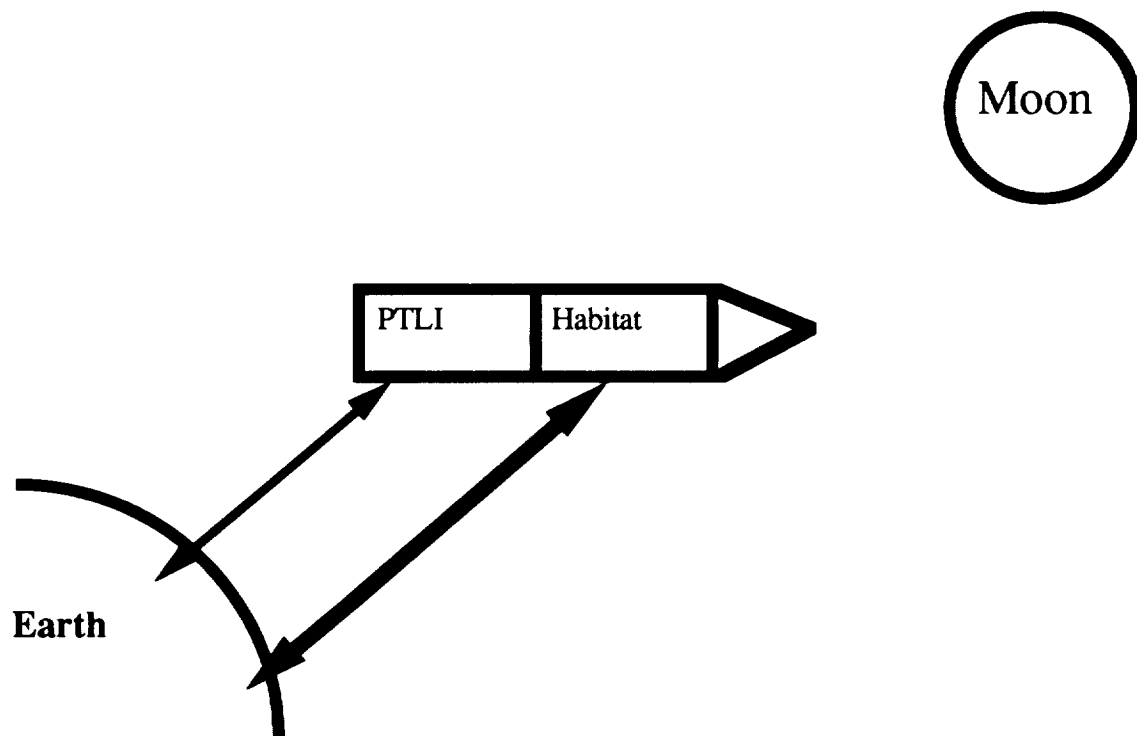


**Figure 4-2**  
**Communication Links of Precursor in LEO and LTO**

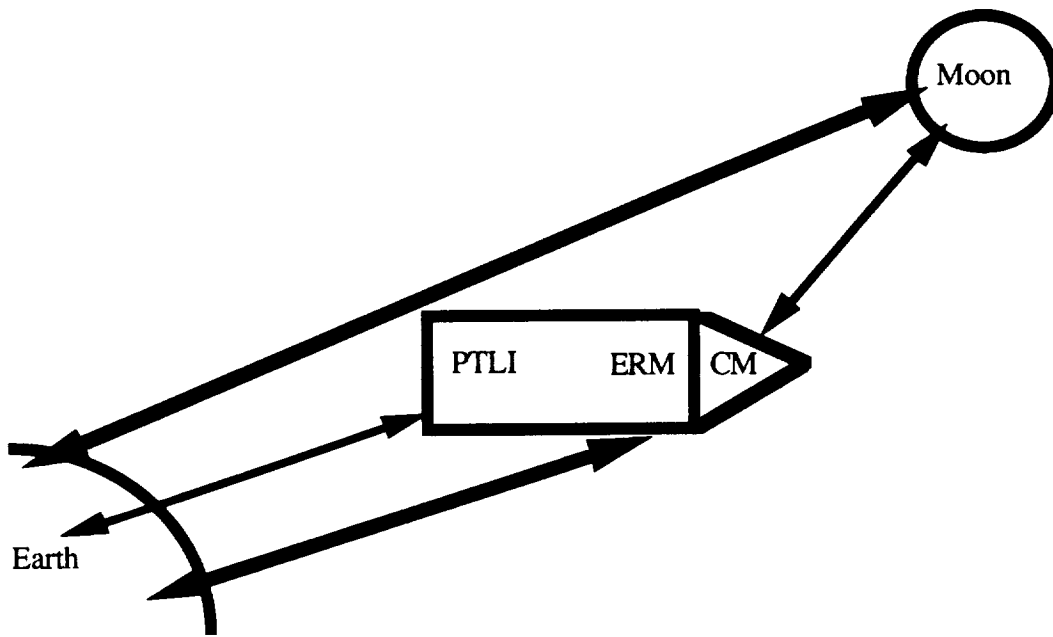


**Figure 4-3**  
**Communication Links on Piloted Mission in LEO and LTO**

During the piloted mission, two links will be maintained through docking maneuvers. The high gain antennas will be deployed from the Earth Return Module (see Figure 4-3). Information will be relayed to the Crew Module via the databus. This antenna will provide the communication link between the Earth and the crew module through lunar landing. Once the piloted vehicle approaches the Moon, the crew module will be able to communicate with the habitat via the low gain antenna system. This link will allow the crew to check out the status of the habitat before landing the crew module and earth return module on the lunar surface.

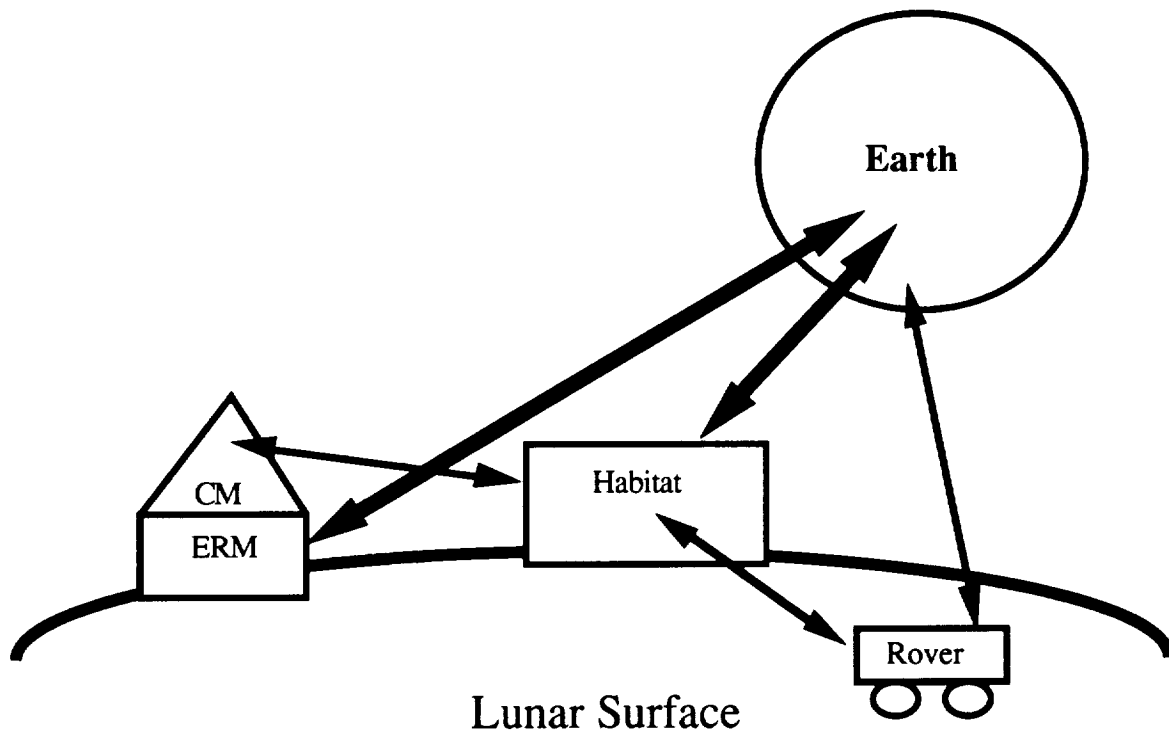


**Figure 4-4**  
**Communication Links on Lunar Surface**

Once the crew has established their presence in the habitat, the communication systems in the crew module will provide a backup to the communication systems in the habitat (see Figure 4-4). Low gain antennas will provide voice and data links between the crew module, the habitat and the lunar rover. The lunar rover will also be equipped with a high gain antenna system for communications with the Earth. This link is necessary because the 50 km range of the rover is likely to remove the lunar rover from the line of sight of the habitat and crew module and there is no atmosphere to bounce a radio signal off on the Moon.

#### **4.2.1 Primary Trans-Lunar Injection and Earth**

Figure 4-5 shows the layout of the C3 equipment on each of the PTLI stages. The four low gain antennas are located around the vehicle so that at least one antenna pattern will "see" the Earth. Information transmitted from the Earth is sent to a pair of receivers. A pair of receivers is used in parallel to achieve the required reliability. The receivers feed into demodulators which decode the incoming signal and make the information available to

the data processors. The three data processors work in parallel in a voting configuration to process commands to actuators and monitor any sensor information.

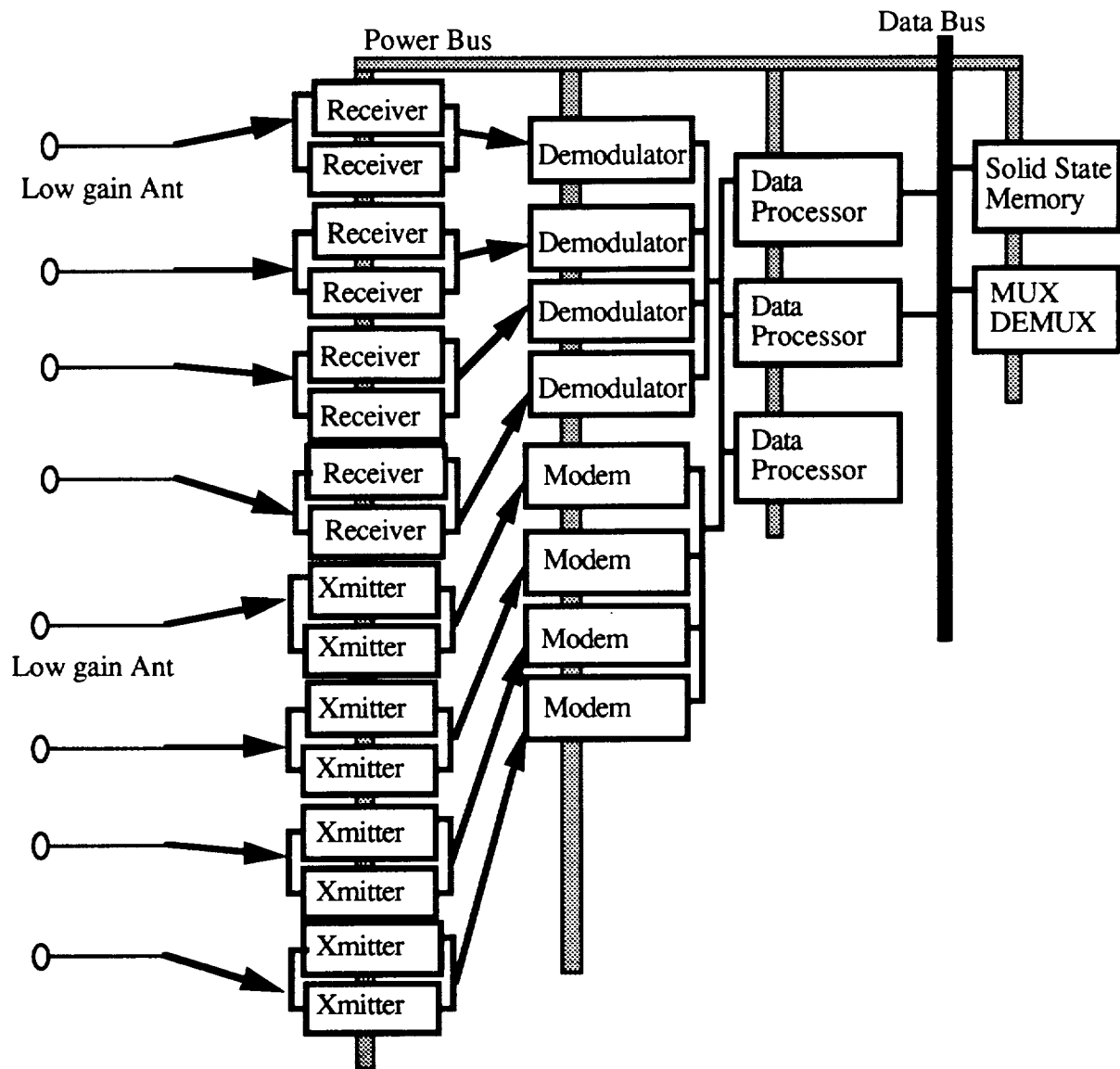


**Figure 4-5**  
**Communications System on PTLI Stages**

#### **4.2.2 Precursor and Earth**

The communications equipment for the precursor mission is located on the habitat with the exception of the high gain antennas which will be located on the Precursor Landing Module (see Figure 4-6). The PLM was chosen for the high gain antennas so that the regolith covering over the BioCan will not interfere with the deployed antennas. Both the



transmitting and receiving high gain antennas are mounted on the same antenna pointing system. Both the high gain and low gain receiving antennas feed into pairs of receivers before turning the signal over to the demodulator for decoding. The three High-Powered Gallium Arsenide Computers run the flight code in parallel in a fault tolerant voting topology. The computers route information and commands to and from the subsystems of the habitat. Information can also be stored for future reference. Sensors are tied to the computers via a databus. Earth-bound information is routed through the modem for coding before being transmitted via transmitting antennas to the Earth.

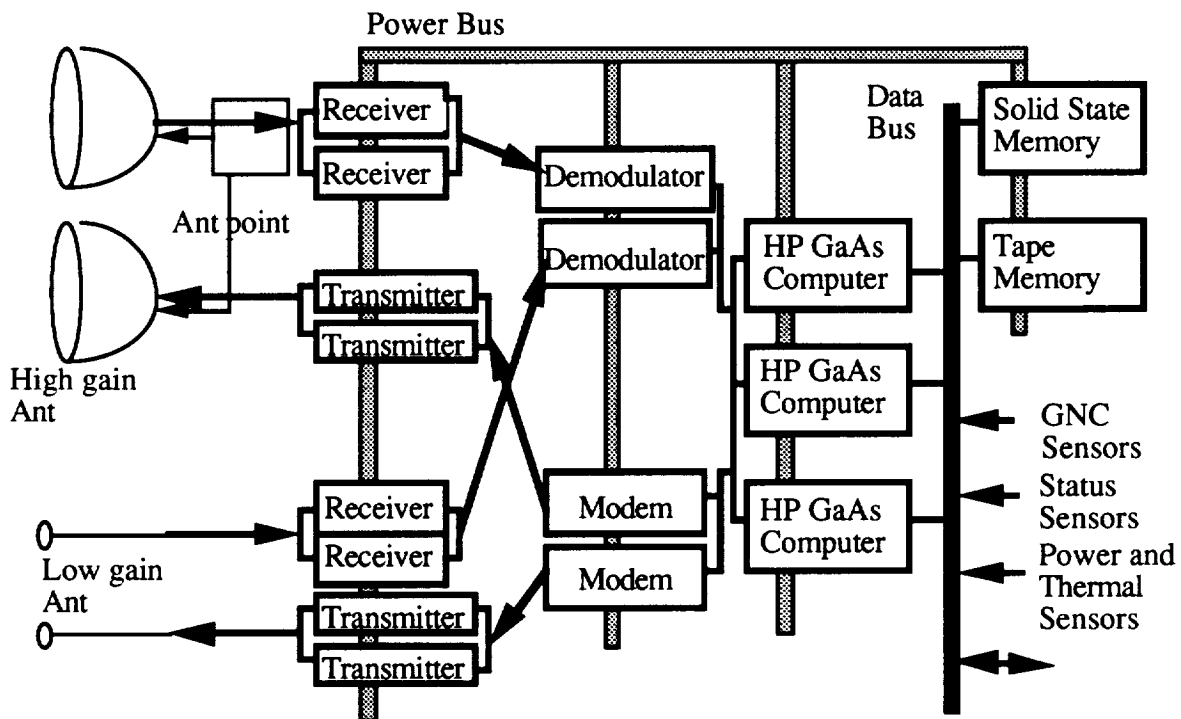


**Figure 4-6**  
**Communications System on Habitat**

#### **4.2.3 Earth Return Module and Earth**

The communications system for the piloted mission is distributed between the Crew Module and the Earth Return Module. The dashed box in Figure 4-7 shows the equipment located on the Earth Return Module. The high gain equipment is located on the ERM because there is more room for it than in the Crew Module, and the high gain equipment is not needed upon reentry when the ERM is ejected from the CM.

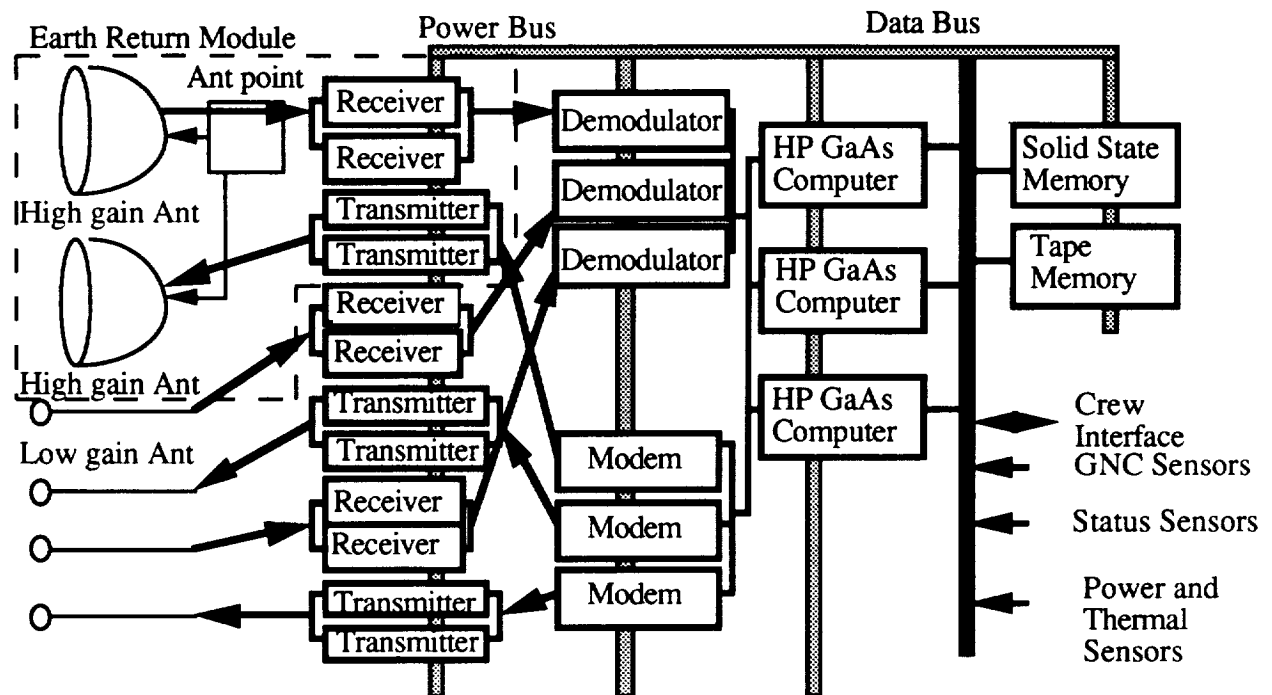


**Figure 4-7**

### **Communications System on Crew Module and Earth Return Module**

#### **4.2.4 Crew Module and Earth**

The crew will communicate with the Earth (LEO and beyond) via the high gain antenna system located on the ERM. The communication system works the same as the communication system on the habitat explained in section 4.2.2 with the addition of the crew interface on the data bus.

#### **4.2.5 Crew Module and Precursor**

When the crew module is on or near the Moon, the low gain antennas on the crew module and the low gain antennas on the habitat will be used to establish a communication link. If this link fails, information can be relayed between the habitat and ERM via the Earth.

#### **4.2.6 Lunar Rover and Earth**

Figure 4-8 shows the communication system on the lunar rover. The high gain antenna is used for a direct link to the Earth. The overall system works the same as explained in section 4.2.2. A Data Processor is used instead of the HP GaAs Computer because not as much computing power is required for the lunar rover. The reliability of the Data Processor is .99 which exceeds the mission success requirement of .95; therefore, only one

data processor is required for the lunar rover. The tape memory was eliminated from the system because solid state memory can store enough on its own.

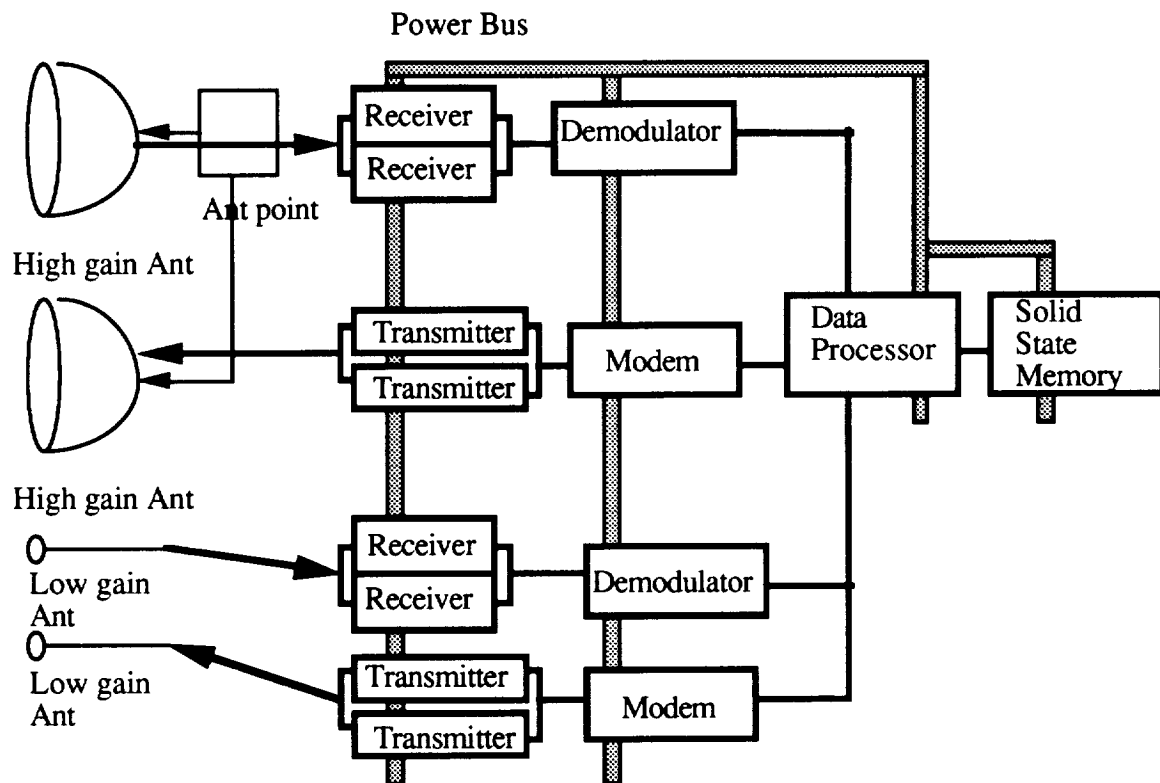


**Figure 4-8**  
**Communications System on Lunar Rover**

### 4.3 Design of Communications Systems

Communication is vital to the success of the mission. The requirements on the communications systems are to provide nearly continuous communications with acceptable reliability and safety margins within the weight and power budgets, structural configuration constraints, and technological limitations imposed on the mission. DSN may be used for communications with Mission Control from launch onward, as was done with the Pioneer missions. For compatibility with DSN, downlink frequencies will be in the 2.2-2.3 GHz band, while uplink frequencies will range from 2.025-2.120 GHz. Table 4-1 gives projected data on DSN capabilities [Weiss, 1992]. If, in the future, more continuous communications capability will be required, the deployment of relay satellites at the Lagrange points between the Earth and the Moon could be used to extend the communications coverage that Columbiad currently provides and would be a good start for

a future Mars mission. Further background theory and information may be found in Appendix III. Table 4-2 lists the distribution of antennae among the different modules of the mission.

**Table 4-1: Projected Operational Parameters for DSN**

**COMMUNICATIONS TECHNOLOGY FORECASTS**

<u>Figure of Merit</u>	<u>1985</u>	<u>1990</u>	<u>1995</u>	<u>2000</u>
<u>Deep Space Communications</u>				
Bit Energy-to-Noise Spectral Density Ratio (dB; BER = $1 \times 10^{-5}$ )	2.3	—	0.2	—
Deep Space Network Performance				
Gain-to-Noise Temperature Ratio (dBi/dBK)	60	63	66	—
Link Data Rate (bps; Jupiter)	$1 \times 10^6$	$3 \times 10^7$	$3 \times 10^8$	—
Antenna Gain (dBi)	72	85	95	110
Effective Radiated Power (dBm)	105	115	125	140
<u>Data Transfer Systems</u>				
Data Rate (Mbps)	90	300	300	1200

**Table 4-2: Antenna Distribution**

Mission Phase	High- Gain		Low- Gain	
	Transmitting	Receiving	Transmitting	Receiving
PTLI*	0	0	2	2
Precursor				
PLM	1	1	1	1
Rover	1	1	1	1
Piloted				
ERM	1	1	0	0
CM	0	0	2	2
<b>Total</b>	<b>3</b>	<b>3</b>	<b>8</b>	<b>8</b>

\* There are two PTLI stages in one complete mission.

#### **4.3.1 Design of the Receiver Systems**

A receiver system converts the electromagnetic energy collected by an antenna into signals which can be processed and interpreted. The general system block diagram is shown in Figure 4-9. The main components are the antenna, the transmission line which carries signals from the antenna to the receivers, the superheterodyne receivers, the amplifier, and the decoding and demodulation units. This system is usable with both high-gain and low-gain antennae.

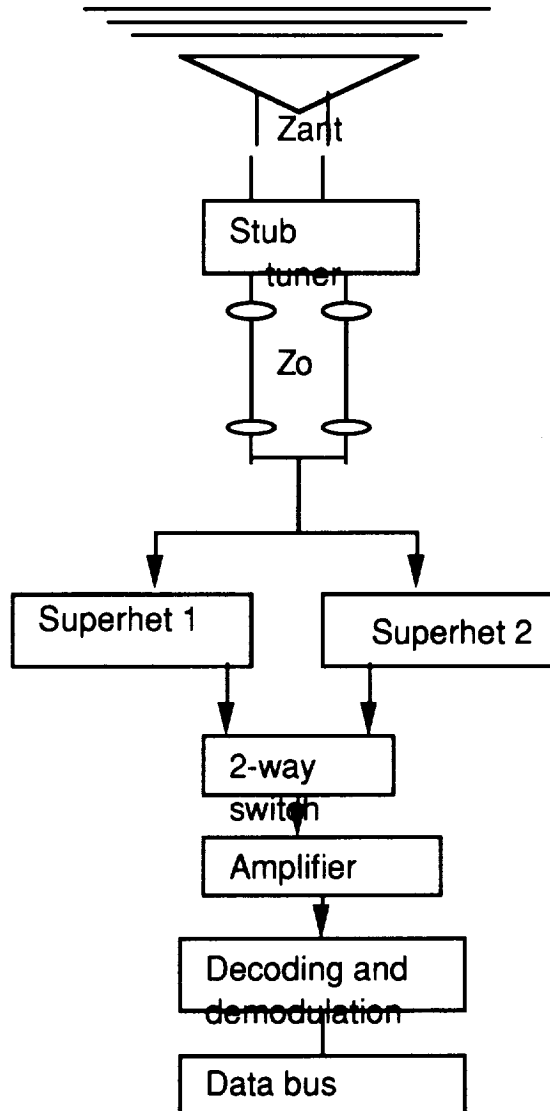


**Figure 4-9**  
**Receiver System Block Diagram**

The antenna has an input impedance  $Z_{ant}$ , while the transmission line has a characteristic impedance of  $Z_o$  which is generally not equal to  $Z_{ant}$ . According to basic transmission line theory (see Appendix III), the impedance mismatch causes the VSWR to be greater than 1, creating dissipative losses as the signal is carried along the line. To reduce these losses, a stub tuner has been added to match  $Z_o$  and  $Z_{ant}$  more closely (Appendix III gives a brief overview of tuning stubs). To increase the system reliability and to provide a measure of redundancy, two superhets have been connected in parallel. The switch, which will be implemented by a multiplexer, selects between the receivers so that the receiver and the decoding and demodulation equipment receives one unambiguous signal. The superhets

are capable of handling signals on the order of tens of picowatts [Verghese, 1992] and thus can process the signals which will be used in this mission.

#### **4.3.2 Design of the Transmitter Systems**

A transmitter system converts data-carrying signals into currents which drive the transmitting antenna. Figure 4-10 shows a block diagram of the transmitter system. The basic components of the transmission system are the antenna, the transmission line, the amplifiers, the transmitters, and the encoding equipment. As was the case with the Receiver System,  $Z_{ant}$  is in general not equal to  $Z_o$  and the VSWR will be greater than one. If the VSWR is high enough, frequency pulling may occur (see Appendix III), changing the transmission frequency as the impedance of the line varies. To prevent frequency pulling and dissipation losses, a stub tuner has been added to the transmission line to provide a better match between  $Z_{ant}$  and  $Z_o$ . To improve the system reliability and to provide a backup, there are two transmitter/amplifier pairs connected in parallel; the switch, realized by a multiplexer, selects between the two transmitters.

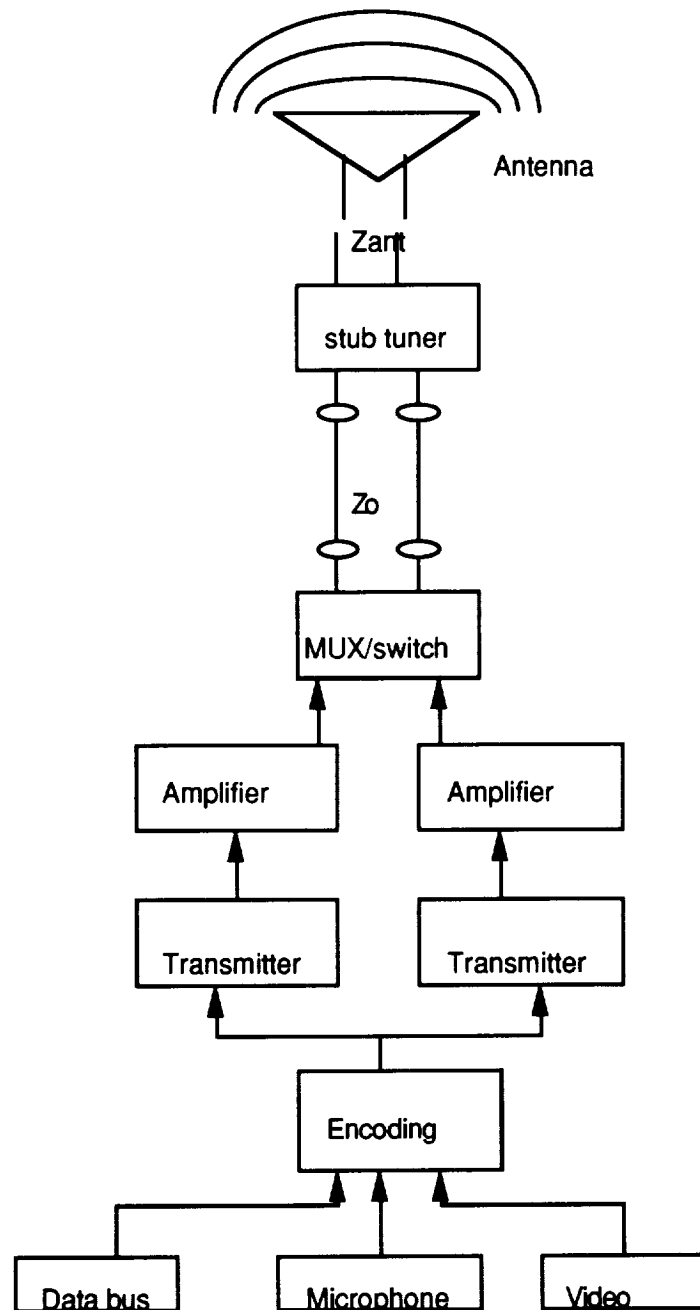


**Figure 4-10**  
**Transmitter System Block Diagram**

Although most of the transmitted data will be sent by the flight computer system, human input interfaces have been provided in the form of microphones for direct voice links, video cameras for video links, and keyboards for communication via computers. The computers are connected into the data bus; the microphone and video camera input are connected to the data encoding equipment.



### 4.3.3 Antenna Design

Four types of antennae will be used on this mission: low-gain receiving and transmitting antennae for use near the Earth and the Moon, and high-gain receiving and transmitting antennae for use beyond LEO and the lunar orbit. The design of the antennae took into consideration issues such as minimization of weight, volume, and power consumption while providing adequate performance margins. For near-Earth communications, Mission Control ground stations will be used; GPS will relay tracking and telemetry data. Outside of LEO and near the Moon, communications and data transfer will be via DSN.

#### 4.3.3.1 Low-gain Antennae

The same type of antenna will be used for both transmission and reception of command data; the GPS receiver is discussed in Chapter 5. For an altitude of 300 km, the expected altitude at LEO, the path losses are approximately 150 dB for both downlinks and uplinks; an estimate of 10 dB signal loss was used for all other attenuations, including thermal noise, atmospheric and weather absorption, line losses, receiver losses, and pointing errors.

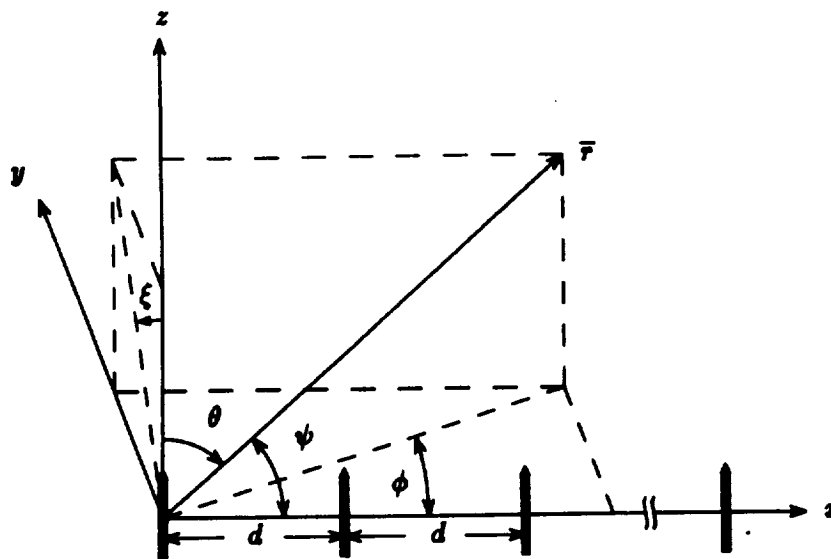
For uplinks, the main constraints on the usable types of antennae are the signal strength provided by DSN. With a projected DSN signal EIRP of 140 dB, the signal which the low-gain antennae will need to pick up is on the order of -20dB. Given the tens of picowatts sensitivity provided by superhets, on the order of -110 dB, polarization mismatch losses between circular and linear polarizations, with a loss of 3 dB, or even between horizontal and vertical polarizations, with a loss on the order of 25 dB, are not a significant problem.

The downlinks, on the other hand, are constrained by the minimum signal power that can be picked up by DSN. Based on TDRSS' capability of picking up signals as weak as approximately -180 dB, it has been concluded that DSN must be able to receive signals at least as faint, and most likely even weaker signals can be received. Using the figure of -180 dB as the minimum signal strength and the projected gain of 85 dB for DSN, the conclusion is that the minimum signal power which is transmitted is about -75 dB. With the 25W of signal power allowed for the transmitters and accounting for polarization mismatch losses, an arbitrarily-designed low-gain antenna may be chosen. For simplicity, therefore, a stub antenna has been chosen.

#### 4.3.3.2 High-gain Transmitting Antennae

For the design of the high-gain antennae, the maximum transmission distance was determined to be the maximum separation between the Earth and the Moon, 384.4 Mm, added to the radius of the Moon, 1738 km, for the maximum range of 386,138 km [Lide, 1990]. Based on this distance, the downlink path loss is 211 dB. Adding in 10 dB for other system losses, the total downlink signal loss comes to 221 dB. If DSN can only receive signals down to -180 dB, then the transmitting signal EIRP must be at least 40 dB. To reduce problems with Faraday rotation, circularly polarized waves will be transmitted. Phased arrays and parabolic reflectors are the most commonly used high-gain antenna types.

A phased array consists of a set of dipoles; Figure 4-11 illustrates a linear array.



Linear antenna arrays.

**Figure 4-11**  
**Linear Phased Array [Kong, 1990]**

The phased array can be controlled electronically. By changing the phases of the dipoles making up the array, the beam can be steered and the shape of the radiation pattern can be altered (see Figure 4-12, which compares the range of the radiation pattern which is detected for a 5-dipole linear array as a function of array parameters). For that reason,

however, phased arrays are more complex and, in order to drive many small antennae, they require more power and weight than a single antenna. The parabolic reflector, on the other hand, is relatively simple. Additionally, the parabolic dish can be foldable, much like an umbrella, with a membrane held by flexible ribs. This foldable antenna would be furled into a compact shape when stowed; stored energy, as in a spring, would open it up. Large objects colliding with the antenna are not a problem [Alexander, 1992]. As Figure 4-13 indicates, the parabolic antenna provides the same channel capacity for less power and weight than the phased array for data rates above 0.1Mb/s. Given that the estimated required data rates are on the order of several Mb/s, the logical choice is therefore the parabolic reflector.

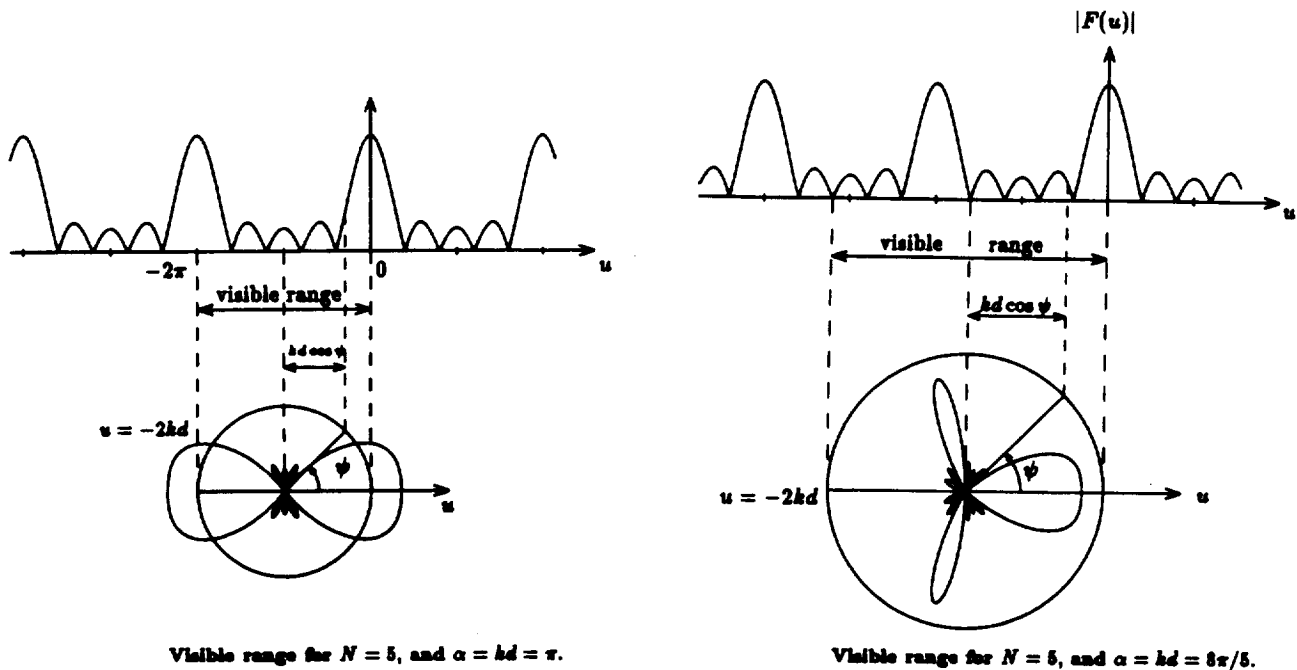
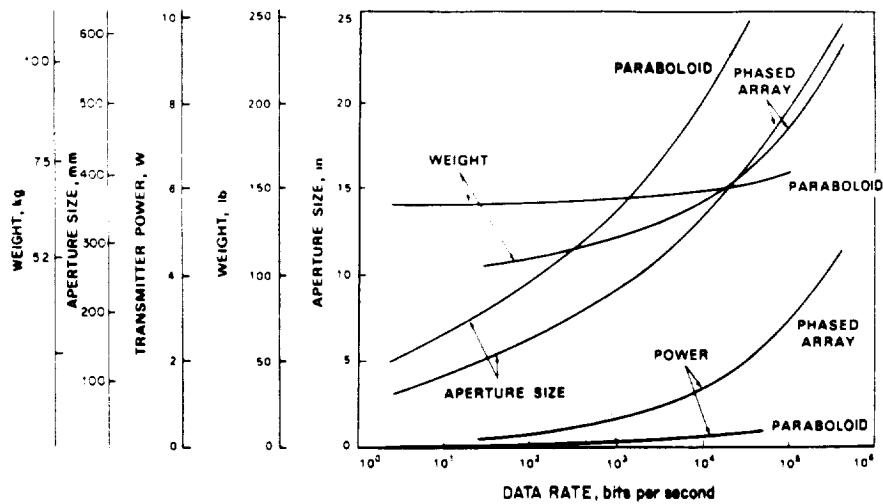


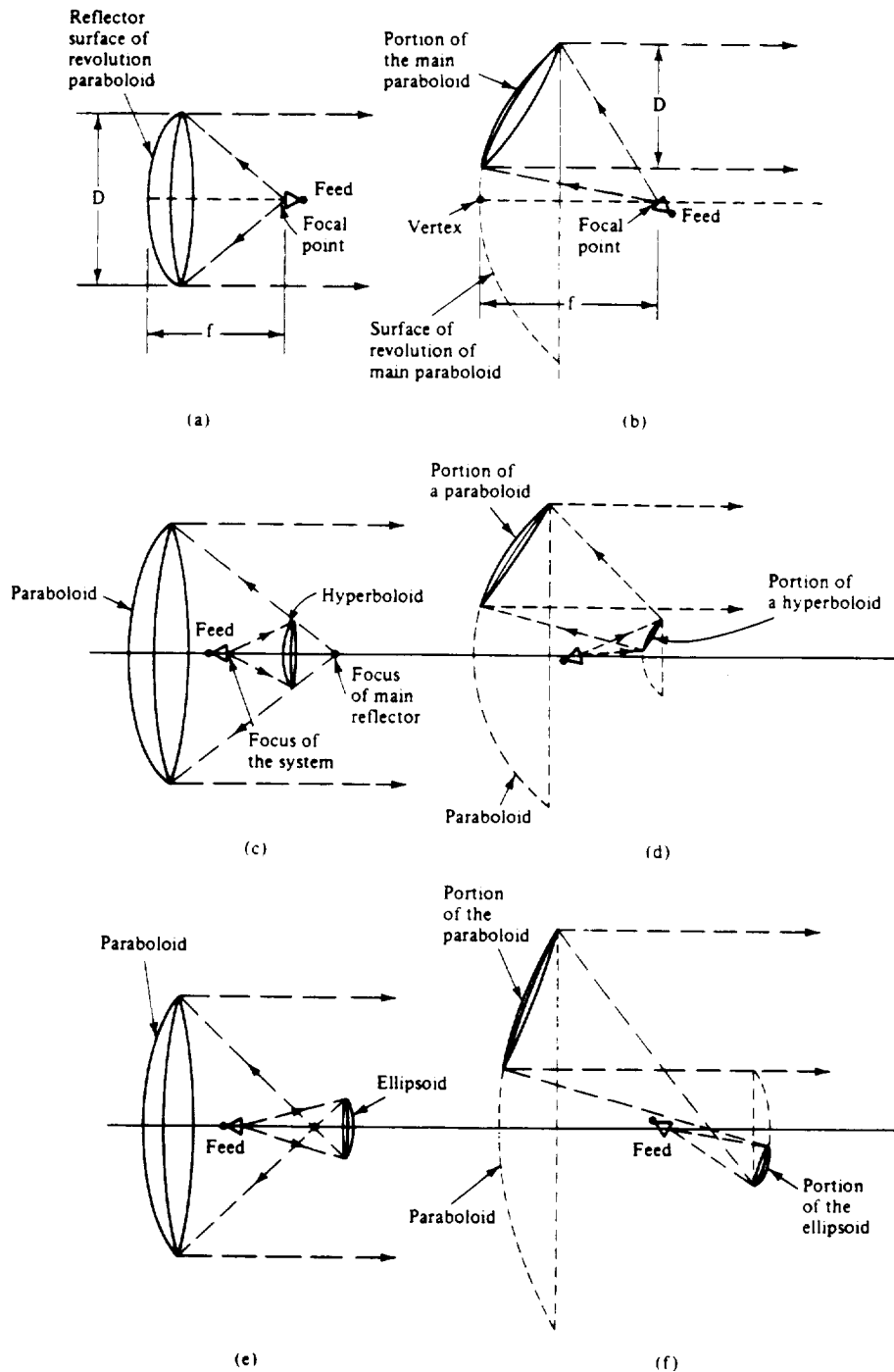
**Figure 4-12**  
**Visible Range for  $kd = \pi$  (left) and for  $kd = 8\pi/5$  (right) [Kong, 1990]**



Phased-array and paraboloid characteristics.

**Figure 4-13**  
**Weight and Power Requirements for Parabolic and Phased Array**  
**Antennae as a Function of Frequency [Johnson and Jasik, 1987]**

Parabolic reflectors may use a single reflector and a feed antenna, as in Figure 4-14a, or multiple reflectors and a feed antenna, as in the Cassegrain configuration in Figure 4-14c and the Gregorian configuration in Figure 4-14e. In a multiple reflector system, the subreflector reflects the waves from the feed antenna onto the main reflector. The Gregorian reflector antenna has a parabolic main reflector and an elliptic subreflector. Since a second antenna will be put on the same arm as the transmission antenna, the Gregorian system was excluded, as will be explained in the next section. The Cassegrain reflector antenna consists of a parabolic main reflector with a hyperbolic subreflector. Although the Cassegrain antenna has higher sidelobes near the main beam and a larger fraction of the aperture is blocked, the transmission line leading to the feed antenna can be made much shorter, there is more flexibility in designing the feed antenna, and the beam can be shaped somewhat by the choice of the subreflector. [Rudge et al, 1982].



(a) Focal-fed symmetrical parabolic antenna; (b) offset-fed paraboloid (no feed blockage); (c) center-fed symmetrical Cassegrain antenna; (d) offset-fed Cassegrain antenna; (e) center-fed symmetrical Gregorian antenna; (f) offset-fed Gregorian antenna.

**Figure 4-14**  
**Single and Multiple Reflector Systems**

The aperture blockage can be reduced by using an offset feed for either the single or multiple reflector systems, as in Figure 4-14b, Figure 4.-14d, and Figure 4.-14f. The aperture blockage is eliminated by moving the feed antenna off to the side, thus increasing the aperture efficiency. Although the signal depolarizes for a linearly polarized feed, there is no degeneration for a circularly polarized feed. In addition, the offset configuration decreases the sidelobes of the main beam. The increase in antenna performance is shown in Figures 4-15 a, b, and c. Antenna pointing is made a little more difficult because of the beam's tendency to squint, or to deviate from its axis of symmetry.

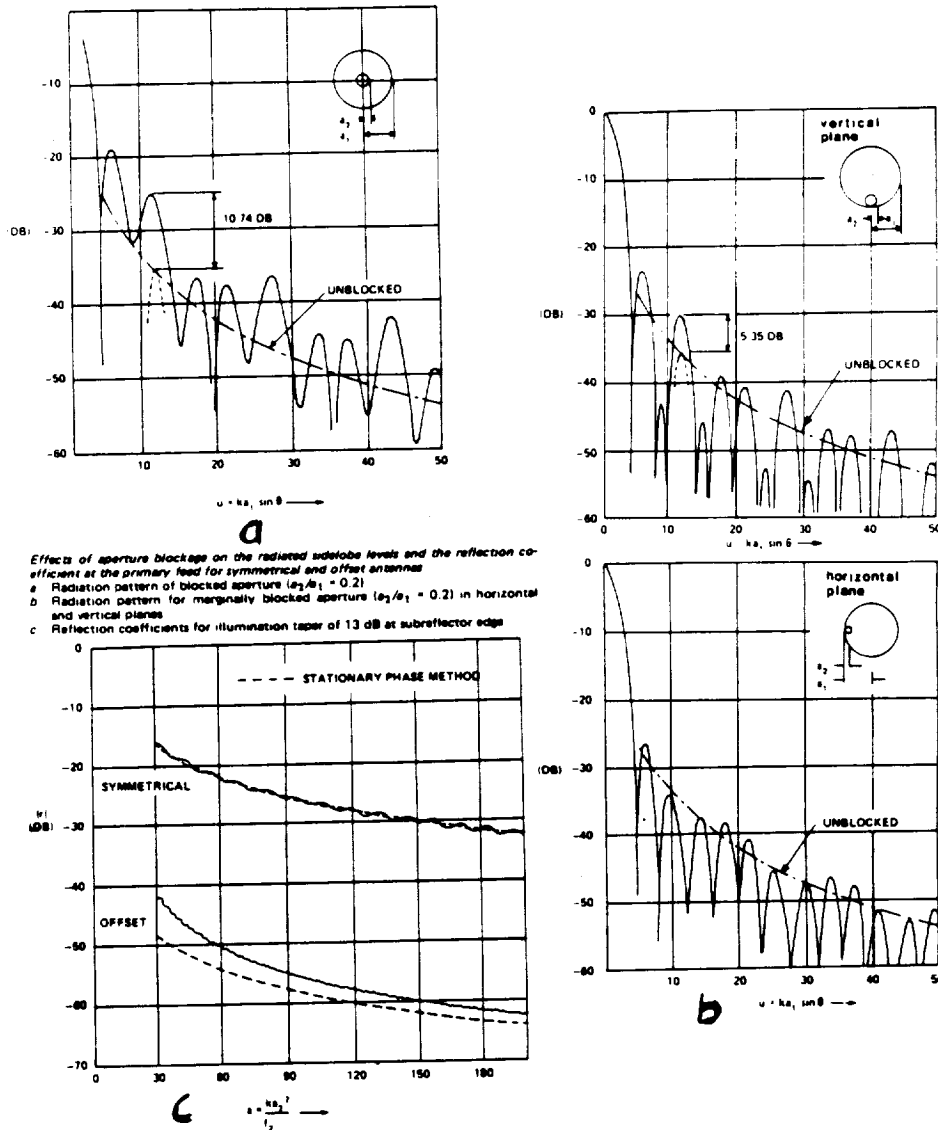


**Figure 4-15**  
**Comparison of Offset and Symmetric Reflector Performance**

A 3m diameter parabolic reflector dish was selected; at the frequencies used for downlinks and with an estimated antenna efficiency of 0.55, the gain of the dish is about 34 dB. If this antenna were driven with 20 W of power, the signal EIRP would be about 47 dB, well over the required power. For these figures, the SNR is about 150/B; the maximum error-free channel capacity of the communications link is then  $7.26 \cdot (\text{link bandwidth})$ . The carrier power to noise power spectral density ratio, C/No in dB, is 23.77.

Since an optimized Cassegrain system can have an efficiency near 0.9, compared to an efficiency of 0.5 - 0.7 for a single reflector, the decision to use a Cassegrain system adds an additional margin in the event of power supply failure; communication to DSN would be possible to at least transmitter powers of 4 W. In addition, the use of the offset subreflector allows an opportunity to add a second high-gain antenna for reception. Therefore, for the high-gain receiving antenna, an offset Cassegrain system with a 3 m main reflector diameter and 20 W transmitter power was selected. Figure 4-16 shows the configuration in both the stowed and deployed positions. The antenna system is contained on a mounting block; gimbals connecting the mounting block and the spring-loaded antenna arm allow 2 or 3 degrees of freedom. Control electronics on the arm point the antenna in the proper direction for transmission.

#### 4.3.3.3 High-gain Receiving Antennae

Given the constraints imposed by the design of the transmitting antenna, the need for compactness in the stowed position, the operating characteristics of DSN, and the relatively low data rates anticipated for reception, the parabolic reflector for the receiver will be much smaller than that for the transmitter. As Figure 4-16 shows, the reflector of the receiving antenna doubles as the subreflector of the transmitting antenna. The dish will be 1 m in diameter; the gain will be about 25 dB, with an EIRP of about 38 dB. This is still well within the ranges of signal strengths that DSN can receive. If the dish can be designed such that it is nearly hyperbolic along its outer surface, then no modifications need to be made. If the shape is not hyperbolic on the outside, then an extra panel of material will need to be added to create the hyperboloid surface required of the subreflector. Figure 4-16 shows the transmitter antenna in both the stowed and deployed positions. The feed antenna for the transmitter antenna is piggy-backed onto the support arm for the receiving antenna; an actuator will control the motion of this arm. An additional actuator will allow the receiving antenna to pivot, thus allowing tweaking for optimum performance.

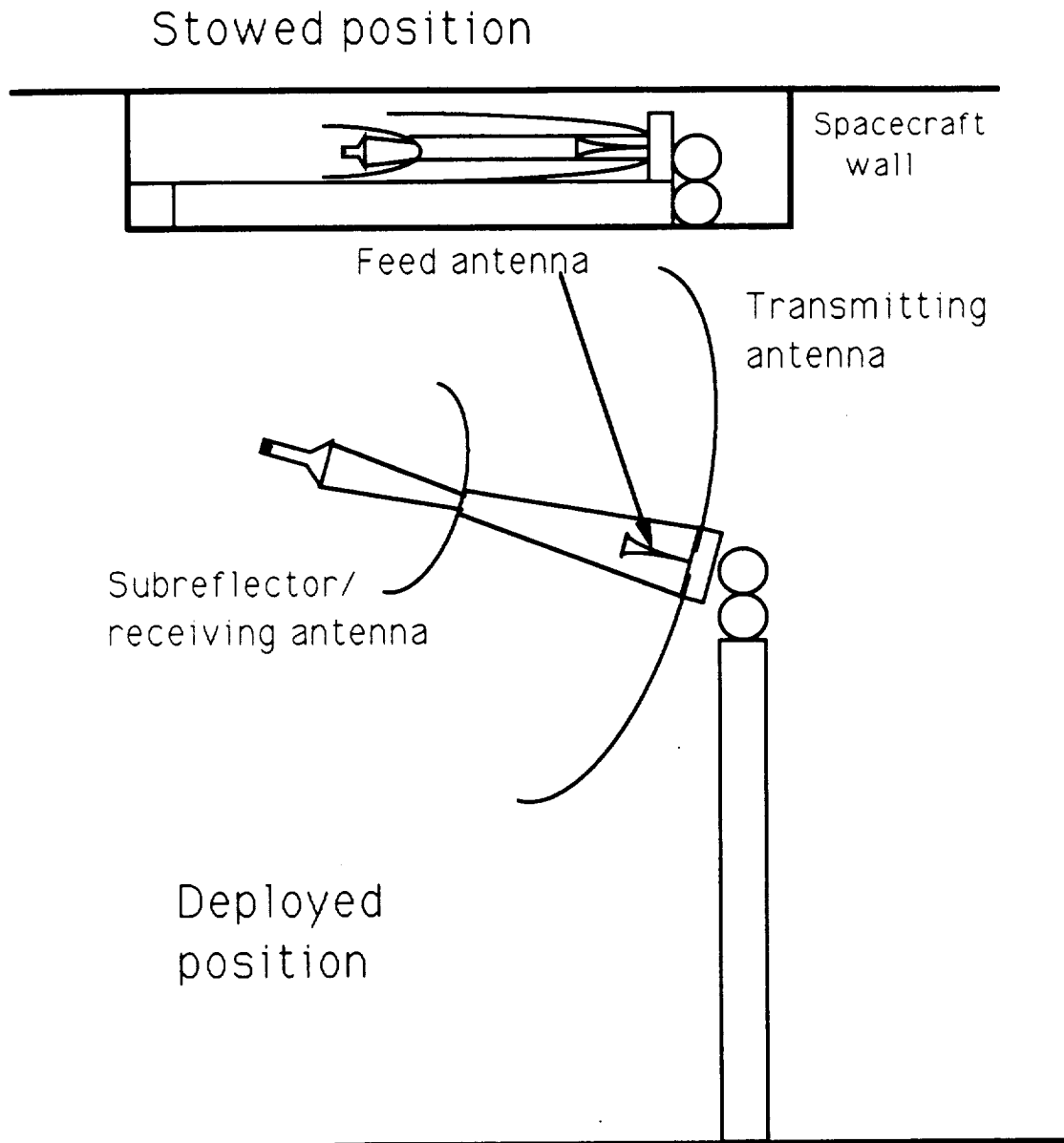


**Figure 4-16**

**System Configuration Selected for Columbiad High-gain Antennae**

#### **4.3.4 Descriptions of Communications Links**

This section expands on the overview given in Section 4.2.



#### 4.3.4.1 Earth to Low Earth Orbit.

Low-gain receiving and transmitting antennae are deployed on the PTLI stages to allow the transmission of commands to and of status data from the PTLI. During this phase of the mission, the guidance and navigation will be through special equipment designed for use with GPS, rather than the generalized communications equipment installed on the PTLI.

The payload modules, the PLM/habitat and the CM/ERM, are also equipped with low-gain equipment. The habitat contains the receiver/transmitter and related equipment for ready access by the astronauts. However, because the habitat will be covered with bags of regolith, the external communications equipment cannot be installed on the habitat. Instead, the antennae will be placed on the PLM, which will not be covered. Placement of the antennae will be as close to the habitat as possible to minimize transmission line losses. Two receiving and two transmitting antennae will be used, as enough position control is assumed to keep the spacecraft properly aligned.

The CM/ERM modules will initially be communicating with Mission Control through the low-gain equipment on the CM. This equipment serves the dual purpose of launch-to-LEO and reentry-landing communications. The CM also has two receiving and two transmitting antennae, both to ensure that at least one antenna of each type will be able to pick up signals and as backups.

Communications via the low-gain equipment will be maintained through docking and will be ceased only after the high-gain antennae have been deployed and their functionality verified. The rendezvous maneuvers will involve the transmission of video data which is used to align and dock the vehicles properly.

#### 4.3.4.2 Low Earth Orbit to Lunar Vicinity

Once the high-gain antennae have been deployed, DSN will be used for communications and monitoring. The PTLI and the payload modules will be connected by a databus; status data from the PTLI will then be sent through the payload modules until separation occurs. The high-gain equipment is deployed on the ERM and the PLM. As with the low-gain equipment, the receivers, transmitters, and related equipment are located in the habitat, while the antenna arm itself is contained in the PLM. The antenna arm deploys through spring action; stored elastic energy opens the reflector dishes, while actuators steer the subreflector and feed antenna. The fine adjustments allowed by the actuators allow for some optimization of the antennae's function.

The high-gain antennae on the PLM/habitat will maintain continuous communication with the Earth except at the end of the flight, when the spacecraft pass behind the Moon. The high-gain equipment on the ERM will be accessible to the astronauts through the data bus connecting the ERM and the CM. The video links will be supported during the flight in the event that an emergency occurs and visual feedback to Mission Control is needed to repair the problem. During the landing of the ERM/CM, Mission Control will monitor the performance of the ERM/CM through the high-gain equipment.

#### 4.3.4.3 Lunar Landing

At landing, the video links supported by the communications system will be used to verify that the landing site is flat and smooth enough for a safe landing. The spacecraft will be landing on the bright side of the moon, ensuring that communication will be possible continuously.

After the landing, the PLM/habitat will lower itself onto the lunar surface, making sure that the antenna arm is on the upper side of the habitat. The antennae will orient themselves to point to the Earth. The low-gain antennae will be used to communicate with the Rover. On the piloted missions, the astronauts will land, then prepare the BioCan for habitation. During this time, caution will need to be exercised to ensure that the antennae are not damaged while the bags of regolith are placed over the habitat. Should damage occur, the high-gain equipment on the ERM, which will be left online, will serve as a backup.

#### 4.3.4.4 Lunar Surface Operations

Lunar surface communications will primarily be concerned with Moon-Earth communication and habitat-Rover communication.

##### 4.3.4.4.1 Habitat

The need for careful placement of the communications equipment has been mentioned above. The receiving antenna will always be on so that any emergency commands or data may be received. Although the transmitter systems could be turned off when not in use to conserve power, the startup transients, warmup time, and lack of immediate communication capacity argue against such shutdowns.

Internal communications within the habitat will be accomplished through a telephone system. The phone system was chosen over an intercom system for several reasons:

increased privacy; possible use for modems connecting computers in later, better-equipped missions; the phones could potentially be connected to the transmitter system for direct voice links. The flexibility provided by the phones outweighs their added cost, weight, and complexity. However, an intercom system should be installed for use in an emergency when time is short and as a backup system.

#### 4.3.4.4.2 Lunar Rover

The Lunar Rover is equipped with a full set of communications equipment: two receiving antennae, one low-gain and one high-gain, and two transmitting antennae, one low- and one high-gain. For operations within the line-of-sight of the habitat, the Rover will use its low-gain antennae. Outside of LOS, however, the Rover must communicate directly to Earth. Should one of the high-gain antennae fail, the other can be pressed into service as the transmitting or receiving, whichever the case may be, antenna if the astronauts move the transmission lines to the appropriate machinery and adjust the tuning stub. Alternatively, the low-gain antennae can be used.

#### 4.3.4.5 Reentry

On the return flight to Earth, the astronauts initially communicate through the high-gain equipment on the ERM. Once the ERM and the CM have decoupled, the astronauts will depend on the communications capability of the CM. Two of the four antennae on the CM are receiving; the other two are for transmitting. The paired antennae assure that, if the CM is properly oriented, at least one of the pair will be able to receive/transmit, and the antennae back each other up.

During reentry, a plasma sheath forms on the spacecraft. The plasma's evanescence causes communications to black out since the waves cannot propagate through the plasma. After the spacecraft has slowed and cooled down enough to eliminate the sheath, communications will again be through the low-gain antennae on the CM. Ground station communications will bring the CM down to the landing site.

#### 4.3.5 Backup Mechanisms for Communications Equipment

The parallel elements in the receiver and transmitter systems provide some measure of backup which was deemed to be enough for the reliability requirements of this mission [Weiss, 1992]. In addition, the linkages between the different modules allow the use of low-gain antennae should the high-gain antennae fail; receiver power calculations show that DSN should be able to receive signals even from the low-gain spacecraft antennae. A way

to backup the CM's low-gain receivers with its transmitters, and vice versa, is being worked out. Given the sensitivity of superhets, receiving a full-power transmission from DSN on the spacecrafts' low-gain antennae appears to be possible. On the lunar surface, the habitat's communications equipment is backed up by the systems on the CM/ERM and on the Lunar Rover. However, the high-gain antennae on the Rover are only backed up by its low-gain antennae; should the Rover be out of either the habitat's or the CM/ERM's LOS, then communications will not be possible. The placement of relay satellites at the Lagrange points between the Earth and the Moon may ameliorate this problem.

#### **4.4 Design of Onboard Computer Systems**

The computing system architecture and fault tolerant topology are designed so that the overall architecture is the same for both piloted and precursor missions. Both PTLI stages will have identical equipment, and the CM/ERM will have the same setup as the habitat/PLM stages. The benefit of using a similar setup with the same equipment for the CM/ERM and the habitat/PLM is that an equipment malfunction on the CM/ERM might be remedied on the lunar surface by stripping equipment from the habitat. The equipment on the habitat could be replaced on subsequent missions.

Figure 4-17 shows the general computer architecture for Project Columbiad. The architecture uses a databus. Each subsystem has access to the databus and the protocol of the databus allows information to be passed between each of the systems, usually via the main computers, giving priority to flight critical information.

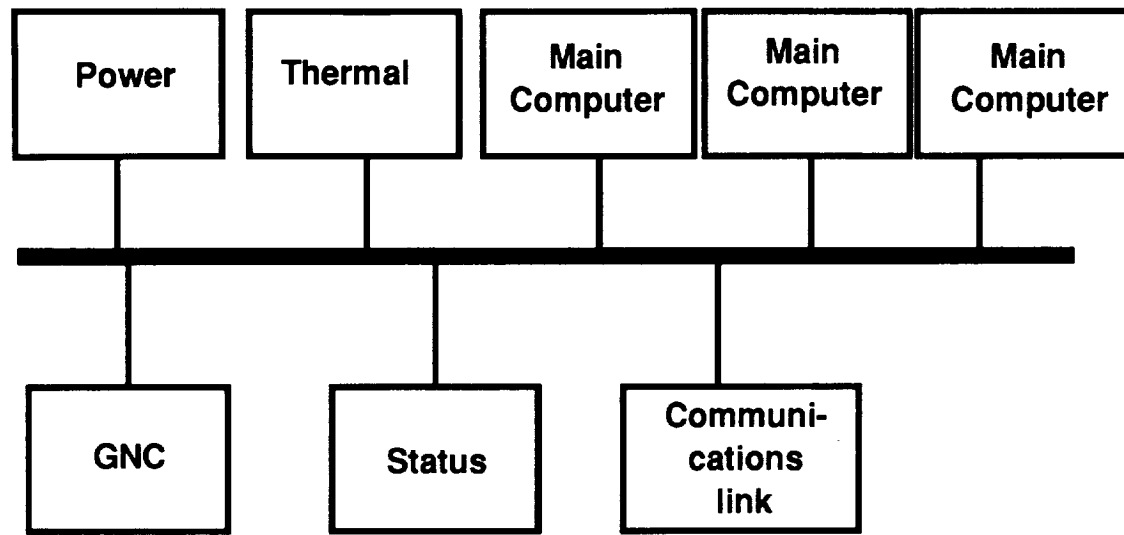


**Figure 4-17**  
**Architecture of Columbiad's Computing System**

The fault tolerant topology used for the computing systems is a voting system in which three computers each process all the information and compare commands before transmitting commands through the databus to the actuator systems. More details on the selection of the fault tolerance design appear in section 4.4.2.

#### **4.4.1 Computer Architecture**

Computer architectures fall into one of two primary categories: centralized computing and distributed computing [Wertz and Larson, 1991]. In a centralized architecture, processors within each subsystem are tied directly to a central processor which manages the information (star topology). In a distributed architecture, each of the processors have access to a common bus or ring and the processors are given control of the bus according to a chosen protocol. Figure 4-18 shows the common centralized star, distributed bus and distributed ring architectures.

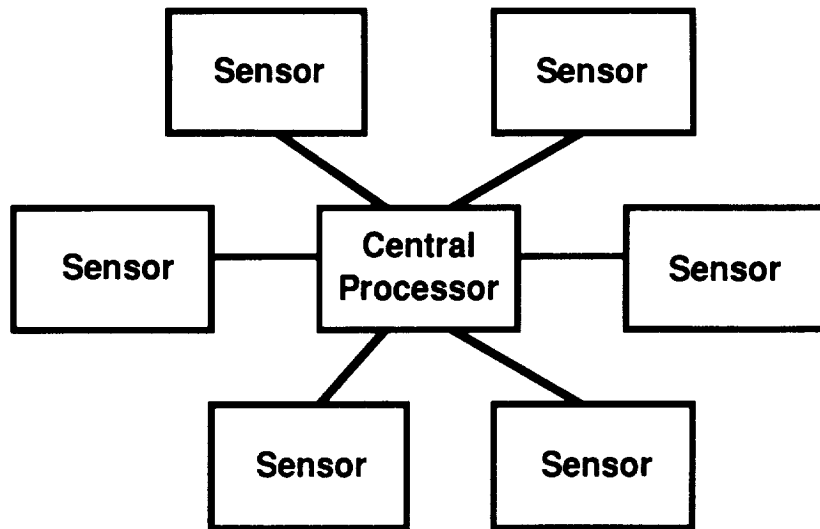


**Figure 4-18a**  
**Star Topology**

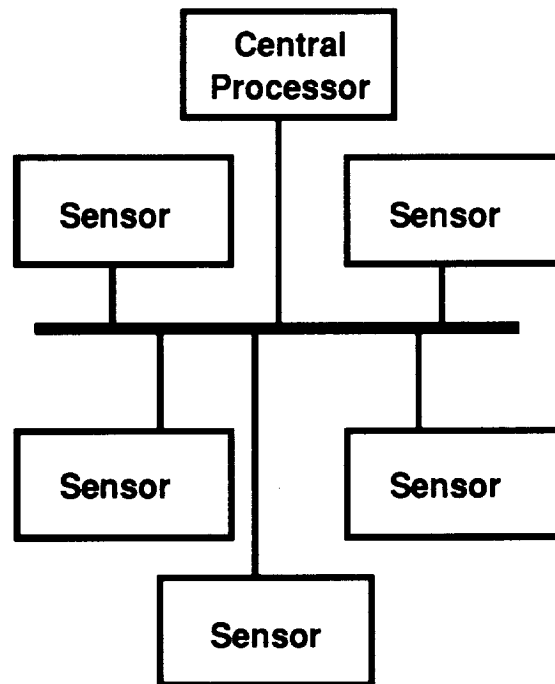


**Figure 4-18b**  
**Linear Data Bus Topology**

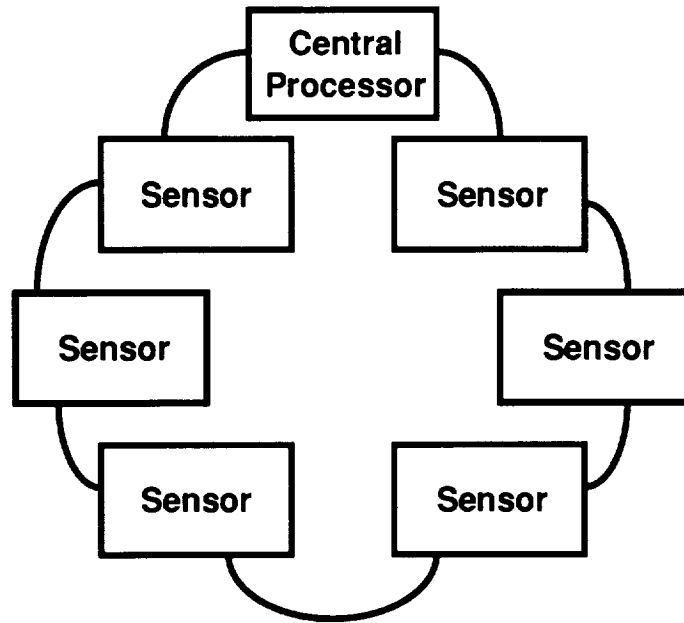


**Figure 4-18c**  
**Ring Topology**

**Figure 4-18**  
**Common Computer Architectures**

The disadvantage of the centralized star configuration is that expanding the number of nodes require both hardware and software changes in the main computer. Since there is only one path between any processor and the central computer, redundant cable must be added for transmission of information between the two processors. The biggest disadvantage is that the central processor is a single point failure because all information must pass through the central processor. Another concern with passing all of the information through the central processor is that it slows down responses to each of the subsystems because the subsystems are competing for processing resources. The advantage of the system is that a problem in one of the processor interfaces will not affect any of the other interfaces (as long as it is not the central processor).

The advantage of distributed systems is that the system can be expanded rather easily with smaller changes in software than in a centralized system. The disadvantage in the ring system shown is that a problem in one of the interfaces interrupts all components on the ring. In the bus configuration, the single point failure is now the data bus. An additional

disadvantage of a star configuration is that additional software is required to manage the protocol for bus access.

These architectures are not yet fault tolerant. A fault in any of these architectures could still lead to mission abort and that is why redundancy needs to be added to the system so that it can withstand a fault in any mission critical system and still continue with the mission; and therefore meet the Level 1 requirements of 99.9% for crew survival and 95% for mission success.

#### **4.4.2 Computer Fault Tolerance**

The on-board computer interfaces with guidance and control functions, status functions, crew systems monitoring functions, and communication functions to name a few. The processors and databus will provide the link between the communications network and the rest of the systems and are, therefore, critical to crew safety as well as mission success. Fault tolerance in the architecture of the computing systems of each of the vehicles will enhance the probability of crew safety and mission success even with a failure within the system.

Three topologies for fault tolerance in computing systems are pair of pairs, voting, and quizzing.

The chosen fault tolerant configuration for Project Columbiad computer systems is the voting configuration which can utilize any odd number of computers (initially). The minimum number of computers used is three computers which each run the flight code separately. A comparator compares the commands from each of the three computers. If one of the computers gives a different command than the other two than the "odd man out" concept applies and the "wrong" computer is disregarded until it is checked out. Figure 4-19 shows the voting configuration.



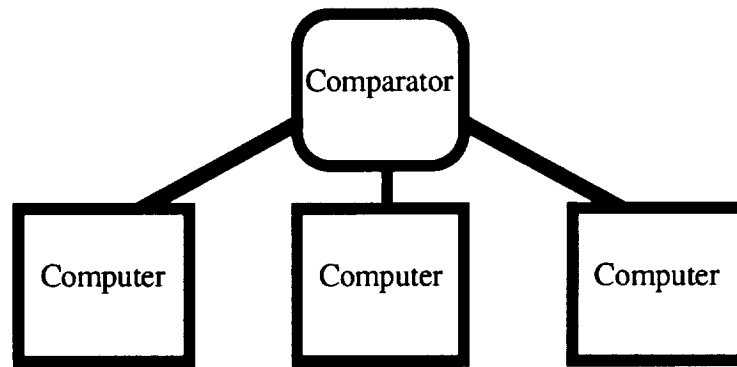


**Figure 4-19**  
**Voting Fault Tolerance**

The second topology is a quizzing computer topology. Two computers run the same flight code. If the two computers come up with different commands a third computer is invoked by running test questions with known answers on both of the computers. The computer that gives a wrong answer in the test sequence is disregarded until corrective measures can be taken on that unit. Figure 4-20 shows the quizzing configuration.

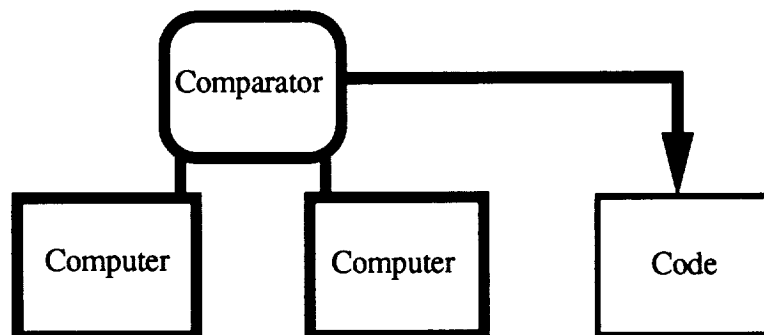


**Figure 4-20**  
**Quizzing Fault Tolerance**

The disadvantage of a quizzing topology is that there could be a delay in issuing a command while the test code is verifying the computers. However, when time is not an issue there is a power consumption advantage of having only two processors operating.

During non-critical phases of the mission, the voting configuration could revert to the quizzing configuration with the third computer either powered down or diverted to scientific payload functions.

The pair of pairs topology is used at a minimum of two pairs of computers (four computers total) with two levels of voting. The first pair of computers both run the same flight code. A comparator compares the results of both computers before relaying commands. The hope is that if one of the computers malfunctions, it will give an "incorrect command" and the two computers' commands won't agree. In this event the comparator switches control over to a second pair of computers which have also been running the code. Figure 4-21 shows the pair of pairs configuration.

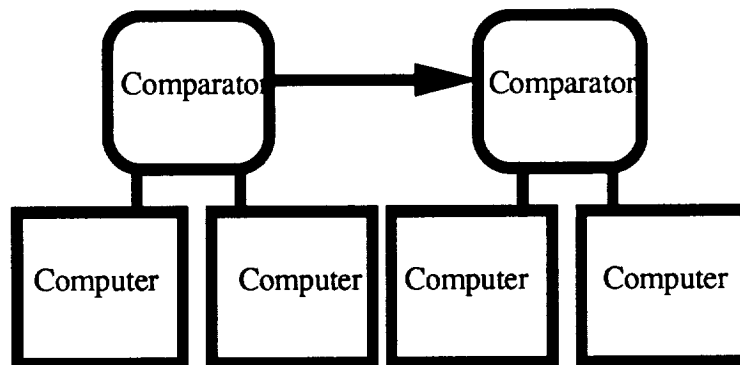


**Figure 4-21**  
**Pair of Pairs Fault Tolerance**

The primary disadvantage of the pair of pairs configuration is that the minimum number of computers would be four and since cost, weight, size and power consumption would all go up, this configuration is inefficient.

#### **4.4.3 Data Bus Fault Tolerance**

Due to the large data rates which will only increase in future missions, an optical network databus will prevent a complete rewiring of the vehicles in the future and thus providing a solid base on which to build the computing network. While wire networks are heavy and limited to data rates in the Gbit range, optical networks can handle data rates in the terabit range. However, due to the nature of optical networks a linear bus topology is extremely limited [DeRuiter]. The linear bus depicted in Figure 4-17 will actually be a multi-node distributed star topology as shown in Figure 4-22 (not to be confused with the centralized star computer architecture).

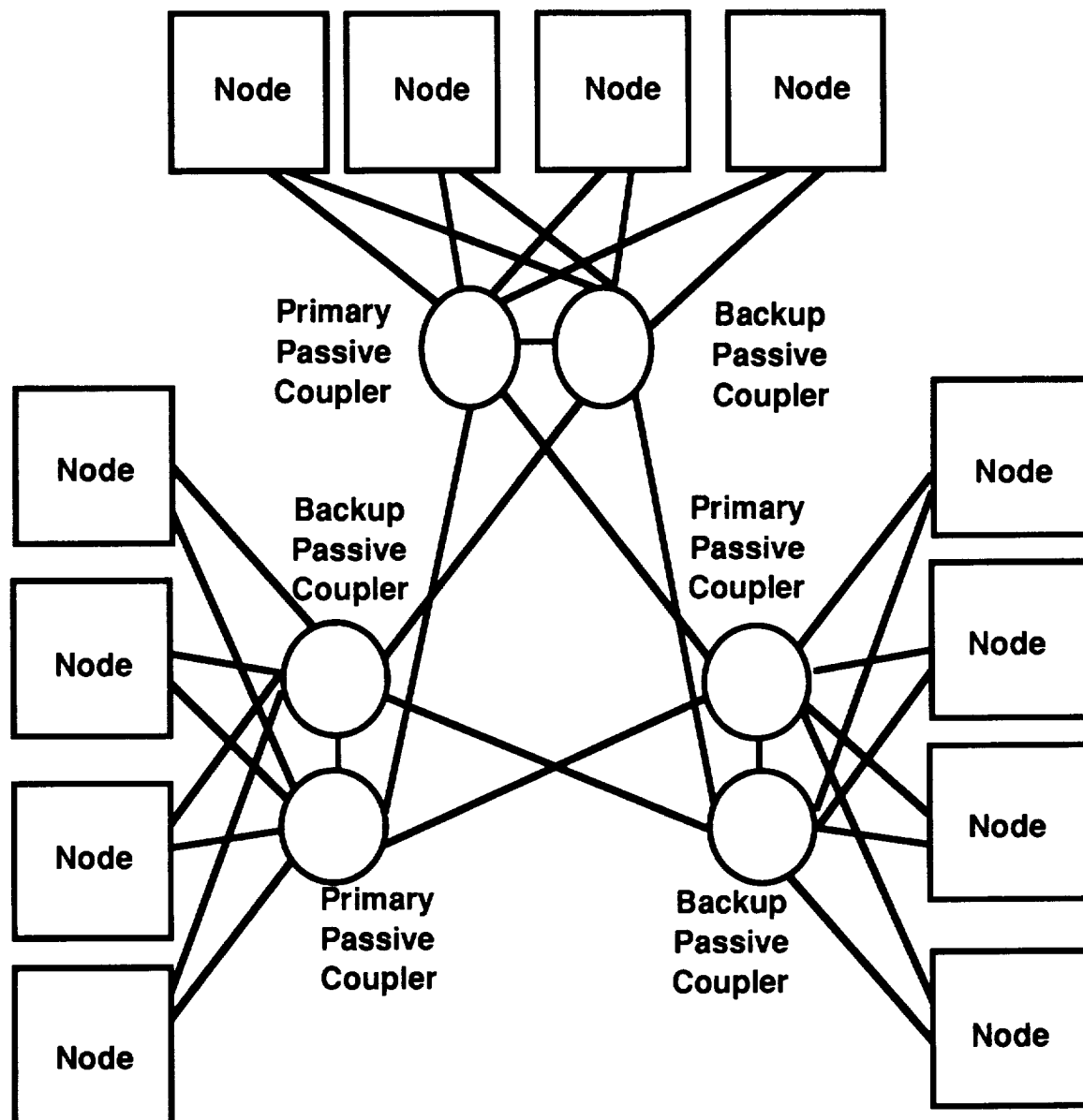


**Figure 4-22**  
**Optical Databus Multi-node Fault Tolerant Topology**

Each node in the multi-node distributed star topology represents one of the subsystem interfaces which would have access to the linear data bus shown in Figure 4-17. The nodes are each connected to a passive star coupler which will connect (via protocol) the nodes with which communication is desired. Since there is a limit to the number of nodes that a coupler can support, one or two of the interfaces connect with other passive couplers which can access even more nodes. Also notice in Figure 4-22 that each node is cross-strapped to a pair of couplers. This cross strapping will allow automatic switch-over at the

component level relieving a system level processor (the main computer) of the management task (i.e., this reduces the executive throughput and eliminates much fault tolerant software).

Protocols for controlling the databus can also improve reliability of the bus. The protocol controls traffic on the bus. This multi-node optical databus will use a transmit upon request protocol which allows nodes that are not in use to be powered down thus reducing power dissipation which improves the reliability.

#### **4.4.4 Processor Sizing**

Processing resources are the computer capabilities provided to the vehicle's various systems for relaying information and distributing commands. The driving factors in sizing a processing system are the memory [Mbits], the throughput [KIPS], and I/O data rates [bps]. The memory measures the storage capacity of information, the throughput measures the number of instructions required to manage information, and the I/O data rates are the number of bits per second that are read in from sensors or commands output to other systems.

##### **4.4.4.1 Data Rate Estimates**

The peak estimate data rate for the entire mission profile is 7 Mbps . This incorporates 1 real time color video channel at 44 Mbps compressed to 8%, 0.5 Mbps of voice link and 2 Mbps for data link. This gives a data rate of approximately 7 Mbps which would only be encountered on the habitat or crew module links.

##### **4.4.4.2 Crew Module Throughput Estimates**

In estimating the required throughput necessary for the CM, first the application functions are listed with their estimated memory and throughput requirements. Most of the application functions estimates were taken from tables in Wertz and Larson, 1991, either by direct correlation or similarity of function.

The operating system software manages the application functions of the computer. Executive software schedules time for the application software to complete its tasks. The throughput of the executive is  $0.3 \times n$  where  $n$  is the number of tasks scheduled per second. The value of  $n$  is shown in Table 4-3 and is calculated by summing up the number of applications at each frequency, multiplying this number by the respective frequencies

and summing up the number of functions per second. Assuming four schedulable tasks per function [Wertz and Larson, 1991],  $n$  is determined.

I/O Device Handler throughput is calculated 0.05 times  $m$ , the number of data words handled per second. The value of  $m$  is calculated by dividing the data rate of 7 Mbps by 32-bit words.

Margin calculations were based on suggested margins in Wertz and Larson, 1991. The uncertainty in software requirements at this stage of design requires a generous margin for growth. 100% of the total software and throughput estimate was allotted for requirements uncertainty. Since software is easier to change than hardware, this margin will also allow for increased software requirements occurring late in the program development. The on-orbit spare is the amount of memory and throughput on launch so that there is still room to add corrections or calibrate systems. As suggested by Wertz and Larson, 1991, 100% of the total software and throughput estimate plus the requirements uncertainty is used. The total estimate of computing requirements is the total software and throughput estimate plus both margin calculations.

**Table 4-3: Crew Module and Earth Return Module Throughput Estimates**

Component	Estimation Source	Required Memory		Freq Hz	Required Throughput KIPS
		Code K words	Data K words		
Application Functions					
Attitude Sensor Processing					
INS	4*Sun sensors	2.00	0.40	4.00	4.00
Star Tracker	W&L Table 16-6	2.00	15.00	0.01	2.00
GPS	Copernicus			1.00	36.00
Joystick				10.00	2.00
Attitude Sensor Processing from ERM					
Star Tracker	W&L Table 16-6*	2.00	15.00	0.01	2.00
Sun sensors	W&L Table 16-6	0.50	0.10	1.00	1.00
Radar Altimeter		0.50	0.10	1.00	1.00
Antenna Beacons	Fast Star Tracker	2.00	15.00	1.00	2.00

<b>Attitude Sensor Processing from LBM</b>					
Laser Docking	ground controlled				
Docking Video	ground controlled				
<b>Attitude Determination&amp;Control</b>					
Kinematic Integration	W&L Table 16-6	2.00	0.20	10.00	15.00
Error Determination	W&L Table 16-6	1.00	0.10	10.00	12.00
Thruster Control	W&L Table 16-6	0.60	0.40	2.00	1.20
Ephemeris Propagation	W&L Table 16-6	2.00	0.30	1.00	2.00
Orbit Propagation	W&L Table 16-6	13.00	4.00	1.00	20.00
<b>Autonomy</b>					
Complex	W&L Table 16-6	15.00	10.00	10.00	20.00
<b>GNC Subtotal</b>		42.60	60.60		120.20
<b>Communications</b>					
Command Processing	W&L Table 16-6	1.00	4.00	10.00	7.00
Telemetry Processing	W&L Table 16-6	1.00	2.50	10.00	3.00
<b>Fault Detection</b>					
Monitors	W&L Table 16-6	4.00	1.00	5.00	15.00
Fault Correction	W&L Table 16-6	2.00	10.00	5.00	5.00
<b>Power</b>					
Power Management	W&L Table 16-6	1.20	0.50	1.00	5.00
<b>Thermal</b>					
Thermal Control	W&L Table 16-6	0.80	1.50	0.10	3.00
<b>Status</b>					
Temperatures	off bus				
Power Supplies	off bus				
Equipment Self Tests	Copernicus/off bus	2.00	15.00	1.00	10.00
<b>Crew Interface</b>					
Graphics Overlays		15.00	15.00	10.00	20.00
<b>Besides GNC Subtotal</b>		12.00	34.50		48.00
<b>Appl Total</b>		54.60	95.10		168.20
<b>Operating System</b>					
Executive	W&L Table 16-7	3.50	2.00	n= 384.44	115.33
I/O Device Handlers	W&L Table 16-7	2.00	0.70	m=2.18e5	10900.00
Built-in-Tests	W&L Table 16-7	0.70	0.40		0.50
<b>Oper Sys Total</b>		176.00	257.80		11490.43

<b>Ttl Software &amp; Throughput Est</b>		230.60	352.90		11658.63
<i>Margin Calculations</i>					
Requirements Uncertainty	100%	230.60	352.90		11658.63
On-orbit spare	100%	461.20	705.80		23317.26
<b>EST of Comp Req</b>	W&L Table 16-8A	922.40	1411.60		46634.53

The totals indicate that the Fairchild Solid State Memory can handle the calculated memory requirements and the HP GaAs Computer which has a capacity of 140 MIPS can handle the 47 MIPS calculated throughput requirements.

#### 4.4.4.3 Earth Return Module Throughput Estimates

Only the high gain antenna system is on the ERM, and all sensors which require monitoring will interface with the databus that leads to the processors on the CM. All processing for the ERM will take place on the CM.

#### 4.4.4.4 Habitat Throughput Estimates

The habitat memory and throughput estimates are calculated in the same manner as the CM memory and throughput estimates are calculated. Differences are the result of different GNC sensors used on each stage. Again the HP GaAs Computer and a Fairchild Solid State Memory can handle the processing requirements of the habitat. See Table 4-4.

**Table 4-4: Habitat Throughput Estimates**

Component	Estimation Source	Required Memory		Freq Hz	Required Throughput KIPS
		Code K words	Data K words		
<i>Application Functions</i>					
<i>Attitude Sensor Processing</i>					
INS	4*Sun sensors	2.00	0.40	4.00	4.00
Star Tracker	W&L Table 16-6	2.00	15.00	0.01	2.00
Radar Altimeter		0.50	0.10	1.00	1.00
Sun Sensor	W&L Table 16-6	0.50	0.10	1.00	1.00
GPS	Copernicus			1.00	36.00
<i>Attitude Determination&amp;Control</i>					
Kinematic Integration	W&L Table 16-6	2.00	0.20	10.00	15.00

Error Determination	W&L Table 16-6	1.00	0.10	10.00	12.00
Thruster Control	W&L Table 16-6	0.60	0.40	2.00	1.20
Ephemeris Propagation	W&L Table 16-6	2.00	0.30	1.00	2.00
Orbit Propagation	W&L Table 16-6	13.00	4.00	1.00	20.00
<b>Autonomy</b>					
Complex	W&L Table 16-6	15.00	10.00	10.00	20.00
<b>Communications</b>					
Command Processing	W&L Table 16-6	1.00	4.00	10.00	7.00
Telemetry Processing	W&L Table 16-6	1.00	2.50	10.00	3.00
<b>Fault Detection</b>					
Monitors	W&L Table 16-6	4.00	1.00	5.00	15.00
Fault Correction	W&L Table 16-6	2.00	10.00	5.00	5.00
<b>Power</b>					
Power Management	W&L Table 16-6	1.20	0.50	1.00	5.00
<b>Thermal</b>					
Thermal Control	W&L Table 16-6	0.80	1.50	0.10	3.00
<b>Status</b>					
Temperatures	pulled off bus				
Power Supplies	pulled off bus				
Equipment Self Tests	Copernicus/off bus	2.00	15.00	1.00	10.00
<b>Applications Total</b>		<b>50.60</b>	<b>65.10</b>		<b>162.20</b>
<b>Operating System</b>					
Executive	W&L Table 16-7	3.50	2.00	n= 268.44	80.53
I/O Device Handlers	W&L Table 16-7	2.00	0.70	m=2.18e5	10900.00
Built-in-Tests	W&L Table 16-7	0.70	0.40		0.50
<b>Oper Sys Total</b>		<b>102.40</b>	<b>117.70</b>		<b>11261.43</b>
<b>Ttl Software &amp; Throughput Est</b>		<b>153.00</b>	<b>182.80</b>		<b>11423.63</b>
<b>Margin Calculations</b>					
Requirements Uncertainty	100%	153.00	182.80		11423.63
On-orbit spare	100%	306.00	365.60		22847.26
<b>EST of Comp Req</b>	<b>Total + Spare</b>	<b>612.00</b>	<b>731.20</b>		<b>45694.53</b>



#### 4.4.4.5 Primary Trans-Lunar Injection Estimates

The estimated memory and throughput requirements for the PTLI stage is shown in Table 4-5 and calculated the same as the CM memory and throughput was calculated. Notice however, the different value for m, the number of data words per second. The value of m for the PTLI stage was calculated using a data rate of 2 Mbps divided by 32-bit words.

**Table 4-5: PTLI Throughput Estimates**

Component	Estimation Source	Required Memory		Freq Hz	Required Throughput KIPS
		Code K words	Data K words		
<i>Application Functions</i>					
<i>GNC</i>					
<i>Attitude Sensor Processing</i>					
GPS	Copernicus			1.00	36.00
Earth sensors	W&L Table 16-6	1.50	0.80	1.00	12.00
Rate Gyros	W&L Table 16-6	0.80	0.50	10.00	9.00
<i>Attitude Determination&amp;Control</i>					
Kinematic Integration	W&L Table 16-6	2.00	0.20	10.00	15.00
Error Determination	W&L Table 16-6	1.00	0.10	10.00	12.00
Thruster Control	W&L Table 16-6	0.60	0.40	2.00	1.20
Ephemeris Propagation	W&L Table 16-6	2.00	0.30	1.00	2.00
<i>Autonomy</i>					
Complex	W&L Table 16-6	15.00	10.00	10.00	20.00
<i>Communications</i>					
Command Processing	W&L Table 16-6	1.00	4.00	10.00	7.00
Telemetry Processing	W&L Table 16-6	1.00	2.50	10.00	3.00
<i>Fault Detection</i>					
Monitors	W&L Table 16-6	4.00	1.00	5.00	15.00
Fault Correction	W&L Table 16-6	2.00	10.00	5.00	5.00
<i>Power</i>					
Power Management	W&L Table 16-6	1.20	0.50	1.00	5.00
<i>Thermal</i>					
Thermal Control	W&L Table 16-6	0.80	1.50	0.10	3.00
<i>Status</i>					

Temperatures	off bus				
Power Supplies	off bus				
Equipment Self Tests	Copernicus/off bus	2.00	10.00	1.00	10.00
<b>Appl Total</b>		36.40	42.60		167.20
<i>Operating System</i>					
Executive	W&L Table 16-7	3.50	2.00	n=312.4	93.72
I/O Device Handlers	W&L Table 16-7	2.00	0.70	m=6.2e4	3125.00
Built-in-Tests	W&L Table 16-7	0.70	0.40		0.50
<b>Oper Sys Total</b>		75.20	86.20		3484.62
<b>Ttl Software &amp; Throughput Est</b>		111.60	128.80		3651.82
<i>Margin Calculations</i>					
Requirements Uncertainty	100%	111.60	128.80		3651.82
On-orbit spare	100%	223.20	257.60		7303.64
<b>EST of Comp Req</b>	W&L Table 16-8A	446.40	515.20		14607.28

The RH32 Data Processor which can handle 20 MIPS will be used to handle the calculated throughput of 15 MIPS. Again the Fairchild Solid State Memory can handle the memory requirements for the PTLI stage.

#### **4.4.5 Data Storage Equipment**

Depending on mission goals and requirements, experimental data will need to be stored. The current design calls for one tape machine in the CM and one in the habitat which can be used to record data. Optical, tape and solid state memories were considered for this purpose. Optical storage provides immediate access to information but still remains the most expensive of the three types. Solid state memories cannot provide the same order of magnitude of storage as optical or tape machines and are also susceptible to soft errors from radiation. Solid state also provides immediate access to information. The tape storage medium provides the most memory of the three media and is the least expensive. The disadvantage with tape is that it is serial access and requires time to access specific information. However, magnetic data compression techniques have increased the density of data on the tape keeping tape as the most economical form of data storage as long as immediate access to information is not a requirement.

## **4.5 Modulation and coding**

In order to transmit the information across the channel, it must be modulated on a carrier frequency. This is important because only a given frequency band is available for the communication link. The information results in deviations of the frequency of the transmitted wave from the carrier frequency. This ensures that the signal can be transmitted on different wavebands depending on the application no matter what the frequencies in the information are.

In order to reduce the probability of undetected errors in the channel it is important that the information being transmitted is coded so that it has redundancies in it. These can be used to detect errors that might occur in the transmitted data because the channel is not ideal. It is also possible to correct errors in the transmitted data. The level of redundancy and the suitability of the code to the channel conditions determine how many errors can be detected and how many can be corrected.

### **4.5.1 Why digital ?**

The information being encoded on the carrier can be in one of two forms.

1. Analog : the signal can take a continuum of values and is defined for all values of time
2. Digital: the signal can only take a set of discrete values determined by the number of bits. The signal is also only defined for a set of time signals. It is therefore discrete both in space and time. Digital systems can be made to capture all the needed information of an analog signal if the sampling rate, the number of bits, and the analog values represented by the bits are chosen wisely.

Digital communication was chosen for the reasons listed below:

1. It is the standard used in existing satellite systems. Both TDRSS and DSN which we will be using use digital communications. We need to be compatible with them.
2. Good methods of encoding the information have been developed for error detection and correction. Encrypting methods have also been developed.
3. There is a lot of flexibility in digital signal processing. There are easy ways to store information so that it can be accessed randomly (RAM). A lot of algorithms have also

been developed for processing digital data and the hardware for the processing has also been improved greatly.

4. Unlike in analog communication, the errors in digital signals can be found and corrected to any desired accuracy. This is very important since the mission will be manned and it is critical that the communication link be reliable to a high accuracy to ensure the safety of the astronauts.

#### **4.5.2 Modulation**

We looked at three different modulation schemes to use to see which was best suited for our application. The three schemes were :

1. QPSK: This stands for quadrature phase shift keying. The signal transmitted within a time interval  $T$  (the reciprocal of the data transmission rate) is one of four signals. These signals are the carrier signal offset by one of four phases. The signals are given by equations 4-1 through 4-5.

$$s_1(t) = \sqrt{2P} \cos(\omega_c t - 45) \quad (4-1)$$

$$s_2(t) = \sqrt{2P} \cos(\omega_c t + 45) \quad (4-2)$$

$$s_3(t) = \sqrt{2P} \cos(\omega_c t + 135) \quad (4-3)$$

$$s_4(t) = \sqrt{2P} \cos(\omega_c t - 135) \quad (4-4)$$

$$\text{i.e. } s_i(t) = \sqrt{P} [\pm \cos(\omega_c t) \pm \sin(\omega_c t)] \quad (4-5)$$

Since one of four symbols can be transmitted at a time, two bits are encoded in a symbol . It is these two bits that determine the sign of the cos and sine in the last equation above. The analog analogue of this is phase modulation.

2. OKQPSK, or offset quadrature phase shift keying. It is similar to QPSK except that the cosine and the sine in the last equation in the previous section are out of phase by one half period. The symbols are therefore of the form given in equation 4-6.

$$s_i(t) = \sqrt{P} [\pm \cos(\omega_c t) \pm \sin(\omega_c (t + T/2))] \quad (4-6)$$

This also encodes two bits in one symbol.

3. FFSK, or fast frequency shift keying. One of two frequencies is transmitted depending on the bit being transmitted. The mean of the frequencies being transmitted is the carrier frequency and the difference between the two frequencies is  $\pi/T$ .

$$s_i(t) = \sqrt{P} \sin(\omega_i t) \quad (4-7)$$

$$i = 1, 2 \quad (4-8)$$

$$\omega_1 - \omega_2 = \pi/T \quad (4-9)$$

The analog analogue of this is frequency modulation.

In choosing between the schemes above, the factors considered were:

1. The effect of thermal noise on the communication link.
2. The effect of band limitation and delay distortion in the channel
3. The degradation of the link as a result of interference by adjacent channels
4. Co-channel interference
5. Phase and amplitude non-linearities present in the amplifier.
6. Ease of modulation and detection.

All this analysis was done assuming that the channel was memoryless and that the noise levels and the transmission power was the same for all the schemes.

#### 4.5.2.1 The effect of thermal noise

Because of ambient noise in space, rain, and in the receiver, the transmitter signal is not the same as the one received at the end of the channel. It is possible that because of noise, a symbol can be mistaken for another if it is distorted enough. The likelihood of this occurring obviously depends on how alike the symbols used in communication are. To get the probability that this happens, it is assumed that a matched filter is used to detect the signals and a comparator decides what the most likely value of the symbol is.

$$r(t) = s_i(t) + n(t) \quad (4-10)$$

where:  $r(t)$  is the received signal  
 $s(t)$  is the symbol that was transmitted  
 $n(t)$  is the noise added to the symbol

It can be shown that for all the modulation schemes listed above, the probability that any bit will be wrong is given by the equation 4-11

$$P_b = 0.5 \operatorname{erfc}(\sqrt{E_b(1 - \rho)/2N_0}) \quad (4-11)$$

where:

$$E_b = \int_0^T s_i(t)s_i(t) dt \quad (4-12)$$

- This is the energy per bit of information and is equal to the power transmitted divided by the data rate

$$\rho = \frac{1}{E_b} \int_0^T s_1(t)s_2(t) dt \quad (4-13)$$

- This is the correlation coefficient and is a measure of how alike the symbols are.
- $N$  is the noise level.

$$\operatorname{erfc}(x) = \frac{2}{\sqrt{\pi}} \int_x^\infty e^{-y^2} dy \quad (4-14)$$

For all the modulation schemes that we looked at the correlation coefficient is -1 and so the effect of thermal noise is not a factor in choosing the modulation scheme. The probability of error in an ideal memoryless channel with white noise is given by equation 4-15.

$$P_b = \frac{1}{2} \operatorname{erfc} \sqrt{\frac{E_b}{N_0}} \quad (4-15)$$

#### 4.5.2.2 Spectra

The shape of the spectrum of the modulation scheme determines the efficiency with which the modulation scheme uses the bandwidth. Of the three modulation schemes, FFSK has the widest main lobe but subsequent lobes fall off faster and so FFSK has the smallest effective bandwidth.

#### 4.5.2.3 Adjacent channel interference

The extent to which the performance of the modulation scheme is affected by interference from adjacent channels is important. The communication link will be two way and so the further apart the carrier frequencies must be to avoid interference, the more complicated the design of the antennae required. Table 4-6 gives the required channel separation for a maximum loss in  $E_b/N_0$  of 1 dB. The channel separation is given in R which is the bit rate in the channel.

**Table 4-6: Adjacent channel power (dB)**

	<b>0 dB</b>	<b>+10 dB</b>
QPSK	4.5 R	13.5R
OKQPSK	5.0R	14.0R
FFSK	1.5R	2.5R

Less separation is required by FFSK for the same performance at both values of interfering channel power.

#### 4.5.2.4 Co-channel interference

Sometimes there is another low power signal within the same frequency band. This could be an unmodulated carrier in the same channel or it could be another transmission at much lower power. It has been shown empirically that FFSK is the most resistant of the three types of modulation to co-channel interference.

#### 4.5.2.5 Phase noise

The regeneration of the carrier at the demodulating end of the channel is not perfect. As a result there are ambiguities in phase which lead to degradations in channel performance. The measure of the vulnerability of a modulation scheme to phase noise in carrier recovery is given by the relationship between the phase reference signal to noise ratio and the probability that a bit will be wrong. It has been found empirically that FFSK needs 2 dB less SNR (signal to noise ratio) for the same probability of error as OKQPSK and 5 dB less SNR for the same probability of error as QPSK. FFSK performs better with an imperfect carrier.

#### 4.5.2.6 Band limitation and delay distortion

The detection filter acts as a band filter and also causes distortion of the delay of different frequencies. This causes a degradation in  $E_b/N_0$ . This degradation is smaller for FFSK than it is for the other modulation schemes.

As a result, FFSK was chosen as the modulation scheme. The differences in the detection and modulating circuitry for the different schemes is not significant.

#### 4.5.2.7 Modulation circuitry for FFSK

It can be shown that the FSK signals can be written as shown in equation 4-16.

$$s(t) = \cos(\psi_k) \cos\left(\frac{\pi t}{T}\right) \cos(\omega_c t) - d_k \cos(\psi_k) \sin\left(\frac{\pi t}{T}\right) \sin(\omega_c t) \quad (4-16)$$

where  $\psi_k$  is the phase at the beginning of the interval of time  $T$ . In this form, it is clear that this can be easily modulated using the structure shown below. This modulation circuitry, shown in Figure 4-23, is very similar to that for QPSK and OKQPSK.

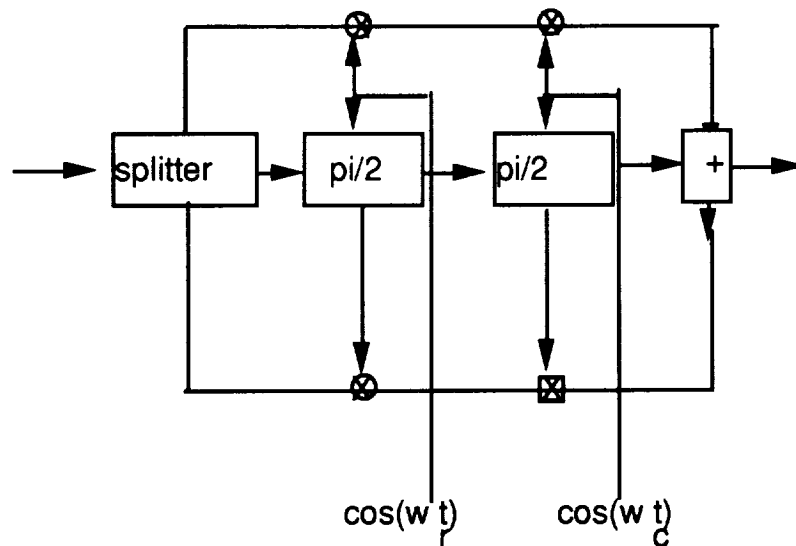


**Figure 4-23**  
**FFSK Modulation Structure**

#### 4.5.2.8 Demodulation Circuitry for FFSK

The general structure of the demodulating circuitry is the same for all the modulation schemes above. The different units required are a carrier recoverer, a clock recoverer , a



unit to detect how like one of the two valid symbols is received, and a combiner. This is shown in Figure 4-24.

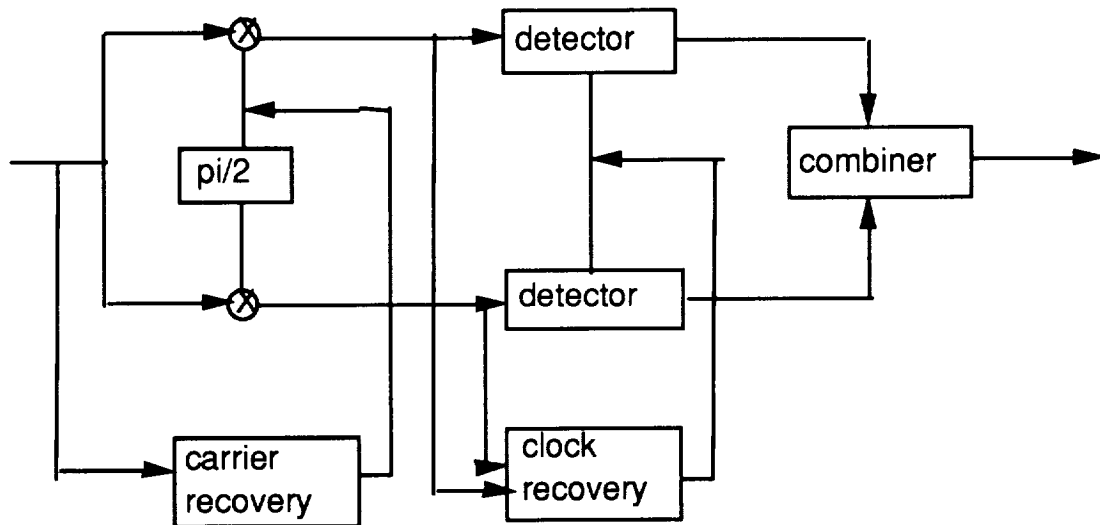


**Figure 4-24**  
**Modulation Circuitry for FFSK**

One of the advantages of FFSK is that the recovery of the clock in the used in the transmission channel is independent of the carrier recovery. This is very important because it means that when the unit is first turned on, it takes much less time for the transients in the clock recovery and transient recovery circuits to settle. The carrier and the clock frequency are related to the transmitted frequencies by equations 4-17 and 4-18.

$$f_c = \frac{1}{4}(2f_2 + 2f_1) \quad (4-17)$$

$$f_{\text{clock}} = 2f_2 - 2f_1 \quad (4-18)$$

This is easily implemented by the circuitry in Figure 4-25.

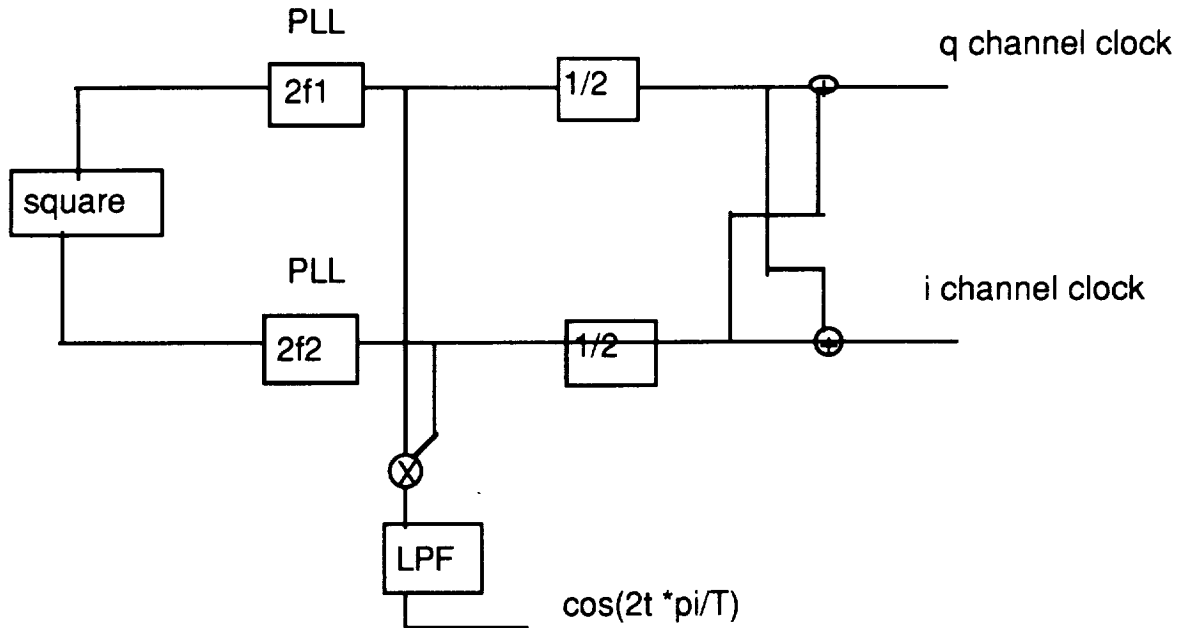


**Figure 4-25**  
**Clock Recovery**

There are problems with the clock and carrier recovery. When a long sequence of ones or zeros is transmitted, it has to recover this information since the received signal does not change. This problem can be solved by either interlacing the signal being transmitted with a random signal or by representing ones and zeros by symbols that change within the time period ( $T$ ). Since the latter method has much less risk of failure, it was chosen over the first method. The disadvantage of using this scheme is that the signal tends to occupy a wider bandwidth as a result.

### 4.5.3 Coding

#### 4.5.3.1 Shannon limit

It was shown by Shannon that there are bounds on the channel capacity placed by the power used in transmission, the ambient noise level, and the bandwidth. This is shown in equation 4-19.

$$c = B \log_2 \left( 1 + \frac{P}{N_0} \right) = B \log_2 (1 + \text{SNR}) \quad (4-19)$$

Where  $c$  is the channel capacity,  $P$  is the power transmitted  $N$  is the noise level, and  $B$  is the bandwidth.

When the bit rate is higher than  $C$  then it can be shown that the probability of error in the channel is bounded by some value greater than zero. When the transmission rate is lower than the channel capacity, an alternative modulation and encoding scheme exists that produces smaller error rates. The Shannon limit does not tell us what this scheme is but it gives us a bound on what to expect.

If the limit of equation 4-19 is found as the bandwidth goes to infinity (see equations 4-20 and 4-21).

$$C_{\infty} = \frac{P}{N_0 \ln 2} \quad (4-20)$$

$$\frac{E_b}{N_0} = \ln 2 \quad (4-21)$$

This means that noise level places a limit on the power used in transmission.

#### 4.5.3.2 Error correction

There are two ways of correcting errors that are in common use.

1. ARQ: (Automatic repeat request) In this mode of error correction, the data is encoded with just enough information to detect errors. No attempt is made to correct the errors. Instead a request for re-transmission is requested on a reverse channel. Since less redundancy is needed to detect errors than to correct them, this scheme has fewer symbol bits in relation to information bits than other schemes.

2. FEC: (Forward error correcting) In this mode, the data is encoded with so much redundancy that errors can be detected and corrected.

We chose ARQ because it is more reliable and robust and its performance is independent of channel conditions. The encoding and decoding of ARQ is also much simpler than that for FEC. There are a lot of good codes developed for ARQ that lead to a very low probability of undetected error.

The disadvantages of ARQ are that a two way channel is required. This is not a disadvantage in our application because we will have a two way channel anyway. The other disadvantage is that large buffers are required at the transmitting end in case of a re-transmission.

There are different implementations of ARQ. The one that we chose is selective repeat ARQ. In this scheme the information is divided into blocks and when there is an error in transmission only the block with the error is re-transmitted. This is very convenient because although we will have high data rates, some of it can be wrong so long as the receiver knows that it is. Most of the data will be video and voice. Errors in this can be tolerated to an extent because the original information can be recovered from context by the user. The telemetry data can have errors so long as the wrong data is known and marked and the errors are not too frequent. As a result, only command and critical application specific information will be re-transmitted.

The measure of merit of an error detection scheme are its throughput and its undetected error probability. The undetected error probability is a function of the code and the probability of error in the channel. The throughput for the scheme described above is given by equation 4-22.

$$\eta = \frac{k}{n}(1 - P_B) = \frac{k}{n}e^{-nP_b} \quad (4-22)$$

k is the number of information bits in a block, n is the block length, and the P's are the probabilities of error in a Block and in a bit.

The throughput reduces with block length but the probability of an undetected error also reduces as a result. As a result there is a trade between throughput and the probability of an undetected error.

#### 4.5.3.3 Code selection

We will use block codes. This means that a block of information bits will be taken and depending on the value, a corresponding symbol that is longer will be sent. This will incorporate redundancy into the design.

The hamming distance between two symbols is the number of bits that are different between them. This is the number of bits that one would have to change in one symbol to make it identical to another. The number of errors that can be in a symbol and be detected by a block code is one less than the minimum hamming distance. The number of errors that can be in a block and be corrected is half of the number of bits that can be detected.

There is a bound on the ratio of the hamming distance to the block length for different values of  $k/n$ . This bound is called the Elias bound and it tells how many errors per block can be detected for different coding ratios. This is plotted in Figure 4-26.

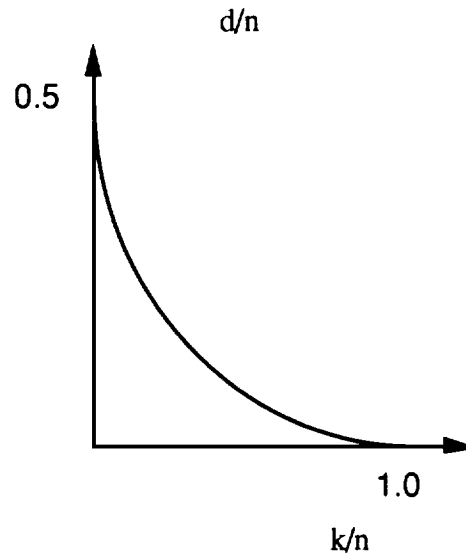


**Figure 4-26**  
**Elias Bound**

The kind of block codes in common use are cyclical. This means that any rotation of the bits of a valid symbol is a valid symbol. If the information streams are written as polynomials in  $x$  with the coefficient of  $x^n$  representing the value of the  $n$ th bit in the information stream, then a polynomial  $g(x)$  can be found so that all the symbols are generated by multiplying the input polynomial with this polynomial. This generator polynomial is unique for an  $(n,k)$  block code. This generator polynomial :

1. Must divide  $x^{n+1}$  exactly

$$x^{n+1} = g(x) h(x) \quad (4-23)$$

2. Is a polynomial of order  $n-k$ . In the case of BCH codes (Bose-Chaudhari-Hocquengheim) the generator polynomial is also the least common multiple of the information polynomials. These are the codes we will use since they work best on a channel with isolated errors.

3. All the code polynomials generated in this way are the product of the generator polynomial and the information polynomial.

$$v(x) = m(x)g(x) \quad (4-24)$$

The encoding is done by calculating the coefficients of the polynomial in the equation above. This is done using shift registers, exor gates, and multipliers. See Figure 4-27.

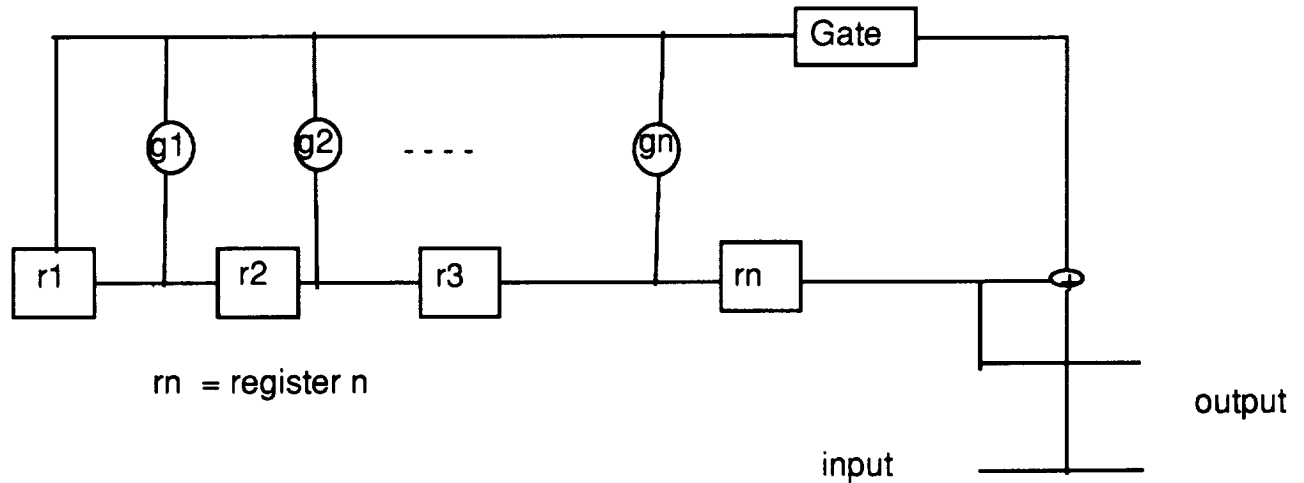


**Figure 4-27**  
**Encoding Block Diagram**

In order to detect the errors, a syndrome polynomial is calculated. This polynomial can tell when there are errors in the stream received. The received signal is given by equation 4-25.

$$r(x) = v(x) + e(x) . \quad (4-25)$$

where  $v(x)$  is the transmitted signal and  $e(x)$  is the error signal.

The error signal can be written out as equation 4-26

$$e(x) = q(x)g(x) + s(x) \quad (4-26)$$

The part of the error that is divisible by the generator polynomial is undetectable since it is a valid symbol. The other part can be detected by the circuit in Figure 4-28.

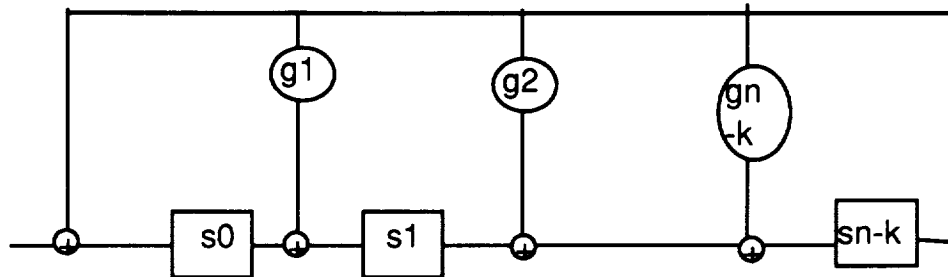


**Figure 4-28**  
**Error Detection Block Diagram**

If the values in the registers after the received symbol has been shifted in is zero then there are no detected errors.

To find the undetected error probability for an  $(n, k, d)$  code with  $n$  as the block length,  $k$  the number of information bits in a block, and  $d$  the minimum hamming distance. If the probability of a single error is  $p$ , the probability distribution for the number of errors in a block is actually a binomial probability distribution with mean  $np$  and variance  $\sqrt{np}$ . For large  $n$ , this can be modelled as a normal distribution with the same mean and standard deviation since the value  $n$  is large for the block codes. To get an undetected error probability of  $10^{-12}$ , see equation 4-27.

$$d = 5 * \sqrt{np} \quad (4-27)$$

The probability of an error in a block is given by equation 4-28.

$$P = 1 - \exp(-np) \quad (4-28)$$

We chose a block size of 511 bits. The number of information bits in a block is 420, and the minimum hamming distance is 22. With an energy per bit to noise level ratio of 8, this satisfies the undetected error probability constraint.

The throughput is given by equation 4-29.

$$\text{throughput} = k \exp(-np) / n \quad (4-29)$$

The hardware to do this has been selected. It will be custom made by Motorola Incorporated. For simplicity and for a reduced development cost the same hardware was

used for the different links. Since the greatest data rate occurs in links that have video, this rate is about 2 Mbs as explained below. Motorola has demonstrated that they can build a modem and codec that is capable of up to 1.5 Gbps. This is the hardware that we will use. The estimated reliability of this hardware is about 0.99 and so there will be a need for redundancy. The modem/codec that is built by Motorola is structured so that it monitors the number of errors. It has a built in microprocessor. If these error rates goes above a certain threshold the modem will test itself to see if it is working well. This is easy to do since the modulator and the demodulator, and the encoder and decoder come together in the same package and are already wired so that one can be the input of the other as shown in Figure 4-29.

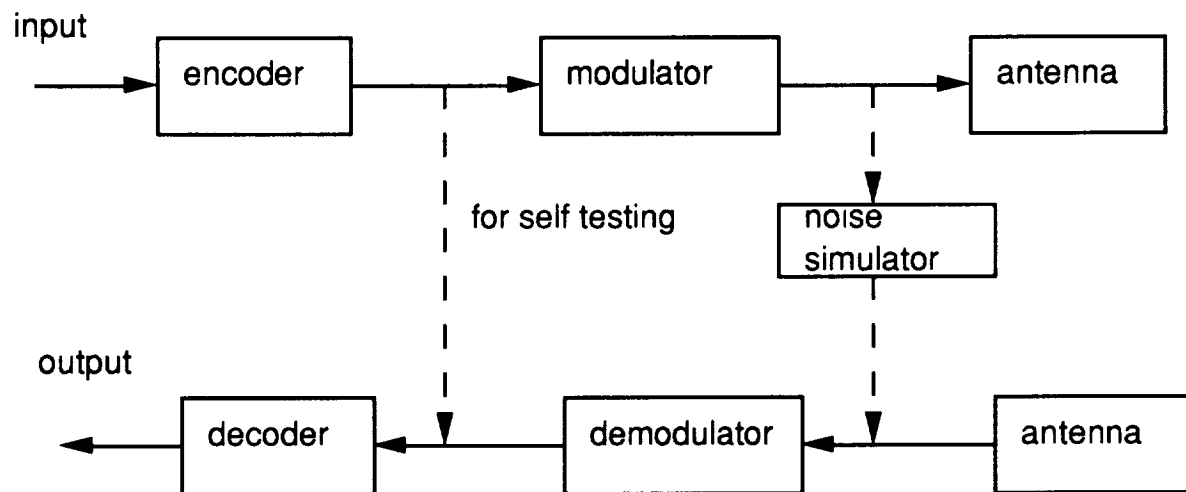


**Figure 4-29**  
**Modem/codec Structure**

Since the reliability of each single unit is less than that required of the system, there will be three of them. Only one of them will be working at any one time but if its error rate increases above a threshold it will bring another on line and test itself to see if it is faulty. The structure of the connections is as shown in Figure 4-30.



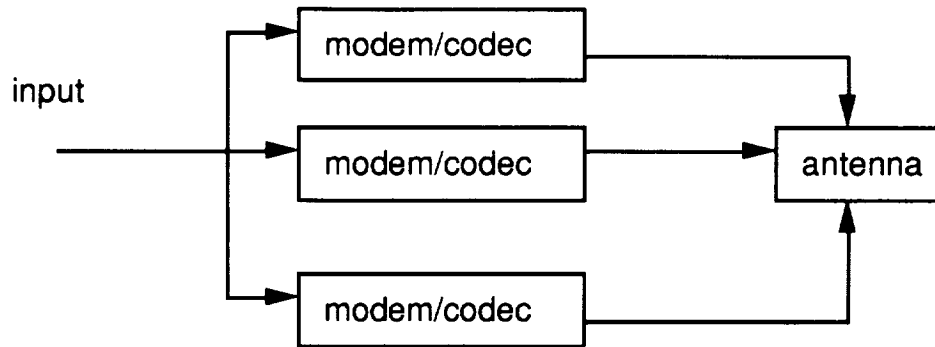


**Figure 4-30**  
**Reliability Schematic**

#### **4.5.4 Video Compression**

For a color video link, a data rate of 44 Mbit/s is required. This is very high compared to the other data rates and it would be the driving factor in the design even if the video is not mission critical. There is a need to reduce this data rate. According to Prof. Lim of MIT's Digital Signal Processing Group, the video signals can be compressed by a factor of 24 without an obvious loss in the quality of the picture. This makes the data rates in the design much more reasonable. However, this technology is new and most of theory and information about it is proprietary. This is the same technology that they plan to use for high definition television and it has been demonstrated.

The basic theory behind the compression is that the energy in the video signal for any one frame is concentrated about very low frequencies (with two dimensional position replacing time in the determination of frequency). The two dimensional frequency transform is taken and the higher frequency values are discarded. The number of bits assigned to the different frequency values is also varied so that there is more precision where it is needed. Similar compression methods are done between frames. The achievable compression rates are a lot higher than for serial signals since video information varies smoothly in three dimensions (2 space and 1 time) and so there is a lot more redundancy in the signal. The eye is also able to smooth and interpolate the picture making it less sensitive to errors.

#### **4.6 Power, Size and Weight for Communications Equipment**

To estimate the power, weight and size of equipment used in communications and information processing systems, Table 4-7, containing the specifications of proposed communication equipment, was compiled. Using this table, the power, weight and

dimensions of equipment for each stage was calculated summing the necessary equipment for each stage together.

**Table 4-7: Communications General Power, Weight and Size Estimates**

Equipment	Power [w]	Weight [kg]	Dimensions [cm]	Size [m <sup>3</sup> ]
HP GaAs Computer	500.00	25.00		3.03E-03
RH32 Data Processor	10.00	7.00	15.2 x 14.0 x 20.2	4.32E-03
MDM-16 MUX/DEMUX		19.50	36.6 x 22.7 x 33.8	2.81E-02
Odetics Tape OHSR	200.00	45.40		7.08E-02
Fairchild Solid State	3.00	6.17	20.1 x 27.9 x 12.2	6.84E-03
Universal Demodulator	13.00	20.40	7.62 x 17.78 x 5.08	6.88E-04
High Data Rate Modem	100.00	10.00		6.88E-04
Antenna Pointing System	33.00	79.80		
High gain antenna	20.00	20.00		3.53E+00
Low gain antenna	10.00	0.50		1.00E-04
Receiver	25.00	1.00		1.00E-03
Transmitter	25.00	1.00		1.00E-03

#### **4.6.1 Crew Module**

The high throughput required for the crew module requires the use of the HP GaAs Computer. The remaining components were chosen based on Figure 4-7.

**Table 4-8: Communications Equipment on Crew Module**  
**Power, Size and Weight Estimates**

Equipment	No.	Power [w]	Weight [kg]	Dim of ea. [cm]	Size [m <sup>3</sup> ]
HP GaAs Computer	3	1500.00	75.00	20.1 x 27.9 x 12.2 7.6 x 17.7 x 5.0	9.09E-03
Odetics Tape OHSR	1	200.00	45.40		7.08E-02
Fairchild Solid State	1	3.00	6.17		6.84E-03
Universal Demodulator	3	39.00	61.20		2.06E-03
High Data Rate Modem	3	300.00	30.00		2.06E-03
Low gain antenna	4	40.00	2.00		4.00E-04
Receiver	2	50.00	2.00		2.00E-03
Transmitter	2	50.00	2.00		2.00E-03
Totals	19	2182	223.77		0.09526

#### **4.6.2 Earth Return Module**

Table 4-9 shows the estimates for the antenna pointing system and the high gain antennas. This equipment interacts with the equipment on the crew module as shown in Figure 4-7.

**Table 4-9: Power, Weight and Size Estimates for Earth Return Module**

Equipment	Qty	Power [w]	Weight [kg]	Dim ea [cm]	Size [m <sup>3</sup> ]
Antenna Pointing System	2	66.00	159.60		0.00E+00
High gain antenna	2	40.00	40.00		7.06E+00
Receiver	2	50.00	2.00		2.00E-03
Transmitter	2	50.00	2.00		2.00E-03
Totals	8	206	203.6		7.064

#### **4.6.3 Habitat**

Table 4-10 shows the equipment on both the habitat and the PLM stages of the precursor mission. All of the equipment is in the habitat except for the high gain antennae and pointing system which are located on the PLM stage. The interactions of the equipment is shown in Figure 4-6.

**Table 4-10: Communications Equipment on Habitat and PLM Stages**  
**Power, Size and Weight Estimates**

Equipment	No.	Power [w]	Weight [kg]	Dim ea [cm]	Size [m <sup>3</sup> ]
HP GaAs Computer	3	1500.00	75.00	20.1x 27.9 x 12.2 7.6 x 17.7 x 5.0	9.09E-03
Odetics Tape OHSR	1	200.00	45.40		7.08E-02
Fairchild Solid State	1	3.00	6.17		6.84E-03
Universal Demodulator	3	39.00	61.20		2.06E-03
High Data Rate Modem	3	300.00	30.00		2.06E-03
Antenna Pointing System	2	66.00	159.60		0.00E+00
High gain antenna	2	40.00	40.00		7.06E+00
Low gain antenna	2	20.00	1.00		2.00E-04
Receiver	4	100.00	4.00		4.00E-03
Transmitter	4	100.00	4.00		4.00E-03
Total	25	2368	426.37	0	7.15906

#### **4.6.4 Primary Trans-Lunar Injection Stage**

The PTLI stage requires minimal communications equipment which only serves to track the location of the stage and monitor status of the stage. The PTLI requires equipment that will allow the precursor payload vehicle to dock with the PTLI stage. Table 4-11 shows the equipment estimates required for the PTLI stage.

**Table 4-11: Communications Equipment for PTLI Stage**  
**Power, Weight and Size Estimate**

Equipment	Qty	Power [w]	Weight [kg]	Dimensions ea [cm]	Size [m^3]
RH32 Data Processor	3	30.00	21.00	15.2 x 14.0 x 20.2	1.30E-02
MDM-16 MUX/DEMUX	1	0.00	19.50	36.6 x 22.7 x 33.8	2.81E-02
Fairchild Solid State	1	3.00	6.17	20.1 x 27.9 x 12.2	6.84E-03
Universal Demodulator	4	52.00	81.60	7.6 x 17.7 x 5.0	2.75E-03
Low gain antenna	8	80.00	4.00		8.00E-04
Receiver	8	200.00	8.00		8.00E-03
Transmitter	8	200.00	8.00		8.00E-03
Totals	33	565.00	148.27		0.06749

## **5 Guidance, Navigation and Control Selection**

### **5.1 Introduction**

The subsystem known as Guidance, Navigation and Control (GNC) is responsible for guiding space craft to whatever destinations specified in the mission profiles and for space craft orientation. GNC is required for orbital maneuvers, insertion into terra-luna trajectory, rendezvous, Earth reentry, and lunar ascent/descent. GNC can be broken down into its three obvious components. Navigation is knowing your present state -- that includes position, velocity, angular rate (within a specified coordinate system)-- and what state you are trying to achieve. Guidance is the process of getting zero range and zero range rate relative to some specific target. In some instances there is overlap between guidance and navigation, thus if something is mentioned under the heading of navigation it may have relevance under guidance also. Control is the maintenance of vehicle state and dynamics, which includes attitude, angular velocities, and vibrations.

### **5.2 Trade Studies and Instrument Selection**

In the Guidance, Navigation and Control system, several trade studies were conducted in order to select the design that optimizes performance while minimizing weight, cost and power. The design must be robust enough to survive two failures to ensure mission success, and three failures for human survivability. Because the guidance, navigation and control (GNC) systems are crucial to the mission, the GNC system needs three levels of redundancy to ensure human survivability. Therefore, instead of the 95% reliability necessary for mission success, GNC needs a 99.9% reliability. This system driver forces weight, cost and size to be essential to the design.

#### **5.2.1 Attitude Determination and Control**

Attitude is defined as the angular orientation of a defined body-fixed coordinate system with respect to a separately defined external frame. Attitude determination involves measuring the orientation of the spacecraft. Attitude control involves returning the spacecraft to a desired position. In attitude determination and control, the Guidance, Navigation and Control (GNC) subsystem is responsible for two functions. First, the orientation of the spacecraft must be determined. Second, the spacecraft must be kept in its desired orientation. To determine the orientation of the spacecraft, several methods are currently available. In order to correct the orientation, two methods are used: jet thruster or momentum absorption. The feedback loop that attitude determination and control follows is shown in Figure 5-1.

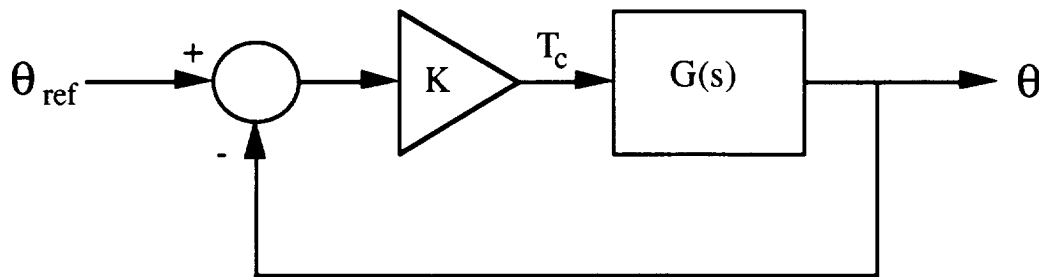


**Figure 5-1**  
**Attitude Determination and Control Feedback Loop**

In this figure,  $\theta_{\text{ref}}$  is the desired orientation of the spacecraft,  $\theta$  is the actual orientation of the spacecraft,  $K$  is the gain that determines  $T_c$ , the correction torque, and  $G(s)$  is the gain of the spacecraft.

### 5.2.2 Coordinate Systems

In order to determine the spacecraft's orientation, a coordinate system must be defined. Five common systems are geocentric, selenocentric, earth-fixed, spacecraft-fixed, local vertical/local horizontal, and ecliptic. *Geocentric inertial* coordinates are centered at the earth and are fixed with respect to inertial space. In this coordinate system, the celestial pole is the  $z$ -axis, and the vernal equinox is the  $x$ -axis. The *selenocentric* coordinate system is centered at the moon. There is also the *egocentric* coordinate system, which believes that the entire mission revolves around oneself. The *earth-fixed* system has the  $z$ -axis on the celestial pole, but the  $x$ -axis is along the Greenwich meridian, i.e., the coordinate system moves with respect to the moon. *Spacecraft-fixed* coordinates are defined about the spacecraft, and are useful for spacecraft maneuvers, from the spacecraft reference frame. *Local vertical/local horizontal* are also defined about the spacecraft, and this coordinate system is also useful for spacecraft activities. *Ecliptic* coordinates are defined in inertial space relative to the sun. This coordinate system is useful for solar system activities. For this mission, the most useful coordinate systems would be geocentric inertial for the Earth's sphere of influence, selenocentric for the Moon's sphere of influence, and spacecraft-fixed for orbital maneuvers.

### 5.2.3 Onboard vs. Ground-based ADCS

The choice for the attitude determination and control system processing is straightforward. It is essential that the orientation of all spacecraft be monitored very closely throughout the mission. If the spacecraft is in orbit around the Moon, the signal would take about 1.25

seconds to travel to Earth. The attitude data would then have to be processed, and a correction signal returned to the spacecraft in another 1.25 seconds. In this time, however, the spacecraft will have continued to rotate, and another correction will be necessary. Ground-based control would be both time and fuel consuming for the trip to the moon.

Onboard processing of attitude feedback is essential for rendezvous and docking. Without on-board processing, rendezvous and docking would be nearly impossible. Also, when the spacecraft goes behind the Moon, there is about half an hour of no communication with Earth. In this time period, no attitude corrections could be made, and attitude data could only be stored. If an abort was necessary on the back side of the Moon, the spacecraft could not be oriented to properly execute the abort procedure.

For the above reasons, on-board processing is necessary for attitude determination and control. In both abort and rendezvous and docking, time is a major constraint on these maneuvers. Less fuel would be consumed with on-board processing, and time response would be much quicker. Ground-based systems may be used to verify on-board calculations, but the primary attitude determination and control data processing should occur onboard.

#### 5.2.3.1 Stabilization

There are three ways to stabilize a spacecraft: passive control, spin control, or 3-axis control. Because the spacecraft must be aligned in certain positions for specific maneuvers, such as lunar transfer insertion, or lunar orbit insertion, passive control cannot be used. Passive control is not very accurate ( $\pm 5^\circ$ ), it can only be used to point to the earth's local vertical, and it does not allow the spacecraft to be reoriented without changing the structure of the spacecraft. Spin control requires that the spacecraft be rotating to maintain stability. Because maneuvers such as docking and midcourse corrections are necessary, spinning also cannot be used. Therefore, in order to allow the spacecraft to be reoriented for orbital maneuvers, midcourse corrections and docking, three-axis control should be used.

#### 5.2.4 Reaction Control System

To counter the disturbance torques and to reorient the spacecraft, a reaction control system is necessary. Various systems are outlined below, and the gas jets are chosen as the method for attitude control and countering disturbance torques.



#### 5.2.4.1 Reaction Wheels

Both momentum and reaction wheels "absorb" the external torques, preventing the spacecraft from being displaced. Reaction wheels, in a three-axis-stabilized spacecraft, nominally run at zero angular momentum. As external torques are exerted on the spacecraft, they are detected by the sensors, and the reaction wheel accelerates to counter the torque and therefore "absorb" the disturbance torque. If too many external torques are applied, the wheel may saturate, i.e., it will not be able to counter any more torque, and the "stored" momentum is "dumped" by using either gas jets or magnetic torquers to bring the rotation of the reaction wheel back to zero. Typically, there is one reaction wheel on each axis of the spacecraft. In order to be redundant, more wheels are added, increasing the overall weight of the actuation system. A typical redundant reaction wheel arrangement would weigh 70 kg, plus the weight of a gas jet system for momentum dumping.

#### 5.2.4.2 Momentum Wheels

Momentum wheels operate almost identically to reaction wheels, except that the momentum wheel is biased at a constant speed, and always turn in the same direction. By adjusting the speed of the momentum wheel, external torques may be absorbed. Momentum wheels also need to be dumped when they become saturated. A typical redundant momentum wheel arrangement would weigh 80 kg, plus the weight of a gas jet system.

#### 5.2.4.3 Magnetic Torquers

Another actuation device is the magnetic torquer. These torquers use magnetic coils or electromagnets to create magnetic dipole moments. These torquers can compensate for minor disturbance torques, and they can also dump momentum from saturated wheels. These torquers rely on the Earth's magnetic field to produce torque, so they are not useful in higher orbits, the trans-lunar orbit, or in lunar orbit. It is not be an efficient use of mass and size allowances to use magnetic torquers for this mission profile.

#### 5.2.4.4 Control Moment Gyros

Control moment gyros (CMG) can produce large amounts of torque, and, if one is placed on each axis, the CMG can provide torque on all three axes. The CMG performs high torque maneuvers rapidly, but requires complex control laws, and it is expensive and heavy. Also, the momentum may have to be dumped from the CMG. CMGs are very noisy, and are resonant at multiples of their operating frequency. A typical redundant CMG system would weigh 150 kg, plus the weight of a gas jet system.

#### 5.2.4.5 Gas Jets

Gas jets produce a thrust by expelling gas. The jets are capable of large torques. The jets may be used in high orbits, and multiple jets may be used for redundancy. However, the jets require fuel, and therefore weight is added to the system, and the life of the spacecraft is limited. Gas jets are more versatile because they can be used not only to control attitude, but also to maneuver the spacecraft over large angles, to adjust orbits, to dump momentum from momentum or reaction wheels, and to control the spin rate and nutation.

#### 5.2.4.6 Choosing a Reaction Control System

Table 5-1 outlines the performance of the various actuators. The table lists the actuation device, its accuracy, its performance, its weight, its power and comments about the actuation device.

**Table 5-1: Typical Characteristics of Actuation Devices**

Actuator Device	Accuracy (deg)	Torque (N-m)	Weight (kg)	Power (W)	Comments
CMG	0.1	25-500	> 40	90-150	quick, noise, costly
Gas Jet	.1	.5-18000	Var.	N/A	quick, fuel, costly
Magnetic Torquer	1-2	.004-.16	.4-50	.6-16	cheap, near earth
M+ R Wheels	.01	.01-1	2-20	10-110	quick, costly

Table 5-1 shows that the magnetic torquer is not very accurate, and that it can only be used near the earth. The CMGs and gas jets have similar accuracy numbers, but the gas jet can provide much more torque if necessary, making the gas jet useful for orbital maneuvers, as well as attitude and control. The momentum and reaction wheels are the most accurate of the systems, but provide low torque only, so momentum dumping, which requires another actuation system, such as gas jets, would have to occur regularly on the flight. Both wheels, when made redundant, would be very heavy and they would require much power. Because the errors due to external torques will be small in trans-lunar orbit, and very large in re-entry, a wide range of correction torques is needed. Gas jets, as shown above, have a very large range of torques. It is also unlikely that the weight of the additional fuel required for the jets to counter external torques would be greater than the weight of either the wheels or control moment gyros.

#### 5.2.4.7 Design Choice for RCS

Therefore, because of the maneuvers that will be required, the gas jets are recommended as the only RCS. Specifically, the Marquardt R4-D will be used for attitude control. This engine weighs 3.63 kg, and delivers a thrust of 490 N with a 2.67 N-sec impulse for a 10 msec burn. This engine is discussed in detail in Chapter 3 of Volume II.

##### 5.2.4.7.1 Theory of Gas Jet Attitude Maneuvers

In attitude maneuvers, the fundamental equation for gas jet control is equation 5-1, which describes the rate of change of angular momentum. [Wertz, 1985]

$$\frac{d}{dt}(I\omega) = N - \dot{m} l^2 \omega \quad (5-1)$$

where **I** is the moment of inertia tensor, **w** is the angular velocity, **N** is the applied torque,  $\dot{m}$  is the rate of consumption of propellant, and **l** is the perpendicular distance from the spin axis to the thruster. For each phase of the mission, the R4-D engine must supply the **N** necessary to correct the unwanted rotation of the spacecraft.

##### 5.2.4.7.2 RCS Thruster Locations

The RCS system provides the necessary translation and orientation control for many of the stages. For a long cylindrical space craft eight RCS thrusters are sufficient for control of all three translation and tree rotation components as shown in Figure 5-2. However, the reliability of the thrusters requires single redundancy, or 16 RCS thrusters.

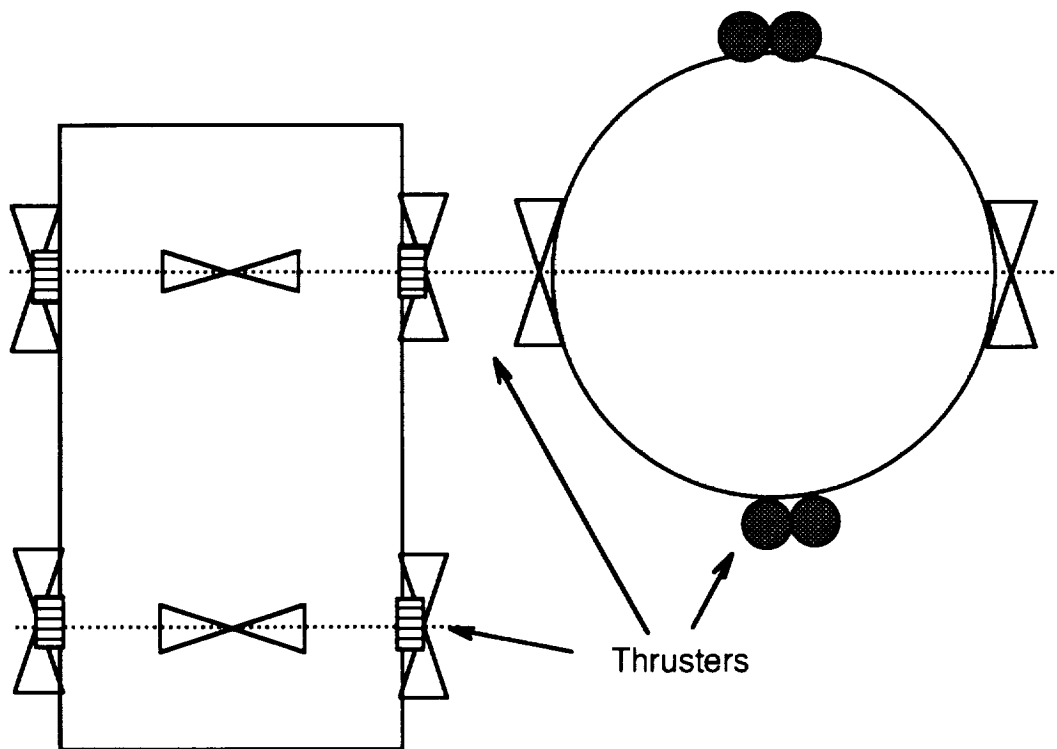


**Figure 5-2**  
**RCS Thruster Locations**

### **5.2.5 Attitude Determination System**

Attitude determination systems use both gyroscopes and sensors to determine the attitude of the spacecraft. Gyroscopes are used for short term determination, and the sensors are used to correct the drift errors in the gyroscopes. Several sensors are discussed below, and designs for each stage are presented.

#### **5.2.5.1 Horizon Sensors**

Horizon sensors use infrared radiation to find the contrast between the cold of space and the heat of the horizon in order to determine spacecraft orientation. The horizon sensor consists of four basic components: a scanning mechanism, an optical system, a radiance detector, and signal processing electronics. Horizon sensors are often accurate to within  $0.02^\circ$  to  $0.03^\circ$ . However, the performance is orbit dependent, the sensors are expensive, and provide only one of the two necessary vectors for determining spacecraft attitude. For the journey to the moon, horizon sensors are not adequate. However, for PTLI stationkeeping in LEO, horizon sensors are a good choice.

The Ithaco Conical Earth Sensor (CES) is typical of horizon sensors. Because the spacecraft is three-axis stabilized, the horizon sensor must have a rotating head. The Ithaco CES meets this requirement, and can be used at the 275 km altitude specified for the orbit of the PTLI stage. The Ithaco CES is accurate to less than  $0.1^\circ$  for LEO. It has a mass of 2.5 kg, and it requires 8 Watts at 52 Volts DC for a digital interface. The sensor is 0.11811 m by 0.075 m by 0.099 m, and its electronics are 0.1778 m x 0.1778 m x 0.1651 m. The CES provides two axis attitude determination for the spacecraft.

#### 5.2.5.2 Sun Sensors

Sun sensors also define only one vector of the spacecraft attitude, and must be used with another system, such as a horizon sensor, in order to determine the attitude. Although sun sensors are accurate ( $\approx 0.01^\circ$ ) and very reliable, they can only be used intermittently. The sun sensor has a field of view of  $\pm 64^\circ$ . The data for some of Adcole's most accurate sun sensors are shown in Table 5-2.

**Table 5-2: Characteristics of Adcole Sun Sensors**

Model Number	# of Axes	Accuracy (deg)	Field of View	Size (m)	Mass (kg)	Power (W)
16932	2	.017	$64^\circ \times 64^\circ$	.097x.104x.025	.372	1.736
electronics				.198x.114x.064	1.161	
18960	2	.017	$64^\circ \times 64^\circ$	.084x.110x.025	.351	1.8
electronics				.206x.157x.030	.455	
17061	1	.05	$100^\circ \times 100^\circ$	.109x.64x.028	.322	.7
electronics				.102x.086x.051	.517	

Model number 18960 appears to be the best choice for a sun sensor, since it minimizes size and weight, at the same power and accuracy as model number 16932.

#### 5.2.5.3 Star Trackers

The most accurate sensor is the star tracker, which can be accurate to  $0.001^\circ$ . The star sensor may follow one star, which is a tracker, or it can identify stars in its field of view, a mapper. Trackers may either be fixed or gimballed. The gimballed tracker is much heavier, and it will not be used for this mission. The star tracker or mapper fixes on a specific star, and uses it to determine spacecraft orientation. In the star mapper, a  $5^\circ$  to  $10^\circ$  field of view

(FOV) is sent through an optical system and converted to electrical signals by a charge coupled device (CCD) that is essentially a photosensitive element [Wertz, 1985]. A smaller, instantaneous field of view (IFOV) of the FOV is scanned by the sensor electronics. When the desired star is located, the mapper fixes on it, and determines the location of the star with respect to star tracker. By checking with the star catalog and ephemeris, the attitude and location of the spacecraft with respect to inertial space can be determined. The star tracker must be shielded from stray light, and can only be used away from the sun, usually  $30^\circ$  to  $60^\circ$  from the sun. The tracker is subject to many errors, such as temperature variations and the velocity of the spacecraft, which can be removed during data processing.

#### 5.2.5.4 Magnetometers

Magnetometers can also be used to determine spacecraft attitude. These are not as reliable as the other sensors, and are only useful in Earth orbit. Because the strength of the magnetic field decreases by  $1/r^3$ , it is less effective at higher altitudes. The magnetometers are only accurate to about  $0.5^\circ$ . Therefore, these will not be used on this mission.

#### 5.2.5.5 Optical Sensor Choice

Because size, weight and accuracy are essential issues for the sensor choice, the star tracker should be the sensor used, with perhaps a sun sensor to provide a crude initial alignment of the spacecraft. By properly selecting catalog stars, the star tracker may be used throughout the mission. Although the star tracker is slightly more expensive than the other sensors, it provides the necessary accuracy without too much additional weight or size. The CT-601 Solid State Star Tracker, made by Ball Brothers, is cylindrical with a .1778 m diameter, with a length of .2946 meters, has a mass of 8.77 kg, and requires 10 W, including electronics. The CT-601 can track 5 stars simultaneously, and determine their position in less than 5 seconds. The CT-601 is a reliable tracker that has flown on every STS mission.

#### 5.2.6 Gyroscopes

The processing time for these optical sensor systems is burdensome, and the systems are not able to track the spacecraft attitude rapidly. Gyroscopes can be used to provide attitude data between star sensor updates. Because gyroscopes only measure change in attitude, and not absolute attitude, and because they have a time dependent error, a sensor system is still necessary to update the spacecraft attitude. Gyroscopes are very accurate for short term attitude determination, but, because of a bias error, their accuracy degrades over time. The two main types of gyroscopes are electromechanical and laser gyroscopes. A subset of

the laser gyroscopes, the fiber optic gyroscope, has recently reached levels of high performance at a minimum weight. Table 5-3 presents the data on a single attitude reference unit (3 gyroscopes plus electronics) for electromechanical, ring laser and fiber optic technologies.

**Table 5-3: Attitude Determination Gyroscope Assembly**

Characteristic	Electromech.	Fiber Optic	Ring Laser
Bias (°/hr)	.05	.01	.002-.008
Size (ARU) (m <sup>3</sup> )	6.88x10 <sup>-3</sup>	10 <sup>-3</sup>	1.64x10 <sup>-3</sup>
Weight (kg)	4.18	1	2.25
Power (W)	25	9	10

The data for the electromechanical ARU was taken from the Northrop ARU used in the Space Shuttle. The data for the fiber optic gyroscope was based on the Litton EDM-2 [Pavlath, 1988] and the Honeywell Prototype Fiber Optic Gyroscope [Bielas et al., 1988]. The data for the ring laser gyroscope ARU was taken from the Honeywell Pointing and Stabilization System using the ring laser gyro GG1320.

#### 5.2.6.1 G-sensitive Errors in Gyroscopes

Besides these characteristics of the gyros, the electromechanical gyros have acceleration sensitive bias terms (not given by Northrop) that would further affect the accuracy of the measurement during high g maneuvers. These errors would have to be corrected by subtracting off the g-sensitive error using accelerometer data. This process increases computing time and rotation measurement errors. The laser gyroscope does not suffer from these g-sensitive errors, so the only errors in laser gyro measurements are bias error, scale factor error, and random walk. The scale factor error for the fiber optic gyroscope (FOG) is less than 100 ppm, and the random walk, another error source, is less than .005 °/hr. If a sensor, such as a star tracker, has measurements taken every 12 minutes, the accumulated error due to bias and walk in the FOG at the end of 12 minutes will be .004°, as shown in equation 5-2.

$$\epsilon = \sqrt{.005^2 * \frac{12}{60}} + .01 * \frac{12}{60} = .004^\circ \quad (5-2)$$

The ring laser gyroscope Honeywell GG1320 has a scale factor error of less than 1 ppm with a random walk of .002-.008 deg/√hr. For the same star tracker sampling rate, the accumulated error in the ring laser gyro would be .0013°, as shown in equation 5-3.

$$\epsilon = \sqrt{.002^2 \frac{12}{60}} + .002 \frac{12}{60} = .0013^\circ \quad (5-3)$$

If the update time is reduced, the accumulated error will decrease. The minimum error is determined by the accuracy of the star tracker. The accumulated error in the laser gyroscopes will be the same for all maneuvers throughout the flight. However, the electromechanical gyroscopes would also be subject to acceleration errors during liftoff, orbital insertion, orbital maneuvers, and midcourse corrections, so that the measurement error will change for various maneuvers. For the same 12 minute span, assuming no acceleration, the error due to bias only in the Northrop ARU is .01°, which is significantly higher than the laser gyroscope errors.

#### 5.2.6.2 Cost and Reliability of Gyros

While the laser gyros surpass the electromechanical gyro in performance, weight, size and power, the issues of cost and reliability must still be resolved. The electromechanical gyro, in order to achieve high performance, has high production costs. However, because it has been developed over 30 years, the research costs are fairly low. Ring laser gyroscopes (RLG), have been developed since the 1970s, and are quite reliable. Honeywell has implemented RLGs in many of its inertial measurement units for defense and space applications. They are less expensive than electromechanical gyroscopes, and RLGs would make an excellent alternative system to FOG at a minimum mass and size penalty. The FOG is in a completely different situation. While FOGs such as the Litton EDM-2 show excellent performance, FOGs are still in the developmental stage, and more research may be necessary in order to improve reliability. Scientists agree that the potential for high reliability of the fiber optic gyroscope exists [Pavlath, 1988] [Bielas et al., 1988]. On the other hand, the production costs of FOGs are very low. The FOG is also lighter and smaller than the RLG, and may reach the same levels of accuracy of the RLG. Since Project Columbiad has at least an eight year schedule, it is recommended that the fiber optic gyro be used for attitude determination and navigation because of its mass, size, cost and power savings.



### 5.2.6.3 Theory of Laser Gyroscopes

The Sagnac Effect is the principle of both ring laser and fiber optic gyroscopes. The Sagnac effect refers to two beams of light that are propagating 180° out of phase in opposite directions around a closed path. If this path is not rotating in inertial space, then the times required for each beam to travel the path are equal, and the waves will completely interfere at the end of the path. If the loop is rotating, then the beam of light that is travelling in the same direction of rotation has a longer path to travel. The path difference is given by equation 5-4 [Martin, 1990].

$$\Delta L = \frac{4\pi R^2 \omega}{c} \quad (5-4)$$

This path difference results in a phase difference between the two beams that allows the rate of rotation of the spacecraft to be determined. Therefore, all laser gyroscopes are rate gyroscopes.

### 5.2.7 Attitude Determination and Control Final Design

From the above trade studies, the proposed attitude determination and control system will consist of reaction control jets (specified by Propulsion to be the Marquardt R-4D). For attitude and determination, each stage will have specific needs that require different sensors. For the PTLI, horizon sensors, sun sensors and fiber optic gyros will be used to determine attitude. For the ERM and CM, as well as the precursor, star trackers, a sun sensor and fiber optic gyroscopes will be used. The final design of the ADCS system is discussed in the chapter of each stage. Estimates of accumulated errors due to gyro bias and random walk are based on the Litton EDM-2 performance in 1988, as presented by Pavlath.

### 5.2.8 Accelerometers

During powered flight maneuvers, such as rendezvous and docking, lunar landing, lunar ascent, and Earth reentry, position updates from the earth are not useful for tracking the spacecraft. In these maneuvers, accelerometers are used to measure the specific force along the spacecraft axes. Specific force is the force per unit mass that is felt by a body; this usually consists of a gravity component and a D'Alembert component due to the actual acceleration of the body. The governing equation for accelerometers is equation 5-5.

$$\mathbf{f} = \mathbf{g} - \mathbf{p}_i^2 \mathbf{R} \quad (5-5)$$

where  $\mathbf{f}$  is the measured specific force,  $\mathbf{g}$  is the gravitational acceleration, and  $\mathbf{p}_i^2\mathbf{R}$  is the inertial acceleration of the spacecraft. A gravity profile is needed so that the  $\mathbf{g}$  can be subtracted from the specific force to yield the inertial acceleration. The accelerations due to the inertial acceleration are then integrated to determine velocity, and integrated again to determine position. With accelerometers, the position of the spacecraft can be determined onboard. Accelerometers will be mostly used during rendezvous and docking, lunar landing, lunar ascent, and earth reentry. During these maneuvers, position updates from the earth will not occur often enough to guarantee a successful maneuver.

Just as gyroscopes are evolving to technologies that enhance performance and reliability at a lower cost, accelerometers are making a similar transformation. Traditionally, electromechanical accelerometers have been used to detect accelerations. Recently, the solid state accelerometer has achieved levels of performance approaching that of the electromechanical accelerometer.

#### 5.2.8.1 Theory of Solid State Accelerometers

The solid state accelerometer uses the piezoelectric properties of quartz to detect acceleration. When an acceleration is directed in the direction of the quartz beam, the resonant frequency of the beam changes, and this change can be converted into an acceleration along that axis. In Figure 5-3, there are two quartz beams shaped as double ended tuning forks. The mass between the two forks moves along the input when an acceleration is applied, changing the resonant frequency of both beams. This behavior is similar to that of a guitar string. When a guitar string is pulled tighter than its rest state, it vibrates at a higher frequency. If the string is made slacker than its rest state, it vibrates at a lower frequency. By measuring this change, the specific force exerted on the guitar string can be determined.

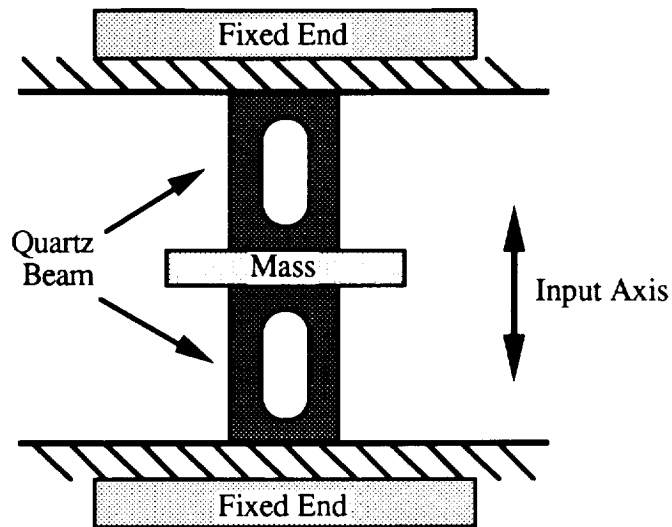


**Figure 5-3**  
**Schematic of a Solid-state Accelerometer**

Solid state accelerometers are expected to match the electromechanical accelerometer in performance, but they will have a higher reliability at lower weight, cost and size. Therefore, the solid-state accelerometer will be used for Project Columbiad, for reasons similar to those outlined in the discussion on fiber optic versus electromechanical gyroscopes. A typical QRA weighs less than 0.400 kilograms, including electronics, uses about 5 W and is about 0.10 m by 0.05 m by 0.05 m.

### **5.2.9 Inertial Measurement Unit**

An Inertial Measurement Unit (IMU) for Project Columbiad is located in the CM, the PTLI and the PLM. By using one design in three places, modularity of design is encouraged, and money is saved. The IMU has been designed to be triply redundant while minimizing total size and mass. The rotation of the spacecraft is measured by six fiber optic gyroscopes, and the acceleration of the spacecraft is measured by six solid-state accelerometers. Star trackers or horizon sensors will be used to update the IMU periodically.

#### **5.2.9.1 Orientation of IMU Components**

The accelerometers and gyroscopes are numbered from 1 to 6, and each component is positioned as shown in Table 5-4. In spacecraft centered coordinates, the angle  $j$  is measured from the positive z-axis and  $q$  is measured counter-clockwise from the positive x-axis.

**Table 5-4: Component Orientation in IMU**

Component Number	j (deg)	q (deg)
1	45	30
2	45	150
3	45	270
4	135	60
5	135	180
6	135	300

In this arrangement, there are twenty possible combinations of the six components to determine either the rotation or the acceleration along the spacecraft axes using any combination of three components. By using two or three combinations simultaneously, a level of fault tolerance is obtained, and malfunctioning components can be easily identified. Malfunctioning components can be eliminated from the data processing until a status check can be made on the component.

#### 5.2.9.2 Component to Spacecraft Coordinates

When all six components in each subsection of the IMU are operating, the transformation matrices,  $T_b$ , from IMU to spacecraft coordinates can be determined using equation 5-6. This equation shows the three components (a, b, c) used to resolve the rotation or acceleration of the spacecraft and the matrix used to transform the inputs from instrument centered to spacecraft centered data. These matrices were generated from equation 5-7, which was iterated for each possible combination of the components.

$$T_{cb} = \frac{1}{\det M_{cb}} M_{cb_{\text{ref}}} \quad (5-6)$$

where,

$$M_{cb} = \begin{bmatrix} \sin \varphi_a \cos \theta_a & \sin \varphi_b \cos \theta_b & \sin \varphi_c \cos \theta_c \\ \sin \varphi_a \sin \theta_a & \sin \varphi_b \sin \theta_b & \sin \varphi_c \sin \theta_c \\ \cos \varphi_a & \cos \varphi_b & \cos \varphi_c \end{bmatrix} \quad (5-7)$$

and the subscript  $a$  represents the first component,  $b$  the second, and  $c$  the third.  $M_{obcof}$  is the cofactor matrix of  $M_{ob}$ , and  $\det M_{ob}$  is the determinant of the matrix.

### 5.2.9.3 Spacecraft to Inertial Coordinates

Once the inputs have been transformed to spacecraft-centered coordinates, the data must be transformed again to inertial coordinates, either the Earth or the Moon. This is accomplished through multiplication by another direction cosine matrix shown in equation 5-8 [Griffin and French, 1991].

$$T_{BI} = \begin{bmatrix} C\psi C\theta + S\psi S\theta S\phi & S\psi C\phi & -C\psi S\theta + S\psi C\theta S\phi \\ -S\psi C\theta + S\psi S\theta S\phi & C\psi C\phi & S\psi S\theta + C\psi C\theta S\phi \\ S\theta C\phi & -S\phi & C\theta C\phi \end{bmatrix} \quad (5-8)$$

where,

$C$  = cosine of argument

$S$  = sine of argument

$q = q_0 + dq$  = pitch of spacecraft coordinates with respect to inertial coordinates

$q_0$  = orientation of spacecraft from star tracker update

$dq$  = change in pitch provided by gyroscope output

$j = j_0 + dj$  = roll of spacecraft coordinates with respect to inertial coordinates

$j_0$  = orientation of spacecraft from star tracker update

$dj$  = change in roll provided by gyroscope output

$y = y_0 + dy$  = yaw of spacecraft coordinates with respect to inertial coordinates

$y_0$  = orientation of spacecraft from star tracker update

$dy$  = change in yaw provided by gyroscope output

The terms in this matrix are periodically updated by the star trackers or horizon sensors, so that new initial conditions are put into the matrix.

### 5.2.10 Operation of Attitude Determination and Control System

For attitude determination and control, the IMU will be used with an optical sensor combination to measure the rotation and orientation of the spacecraft. For the PTLI in LEO, the hardware used will be two horizon sensors, a sun sensor and the IMU. For the precursor and piloted missions, four star trackers, a sun sensor and the IMU will be used for the ADCS and INS. Figure 5-4 shows the schematic for controlling the orientation of the spacecraft. This figure is a more detailed diagram of the attitude control scheme shown

in Figure 5-1. The computer takes data from the gyroscopes at 50 Hz and from the optical sensors every 2.5 minutes. During optical sensor updates, such as from the star tracker, the computer uses the stars located by the tracker and the star catalog to determine the actual spacecraft orientation and position, and then the estimates from the gyroscopes are corrected to remove the time dependent bias and random walk errors. After the computer receives the data from the gyros, the inputs are first transformed into spacecraft coordinates, and then into inertial coordinates. The inertial coordinate system will be either Earth or Moon centered, depending on the sphere of influence at the spacecraft position. The ephemeris will contain data concerning the proper inertial coordinate system. The measured inertial orientation is then compared to the desired inertial orientation stored in the ephemeris. If the values are different, the error between the two orientations is calculated, and, if it exceeds a preset tolerance, a proportional signal is sent to the RCS to reorient the spacecraft to the desired orientation.

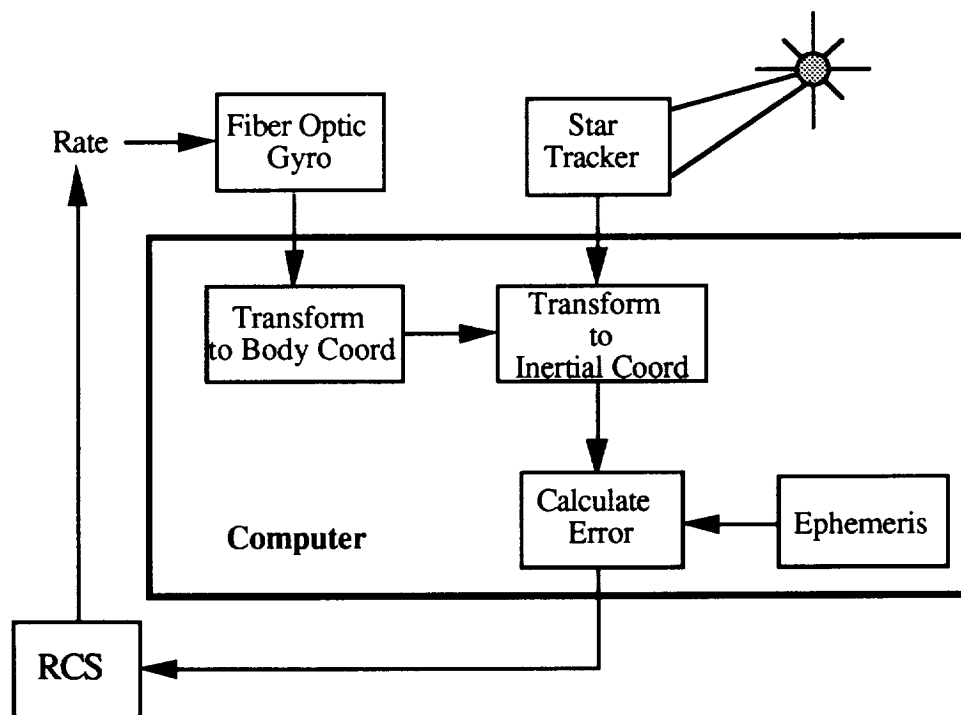


**Figure 5-4**  
**Schematic of Attitude Determination and Control System**

#### **5.2.11 Inertial Navigation**

The process of inertial navigation is very similar to that of attitude determination and control. However, instead of gyroscopes, the accelerometers are sampled at 50 Hz, and both the star trackers and Deep Space Network (DSN) are used to provide the updates to

the computer, as shown in Figure 5-5. The outputs of the accelerometers are transformed into the proper inertial coordinates, and the data are then integrated once to give spacecraft velocity, and then integrated again for position. For maneuvers such as lunar landing, the position and velocity vectors of the spacecraft are compared to the desired vectors stored in the ephemeris. If the error between these two values exceeds a preset limit, a signal is sent to the RCS to correct the discrepancy.

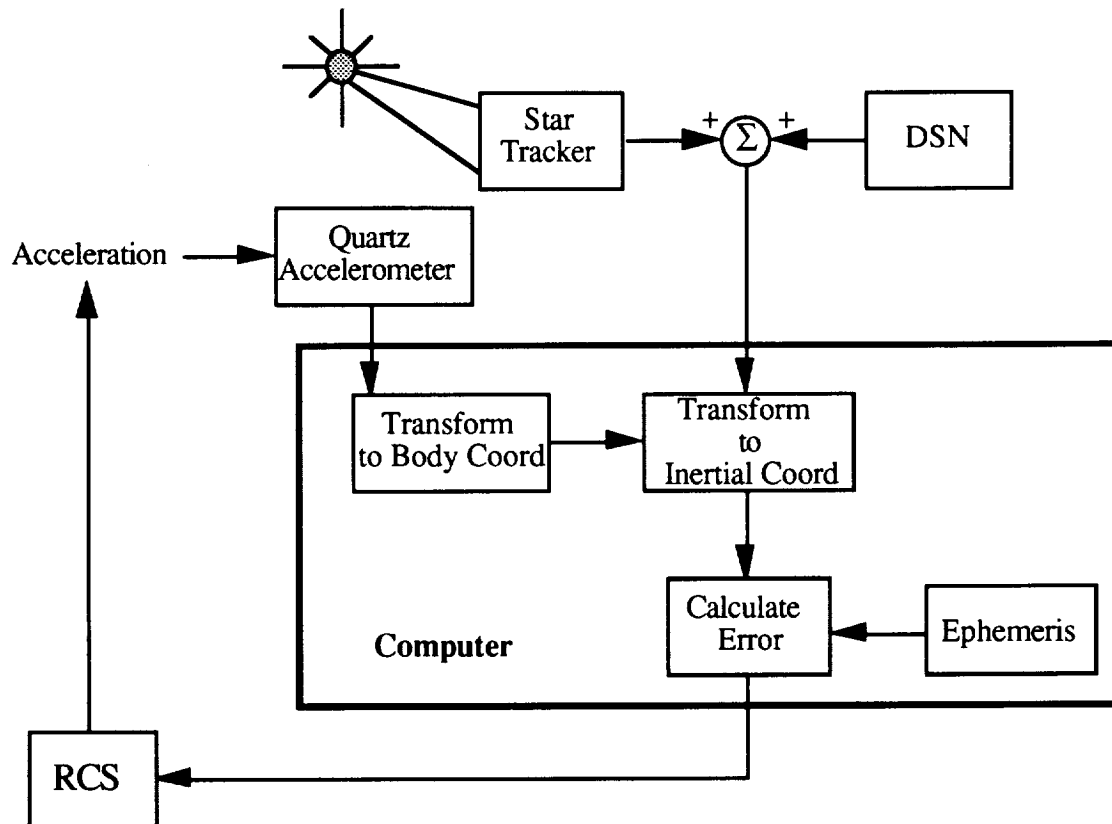


**Figure 5-5**  
**Schematic of Inertial Navigation System**

### **5.2.12 Radar Systems**

Two occasions where radar is necessary is for docking and lunar descent to the moon. Both require accurate distance measurements of range for docking and altitude for lunar descent. In the case of lunar landing, there are several possibilities for measurement. The first is ground tracking from the Earth; however, this does not prove feasible for real-time control. The second is INS. These INS estimates will be based on current data in low lunar orbit. The third altitude measurement uses radar altimeters. In the Apollo missions, the data from both the INS and radar altimeters were combined where the INS

measurements were weighted more heavily at high altitudes and the radar altimeter was weighted more heavily at lower altitudes. A similar measurement methodology will be used in lunar descent. The main criterion for selection is performance.

A radar system, typically, transmits electromagnetic waves which are reflected off of an object. Then it collects those reflections which impinge on the receiving unit. The effectiveness of a radar is determined by the amount of power received  $P_r$ , which is given by the *radar equation*., equation 5-9,

$$P_r = P_t G^2 l^2 s / (4\pi^3) R^4 \quad (5-9)$$

where  $P_t$  is the transmitted power,  $G$  is the antenna gain,  $R$  is the slant range from the transmitter to the target area,  $s$  is the effective backscatter area of the target element, and  $l$  is the wavelength of the carrier pulse. Also important is the *signal-to-noise ratio* (SNR) given by the equation 5-10:

$$\text{SNR} = P_t G^2 l^2 s / (4\pi^3) R^4 (kTB)l, \quad (5-10)$$

where  $k$  is Boltzmann's constant,  $T$  is the system-noise temperature,  $B$  is the receiver bandwidth, and  $l$  is the measure of system losses.

#### 5.2.12.1 LADAR v. Microwave

There are two types of radar systems investigated for use as altimeters, conventional microwave and laser radar (LADAR). LADAR is the cutting edge of radar technology. It's narrow beamwidth--about 10 mrad--and high frequency carrier (wavelength 0.7 $\mu$ m) allow for colossal accuracy. Proponents of LADAR claim reduced weight, cost, and power usage as compared with conventional systems. The microwave systems are similar to those used on Apollo but reflect today's technological advances [Bachman, 1979].



### **5.2.13 Docking Radar**

Docking radars work on much the same principle as radar altimeters. In addition to range information, docking radars provide range rate and angular rate. Docking procedures also require that these radar have high measurement accuracies. The accuracies necessary for docking are mentioned in section 5.3.3.

For the docking system being designed, it is possible to use either microwave or LADAR. However, LADAR provides much better accuracy and range (even greater with the use of retro-reflectors) in addition to lower power consumption. The radar system mentioned is not an off the shelf component. A subcontractor must be hired to build the system; however, the design does not require any cutting-edge technology. A feasible docking radar can determine range and angular position with accuracies of  $\pm 3$  cm and  $\pm 0.1^\circ$ , respectively. These accuracies could change depending on type of laser system used. Ultimately, the system must be designed for a reliability of 0.999.

### **5.2.14 Laser Retro-Reflectors**

A retro-reflector is a passive optical-device used in conjunction with laser systems. The retro-reflector is capable of reflecting back an incident beam at its incident angle. Essentially, the beam is bounced back from the optics to the source point with very low signal degradation.

A basic corner-cube reflector provides  $23^\circ$  FOV [C. Bachman, 1979], which is adequate for this mission. Retro-reflectors have been made for optics benches all over the world and even for the Apollo mission. They are not off-the-shelf components and must be manufactured for specific use in space.

### **5.2.15 Visual Targets**

The visual target for docking will be painted on the interface surface of the PTLI. This target will be used in conjunction with a video camera for the case of failure of the autonomous docking mode. Since the edges are easier for humans to detect than solid surfaces, the cross hair pattern shown in Figure 5-6 was chosen. The pilot will use the part of the docking interface at the center of the visual target. Because the docking interface protrudes from the surface of the PTLI, the surface will have a three dimensional geometry allowing the pilot or mission control to adjust the space-craft attitude.

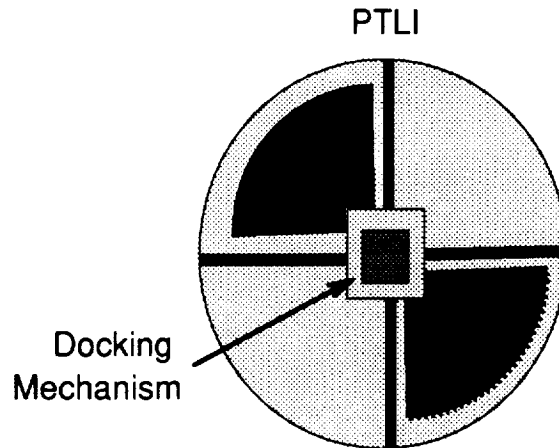


**Figure 5-6**  
**Visual Target Surrounding Docking Interface**

#### **5.2.16 Video Cameras**

Failure of the primary docking mode and lunar landing both require a video interface with the pilots. The video cameras chosen are charge coupled devices (CCD). They are small and light. Because they are readily available, off-the-shelf components, they run on NTSC standard at 30 frames/s, compatible with CRT displays.

#### **5.2.17 CRT Displays**

Cathode Ray Tubes (CRT) displays are necessary to display video for failure-mode-docking and lunar landing. The CRT displays are directly compatible with the video cameras. The CRTs display in color.

#### **5.2.18 LCD Displays**

LCD displays were sought after because of they're light weight, small volume, and reduced power consumption. These are the same types of displays that are used on the Boeing 777 fly-by-wire aircraft.

#### **5.2.19 External Spacecraft Tracking**

While vehicle attitude may be determined relatively easily by a spacecraft using star, earth, and sun sensors, accurate translational measurements are quite difficult to obtain. For this reason, several tracking methods will be employed which take advantage of external sources for accurate measurement of spacecraft position and velocity.

#### 5.2.19.1 The Global Positioning System

The Navstar Global Positioning System (GPS) can be used for highly accurate spacecraft position and velocity measurements in the vicinity of the Earth to an altitude of about 1800 kilometers [AGARD, 1988]. The state of a single object can be instantaneously determined with a position accuracy of less than 30 meters [Bar-Sever, 1990] and a velocity error of less than 6 centimeters per second [AGARD, 1988]. If integrated over a few hours, the position error estimates can be brought down to less than three meters. The relative position of two active, cooperating bodies can instantaneously be found with a three sigma error of less than 10 meters [AGARD, 1988].

#### 5.2.19.2 Ground Tracking

The Deep Space Network (DSN) is a system of large Earth-based antennas which will be used for direct communication with the Columbiad spacecraft. In addition to communication, this system will be used to track the vehicle's position and velocity when it is beyond the range of GPS, and will be used as a backup in case of a failure of the GPS antenna. A single DSN antenna can determine the position and velocity of an object in space very accurately. The antenna can measure the angle of the line-of-sight to a coasting body to less than  $0.0035^\circ$ . The object's range can be determined to within 5 meters while its velocity can be found from doppler readings to an accuracy of about 10 centimeters per second [Jet Propulsion Laboratory, 1980]. The angular error of  $0.0035^\circ$  corresponds to a cross-range error of about 24 kilometers at lunar distances; however, analysis has shown that measurements taken from three widely separate points on the Earth can reduce this error to approximately 1 kilometer. DSN antennas are located in Spain, Australia, and California.

DSN can also be used as a backup for the GPS system described above. Its accuracies are very similar to GPS accuracies for vehicles in Low Earth Orbit. The only drawback of using this system is that a communication link with Earth is required.

#### 5.2.19.3 Pre-Deployed Navigation Aids

In an effort to improve position and velocity navigational accuracies on and around the moon, pre-deployed navigation aids will be implemented on the Columbiad mission. The use of such aids will allow for better landing and launch accuracies on the lunar surface, and will be a long lasting aid for future missions with a reasonable one-time cost.

Lagrange point satellites, a lunar version of GPS, and Lunar surface aids were all considered. Lagrange point satellites were found to be somewhat useful; however, they have a large cost, their best accuracy is during midcourse rather than landing and launch, and they are not very effective in measuring spacecraft deviations out of the lunar orbital plane. Lunar GPS was found to be much more useful for surface operations, however, its enormous cost makes this option unrealistic at this time. For these reasons, accurate yet relatively inexpensive lunar surface aids similar to aircraft navigation aids on Earth will be used by Project Columbiad.

Looking at cost, complexity, and navigational accuracy, it was determined that a set of two transponder ranging beacons on the lunar surface forming a line perpendicular to the spacecraft horizontal velocity on final approach or launch (see Figure 5-7) is the best solution for improved navigation. Assuming the vehicle has a radar altimeter and a rough lunar map on board, two beacons with a separation of 50 kilometers will give enough additional information to greatly reduce the errors in all three dimensions. To ensure that any spacecraft flight direction will have two beacons forming a line roughly perpendicular to it, three beacons in a triangular formation around the nominal landing site will be the desired configuration (see Figure 5-8).

During final descent, the spacecraft will be located within the triangle formed by the three beacons, giving even greater accuracies. At least two beacons will be visible by the spacecraft down to an altitude of 180 meters, at which point inertial navigation, altimeter information, and video data will be satisfactory for position and velocity determination.

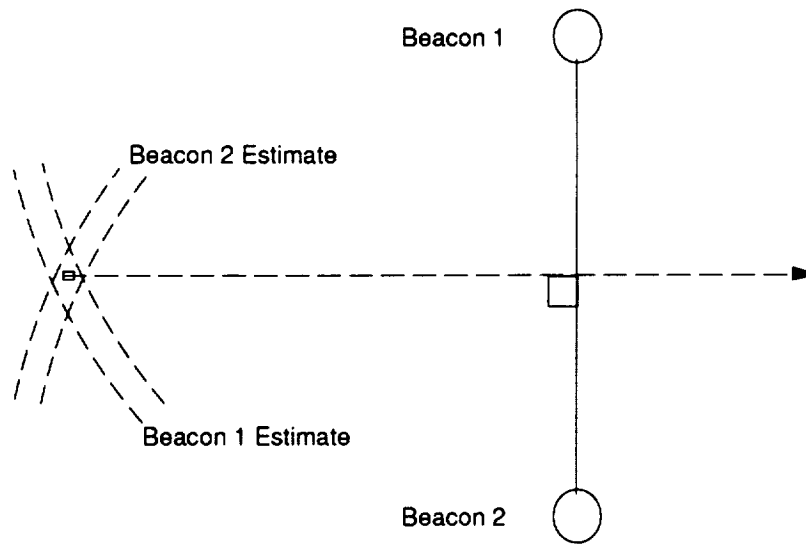


**Figure 5-7**  
**Optimal Transponder Beacon Orientation**

Beacons ○

△ Nominal Landing Site

**Figure 5-8**  
**Optimal Beacon Configuration**

#### c3.5.2.20. Conclusion

In conclusion of GNC design, all the instrumentation has been placed in the Table 5-5 below.

**Table 5-5: GNC Instrumentation Breakdown**

system	no. of systems	subsystem vendor	weight (kg)	volume (m3)	power (W)	power profile
<b><u>FOR EACH MISSION</u></b>						
<b><u>PTLI</u></b>						
1. earth sensors	2	GNC	3.5	0.001	8	Continuous until the end of Rendezvous
2. GPS	2	GNC	5.0	0.010	10	
3. INS	1	GNC	7.5	0.010	40	
4. RCS	16	Propulsion				
5. telemetry and command radar		C3				
6. small hardware board		C3				
<b><u>LBM</u></b>						
1. docking laser radar	1	GNC	18.0	0.010	30	during Rendez- vous (~ 1.5 hrs.)
2. docking video camera	1	GNC	4.0	0.010	20	
<b><u>FOR PILOTED MISSION</u></b>						
<b><u>ERM</u></b>						
1. star trackers	3	GNC	25.0	0.100	5	Continuous from earth launch until end of Moon-to -Earth coast
2. sun sensors	1	GNC	1.0	0.001	2	
3. radar altimeters	3	GNC	15.0	0.010	25	
4. antenna beacons	2	GNC	3.0	0.010	20	
5. RCS	16	Propulsion				
<b><u>CM</u></b>						
1. INS	1	GNC	7.5	0.010	40	Continuous for whole mission
2. CRT Display	2	GNC	10.0	0.125	100	
3. Liquid Crystal Displays	2	GNC	3.0	0.040	10	
4. GPS	2	GNC	5.0	0.010	10	
5. landing video cameras	4	GNC	3.0	0.002	20	lunar landing .5h
7. RCS	8	Propulsion				
8. telemetry and command radar		C3				
9. main guid. computer		C3				

## **FOR PRECURSOR MISSION**

### **Habitat & Power Module**

1. INS	1	GNC	7.5	0.010	40	Continuos from Earth launch to Lunar landing
2. radar altimeters	3	GNC	30.0	0.100	100	
3. star trackers	3	GNC	25.0	0.100	5	
4. sun sensors	2	GNC	1.0	0.001	2	
5. GPS	2	GNC	5.0	0.010	10	
6. antenna beacons	2	GNC	3.0	0.010	20	
7. RCS	16	Propulsion				

### **5.3 Precursor Mission**

This section outlines the GNC operations for each phase of the precursor mission.

#### **5.3.1 Launch**

The launch vehicle will be completely responsible for control of the spacecraft during launch. It will also be expected to keep track of the position, velocity, attitude, and angular rates of the Columbiad vehicle; however, as a backup, the inertial navigation system of the Columbiad vehicle will be used during launch.

#### **5.3.2 PTLI Stationkeeping**

##### **5.3.2.1 PLTI Attitude Determination**

On the PTLI stage two Earth sensors and a sun sensor will be used with the IMU configuration discussed in 5.2.2 to determine the attitude of the stage. The sensor inputs will be downloaded to the ground to be processed. The Earth sensors and sun sensor will nominally take data every 2.5 minutes, and the IMU inputs will be sampled at 50 hertz.

##### **5.3.2.2 PLTI Translational Navigation**

The Global Positioning System will be used to track the position and velocity of the PTLI stage (see section 5.2.3.1). In case of a failure of the GPS antenna or unavailability of GPS, ground tracking will be done using the Deep Space Network (see section 5.2.3.2).

### 5.3.2.3 PLTI Guidance and Control

During the period between the two launches required for each mission, the PTLI stage will be required to remain in orbit, keeping constant communication with the Earth. The guidance required for three-axis stationkeeping will primarily be done from the ground with some autonomous capability in case of a broken communication. Control will be done with reaction control thrusters. Quick response is not necessary for attitude control because the stage will not experience large rotation rate changes, and the delay between the ground and the PTLI stage is minimal.

The control system during nominal stationkeeping will operate by comparing actual and desired angular positions and rates. The limitations of the reaction control thrusters make it impossible to achieve the exact desired conditions. In order to keep the system from limit cycling and wasting fuel by trying to reach an exact condition, a control method referred to as "bang-bang" control is used.

#### 5.3.2.3.1 Bang-Bang Control

Bang-bang control is performed independently on each of the three spacecraft axes. The computer uses navigational sensors to determine angular position and velocity about each axis. These values are compared to their guidance determined desired values, and a basic algorithm is used to determine whether negative, positive, or no thrust is required. The algorithm (see Figure 5-9) is chosen considering the desired speed of response, the vehicle moment of inertia, and the required angular accuracy. The first two determine the equations of the dividing lines and the third determines the size of the "dead zone" [NASA,1967].



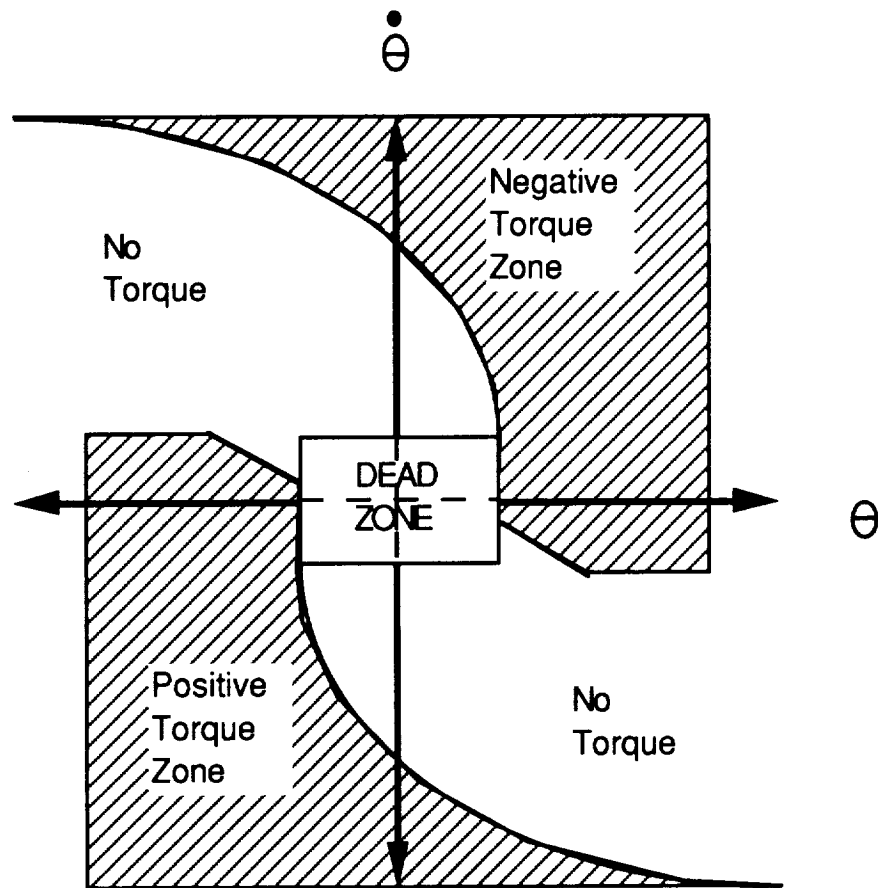


**Figure 5-9**  
**Bang-Bang Controller**

#### 5.3.2.3.2 Emergency Attitude Acquisition

In case of a communication break between the PTLI stage and the Earth due to an anomalous attitude, the vehicle will be capable of autonomously orienting its Earth sensor toward the Earth, reestablishing communication. The on board processor will use the rate gyro data to zero angular rates and initiate an earth acquisition sequence using the Earth sensor. The pitch rate will be set to 1/2 RPM, then the roll rate will be set to 12 RPM. Since the Earth sensor has a 30 degree field of view and the sun sensor has a 64 degree field of view, both sensors will cross their respective targets within two minutes. Recording the relative positions of these heavenly bodies will allow the vehicle attitude to be determined well enough to reacquire the Earth in the Earth Sensor.

### 5.3.3 Earth Orbit Rendezvous

#### 5.3.3.1 Docking

Docking is considered a part of orbital proximity operations between a chaser vehicle (CV) and a target vehicle (TV). More precisely, however, docking is the act of rigidly interfacing two spacecraft. The TV in both the precursor mission and the piloted mission is the PTLI stage. The CV consists of the PLM and the LBM in the Precursor mission and the CM, ERM, and LBM in the piloted mission.

The two different missions are exactly the same in their rendezvous configurations. Because the Precursor mission is unmanned it will be necessary to make docking automated. To keep the missions modular, the piloted mission will have the same automated docking system. There will be similar visual backup systems on both missions such that the ground control in the Precursor mission and the pilots in the piloted mission can take over the case of the primary system failure.

#### Docking Zones

There is a zone around the TV where effects of orbital mechanics are negligible on proximity operations. This zone is cylindrical and extends several kilometers ahead and behind the TV, while the radius is several hundred meters. According to Brody, NASA protocol defines the end of the rendezvous zone as the beginning of the docking zone, from 1000 meters in front to 1000 meters behind the TV [Brody, 1990]. This zone is not hard and fast as it was developed for Apollo and the Space Station (which will have many more vehicles in station-keeping). Although our GPS system will have greater positioning accuracy compared to previous missions, the same NASA standards will be maintained.

#### 5.3.3.1.2 Docking Accuracies

In Adkin's research on docking, he uses accuracies shown in Table 5-6. These accuracies are actual empirical data from the Gemini program [Adkins, 1986]. Though they are thirty years out of date, they establish the minimum accuracies that the guidance and control software must maintain for successful docking. Adkins also cites work done by Matra Espace (1985) in determining the influence of the docking environment on achievable accuracies.

**Table 5-6: Docking Requirements/Accuracies**

STATE MEASUREMENTS	GEMINI	MATRA ESPACE	LADAR REQS.	FINAL SPECS (on ladar)
range resolution			0.01 m	0.01 m
range accuracy			$\pm 0.1$ m	$\pm 0.1$ m
range rate	0.23 m/s	0.15 m/s	0.03 m/s %	.03m/s%
range acceleration	1 g			
angular pos. accuracy	0.25°	0.25°	$\pm 0.1^\circ$	0.25°
angular rate accuracy			$\pm 0.03^\circ/\text{sec}$	$\pm 0.03^\circ/\text{sec}$
lateral displacement	5 cm	0.23 m		0.23 m
lateral velocity		0.06 m/s		0.06 m/s
lateral acceleration	0.5 g			
maximum force	depends on the dock ing interfaced			

Environmental effects included differential drag, fuel slosh, etc. Matra concluded that it was possible to obtain errors of 2 cm translation error and 0.25 degrees angular error, even with noisy, nonlinear control [Brody, 1990].

#### 5.3.3.1.3 The 0.1% Rule

A major rule established by NASA is the 0.1% rule. The rule is simply that the CV must close in on the TV at a rate that is 0.1% of the range. Thus, if the CV is 1000 meters out, it can close in no faster than 1 meter per second; after 100 seconds it would be at 900 meters and could close in no faster than 0.9 meters per second. For this example a docking procedure could take up to an hour. It was determined by Brody out of NASA Ames, that this rule is overly conservative (from a remote pilot standpoint). Nevertheless, the rule is probably conservative overall; and an autonomous system could handle a 1% or 2% rule more efficiently.

#### 5.3.3.1.4 Docking System

The choice of hardware is based on comments made by Adkins about instrumentation developed for the future: "Prototype laser radar units have been shown to yield range accuracies of  $\pm 1$  cm. These units can be directed at a mosaic of reflectors in a known pattern. Differences in the range to various reflectors in the mosaic can then be used to compute relative angles of the pattern to the tracking ship (Rockwell, 1985)" [Brody,

1990]. A system has actually been designed which surpasses the specifications given in Table 5-6 [Bachman, 1979]. Unfortunately, there is very little information about the LADAR system; it does mention the physical characteristics: 30 kilograms, 0.001 cubic meters, 100 watts. An additional part of the design of the laser docking system is the array of retro-reflectors.

The main purpose of the retro-reflectors is to passively maintain the strength of the beam when it hits the TV; these are known as cooperative targets. Moreover, an array of retro-reflectors can be used to determine attitude at far ranges, while at close proximity a tracking of a single retro-reflector determine attitude and range.

A visual system is implemented as a backup to the automated LADAR system; a video monitor is imperative. Pilots or ground control will be able to adjust attitude using visual markers. The GPS system could be used for range/range-rate determination. From video it would be possible to make very precise alignments before interfacing. Figure 5-10 shows all the instrument interfacing to the guidance computer.

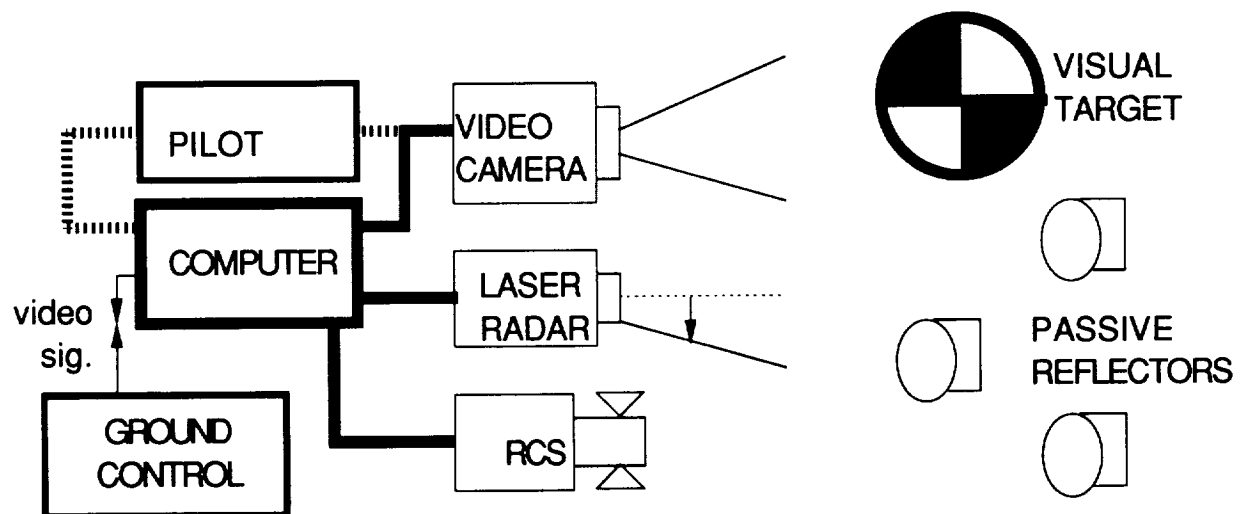


**Figure 5-10**  
**Instrumentation Layout**

### **5.3.4 Trans-Lunar Injection**

#### **5.3.4.1 Trans-Lunar Injection Navigation**

For the TLI burn, the spacecraft position and attitude will be determined autonomously. Immediately prior to the initiation of the TLI burn, the IMU will be updated with accurate position, velocity and attitude data as described in section 5.3.3. Throughout the burn, the gyroscopes and accelerometers alone will determine the state vector of the spacecraft.

#### **5.3.4.2 Trans-Lunar Injection Guidance**

The guidance for trans lunar injection will be implemented by the main on-board computer. It is important to note that the guidance law prescribed here is software based, and therefore its implementation can be easily changed in the future with little or no effect on the rest of the spacecraft design. The decision on a guidance law was based on a trade study between code complexity, computer power required, and fuel required for the maneuver.

The trans lunar injection is a powered flight maneuver, meaning thrust is the dominant force on the vehicle. The goal of this type of guidance scheme is to determine the desired direction, and magnitude if controllable, of the vehicle thrust vector. The required end state of the spacecraft is a given orbit, not a specific final position and velocity, so a Present-Velocity-Required (PVR) guidance approach is sufficient. [Hall,1991]

##### **5.3.4.2.1 Present Velocity Required Guidance**

The theory behind PVR guidance is that, for a given position, a required velocity can be found which will put the spacecraft on its desired orbit. The guidance computer vectorially subtracts the spacecraft velocity ( $\mathbf{V}$ ) from the velocity required ( $\mathbf{V}_r$ ) to obtain the velocity-to-be-gained ( $\mathbf{V}_g$ ). The goal is to reduce the velocity-to-be-gained to zero using the least fuel possible. [McKay]

It turns out that reducing  $\mathbf{V}_g$  explicitly, or simply thrusting in the direction of  $\mathbf{V}_g$ , is not the most fuel efficient method of steering. An implicit approach to the problem is to figure out what the time derivative of the velocity-to-be-gained is and, if possible, let it drive itself to zero without thrusting. Equation 5-11 is the governing equation for implicit PVR guidance. [Hall,1991]

$$d\mathbf{V_g}/dt = -\mathbf{Q} \mathbf{V_g} - \mathbf{a_T} \quad (5-11)$$

where  $\mathbf{a_T}$  is the thrust acceleration  
and  $\mathbf{Q} = \begin{bmatrix} \partial V_{rx}/\partial x & \partial V_{rx}/\partial y & V_{rx}/\partial z \\ \partial V_{ry}/\partial x & \partial V_{ry}/\partial y & V_{ry}/\partial z \\ \partial V_{rz}/\partial x & \partial V_{rz}/\partial y & V_{rz}/\partial z \end{bmatrix}$  (3 X 3 matrix)

The PVR guidance scheme which will be implemented on the Columbiad mission is cross-product steering. The idea behind this is to keep the  $\mathbf{V_g}$  vector from rotating by keeping it parallel to its time derivative vector. This way the magnitude of the velocity-to-be-gained is forced to constantly decrease with relatively little thrust. The computer keeps the two vectors parallel by driving their cross product to zero (see equation 5-12).

$$\mathbf{V_g} \times d\mathbf{V_g}/dt = \mathbf{0} \quad (5-12)$$

There are other steering laws which require even less fuel than cross-product steering, however, these methods require much more computer power, introduce unnecessary algorithm complexity, and do not save enough fuel to justify their use.

The purpose of the control system in a powered flight maneuver is to orient the vehicle thrust vector in the direction prescribed by the guidance system. This is done by angling the main thrusting engines. In the actual computer implementation of cross product steering, the vector solution to the cross product in equation 5-12 is found, and this vector is used as feedback to drive the attitude of the spacecraft [Battin, 1991] .

#### 5.3.4.3 Trans-Lunar Injection Control

Control of the spacecraft during the burn will be performed by angling the gimbaled main engines. The vehicle will be aligned to the proper attitude before the burn begins by using its reaction control thrusters.

### 5.3.5 Lunar Transfer Orbit

#### 5.3.5.1 Lunar Transfer Orbit Navigation

In the lunar transfer orbit (LTO), the spacecraft attitude, position, and velocity vectors will be constantly monitored by the IMU, with measurement corrections provided by the star trackers and DSN, as discussed in Section 5.2.3. One unusual feature of LTO is that the

spacecraft must be rotated about its yaw axis during flight for thermal reasons. Also, the vehicle will be required to change its attitude prior to midcourse correction and Lunar Orbit Injection (LOI) burns. These maneuvers must be accounted for in the star tracker ephemeris.

When the spacecraft enters the Moon's sphere of influence, the inertial coordinate system must be changed from Sun-centered to Moon-centered coordinates. For this conversion, the location and orientation of the spacecraft must be converted to the Moon-centered coordinate system.

#### **5.3.5.2 Lunar Transfer Orbit Guidance and Control**

The guidance during LTO will be implemented by the main on-board computer. It is important to note that the guidance laws prescribed here are software based, and their implementation can be easily changed in the future with little or no effect on the rest of the spacecraft design. The decision on guidance laws were based on trade studies between code complexity, computer power required, and fuel required for maneuvers.

For the majority of midcourse flight, attitude control alone is needed in order to keep navigational sensors and communication equipment pointed in the right directions. This will be done by the RCS system using relaxed "bang-bang" control (see section 5.3.2). One or two small changes in translational velocity (on the order of 10 meters per second each) may be required for correction during the three day flight. To do this, the RCS thrusters will line the vehicle up in the direction of the velocity to be gained and the main thruster will briefly fire. RCS jets will finally be used to line up the vehicle before the lunar orbit injection.

#### **5.3.6 Lunar Orbit Injection**

##### **5.3.6.1 Lunar Orbit Injection Navigation**

For the LOI burn, the spacecraft position and attitude will be determined autonomously. Immediately prior to the initiation of the LOI burn, the IMU will be updated with accurate position, velocity and attitude data as described in section 5.3.5. Throughout the burn, the gyroscopes and accelerometers alone will determine the state vector of the spacecraft.

#### 5.3.6.2 Lunar Orbit Injection Guidance and Control

Lunar orbit injection is a powered flight maneuver, meaning thrust is the dominant force on the vehicle. The goal of this type of guidance scheme is to determine the desired direction, and magnitude if controllable, of the vehicle thrust vector. The required end state of the spacecraft is a given orbit, not a specific final position and velocity, so a Present-Velocity-Required (PVR) guidance approach is sufficient. Guidance and control for these mission phases will be the same as for the trans lunar injection phase (refer to 5.3.4).

#### 5.3.7 Lunar Descent

##### 5.3.7.1 Lunar Landing Navigation

Immediately before the initiation of lunar landing, the IMU will be updated as accurately as possible using DSN, the star trackers, and the Lunar transponder beacons. The IMU will be the only navigation and attitude system for the initial lunar descent orbit. As the vehicle approaches the final landing site and comes within line of sight of the Lunar beacons, these will be used to further aid in position and velocity determination.

During the final vertical descent phase of landing, a radar altimeter system and video camera will be used for Navigation. The altimeter system will give highly accurate velocity and position estimates. The camera will allow for ground determination of the final landing site, since the altimeter system cannot ensure that the vehicle will not land on a small boulder. Ground command will be capable of controlling horizontal position and velocity directly while the on-board computer controls the vertical velocity and attitude of the spacecraft.

##### 5.3.7.2 Lunar Landing Guidance

The final lunar descent burns will be powered flight maneuvers, however, since the end state of each of these burns is critical, position constrained guidance must be employed.

###### 5.3.7.2.1 Position Constrained Guidance

For this phase of the flight, we have chosen to use "nominal following control". This type of guidance utilizes a pre-computed nominal trajectory and uses simple feedback to keep the vehicle on this path. This method is limited because it requires a very specific initial condition and uses more fuel than other methods; however, it is far simpler than other methods to implement electronically and the guidance code is more reliable.



#### **5.3.7.3 Lunar Descent Control**

During the powered flight of lunar descent, the main thrust vector direction will be controllable to four degrees from axial to give control over the attitude of the spacecraft. Also, the main engines will be throttlable to ensure a soft landing on the lunar surface. The purpose of control loops will be to follow as closely as possible the guidance prescribed by the main computer.

### **5.4 Piloted Mission**

This section outlines the GNC operations for each phase of the piloted mission.

#### **5.4.1 Mission Similarities**

The piloted mission operations are similar to those for the precursor mission, except for the mission phases discussed below.

#### **5.4.2 Lunar Landing**

The piloted lunar landing phase will be identical to the precursor phase, except that the pilots will control the horizontal position and velocity of the spacecraft. This will be done using a monitor, the video camera, and a simple joystick. Having the pilots perform this task will eliminate the four second time delay associated with Earth communication.

#### **5.4.3 Lunar Launch**

##### **5.4.3.1 Lunar Launch Navigation**

For lunar launch, the ascent will be inertial with position and velocity updates from the Lunar transponder beacons. Once the spacecraft has reached a low lunar orbit, the gyros and accelerometers will have their time dependent errors further corrected by star tracker and DSN inputs.

##### **5.4.3.2 Lunar Launch Guidance and Control**

Lunar launch will be performed using position constrained powered flight guidance. Nominal following control will be used to bring the spacecraft to the desired low lunar orbit (see section 5.3.8). Control will be performed using the throttlable and gimbalable main engines.

#### **5.4.4 Trans Earth Injection**

##### **5.4.4.1 Trans-Earth Injection Navigation**

TEI navigation will be implemented in the same way as TLI navigation (see section 5.3.4). Inertial navigation will be used throughout the burn. The inertial coordinate system must be changed back from Moon-centered to Sun-centered when the spacecraft leaves the Moon's sphere of influence.

##### **5.4.4.2 Trans-Earth Injection Guidance**

The TEI burn will be identical to the TLI burn from the standpoint of guidance and control. PVR guidance will be implemented using cross product steering, and RCS jets will be used to initially align the main thrust vector as required (refer to section 5.3.4).

#### **5.4.5 Earth Transfer Orbit**

##### **5.4.5.1 ETO Navigation**

ETO navigation will be done almost identically to LTO navigation (see section 5.3.5). The main exception is that, since reentry conditions are so critical, GPS will be used to update the exact position and velocity of the vehicle. In the few moments after the ERM is released and prior to reentry, only inertial and GPS measurements will be performed.

##### **5.4.5.2 ETO Guidance and Control**

The return midcourse flight will be almost identical to the midcourse flight to the Moon. Bang-bang control will be used to maintain the proper attitude and the ERM will be used for small correction burns (see section 5.3.5). More fuel will be used on the return flight since the end point constraint is so critical.

#### **5.4.6 Reentry Navigation, Guidance and Control**

##### **5.4.6.1 Reentry Navigation**

Immediately before ERM separation, the IMU will be updated using star trackers and DSN. During reentry, the CM will be controlled autonomously through the plasma induced blackout, and then ground tracking and GPS will be used to monitor the position and velocity of the spacecraft until touchdown. Throughout the entire reentry, the gyroscopes will be used to control the attitude of the spacecraft.

#### 5.4.6.2 Reentry Guidance and Control

Reentry guidance is very different from any other type of guidance prescribed for this mission. During reentry, the primary force on the vehicle is aerodynamic lift and drag. The reentry path will need to be predetermined, however, small errors will tend to propagate. Since the end state is highly restricted, corrections will have to be made throughout the Earth approach. For this reason, a multiple-mode guidance scheme will be used [McKay].

Multiple-mode, as the name implies, uses several guidance schemes during reentry to serve several purposes. The process of reentry is typically broken up into five modes: pre-entry, initial pull-up, controlled climb, ballistic skip / high altitude cruise, and final glide.

##### 5.4.6.2.1 Pre-Entry

Pre-entry includes the last minute corrections made to ensure atmospheric entry conditions are satisfactory. Coming in at too steep an angle will cause the vehicle to burn up, and coming in at too shallow an angle will cause it to skip off the atmosphere and careen irreversibly into space. The ERM is used to make these final burns before it is separated from the command module.

##### 5.4.6.2.2 Initial Pull-up

Initial pull-up is the most critical mode in terms of safety, since this is the time the vehicle is most likely to exceed maximum loads. Much of the kinetic energy is dissipated during this phase. The guidance system ensures the vehicle remains within the physical limits of the vehicle while still managing to shed this kinetic energy. Control of the spacecraft during this and all other modes is performed by using reaction control jets except where noted otherwise. The RCS jets can easily roll the spacecraft, allowing for climbs, dives, and turns in both directions. Minimal pitch and yaw control is also possible using the RCS jets.

##### 5.4.6.2.3 Controlled Climb

When the attitude rate becomes zero or slightly positive, the controlled climb mode begins. The vehicle typically climbs to an altitude which will allow it to dissipate just enough energy to reach the target without exceeding it. The final altitude of the climb is a pre-computed function of the range to target.

#### 5.4.6.2.4 Ballistic Skip / High Altitude Cruise

The final altitude of the climb can either be above or below the "top" of the atmosphere, resulting in a ballistic skip or a high altitude cruise respectively. In a ballistic skip, the atmospheric exit condition essentially dictates the landing site. In a high altitude cruise, calculations can be made in flight to find the final landing point given the current altitude and corrections can be made in flight. A high altitude cruise would, of course, be the desired path, and a ballistic skip would only be used if the vehicle were expected to fall significantly short of the target.

For the current design, the high altitude cruise of the flight is characterized by large oscillations which will be quite difficult to guide. For this portion, the ground will be given general control of the vehicle. Complex, high speed computer code will take the current vehicle state vector and use predicted final value control (a complicated version of position constrained guidance) to decide when the roll maneuvers of the crew module need to occur.

#### 5.4.6.2.5 Final Glide

The final glide comes when the vehicle has lost most of its kinetic energy and can no longer maintain a constant altitude. At this point, the vehicle glides into its target as well as it can using its parachutes.

### 5.5 Lunar Operations

Navigation on the lunar surface is an integral part of the lunar rover operations. Most of the rover operations will occur outside visible sight of the BioCan. This will preclude using a beacon for navigation. The easiest form of navigation possible is inertial navigation. Using the rover's computer and an INS, it is possible to integrate INS output in real-time to establish a position. This position can then be displayed to the driver via an LED display.

The main problem with INS is the drift rate errors that the gyros introduce in velocity measurements and the computed position. To decrease the effect of the INS, it is necessary to zero-out the INS. When the rover has no velocity, that is, when it is stopped, the INS drift rate can be initialized precisely to zero. Thus, the more often the INS is initialized, the less error accumulates. Nevertheless the errors are much more than 1km/hr. In addition to gyro drift, errors can also be introduced due to the unevenness of terrain. These error can be alleviated by filtering the out the gyro readings [Artemis, 1989].

Once the rover is within a 1 km range of the habitat, it is possible to activate transponder beacon guidance. The beacon signal allows the rover to determine bearing and range.

In the event of a rover malfunction, it is necessary to return the astronauts safely to the habitat. The astronauts will be able to unplug the rover computer and the INS package. The INS package and a portable battery pack will clip on to the computer. Altogether it will have a mass of about 25 kg, easily portable. As with the rover, the astronauts will have to stop occasionally to zero-out the INS, for the same reasons given for the rover.

## **6 Power and Thermal Control Hardware Selection**

While in pursuit of the optimization of PTC hardware designs, many decisions and choices came to light which had to be thoroughly evaluated in trade studies. The following is a complete overview of the decisions and trade studies which were conducted among design options in PTC hardware. The first group of studies is an examination of miscellaneous power hardware options which pertain to several applications throughout the Columbiad hardware; the next two sections pertain respectively to the power hardware of the spacecraft and of the lunar surface equipment. Last is an examination of the issues of cryogenic propellant and reactant storage.

### **6.1 General Power Hardware Selection, Issues, and Trade Studies**

#### **6.1.1 Choice of Conductor**

An important trade study was done to choose the material which will be used for any long conductors included in the final design. This choice will be made partly on the basis of which metal has the highest conductivity for the lowest density. High conductivity is desirable because it results in low power loss along the length of the cable, while low density is desirable because less mass needs to be transported on the mission in the form of cabling with a normal or large cross-sectional area. Table 6-1 shows a list of the three top candidates for the choice of metal for wiring.

**Table 6-1: Conductor Properties**

	conductivity ( $1 / \Omega\text{m}$ )	density (kg/cu.m)	conductivity per density
aluminum	$3.77 \times 10^7$	2650	14240
copper	$5.99 \times 10^7$	8960	6683
silver	$6.29 \times 10^7$	5990	5990

It can be seen from the table that when minimizing mass for transportation is a strong driver, aluminum becomes the conductor of choice since its very low density strongly compensates for its relatively low conductivity.

### **6.1.2 Power Conversion: Transformers, Inverters, Regulators**

Conversion from the DC power of the solar arrays and fuel cells to AC, if the task becomes necessary, will be accomplished with an inverter. Typical inverters have performance parameters of .272 kg per kW converted and 96.5% to 98% efficiency. Voltage regulators typically require .9 kg/kW and 98% efficiency. Transformers may also be needed for some tasks of power conditioning. Typical performance numbers for transformers are .91 kg per kW converted and 98.5% efficiency.

### **6.1.3 Electrical Storage Survey and Selection**

Electrical energy storage devices will be required in several applications throughout the Columbiad hardware. A preliminary survey of these devices was conducted to choose the best such systems and to match up specific storage devices with specific applications.

The two basic types of electrical storage devices are fuel cell systems and sealed cell battery packs. An overview of these devices is shown in Table 6-2.

**Table 6-2: Electrical Storage Devices**

#### **Sealed electric cells**

- Silver-Zinc cells: high performance, very limited rechargeability, specific energy = 150 to 175 W-hr/kg, 50% allowable depth of discharge
- Lithium-based cells: specific energy = 450 Whr/kg, very limited rechargeability, 100% allowable DOD
- Sodium Sulfur cells: high performance, good rechargeability, specific energy = 150 to 210 Whr/kg, 80% allowable DOD, still in developmental stage
- Nickel-cadmium cells: specific energy = 25 to 30 W-hr/kg, 15 to 20% allowable DOD, long cycle life, large acquired data base on all aspects of behavior of Ni-Cd cells, by far most widely used cells in aerospace
- Nickel hydrogen: specific energy = 30 to 45 W-hr/kg, long cycle life, 30 to 40% DOD, require greater volume than Ni-Cds, up and coming replacement for the Ni-Cd cell

#### **H<sub>2</sub>-O<sub>2</sub> Fuel Cells**

theoretical max specific energy = 3630 W-hr/kg, typical discharge efficiency of 60 to 70%, electrolytic recharge efficiency of 70 to 80%, typical fuel cell hardware specific power of 147 W/kg, typical cell voltage = 1.0 V at room temp.; produces essentially pure water, can be consumed or otherwise used by astronauts, requires cryogenic or gaseous storage system for reactants

From the statistics in Table 6-2, one can see that the fuel cell system can easily store more energy per system mass, greater by a factor of ten, than the capability of the sealed cell units. However, the fuel cell system also has greater complexity, requiring external plumbing and gaseous or cryogenic storage of its reactants, while the sealed cells come as a single sealed unit. Therefore, for applications where the volume and complexity of a cryogenic storage system can be accommodated such as in spacecraft stages or the lunar power plant, fuel cells will be used. Conversely, in situations where a compact, less complex means of storage is desired, sealed cells will be used. If rechargeability is not necessary, the high-energy Lithium-based cells such as Lithium thionyl chloride will be chosen; if rechargeability and longer life is desired, the Sodium sulfur cells with the second highest energy capability will be employed.

#### **6.1.4 Bus Voltage Selection**

To transmit a given amount of power through a conductor, higher voltage is chosen so that currents will be lower. Lower currents mean that smaller gauge wire can be used (lower cross-sectional area and less mass) and still not drive up the energy dissipated in the conductors. On the other hand, in spacecraft one encounters lower ambient gas pressures and smaller equipment dimensions, so if potentials are too high, arcing, a dangerous loss mechanism, can occur. These two driving and opposed factors, desired low currents versus arcing potentials, combine to set the typical bus voltage of a spacecraft in the range of 30 to 40 volts DC. PTC decided that the Columbiad spacecraft will mimic the Space Shuttle in choice of bus voltage at 32 volts DC.

Land-based or larger-scale power transmission is typically done with high-voltage, high-frequency alternating current, chosen to avoid and prevent the development of loss-incurring currents over long lengths of conductor. The Space Station Freedom originally was slated to provide power in the unprecedented style of 440 volts AC, 20kHz. However, after continued studies the Station was brought back to a lower voltage DC format. PTC decided that the Columbiad lunar surface hardware will operate with a common bus voltage also of 32 volts DC, to promote compatibility and power sharing between the lunar equipment and the moon-faring spacecraft of Project Columbiad.

All power sources of Columbiad will be designed to output a source voltage of 32 volts DC, but will also be fitted with DC to DC converters to provide 15 volts and 5 volts for equipment calling for these other common voltage levels. Thirty-two volts will be used for



operating higher-power devices, such as valves and actuators which call for the higher voltage, 15 volts is assigned for purposes of housekeeping tasks, and five volts is supplied for powering digital equipment.

#### **6.1.5 Power Distribution Characteristics**

Circuitry for power distribution should have several safety characteristics built into its design, including surge protection, fault isolation and the ability to switch-bypass failed units, and circuit breakers at the main power source as well as out at the low level supplies. A chassis ground design will not be implemented to isolate the power system and electrical apparatus from external noise sources such as upper atmospheric plasma-induced and radiation-induced charging, lightning strikes, etc.

#### **6.1.6 Power Systems Safety Factor Definition**

As handed down from Systems Engineering, all power systems will incorporate a factor of safety of 1.1. This factor has two separate meanings: 1) Power supplies and power conversion devices must be capable of supplying 1.1 times the maximum expected power needed over the supply's duration of use; 2) Electrical energy storage devices must be capable of supplying 1.1 times the total energy they will be expected to supply over the duration of their use.

### **6.2 Lunar Surface Power Plant Selection**

#### **6.2.1 Introduction**

One of the larger hardware units which is called for on the lunar surface is a large power plant. This plant must have the ability to provide power for all operations on the lunar surface, which include life support, communications, and scientific experiments in the habitat, operation of the lunar rover and of lunar construction equipment, and possibly future manufacturing applications. Furthermore, the plant may be able to support the piloted mission command module during the astronauts' stay on the surface.

Since a major objective of Project Columbiad is to allow for future expandability of the lunar base, it was important to design a power plant which could support the activities which were certain to occur and then scale up the plant to allow for future needs. This essentially meant including an additional availability of power for which there was as yet no designated use. Determining the type and the scale of the power plant was undertaken by Surface Payloads and Power and Thermal Control.

### **6.2.2 Scale of Lunar Surface Power Plant**

Initial designs for the power plant called for power availability in the range of hundreds of kilowatts up to the 1 megawatt range. This is the range of power which has been assumed in several NASA papers on the lunar power plant topic. As a major objective of Project Columbiad it was considered desirable to emplace on the moon a power plant which was substantially larger than the needs of this first mission, in that this plant would also be ready to provide power for later missions, all of which could tap the ready power supply on the moon. There would be no immediate need to bring additional power supplies to the moon for future scientific apparatus or habitats, and power provision would be unified in a single unit. Furthermore, a large power plant would be highly useful for future lunar-based construction and manufacturing, allowing more rapid expansion and endeavor into these areas.

The essential argument against a large-scale or oversized power plant was that the addition of such a large piece of payload would simply add too much to the cost of Project Columbiad. Too large a plant would make for too large an initial investment in the efforts of the space program to return to the moon.

Given the scope of Project Columbiad, it was deemed much more practical to return to the notion that the project is more of a pioneering mission, and that lunar manufacturing would probably be still more than a decade in the future beyond the project. Before any manufacturing could take place, extensive experimentation with lunar surface material would surely have to be done on the earth. As the moon is an extremely harsh environment, there is much research and testing to be done before industrialization is known to be feasible, and a manufacturing project design would take years after that to be implemented. Hence lunar-based manufacturing was removed from the needs for power provision by the Columbiad plant. The remaining major power needs were life-support and scientific experimentation, similar to those of Space Station Freedom. Noting that the Station is slated to provide a 40 kilowatt capability, it was decided that first cut designs for the power plant should be scaled back to be on the order of 100 kilowatts.

### **6.2.3 Trade Study: Type of Power Plant**

A search through all the recent literature regarding lunar-based power plants revealed that three main types of sources are generally considered: nuclear, solar photovoltaic and solar thermal dynamic. Nuclear power plants operate through the chain-reaction fission of a heavy element such as Uranium-235 which releases large amounts of heat. This heat is typically converted to electricity through a Stirling engine-generator apparatus. Solar photovoltaic plants produce power by converting sunlight directly to electricity in a cell made of a material such as Gallium-Arsenide. Solar thermal-dynamic plants typically function by absorbing solar radiation as heat in a fluid, and then using the heated fluid to run a Brayton engine-generator apparatus to produce electricity. See Table 6-3 for a comparison of typical space-rated power plant performance parameters.

**Table 6-3: Power Plant Performance Parameters**

	specific power (Watts/kg)	system efficiency
Nuclear plant	33	25 to 30%
Solar photovoltaic plant	25 to 100	18 to 24%
Solar thermal-dynamic plant	9 to 15	20 to 35%

Early in the comparison, solar thermal dynamic option was discarded for two important reasons. First, the system puts out a specific power of less than half those of the other two types of systems, which means one could expect the system mass of the thermal dynamic system to be twice as large as the others. The dynamic system was also discarded because it has the disadvantage of requiring a mechanical Brayton engine and thermodynamic cycle which creates greater system complexity and reduced reliability, and more development difficulties. Hence, only the photovoltaic and nuclear systems were pursued in greater detail.

#### **6.2.3.1 Power Plant System Mass Comparison**

The first major point of comparison between the two systems was that of total system mass. One of the top drivers of the design was to minimize the mass and therefore the cost of transporting the system to the moon. The power plant had the potential to be one of the most massive pieces of payload of Project Columbiad, and each piece of payload mass has heavy consequences which propagate all the way back to the launch vehicle in terms of additional propellant, etc. Therefore a system mass analysis was carried out by creating

models of each of the two types of systems, each based upon a published paper on that type of lunar power plant. The solar plant reference paper was written in 1990 at the University of Washington and was entitled, "A 1-Megawatt Solar Lunar Power Plant." The nuclear plant reference paper was developed at the NASA Lewis Research Center in 1989 and is entitled "SP-100 Power System Conceptual Design for Lunar Base Applications."

The following system mass breakdown models were generated by scaling down the system components which were linearly proportional to power output, and then adding these scaled-down numbers to the fixed parameters. (See Table 6-4)

**Table 6-4: Preliminary Power Plant Mass Breakdowns**

1) Solar plant (based upon numbers from U. of Washington paper)	
Characteristics: 100 kW output during daytime, 30 kW output during lunar night	
Component	Mass (kg)
Solar array	1625
Electrical Storage	6024
Power Transmission, Conditioning	950
Backup Power	2856
TOTAL	11455 kg (+construction equipment)

2) SP-100 nuclear plant (based upon numbers from NASA SP-100 paper)	
Characteristics: 100 kW nominal; 150 kW with single redundant Stirling engine online	
Component	Mass (kg)
Reactor and low level shielding	2045
Heat transport equipment	765
Power conversion	734
Heat rejection	884
Power management and dist.	1650
Cabling	917
Surface Structure	1684
Backup Power	2856
TOTAL	11535 kg (+construction, excavation equipment)

As can easily be noted, for similar output characteristics the solar power plant and the nuclear power plant require roughly equal total system mass. This allows more flexibility in the choice of the type of plant, and allows for more attention to be given to the plethora of other considerations in the type-of-plant-decision. As will be seen, these considerations include expandability, maintainability, required manpower, environmental issues, and others.

#### 6.2.3.2 Additional Comparative Considerations of Power Plant Choice

The following is a list with discussion of the additional points of interest with respect to the nuclear plant versus solar plant decision.

1) System safety: The nuclear plant would raise serious safety concerns over the handling, disposal, and containment of radioactive waste, astronauts' exposure to radiation, and the potential for reactor explosion, whereas the solar plant produces no toxic waste or radiation and has a reduced likelihood of explosive failure.

2) Astronaut-assisted versus autonomous operation: In the nuclear studies surveyed, it was generally assumed that several astronauts would be continuously on hand for the monitoring and control of the plant, whereas the solar power plant would be more amenable to autonomous operation. Project Columbiad will not leave any astronauts on the lunar surface, while later missions will have the option of doing so.

3) System complexity: The nuclear plant has a greater overall system complexity, with a nuclear chain reaction and a dynamic power cycle and mechanical engines, while the solar plant has the simple components of solar cells for day operation and highly reliable fuel cells for night operation.

4) System lifetime and reusability: A standard reactor lifetime before decommissioning lasts about 30 to 40 years, after which the reactor is too contaminated for continued use. The solar plant would experience solar cell degradation over several decades and the panels would have to be replaced, but the rest of the structure and components would still be usable.

5) Refuelling: The nuclear reactor would have to be refuelled every seven to ten years with a shipment of uranium from the earth. Assuming the solar plant's cryogenic storage

system was effective, the replenishing of reactants for the night power fuel cell system would require substantially less mass from the earth over time.

6) System Deployment Difficulty and Setup Time: The nuclear reactor would need a separate landing stage to emplace it upon the lunar surface several kilometers away from the habitat for radiation considerations. In addition, the reactor would have to be buried 4 meters down under the surface to provide shielding, so additional excavation hardware would have to be included with the power plant. A solar power plant can be designed to be constructed by astronauts with no heavy lifting equipment, since no individually large units need to be moved. The hardware can be broken down into more manageable units.

Conclusion: In light of the above considerations, especially the safety, manpower, and setup issues, it was decided that the Columbiad lunar plant should be a solar power plant. The nuclear option seems to become acceptable only for much higher power applications, where the nuclear reactor constraints are mitigated by the preference for handling one singular heavy hardware unit as opposed to setting up an unacceptably large number of solar panels. Therefore, Project Columbiad will call for the emplacement of a Solar Lunar Power Plant (SLURPP) on the lunar surface for supplying power to the BioCan habitat, rovers, and scientific apparatus.

### **6.3 Spacecraft Power Hardware Selection and Trade Studies**

#### **6.3.1 Power Supply Placement on Vehicle Stages**

Initial designs called for an individual fuel cell power supply to be placed in every vehicle stage. (See Table 6-5) It was then realized that most of these fuel cell systems would never be operating simultaneously, so there were too many redundant power supplies.

Furthermore, when a stage was jettisoned, a useful power supply was dumped along with the empty stage. This configuration was extremely wasteful of mass. It was first decided that power supplies should be placed in the highest stages (PLM and CM; later PLM and ERM), drawing their reactants from the LOX-LH<sub>2</sub> propellant tank of that stage, and sending power down to all other stages that needed supply.

**Table 6-5: Vehicle Stages**

Precursor Mission	Piloted Mission
PLM	CM
LBM	ERM
PTLI	LBM
	PTLI

Another realization was that the PTLI needed to have its own power supply in both the precursor and piloted missions because of the separation time between earth launches. One launch will put the PTLI in orbit, and a second launch will bring up the other half of the vehicle for assembly of the two halves in LEO. While the PTLI waits in LEO for the second launch, it will need power for C3, GNC, and other subsystem concerns, so it must have its own power supply.

The last major consideration of power supply placement is the issue of a supply for the Crew Module of the piloted mission. Since the CM is very much volume restricted, it was decided that the main power supply should be placed in the ERM just below the CM. The CM would draw most of its power from the ERM but would also be fitted with a smaller sealed Lithium cell supply for power during reentry, after the ERM has been jettisoned.

The ultimate result of this study was the elimination of two of the stage power plants, the one in each of the Lunar Braking Modules of the two missions. The primary power stages (i.e. the ones with fuel cell power plants) are the PTLI, the ERM, and the PLM. Thus a modest mass savings of approximately 50 to 100 kilograms was achieved, accompanied by a cost savings of the price of the two extraneous power plants.

### **6.3.2 Wraparound Solar Array on Primary Vehicle Power Stages**

Another concept which was studied was the notion of installing a wraparound solar array on each of the vehicle power stages to lessen their dependency on fuel cells. The main inspiration for this idea comes from the fact that the vehicle will be bombarded at all times with the sun's energy, and it would be convenient to tap that energy rather than carry the energy along in the form of fuel cells and reactant mass. The factor that limits the decision would be that the equipment mass needed to tap the solar energy plus the added system

complexity might make the compact, highly reliable, and more easily integrable fuel cell system more attractive.

Several issues related to the stages' solar cell concept were examined:

- The stage designs would have to include fairings for array protection during launch which would require additional mass.
- The fairing ejection system would be critical and power generation would be dependent upon successful jettisoning of fairings to uncover the solar arrays.
- Arrays covering the spacecraft surface could lead to a thermal control complication, since there could no longer be a high-reflectivity coating everywhere on the stages. Noting that the best arrays are only 23.5 percent efficient, a large fraction of the incoming radiation must become heat.
- One would have to carefully control vehicle orientation during its entire trajectory, to effectively track the sun and maximize the array projection area. Another important concern would be to ensure that the vehicle would not be eclipsed by the earth or moon during its trajectory.
- Sole reliance on arrays for power would cause power generation system to be dependent upon the success of the RCS system, since there would be a need to control vehicle attitude to get maximum projection area.
- Solar cells are composed of fragile, brittle material which could get broken or degraded during launch loads; the outside skin of the vehicle is designed and allowed to buckle during launch and this could destroy solar panels mounted on the outer skin. Another option would be to add structural mass to the outside skin at critical regions to reinforce the solar arrays.

Since the stages' fuel cell system masses are relatively low and fully satisfy the power needs, the only way it would be reasonable to implement the solar cell concept would be if confidence in the proposed system were high enough to go with solar panels only, and if the overall mass of that configuration would be less than that of the fuel cells. Also, it would be unacceptable to substantially compromise the thermal control provided by the outside reflective coatings. If these criteria could not be met, then it would be wise to include only the fuel cell systems for power generation. The proposed fuel cell system would be highly similar to that used on board the space shuttle, and that system has never experienced a major failure or serious performance degradation in flight.



After extensive study it was decided that the vehicle stages' solar wraparound arrays are an undesirable option. The power generation system is too fundamentally important to let its success be wholly dependent upon fairing ejection, the RCS system, and the brittle, fragile material of the solar panels. Furthermore, the arrays would have required increased structural mass for backing the brittle cell material during launch loads. Hence, it was deemed wise to design the stages' power plants with the tested fuel cell system.

### **6.3.3 Integration of Lunar Power Plant with Payload Landing Module**

Another important vehicle power plant concept is to integrate the Lunar Power Plant night operation fuel cell system with the Payload Landing Module as much as possible, to reduce the amount of design development necessary, and to make use of the payload lander structure and power system. Since the lander needs to carry the LOX and LH2 of the Power Plant somewhere on board the vehicle, it makes sense to combine the Power Plant tanks along with the vehicle propellant tanks, making use of the PLM structure and requiring development of one cryogenic storage system instead of two. Furthermore, it is sensible to place all the fuel cells of the lander and the Power Plant together, again to make use of the PLM structure and to make a need for only one thermally-controlled environment instead of two separate ones. In effect, after the lander touches down and deploys the payload, the lander will then be part of the Lunar Power Plant.

### **6.3.4 Integration of Fuel Cell Reactant Tanks with Propellant Tanks**

Another important issue was that of integrating the fuel cell LH2 and LOX cryo-tanks with the propellant tanks of the primary power stages. Initially it seemed to be a good idea to combine the cryo systems, to simplify the overall design and have one pair of cryo-storage tanks. One risk of the scheme of tapping fuel for the fuel cells before the fuel is used as propellant was that a valve failure could cause the vehicle to lose all its propellant. Several valve schemes were developed wherein each "valve" was actually several valves in series and parallel for multiple redundancy.

Examination of other system parameters shed light on the decision. The cryogenic storage temperatures of the two temperatures were slated to be equal, but the pressures were not. It turned out that the propellant tanks are to be pressurized substantially lower than needed for the fuel cells (40 psi compared to 100 psi). To bring all of the tanks up to the higher pressure would have meant more than doubling the tank structural masses to handle the increased stresses. Hence the following decisions were made: No propellant tank would be pressurized to the higher pressure to save mass; There will be separate, small, higher-

pressure tanks for the propulsion stages' fuel cell power plants to avoid having to add a pump into the system to provide the correct pressure to the fuel cells. Only the PLM, where fuel cell reactants account for over half of the cryo fluids, will have integrated lower-pressure tanks and will use a static heating unit to raise the pressure of the cryo fluid up to the needed input pressure of the fuel cells.



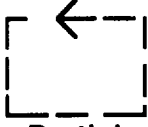

#### **6.3.5 Power Dependency of ERM/CM on Solar Lunar Power Plant**

The last major issue of discussion was the level of power dependency of the ERM/CM on the lunar power plant during the ERM/CM's 28 day stay on the moon. The ERM had previously been designed to carry power capability for itself and the CM only for use during transit to and from the moon, and to link up with the Solar Lunar Power Plant (SLURPP) for power during the lunar stay. The vehicles were all propulsively designed to be able to access any location on the moon, while the piloted vehicle was being designed with the concept in mind that the same vehicle design would be used repeatedly for later missions to the moon. The combination of these two facts lead to the notion that later piloted missions may be desired which do not return to the site of the BioCan and the lunar power plant, but to explore other surface regions, in which case the power dependency of the ERM on the power plant is a restrictive limitation. After study, it eventually was concluded that the capability of piloted missions to travel to other lunar locations besides that of the BioCan were not considered to be an objective of the hardware of Project Columbiad. However, it was also decided that the ERM/CM should be independent of the lunar power plant during its stay on the moon in the interest of redundancy and in case of emergency.

#### **6.4 Cryogenic Storage**

The long duration of Project Columbiad's proposed mission, coupled with our use of cryogenic fuels in our propulsion system, makes it necessary to provide a form of storage for these materials. The Propulsion and Thermal Control (PTC) sub-sub-system group examined many of the most efficient options available.

### 6.4.1 Storage Options

Storage Methods				
				
	Passive	Refrigeration	Partial Reliquefaction	Total Reliquefaction
Reliability	1	2	2	1
Cost	2	3	4	1
Performance	3	3	2	1
Safety	2	2	2	1
<hr/>				
Total	8	10	10	4
Power (kw)	0.22	0.55	5.32	2.13

J.Schuster, "LONG TERM CRYOGENIC STORAGE FACILITY SYSTEMS STUDY",  
NASA Conference Publication 2465, 1987

**Figure 6-1**  
**Evaluation of Storage Methods**

We began by looking at the storage methods suggested in the article "Long Term Cryogenic Storage Facility Systems" by Dr. J Schuster, published in NASA Conference Publication 2465, 1987. In this article, the author evaluates four such systems on the bases of performance, reliability, cost, and safety. The summary of his analysis is given in figure 6-1. The lowest ratings are the most favorable; according to Schuster, a system which provides for total reliquefaction of boiled-off fuels is the most desirable, with purely passive thermal control systems following as a distant second, while the 'refrigeration' and 'partial reliquefaction' systems are rated last.

The names used to designate these four systems are slightly misleading, in that they are not mutually exclusive; all four use passive multi-layer insulation [MLI], while the last three employ some refrigeration as well; however, the names used underline the most important aspects of each system.

The systems were designed to hold 22.7 tonnes of liquid hydrogen [LH2] and a like amount of liquid oxygen [LOX] for a period of 28 days. All four employ 10.2 centimeter

thick coated DAK/Dacron net MLI, and a coupled vapour-cooled shield [VCS], which requires some power to run pumps and compressors (hence the power requirement given for the passive MLI option). The tanks are pressurized to 20 psia, with a diameter of 4.42 m, and made out of 2219-Aluminum.

#### 6.4.1.1 Passive Control

The passive control option described by Schuster requires 12.6 tonnes total structure and insulation, and 220 Watts of power. It also receives a favourable rating in terms of the risks involved in development, since the technology involved has already enjoyed extensive use in modern spacecraft. However it also results in a propellant loss rate of 143 kg of LH2 per month, leading Schuster to give it a low grade on performance. It is reliable, fairly safe, and fairly inexpensive.

#### 6.4.1.2 Refrigeration System

The proposed refrigeration system is considerably more bulky than the purely passive one, with a dry mass of 14.4 tonnes. It also requires more power -- 550 Watts -- while losing fuel at the rate of 93.9 kg of LH2 per month. Although this represents a slight improvement over the passive system, this is not enough to offset the huge disadvantages inherent in the system, which would require extensive development in order to be viable. It also is more complex and more expensive than the first option.

#### 6.4.1.3 Partial Reliquefaction

Schuster's third concept combines the approaches used in his second and last concepts, by refrigerating the fuel and reliquefying any of it that boils off. This system has a dry weight of 14.3 tonnes, or 100 kg less than the pure refrigeration concept, and offers the advantage of total fuel recovery. The main disadvantages are that it is doubly expensive and complex when compared to the others, needs further development, and requires over 5 kWatts of power -- nearly ten times that used in the refrigeration system.

#### 6.4.1.5 Total Reliquefaction

The last concept proposed is one which relies on a reliquefaction plant to recover all fuel that may boil off. According to Schuster, such a system would have a mass of 14.1 tonnes, and require 2.13 kWatts of power. It would be safe, reliable, less difficult to develop than options 2 and 3, and over the long term would be more cost-effective than option 1. This system gets Schuster's highest rating on all counts.

### 6.4.2 Calculations

After looking at the benefits and disadvantages of these four proposals, we decided to concentrate on passive insulation as the most practical system for our purposes. The refrigerative and partial reliquefaction concepts were clearly not desirable options. Although the total reliquefaction system was a good choice, we have decided it is not suitable for Project Columbiad. Its supposed long-term cost advantage is moot for our mission, while the additional weight and power requirements are all the more burdensome for a lunar mission. Finally, the prospect of being forced to wait three or more years for the development of a zero-G LH2/LOX condensor system and other necessary components convinced us to rely primarily on multi-layer insulation for cryogenic storage.

#### 6.4.2.1 Boundary Conditions

In order to decide how much insulation is necessary, a number of boundary conditions have to be determined. It is necessary to determine the temperatures at which the fuels must be maintained, the heat flux which the craft can be expected to encounter at various points of the mission, and the maximum heat flux which can be allowed into the tanks if design requirements are to be met.

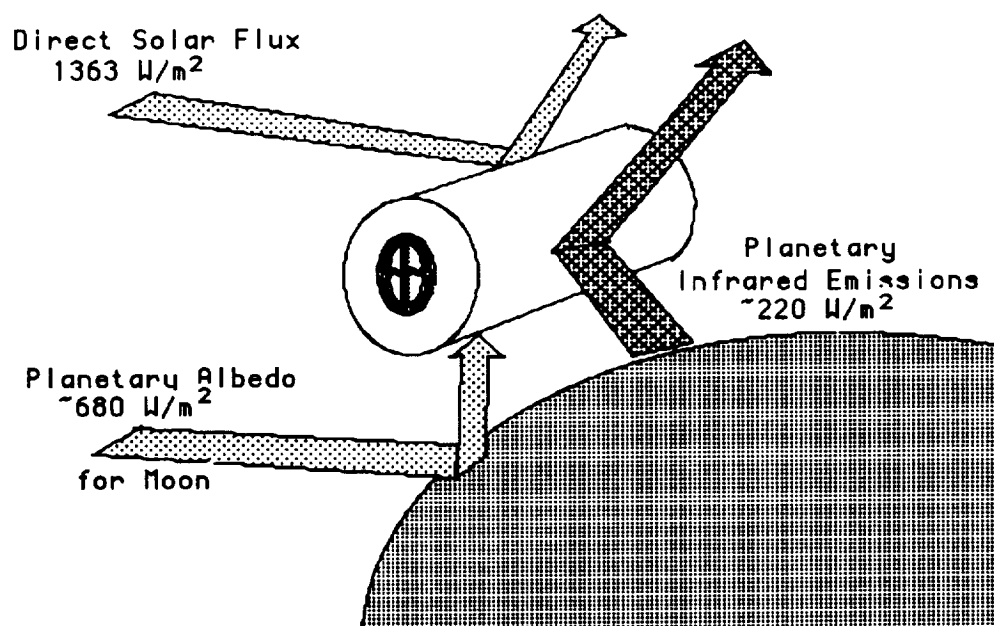


**Figure 6-1**  
**Expected Sources of Heat Flux**

There are several possible sources of heat which may contribute to the flux into the Columbiad spacecraft. The most important one is the sun itself, which can be expected to contribute on the order of 1400 Watts per meter squared of flux. For periods when the spacecraft is in orbit about a planetary body, the albedo from the planet will also be significant -- adding as much as one half of the flux due to direct sunlight. A planet will also generate an infrared flux of its own, on the order of 200-250 Watts per meter squared. Together, this means that the spacecraft may have to deal with as much as 2263 Watts per meter squared at some points of its journey.

#### 6.4.2.1.2 Spacecraft Surface Temperature

The main principle behind the use of multi-layer insulation is that of radiative heat transfer. Any given body in vacuum will radiate heat to its surroundings at a rate which increases as the square of the square of its temperature:

$$q = esT^4 \quad (6-1)$$

Here  $q$  is the heat flux,  $e$  is the emissivity of the material in question,  $s$  is the Stefan-Boltzmann constant ( $5.67 \times 10^{-8}$  Watts/m<sup>2</sup>-K<sup>4</sup>), and  $T$  is the temperature of the body. For a steady-state situation, this heat flux leaving the body will be equal to the heat flux entering the body. Using this fact, we can calculate the temperature of the body's surface, thus determining an important boundary condition.

#### 6.4.2.1.3 Fuel Boiling Points and Heats of Vaporization

**Table 6-5: Boiling Points and Specific Heats of Vaporization of Fuels**

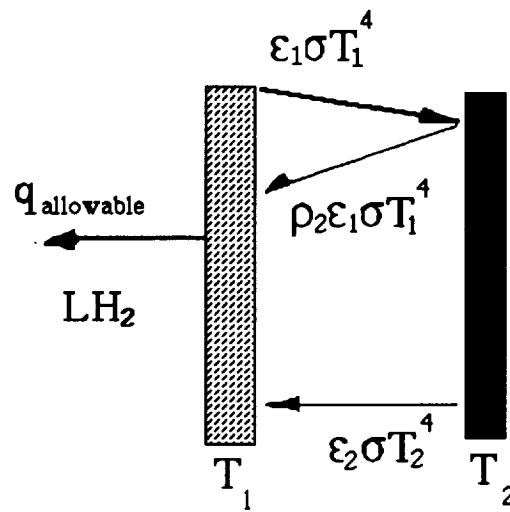
Fuel	Boiling Point	Latent Heat of Vaporization
N <sub>2</sub> O <sub>4</sub>	261.5 K	413 KJ/kg
N <sub>2</sub> H <sub>4</sub>	386.4 K	1256 KJ/kg
LH <sub>2</sub>	20.4 K	446 KJ/kg
LOX	90.0 K	213 KJ/kg

Table 6-5 shows the boiling points and specific heats of vaporization of the fuels employed in Project Columbiad's propulsion systems. These boiling points serve as the boundary conditions for the maximum temperature of the innermost layer of insulation.

The heat of vaporization is necessary to calculate the maximum heat flux allowable into each tank. When the acceptable boiloff rate has been determined, it is multiplied by the fuel mass and heat of vaporization in order to find the total heat which can be allowed in. This total is then divided by the time necessary for the mission and the surface area through which heat can pass in order to find the maximum heat flux allowable at the tank surface.

#### 6.4.2.2 MultiLayer Insulation Design

##### 6.4.2.2.1 Primary Design Considerations



**Figure 6-2**  
**The Innermost Layers**

Using the allowable heat flux determined in 6.4.2.1.3, it is possible to begin actual analysis of the multilayer insulation. MLI generally consists of layers of a thin plastic such as teflon, kapton, or mylar, sprayed with a coating of reflective metal on one side and separated by spacers of some sort. This means that each side of a given layer exhibits very different radiative properties from the other.

At the tank/insulation interface, we know the maximum temperature and heat flux. Using the fact that for steady state heat transfer, equal amounts of heat are flowing into and out of the insulation layer nearest the tank wall:

$$q_{\text{out}} = q_{\text{allowable}} + e_1 s T_1^4 \quad (6-2)$$

$$q_{in} = a_1 e_2 s T_2^4 + a_1 e_1 s T_1^4 [1/(1-r_1 r_2)] \quad (6-3)$$



Since we already know  $q_{\text{allowable}}$  and  $T_1$ , if we have values for the absorptivities  $a$  and reflectivities  $r$  for each side of a layer, the only unknown remaining is the temperature  $T_2$  of the next layer, and we can solve for it.

The solution for the subsequent layers becomes a bit more complicated. Heat flows in from the first layer and third layer, which also reflect back part of the radiation from the second layer itself:

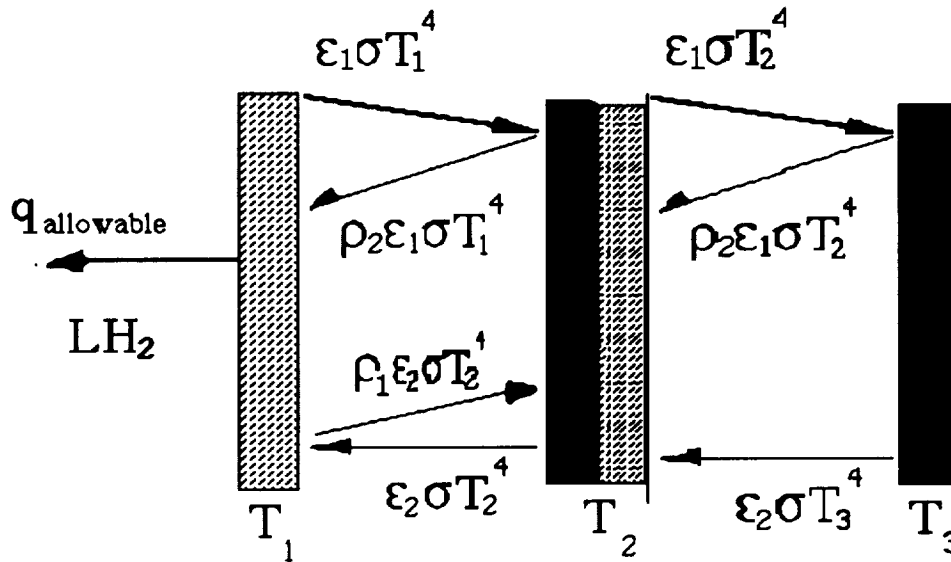


**Figure 6-3**  
**Subsequent Layers**

$$q_{\text{out}} = (e_1 + e_2)sT_2^4 \quad (6-4)$$

$$q_{\text{in}} = a_1 e_2 s T_3^4 + a_1 e_1 r_2 s T_2^4 [1/(1-r_1 r_2)] \\ + a_2 e_2 r_1 s T_2^4 [1/(1-r_1 r_2)] + a_2 e_1 s T_1^4 \quad (6-5)$$

Again making use of the relation  $q_{\text{in}} = q_{\text{out}}$ , and realizing that the temperature  $T_3$  is the only variable left, we can find  $T_3$ . This process can be repeated  $n$  times indefinitely until  $T_n$  is equal to the outside surface temperature found in 6.4.2.1.2.

#### 6.4.2.2.2 Secondary Design Considerations

Other factors which must be accounted for in the design of a cryogenic insulation system include the manner in which it is attached to the tank, the loads to which the insulation may be subjected, and the factor of safety which is to be employed.

The method of attaching the insulation which we will use is described in NASA Special Publication NASA SP-5027, *Thermal Insulation Systems: A Survey*, by Peter Glaser, Igor Black, Richard Lindstrom, Frank Ruccia, and Alfred Wechsler (NASA, 1967). It consists of a series of tacks spaced in a square pattern 1.25 inches on each side from center to center. The tacks are shielded from the insulation surface by glass disks measuring 0.25 inches in diameter and 0.008 inches in width. This should provide us with sufficient structural integrity for the insulation to withstand the loads generated in Project Columbiad without tearing; and we chose 1.15 as a reasonable factor of safety.

#### 6.4.2.3 Trade Studies

##### 6.4.2.3.1 Assumptions

In all trade studies, the outside temperature was set at 300 K. We assumed that this was an average temperature all the way around the tank, and constant throughout the trip. The LH2 tanks were all assumed to be cylindrical in shape, with a diameter of 5.6 m, while the LOX tanks were uniformly assumed to be spherical. The density of all plastics was estimated at  $50 \text{ kg/m}^3$ , while that of aluminum was set at  $2700 \text{ kg/m}^3$ . The duration of the mission was set at 4 days for the first two stages, and 32 days for the last. The optical qualities of insulation types were taken from the International Space University's publication Introduction to Space Life Science, from Dr. Giovanni Fazio's article "Hazards of Space: Vacuum, Temperature, and Microgravity".

**Table 6-6: Properties of Selected Materials**

INSULATION	a	e	a/e
Aluminized Mylar			
0.25 mils thick	0.14	0.36	0.39
1 mil thick	0.16	0.54	0.30
2 mil thick	0.17	0.70	0.24
5 mil thick	0.18	0.75	0.24
Aluminized Kapton			
1 mil thick	0.36	0.54	0.67
3 mil thick	0.44	0.78	0.38
5 mil thick	0.53	0.80	0.66
Aluminized Teflon			
1 mil thick	0.15	0.60	0.25
2 mil thick	0.15	0.66	0.23
5 mil thick	0.15	0.78	0.19
Silvered Teflon			
1 mil thick	0.06	0.52	0.09
5 mil thick	0.09	0.80	0.11

A trade study of these insulation materials follows.

**6.4.2.3.2 Trade Study of Selected Materials**

For the material trade study, the acceptable propellant loss was set at 4% over a period of 32 days, for the 17 825 kg of fuel used in the ERM.

**Table 6-7: Material Trade Study Results**

INSULATION	Layers for LH2	Layers for LOX	Total Mass(kg)
<b>Aluminized Mylar</b>			
0.25 mils thick	185	126	380.26
1 mil thick	160	104	1217.43
2 mil thick	148	94	2208.23
5 mil thick	147	93	5484.63
<b>Aluminized Kapton</b>			
1 mil thick	215	139	1691.36
3 mil thick	233	145	5433.66
5 mil thick	-----	-----	-----
<b>Aluminized Teflon</b>			
1 mil thick	152	98	1148.30
2 mil thick	147	94	2194.89
5 mil thick	139	88	5156.34
<b>Silvered Teflon</b>			
1 mil thick	145	96	1096.33
5 mil thick	129	81	4740.49

It is evident from these results that the added radiative thermal properties which accrue to thicker metal films are not sufficient at Columbiad's level to offset the extra mass which they require.

#### 6.4.2.3.3 Trade Study of ERM Stage

The next trade study pursued was to determine how much differing rates of fuel loss affect the total extra mass necessary to protect the fuel necessary for mission success.

The trip duration was set at 32 days, the total fuel mass at 17 825 kg, and 0.25 mil thick film aluminum mylar was used as the insulation. The results are given in Table 6-8.

% loss is the percentage of fuel allowed to boil off; Layers LH2 is the number of MLI layers needed to shield the fuel; Total Mass is the mass of the insulation ; and extra % is the percentage ratio of the sum of insulation mass and fuel boiled off, divided by the mass of fuel remaining, since this seemed the best measure of efficiency.

**Table 6-8: Results of ERM Stage Trade Study**

% loss	Layers LH2	Total Mass (kg)	extra %
0.010	276	472.3	2.6600
0.025	273	467.3	2.6470
0.050	268	458.9	2.6259
0.075	264	452.3	2.6143
0.100	260	445.6	2.6027
0.125	257	440.7	2.6006
0.150	253	434.1	2.5890
0.175	252	432.5	2.6087
0.200	250	429.2	2.6130
0.300	243	417.1	2.6483
0.400	237	407.4	2.6961
0.500	232	398.74	2.7512

**6.4.2.3.4 Trade Study for LBM and TLI Stages****Table 6-8: Results of LBM and TLI Trade Study**

% loss	Layers LH2	Total Mass (kg)	extra %
0.010	258	757.70	1.663
0.025	243	717.17	1.5910
0.050	229	680.15	1.5355
0.075	220	656.56	1.5094
0.100	214	640.90	1.5006
0.125	209	627.93	1.4977
0.150	205	617.58	1.5004
0.175	201	606.19	1.5009
0.200	198	598.47	1.5092

The next trade study was very similar to the second, except that it was performed for larger fuel masses and a trip duration of only 4 days, rather than 32. In spite of these differences,

the results were not dramatic. The optimum loss rate of one eighth of one percent is almost exactly the same as the 0.15 percent of trade study 6.4.2.3.3.

### **6.4.3 Conclusions**

Based on these trade studies, it was decided to adopt certain standards in the design of Project Columbiad's cryogenic storage systems.

The insulation itself is made of mylar sheets of 0.014 inch (0.356 mm) thickness, with a 0.00025 inch (6.35 microns) reflective aluminum shield on one side only. The spacing between layers is set at 0.014 inches (again, 0.356 mm), and it is attached to the tanks as described above in section 6.4.2.1.2. The design for each stage allows for a 0.175 % fuel mass boiloff over the course of its flight, with the exception of the PLM stage, where it was decided to allow 10% boiloff over the course of 10 years -- or 0.083% per month. These assumptions were also used in designing insulation for the fuel used by Columbiad's power cells, as noted in Volume III, 3.3.3.2 and 5.3.3.2.

The final design for cryogenic storage in each stage is detailed exactly in each stage report; however, to summarize briefly:

- The PTLI stage requires 1660 kg of mass, with insulation 17.44 cm thick around the tanks.
- The LBM stage requires 959 kg of mass, with insulation 13.92 cm thick around the tanks.
- The ERM stage requires 527 kg of mass, with insulation 17.65 cm thick around the tanks.
- The PLM stage requires 673 kg of mass, with insulation 16.29 cm thick around the tanks.

## **7 Crew Systems Selection**

Crew systems includes crew provisions, environmental control, spacesuits, and medical monitoring. Each of these systems is broken down in this chapter. The trade studies and methods of selection are discussed in depth.

Crew Systems has the primary goal of providing a livable environment for the astronauts. The crew systems requirements include a 99% reliability. This reliability will be achieved by having systems that have a 99% reliability or by providing three levels of redundancy in the system [Shea, 1992]. Some systems have a 95% reliability and when three systems are connected in parallel then the net reliability will be the desired 99%. Crew systems has also established a factor of safety of 1.5 for all consumables. These two aspects, reliability and safety factor, affect crew systems' drivers. The drivers are mass, volume, and power requirements.

### **7.1 Crew Provisions**

The basic necessities of survival for the astronauts were based on daily requirements for each astronaut. The numbers were calculated from different sources and with various engineering techniques. The daily requirements for human survival include [Shipman, 1989]:

Oxygen = 0.91kg/person/day  
Nitrogen = 0.6kg/person/day  
Drinking water = 1.68 kg/person/day  
Wash water = 0.95 kg/person/day  
Food (dry weight) = 0.61 kg/person/day.

Thus, the total amounts for daily oxygen, daily nitrogen, drinking water, wash water, and food were calculated by the following equation 7-1.

$$\begin{aligned} &(\text{Daily level}) \times (\text{Factor of safety}) \times (\text{Number of people}) \\ &\times (\text{Number of days}) = \text{Total mass of consumable} \end{aligned} \quad (7-1)$$

The crew provision totals for the crew module are given in Section 6.3.1 of Volume III. The totals for the habitat are given in Subsection 8.1.3.1 of Volume III. However, the habitat values for daily oxygen and wash water are different than the totals given by the above equation. This is due to the oxygen reclamation and wash water recycling systems which are described in Subsections 7.2.1.4 and 7.2.2.1 of this Chapter. The values for volume requirements were calculated in a similar fashion. However, the volume numbers

for the oxygen, nitrogen and water are not given since these consumables are stored in tanks. The tanks and volumes are described in Subsections 7.2.1.5 and 7.2.2.2. The values for the crew, clothing, sleepers, medical kit, and toiletries were based on a NASA 90-day regenerative life support study [Pearson, 1971 and Joels, 1982].

Additional crew provisions include cabin air and EVA oxygen. The cabin atmosphere trade study is examined in Subchapter 7.7. The EVA required oxygen is described here to provide a total for the crew provisions. The required EVA oxygen level is 0.157kg/hour [Harding, 1989]. The total EVA oxygen for the habitat was calculated by allocating twenty-eight days of EVA operation at sixteen person-hours of EVA per day for the habitat and sixteen total hour of EVA oxygen for the Crew Module. A factor of safety of 1.5 was also allocated for.

## **7.2 Environmental Control**

The Crew Module utilizes a completely non-regenerative environmental control system. Trade analyses easily show that it is less costly, in terms of mass, to take all the supplies that you need for a six day mission than to use regenerative equipment. Utilizing supplies on a once through basis is also less costly since no additional cost of equipment development is incurred. Basically, the only cost is the mass to the lunar surface and back to the Earth.

The habitat crew environment is engineered to provide the most comfortable conditions for the astronauts. The environmental factors include atmosphere, water management, and waste management. The habitat will utilize a semi-regenerative system as pictured in Figure 7-1. A more complete diagram is provided in Subsection 8.1.3.2 of Volume III. The system is regenerative in oxygen reclamation and wash water recycling. The following sections provide a complete analysis of the environment control system selection and trade study descriptions.



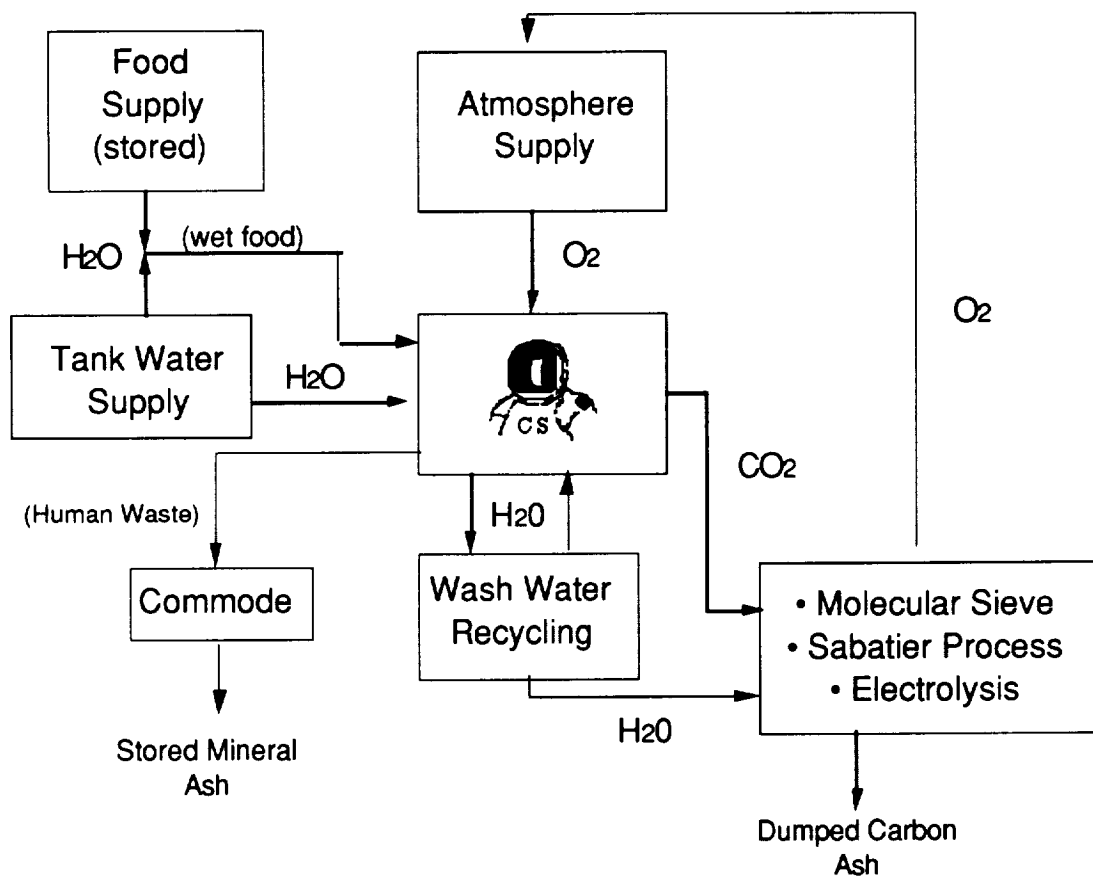


**Figure 7-1**  
**Habitat Semi-Regenerative Environment System**

### 7.2.1 Atmosphere

An Environmental Control and Life Support System (ECLSS) will maintain gas pressurization, gas content, temperature and humidity in the Crew Module and lunar habitat. The selection of these atmospheric parameters will be identical on the module and habitat, and will be based upon the physiological requirements necessary to ensure human safety and well-being.

ECLSS components will be installed to remove carbon dioxide from the atmosphere and maintain habitable proportions of oxygen and nitrogen. In addition, the application of a semi-regenerative oxygen reclamation system will be discussed for use on the lunar habitat.

### 7.2.1.1 Requirements

Human physiological limitations will define the requirements for atmospheric pressure, gas content, temperature and humidity ranges. This will prevent the development of deleterious physiological conditions and ensure optimal crew health and performance throughout mission Columbiad.

#### 7.2.1.1.1 Pressurization

In order to sustain the lives of the human crew, acceptable static pressures in the crew environment must be maintained. While a minimal atmospheric pressure of 0.06 atm at 37°C is required to prevent the vaporization of body fluids, human tolerance for extremely high pressures is limited. Detrimental physiological conditions arise primarily from the rate and magnitude of pressure *change* rather than the absolute value of atmospheric pressure. Barotrauma, Explosive Decompression Syndrome and Dysbarism are three potentially fatal conditions which will be prevented through the maintenance of an appropriate atmospheric pressure in the Crew Module and lunar habitat.

**Barotrauma** occurs when gas becomes temporarily trapped in the middle ear or sinuses, in a decayed tooth, or in the gut. This gas buildup alters the pressure differential across the walls of these cavities, resulting in pain and tissue injury. Susceptibility to Barotrauma increases

- (1) during respiratory infection when passages normally permitting pressure equilibration of the ears and sinuses is obstructed,
- (2) when poor dental care results in tooth cavities, or
- (3) when diet allows large quantities of gas to form in the gut.

These predisposing factors can be controlled through preflight astronaut medical screening, adequate personal hygiene and proper nutrition. However, barotrauma can best be avoided by limiting the rate of pressure change in the environment. Rapid pressure changes exacerbate the symptoms significantly. Decompression rates of 0.007 atm/sec or slower are acceptable. A maximum decompression rate of 0.07 atm/sec is acceptable only during emergency situations.

**Explosive Decompression** is a potentially fatal condition which occurs when the environmental pressure drops so rapidly that a transient overpressure develops in the lungs and other air cavities. At pressure differentials as low as 0.11 atm, a positive pressure in the lungs will force large quantities of gas into the bloodstream, resulting in the immediate

severing of blood vessels, an air embolism, and symptoms similar to those of a stroke. These high decompression rates will necessitate immediate protection with an IVA space suit and subsequent mission abort.

**Dysbarism** occurs when the partial pressure of dissolved gases in the tissues exceeds ambient pressure. Because of this pressure differential, bubbles form underneath the skin, causing pain in joints and muscles, pain in the lung area, neurological difficulties, and circulatory collapse. Because of the high rate at which tissues utilize oxygen, O<sub>2</sub> will not contribute significantly to the formation of bubbles in tissue. However, the buildup and bubbling of dissolved diluent gases (like nitrogen) in body tissues are inevitable and must be lowered prior to decompression. It is therefore a common procedure to prebreathe 100% oxygen for an extended period of time to displace the diluent gas in the tissues. However, dysbarism is not a threat, and oxygen prebreathe is *not necessary*, when the diluent gas concentration in the atmosphere is low enough that:

$$\frac{\text{Partial Pressure of Diluent Gas}}{\text{Total Final Pressure}} \leq 1.5 \quad (7-1)$$

#### 7.2.1.1.2 Gas Content

The habitability of the environment is largely dependent on the partial pressures of component gases consumed by the crew members. ECLSS subsystems will be installed to achieve the required oxygen and diluent gas levels for crew consumption in the capsule and lunar habitat. Removal of carbon dioxide waste and other hazardous gases will also be required to maintain optimal crew health and performance.

**Oxygen Requirement.** Consumed oxygen gas transfers to the blood stream at the lung alveoli where the partial pressure of oxygen is diluted by carbon dioxide and water vapor . At any elevation, oxygen partial pressure at the alveoli (p<sub>A</sub>O<sub>2</sub>) can be calculated as follows:

$$p_{AO_2} = f_{iO_2} \times (p_B - 47) - p_{CO_2} \times \left( f_{iO_2} + \frac{(1 - f_{iO_2})}{0.85} \right) \quad (7-2)$$

where

f<sub>i</sub>O<sub>2</sub> = Oxygen fraction in breathing atmosphere

p<sub>B</sub> = Barometric pressure of breathing mixture

0.85 = Respiratory exchange ratio (assumed)

pCO<sub>2</sub> = Partial pressure of carbon dioxide.

At low alveolar partial pressures, **hypoxia** occurs; insufficient oxygen reaches body tissues. Without acclimation to a low  $O_2$  environment, measurable effects of hypoxia occur at  $p_{AO_2}$  lower than 0.11 atm . As shown in Table 7-1, the central nervous system, including the brain and eyes, are particularly sensitive to oxygen deficiency.

**Table 7-1: Effects of Insufficient Oxygen**

Alveolar Oxygen Partial Pressure (atm)	Effect
0.11	Low-illumination Color Vision Threshold. Loss of night vision.
0.09	Declining mental performance. Hallucinations, excitation, apathy.
0.05	Visual, mental, and motor impairment. Loss of memory and paralysis.
<0.5	Loss of consciousness. Death in 90 to 180 seconds.

After a long exposure to high alveolar oxygen partial pressure, oxygen becomes toxic. For ambient oxygen partial pressure ( $p_{O_2}$ ) exceeding 0.25 atm, the overconsumption of oxygen (**hyperoxia**) causes a slow  $O_2$  buildup around the alveoli after 300 hours. This has been responsible for substernal distress, coughing and a decrease in lung vital capacity by 500-800 ml. As shown in Figure 7-2, convulsions, fainting, and dizziness will occur in a  $p_{O_2}$  environment exceeding 2.6 atm within 10 hours. Figure 7-3 indicates the volume of oxygen required to prevent the occurrence of hypoxia or hyperoxia for a given atmospheric pressure.

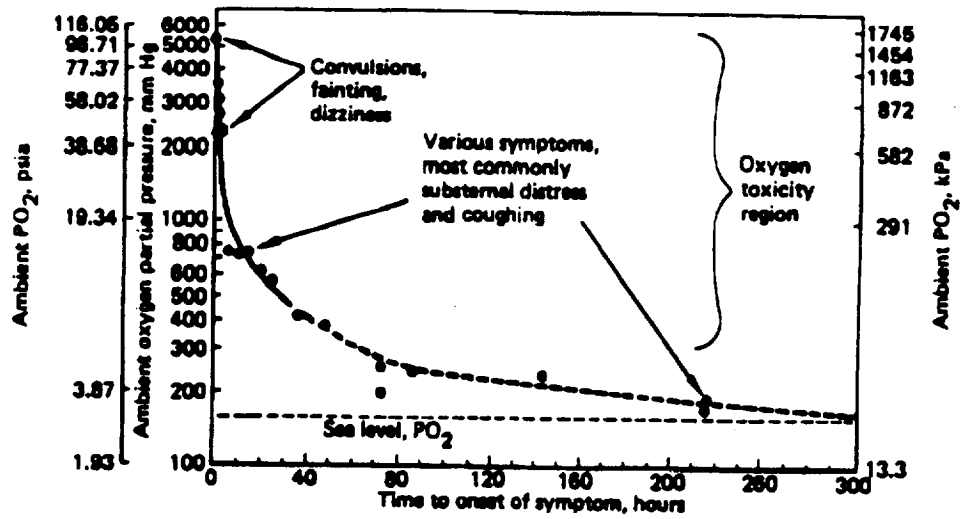


**Figure 7-2**  
**Approximate Time of Appearance of Hyperoxic Symptoms for**  
**an Ambient Oxygen Partial Pressure [NASA-STD-3000, 1987]**

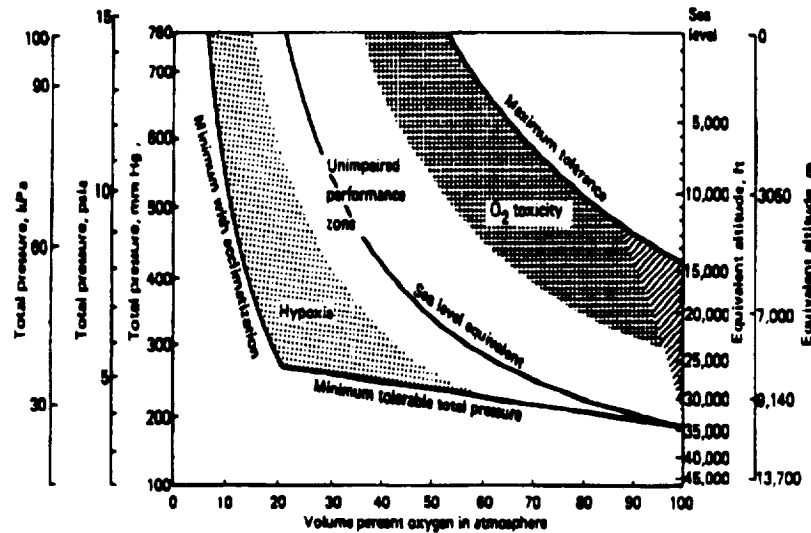


**Figure 7-3**  
**Oxygen Requirement Per Total Atmospheric Pressure**  
**for the Prevention of Hyperoxia and Hypoxia**  
**[NASA-STD-3000, 1987]**

**Gas Diluent.** The addition of diluent gas to the cabin atmosphere will be provided in order to:

- (1) Increase cabin total pressure without the risk of hyperoxia,
- (2) Prevent the collapse of gaseous pockets in the middle ears and lungs of the crew by decreasing the rate of gaseous absorption, and
- (3) Suppress the fire hazard of 100% oxygen.

Because of the high flammability of hydrogen gas, this will not be used as a gas diluent. Potential diluents He, Ne, N<sub>2</sub>, Ar, Kr and Xe were considered with regard to their physical properties, toxicity and availability.

Table 7-2 indicates the density and thermal conductivity of these potential diluents. Low density gases induce an increase in human voice frequency at high percentages, reducing speech intelligibility. Gases of high thermal conductivity will present difficulty in thermal regulation. Atmospheres using such gases necessitate the maintenance of air temperatures higher than normal for subjects at rest. The low density and high thermal conductivity of

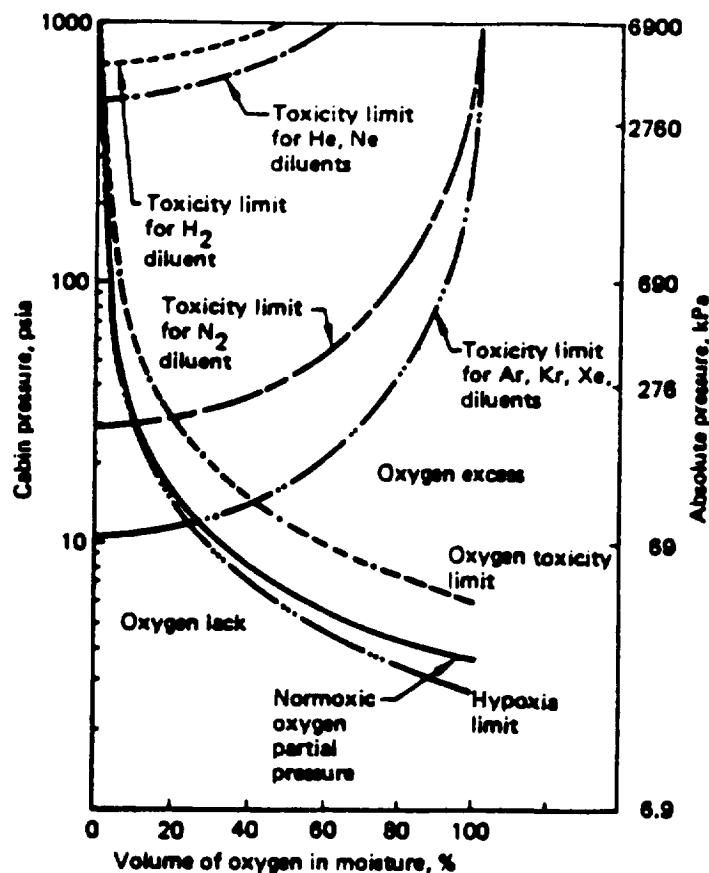
helium make this gas particularly undesirable for use as an atmospheric diluent in the Columbiad Crew Module and BioCan.

Figure 7-4 indicates the toxicity limits of these diluents for a given percent volume of atmospheric oxygen.

**Table 7-2: Physical Properties of Potential Diluents**

Diluent	Density (kg/m <sup>3</sup> )	Thermal Conductivity (Kcal/m.hr °C)
Helium	0.178	0.125
Nitrogen	1.251	0.013
Neon	0.900	0.010
Argon	1.784	0.026
Krypton	3.708	0.045
Xenon	5.851	0.085

Note: Density and thermal conductivity values correspond to 1 atm and 0 °C.



**Figure 7-4**  
**Toxicity Limits of Potential Diluents**  
 [NASA-STD-3000, 1987]

**Carbon Dioxide and Other Crew Cabin Gases.** Monitoring of carbon dioxide, water vapor, and atmospheric toxins in the crew cabin will be required because of the adverse physiological conditions which will result from the buildup of these gases.

The partial pressure of **carbon dioxide** ( $p\text{CO}_2$ ), will be maintained *below* 0.01 atm. Although long-term exposure to  $\text{CO}_2$  near this concentration significantly alters the acid-base balance of the body, no outward symptoms are apparent. At approximately 0.01 atm, crew members will begin to exhibit temporary increases in motor activity, euphoria and sleeplessness followed by headache and sluggishness. Acute exposure to  $\text{CO}_2$  concentrations exceeding 0.01 atm may result in body temperature reduction, increased urine production, dizziness, fatigue and a loss of consciousness.



**Carbon monoxide** from crew metabolism, material offgassing, and material thermodegradation will be limited to a maximum of 60 volumes per million. Higher concentrations may result in severe headache, extreme fatigue, loss of consciousness, coma and death.

**Ozone** produced by electric motors or ultraviolet light rays from the onboard lighting system will be limited to 0.3 ppm. Higher concentrations cause sleepiness and bronchial irritation while exposure to 1.5 ppm has been described as intolerable.

#### 7.2.1.1.3 Temperature and Humidity

Cognition, psychomotor performance and human efficiency are greatly dependent on atmospheric temperature and humidity.

Systems must be implemented to avoid potentially fatal conditions associated with improper thermal regulation of the environment. The dry bulb temperature of the capsule and BioCan must be sufficient to allow the maintenance of a core body temperature between 36-40 °C. Body temperatures higher than this will result in heat exhaustion or heat stroke while temperatures below this will induce hypothermia. The amount of clothing worn and physical activity performed alter human tolerance to these parameters.

A high humidity environment promotes microbial and fungal growth. Drying of eyes, skin, and mucous membranes in the nose and throat, are likely to occur in a low moisture environment. The development of respiratory ailments is an added concern of low humidity since drying of protective respiratory tract cilia often occurs.

The interplay of dry bulb temperature with humidity greatly influences human responses to the thermal environment. Increased temperature tolerance is associated with decreased relative humidity. Temperatures up to 30 °C are comfortable for lightly clothed, sedative crew members in an atmosphere of 10% humidity. Seventy percent humidity decreases this tolerance level to 25 °C. The relationships between temperature, relative humidity and water vapor pressure in the crew atmosphere are shown in Figure 7-5.

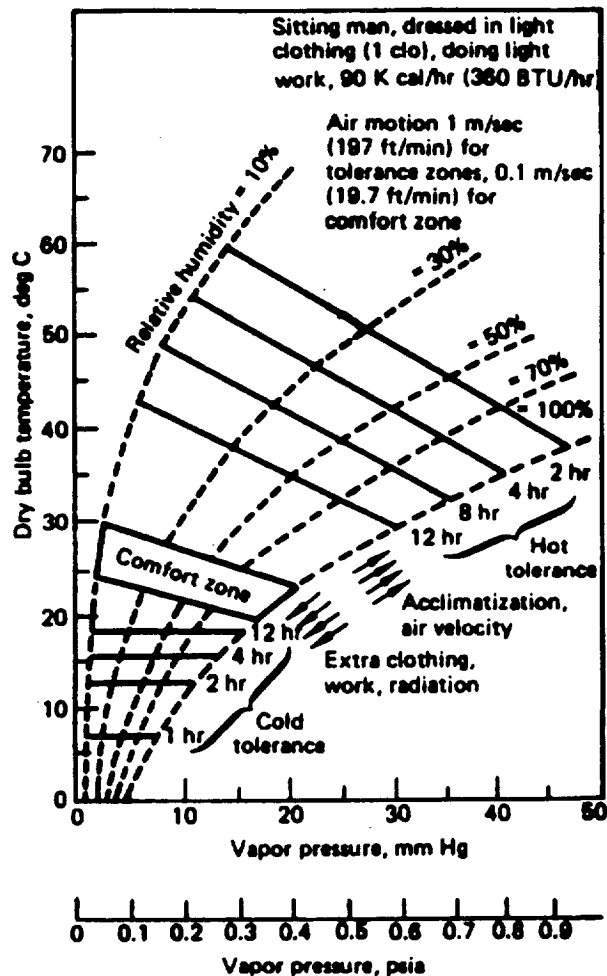


**Figure 7-5**  
**Thermal Environment Requirements for Human Comfort**

#### 7.2.1.2 Selection of Cabin and Lunar Habitat Atmosphere

**Pressurization and Gas Composition.** A total pressure of 0.34 atm was selected for the Columbiad Crew Module and BioCan environments. Sixty-four percent (64%) of the total gas volume will be composed of oxygen, resulting in an oxygen partial pressure of 0.22 atm. This value is sufficient for the prevention of hypoxia and hyperoxia.

The addition of diluent gas (partial pressure of 0.12 atm) is necessary to design an environment which is compatible with the total 0.34 atm pressure attained by the 100% oxygen IVA and EVA spacesuits (as discussed in Subchapter 7.4). If compatibility is achieved, the need for a slow airlock decompression and 100% oxygen prebreathe will not be necessary prior to EVA activities. This compatibility is especially important because it

allows the immediate donning of a spacesuit during an emergency rapid decompression and abort. Dysbarism is not a danger with this small diluent gas partial pressure since the ratio of the nitrogen partial pressure to the total final pressure is 0.35, less than the maximum acceptable value of 1.5.

Thirty-six percent (36%) nitrogen by volume was chosen specifically as a diluent for its low density, low thermal conductivity and high availability. This nitrogen partial pressure (0.12 atm) is non-toxic and provides adequate speech intelligibility, thermal regulation and fire suppression.

Carbon dioxide buildup will be restricted to non-toxic levels under 0.01 atm.

**Temperature and Humidity.** A thermal environment which is conducive to optimal crew health and performance will be provided in the crew cabin and lunar habitat. Temperature will be maintained between 17.8 - 27.2 °C. To limit the exacerbating effects of humidity at higher temperatures, the partial pressure of water vapor ( $p_{H_2O}$ ) will be maintained between 0.008 - 0.018 atm (40 - 50% Relative Humidity). A summary of the above stated parameters is shown in Table 7-3.

**Table 7-3: The Cabin and Lunar Habitat Atmospheres**

Parameter	Value
Total Pressure	0.34 atm
-- Oxygen Partial Pressure	0.22 atm
--Nitrogen Partial Pressure	0.12 atm
--Carbon Dioxide Partial Pressure	<0.01 atm
--Water Vapor Partial Pressure	0.008-0.018 atm
Dry Bulb Temperature	17.8 - 27.2 °C
Humidity	40 - 50 %

#### 7.2.1.3 Carbon Dioxide Removal

Various methods of carbon dioxide removal were studied. These included lithium hydroxide, solid amines, hydrogen-depolarized cells, and molecular sieves. Lithium hydroxide has proven to be effective in many of the space missions flown to date. Also, a NASA study [Pearsons, 1971] showed that a molecular sieve works well with oxygen

reclamation (see Subsection 7.2.1.4). Thus, the crew module will use lithium hydroxide because of its ease of use, the Crew Module's non-regenerative environment, and the mass and volume restraints. The habitat, on the other hand, will utilize a molecular sieve (see Subsection 7.2.1.4).

Carbon dioxide will be removed from the crew module's atmosphere by use of a lithium hydroxide (LiOH) system similar to the Space Shuttle [Joels, 1982 and Pearson, 1971]. The system has lithium hydroxide cartridges which adsorb the carbon dioxide out of the air. The chemical equation (Equation 7-3) is



The carbon dioxide reacts with the lithium hydroxide to produce lithium carbonate and water vapor which are both waste products. The waste is stored in the cartridges. These cartridges must be replaced every 12 hours during operation. The estimates for the system are 20 kg and 0.2 m<sup>3</sup> (see Section 6.3.2 of Volume III).

#### 7.2.1.4 Oxygen Reclamation

Figure 7-1 (Subchapter 7.2) roughly illustrates that oxygen is recycled from carbon dioxide waste and reentered into the atmosphere supply in the habitat (note: the Crew Module uses a completely non-regenerative environmental control system). The oxygen reclamation system was chosen after a trade analysis revealed an eventual savings in mass and cost. The system is further broken down (with mass values in kg) in Figure 7-6 [Pearson, 1971].

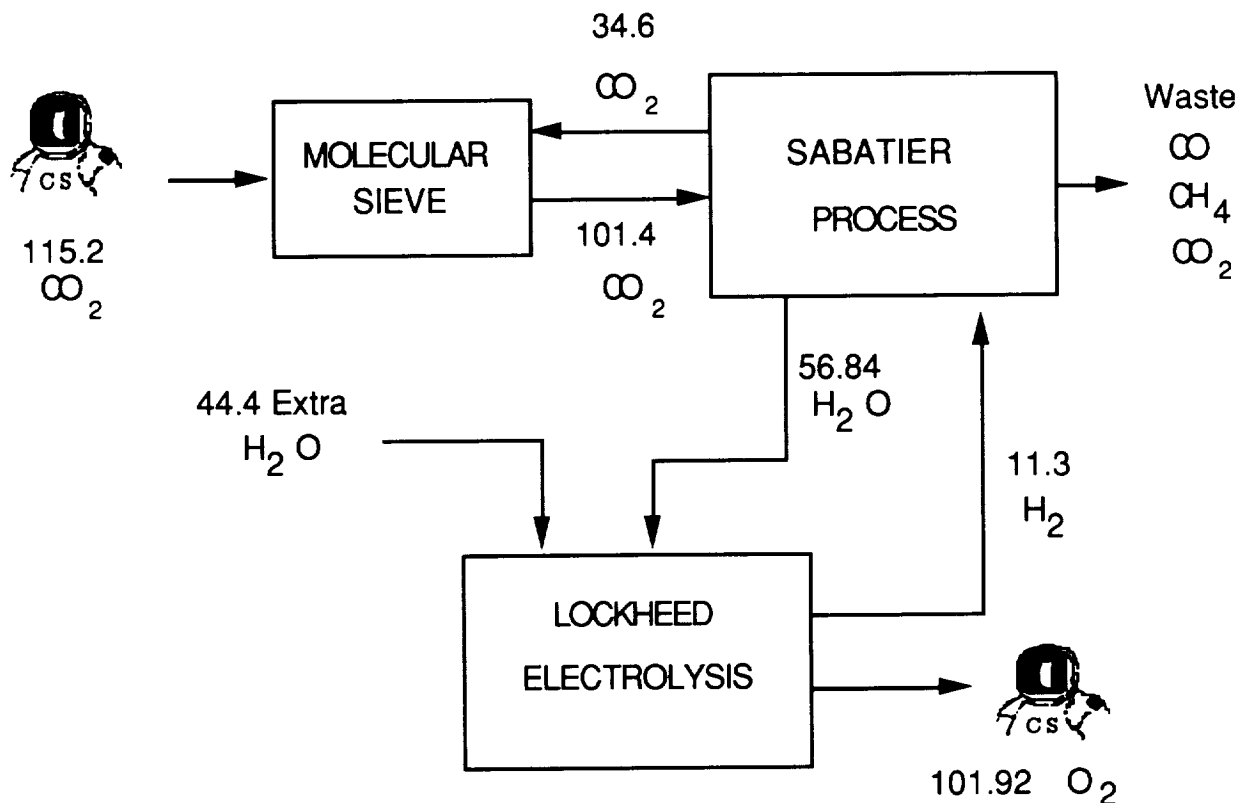


**Figure 7-6**  
**Oxygen Reclamation System**

The oxygen reclamation system works in a simple manner. The astronauts exhale carbon dioxide. The molecular sieve adsorbs the carbon dioxide from the air. The carbon dioxide is then combined with hydrogen in the Sabatier Processor. The Sabatier process converts the carbon dioxide and hydrogen to water. It also produces wastes of carbon dioxide, carbon monoxide, and methane gas. These waste gases must be vented from the habitat. The water produced from the Sabatier process is sent to The Lockheed Electrolysis machine. The electrolysis process produces oxygen for the astronauts and hydrogen to run the Sabatier Process. In order to produce the level of oxygen shown and to initiate the electrolysis process an additional 44.4 kg of water is necessary.

The mass trade analysis was a trade-off between bringing all the necessary daily oxygen to the moon and utilizing the oxygen reclamation system, (thus bringing less oxygen to the moon). If no oxygen is recycled then the habitat needs 152.85 kg of oxygen for the 28-day four man mission [see Subchapter 7.1]. The oxygen reclamation system equipment has a

total mass of 230.2 kg (see Subsection 8.1.3.2 of Volume III). However, an additional 50.93 kg is required since the reclamation system only produces 101.92 kg of oxygen over 28 days and not the necessary 152.85 kg. Thus, the total reclamation system mass is 281.13 kg. In order for redundancy and protection, the first mission to the moon will take the total daily oxygen needed and the oxygen reclamation system. The total mass for the first mission is equal to 230.2 kg (the reclamation system mass) and 152.85 kg (for daily oxygen) which provides a grand total of 383.05. Note that the extra 50.93 kg of oxygen needed with the reclamation system is included in the 152.85 kg daily oxygen value. Thus, the oxygen reclamation system incurs a net loss of 230.2 kg on the first flight. However, on recurring flights there will be a mass savings. On recurring flights, (without taking the 152.85 kg of daily oxygen) the required mass will be equal to 74.33kg ( 50.93 kg oxygen + 23.4 kg water). The 50.93 kg of oxygen plus the 101.92 kg of oxygen produced by the reclamation system provide the necessary 152.85 kg of oxygen. The 23.4 kg of water provides the 44.4 kg of water needed for electrolysis with water recycling (as described in Subsection 7.2.2.1). This recurring mass of 74.33 kg is a savings of 78.52 kg over the 152.85 kg of oxygen with no reclamation. Thus, the first mission has an extra 230.2kg but recurring missions have 78.52 kg less; thus, the mass break-even point is three missions with using the oxygen reclamation system.

A cost analysis was also done. This oxygen reclamation system was used by NASA Langley in 1970. However, development and improvement costs will equal at most \$5 million. If it costs about \$40,000 to send one kg to the moon (see Volume IV), then with the 78.52kg savings on recurring missions with the oxygen reclamation system, an additional two missions is required after the mass break-even point to have a cost break-even. Thus, the cost break-even point is five missions. After the fifth mission the oxygen reclamation system will save  $(78.52\text{kg}) \times (\$40,000/\text{kg}) = \$3.2$  million per mission.

In conclusion, the oxygen reclamation system is a good idea. The mass break-even point is three missions and the cost break-even point is five missions. With the intention of Project Columbiad, these are good numbers. Also, with longer lunar missions and Martian missions the savings with the oxygen reclamation system will increase.

#### 7.2.1.5 Oxygen and Nitrogen Tank Design

Three methods exist for storing atmosphere gases for spacecraft applications. These are high-pressure storage at ambient temperature, super-critical storage at cryogenic temperature, and sub-critical storage at cryogenic temperature. High pressure gaseous

storage is usually heavier than cryogenic storage because of the heavy vessels dictated by the nature of high pressure storage. The primary advantages of high pressure storage are that the equipment is relatively simple and the gas is readily available for the requirements of rapid repressurization and emergency operation. Cryogenic storage generally entails lower tankage weight due to the smaller volumes required when the gas is stored in a liquid form and the lower working pressures which permit thinner vessel walls. However, a major disadvantage of cryogenic storage is the complexity of the overall system. With the above mentioned methods of storage and advantages and disadvantages of each, the cryogenic method of storage was chosen due to mass and volume restraints in the crew module and the habitat.

Specifically, the method of sub-critical storage at cryogenic temperature was selected. Liquid oxygen boils at 154.8° K and liquid nitrogen boils at 126.2° K [Van Wylen, 1985]. The cryogenic storage temperatures for liquid oxygen and nitrogen are 88.6° K [Fleener, 1992]. The actual method and technique of cryogenic storage is described in Subchapter 6.3. The technique used to design the actual tanks is provided in the following paragraphs.

The tanks were optimized for minimum weight [Ashby & Jones, 1980]. The hoop stress equation (equation 7-4) and the equation for mass of a sphere skin (equation 7-5) were combined. A structural safety factor of 1.4 (equation 7-6) was also included. Thus, the masses of the tanks were calculated (equation 7-7). The radius of the tanks were designed by considering the volume constraints of the habitat and the crew module. The volumes of the tanks were also calculated (equation 7-8).

$$\sigma = \frac{Pr}{t} \quad (7-4)$$

$$M_{\text{sphere skin}} = 4\pi r^2 t \rho \quad (7-5)$$

$$\sigma = \frac{\sigma_y}{\text{F.O.S.}} = \frac{2\pi Pr^3 \rho}{M} \quad (7-6)$$

$$M = 2.8\pi Pr^3 \left( \frac{\rho}{\sigma_y} \right) \quad (7-7)$$

$$V_{\text{tank}} = \frac{4}{3}\pi r^3 \quad (7-8)$$

Each tank is made of graphite epoxy because of its superior strength to weight ratio. This gives a mass savings of 172% over aluminum. The tanks were designed against yield (Equations 7-4 to 7-8). Fatigue failure is not a problem since there is a low number of pressure cycles (one per mission) for each tank. Corrosion is not a problem either because graphite epoxy does not react with nitrogen nor oxygen. Also, graphite epoxy is not affected by the low cryogenic temperatures [Graves, 1991]. Fracture toughness calculations (equations 7-9 to 7-13) [data from Ashby & Jones, 1980, Joels 1982, and Ball Aerospace Corporation, 1992] show that each tank will leak before it breaks. This allows time for detection of leaks and solution methods of pressure reduction or piping bypass to be implemented.

$$K = \sigma\sqrt{\pi a} \quad (7-9)$$

$$\sigma = \frac{Pr}{t} \quad (7-10)$$

$$K_{\text{CG/E}} = 32 \frac{\text{MN}}{\text{m}^{3/2}} \quad (7-11)$$

$$a_{\text{G/E}} \approx 5 \times 10^{-4} \text{ m} \quad (7-12)$$

$$K < K_c \text{ no fast fracture} \quad (7-13)$$

The design K was 17 MN/m<sup>3/2</sup> which is below the critical K for fast fracture. A cost trade was done and showed that the extra cost in graphite epoxy material is easily surpassed by the cost saved in transporting less mass to the lunar surface.

To achieve three levels of redundancy, the total oxygen for the habitat and crew module is divided up between three identical tanks. The same is done for nitrogen. Final mass and volume values are presented in Section 6.3.2 and Subsection 8.1.3.2 of Volume III. The same size tanks are used in both the habitat and the Crew Module due to the fact that the Crew Module has enough volume space to allot for this. This cuts down on the development cost. Also, the Crew Module could be supplied with additional oxygen and nitrogen if necessary. This will be necessary for recurring missions (Subsection 8.1.1.7 of



Volume III). Thus, for recurring missions, the crew module will be able to take some of the necessary oxygen and nitrogen to the moon.

#### 7.2.1.6 Other Atmospheric Control Aspects

The other atmospheric control aspects include a thermal control system, atmospheric supply and control equipment, a humidity control system, and fire suppression and detection equipment. These systems are based on the NASA study [Pearson, 1971] and updated information provided from AiResearch [Shewfelt, 1992]. The specific components and mass, volume, and power budgets are described in Section 6.3.2 and Subsection 8.1.3.2 of Volume III. Table 7-4 shows the suppliers for the environment control systems.

**Table 7-4: Suppliers/Contractors for Environmental Control Systems**

<b>Equipment Contractor</b>	<b>Specific Life Support Component</b>
McDonnell Douglas Aerospace Corp.	Sabatier reactor
	Breadboard two-gas control
	Wash water recovery system
	Humidity control system
Ball Aerospace	Oxygen tanks
	Nitrogen tanks
Lockheed	Electrolysis system
Perkin-Elmer Aerospace	Mass spectrometer
Oregon Freeze Dry	Freeze dried foods
AiResearch - Allied Signal	LiOH system
	Thermal control system
	Molecular sieve
	Fire suppression and detection system
	Commode

#### 7.2.2 Water Management

The Crew Module does not recycle water by any method. The water tank design is described in Subsection 7.2.2.2. For the required amount of water and reliability, the crew module will have two water tanks. Each tank has a reliability of 98% and thus, a system of two tanks in parallel meets the required 99% reliability requirement.

The habitat recycles wash water as described in Subsection 7.2.2.1. For the required amount of water, six water tanks will be used in the habitat. These six tanks provide a redundancy level of six and with their separate 98% reliability, they easily produce a 99% reliability when connected in parallel.

#### 7.2.2.1 Wash Water Reclamation

A trade analysis was performed to determine if wash water recycling produced a mass savings. The wash water reclamation system used was based on a NASA Langley 90-day regenerative life support system study [Pearson, 1971]. The system utilizes filtration techniques and has a 90% recyclability over a one month mission. Based on 0.95kg/person/day for a 28-day mission with a safety factor of 1.5, the total wash water required is 159.6 kg [Shipman, 1989]. The first mission costs an extra 28.9 kg in mass. This additional mass includes a redundancy level of three (with system mass given in Subsection 8.1.3.2 of Volume III) by taking three separate wash water recovery systems. However, in just the second mission there is a 75.6 kg savings in mass. Thus, the mass break-even point is two missions. The system is currently in production and improvement costs will be minimal compared to sending 75.6 kg to the lunar surface. The water management budgets are shown in Subsection 8.1.3.2 of Volume III. The trade shows that a lot is saved by recycling wash water. Urine/waste water recycling is not economical for a 28-day mission. Also, the water recovery system does not produce pure enough water for drinking.

#### 7.2.2.2 Water Tank Design

The NASA Langley 90-day regenerative life support system study provided information on water tanks. Each tank has a capacity of 56 kg of water, a mass of 18.17 kg, and a volume occupancy of 0.057m<sup>3</sup>. With the amount of water required (Subsection 6.3.2.2 and Paragraph 8.1.3.2.2 of Volume III), the crew module requires two water tanks while the habitat requires six water tanks. These tanks have a reliability of approximately 98% each [Pearson, 1971].

### **7.2.3 Waste Management**

The waste management system must properly dispose of or process all waste products. The Columbiad mission should include systems which reclaim wash water for reuse, a commode for human waste disposal, air filters to reduce atmospheric particulate count, and a toxin detection system.

The Space Shuttle WCS, nicknamed the 'Slinger', represents the only fully operational U.S. human waste system. It is capable of processing biowaste from male and female astronauts in 0-g and 1-g conditions. This is accomplished with the use of a suction which pulls all waste into a lower chamber. There a spinning blade system spews waste matter around the inside of a storage tank. This tank is subsequently exposed to the vacuum of space, freeze-drying the layer to the tank wall. The tank must be periodically emptied. Potentially this could be done remotely with a mechanical scraper, though such a technique is not currently used.

An alternative to the current Shuttle commode system is the Allied-Signal commode [Shewfelt, 1992]. This unit consists of a collection chamber, a piston for waste compaction, a mechanism for providing a bacterioid paper covering for the piston for each use, and an accumulation chamber for storing waste. Solid wastes and wipes are drawn into the collection chamber by means of airflow through holes under the commode seat. The airflow is induced by a fan integrated into the commode unit. The piston is covered with a fresh bacteriocidal paper cover, and then the piston pushes the waste and wipes into the accumulation chamber. This results in compaction of the material. A manual crank backup is provided in case of motor failure. For long-duration missions, accumulation chambers can be switched in and out. Urine is collected separately through the use of specialized funnels for male and female astronauts. Urine and air is directed into a fan/separator and rotating centrifuge bowl which separates liquid from air. The liquid can be stored or ejected while the air is passed through an odor/ bacterial filter and then can be reused. Though this system is new, a manually controlled version was tested aboard STS-35 as well as in numerous ground- and KC-135 tests.

Reports from the Shuttle commode have been mixed, the astronauts generally all disappointed with certain elements. In particular, the odors from waste materials have been known to linger in the cabin. Also, the unit cannot be easily cleaned while on orbit, and is difficult to clean even when on the ground. The unit does not include any option to replace

storage cannisters as of yet. Aside from these problems, the system requires little extra operation beyond what would be necessary for an Earth-based toilet.

Tests of the Allied-Signal commode appear to be much more favorable [Brasseaux, Thornton, Whitmore, 1991]. The system required no more user involvement than with Earth toilets, aside from cranking the piston to compact waste material (which is motorized on ground and will be on future flight models). Occasionally, it is desirable to run a clean pad through with spray detergent to remove residual fecal films, which is not above and beyond comparable Earth toilet maintenance. Seat and thigh restraints worked normally, and the large seat orifice received favorable comment. Despite minimal suction and O-ring sealing on the test unit, odors were not present. Future tests will incorporate an air path through a charcoal filter and more complete sealing which will eliminate the need for a vacuum and further reduce the potential for odor escape. Inspection of the waste accumulation chamber revealed undesirable voids in the waste/pad layers. This problem can probably be eliminated with a higher compaction pressure and a directed airstream through the chamber.

Due to the favorable results from preliminary Allied-Signal tests with respect to efficient waste storage, ability to replace/clean the storage chamber during the mission, lack of odor, and minimal maintenance, it is recommended that the Columbiad mission incorporate the Allied-Signal commode unit over the current Space Shuttle commode. The Shuttle unit would have to be greatly redesigned to be compatible with Columbiad, particularly for the long-term habitat system. However, the Shuttle unit should still be considered as an alternative system on which to base a Columbiad commode in case of prohibitive scheduling slips/overriding cost on the Allied-Signal unit.

In addition to the commode, the crew module and habitat must address other solid wastes, particularly for garbage related to food packaging. An effort must be made to eliminate non-reusable and non-consumable items so as to reduce waste that needs to be processed. For example, freeze-dried foods should be packaged in thin plastic and then placed in reusable platters for consumption. That garbage which is collected must be compacted and stored, buried on the lunar surface or, if possible, burned and discarded as ash. Fumes from collected trash could be processed in the molecular sieve system (see section 7.2.1.3). However, considering the power requirement of a frequently operating burner, such a system should probably be avoided. Columbiad should take the stance of environmental awareness however, and investigate non-damaging techniques for waste burial.

It is important to minimize the potential for toxic hazards which come from storage tank leaks, crew waste product spill, particulates in the atmosphere, spilled food, leaks from flight apparatus, products from cabin fire, outgassing of cabin structural materials, or the accumulation of lunar dust within the habitat during the lunar stay. The control of such spills and accumulation can be accomplished through the use of portable vacuum systems and hazardous material containment bags which will prevent re-leakage. Filters should be incorporated into all air processing systems to prevent circulation of such contaminants as lunar dust and dead skin particles.

### **7.3 Radiation Requirements**

Radiation represents the single greatest natural hazard of spaceflight. Each stage of Columbiad exposes the astronauts to severe radiation environment. The responsibilities of Crew Systems include defining the radiation environment and determining the safe intake level limits.

#### **7.3.1 Human Radiation Tolerance**

The human body is particularly vulnerable to radiation in certain areas. The most critical body elements are the bone marrow, the skin, lenses of the eyes, and the reproductive organs. Scientists have established what are considered to be healthy annual limits. The standard units of measure of radiation intake are as follows [Hall,McCann,1987]:

**Rad-** defined as the amount of any kind of radiation which deposits 100 ergs per gram. This unit is not limited to any particular material and is the basic unit for both living organisms and inert substances.

**REM (Roentgen Equivalent Man)-** defined as the amount of radiation which produces the same biological effect as 1 Rad of X- or gamma rays. It is related to the Rad by the relationship:

$$\text{Rem} = \text{Rad} \times \text{RBE}$$

where RBE is the Relative Biological Effectiveness. The concept of biological effectiveness was introduced because it was found that energy deposition alone did not fully explain the damage produced in biological specimens. It was observed that the biological effects varied for different types of radiation or even different energies of the same type.

The annual limit placed on U.S. radiation workers is 5 Rem per year. However, this limit

**Table 7-5: Radiation Exposure Limits Recommended  
for Spaceflight Crewmembers**

	Bone Marrow	Skin	Ocular Lens
<u>Constraint</u>	<u>(Rem at 5 cm)</u>	<u>(Rem at 0.1 mm)</u>	<u>(Rem at 3 mm)</u>
1 year average daily dose	0.2	0.6	0.3
30-day maximum	25	75	37
Yearly maximum	75	225	112
Career limit	400 (death)	1200	600

takes into consideration that the dosage will be repeated year after year. Also, radiation workers are not expected to take on the level of danger associated with space exploration. In Table 7-5, we see the limits established by space medicine specialists. We see that restrictions on bone marrow intake are the most limiting, and so sets the upper bounds of the Columbiad mission. The limit established is 25 Rem over the entire 34-day mission.

### **7.3.2 Types of Radiation**

Astronauts on Columbiad mission can expect to encounter many different types of radiation. The first is that trapped in the Earth's Van Allen belts. Primarily composed of protons but also of electrons, this radiation surrounds the Earth as a result of the geomagnetic field. The highest radiation concentrations occur at both the 240 - 965 km altitude and the 7965 - 42,845 km altitude. The energy of these particles can be as high as 30 keV, and the flux results in roughly 1.14 Rem if flying directly through the belts.

The second variety of radiation has its origin from elsewhere in our galaxy and from other galaxies as result of cosmic explosions. Termed galactic cosmic radiation, it consists of low intensity but extremely high-energy particles (roughly 1 GeV), primarily protons (85%), alpha particles (13%), and heavy nuclei (2%). This radiation results in anywhere from 0.165 to 0.265 Rem per day.

The third type of radiation, due to solar flare activity, is much more rare. Large solar flares occur only a few times within the 4 to 6 year period of high sunspot activity in the eleven year solar cycle. The danger is in the intensity of the radiation against which normal spacecraft shielding is useless. Though the flare activity is sporadic and unpredictable, astronomers observing the sun can spot the 30- to 50- minute long flares and warn the

astronauts. Though the electromagnetic radiation reaches the Earth in roughly eight minutes, the most harmful particle radiation may take as long as 48 hours to arrive in the Earth's vicinity. This gives the crew plenty of time to seek shelter in a safe haven. Obviously, solar flare radiation is primarily a concern during the long period of lunar stay, rather than during the relatively short flight to and from the Moon.

### **7.3.3 Capsule Radiation Design Considerations**

The capsule should take into consideration the two trips through the Van Allen belts and the daily intake from galactic cosmic rays. However, due to the brief nature of the Earth-Moon transit, it has not been recommended to provide the heavy armor necessary to guard against solar flare radiation due to excessive weight.

### **7.3.4 Habitat Radiation Design Considerations**

The lunar habitat will automatically include shielding against daily galactic cosmic radiation. However, due to the long duration of lunar stay, it has been recommended that the lunar habitat include some form of safe haven to ensure crew survival during possible intense solar activity. This could take the form of a pre-fabricated metallic safe haven or alternatively through the loading of lunar regolith upon the habitat. This design philosophy varies from that imposed on the Crew Module (see section 7.3.3).

## **7.4 Spacesuits and Other Garments**

**Table 7-6: Columbiad Spacesuits and Crew Garments**

Unit	Quantity (CM/Hab)	Mass (kg/unit)	Volume (m <sup>3</sup> /unit)	Power (W/unit)
IVA Pressure Suit	4/0	10.2	0.5	-
IVA Overgarment/Boots	4/0	11.4	0.03	-
IVA Suit PLSS	4/0	8.0	0.015	20
EVA Hardsuit (AX-5)	0/5	81.8	2.0	37
Rescue Ball	1/2	2.0	0.128	-
Undergarments	1wk/3wks	1.0	0.005	-
Flight Suit/Shoes	1/3	2.0	0.005	-

Table 7-6 lists all of the final choice garments included on both the Crew Module and Lunar Habitat. The following sections briefly describe the Crew Systems garment package design requirements and reasoning for the choice of each garment.

#### **7.4.1 Crew Capsule Garments**

Astronauts must be protected from hazards at every phase of the mission. Besides the obvious hazards during lunar EVA, Columbiad crewmembers must be prepared to face launch and reentry loads, possible ejection abort, water or other environmentally hazardous landing, and cabin depressurization, not to mention simply keeping comfortably warm during Earth-Moon transit. The intravehicular wear includes human waste management, thermal undergarments, Earth environmental protection, anti-g protection, and full pressurization.

##### **7.4.1.1 IVA Undergarments**

Columbiad crewmembers shall wear a variety of undergarments to remain comfortable both within the IVA pressure suit as well as during non-critical Earth-Moon transit phases when the IVA suits are doffed. Underwear is particularly critical since it comes in direct contact with the skin. It must be, most importantly, non-irritating. Also, the material must allow the free passage of heat convected, radiated, or evaporated from the crewmember. Finally, it must be lightweight, elastic and be nearly wrinkle-free. Though cotton and linen have desirable properties, the addition of man-made fibers has shown to increase clothing durability. The commercial fabric Capellene is an example. For long term IVA suit wear, particularly during the launch, reentry, and capsule-to-habitat transfer phases, the crew will also don a garment similar in design to the Apollo Fecal Containment System (FCS) which holds up to 1 L of waste matter if defecation becomes inevitable during these mission phases. During Earth-Moon transit, crew garments should include a flight suit similar to the current cobalt blue Space Shuttle pants/jacket combination. These are particularly functional as they include pockets with zippers Velcro patches which allow crewmembers to stow small personal items such as notebooks, pens, scissors, and flashlights while in low-g.

##### **7.4.1.2 IVA Spacesuit**

The choice to include a specialized IVA suit as part of life support equipment was made for several reasons. First, with the extensive lunar EVA schedule planned, in which astronauts may perform four hours of EVA per day for 28 days, it was deemed imperative to include a very specialized, durable spacesuit for the lunar stay. These EVA suits would, by nature of



all its extra protective layers, be very bulky and would likely interfere with minute-by-minute crew operations during launch and landing phases. With the decision to go with off-the-shelf ejection seats, which are restricted in size, over a nose mounted escape tower, the constraints on spacesuit bulkiness grew particularly critical. However, the fact remained that it is important to provide backup life support for all possible contingencies, particularly cabin depressurization. The best solution was a suit which would already be compatible with ejection seats in high altitude reconnaissance aircraft, as well as allow enough dexterity for the coordinated actions associated with flying. The best option available is a suit similar to those used on initial Space Shuttle flight tests, which in turn was a readaptation of the Air Force full pressure suit flown on SR-71 missions (see Vol III section 6.3.3.2 for design details).

#### 7.4.1.3 Habitat-Capsule Transfer

In addition to the specialized EVA suit, which is too bulky to include on the Crew Module, an IVA pressure suit coverall and abrasion resistant booties should be included on the crew capsule for use in the capsule-to-habitat and habitat-to-capsule transfer at the beginning and end of the lunar stay. Because the IVA suits are designed primarily to be used during relatively motionless in-capsule phases of the mission as well as for atmospheric abort, they have not been designed for the intense thermal and abrasive environment of the lunar surface. An overgarment and protective footwear will provide protection for the brief EVA expected at the immediate beginning and end of the lunar stay. In addition, a portable life support system backpack must be included for these brief transfer phases to supply oxygen and remove heat and waste carbon dioxide. Scientists at Johnson Space Center have readapted the current Shuttle EMU fabric layup allowing engineers to design alternative protective overgarments. This represents the best fabric spacesuit layup designed to date, and has been chosen as the base material for the IVA Spacesuit Overgarment (see Vol III section 6.3.3.3 for design).

### 7.4.2 Habitat Garments

#### 7.4.2.1 IVA Garments

Crew garments on the lunar habitat will be identical to those worn while in Earth-Moon transit. These include thermal underwear made of Capellene (Constant Wear Garments), flight jacket and pants, and tennis shoes (see section 7.4.1.1). In addition, it is desirable to provide warmer layers, for instance sweatshirts, and cooler garments such as t-shirts and shorts to allow greater freedom among crewmembers for personal comfort.

#### 7.4.2.2 EVA Spacesuits

A large portion of time on the lunar surface will be spent performing EVA. Therefore, providing the astronauts with an EVA spacesuit capable of protecting them from the harsh conditions of the lunar surface is a priority. This performance level must be maintained over long-duration EVA, and should allow all four crew members to perform excursions every Earth day for the 28 day lunar visit. We must protect against thermal, radiation, micrometeoroid, pressure, abrasive, chemical, and electrostatic hazards that might be encountered. Beyond basic protective concerns, the spacesuit must provide life support independent of the spacecraft and remain compact and light. Finally, the astronaut must be able to perform mission tasks over many hours without excessive fatigue. Therefore, unrestricted motion, high visibility, and comfort are design requirements.

Crew systems efforts in choosing a spacesuit for lunar excursions included an examination of the Apollo suits as well as the currently used Space Shuttle Extravehicular Mobility Unit (EMU) to determine if these would be acceptable for Columbiad. The Apollo was a highly successful spacesuit which used a typical multi-layered fabric design to combat the various harmful properties of the lunar surface. However, these suits had problems which we would like to avoid for the return to the Moon. First, being entirely constructed of fabric, the Apollo suits are vulnerable to tearing and chemical degradation, particularly over extended use. Secondly, the Apollo suit joints were not entirely volume conservative, causing resistance to every movement due to internal pressure increase. Lastly, the Apollo suits utilize technology that is nearly 30 years old, for example of fabrics. The knowledge gained during research for the Space Shuttle suit should be used for the EVA suit which may be standard for lunar and possibly Mars missions for the next 20 years.

Crew systems also examined the Space Shuttle EMU. Again, the suit is constructed of a multi-layered fabric, though its torso is reinforced with fiberglass. It is highly modular, allowing pieces to be mixed to cater to a wide range of human proportions. This suit has also had a very successful record, but is still not ideal for a future lunar EVA suit. One of its greatest problems is that it is only rated for 0.29 atm, slightly incompatible with desired cabin atmospheric pressures. It is desirable to completely eliminate time consuming pre-breathing or decompression procedures. We also wish to have a thicker atmosphere than in the Shuttle suits to allow greater work capacity over longer hours. Therefore, the EMU as it exists is incompatible with Columbiad design requirements. Finally, the EMU and its associated PLSS weighs approximately 110 kg, too heavy for extended weighted

operations. Again we decided that a spacesuit which could conceivably be used over the next 20 years should utilize the most advanced protection methods and should be very mobile. We found the prototypes for such a suit in a study currently being conducted by NASA Ames.

The NASA Ames AX-5 and Mark-3 hardened suits, designed for Space Station Freedom construction, can be readapted for use on the lunar surface. Their protective qualities against micrometeoroid impact, abrasion, and lunar surface impact, high pressure capability, as well as their highly mobile, constant-volume joint design make readaptation design a better option than using the Shuttle EMU as the base system. See Volume III section 8.1.3.3 for the EVA Spacesuit design details.

If NASA coordinators project that with redesign and testing the Ames-derived suits cannot be ready for Columbiad's maiden voyage, Crew Systems recommends a readaptation of the current Space Shuttle EMU for the lunar surface. The system may be sufficient for expected EVA with the addition of several features. Long-term abrasion can be combatted with the addition of either an integral protective fabric/solid layer or a protective overgarment similar to that we expect to use for the IVA suits. However, both of these options may be too bulky to make them worthwhile. Furthermore, the pressure bladder and joints may have to be modified to allow for a 0.34 atm internal pressure. Oxygen capacity for the EMU PLSS will probably have to be increased by about an hour's worth of oxygen. The benefit to this option is the amount of experience NASA has already acquired on the suit's performance. Many of the system's quirks have probably already been ironed out. However, the addition of new equipment may create a whole host of new problems.

#### 7.4.2.2.1 Metabolic Requirements

While providing a pressurized oxygen atmosphere for each crew member, the EVA life support equipment must also support a comfortable thermal environment. In order to prevent heat exhaustion, the EVA spacesuit and portable life support system (PLSS) must have the capacity to dissipate the metabolic heat production of the Columbiad crew during lunar surface activities. Metabolic rates exhibited by the Commander and Lunar Module Pilot during Apollo 11 lunar surface EVAs is shown in Table 7-7. For the initial Columbiad mission, the crew is expected to exhibit similar EVA metabolic rates.

**Table 7-7: Crew Metabolic Rates During Apollo 11 Surface EVAs**

Work	Mean Rate (kJ/hr)	Mean Rate (kcal/hr)
ALSEP Deployment	1018	244
Geological Sampling	1018	244
Overhead	1123	270
LRV Operations	518	123
Sedative (BMR)	175	41
All Activities	980	234

Key:

Overhead = tasks required for each EVA such as egressing, ingressing vehicle which are not directed toward the specific mission objective

ALSEP = Apollo lunar surface experiment deployment

LRV = Lunar roving vehicle

BMR = Basal Metabolic Rate

The liquid cooling garment of the EVA spacesuit and PLSS has the capability of suppressing perspiration at sustained work rates as high as 2100 kJ/hr. Thus, between 60 and 80% of the heat generated by metabolism was successfully dissipated. Additionally, a daily food intake of 2800-3000 kcal was found to be sufficient for sustaining five to seven hours of Apollo lunar EVA activity. However, a better understanding of metabolic requirements on the lunar terrain will be necessary to adjust future lunar EVA suit designs, work scheduling and nutritional requirements. This will better prevent dehydration and excessive fatigue.

**Metabolic Rate Monitoring.** To ensure that crew members do not experience high work rates beyond the capability of EVA life support equipment and daily caloric intake, metabolic rates during human lunar activities must be monitored. The following data will be transmitted to mission control from each crew member performing lunar EVA:

- electrocardiogram data
- oxygen bottle pressure
- liquid cooling garment coolant-water entry

Using this data, approximate metabolic rates will be calculated by averaging the results of the following:

- a correlation between ECG signal and a bicycle ergometer workload established on the lunar habitat for each crew member
- a record of the decrease in oxygen bottle pressure per time (including a correction factor for an assumed rate of suit leakage)
- a calculation of the difference in coolant water temperature flowing into and out from the liquid cooling garment, multiplied by an assumed water flow rate.

#### 7.4.2.2.2 Medical Monitoring

Without the protection of the BioCan environment, biomedical monitoring of crew members performing lunar surface EVA is critical for human safety. Real-time comprehensive monitoring of physiological status will provide important data for medical personnel at mission control to ensure proper functioning of EVA life support. Data is also needed to establish work scheduling limitations. For example, overwork was partially responsible for the cardiac arrhythmias that were detected when monitoring the Apollo 15 crew.

The **Operational Bioinstrumentation System** shown in Figure 7-7 will be assembled in the *biobelt* and worn underneath the spacesuit during lunar surface EVA. This includes three signal conditioners of equal size (5.84 cm x 3.81 cm x 1.04 cm) providing electrocardiogram (ECG), impedance pneumograph (ZPN), and body temperature (BTS) data. Electrodes will be attached to the crew member by double-back adhesive tape at the areas indicated in Figure 7-8. ECG data will provide a means for approximating metabolic rate (as discussed in paragraph 7.3.2.2.1) and detecting abnormal heart electrical activity. Breathing will be monitored with ZPN data that provides information on thoracic movements and lung volume changes. Finally, overheating will be detected by relaying data on body temperature. More specific details on the biobelt assembly will be discussed in Volume III: Subsection 8.1.3.4.

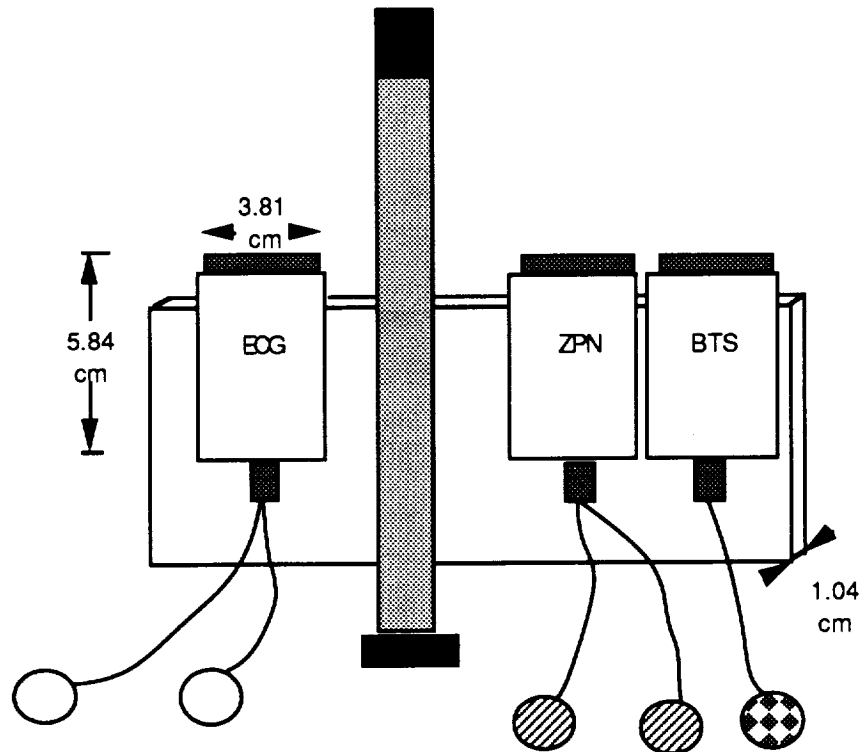


**Figure 7-7**  
**Biobelt Assembly for EVA Medical Monitoring**

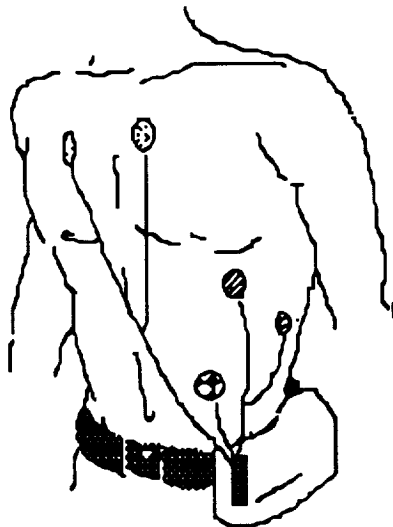


**Figure 7-8**  
**Biobelt Assembly Electrode Placement**

### **7.4.3 Personal Rescue Spheres**

It is vital that crew of Columbiad be able to transfer from Crew Module to Habitat and vice versa without the use of spacesuit given one or more spacesuit malfunctions. As part of the Space Shuttle program, a rescue concept was conceived utilizing a pressurized, protective, and compact fabric sphere into which an astronaut can zip his or herself into quickly [Harding,1989]. After entry, the sphere is inflated with oxygen, making it 0.8m in diameter. The sphere includes a Personal Oxygen System and a window. Though the enclosed astronaut cannot move on his own, the sphere can be carried by another astronaut who is suited for transfer between vehicles. Aside from the Habitat-to-Crew Module transfer concept, the idea could be carried further to include transfer from Crew Module to rescue vehicle in LEO if severe spacecraft malfunction occurs post-launch or pre-reentry.

### **7.5 Medical Monitoring in the Crew Module**

Medical studies from Apollo and Skylab have been performed to determine the effects of zero-gravity on the human cardiovascular, musculoskeletal, vestibular, respiratory and endocrine systems. Observed inflight results from the Apollo mission include:

- 1.5-2 liter headward fluid shift (Lower Body Negative Pressure)
- 4-9% reduction of blood plasma volume
- 2-10% reduction of red blood cell mass
- 10% decrease in vital capacity (lung volume)
- Reduction in hormone volumes controlling excretion
- Vestibular disturbances (vertigo, dizziness, motion sickness)

The conditions listed above did not endanger the lives or work performance of the astronauts and were found to be self-limiting. These symptoms ceased and in some cases reverted back to normal within 30 days of flight. Because of the short transit time between the earth and moon, bioinstrumentation related to monitoring these minimal threat conditions will not be carried on-board the capsule in an effort to decrease capsule mass and maximize cabin volume for crew movement. However, deleterious and non-adaptive conditions experienced by Apollo and Skylab astronauts are of concern on this mission. Rapid "g"-variations and weightlessness have been shown to threaten the health of the cardiovascular and musculoskeletal systems. Consequently, biomedical monitoring must be conducted on the crew capsule to record the status of these physiological systems.

### 7.5.1 Cardiovascular Effects of Rapid "G"-Variations

The human heart responds to the environment in ways which achieve equilibrium with external demands. Multiple-g acceleration forces observed during crew capsule launch and reentry impose considerable increases in heart rate. In contrast, the human body normally responds to severely reduced gravitational loading during weightlessness with a low heart rate and increased blood pressure. In the Columbiad mission, multiple acceleration forces encountered during launch are followed immediately by several days of inflight weightlessness. Habitation in the lunar environment imposes a needed adjustment from weightlessness to one-sixth-g. Furthermore, exposure to multiple-g acceleration forces encountered during earth reentry after three days of weightlessness requires subsequent adjustment to postflight terrestrial gravity. These sudden alterations in gravitational external demands stress the cardiovascular system and have the potential of inducing cardiac irregularities and orthostatic hypotension.

#### 7.5.1.1 Detection of Cardiac Irregularities

Benign premature ventricular contractions have been observed occasionally by crew members during previous space missions. An unusually high frequency of cardiac arrhythmia was observed from both the Commander and Lunar Module Pilot on Apollo 15. Although the exact cause of these irregularities is not known, the presence of this potentially dangerous condition necessitates the monitoring of heart rate and cardiac electrical activity.

On the crew capsule, cardiovascular monitoring of all crew members must be conducted with a multichannel electrocardiogram (ECG). Electrodes worn underneath flight clothing will allow for the continuous monitoring of the crew immediately before, during, and at least one hour after earth and lunar launch, reentry and landing. Rapid g-load variations during these periods may induce potentially hazardous physiological stresses.

#### 7.5.1.2 Prevention of Orthostatic Hypotension

In a weightless environment, the shift of fluid volume toward the upper body (lower body negative pressure) is interpreted by central mechanoreceptors as a relative increase in fluid volume. This triggers diuresis, resulting in a decrease in blood volume. With the low blood volume and low external gravitational demand, blood pressure increases during weightlessness while heart rate decreases. A sudden exposure to lunar or earth gravity after an extended period of weightlessness often results in *orthostatic hypotension*.

Fainting spells are symptomatic of this condition since the sudden exposure to an increased



gravitational load yields an abrupt drop in blood pressure accompanied by a sharp increase in pulse rate. Consequently, the circulatory system fails to supply a sufficient amount of blood to the brain. A lower body positive pressure garment (anti-g IVA suit) will be worn before and during earth and lunar landing in order to increase blood supply to the brain.

### 7.5.2 Musculoskeletal Effects of Microgravity

One of the most serious physiological hazards of spaceflight is irreversible musculoskeletal atrophy. Chronic exposure to zero-gravity decreases the external demand on muscles and results in a gradual decomposition of protein. Bone strength, density and mass also decline under reduced gravitational loading.

Muscle atrophy and bone demineralization have been confirmed through urinalysis and blood sampling from Apollo and Skylab biomedical studies. The appearance of abnormally high concentrations of calcium, phosphorus and nitrogen in the fluid samples from these crews indicate that the primary elements of the musculoskeletal system were expelled as waste. Studies of a Skylab 2 crew recorded an average bone mineral loss of only 0.01% per day in a weightless environment. Therefore, loss of bone mineral on the Crew Module during the three-day transit between earth and moon will be negligible.

Noticeable loss of muscle strength *will* be expected upon the initial exposure to one-sixth-g lunar gravity. In order to maintain muscular strength for extravehicular activities immediately after lunar landing, the MK- I exerciser will be used on the Crew Module to maintain arm strength during the three day transit in zero- gravity. This isokinetic exerciser, shown in Figure 7-9, retards the speed at which the user can move. As the user applies maximum effort, the MK-I automatically varies opposing resistance to maintain movement at a constant, pre-selected value. The effectiveness of this lightweight and compact device was proven on Skylab missions when three sets of twelve repetitions were performed per crew member per day.

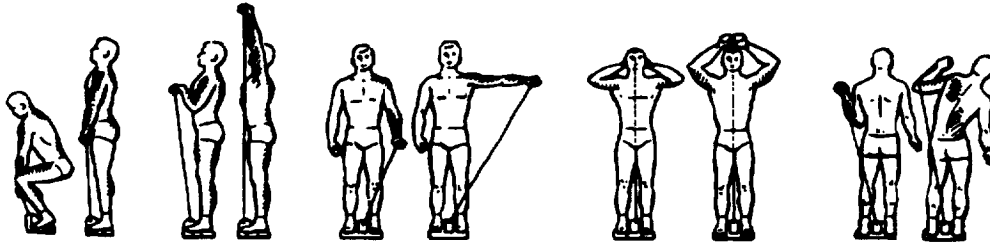


**Figure 7-9**  
**MK-I Exercise Positions**  
**[Johnston and Dietlein, 1977]**

### **7.5.3 Inflight Medical Support**

A medical kit will be supplied on the crew capsule to treat minor injuries and inflight illnesses encountered during capsule habitation. The list of medications in Table 7-8 was compiled from the inflight medical needs of astronauts on Apollo and Skylab. The amount of each item supplied was based upon the frequency at which particular illnesses occurred.

Vitamins, amino acids and mineral dietary supplements will be needed to promote the retention of fluids and electrolytes often lost in a zero-g environment. Potassium supplements are particularly important since a deficiency of this mineral has been linked to arrhythmias on Apollo 15.

**Table 7-8: Inflight Medical Support**

Item	Amount Supplied
Methylcellulose Eye Drops	1
Skin Cream	1
Neosporin (antibiotic ointment)	1
Actifed	30
Lomotil (diarrhea medication)	20
Tetracycline (250 mg)	10
Ampicillin	10
Tylenol	15
Benadryl (antihistamine)	10
Seconal (insomnia medication)	15
Scopolamine/Dexedrine (motion sickness)	15
Demerol (pain medication)	2
Lidocaine (cardiac medication)	10
Atropine (cardiac medication)	10
Other Equipment:	
Compress-bandage	2
Bandaid	5
Tweezers	1
Scissors	1
Oral Thermometer	1

### **7.6 Medical Monitoring on the Lunar Habitat**

While Apollo and Skylab missions provided ample information on the human physiological responses to zero-g environments, extensive biomedical research on the effects of one-sixth-g has never been performed. Data on human tolerance of the lunar environment must be collected in order to (1) define medical risk factors which may aid in astronaut selection, (2) define countermeasures to adverse physiological conditions, and (3) aid in the development of work schedules and nutritional requirements for optimal crew performance. Therefore, the medical monitoring conducted during the 28-day lunar habitation will be much more comprehensive than that performed on the Crew Module.

### **7.6.1 Monitoring Cardiovascular Deconditioning**

Significant cardiovascular deconditioning is not a threat during the short duration of Crew Module habitation. While the main concern on the Crew Module is the detection of immediate cardiac abnormalities during rapid acceleration changes (see Section 7.5.1), habitat monitoring will concentrate on gradual, long-term effects of one-sixth-g.

Heavy leg exercise performed on the habitat **treadmill** (discussed in Section 7.6.2) and **bicycle ergometer** can effectively stress the cardiovascular system in microgravity by increasing blood circulation in lower extremities. Simultaneous biomedical monitoring must be performed *during exercise* on either equipment in order to detect potential decreases in exercise capacity throughout the 28-day duration. Data on oxygen consumption, carbon dioxide production, lung volume and respiratory exchange will be collected with a metabolic analyzer. Coupled with electrocardiogram data, the results of this analysis may also be used to approximate metabolic rates of crew members performing lunar surface EVAs (as mentioned in Paragraph 7.3.2.2.1).

### **7.6.2 Monitoring Musculoskeletal Atrophy**

Slow musculoskeletal atrophy is inevitable under the reduced gravitational loading of the one-sixth-g lunar environment. Resistive forces encountered in the EVA spacesuit during surface activities necessitates the use of MK-I exercisers on the habitat to maintain arm strength (see Section 7.5.2). The rate of trunk and leg muscle atrophy will be decreased by walking or running on an angled treadmill under gravitational loading, as shown in Figure 7-10. An equivalent 80 kg weight is provided by the attached bungees.

Despite the inclusion of exercise equipment to hinder muscle degradation, long-term exposure to microgravity will require physical and chemical analyses to record actual musculoskeletal status. The presence of a lunar gravity makes a standard terrestrial scale suitable for recording rapid decreases in **body mass** on the lunar habitat. **Blood and urine analyses** will be conducted three times per week to trace abnormally high concentrations of nitrogen, phosphorous and calcium in body fluids. The correlation between both of these parameters can provide an accurate indication of muscle and skeletal tissue breakdown.

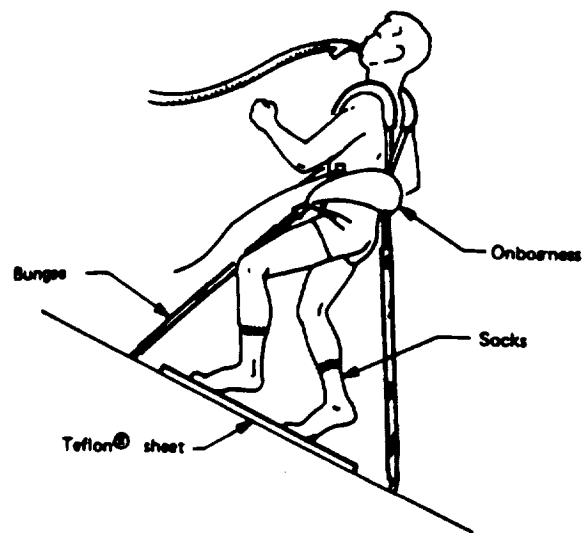


**Figure 7-10**  
**The Angled Lunar Habitat Treadmill**  
**[Johnston and Dietlein, 1977]**

**Exercise program.** An exercise program on the lunar habitat must be implemented to: (1) effectively reduce muscle, joint, and bone atrophy, (2) minimize reductions in heart size or mass, and (3) maintain coordination and exercise capacity. The minimum exercise requirements of each crew member on the lunar habitat are shown in Table 7-9. Long-term Soviet and American missions have shown that more strenuous exercise further reduces physiological deconditioning.

**Table 7-9: Minimum Exercise Requirements on the Lunar Habitat**

Exercise Target	Equipment	Duration
Arm Strength	MK-I	2-3 sets of 6-12 maximum repetitions per day
Leg Strength and Endurance, Prevention of calcium and mineral loss, neuromuscular coordination, joint and tendon integrity	Angled Treadmill (with Gravitational Loading)	30 min/day @ 6-7 mph
Cardiovascular Endurance	Ergometer/ Treadmill	30 min/day

### **7.6.3 Habitat Medical Support**

A daily private crew voice communication channel will be installed to allow the relay of crew health concerns and biomedical data (electrocardiogram, body mass, metabolic analysis and fluid chemistry results) to medical specialists at Mission Control. These personnel will be staffed in order to:

- advise in emergency medical situations,
- analyze telemetered data for possible work schedule revisions
- continuously monitor EVA spacesuit activities, and
- provide recommendations for future missions regarding crew health.

A medical kit similar to that used on the crew capsule will be supplied on the lunar habitat (see Section 7.5.3). As shown in Table 7-10, the amount of each item supplied has been increased to support the longer duration of lunar habitation.

**Table 7-10: Habitat Medical Support**

Item	Amount Supplied
Methylcellulose Eye Drops	2
Skin Cream	2
Neosporin (antibiotic ointment)	2
Actifed	60
Lomotil (diarrhea medication)	50
Tetracycline (250 mg)	30
Ampicillin	30
Tylenol	45
Benadryl (antihistamine)	30
Seconal (insomnia medication)	30
Scopolamine/Dexedrine (motion sickness)	20
Demerol (pain medication)	5
Lidocaine (cardiac medication)	30
Atropine (cardiac medication)	30
Other Equipment:	
Compress-bandage	4
Bandaid	15
Tweezers	1
Scissors	1
Oral Thermometer	1
Analytical kits:	
Urinalysis	55
Blood Chemistry	55

## **7.7 Additional Crew System Concerns**

### **7.7.1 Mass of Cabin Air**

A study was done to determine the mass of the cabin atmosphere (.34 atm and 64% oxygen, 32% nitrogen). The ideal gas law was used to determine the partial densities of oxygen and nitrogen to provide a 64% oxygen and 36% nitrogen mixture at 0.34 atm. Thus, the partial densities are .140kg/m<sup>3</sup> for nitrogen and .284 kg/m<sup>3</sup> for oxygen. The partial densities were then multiplied by the habitable and pressurized volume of the crew

module ( $15\text{m}^3$ ) and the habitat ( $200\text{m}^3$ ) to obtain the needed mass of the oxygen and nitrogen to obtain the desired characteristics of the cabin air. These totals are 4.26 kg of oxygen and 2.1 kg of nitrogen for the Crew Module and 56.8 kg for oxygen and 28 kg for nitrogen for the habitat.. For redundancy these numbers were multiplied by a 1.5 factor of safety and two additional supplies of each are stored in tanks. These additional supplies provide protection against cabin depressurization or air loss by other means. The final mass values for cabin atmosphere supply are 19.17 kg of oxygen and 9.45 kg of nitrogen for the crew module and 255.6 kg of oxygen and 126 kg of nitrogen for the habitat.. This information is also provided in the tables of Section 6.3.2 and Subsection 8.1.3.2 of Volume III.

### **7.7.2 Other Equipment**

The habitat and the crew module require additional equipment for operation which has not been stated in the previous trades and selection sections. Table 7-11 contains the additional equipment required for the Crew Module, whereas, Table 7-12 contains the additional equipment required for the habitat. Much of the equipment is self-explanatory.

**Table 7-11: Additional Equipment for The Crew Module**

	Mass (kg)	Volume (m3)	Power (watts)
<b>Other Equipment TOTAL</b>	<b>33.5</b>	<b>0.12</b>	<b>200</b>
Lighting	4	0.01	200
Tools, cleaning equipment	29.5	0.11	-

**Table 7-12: Additional Equipment for The Habitat**

	Mass (kg)	Volume (m3)	Power (watts)
<b>Other Equipment TOTAL</b>	<b>160</b>	<b>1.77</b>	<b>1506.3</b>
Hardsuit Recharge System	50	1.5	500
Lighting	10	0.1	450
Tools, cleaning equipment	100	0.17	
Housekeeping			556.3



#### 7.7.2.1 Spacesuit Checkout and Recharge System

The astronauts will be conducting numerous EVAs over the course of their lunar stay. This activity will most likely weigh heavily on the EVA hardsuits, and will necessitate frequent checkovers to detect damaged or malfunctioning equipment before EVA. Also, it is imperative that Portable Life Support System backpack batteries and oxygen tanks can be quickly recharged, reducing EVA turnover time. Allied-Signal has designed a system for use on the Space Station Freedom called the Service and Performance Checkout System (SPCS) which provides a system checkout for pre- and post-EVA, as well as recharge for the oxygen and power supplies. Such a unit would necessarily have to be reconfigured for use on the lunar habitat and with the EVA hardsuits depending on the exact PLSS system used.

## **8 The Status Group**

The primary purpose of status can be summed up in two words: monitor and maintain. The status group must be able to continually monitor the performance of a spacecraft's systems. The group's ability to detect possible problems will depend upon the use of various instruments such as thermocouples, pressure gauges, and flow meters. It will also depend upon the group's ability to quickly gain access to failure data on operating time, environments, and failure rate. This will allow the status group to determine whether or not any system is maintaining its desired level of performance. With the use of artificial intelligence and computer aided engineering and design techniques, the status team should be able to identify and isolate a faulty unit or component.

Once a problem has been diagnosed, the status group must be able to maintain the system by easily removing and replacing the faulty component. Furthermore, the group must show that all systems are fully functional after repair activities are accomplished. This step must be done without allowing any safety hazard which might jeopardize the mission.

Status engineers have to assess the feasibility of any test or monitoring activity in terms of limitations that are imposed by costs and scheduling. The team must tackle challenges such as accessibility to faulty units and replacement parts, the ease of removal and repair, and the frequency of repairs. Status must decide such things as which components require spare parts, how many of them to stock, and where they should be kept.

Since the development of the Space Transportation System (STS), there has been an even greater emphasis placed on the role of status. Earlier systems were not maintainable once they had been sent into orbit. But concepts such as reusability, streamlining, downsizing, and automation have led to an evolution in which the status team has developed into an efficiency and quality assurance watchdog. In essence, status should promote overall efficiency while maintaining superior quality (see Volume 4, section 1.7.3.4).

### **8.1 Testing**

One of Status' main functions is the design and application of required tests for the qualification and verification of the launch system. As a result, this group plays a key role in the design and development of the launch vehicle. The Status design tests are a significant factor in determining the confidence and the reliability of the entire system. A typical test series consists of design development, qualification, and acceptance tests. It is

through these tests that the project engineers can determine if a system or component was built correctly.

The design development tests (DDT) are implemented once a preliminary design has been presented. Such tests can provide valuable insight into the reasonability of the structural design approach. They can provide essential data such as the various modes of failure. The DDT is particularly useful in analyzing a component for which there is little confidence in its structural capability. Such a situation usually arises when a new manufacturing process is employed.

Qualification tests are usually implemented after the presentation of a final design. They are used to show that the requirements of the design have been met. In the qualification tests, flight quality components and systems are subjected to loads and durations which greatly exceed the anticipated in-flight values. These tests provide a favorable confidence level for the acceptable performance of a tested unit, as well as to any similarly constructed unit, in the predicted service environment.

Acceptance tests are very similar to qualification tests. However, they are mainly used to prove the quality of the manufacturing process used in the production of flight hardware. These tests are the final step in the flight verification process. A unit which meets the test criteria is ready for flight.

### **8.1.1 Ground Testing**

The ground testing of a large space structure is a key aspect of the verification procedure. It is a major step in the certification of the launch system because it is a true representation of the mission environment. In fact, the large size of the test structure presents a number of challenges in the successful application of the tests. The dynamic characteristics of the body are affected by such forces as gravitational stiffening, low resonant frequencies, and high modal densities. Furthermore, analysis of the structure is complicated by air damping and small motions due to wind loads and operations noise. In addition, the nonlinearities and intricate mechanical links of the component, which is characteristic of a space structure, adds to the overall complexity. However, there is a test philosophy which allows for the successful implementation of the ground test.

### **8.1.2 Ground Test Philosophy**

An efficient ground test incorporates several analytical procedures. In addition, the ground tests for a spacecraft should be slightly different than the ground test for a large, space erected structure. First, for a spacecraft, the use of a scale model test can be very effective because it permits structural analysis without the inhibiting gravitational and size effects. Secondly, the complexities of various mechanisms, such as joints, can be overcome through the use of element tests. Another technique which can be utilized is the testing of sub-structures. This allows the actual structure's dynamic response to be studied in spite of the various size related complexities. Fourth, experience has shown that modeling the vehicle with a linearized representation can ameliorate the problems that accompany small orbital motions. Finally, the designer of the ground test should be open to the fact that in some cases certain complexities can not be avoided. Thus, certain ground test sequences will have to be studied separately. All of these techniques, as a whole, are geared toward the analytical verification of the spacecraft using models or sub-structures.

The design and verification of a large space erected structure is slightly different than that of the spacecraft in that the structure does not employ the use of a prototype. It relies more upon analysis than it does on ground verification.

### **8.1.3 Countdown Demonstration Test**

The countdown demonstration test (CDT) is a precursor of the systems integration test (see section 8.1.6). In this test, the vehicle is exposed to the actual launch conditions without regard to actual liftoff. The climax of this test is firing of the engines to determine flight readiness. The CDT is meant to determine if the system is fully integrated; it provides confidence in the critical elements which are being tested together for the first time. A typical countdown demonstration test will try to achieve several goals.

First, it will use all the systems, sub-systems, and components of the launch system, as well as the necessary personnel and launch facilities. Second, the countdown provides the opportunity to determine the launch vehicle's ability to provide propellants at the intense conditions of engine firing. Third, the CDT is very useful in correlating the performance of the propulsion system and its interfaces. In addition, the CDT allows the flight operations personnel to assess the monitoring capability of the avionics equipment under launch vibration loads. Fourth, the test evaluates the validity of using design modeling methods to extend analysis from the test facilities to the launch facilities. Finally, a countdown simulation allows for the evaluation of the information acquisition systems and data reduction methods.

#### **8.1.4 Astronaut's Role in Testing**

Prelaunch tests and activities are geared toward the verification of the readiness of all flight systems. This has a significant impact on the confidence given to the flight hardware and the success of the mission. It is therefore essential that these tests are run properly and accurately. One factor that can influence this is the presence of the astronaut. In this section, the role of the astronaut in the preflight testing procedures will be briefly summarized.

Preflight activities are a major component of an astronaut's training procedure. They allow the pilot to become familiar with the the layout of the vehicle (especially the escape hatches) and its systems. It is important for an astronaut to feel comfortable with the vehicle and to get a feel for the handling of the controls. The countdown simulation provides the astronaut with the chance to test his/her familiarity with the various in-flight procedures such as vehicle health monitoring and launch checkout tasks. In addition, the astronaut becomes more confident with the abilities of the support and flight operations personnel. From an engineering standpoint, the presence of the astronaut is necessary for an accurate representation of actual launch configuration. The success of the mission is greatly dependant upon the astronaut's ability to carry out the flight experiments or cargo deployment. Everything must be geared toward the comfort of the astronaut.

#### **8.1.5 Pre-launch Testing**

Although it is present from the first leg of construction, the presence of the status group is most prevalent during the final days before the launch. It is during this time in which the launch facilities and all launch operations are focused upon the primary status function-testing and verification. The testing procedures are based upon those that were used in the first space launches such as Gemini and Apollo. The tests are grouped into several general categories: 1. Electrical Systems 2. Telemetry 3. Radio Frequency (RF) and Tracking 4. Measurements 5. Mechanical Systems 6. Guidance and Control Systems and 7. Vehicle Systems. Furthermore, each group is divided into even smaller categories. The vehicle systems tests encompasses such activities as simulated flight tests, cooling systems tests, static firing, and fuel tank pressurization. On the average, these tests require 4 to 8 hours, but a few of them will require 2 or 3 days.

The effectiveness of the status group depends upon its ability to follow and adhere to a defined set of procedures in the testing phase. The testing of the engines and the calibration

of measuring devices and telemetry fall under such guidelines. The engine tests require a low level nitrogen purge of the liquid oxygen dome. This step will usually commence before loading the propellant and continue until just before engine ignition. The nitrogen purge is designed to prevent contaminants from entering the nozzle of the thrust chamber and flowing up to the injector plate. It also helps to keep the area dry. In the event that the launch should be scrubbed, a nitrogen purge is used to remove all of the liquid oxygen thereby preventing the possibility of an explosion. This same technique can be incorporated to purge the liquid oxygen injector manifold, liquid propellant gas generator, and fuel injector manifold of the thrust generator to prevent harmful refuse from entering the thrust chamber.

The calibration of measuring devices and the telemetry is usually done by two separate groups within status. The measuring group must calibrate a number of black boxes which are signal conditioners that magnify an impulse until it can be read on a certain scale. During the tests, these amplifiers bypass the telemetry systems in order to obtain a more accurate sense of their reliability. The testing procedure employs a five step sequence in which instrument readings (pressure valves, thermocouples, flow meters, etc.) are taken at 0%, 25%, 50%, 75%, and 100% of their maximum values. Once testing is completed, the measuring and telemetry systems are connected with RF links.

The calibration of the telemetry systems is an ongoing process. The major component of this process is the RF compatibility test. During this test, the service structure is moved away from the pad and the vehicle stands alone. A total diagnostic of the radio systems is performed. In addition to assuring the reliability of these components, the test is also used to certify that there are no disturbance signals to interfere with communications or the command destruct system. During the tests, power is sent to the RF systems. This allows them to transmit signals to the various receiving stations for radar and command & control.

#### **8.1.6 Integrated Systems Tests**

The Integrated Systems Test is the most crucial step of the checkout procedure. It is composed of three separate tests. First, the overall test (OAT#1) includes the mechanical systems and electrical networks tests. The major highlight of OAT#1 is the initial run of the launch vehicle's sequencing system. This is the relay logic network that takes over control of the final moments of the launch sequence. Second, there is the Plug Drop Test (OAT#2). In this test, the spacecraft is placed on internal power and its attachment to all ground support systems is removed. This test is used to determine the reliability of part

of the crew safety design. Finally, there is the Guidance and Control Test(OAT#3). In this phase, all of the launch vehicle's and support vehicle's systems are linked and tested. This is the ultimate check that is used as a verification of all previous activities. It involves advance work by the launch teams in vehicle networks, ground networks, mechanical, electrical support, measuring, RF, and navigation. Their activities will be linked through the LOX loading tests, Plug Drop, Engine Swivel, and Simulated Test Flight.

The activities of the launch facility on launch day are placed in the hands of status. On this day, all actions are procedural and methodical. This is the monitoring phase for status. It is status' job to ensure that all systems are performing as expected. If a system is not performing properly, it must be identified and its faulty component must be isolated.

The status mechanical team will usually be the first team present on launch day. Its tasks are basically to inspect high pressure gas panels, cable masts, and fuel masts and to prepare the hold down array for launch. The propellant team pressurizes the helium bottles, checks out the fuel facility, and loads the fuel. Even this process is subject to regulations. The tanks are usually filled to 10% of their necessary capacity through a very time consuming process. During this "slow fill", the tank level is filled at a rate of 750 liters/minute. This is done to determine if there are any leaks present. When they are confident that no leaks are present, a "fast fill" stage is then used to increase the tank level at a rate of 7570 liters/minute. When the tank has reached the 97% capacity level, the "slow fill" method is once again used . In addition, the tanks are pressurized to about half of the operating pressure in order to detect the presence of any leaks. Leaks are detected through the use of pressure drop off time and switch cycle measurements. The tanks are filled to a level that is slightly more than the designed takeoff level due to fuel drainage during these last minute tests. The excess will be drained after final density measurements are taken, just before launch.

During the countdown, the launch facilities will require an enormous amount of power that is essentially free of typical fluctuations. The electrical components and telemetry channels of the vehicle and launch facilities will usually be turned on nine and a half hours before the launch. There is usually a one hour long check of the radar systems and a recheck of instrument calibrations. At six hours before the launch, the liquid oxygen tanks will be filled to the 10% level (see Volume 3, section 2.4.3, Table2-5). In addition to checking for leaks, this step is used to pre-cool the fuel transfer lines for the fast flow (9500 liters/min/minute) of liquid oxygen. Testing of the Command and Communication system

will typically begin at four and a half hours before the launch. During this phase, the flight control operators have two major functions. First, they must test dynamic response capabilities (pitch, roll, & yaw) of the launch vehicle and/or payload vehicle. Secondly, the vehicle must be placed on internal power to test the performance of various systems. Once this has been done, the vehicle will be returned to internal power. No step shall be considered complete without the authorization of a status safety officer. In the closing moments of the launch, checks of telemetry and radar are continued. Pressures are monitored. Temperatures and voltages are checked. Status' most visible function will have been completed once the vehicle has been placed in orbit.

## **8.2 Sensors**

Determining the status of the various components requires an alignment of sensors. Many of the components require similar sensors. Power and temperature ranges are common requirements for all electrical and many non-electrical components. Here is a list of the most common types of sensors, and their operating ranges. From here on they will be known as temperature, pressure, current, strain sensors and will have the conditions shown in Table 8-1.

**Table 8-1: Sensor Characteristics**

<u>Type of Sensor</u>	<u>Operat. Range</u>	<u>Data Rate</u>
temperature sensor	15-20 C	0.1 Hz
Pressure Transducer	1 atm	0.1 Hz
current sensor	part specific	1 Hz
strain gauges	2000micro	0.1, 10 Hz
tank pressure sensors	tank specific	0.1, 10 HZ
feed line sensors	line specific	0.1 , 10 Hz

Excluding very specific sensors and hopefully some new technology for determining tank fill percentage, most systems would require some combination of the above sensors. Sensors will also be redundant, with a minimum of two at each critical point. The processors will then proceed with weeding out the bad data. Sensors with two values are for systems like propulsion which require closer monitoring during operation, but much less during quiescence.



The next is an example of how a specific part may be monitored. Due to the large number of components, there will not be detailed layout for each part. Instead, the status sections will deal more with conditions which must be fulfilled during each stage for the successful completion of the mission. For a breakdown of the components for each system and how they are monitored see Appendix III.

An example of sensor configuration is the sensing for the solar arrays for the precursor:

#### Temperature Sensors

- two per panel
- can be used to control the orientation of the arrays to allow optimal orientation with respect to the sun.

#### Current Sensors

- three per panel
- to monitor the output of the array, used to control orientation and to check for malfunctioning panels

#### Extension Sensors

- one for each joint which requires assembly
- to assure that the structural portions of the arrays are properly assembled

#### Motor sensor

- to assure that the tracking motor is functioning properly
- to check orientation and current

### **8.3 Importance of Documentation**

When testability is incorporated in the design, the design and its test methods should be properly documented with:

1. Schematic diagrams
2. Relevant waveform/timing diagrams
3. Wiring diagrams and wiring run lists

4. Assembly drawings and parts lists
5. Copies of manufacturer's specification sheets for all components contained on the UUT (Unit Under Test)
6. UUT functional description and theory of operation
7. Voltage/resistance chart of UUT nodes
8. List of test equipment required
9. Equipment performance specification and test procedures, include here any and all comments on failure modes. Well documented failure modes can greatly decrease the repair/debugging time.
10. Test Flow
  - Block diagram
  - Brief description of tradeoffs (reasons for decisions)
  - Faults found at each test level (including method of measurement)
11. Interface
  - Graphic description of interface
  - Schematic
  - Wiring diagram
  - Nodal cross-reference
  - Assembly diagram (include assembly drawing, bill of materials, assembly instruction, etc. )

By making this level of documentation available at all levels of manufacture, assembly, and usage, the implementation and repair times can be greatly reduced, directly translating into a savings of manpower and cost.

#### **8.4 Failure Studies**

It is the job of Status to seek out, understand, and eliminate the various causes of failure in the launch system. Although the group is most visible during the actual flight operations, the analysis of failure, its roots, and its required corrective measures actually begins in the

design and development stages. This process is vital to assuring the reliability and success of the launch project.

A failure occurs when a component does not meet its performance specifications. Failures can be grouped under two major headings: Relevant and Non-relevant. Relevant failures are primarily used to determine the mean time between failure (MTBF) of the various components. They are also a key factor in the accept/reject criteria of several acceptance tests. Most failures that occur during the reliability tests are classified as relevant failures. A test is not classified as being relevant if an externality, that is not part of the test requirement, were responsible for the failure. Some typical relevant failures include design/workmanship failures, failure due to wear, multiple failures, and failures of the built-in tests. Failures due to wear or constraints are classified as relevant only when a unit fails before its specified lifetime. In the case of multiple failures, if the failure of one part is responsible for the failure of another, the latter(dependant) failure is not classified as relevant.

Non-relevant failures also come in various forms. They can be the result of the improper installation of test units. Also, failures in the operation of testing or monitoring equipment, human error on the part of the test operators, and dependent failures all fall under this heading.

It is possible to reclassify a failure from relevant to non-relevant status. This process has several requirements. First, reclassification must be authorized by the appropriate test or reliability engineer. Second, the failure must be remedied in such a way as to meet all specifications. Finally, data must be collected and analyzed to assess the effectiveness of the corrective actions.

#### **8.4.1 Handling of Failure Data**

The successful use of failure data will depend upon the means of data display, storage, and organization. An ideal system should display the retrieved data in such a way as to allow the engineer to get a full grasp of the problem. The system should also provide such vital details as a summary of the failure and its current status. In addition, such a system can be used to forecast possible performance trends by providing failure data of similar components. With such information, the test engineer is now able to estimate the required level of necessary corrective action. Finally, the documentation of all failures in this model system should be standardized, concise, and thorough. Some of the more important pieces

of information in the documentation include the failure, the time of the failure, the location of the failure, and corrective measures.

Once the cause of a failure is understood, an appropriate course of action to correct it should be carried out by the proper personnel. This corrective action should be fully documented so that it can be correctly implemented. Also, the corrective action should be monitored to assure that it does not create more problems than it solves.

#### **8.4.2 Failure Mode Analysis**

The main function of the testing program is to provide confidence in the reliability of the various launch systems and components. However, the reliability of any structure or component is also a function of the quality of the manufacturing processes. For example, a study of the reliability growth histories reveals a very interesting fact. Most launch vehicle failures occur during the early period of the vehicle's operational life. Furthermore, manufacturing related errors have been responsible for the majority of solid rocket booster operational failures. Project Columbiad's launch vehicle, which is still in the design phase, will employ the service of several shuttle derivative SRBs. Hence, it is vital to the mission's success that the reliability of the SRB's is assured. The efforts to improve this reliability should be focused upon the the reliability program at the manufacturing and fabrication level. The quality of the product is indicative of the quality of the manufacturing techniques which produce it.

The reliability of most manufactured products could be significantly enhanced through the implementation of process related initiatives which are based upon the principles of a probabilistic design analysis. This method, developed by NASA, is used to study various failure modes through the use of mathematical models. The Failure Mode Effect and Criticality Analysis (FMECA) is an offshoot of this technique. FMECA has several functions. First, it determines all the possible ways in which a failure can occur. Second, it can identify the sources of a failure or failure system. Finally, the FMECA can assess the impact that the failure will have on other systems and the overall mission.

The application of a FMECA is dependent upon the stage of the design process. A functional FMECA (FFMECA) uses the history of similar designs to determine or guess a failure mode. The FFMECA is usually done in the incipient phases of the design process and often plays a significant role in determining reliability vs. cost, weight, and performance tradeoffs. During the production phase, a process FMECA (PFMECA) is

used to ensure that the finished hardware is free of built in failures which are indicative of a faulty process. The PFMECA analyzes the manufacturing steps and techniques, maintenance techniques, process controls, and other criteria which could affect the system's reliability. In addition to these, a FMECA can be used during the operational phase of a unit to determine risk factors and to provide a listing of the most critical items.

Anomalies in the manufacturing stage can also be eliminated with the use of statistical quality control (SQC). Under this philosophy, discrepancies in the "measurable indicators of quality" of a manufactured product are sought after and ameliorated. SQC has been shown to be very effective in assuring that the quality on the Nth unit is the same as the quality of the qualification unit. It is a cost saving technique that eliminates the need for any unnecessary testing. For example, the traditional method of testing an SRB has been to fire each unit. However, the cost of numerous tests and scheduling constraints makes this undesirable for future launch programs. Through SQC testing and reliability can be demonstrated at low cost.

#### 8.4.2.1 Ranking Failure Modes

Criticality is a measure of the relative importance, from a reliability viewpoint, of each failure mode. Criticality ranking achieves several things. First, it allows the test engineer to determine which factor should be focused upon more heavily. Second, ranking allows the production engineer to determine if changes in the manufacturing or handling process is needed. Third, it provides a data base upon which future test acceptance standards can be established. Finally, criticality ranking helps the testing and reliability engineers determine when a corrective action should be provided.

There are a number of analytical tools that are available for the calculation of a failure's criticality ranking. In general, these equations are expressed as functions of either component reliability or failure rate. One such expression is

$$CR = P_L * Q * F_r \quad (8 - 1)$$

CR is the dimensionless criticality ranking.  $P_L$  represents the damage that is likely to occur from a given failure mode.  $Q$ , which is equal to 1 minus the reliability, represents the probability of component failure.  $F_r$  represents the likelihood that a unit will fail in the indicated failure mode. Most of these values can be obtained from various sources. Tables

or estimates from past data can be used to determine reliability. Failure rate data can be obtained from sources such as MIL-HDBK-217 and industrial indices.

Off line quality control (OLQC), the most efficient type of SQC, is used to determine the relative importance of those failures that are believed to influence the quality of a unit. OLQC allows each factor to be ranked and helps focus the efforts of the unit variation reduction methods.

A definitive procedural approach for doing a FMECA does not exist. Each FMECA is fitted to meet the testing needs of the component or subsystem under study. However, there are several recommended practices:

1. The definition of the system and its requirements must be presented.
2. All assumptions that are used in the analysis should be clearly presented from the start.
3. The sequence of critical events in the analysis should be established and illustrated.
4. The requirements of the FMECA worksheet (modes of failure, their effects, failure detection methods, etc.) should be clearly presented.
5. The criticality of each failure mode should be determined.
6. Corrective actions and recommendations for uncorrectable problems should be presented.

### **8.5 Efficient Maintenance Techniques**

Launch operations can be significantly improved with the use of a revised maintenance program which is based upon standard airline operation techniques. This reliability centered procedure works on the premise that hardware failure is usually the result of cycle use, environmental exposure, or accidents. Whatever the cause, hardware is redesigned until its performance is acceptable. This technique, in conjunction with space vehicle processing activities, can be used to improve both the reliability and maintainability of hardware at reasonable costs. Furthermore, this method allows for the analysis of failure modes. With this knowledge, schedules can be modified to include provisions for expected maintenance based on a historical data base.

Another facet of efficient maintenance handling is the procurement and inventory of spare parts. Ideally, a parts procurement program would determine a need versus current inventory status of various parts. The STS incorporates such a program in the Shuttle

Inventory Management System (SIMS) which controls the acquisition of spare parts. Spares management is usually handled by the vehicle design centers. At Kennedy Space Center (KSC), the proposed launch site of Project Columbiad, the upkeep of line replaceable units (LRU) is handled in the facilities' shops and labs.

### **8.5.1 Definitions**

Spare parts refers to any material that is needed or will be needed to replace any assembly, subassembly, component, etc. during the operation, maintenance, repair, or overhaul of a piece of equipment.

The Spare Parts Selection List (SPSL) lists all spare parts and the price of their procurement or fabrication.

The Priced Spare Parts List (PSPL) is the final and approved version of the SPSL. It includes total quantities and firm unit and total prices.

Repair refers to the partial disassembly, modification, and test of various components or spares. It typically includes day-to-day maintenance that is performed at the test or launch site.

Overhaul will usually be performed at the manufacturing facilities of the vehicle. It involves the total disassembly and maintenance of components which have deteriorated or worn out.

Modification occurs when a component is physically altered in an effort to change its performance.

### **8.5.2 Program**

The development of an SPSL is the first major step of the maintenance program. This will depend upon several things. First, it is essential that all procurements are based upon the guideline of providing required support at the lowest possible inventory level. This should minimize the potential for obsolescence that may be caused by design or engineering changes. Furthermore, the driver for determining inventory levels should be the anticipated utilization. Any shipment which surpasses this level should only be made if it is clearly in the best interest of the program. Second, inventory costs must be minimized. This can be done accomplished by stocking the relatively low cost items (repair/overhaul and modification kits) instead of the relatively high cost items (assemblies and modules). In addition, the economical use of repair and modification practices can also lower the stock level. Thirdly, in some cases, existing assets can be drafted into service. Some of these include test components or equipment that may no longer be in use.

Launch maintenance efficiency could be markedly improved through the use of a "critical-to-launch" spare parts list. Such a list would detail the availability and quantities of launch critical replacement components during the 30-day period prior to a scheduled launch. In addition to this, a spare parts modification program (SPMP) could provide the flexibility that is required of a successful maintenance program. Such a program would assure the continued compatibility of the spares design program with the continually changing launch configuration.

One of the simplest means of improving operations efficiency is through the re/training of of flight personnel . This can allow tasks that are handled by professionals or engineers to be done by technicians at a lower cost.

### **8.6 Industry Streamlining Efforts**

The desire to produce reliable and cost effective launch vehicles is a growing trend in the design of current launch systems. McDonnell Douglas has created a new Streamlining program and has successfully implemented it in the design of its Payload Assist Module (PAM). This program can be used as a model and starting point for future projects.

The Streamline Program of the McDonnell Douglas Technical Services Company has been employed by the STS as a quality and productivity enhancement device which promotes drive and ingenuity in reducing launch flights. The program is built upon two major premises. First, the commitment of management is absolutely essential. Workers can not be expected to respond without committed leadership. Second, it is essential to provide a nurturing environment for the workforce. This can be done through the use of incentives and a system for recording and reporting progress to the employees and the customers. Formal meetings can be used as a forum for discussions and the reception of suggestions. Furthermore, standardization and automation can facilitate cumbersome procedures. However, the workforce must be informed that these cost cutting measures will not threaten their job security and will allow them to be used in a more productive capacity. The application of these ideas can have a substantial effect on the status group. This can be seen in the development of the PAM.

The payload assist module is designed to economically augment the payload carrying capability of the space shuttle. It can send a Delta class satellite into geosynchronous transfer orbit after being released from the shuttle at a less energetic orbit. The efficiency of the PAM concept is the result of several cost saving steps. First, in the prelaunch



checkout, circuits that are not going to be used in the mission are not tested. The usual practice has been to test all flight circuitry. Second, there are several modifications in the sequence control assembly verification. It is customary to operate all systems in such a way that the software packages are sent through all possible scenarios. This step is used to provide confidence in the flight software, even though verification was attained earlier. The PAM gets away from this software oriented approach by using a bit-by-bit read/write verification of the memory in which the flight software is present. Third, the PAM does not use the Vehicle Processing Facility (VPF) test on missions where the spacecraft and vehicle have designs that are similar to those of a previous mission. VPF testing is primarily used to detect any possible difficulties that may arise in the cargo element/shuttle interface. The PAM system has shown that elimination of VPF testing adds minimal risks to problem detecting capability while not increasing the overall flight risk.

The Space Transportation Automated Reconfiguration (STAR) system is another automated system designed to improve the efficiency of the STS. This IBM designed program is a substantial departure from the usual launch preparation methods of the shuttle program. STAR, an integrated software system, incorporates an assembly line type of process by providing quality assurance and automation. It is indicative of an autonomous system that can produce rapid response to changing needs while keeping quality up and costs low.

The major feature of the STS has been its adaptability to meet various mission requirements. However, modifications to the shuttle for each mission are costly and very slow. The reconfiguration tools that are employed depend upon enormous software challenges that are extremely labor intensive. In addition, these challenges often require efforts that stress the use of research and development for integration and verification. As a result, each mission usually requires customized systems and could not reuse previously defined data. In this era of rapidly increasing commercial flights, the challenge is to meet these mission specific requirements as efficiently as possible. The STAR system can meet these requirements.

The STAR system seeks to make launching a more standardized and less mission intensive procedure. It accomplishes this through several ways. First, it identifies and analyzes the effects of the mission drivers. These include the launch site, launch date, launch vehicle, flight trajectory, and cargo characteristics. In the end, each driver is linked with a fundamental parameter which is independent of the mission. Second, a flight independent baseline requirement is produced by an automated integration and verification function

which selects and groups key components. This allows research and development to concentrate on future needs, thus minimizing its role in each flight. Furthermore, automation and streamlining are fostered. It is even possible that these forces may promote the reuse of stored components.

The STAR system divides the flight configuration requirements into smaller units that are independent of the mission. The management and payload data are two such units. These units are then integrated into higher level units. The requirements are met by integrating only the highest level units that are needed to define its contents. The software of the STAR system is designed to strengthen the controls on configurations data, quality, and error detection capabilities. It does this through the use of data access control which only permits authorized users to access or modify any data. All of these features combine to make components that are independent of flight requirements and are reused on future flights. It is quite evident that the success of future STS flights will depend on the development of programs such as STAR and their ability to make space travel as efficient as possible. The status group must work to incorporate these new technologies within current and future programs as smoothly as possible.

### **8.6.1 Advanced Technologies**

In the future, Status' ability to monitor and maintain the health of launch vehicles will depend upon the use of advanced technologies. The use of artificial intelligence in space systems will be critical in the effort to provide high reliability at low cost. What follows is a brief description of the functions and development of several vehicle health monitoring technologies that are being studied at Kennedy Space Center, Rocketdyne, Marshall Space Flight Center, and Aerojet.

Dynamic causal models provide summaries of the cause and effect relationships between the units of every subsystem. They can be used to investigate systematic failure modes and can aid engineers to design and assess their failure detection methods. In addition, it can be used to study the interaction between subsystem components and certain monitoring equipment. A fault detection, identification, and reconfiguration (FDIR) system which provides a dynamic causal model can be fully developed within a three year period at a total cost of 750 thousand dollars.

An automated preflight checkout can eliminate unnecessary expenditures in launch operations while providing confidence in the reliability of the checkout process. This

process is usually performed by hand (Shuttle ground operations require about 6000 people). A fully automated checkout system using current technologies can be developed within two years. The required funding through a demonstration of a prototype is estimated to be about four million dollars.

An automated engine fault diagnosis and maintenance processing system can reduce the amount of time that is spent searching for the source of a failure. It can also detail the processing procedures for a corrective action. Such a system could be developed within three years at a cost (up to implementation) of 2.5 million dollars.

Automated sensor failure detection can quickly provide detection of sensor data errors. This prevents false alarms and unnecessary or improper corrective actions. Development of software for this system could be developed in 1.5 years at a cost of 0.5 million dollars.

On-board, real time hydrogen leak detectors can be used during pre-flight checkout and in flight as an indicator of a possible structural failure. Their development (through prototype testing) can be achieved at a cost of one million dollars in three years.

## REFERENCES:

- Adkins, S.P., Performance Effects of Display and Control Augmentation on a Simulated Manual Orbital Docking Task, MIT M.S. 1986.
- Admad, M. and J. Carpinelli, "A Methodology for Designing Spacecraft Onboard Computer Systems," AIAA Computers in Aerospace VII Conference, no. 89-2986, 1989.
- AGARD. *The Navstar Global Positioning System*, no.161. 1988.
- Agrawal, B. N., *Design of Geosynchronous Spacecraft*. Prentice-Hall, 1986.
- Alexander, H. L., Personal communication. Department of Aeronautics and Astronautics, MIT, March 1992.
- Allen, David H., and Haisler, Walter E. *Introduction to Aerospace Structural Analysis*. John Wiley & Sons. 1985.
- Apollo News Reference*.
- Ashby , Michael F. and David R H Jones, *Engineering Material I: An Introduction to their Properties and Applications*. Pergamon Press, 1980.
- Baccini, H., et al., "Hermes Safety and Rescue," *Space Safety and Rescue 1986-1987* (AIAA Science and Technology Series), vol. 70, 1988.
- Bachman, C.G., *Laser Radars Systems and Techniques*. Artech House, Inc., Dedham, MA, 1979.
- Battin, Richard H., *An Introduction to the Mathematics and Methods of Astrodynamics*. AIAA, 1987.
- Bar-Sever, Yoaz E., et al. "GPS-Based Orbit Determination and Point Positioning Under Selective Availability." Proceedings of 3rd International Technical Meeting of the Satellite Division of the Institute of Navigation, Colorado Springs, CO, Sept 19-21, 1990.
- Benson,C.,et al., "Moonport: A History of Apollo Launch Facilities and Operations", NASA History Series, 1978, N79-12127.
- Bielas, M.S., Dankwort, R.C., El-Wailly, T.F., and Stokes, L.F., "Test Results of Prototype Fiber Optic Gyros," Proceedings of the National Technical Meeting, Institute of Navigation, 1988.
- Blevins, Robert D. *Formulas for Natural Frequency and Mode Shape*. Krieger Publishing Company. 1984.
- Brody, A.R., "Evaluation of the '0.1% Rule' for Docking Maneuvers", *Journal of Spacecraft*, Vol. 27, No. 1, Jan.-Feb. 1990.

- Brody, A.R., "Spacecraft Flight Simulation: a Human Factors Investigation Into the Man-Machine Interface Between an Astronaut and a Spacecraft Performing Docking Maneuvers and Other Proximity Operations," MIT M.S. 1987.
- Bruhn, E.F. *Analysis and Design of Flight Vehicle Structures*. Tri-State Offset Company. 1973.
- Bryan, C.E., "Ground Processing of The McDonnell Douglas Payload Assist Module," McDonnell Douglas Astronautics Company, NASA Series N86-15196.
- Column Research Committee of Japan. *Handbook of Structural Stability*. Corona Publishing Company. Tokyo. 1971.
- Connors, Mary, et. al., *Living Aloft: Human Requirements for Extended Spaceflight*. NASA, 1985.
- Dalton, J. et al, "Data Storage Systems Technology for the Space Station Era," *Space Information Systems in the Space Station Era*, pp. 80 - 91, 1987.
- DeRuiter, J., "Fault-Tolerant Techniques for High-Speed Fiber-Optic Networks," Space Communications Technology Conference Onboard Processing and Switching, NASA publication 3132, November 1991.
- Dhargavaq, Vijay, *Digital Communications by Satellite*, Wiley 1981.
- Fleener, T. N., Product Literature and Information. Ball Aerospace Electro-Optics/Cryogenics Division, April 1992.
- French, James and Griffin, Michael, ed., *Space Vehicle Design*, 1991.
- Frisbee, R.H., *Spacecraft Propulsion Systems - What They Are and How They Work*, Astronautics Notebook, 1989
- Gollapudy, C. "Performance Analysis of MIPS Computers," AIAA Computers in Aerospace VII Conference, no. 89-2966, 1989.
- Graves, Michael. Personal communication. Department of Aeronautics and Astronautics, MIT, February, 1992.
- Graves, M.J., Discussion by Professor Michael Graves. Department of Aeronautics and Astronautics, MIT, April 1992.
- Hall, S. B., and McCann, M. E., *Radiation Environment and Shielding*, NASA N87-17780, 1987.
- Hall, S.R., Lectures by Professor Hall. Department of Aeronautics and Astronautics, MIT. Spring 1991.
- Hankey, Wilbur L., *Re-Entry Aerodynamics*, AIAA Education Series, AIAA, Washington DC, 1988.
- Harding, Richard, *Survival In Space*. Routledge Publishing, 1989.

- Hecht, H. and Hecht, M., *Reliability Prediction for Spacecraft*, RADC Report RADC-TR-85-229. Rome Air Development Center, NY: Department of Defense, December, 1985
- Hempsell, C.M., "Multi-Role Capsule System Description," *British Interplanetary Society Journal*, vol. 42, Feb 89.
- Hoerner, Sighard F., *Fluid-Dynamic Drag*, by Author, 1965.
- Jet Propulsion Laboratory, "The Deep Space Network Progress Report." April 15, 1980.
- Joels, K. M., Kennedy, G.P. and Larkin D., *The Space Shuttle's Operator's Manual*. Ballantine Books, 1982.
- Johnson, R. C., and Jasik, H., *Antenna Applications Reference Guide*. McGraw-Hill, Inc., 1987.
- Johnston, Richard S., et. al., *Biomedical Results of Apollo*. NASA, 1975.
- Johnston, Richard S. and Lawrence F. Dietlein, *Biomedical Results from Skylab*. NASA, 1977.
- Kennedy, F.G.W *Impact of Nuclear Thermal Propulsion on The NASA 90-day Study's Baseline Missions for the Space Exploration Initiative*, MIT M.S. Thesis © 1991.
- Kourepennis, Anthony. Discussion on solid-state accelerometers. C.S. Draper Laboratory, April 1992.
- Kong, J. A., *Electromagnetic Wave Theory*. John Wiley & Sons, Inc., 1990.
- Larson, Wiley J. and Wertz, James R., ed., *Space Mission Analysis and Design*. Kluwer Academic Publishers, 1991.
- Lide, D. R., editor-in-chief, *CRC Handbook of Chemistry and Physics*. CRC Press, Inc., 1990.
- Lim, James, *Two Dimensional Signal and Image Processing*, Prentice Hall 1990.
- Lin, Shin, *Fundamentals Error Control Coding*, Wiley 1978.
- Lo, Y. T., and Lee, S. W., editors, *Antenna Handbook*. Van Nostrand Reinhold Company, 1988.
- Lofland, W.W., "Orbiter Emergency Crew Escape System," NASA Document N80-23499, 1980.
- Man-System Integration Standards (NASA-STD-3000)*, Volume I. NASA, 1987.
- Maral, G. and Bosquet, M, *Satellite Communications Systems*. John Wiley & Sons, 1986.
- Martin, Graham J., "Ring Laser Gyro Principles and Techniques," Analysis, Design and Synthesis Methods for Guidance and Control Systems AGARDograph no. 314, June 1990.

McCormick, Barnes W., *Aerodynamics, Aeronautics, and Flight Mechanics*, John Wiley & Sons, Inc., 1979.

McKay, Walter, et al., *Principles of Flight Guidance*. Massachusetts Institute of Technology Department of Aeronautics and Astronautics. date unknown.

McNeil-Shnedler Coporation. *MSC/pal 2 User Manual*.

MIL-HDBK-217

MIL-HDBK-764

MIL-STD-1538

MIL-STD-2074

MIL-STD-2155

NASA, *Apollo Guidance System Operation Plan AS-206*, volume1. MIT Instrumentation Laboratory., January 1967.

NASA Space Vehicle Design Criteria:Structural Design Series,1970 . NASA SP 8043-8045.

NASA Space Vehicle Design Criteria: Pressurization Systems for Liquid Rockets, 1975. NASA SP 8112

NASA Space Vehicle Design Criteria: Liquid Rocket Lines, Bellows Flexible Hoses, and Filters, 1977. NASA SP 8123

Newman, A., Memo on National Launch System Reliability. Department of Aeronautics and Astronautics, MIT, 9 Mar 92.

Nicogossian, Arnauld E., *Space Physiology and Medicine*. NASA, 1985.

O'Connor, B., "Safety and Rescue During STS Operations," Proceedings of the Workshop on Crew Safety and Rescue in Space, ESA SP-300, Aug 89.

Oppenheim, Alan V. and Ronald Schafferr, *Discrete Time Signal Processing*, Prentice Hall 1989.

Pavlat, G.A. "Inertial Grade Fiber Gyros," Proceedings of the National Technical Meeting, Institute of Navigation, 1988.

Pearson, Albin O. and David C. Grana, *Preliminary Results from an Operational 90-Day Manned Test of a Regenerative Life Support System*. NASA Langley, 1971.

Pitts, John A., *The Human Factor*. NASA, 1985.

"Research on Man-Machine Relationships In Pre-launch Checkout of Advanced Space Vehicles". NASA: Quarterly Progress Report Number 1, 1965. N65-12729.

- Regan, Frank J., *Re-Entry Vehicle Dynamics*, AIAA Education Series, AIAA, Washington DC, 1984.
- Robbins, H., *An Analytic Study of The Impulsive Approximation*, AIAA Journal, August 1966.
- Rowley, V. M., Effects of Stereovision and Graphics Overlay on a Teleoperator Docking Task, MIT M.S. Thesis 1989.
- Rudge, A. W., Milne, L., Olver, A. D., and Knight, P., editors, *The Handbook of Antenna Design*. Peter Peregrinus, Ltd., 1982.
- SAE Aerospace Resource Document 50013, "SRB Reliability Guidebook", July 2, 1991.
- Schelkunoff, S. A., *Antennas*. John Wiley & Sons, Inc., 1952.
- Shen, L. C. and Kong, J. A., *Applied Electromagnetism*. PWS Engineering, 1987.
- Shewfelt, K.M., Personal communication and literature provided by Mr. Kurt M. Shewfelt. AiResearch Los Angeles Division, Allied-Signal Aerospace Company, April 1992.
- Shipman, H. L., *Humans In Space: 21st Century Frontiers*. Plenum Press, 1989.
- Stahle, C.V., "Analysis and Testing of Large Space Structures", Space Systems Division, General Electric Company, N83-18825
- Stette, Gunnar, "Broader Communication Bands," Bridging the Communication Gap, AGARD proceeding no. 487, September 1990.
- Strategic Avionics Technology Working Group. Vehicle Health Management Panel. June 11, 1991.
- Stutzman, W. L. and Thiele, G. A., *Antenna Theory and Design*. John Wiley & Sons, 1981.
- Sutton, G.P. *Rocket Propulsion Elements: An Introduction To the Engineering of Rockets*, John Wiley and Sons, New York ©1989
- Thornton, Brasseaux, Whitmore, *Flight Test of an Improved Solid Waste Collection System*, SAE paper presented at ICES 1991.
- Transition to the Space Shuttle Operations Era* by The Space Shuttle Engineering Staff, Integrated Operations Department. William F. Edson, Jr., Director
- University of Minnesota, Final-Report: Biconic Cargo Return Vehicle with an Advanced Recovery System, University of Minnesota, 1990.
- Verghese, G., Lecture by Professor George Verghese. Department of Electrical Engineering and Computer Science, MIT, April 1992.
- Van Wylen, G.J. and R.E. Sonntag, *Fundamentals of Classical Thermodynamics*, 3rd edition. John Wiley and Sons, 1985.



- Weiss, Personal Communication. Department of Aeronautics and Astronautics, MIT, March and April, 1992.
- Wertz, James R., *Spacecraft Attitude Determination and Control*. D. Reidel Publishing Company, 1985.
- Whitehurst, T.N., Jr., "Space Shuttle Orbiter Ejection Seat Survey," 24th Annual SAFE Symposium, 1986.
- Wiesel, William, *Spaceflight Dynamics*. McGraw-Hill Book Company, 1989.
- Wine, J. and T. Rasset, "An All GaAs High Performance Computer," AIAA Computers in Aerospace VII Conference, no. 89-2965, 1989.
- Wolfram, Stephen. *Mathematica: A System for Doing Mathematics by Computer*. Addison-Wesley. 1991.

## APPENDIX I Spacecraft Propulsion Theory

### ABBREVIATIONS AND SYMBOLS

Symbol	Quantity	Units
$F_T$	thrust force	[N]
$P$	power	[W]
$\dot{m}$	mass flow	[kg / s]
$M_s$	Spacecraft structural mass	[kg]
$M_p$	Propellant mass	[kg]
$M_L$	Payload Mass	[kg]
$M_o$	Total initial mass of spacecraft before burn ( $M_o = M_s + M_p + M_L$ )	[kg]
$M_f$	Mass of spacecraft after burn ( $M_f = M_o - M_p$ )	[kg]
$n_i$	molar fraction of species i	[moles]
$M_m$	molecular mass	[kg / kmol]
$p_c$	combustion chamber pressure	[Pa]
$p_e$	exhaust gas exit pressure	[Pa]
$p_a$	Ambient pressure	[Pa]
$T_c$	combustion chamber temperature	[K]
$u_e$	exhaust gas exit velocity	[m / s]
$c$	effective exhaust velocity	[m / s]
$c^*$	characteristic velocity	[m / s]
$A_e$	nozzle exit area	[m <sup>2</sup> ]
$A_t$	nozzle throat area	[m <sup>2</sup> ]
$I_{sp}$	specific impulse	[s]
$C_F$	thrust coefficient	dimensionless
$\gamma$	specific heat ratio	dimensionless

### CONSTANTS

$R$	Universal gas constant	8.314 kJ / kmol / K
$R_s$	Specific gas constant	$R_s = R / M_m$

### Definitions And Fundamentals

Spacecraft propulsion is accomplished by rocket engines, which produce a thrust force  $F_T$  by the ejection of a stored propellant at some mass flow rate  $\dot{m}$ . The fundamental equation for rocket thrust is given by equation I-1.

$$F_T = \dot{m}c \quad (I-1)$$

The quantity  $c$  is the effective exhaust velocity of the given by equation I-2

$$c = u_e + \frac{A_e}{\dot{m}} (p_e - p_a) \quad (\text{I-2})$$

where  $u_e$  is the actual exit velocity of the combustion gases,  $A_e$  is the nozzle exit area,  $p_e$  is the exit pressure of the exhaust products and  $p_a$  is the ambient pressure. The value of  $u_e$  may be predicted from the properties of the combustion products and the combustion and exit pressures as in equation I-3

$$u_e = \sqrt{\frac{2\gamma}{(\gamma - 1)} R_s T_c \left( 1 - \left[ \frac{p_e}{p_c} \right]^{\frac{\gamma - 1}{\gamma}} \right)} \quad (\text{I-3})$$

Here  $\gamma$  is the average specific heat ratio of the combustion products,  $R_s$  is their specific gas constant, and  $T_c$  and  $p_c$  represent the combustion temperature and pressure, respectively.

Equation I-3 shows that the thrust produced by a rocket engine is not only dependent upon  $A_e$  and the difference between the exit and ambient pressures, as is implied by the general expression for  $c$  in equation I-2. The chemical composition of the propellants, along with the pressure and temperature of the propellants during combustion, determine the values of the exhaust mass flow and exit velocity. All other things equal, a rocket will achieve maximum thrust when the pressure of the exhaust gases exiting the nozzle equals the ambient pressure.

The primary measure of propulsion system performance capability is the velocity change,  $\Delta V$ , that it can produce. The relationship is quantified by the *rocket equation*, which relates the mass of the initial mass  $M_o$  of the spacecraft to its final mass  $M_f$  after the velocity increment is given in equation I-4.

$$\Delta V = c \ln \left( \frac{M_o}{M_o - M_p} \right) = c \ln \left( \frac{M_o}{M_f} \right) \quad (\text{I-4})$$

where  $M_p$  is the mass of the propellant expended during the burn. This equation assumes zero losses due to aerodynamic drag or gravity, and is thus a limiting ideal case.

The impulse  $I$  is the total change in momentum of the expelled propellant and is given by equation I-5.

$$I = \int_0^{t_b} F_T dt = \int_0^{t_b} \dot{m} c dt = M_p c = M_o (1 - e^{\Delta v/c}) c \quad (I-5)$$

The upper limit of the integral,  $t_b$ , is the rocket motor burn time. The efficiency of a rocket engine is generally assessed with a quantity known as the specific impulse,  $I_{sp}$ , formally defined as the engine thrust divided by the propellant mass flow rate. See equation I-6.

$$I_{sp} = F_T / \dot{m} g = I / M_p g = c / g \quad (I-6)$$

Thrust and more particularly specific impulse are the two basic parameters of rocket engine design. Specific impulse is a function primarily of the square root of the ratio of the expelled propellant's combustion temperature,  $T_c$  and average molecular mass  $M_m$ . The governing equation for the theoretical prediction of the specific impulse is given by equation I-7.

$$I_{sp} = \frac{1}{g} \sqrt{\frac{2\gamma}{\gamma-1} \frac{R T_c}{M_m} \left(1 - \left[\frac{p_e}{p_c}\right]^{\frac{\gamma-1}{\gamma}}\right)} \quad (I-7)$$

where  $R$  is the universal gas constant, and all the other variables are defined as before. For the case of ideal expansion into a vacuum ( $p_e = p_a = 0$ ), the expression for specific impulse simplifies to equation I-8

$$I_{sp} = \frac{1}{g} \sqrt{\frac{2\gamma}{\gamma-1} \frac{R T_c}{M_m}} \quad (I-8)$$

Specific impulse may be thought of as the amount of impulse delivered per unit mass of propellant, or "kick" per kilogram. A high specific impulse is therefore a figure of merit for any propulsion system, and is universally accepted as a baseline for the estimation of system performance. The benefits derived from a high  $I_{sp}$  drive the designer to higher combustion temperatures and lower molecular weights.

The characteristic velocity  $c^*$  is a measure of the energy available from the combustion process and is given by equation I-9.

$$c^* = \frac{\dot{m}}{p_c A_t} = \left[ \frac{1}{\gamma} \left( \frac{\gamma+1}{2} \right)^{\frac{\gamma+1}{2(\gamma-1)}} \right] \sqrt{\gamma R_s T_c} \quad (I-9)$$

The characteristic velocity is a measure of the performance in rocket combustion chamber or how efficiently the chemical propellants are converted to total pressure from the hot gases. It is mostly dependent upon the chemical properties of the propellant.

Another important parameter in the evaluation of rocket performance is the dimensionless thrust coefficient,  $C_F$ , given by equation I-10.

$$C_F = \frac{F}{p_c A_t} = \sqrt{\frac{2\gamma^2}{(\gamma-1)} \left(\frac{\gamma+1}{2}\right)^{\frac{\gamma+1}{\gamma-1}} \left(1 - \left[\frac{p_e}{p_c}\right]^{\frac{\gamma-1}{\gamma}}\right)} + \frac{A_e}{A_t} \left(\frac{p_e}{p_c} - \frac{p_a}{p_c}\right) \quad (\text{I-10})$$

The thrust coefficient is a measure of the efficiency of converting the energy to exhaust velocity and therefore characterizes nozzle performance. It is a measure of how efficiently the total pressure energy from the hot combustion gas is accelerated to maximum exhaust velocity which results in the highest values of thrust and  $I_{sp}$  for a given set of operating conditions in the combustion chamber. Like  $I_{sp}$ , it reaches a theoretical maximum for a complete expansion of the exhaust products into a vacuum.

## APPENDIX II Communications Theory and Background

A brief review of the physics behind antenna systems is given here.

### Basic Electromagnetics

Maxwell's equations for a generalized medium are

$$\nabla \times E = i\omega\mu H - M \quad (\text{II-1})$$

$$\nabla \times H = -i\omega\epsilon E + J \quad (\text{II-2})$$

$$\nabla \cdot B = \rho_m \quad (\text{II-3})$$

$$\nabla \cdot D = \rho \quad (\text{II-4})$$

with an assumed harmonic time dependence of  $e^{j\omega t}$  for the field vectors;

$E$  = electric field vector [V/m]

$H$  = magnetic field vector [A/m]

$B$  = magnetic flux density [T]

$D$  = electric flux density [C/m<sup>2</sup>]

$\epsilon$  = electric permittivity tensor [F/m]

$\mu$  = magnetic permeability tensor [H/m]

$M$  = magnetic current density [V/m<sup>2</sup>]

$J$  = electric current density [V/m<sup>2</sup>]

$\rho_m$  = magnetic charge density [Wb/m<sup>3</sup>]

$\rho$  = electric charge density [C/m<sup>3</sup>]

$\omega$  = angular frequency [rad/s]

$E$ ,  $H$ ,  $B$ ,  $D$ , and  $J$  are related by the constitutive relations

$$D = \epsilon E \quad (\text{II-5})$$

$$B = \mu \cdot H \quad (\text{II-6})$$

$$J = \sigma \cdot E \quad (\text{II-7})$$

where  $\sigma$  is the conductivity tensor [S/m<sup>2</sup>].

$\omega$ , the angular frequency, is  $2\pi f$ , where  $f$  is the frequency in Hz [1/s]. The permittivity, permeability, and conductivity tensors are properties of a given medium which describe an

electromagnetic wave's propagation in that medium. In general, the permittivity and permeability are complex, while the conductivity is usually real.  $M$  is a fictitious magnetic current which is used to develop duals of electrodynamic systems, thus simplifying the mathematics and allowing the use of equivalent sources which generate the same waves. As an example, by substituting  $E \Rightarrow H$ ,  $H \Rightarrow -E$ ,  $\mu \Rightarrow \epsilon$ ,  $\epsilon \Rightarrow \mu$ ,  $J \Rightarrow M$ , and  $M \Rightarrow J$ , (II-1)  $\rightarrow$  (II-2) and (II-2)  $\rightarrow$  (II-1).

In addition, there are continuity equations.

$$\nabla \cdot J - i\omega\rho = 0 \quad (\text{II-8})$$

$$\nabla \cdot M - i\omega\rho_m = 0 \quad (\text{II-9})$$

These are statements of charge conservation.

The wave equation is obtained by crossing  $\nabla$  with (II-1) and substituting in (II-2), then using a vector identity to simplify the equations:

$$\nabla^2 E = \omega^2 \mu \epsilon E - i\omega \mu J + \nabla \times M \quad (\text{II-10})$$

A similar equation can be derived for  $H$ . In a source-free, isotropic, homogeneous, non-dispersive, linear medium such as free space, (II-10) reduces to

$$\nabla^2 E + \omega \mu \epsilon E = 0 \quad (\text{II-11})$$

Similarly,

$$\nabla^2 H + \omega \mu \epsilon H = 0 \quad (\text{II-12})$$

$k$ , the wavenumber describing the wave's propagation, is defined as

$$k^2 = \omega^2 \mu \epsilon \quad (\text{II-13})$$

The  $k$ -vector is defined by

$$k = \hat{x}k_x + \hat{y}k_y + \hat{z}k_z \quad (\text{II-14})$$

in Cartesian coordinates. The velocity of the wave relates to  $k$  through

$$v = \omega/k \quad (\text{II-15})$$

while the frequency of the wave is given by

$$f = v/\lambda \quad (\text{II-16})$$

where  $\lambda$  is the wavelength of the wave.

The power transmitted by a wave is given by the Poynting vector

$$S = E \times H \quad (\text{II-17})$$

The time average power transmitted by the wave is then

$$\langle S \rangle = \frac{1}{2} \text{Re} \{ E \times H^* \} \quad (\text{II-18})$$

where  $H^*$  is the complex conjugate of  $H$ .

### Reciprocity

Let  $J_a$  and  $M_a$  describe a source in the fields  $E_b$  and  $H_b$  generated by source  $b$  which is characterized by  $J_b$  and  $M_b$ . Source  $a$ 's interaction with the fields of  $b$  is described by the reaction

$$\langle a, b \rangle = \iiint dV (J_a \cdot E_b - M_a \cdot H_b) \quad (\text{II-19})$$

$\langle a, b \rangle$  describes how source  $a$  is affected by a drive at source  $b$  and has units of power. A reciprocal system has

$$\langle a, b \rangle = \langle b, a \rangle \quad (\text{II-20})$$



The difference can be written as

$$\langle a, b \rangle - \langle b, a \rangle = \iiint_V dV (J_a \cdot E_b - M_a \cdot H_b - J_b \cdot E_a + M_b \cdot H_a)$$

which can be rewritten as

$$\langle a, b \rangle - \langle b, a \rangle = i\omega \iiint_V dV (E_b \cdot D_a - E_a \cdot D_b + H_a \cdot B_b - H_b \cdot B_a) \quad (\text{II-21})$$

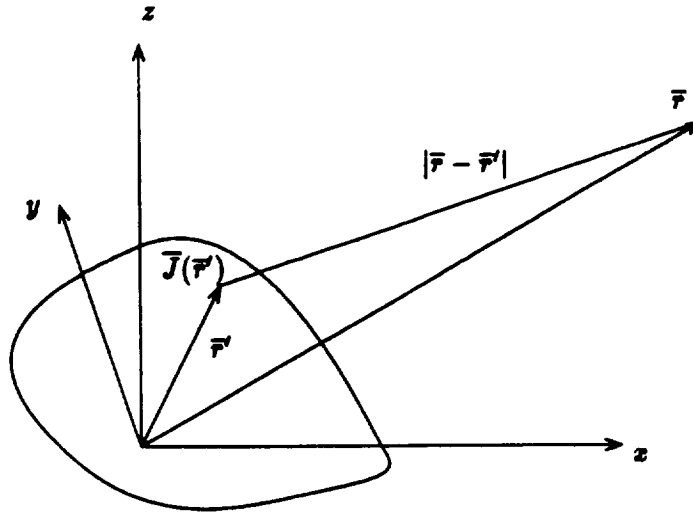
For  $\langle a, b \rangle = \langle b, a \rangle$ ,  $E_b \cdot D_a = E_a \cdot D_b$  and  $H_b \cdot B_a = H_a \cdot B_b$ . Physically, this means that one can, say drive source a to generate a field  $E_a$  which produces a field  $E_b$  at b as its reaction. Suppose that a was then shut off. If b were driven to generate the field  $E_b$ , the field describing the reaction at a would be  $E_a$ . If a and b were antennae, reciprocity means that the radiation pattern for an antenna which is transmitting is the same as the radiation pattern for that antenna when it is receiving. For more details and examples, see [Kong, 1990].

### Radiation source

This is a summary of the detailed treatment given in [Kong, 1990]. A source  $J(r)$  produces a field

$$E(r) = i\omega\mu \iiint_V dV G(r, r') \cdot J(r') \quad (\text{II-22})$$

where  $r$  is the position vector to the observer,  $r'$  is the position vector to the source, and  $G(r, r')$  is a dyadic Green's function describing  $E$  from the given  $J$ . (See Figure II-1)



Observation point  $\bar{r}$  is outside the source region

**Figure II-1**  
**Parameters of Source Radiation Problem**  
**[Kong, 1990]**

$\mathbf{G}(r, r')$  can be written in terms of the scalar Green's function  $g(r, r')$ :

$$\mathbf{G}(r, r') = \left[ \mathbf{I} + \frac{1}{k^2} \nabla \nabla \right] g(r, r') \quad (\text{II-23})$$

where  $\nabla \nabla g = \nabla \times \nabla \times (\mathbf{I} g) + \mathbf{I} \nabla^2 g$ . The scalar Green's function is

$$g(r, r') = \frac{e^{ik|r-r'|}}{4\pi|r-r'|} \quad (\text{II-24})$$

so that

$$\mathbf{E}(r) = i\omega\mu \left[ \mathbf{I} + \frac{1}{k^2} \nabla \nabla \right] \cdot \int \int \int_{V'} dV' \frac{e^{ik|r-r'|}}{4\pi|r-r'|} \mathbf{J}(r') \quad (\text{II-25})$$

If  $kr \gg 1$  and  $|r-r'| \approx r - \hat{r} \cdot r'$ , which is the case where the observer is far from the source (see Figure II-2), then

$$E(r) \approx i\omega\mu \left[ \mathbf{I} + \frac{1}{k^2} \nabla \nabla \right] \frac{e^{ikr}}{4\pi r} \iiint dV' J(r') e^{-ik \cdot r'} \quad (\text{II-26})$$

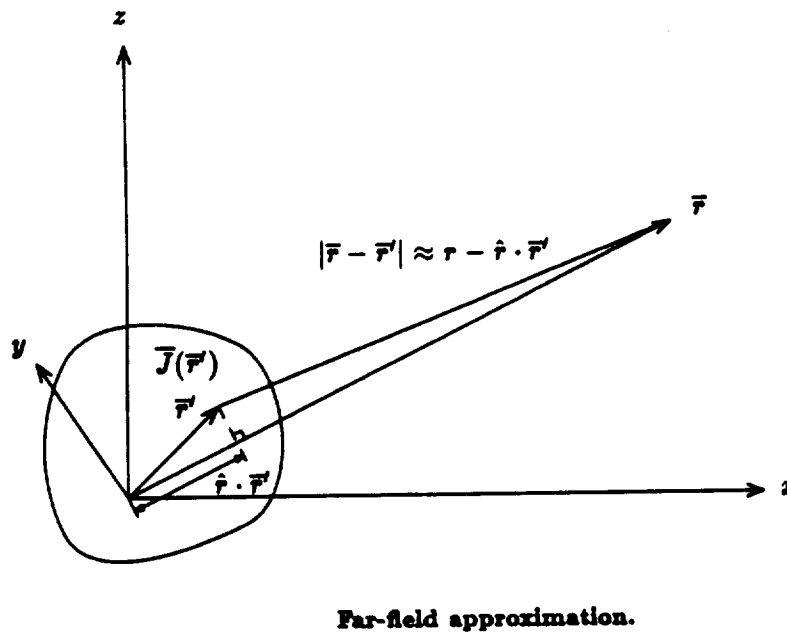


**Figure II-2**  
**Parameters for Radiating Source in the Far Field**  
**[Kong, 1990]**

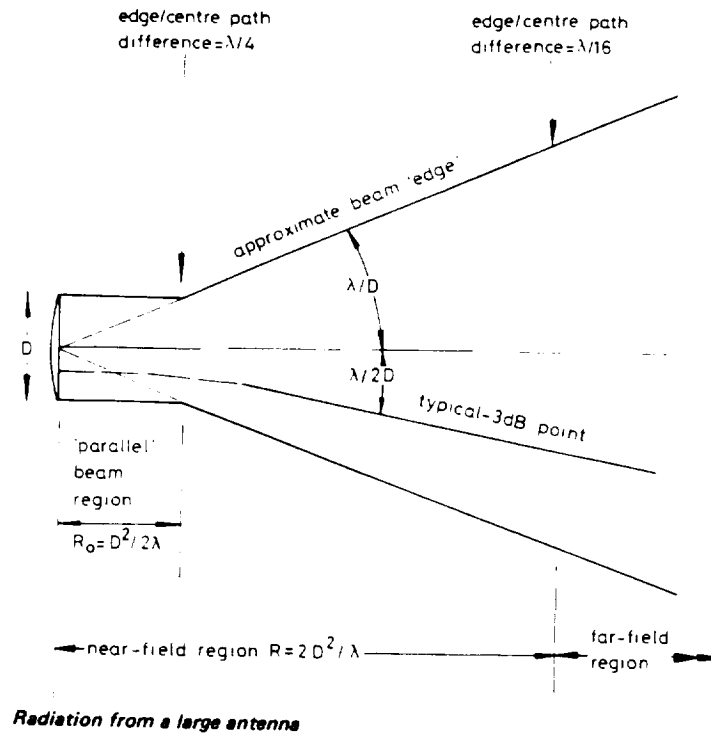


**Figure II-3**  
**Near- and far-field Regions of a Large ( $D \gg \lambda$ ) Antenna**  
**[Johnson and Jasik, 1987]**

The vector current moment  $f(\theta, \phi)$  can be defined in spherical coordinates:

$$f(\theta, \phi) = \iiint dV' J(r') e^{ik \cdot r} \quad (\text{II-27})$$

In practice, simpler expressions can be used. For example, a Hertzian dipole of length  $l$  with  $J(r') = \hat{z}Il \delta(r')$  and moment  $p = ql$ , oscillating at angular frequency  $\omega$  has  $Il = -i\omega p$ . In this case,

$$f(\theta, \phi) = \hat{z}Il = (\hat{r}\cos\theta - \hat{\theta}\sin\theta)Il$$

so  $f_\theta = -Il \sin\theta$ . The far field is

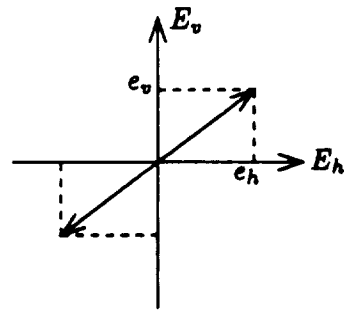
$$E(r) = \hat{\theta}i\omega\mu \frac{e^{ikr}}{4\pi r} f_\theta = -\hat{\theta}i\omega\mu Il \frac{e^{ikr}}{4\pi r} \sin\theta$$

### Wave polarization

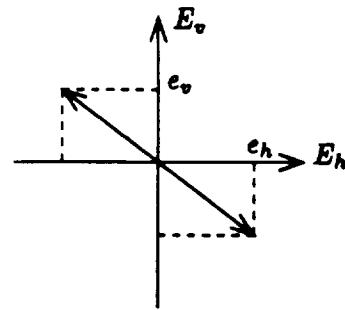
The polarization of a wave is determined by the motion of its tip, at a fixed point in space, as time passes. The wave propagates in the direction of the  $k$ -vector. The  $E$  field can be written as  $E = E_h + E_v$  where  $E_h$  is the component defined to be horizontal with respect to  $k$ , and  $E_v$  is the vertical component;  $k$ ,  $\hat{h}$ , and  $\hat{v}$  are mutually perpendicular.

$$E(t) = \hat{h}E_h + \hat{v}E_v = \hat{h}e_h \cos(\omega t - \psi_h) + \hat{v}e_v \cos(\omega t - \psi_v) \quad (\text{II-28})$$

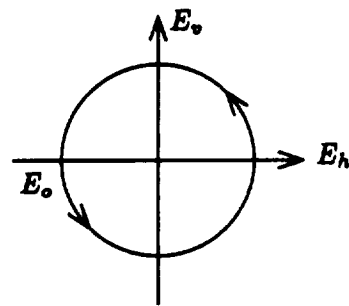
where  $e_h$  and  $e_v$  are the positive amplitudes and  $\psi_h$  and  $\psi_v$  are the phases of  $E_h$  and  $E_v$ , respectively. By changing the values of  $\omega t$ , the movement of the tip of  $E(t)$  may be traced. Figure II-4 illustrates the possible linear and elliptic polarizations, while Figure II-5 shows how the wave appears as it propagates in the  $-\hat{z}$ -direction.



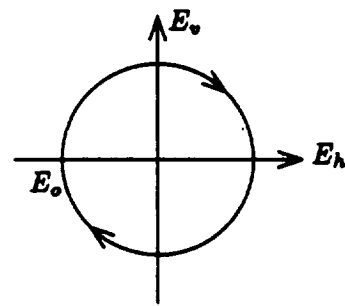
a. Linear Polarization



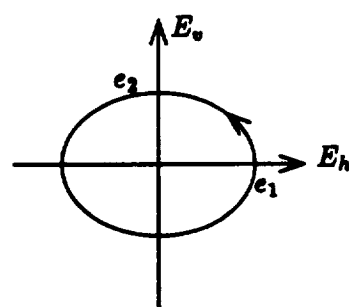
b. Linear Polarization



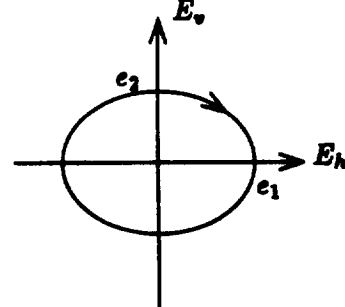
c. Right-hand  
circular polarization



d. Left-hand  
circular polarization



e. Right-hand  
elliptical polarization



f. Left-hand  
elliptical polarization

**Figure II-4**  
**Wave Polarizations; Direction of Propagation is out of the page**  
**[Kong, 1990]**

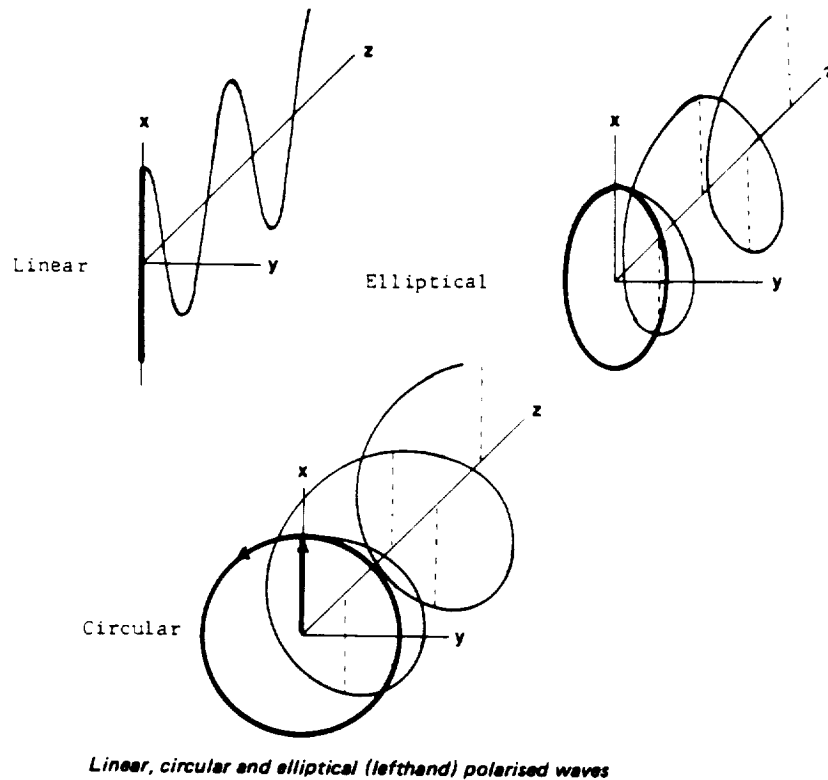


**Figure II-5**  
**How a Wave of Given Polarization Appears as it Propagates Along**  
**the Z-axis [Rudge, et al, 1982, volume I]**

### Antenna theory

An isotropic radiator transmits power equally in all directions; by reciprocity, it also receives equally well from any direction. In practice, antennas are not isotropic. Instead, the strength of the transmission depends on the direction of the receiver. One measure of an antenna's performance is its gain.

$$G = \frac{\eta 4\pi f^2 A_p}{c^2} = \frac{4\pi A_e}{\lambda^2} \quad (\text{II-29})$$

where  $\eta$  is the antenna efficiency,  $A_p$  is the physical aperture area of the antenna,  $f$  is the transmission frequency, and  $c$  is the speed of light. The antenna efficiency is a measure of how well the antenna uses its physical area. 0.5 is a good value for a first-cut estimate of gain; the efficiency typically ranges from 0.5 to 0.7 for a parabolic reflector.  $A_e$ , the effective aperture area, is the product of  $A_p$  and  $\eta$ . The gain is proportional to the ratio of the maximum radiation intensity and the total power input to the antenna.

The beamwidth is the angle between half-power points relative to the power on the boresight axis. It is a critical parameter in antenna pointing accuracy.

If a transmitter transmits  $P_t$  W, then the power flux density is

$$F = \frac{P_t G_t}{4\pi R^2} \text{ W/m}^2 \quad (\text{II-30})$$

where  $R$  is the distance from the source in meters. The effective isotropic radiated power (EIRP) is

$$\text{EIRP} = G_t P_t \quad (\text{II-31})$$

The EIRP is the power which an isotropic radiator would need to transmit if it had the same flux density as an antenna with gain  $G_t$ . A receiving antenna intercepts the power flux from the transmitter. The amount of flux intercepted is

$$P_r = P_t G_t G_r \left( \frac{\lambda}{4\pi R} \right)^2 \text{ W} \quad (\text{II-32})$$

This result is the Communication Equation. The  $\left( \frac{\lambda}{4\pi R} \right)^2$  factor is the path loss  $L_p$ ; it is a measure of how the power flux decreases as the wave propagates away from the transmitter.

### Noise considerations.

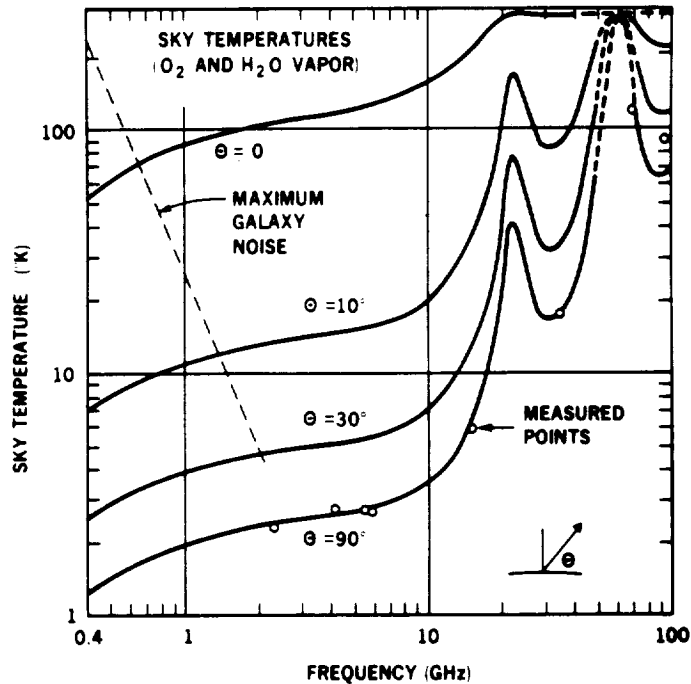
So far, ideal transmission and reception, in a noise-free environment, has been assumed. For radio-frequency (RF) communications, thermal noise must not be ignored.

$$P_N = k T_s B \quad (\text{II-33})$$

where  $P_N$  is the thermal noise power,  $k$  is the Boltzmann constant ( $1.35\text{E-}23 \text{ W*s/K}$ ),  $T_s$  is the equivalent system noise temperature, and  $B$  is the bandwidth of the signal.  $T_s$  includes not only the device temperature, but also accounts for noise from other thermal sources, such as blackbody radiation from the sun, earth, and the sky, and from nonthermal noise sources as well. A figure of  $T_{\text{sdB}} = 31 \text{ dB}$  is given in [Wertz and Larson, 1991]; this translates to a noise power of  $1.7\text{E-}20 * B \text{ W}$ . Figure II-6 plots sky temperature, while Figures II-7, II-

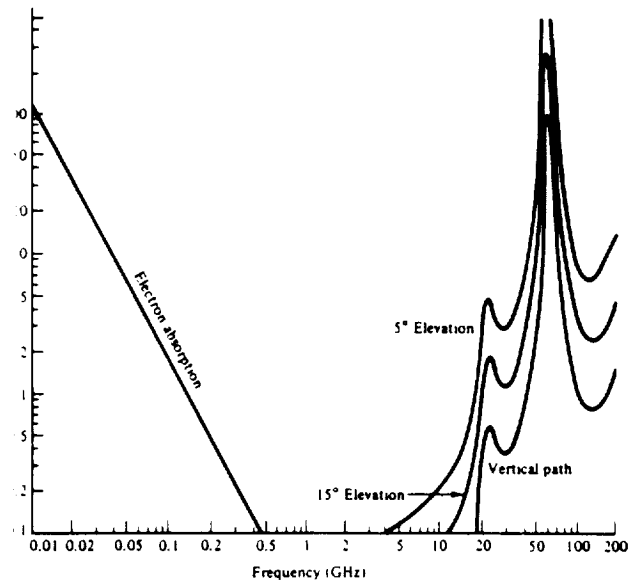


temperature, while Figures II-7, II-8, and II-9 plot atmospheric absorption as a function of frequency.



*Maximum galaxy noise and calculated atmospheric sky noise for various elevation angles as a function of signal frequency. Measured points agree with calculated values*

**Figure II-6**  
**Sky Temperature vs. Frequency (from [Rudge, et al, 1982])**



Absorption in the atmosphere caused by electrons, molecular oxygen, and Jensen's water vapor (Ref. 11).

**Figure II-7**  
**Atmospheric Absorption vs. Frequency [Agrawal, 1986]**

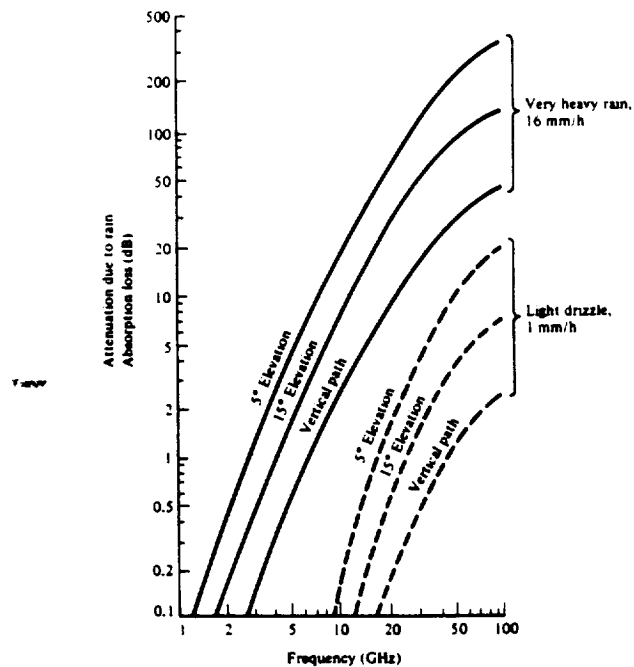


**Figure II-8**  
**Absorptive Losses due to Rain vs. Frequency [Agrawal, 1986]**

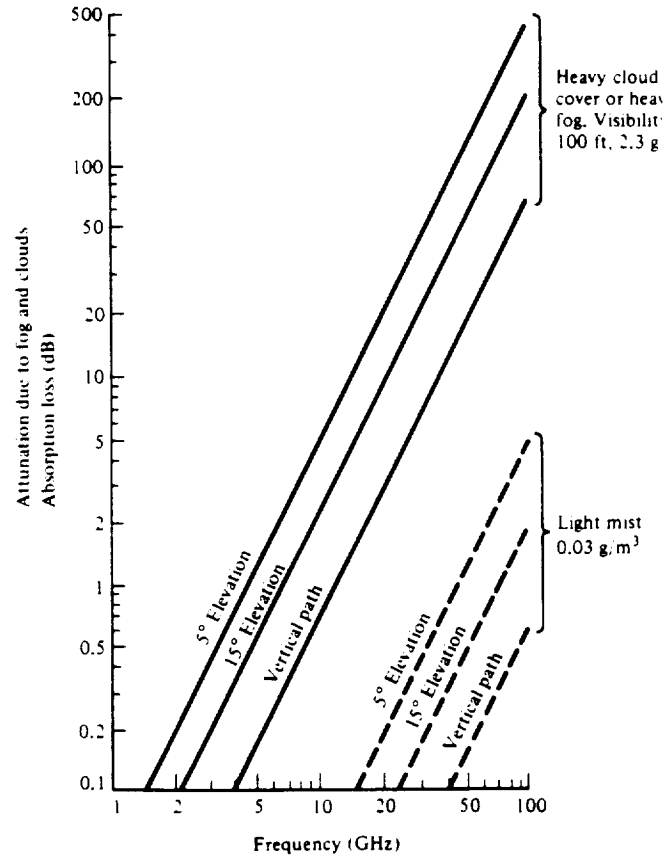


**Figure II-9**

**Absorptive Losses due to Fog and Clouds vs. Frequency [Agrawal, 1986].**

By taking the ratio of the received power and the thermal noise power, the signal-to-noise ratio (SNR) can be found:

$$\text{SNR} = \left(\frac{1}{4\pi}\right)^2 \left(\frac{1}{k}\right) \left(\frac{\lambda^2}{BR^2}\right) G_t P_t \left(\frac{G_r}{T_s}\right) \quad (\text{II-34})$$

The SNR affects the error-free channel capacity of a communications link, C

$$C = B \log_2(1 + \text{SNR}) \quad (\text{II-35})$$

where B is the link bandwidth in Hz.

### Random surface error losses

A real antenna's surface will not be perfect; the surface roughness and irregularity leads to the gain/loss factor,  $g$ .

$$g = e^{\left( \frac{-4\pi^2 E_{rms}^2}{1 + (D/4F)^2} \right)} \quad (\text{II-36})$$

where  $E_{rms}^2$  is the average surface error, in fractions of the wavelength,  $D$  is the antenna diameter, and  $F$  is the antenna's focal length. Figure control, or the maintenance of an accurate surface, is very important for phased-array and parabolic antennae.

### Polarization losses

Antennae radiate either linearly polarized or circularly polarized waves. A linear polarization may be either vertical or horizontal; a circular polarization may be left- or right-handed. If the polarizations do not match between the receiving and transmitting antennas, the receiving antenna will receive only a fraction of the power that the transmitter sends out. Let  $E_r(t)$  describe the polarization of the receiving antenna and  $E_t(t)$  describe the polarization of the transmitting antenna. By defining the unit complex polarization vectors

$$u_r = \frac{E_r(t)}{|E_r(t)|} \quad (\text{II-37})$$

$$u_t = \frac{E_t(t)}{|E_t(t)|} \quad (\text{II-38})$$

the polarization efficiency,  $p$ , can be defined as

$$p = |u_t^* \cdot u_r| \quad (\text{II-39})$$

$$p_{dB} = 10 \log_{10} p \quad (\text{II-40})$$

$p$  is a measure of how well the receiving antenna picks up the incoming signal from the transmitting antenna. If  $u_t^* \perp u_r$ , then theoretically no signal will be received, whereas if  $u_t^* // u_r$ ,  $p = 1$ .

Another type of loss affecting linearly polarized waves is the loss due to Faraday rotation. Wave propagation along  $\hat{Z}$  in a gyroscopic medium is described by

$$\begin{pmatrix} u^2 - v\kappa & i v \kappa_g \\ -i v \kappa_g & u^2 - v\kappa \end{pmatrix} \begin{pmatrix} D_1 \\ D_2 \end{pmatrix} = 0 \quad (\text{II-41})$$

where

$$E = \gamma D \quad (\text{II-42})$$

$$H = \kappa B \quad (\text{II-43})$$

$$\kappa = \begin{bmatrix} \kappa & i\kappa_g & 0 \\ -i\kappa_g & \kappa & 0 \\ 0 & 0 & \kappa_z \end{bmatrix} \quad (\text{II-44})$$

The wave decomposes into two opposite-handed circularly polarized waves propagating at different velocities; the phases of the waves once they have travelled a distance  $Z_0$  through the gyrotropic medium are

$$\phi_1 = \frac{\omega Z_0}{\sqrt{v(\kappa - \kappa_g)}} \quad (\text{II-45})$$

$$\phi_2 = \frac{\omega Z_0}{\sqrt{v(\kappa + \kappa_g)}} \quad (\text{II-46})$$

An observer watching the wave approaching will see a rotation of  $(\phi_2 - \phi_1)/2$  [Kong, 1990]. A linearly polarized wave will therefore have a different orientation after passing through the medium, whereas a circularly polarized wave is unaffected.

#### Brief overview of transmission line theory

A z-directed coaxial transmission line is characterized by

$$V(z) \propto V_0 \ln \frac{b}{a} e^{ikz} \quad (\text{II-47})$$

$$I(z) \propto 2\pi V_0 \sqrt{\frac{\epsilon}{\mu}} e^{ikz} \quad (\text{II-48})$$

$$\frac{dV}{dz} = i\omega L I \quad (\text{II-49})$$

$$\frac{dI}{dz} = i\omega C V \quad (\text{II-50})$$

where  $V$  is the line voltage,  $I$  is the line current,  $V_0$  is the applied voltage,  $b$  is the inner diameter of the outside conductor, and  $a$  is the diameter of the inner conductor;  $L$  is the inductance per unit length of the line and  $C$  is the capacitance per unit length of the line.  $L$  and  $C$  are given by

$$L = \frac{\mu \ln \frac{b}{a}}{2\pi} \quad (\text{II-51})$$

$$C = \frac{2\pi\epsilon}{\ln \frac{b}{a}} \quad (\text{II-52})$$

The characteristic impedance of the line is

$$Z_0 = \sqrt{\frac{\mu}{\epsilon}} \frac{1}{2\pi} \ln \frac{b}{a} \quad (\text{II-53})$$

On the line, the voltage is the sum of forward and backward travelling waves:

$$V = V_+(e^{ikz} + \Gamma_L e^{-ikz}) \quad (\text{II-54})$$

$\Gamma_L$  is the reflection coefficient defined by

$$\Gamma_L = \frac{Z_L - Z_0}{Z_L + Z_0} \quad (\text{II-55})$$

where  $Z_0$  is the impedance of the transmission line and  $Z_L$  is the impedance of the load, in this case an antenna. The impedance of the transmission line is also a function of position and frequency.

$$Z(z) = Z_0 \frac{e^{ikz} + \Gamma_L e^{-ikz}}{e^{ikz} - \Gamma_L e^{-ikz}} \quad (\text{II-56})$$

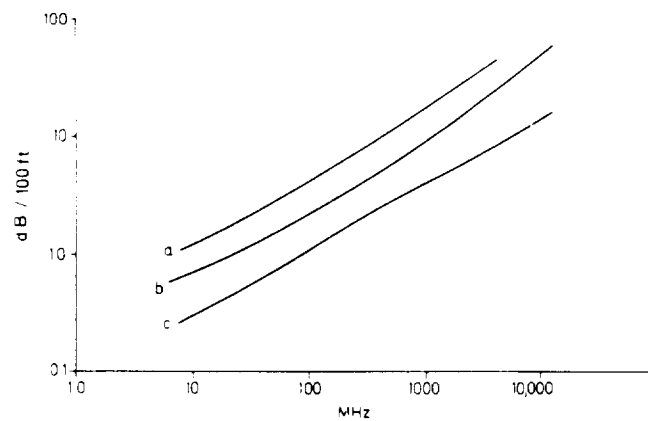
The ratio of the maximum voltage to the minimum voltage is the voltage standing wave ratio (VSWR):

$$\text{VSWR} = \frac{1 + |\Gamma_L|}{1 - |\Gamma_L|} \quad (\text{II-57})$$

Ideally,  $\text{VSWR} = 1$ ; i.e., the load is matched and all of the power carried by the transmission line is transmitted to the load. In general, however,  $Z_0 \neq Z_L$  and  $\text{VSWR} > 1$ . If the VSWR is low, then reflections produce dissipative losses. However, if the VSWR is high enough, the impedance will begin to vary along the transmission line. The variation in impedance is frequency-dependent, through the  $e^{ikz}$  factors; the signal's frequency may be forced to match the variations in impedance. This is known as "frequency pulling" and it is a problem if it keeps the transmitter of the spacecraft from producing signals at a stable frequency.

To reduce the VSWR, the impedance of the antenna can be matched to the transmission line impedance by using a stub tuner, which is a short-circuited shunt line attached to the main line. By varying the length and position of the shunt, a shunt admittance is added to the impedance which allows  $Z_L$  to be matched more closely to  $Z_0$ .

Coax cables also introduce ohmic losses (see Figure II-10). At the S band frequencies, losses are on the order of 10 dB per 30.5 m of cable length. For this reason, transmission line lengths must be minimized.



*Variation of attenuation with frequency*  
 (a) For small solid polythene cable RG-58B/U  
 (b) For medium solid polythene cable RG-213/U  
 (c) For semi-airspaced cable of same DOD as (b)

**Figure II-10**  
**Coax Cable Attenuation vs. Frequency and Cable Type**  
**[Rudge, et al, Volume 2, 1983]**



## **APPENDIX III Status and Monitoring Methods and Definitions**

### **Definitions and Benefit Breakdown**

Health Management - the measurement, assessment, communication and follow-up actions needed to know that a system is in working order and the recommendation of action to take if it is not

Condition Monitoring - real-time measurement of system operation (at all levels) for the determination of whether or not the system and its elements are operating nominally

Safety monitoring - real time measurement of system and element operation to determine if the system and its elements are operating within safety limits

Checkouts - test to verify that the system configuration meet mission-specific requirements (integration and prelaunch checkout); test to determine current system configuration status for future mission (post-launch checkout)

Failure diagnosis/ isolation - assessments that detect and isolate the on-line failure of a system or its elements and produce recommended recovery and maintenance action (this includes BIT)

Predictive diagnosis - assessments that determine if and when a system or its elements are going to fail

Preventive diagnosis - assessments that determine and produce recommended scheduled maintenance action (ground) and control actions (in-flight) required to keep a system and its elements operational

Explanation and recommendation - the ability to describe causes of detected/isolated, predicted and/or preventive events and to recommend action required to correct these events

Integrated maintenance database - a database integrating system, failure, repair, and historical data to support and provide maintenance aids required to verify and correct diagnostic assessments.

## Testing and Documentation Terminology

Ad-Hoc Test Approach	Add control and visibility points after initial design
Structured Test Approach	BISR, Scan Chain, LSSD, etc. - commercially available
Ambiguity Group	A collection of components which have the same fault signature (reading)
Baysien Process	Used to determine the probability of intermittent fault during a specific length of mission
Boundary Scan	A structured test built into an IC's circuitry
Built-in Test (BIT)	When a piece of equipment can automatically detect its own failures
Cannot Duplicate	An operation system fault which shows up once and cannot be duplicated under test conditions
Cluster Test	Testing more than one device simultaneously
Combinational Circuit	An electronic circuit with an output which is dependent on its present input signal states only. Its output is not dependent on any previous signals or states.
Component	A physical piece of hardware
Controllability	The ability of a device to maintain certain signal states or values.
Diagnostics	Finding a fault that has occurred

Failure	When an item is not longer able to perform its function
False Alarm	When diagnostics indicate that a failure has occurred when in fact, the item is working properly
False Alarm Rate	How often false alarms occur
Feedback Loop	When the output of a circuit is part of the input
Functional Test	Testing technique where tester manipulates and monitors signals from the UUT (Unit Under Test) I/O connector
Glue Logic	Components used to tie VLSI and VHSIC logic together
Hamming Code	Linear block code that can be used to detect or correct errors during data transmission
Hybrid	Combining more than one technique in one item
Incircuit Test	Where test equipment can simultaneously accesses each node in a circuit card so that individual components can be tested
Initialization	Setting the circuits before beginning a test
Intermittent Fault	A fault that is present some of the time, usually with no known or preventable reason
Level Sensitive Scan Device	A technique for scanning structures
Life Cycle Cost	Development, manufacture, installation, operation, maintenance, and replacements cost of a design over the useful lifetime

Linear Replaceable Unit (LRU)	The components that make up a single replaceable part. This is the part which will be replaced if any component in it is not functioning. This usually set the limit for required accuracy in testing.
Node	Electrical connection between two or more components
Observability	Degree to which a signal can be monitored
Off-line BIT	BIT that runs periodically in the background of functioning equipment
On-line BIT	BIT that runs once at power-up and whenever commanded by a controller
Prognostics	Detecting faults before they occur
Random Access Scan	Randomly run fault tests
Smart BIT	Measure stress parameters with performance to decide if fault is due to over-stress of fault-free equipment.
Synchronous	Several signals are synchronous if each signal is an integer multiple of the fastest signals frequency and a well defined phase relationship exists between them
Testability	The degree to which a design lends itself to simple and thorough testing
Unit Under Test (UUT)	Unit being tested

Very High Speed Integrated Circuit  
(VHSIC)

Very Large Scale Integration  
(VLSI)

### Benefits of VHM

Since VHM comes at a cost in terms of weight, development time, and production cost, there must be some benefit to installing this kind of a system. Installing a complex VHM system must have the following effects, or the system is excess weight.

- increased automation
  - streamline vehicle checkout
  - reduce ground/flight crew requirements
- better failure/error detection methods
  - enhance troubleshooting
  - reduce hardware costs
  - improve probability of mission success
  - reduce maintenance cost
- improve decision making (electronic and human)
  - quickened response time
  - provide consistent, reliable decisions
  - improve probability of mission success
- improve reliability
  - reduce hardware costs
  - improve probability of mission success

Implementing a monitoring system is useless if it does not 'pay its way' in term of increased mission performance and safety. When designing a VHM system, it is always important to ask if the modification is an improvement in term of simplicity and cost. If it represents a neat gizmo with no additional benefit in terms of reliability, performance, or

safety, then it has no place in the design. If simply putting enough components on-line at all time to assure that at least one of them is still working at the end of the mission requires less mass and power than putting in a unit for failure detection and switching over, the VHM system represents an unnecessary complication. Another example of a useless monitoring system is one that can isolate a fault to a lower component level than can feasibly be replaced during the mission. However, close monitoring of any potentially dangerous system is never a waste. Being able to get accurate data on the functioning of the propulsion system, especially the cryogenic tanks and the combustion chamber is always of utmost importance.

Using the above criteria, this is a list of drivers for the design of an onboard monitoring system

#### Repair and Replacement

- To ensure that at any point during the mission, the safety specifications are not violated, only one level of redundancy will be replaced at a time
- Physical placement should make replacement easy
- Use the expected lifetime of component to determine the necessary level of redundancy for a specific mission length, factoring in that a component may not be on for the entire duration of the mission

#### Anomaly Handling

- Health monitoring should be viewed as a passive system and not used to substitute for redundancy or hazard warning systems
- Never give a false positive, voting may be a good way to avoid this
- a clear and concise display, which indicates any out of spec readings
- if something can be indicated as going wrong, there should be a way to fix it.

## Periodic Maintenance

- set up scheduled maintenance based on history of time between failures
- the schedule should preserve the required levels of safety at all time during the mission
- degradation over time should be documented and changes to the maintenance schedule should be made based on this history

This last requirement is the most important, if the VHM causes as many problems as it solves, it is not a viable solution.

Display and Controls- for monitoring system status and to alert for failure, should also allow for acoustical warnings. Available, accessible and readable during an emergency. Controls for critical functions must not be able to be inadvertently changed.